THE UNIVERSITY OF WARWICK

University of Warwick institutional repository: http://go.warwick.ac.uk/wrap

A Thesis Submitted for the Degree of PhD at the University of Warwick

http://go.warwick.ac.uk/wrap/36685

This thesis is made available online and is protected by original copyright.

Please scroll down to view the document itself.

Please refer to the repository record for this item for information to help you to cite it. Our policy information is available from the repository home page.

12

SANDWICH INJECTION MOULDING WITH THERMOSET MATERIALS

by

SUBONGKOJ KIATMANAROJ

A thesis submitted in partial fulfilment of the requirements for the degree of
Doctor of Philosophy in Engineering

University of Warwick, Department of Engineering
May 2004

Dedication

To my mom, my dad and my brother

Contents

Contents.....i
List of Figures.....v
List of Tables.....xii
Acknowledgements.....xiv
Declaration.....xv
Abstract.....xvi
Abbreviations.....xvii

CHAPTER 1 INTRODUCTION.....1

CHAPTER 2 CO-INJECTION MOULDING.....6
2.1 Introduction.....6
2.2 History of Co-injection Moulding.....7
2.3 Sequential and simultaneous co-injection moulding processes.....17
2.3.1 Sequential co-injection moulding process of a single-channel moulding machine.....18
2.3.2 Sequential co-injection moulding process of a mono-sandwich moulding machine.....21
2.3.3 Simultaneous co-injection moulding process.....24
2.4 Different machine structures and injection unit arrangement.....26
2.5 Criteria of selecting raw materials.....29
2.6 Applications of sandwich moulding.....31
2.7 Previous studies in co-injection moulding process.....33
2.7.1 Experiment works.....33
2.7.2 Simulation works.....38
2.8 Related works on thermoset co-injection moulding.....41
2.9 Conclusions.....42

CHAPTER 3 THERMOSETTING PLASTICS AND MOULDING.....44
3.1 Definition.....44
3.2 Cross-linking and curing.....46

3.3 Flow behaviour of thermoset.....49
3.3.1 Rheological behaviour.....50
3.3.2 Rheological behaviour of thermoset.....54
3.3.3 Flow effects of thermoset in the mould.....56
3.4 Thermoset moulding processes.....58
3.4.1 Compression moulding.....59
3.4.2 Transfer moulding.....60
3.4.3 Injection moulding.....60
3.5 Thermoset components.....63
3.5.1 Automotive industry.....63
3.5.2 Electronic industry.....65
3.5.3 Housing for domestic appliance, business machine and kitchen ware.....66
3.5.4 Fuel cell.....66
3.6 Recycling of thermosets.....67
3.7 Conclusions.....70

CHAPTER 4 THERMOSET CO-INEJECTION MOULDING.....73
4.1 Introduction.....73
4.2 Process description.....75
4.3 Thermoset co-injection moulding machine.....77
4.3.1 Feeding unit.....77
4.3.2 Barrel, screw and nozzle.....79
4.4 The manifold system.....81
4.5 Thermoset mould.....85
4.5.1 The feed system.....85
4.5.2 Mould temperature control.....91
4.5.3 Ejection.....92
4.6 Related works in thermoset injection moulding.....94
4.7 Conclusions.....98

CHAPTER 5 MATERIAL EXPERIMENTS.....100
5.1 Introduction.....100
5.2 Gel test.....101

5.3 Melt flow index test.....104
5.4 Viscosity by capillary rheometer.....107
5.5 Conclusions.....111

CHAPTER 6 INJECTION MOULDING EXPERIMENTS.....113
6.1 Machine and tooling.....113
6.2 Mould.....115
6.3 Materials.....116
6.4 Experiments.....116
6.4.1 Single injection moulding of BMC.....117
6.4.2 Single injection moulding of Interpon 119
6.4.2.1 Effect of mould temperature.....120
6.4.2.2 Effect of manifold temperature.....125
6.4.3 Sandwich injection moulding of BMC and Interpon.....130
6.4.3.1 Initial experiment.....130
6.4.3.2 Increasing core injection delay time and skin metering stroke.....136
6.4.3.3 Roughness of the thermoset sandwich injection mouldings.....147
6.5 Conclusions.....152

CHAPTER 7 MANIFOLD SYSTEM DESIGN AND IMPROVEMENT.....155
7.1 Introduction.....155
7.2 The existing manifold system.....156
7.2.1 Design concept.....156
7.2.2 Problems during injection moulding.....159
7.3 New manifold system design concept.....162
7.4 Conclusions.....167

CHAPTER 8 THERMOSET INJECTION MOULDING SIMULATION.....168
8.1 Introduction.....168
8.2 Moldflow® simulation of the existing manifold system and the tray.....171
8.2.1 Result of Moldflow simulation of the existing manifold system
and the tray.....173
8.2.2 Effect of mould temperature and injection speed on material temperature....177

8.3 Moldflow® simulation of the tray.....187
8.4 Moldflow® simulation of the new manifold.....191
8.5 Maximum shear rate during simulations of the tray mould, the existing manifold and the new manifold system.....197
8.6 Conclusions.....199

CHAPTER 9 CONCLUSIONS.....202
Recommendation for future work.....204

REFERENCES.....206

APPENDICES
Appendix I: New manifold drawings.....212
Appendix II: Example of Moldflow® simulation screen outputs.....221
Appendix III: Melt temperature-time plots results of the existing manifold.....246
Appendix IV: Melt temperature-time plots results of the new manifold.....262
Appendix V: Papers published in Progress in Rubber, Plastics and Recycling Technology
Sandwich Injection moulding of thermosetting materials
Part I: Initial experiments.....279
Sandwich Injection moulding of thermosetting materials
Part II: Effects of moulding parameters.....293

List of Figures

CHAPTER 1

Figure 1.1 Cross section of a sandwich moulding shows skin and core layers.....2

CHAPTER 2

Figure 2.1 Sandwich moulding and the fountain flow effect.....6

Figure 2.2 Single channel technique.....8

Figure 2.3 Principle mould filling diagram of the single-channel nozzle co-injection moulding process.....9

Figure 2.4 Battenfeld's two-channel nozzle.....10

Figure 2.5 Principle mould filling diagram of the simultaneous co-injection moulding process.....11

Figure 2.6 Billion's three-channel nozzle.....12

Figure 2.7 Kortec's three-channel nozzle.....12

Figure 2.8 Mono-sandwich injection moulding.....13

Figure 2.9 3K-injection moulding system.....15

Figure 2.10 Addmix co-injection system.....15

Figure 2.11 Twinshot co-injection system version I.....16

Figure 2.12 Twinshot co-injection system version II.....17

Figure 2.13 The different techniques for co-injection moulding process.....18

Figure 2.14 Principle mould filling diagram of the mono-sandwich co-injection moulding process.....23

Figure 2.15 Overview of the available standard arrangements of the injection unit..27

Figure 2.16 Design of a six-component injection moulding machine of Ferromatik Milacron.....29

CHAPTER 3

Figure 3.1 The simplified 2D model of a.) Cross-linked network polymer and b.) Thermoplastic polymer.....46

Figure 3.2 Viscosity and time of a thermoset at a constant temperature.....47

Figure 3.3 Effect of temperature on gel time of a thermoset polyester.....48

Figure 3.4 Effect of temperature on viscosity and time of thermoset.....48

Figure 3.5 Simple shear experiment.....50
Figure 3.6 The characteristic behaviour of Newtonian and non-Newtonian fluid....51
Figure 3.7 Flowing of fluid in the mould; A: Newtonian fluid, B: non-Newtonian fluid and C: high fibre-filled polyester melt.....56
Figure 3.8 The fountain flow pattern of polymer in the mould.....57
Figure 3.9 The fountain flow affects the short fibre orientation of a glass-polypropylene, showing the short fibre oriented parallel to the flow.....58
Figure 3.10 Diagram of compression moulding operations.....59
Figure 3.11 Simplified diagram of a transfer moulding machine.....60
Figure 3.12 Diagram of a fuel cell stack.....66

CHAPTER 4

Figure 4.1 Effects of various stages of thermoset injection moulding.....74
Figure 4.2 Diagram of the thermosetting co-injection moulding machine.....75
Figure 4.3 Moulding cycle of thermoset co-injection moulding.....77
Figure 4.4 Stuffer unit: a.) Loading BMC into hopper and b.) Fully loaded hopper.78
Figure 4.5 General characteristic of a thermoset screw and barrel.....80
Figure 4.6 Recommended steel for thermoset barrel system showing ANSI grades and CPM® grades.....81
Figure 4.7 a.)The manifold for thermoset co-injection moulding machine. (The halves are placed between the injection unit and the heated mould.) and b.) The cross-section of the manifold nozzle.....82
Figure 4.8 The feed system.....86
Figure 4.9 Plane surface sprue.....86
Figure 4.10 Curved contact surface sprue.....86
Figure 4.11 Cross-sections for runners a.) Favourable runners b.) Unfavourable runners.....88
Figure 4.12 Different types of gate in used in injection moulding.....89
Figure 4.13 Ejector pin positions: a.) Good position and b.) Bad position.....93
Figure 4.14 Acceptable ejector position with inclined angles to facilitate demoulding.....93
Figure 4.15 Cycle temperature change on the mould surface during injection moulding of a thermoset.....96

CHAPTER 5

Figure 5.1 Gel time results of BMC and Interpon.....103

Figure 5.2 Melt flow indexer simplified diagram.....105

Figure 5.3 Capillary rheometer simplified diagram.....108

Figure 5.4 Diagram of the nozzle for the inline measuring system.....109

Figure 5.5 Relationship between viscosity and shear rate of BMC and Interpon...110

CHAPTER 6

Figure 6.1 a.) The manifold system and b.) Cross-section of the manifold during injection moulding process.....115

Figure 6.2 Front and side view of the tray moulding.....116

Figure 6.3 Front and back of a BMC full moulding.....118

Figure 6.4 Interpon moulding at 140°C mould temperature.....121

Figure 6.5 Interpon moulding at 150°C mould temperature.....121

Figure 6.6 Interpon moulding at 160°C mould temperature.....122

Figure 6.7 Comparing the three mouldings, 140, 150, 160°C mould temperature...122

Figure 6.8 Some flow marks at the edge near the top of the moulding from Figure 6.6.....123

Figure 6.9 Some flow marks at another side of the moulding from Figure 6.6.....124

Figure 6.10 Interpon moulding at 65°C manifold temperature.....126

Figure 6.11 Interpon moulding at 70°C manifold temperature.....126

Figure 6.12 Interpon moulding at 80°C manifold temperature.....127

Figure 6.13 Interpon moulding at 90°C manifold temperature.....127

Figure 6.14 Comparison of Interpon mouldings at varied manifold temperature...128

Figure 6.15 Diagram of injection settings for sandwich injection moulding of BMC and Interpon.....131

Figure 6.16 The injection velocity diagram of Interpon. The co-ordinate represents the screw velocity when it reaches 8-mm metering stroke.....132

Figure 6.17 Thermoset sandwich moulding from the setting in Table 6.3.....134

Figure 6.18 Back view of the moulding from the setting in Table 6.3.....135

Figure 6.19 Front and back of the sandwich moulding of Interpon and BMC when using 0.5-second delay time, 6.0mm switchover point and 30:50 skin/core ratio.....136

Figure 6.20 Front and back of the sandwich moulding of Interpon and BMC when using 1.5-second delay time, 6.0mm switch over point and 140:50 skin/core ratio.....137

Figure 6.21 Comparison of the three sandwich mouldings produced by the novel co-injection moulding machine 138

Figure 6.22 Cross sections of the sandwich injection mouldings; section A and section B are magnified and shown in Figure 6.23 and 6.24, respectively.....140

Figure 6.23 Magnified view of section A in Figure 6.22.....141

Figure 6.24 Magnified view of section B in Figure 6.22.....142

Figure 6.25 Molecular flow at the moulding skin when injecting a thermoset material from a.) Central sprue gate and b.) Side sprue gate.....144

Figure 6.26 The cut sample used to measure roughness of the surface.....147

Figure 6.27 Graph shows the roughness of a moulding surface.....148

Figure 6.28 Example of data output from surface profile.....148

CHAPTER 7

Figure 7.1The existing manifold system a.) Side view and b.) Isometric view.....157

Figure 7.2 Positions of cartridge heaters and thermocouples in moving and fixed platens of the existing manifold system.....158

Figure 7.3 Possible cause of the problems during single injection moulding of Interpon and sandwich injection moulding.....159

Figure 7.4 The new manifold system a.) Side view and b.) Isometric view.....163

Figure 7.5 Close-up view of the new nozzle design.....166

CHAPTER 8

Figure 8.1 The meshing model of the tray and the existing manifold runner.....172

Figure 8.2 Melt temperature of the material at different positions in the mould and manifold. The mould and manifold is at 80°C and injection time is 2 seconds.....174
Figure 8.3 Melt temperature of the material at different positions in the mould and manifold. The mould and manifold is at 90°C and injection time is 2 seconds.....175
Figure 8.4 Melt temperature of the material at different positions in the mould and manifold. The mould and manifold is at 120°C and injection time is 2 seconds.....175
Figure 8.5 Cured layer fraction results at 120°C mould temperature (left) and 130°C (right) (Injection time 4 seconds).....175
Figure 8.6 Melt temperature of the material at different positions in the mould and manifold. The mould and manifold is at 80°C and injection time is 3 seconds.....178
Figure 8.7 Melt temperature of the material at different positions in the mould and manifold. The mould and manifold is at 90°C and injection time is 3 seconds.....178
Figure 8.8 Melt temperature of the material at different positions in the mould and manifold. The mould and manifold is at 100°C and injection time is 3 seconds.....179
Figure 8.9 Melt temperature of the material at different positions in the mould and manifold. The mould and manifold is at 110°C and injection time is 3 seconds.....179
Figure 8.10 Melt temperature of the material at different positions in the mould and manifold. The mould and manifold is at 120°C and injection time is 3 seconds.....180
Figure 8.11 Melt temperature of the material at different positions in the mould and manifold. The mould and manifold is at 130°C and injection time is 3 seconds.....180
Figure 8.12 Time and temperature curve of a thermoset polyester in the sprue end when varying mould temperature. Injection time is 3 second.....183
Figure 8.13 The melt temperature during injection and curing phase of a thermoset.....184

Figure 8.14 Fusion model of the tray.....187
Figure 8.15 The melt temperatures at the mould sprue end at varied injection time when the manifold and mould were set at 120°C.....189
Figure 8.16 The melt temperatures at the mould sprue end at varied injection time when the mould was set at 120°C.....189
Figure 8.17 Percentage of filling at different injection time when the mould was set at 130°C and 140°C 190
Figure 8.18 Process of designing the new manifold system.....192
Figure 8.19 Meshing model of the new design manifold and the tray mould.....192
Figure 8.20 Melt temperature at different positions of 120°C mould temperature
Figure 8.20 a.) 1-second injection time.....194
Figure 8.20 b.) 2-second injection time.....195
Figure 8.20 c.) 3-second injection time.....195
Figure 8.20 d.) 4-second injection time.....196
Figure 8.20 e.) 5-second injection time.....196

APPENDIX III Moldflow® simulation results Injection time-Melt temperature plots of the existing manifold system and the tray moulding
Figure App3.1 Injection time-melt temperature plot at 1-second injection time and mould temperatures is varied from 80 to 130°C.....246
Figure App3.2 Injection time-melt temperature plot at 2-second injection time and mould temperatures is varied from 80 to 130°C.....249
Figure App3.3 Injection time-melt temperature plot at 3-second injection time and mould temperatures is varied from 80 to 130°C.....252
Figure App3.4 Injection time-melt temperature plot at 4-second injection time and mould temperatures is varied from 80 to 130°C.....255
Figure App3.5 Injection time-melt temperature plot at 5-second injection time and mould temperatures is varied from 80 to 130°C.....258

APPENDIX IV Moldflow® simulation results Injection time-Melt temperature plots of the new manifold system and the tray moulding
Figure App4.1 Injection time-melt temperature plot at 1-second injection time and mould temperatures is varied from 80 to 130°C.....262

Figure App4.2 Injection time-melt temperature plot at 2-second injection time and mould temperatures is varied from 80 to 130°C.....265
Figure App4.3 Injection time-melt temperature plot at 3-second injection time and mould temperatures is varied from 80 to 130°C.....268
Figure App4.4 Injection time-melt temperature plot at 4-second injection time and mould temperatures is varied from 80 to 130°C.....271
Figure App4.5 Injection time-melt temperature plot at 5-second injection time and mould temperatures is varied from 80 to 130°C.....274

List of Tables

Chapter 2

Table 2.1 Operating sequence of the single-channel moulding machine.....19

Table 2.2 Operating sequence of the mono-sandwich moulding machine.....21

Table 2.3 Operating sequence of the simultaneous co-injection moulding machine.25

Table 2.4 Compatible and incompatible thermoplastic material combinations.....31

Chapter 3

Table 3.1 Classification of thermosetting materials.....45

Table 3.2 Advantages and disadvantages of different thermoset moulding method..62

Chapter 4

Table 4.1 Operating sequence of thermoset co-injection moulding.....83

Chapter 5

Table 5.1 Composition of BMC G7B5580.....100

Table 5.2 Interpon melt flow indexes (g/10min) and standard deviation at three temperatures.....106

Chapter 6

Table 6.1 Specification of BA2000/630+630 thermoset co-injection moulding machine.....114

Table 6.2 Machine condition settings for BMC injection moulding.....117

Table 6.3 Settings for single injection moulding of Interpon.....119

Table 6.4 Settings for sandwich injection moulding of Interpon and BMC.....130

Table 6.5 Summary of all injection moulding experiments.

Table 6.6 The roughness of the thermoset sandwich injection mouldings.....149

Chapter 7

Table 7.1 Operating sequence of the new manifold system.....164

Chapter 8

Table 8.1 Conclusion of the polyester mould filling simulation. Using the manifold and the tray as a single mould.....173

Table 8.2 Conclusion of the polyester mould filling simulation of the tray mould..188

Table 8.3 Conclusion of the polyester mould filling simulation. Using the new designed manifold and the tray as a single mould.....193

Table 8.4 The Maximum shear rate during injection moulding simulations of the tray, the existing manifold and the new manifold system.....197

Acknowledgements

The author is grateful to Dr Gordon F. Smith for his guidance and assistance and also would like to thank Dr Vannessa Goodship for her support and useful suggestion throughout the duration of this project.

I would like to express my appreciations to the British Industrial Plastics Ltd, Akzo Nobel Powder Coating Ltd and Synres-Almoco BV for all of their materials that were used in this project.

All experiment works could not be completed without technical support from Mr Wal Cosgriff and Mr Graeme Thacker.

Acknowledgements are due to the National Metal and Materials Technology Centre (MTEC), the ministry of Science, Technology and Environment of Thailand for their sponsorship of my studies.

Lastly, this thesis would not be completed without encouragement from my family. I would like to thank for their love and support throughout the time whilst I have been studying in UK.

Declaration

I declare that all the work described in this thesis was undertaken by myself otherwise acknowledged in the test and that none of the work has previously been submitted for any academic degree. All sources of quoted information have been acknowledged by means of references.

Subongkoj Kiatmanaroj

Abstract

This project aimed to study the feasibility of making a thermoset sandwich injection moulding from a novel thermoset co-injection moulding system. Two thermoset polyesters, BMC and a powder coating, were used for all experiments. Flow and cure of those materials in a newly designed manifold system were studied and some thermoset sandwich injection mouldings have been produced. Despite producing novel co-injection mouldings using two thermoset materials together, the results showed that the existing system was not applicable for large-scale production of sandwich parts and needed some improvements.

The experiments on the moulding materials and single injection of each material gave temperature windows and settings for the co-injection moulding. The results from all experiments indicated that temperature and the time of applying heat to a thermoset material were very important to its flow ability and formation. Especially when producing a sandwich moulding, adequate heat and time was necessary for the skin material to form a sufficient layer to cover the core material. Investigation of the sandwich moulding cross-sections showed that applying more core injection delay time could help to increase the skin thickness. Surface assessment indicated that the surface quality was also improved when the skin layer was thicker. However, core break-through at the position opposite to the mould gate was found in all sandwich mouldings showing that the type of mould gate was also important. A central sprue gated mould used in these experiments was found to be not suitable for producing a sandwich component using this machine configuration.

A new manifold design was proposed and was compared to the existing manifold designed by using a simulation software package from Moldflow®. Thermoset single injection moulding simulation was used to help to understand the flow and cure of a thermoset material in both manifold designs. It was shown that the new manifold system design was an improvement on the existing one.

Abbreviations

ABS	Acrylonitrile-butadiene-styrene
ASA	Acrylic-styrene-acrylonitrile
BMC	Bulk moulding compound
EVA	Ethylene vinyl acetate
PA6	Polyamine 6 or nylon 6
PA66	Polyamine 66 or nylon 66
PBT	Polybutylene terephthalate
PC	Polycarbonate
PE-HD	High-density polyethylene
PE-LD	Low-density polyethylene
PET	Polyethylene terephthalate
PMMA	Polymethyl methacrylate (acrylic)
POM	Polyoxymethylene (acetal)
PP	Polypropylene
PPO mod.	Modified Polyphenylene oxide
PS-GP	Polystyrene General purpose
PS-HI	Polystyrene High impact
PVAC	Polyvinyl acetate
PVC	Polyvinyl chloride
SAN	Styrene acrylonitrile copolymer
TPU	Thermoplastic polyurethane

Chapter 1

Introduction

Injection moulding of plastics is a successful process in the plastic industry as it has faster production rates compared to other types of plastic manufacturing. A wide range of materials including thermoplastics and thermosets can be injected through a nozzle and transformed into many useful finished components within a few minutes. With new techniques and technologies nowadays, it allows the usage of plastics in many applications, which expands the market from domestic general purposes, for example, a toaster and a kettle to heavy duty usage, such as high voltage electrical boxes and covers. More importantly, some metal parts in the automotive industry are being replaced with plastic components, such as engine covers and vehicle panels in order to produce a better fuel consumption vehicle. Some of these applications require additives to improve the components' properties and prevent them from environmental degradation. For example, foaming agent may be used for reducing shrinkage of a thick but lightweight part and for the purpose of strength improvement, glass fibres are added. However, adding those additives to the materials can be disadvantageous. The rough surface of parts filled with glass fibres or foaming agent is unsatisfactory in some cases when appearance is important. Consequently, an additional process is needed in order to finish the parts and thus increase the production time and cost.

One of the plastic moulding technologies called the co-injection or the 2K-injection moulding is an optional solution[1-3]. The process combines the main and the secondary operations; plastic injection moulding and surface finish treatment together. It produces a thermoplastic component from two materials but presents only one plastic outside while the other is encapsulated. Because of this unique characteristic, the product can be made with its unwanted surface covered completely at the same time. As a result, sometimes the process is referred to as a sandwich injection moulding. This technology is also useful for plastic recycling. The used material is injected as the inner layer called 'core layer' covered by virgin material outside called 'skin layer' (see Figure 1.1). Sometimes, to reduce production cost, cheaper material can also be a 'core' and is coated by a more expensive 'skin'. Another example of its useful application is in-mould painting components when an unpainted plastic part can be coated by a colour material during the machine process.

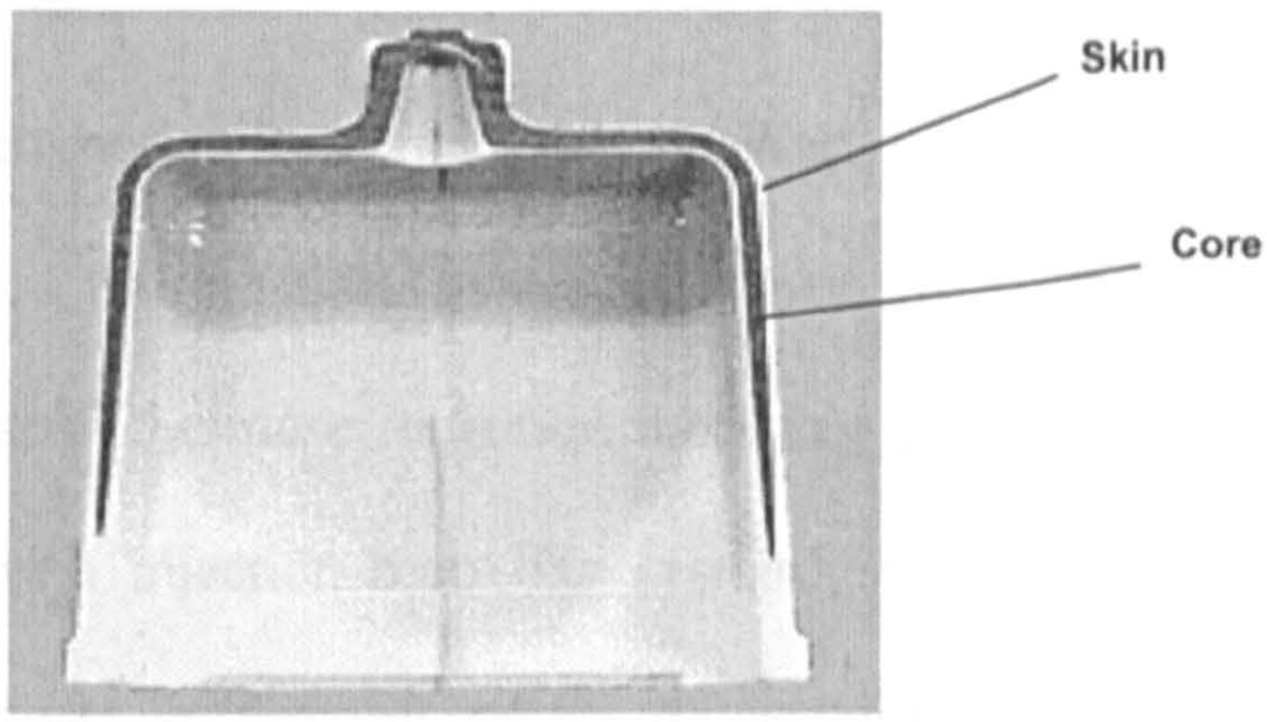

Figure 1.1 Cross section of a sandwich moulding shows skin and core layers.

The sandwich injection moulding technology is very successful today but is limited to thermoplastics. The process of sandwich injection moulding should also be possible for thermosets, even though it is more difficult since controlling temperature

and cross-linking is a problem. The use of recycled materials as the sandwich's core is very interesting in term of thermoset recycling. Apart from the existing recycling methods, such as (i) mixing some regrind material with the virgin polymer[4-6] and (ii) reusing the glass fibre[7], the sandwich technique could offer a further alternative of incorporating the regrind in the core so as not to affect the skin properties.

Another useful application of the sandwich technology is to coat a glass-filled thermoset with a paint material. Thermoset materials are notoriously difficult to paint. Post mould, the monomer often "pops" from the surface and ruins the aesthetics, thus a masking coat is often used. Even so, "popping" can occur in the paint oven. Sandwich moulding skin could be used to mask and protect the surface from this effect whilst providing the paint. As with the thermoplastic case, a coloured component can be made in one cycle without the need for a paint line. However, until this work, no co-injection moulding of thermosets has been reported.

At the International Automotive Research Centre in Warwick Manufacturing Group, University of Warwick, a new manifold system was specially designed and installed on a Battenfeld two-barrel thermoset injection moulding machine to function as a novel thermoset sandwich injection moulding system. Since there were no exact design rules for a thermoset co-injection system, it was built on a general design and it was likely that the system needed some improvements.

The aim of this project was to study the feasibility of making a thermoset sandwich injection moulding from the newly designed manifold system and machine with regard to how thermosets flow and cure in the system. Two thermoset polyesters, a

bulk moulding compound (BMC) from British Industrial Polymer and a black conductive powder coating (Interpon) from Akzo Nobel were used in all experiments, respectively as the moulding core and skin. This study will focus on the following.

- To produce novel thermoset co-injection mouldings.

To achieve this first aim, the following objectives are necessary.

- To study the filling and curing of thermoset polymers when co-injected from the injection units through the new manifold into the mould.
- To study the effect of temperature during co-injection of BMC and Interpon on the mould filling and curing of the materials in the manifold system.
- To determine the effect of time of injection to the formation of skin and core layers in sandwich moulding component.
- Design a new manifold system to improve the existing system

The thesis is divided into 9 chapters. Chapter 2 contains a literature review on co-injection or sandwich injection moulding technology since it was invented. All different techniques to produce a sandwich component are explained with diagrams showing how each system works. Previous research including experiment and simulation are also discussed at the end of this chapter.

Chapter 3 contains information on thermoset material properties. This includes the characteristics of how these materials cure and flow. Moulding techniques for thermosets and their applications are provided.

Chapter 4 describes the thermoset co-injection moulding machine, including a process description and the general machine design from the feeding units, injection units and manifold system to the mould. The current work related to the thermoset co-injection moulding is explained at the end of this chapter

Chapter 5 details the experiments on two thermoset materials, BMC and Interpon, which were used as core and skin for the sandwich moulding experiments. This chapter focuses on how these materials react to the change of temperature and shear rate in terms of curing and flowing.

Experiments on the thermoset co-injection moulding are provided in Chapter 6. These include single injection moulding of each material and sandwich injection moulding. Results of all experiments are shown and the problems, which occurred during the experiment, are discussed.

Chapter 7 explains the mechanical design of the existing manifold system. Some problems that occurred during injection moulding are pointed out and described. Later in this chapter, a new manifold design is proposed.

The existing manifold system and the new one are compared using Moldflow Plastic Insight® 4.1, a simulation programme in Chapter 8. Flowing of a thermoset material through each design at the same machine condition setting is studied and discussed.

Chapter 9 draws the conclusions on the work and makes suggestions for further work.

Chapter 2

Co-injection moulding

2.1 Introduction

Co-injection moulding, which is also sometimes called 2K-injection or sandwich injection moulding is a process for producing sandwich structure plastics. The machine is used to inject two or more different but compatible thermoplastic materials into a mould. As illustrated in Figure 2.1, once the first polymer melt flows into the mould and touches the walls, it will form a film or a thin frozen layer with some viscous liquid material flowing faster near the centre and slower near to the film. This is a characteristic of polymer flow in an injection mould, called '*Fountain Flow*'. Followed by the second material, which penetrates to the first material and forces it to flow further into the mould, a skin-core layered moulding is produced.

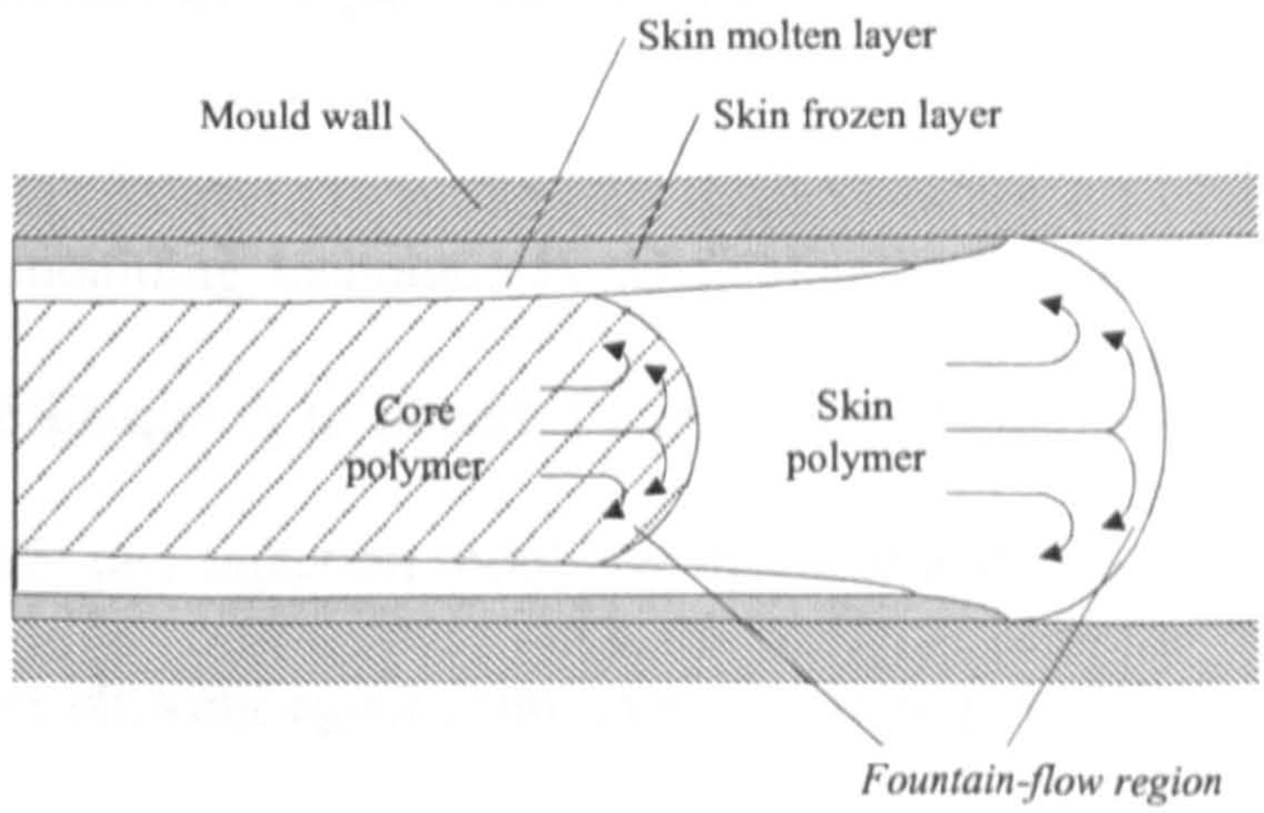

Figure 2.1 Sandwich moulding and the fountain flow effect

This process can be sequential or simultaneous injection dependent on the machine settings. For sequential injection moulding, skin and core materials are injected sequentially or orderly; one follows another while for simultaneous injection moulding, skin and core materials can be injected almost at the same time or overlap each other. These will be explained in detail in section 2.3. In this chapter, the applications of sandwich moulding will also be described followed by many types of co-injection moulding machines, guidelines for material selection and previous studies in this subject.

2.2 History of co-injection moulding

The co-injection moulding technology was invented in 1970 by ICI[3,8-10], one of a group of companies including Asahi-Dow Corporation, Borg Warner Chemicals, Allied Chemical, USM and AMF, who were developing many new techniques for thermoplastic foam processing. At that time, producing a part with lower material density and acceptable mechanical properties had been achieved but an improvement in the surface smoothness of the parts was needed.

ICI's co-injection moulding technique is schematically shown in Figure 2.2. The objective of this technique is to obtain a part with a smooth surface from a solid surface injected from one injection moulding machine and fill the moulding's core by a material with a blowing agent from another. These polymer melts are injected sequentially into a cold mould through an adjustable valve. It is called the ***Single Channel Technique*** as the materials are injected through only one channel. The first polymer injected forms the skin layer and surrounds the core, which is injected afterwards. The valve in front of both nozzles functions as a gate to switch between

those two materials after getting the required amounts of plastics from each barrel. In order to change the thickness of skin, injection moulding parameters, such as injection velocity, melt temperature, mould temperature, and melt viscosities are varied.

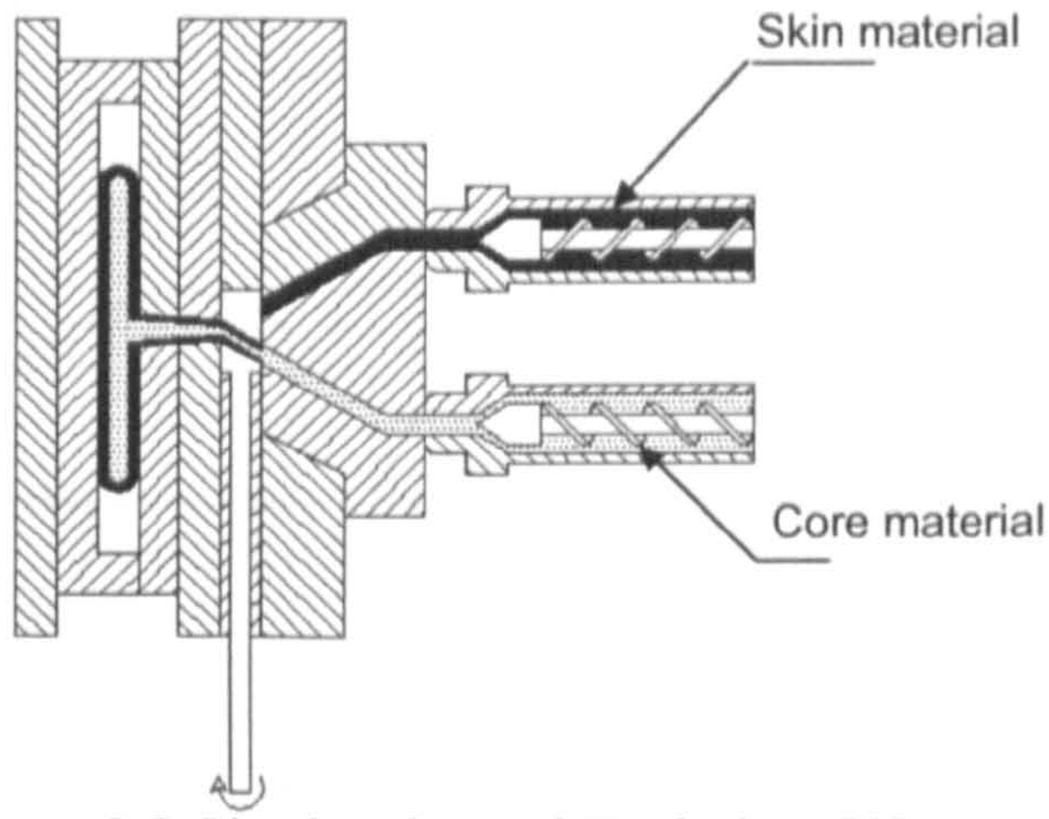

Figure 2.2 Single Channel Technique[9]

A disadvantage of the method is that when switching from injection of skin to core, the mould cavity pressure drops, so the melt front comes to a temporary stand still as shown in Figure 2.3. This is revealed on the finished part as a shadow marks or gloss marks. If requirements for the surface finish are high, it might be necessary to paint the part after moulding. Details of how this technique works is described more fully in section 2.3.1.

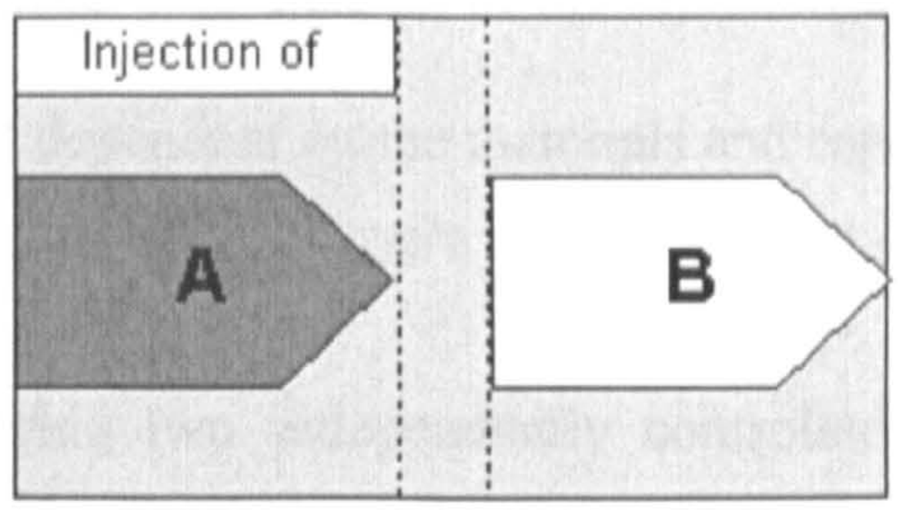

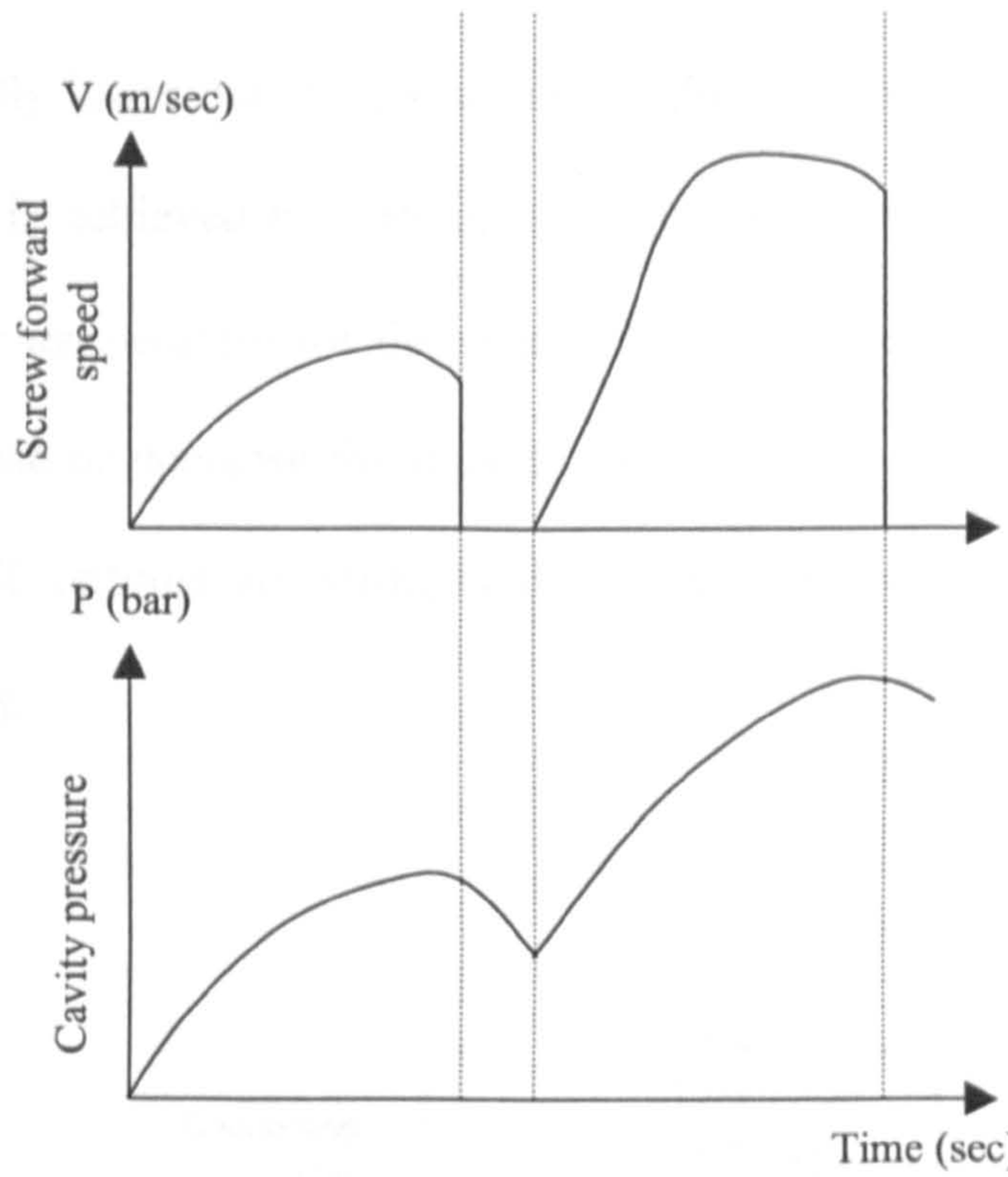

Figure 2.3 Principle mould filling diagram of the single-channel nozzle co-injection moulding process

In the mid 1970's, a new nozzle design from Battenfeld called the ***Two Channel Technique*** was developed in order to solve the pressure difference during the switching of two materials[3,11] (Figure 2.4). This special nozzle was designed to fit a machine with two injection units. It is equipped with two separate, concentric channels that can be independently operated, opened and closed, hydraulically. As a result, it allows injection of skin and core simultaneously, which helps avoid gloss marks by maintaining a smooth flow velocity (see Figure 2.5). Typically the duration

of the simultaneous phase is 25 percent of the injection time for the skin component. The duration is varied dependent on the materials and especially mould geometry.

An advantage of having two independently controlled injection units is that an optimum distribution of core material can be obtained. Normally skin viscosity should be slightly lower than core viscosity. If the same material is used in sandwich moulding, this is achieved by varying the machine's settings. For example, adjust 20-30°C higher temperature for the skin to lower its viscosity. In some cases, it is useful to increase or decrease the injection velocity and injection delay time of the core. Again, all settings are strongly dependent on both material properties and mould geometry.

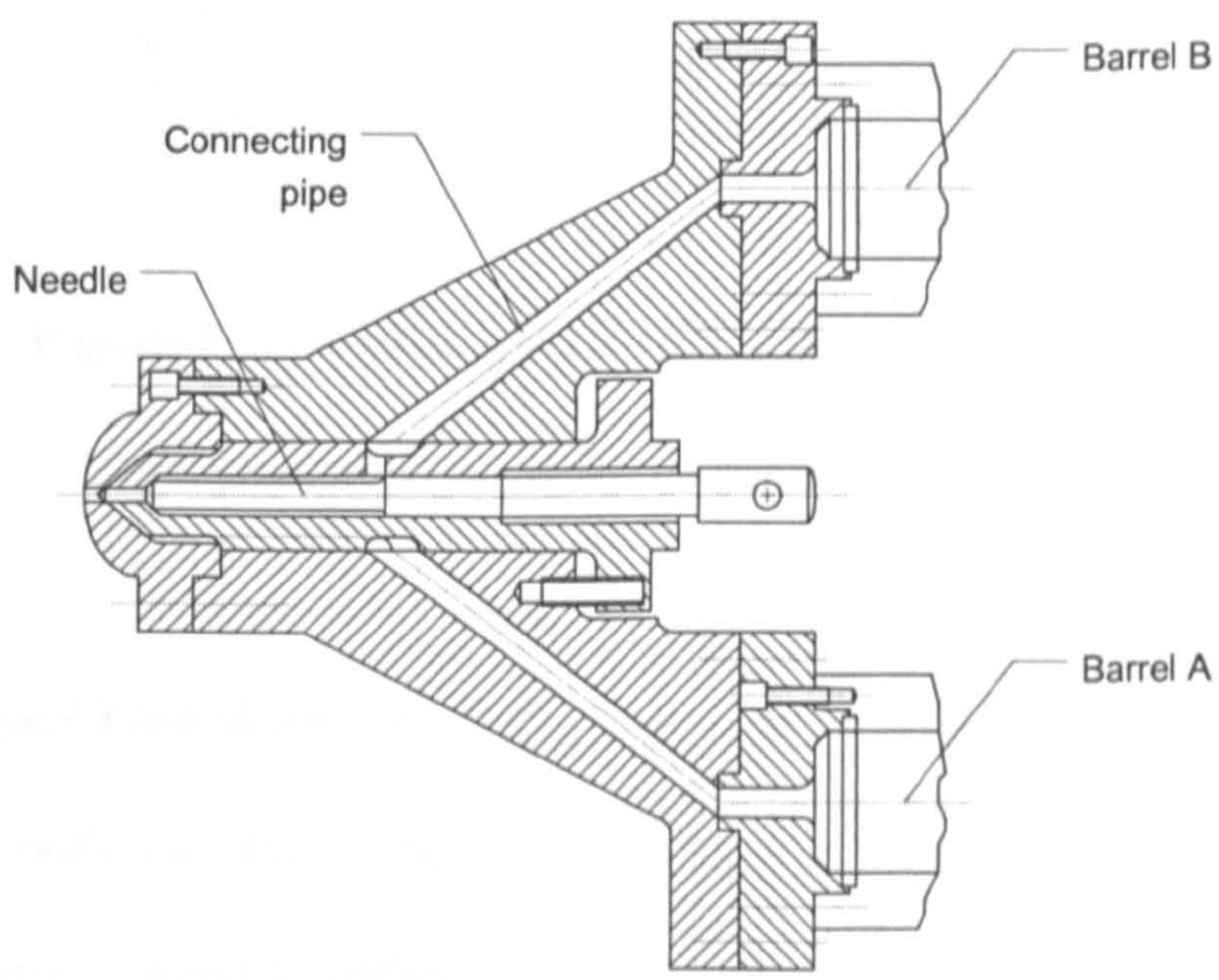

Figure 2.4 Battenfeld's two-channel nozzle[12]

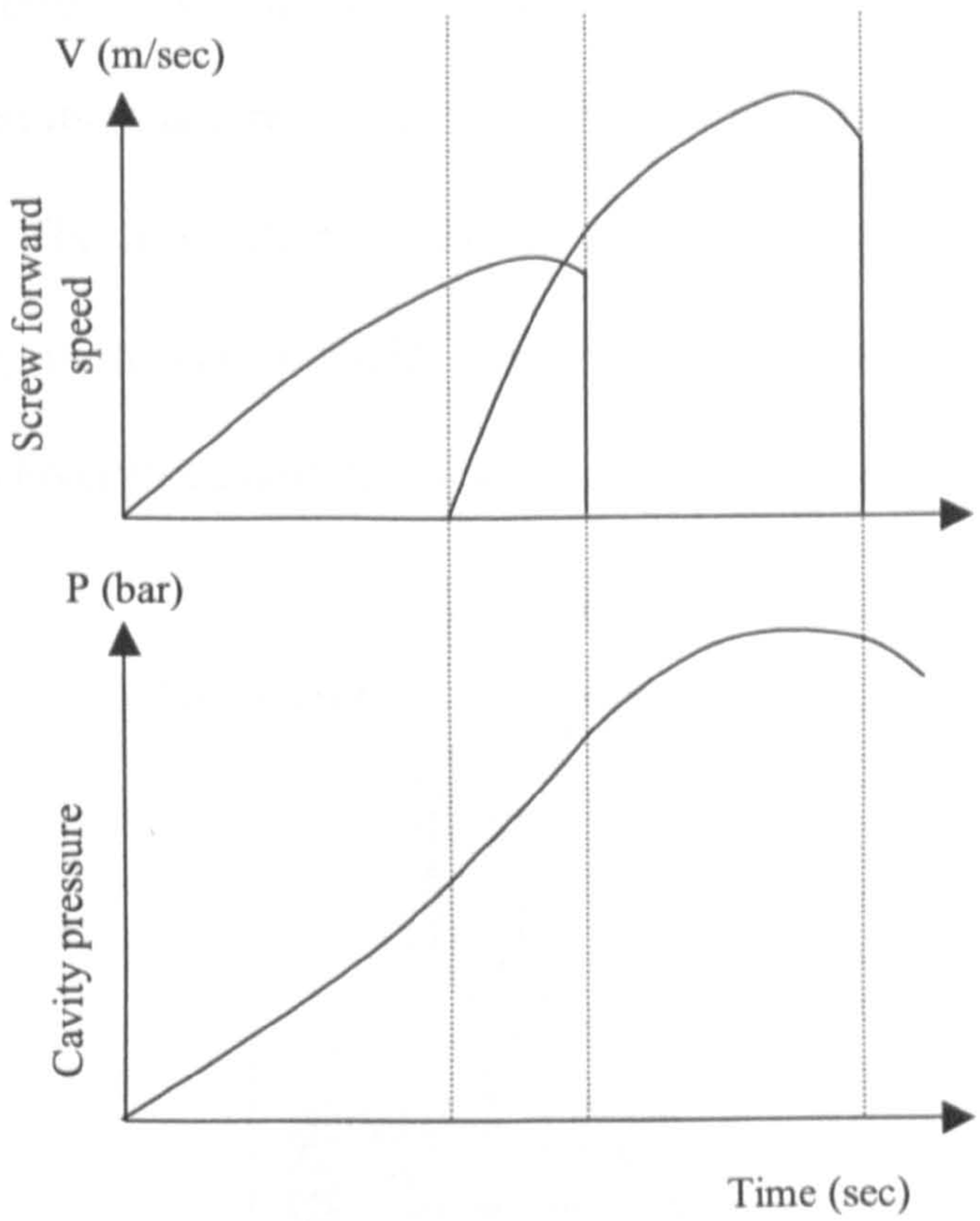

Figure 2.5 Principle mould filling diagram of the simultaneous co-injection moulding process

The ***Three Channel Technique*** is used to solve some problems that may occur when producing parts with the Two Channel Technique. Similar to the Two Channel Technique, an extra channel is applied to the nozzle to produce the third passage for the third material. As shown in Figure 2.6, the third channel of Billion's three-channel nozzle is used to inject a compatibiliser, which forms some chemical bonds between skin and core. This can be used in the case that the two polymers are not

compatible or material layers cannot stick to each other, which leads to unsatisfactory mouldings. The use of compatibiliser overcomes this problem.

A problem that is normally found in a central gate designed mould is the skin thickness at the position opposite of the gate is too thin. It is because the highest pressure is developed there and results in the core melt pushing some skin melt to the edge of the mould. The three-channel nozzle designed from Kortec gives another channel for injecting more skin material into the mould as shown in Figure 2.7. It adds additional skin layer there and thus gives a more stable skin thickness.

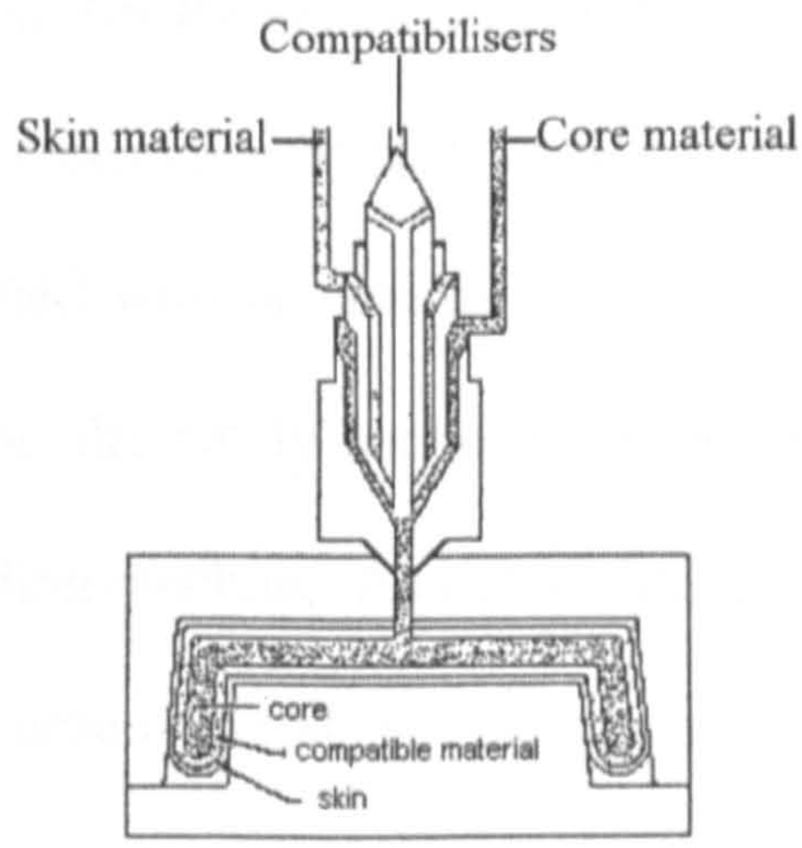

Figure 2.6 Billion's three-channel nozzle[13]

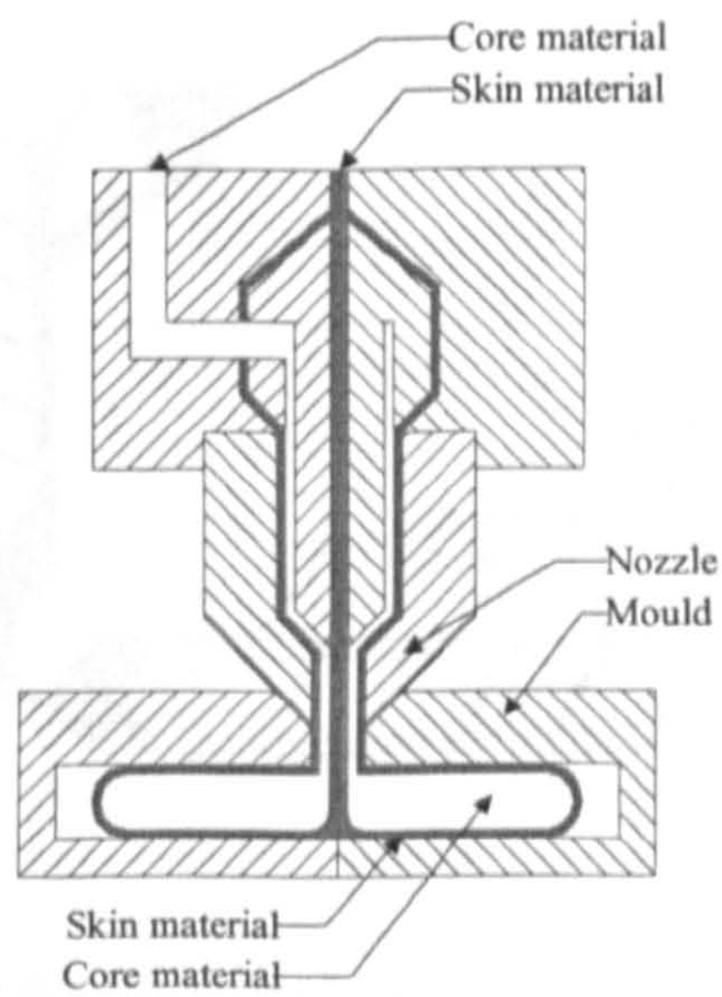

Figure 2.7 Kortec's three-channel nozzle[14]

Patented in 1995, Ferromatik Milacron invented a new apparatus for the sandwich method of injection moulding, called the ***Mono Sandwich Technique***[15]. As claimed in the patent, typical injection moulding apparatus designed to produce sandwich mouldings have employed two injection units. Machines of this type have disadvantages involving the high initial cost of the required components and associated control capacity for close operation monitoring to ensure that the volume flow of material is constant through the nozzle into mould when changing between the skin material and the core material.

Ferromatik Milacron proved that the sandwich injection moulding was possible by a single injection unit. The machine is simple as it is based on a standard injection moulding machine combined with an auxiliary plasticising unit, which has a hot runner manifold that can be alternately connected to or disconnected from the main injection unit of the moulding machine. As shown in Figure 2.8, two material melts are layered in the barrel. These materials are injected into the mould cavity within a single injection stroke. The details of how this technology works will be described in section 2.3.2.

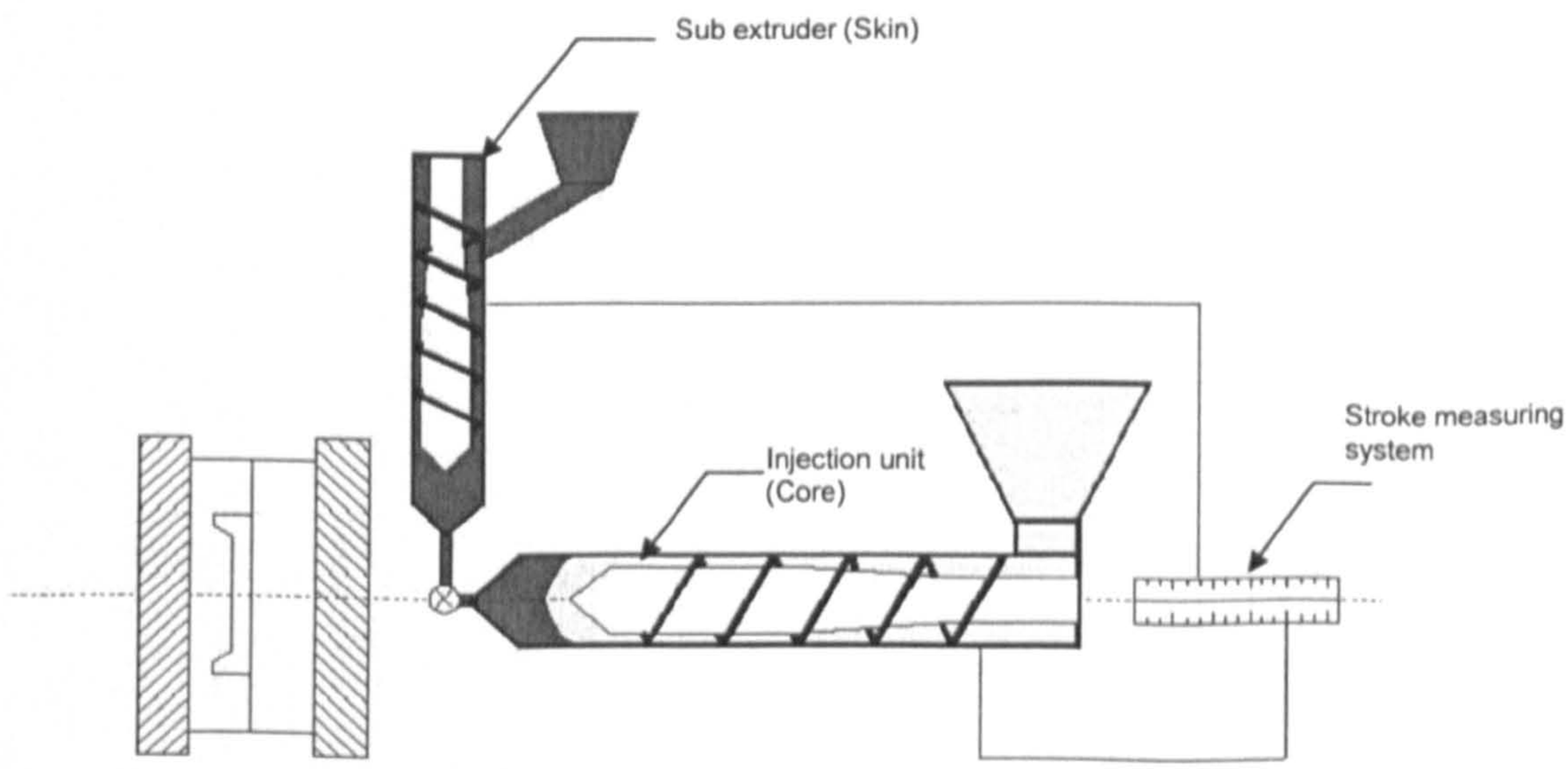

Figure 2.8 Mono-sandwich injection moulding

A strong advantage of Ferromatik's technique is very thin parts are possible[3,16]. In other words, a very high core content around 65-75 percent by volume can be produced, which is somewhat higher than for the two-channel technique, which can use 55-60 percent core volume[2]. Because the machine is based on a normal injection moulding machine, it is easy to control and operate. However, since there is only one injection unit, materials used in this machine have to be similar in terms of operating temperature. Also the lack of detailed control of the injection process makes the moulding of complicated shaped parts more difficult.

Presently, Battenfeld and The International Automotive Research Centre of The University of Warwick are developing a new three-material injection moulding machine, which is designed based on a co-injection moulding or the two channel technology, by adding an extra injection unit placed vertically from the top. An intermediate platen is placed to link between those units as shown in Figure 2.9. The platen, called a manifold system, is similar to the one that was used in the thermoset co-injection machine in this research and will be described in the next chapter.

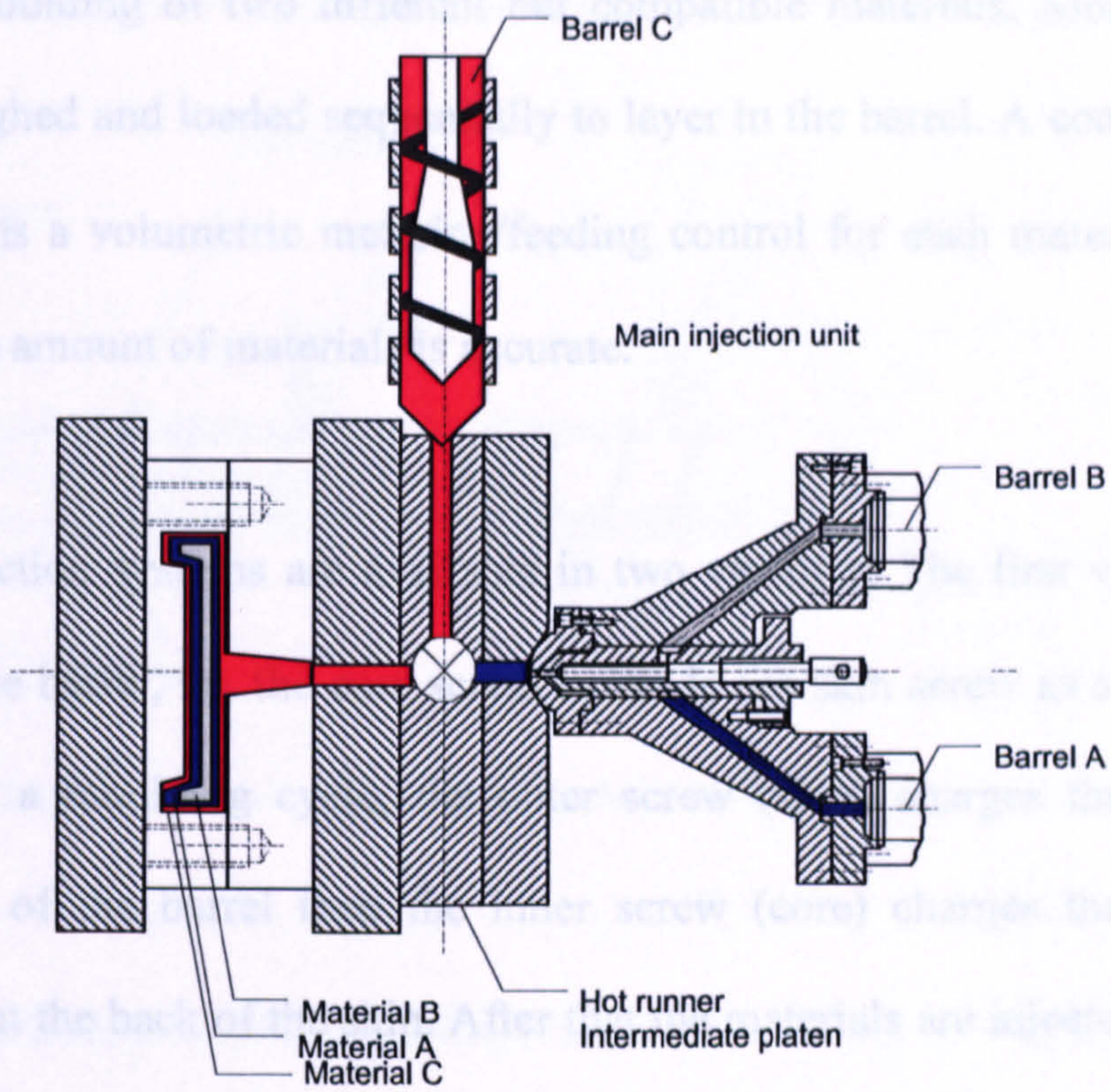

Figure 2-9 3K-injection moulding system

Currently in the co-injection moulding industry, there are new machine and nozzle designs, which have been developed from the mono-sandwich techniques. These are illustrated in Figure 2.10, a co-injection system from Addmix and 2.11 and 2.12, co-injection systems from Twinshot Technologies.

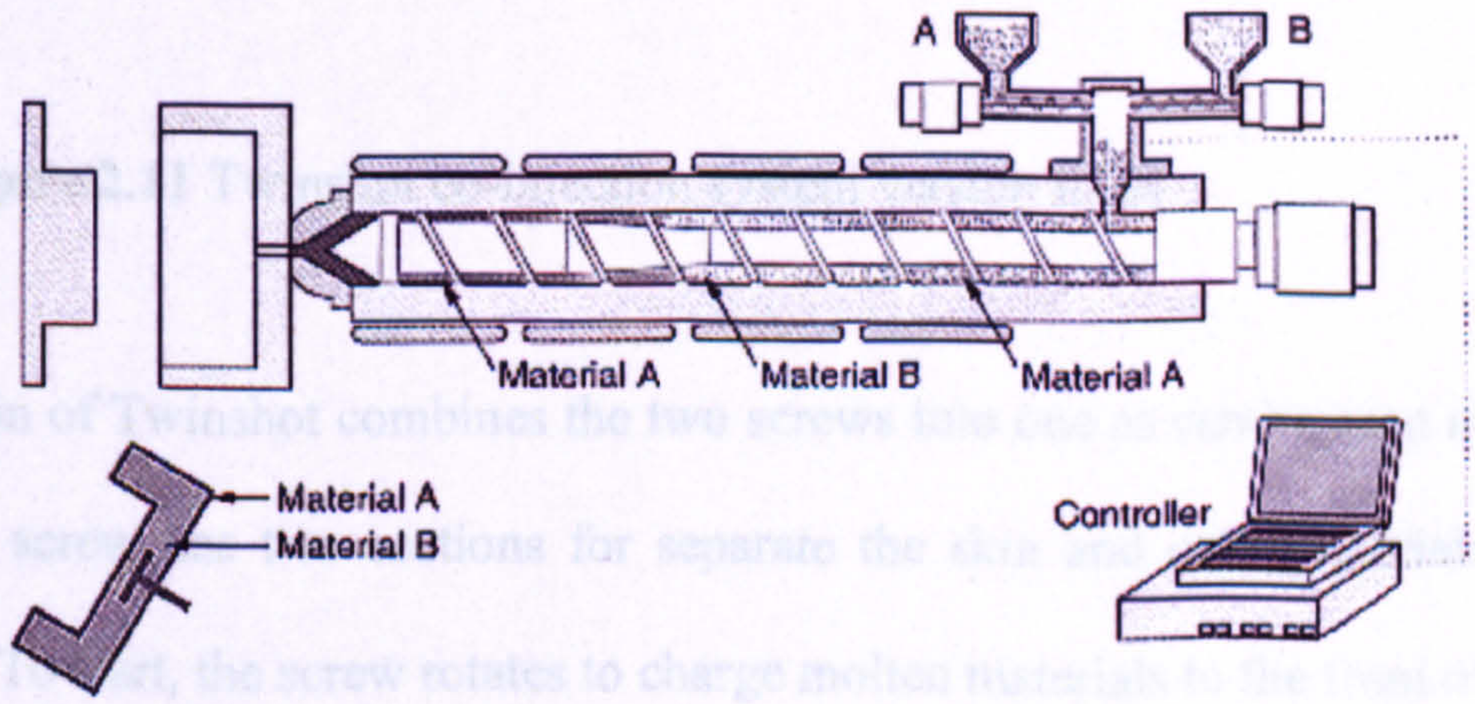

Figure 2.10 Addmix co-injection system[17]

The Addmix co-injection system, as shown in Figure 2.10, uses one injection unit to mould a sandwich moulding of two different but compatible materials. Moulding skin and core are weighed and loaded sequentially to layer in the barrel. A computer system, which contains a volumetric metering/feeding control for each material, is used to ensure that the amount of materials is accurate.

The Twinshot co-injection systems are available in two versions. The first version uses two screws in one barrel, i.e. the core screw is inside the skin screw as seen in Figure 2.11. To start a moulding cycle, the outer screw (skin) charges the skin material to the front of the barrel then the inner screw (core) charges the core material and layers it at the back of the skin. After that the materials are injected into the mould and form a sandwich moulding.

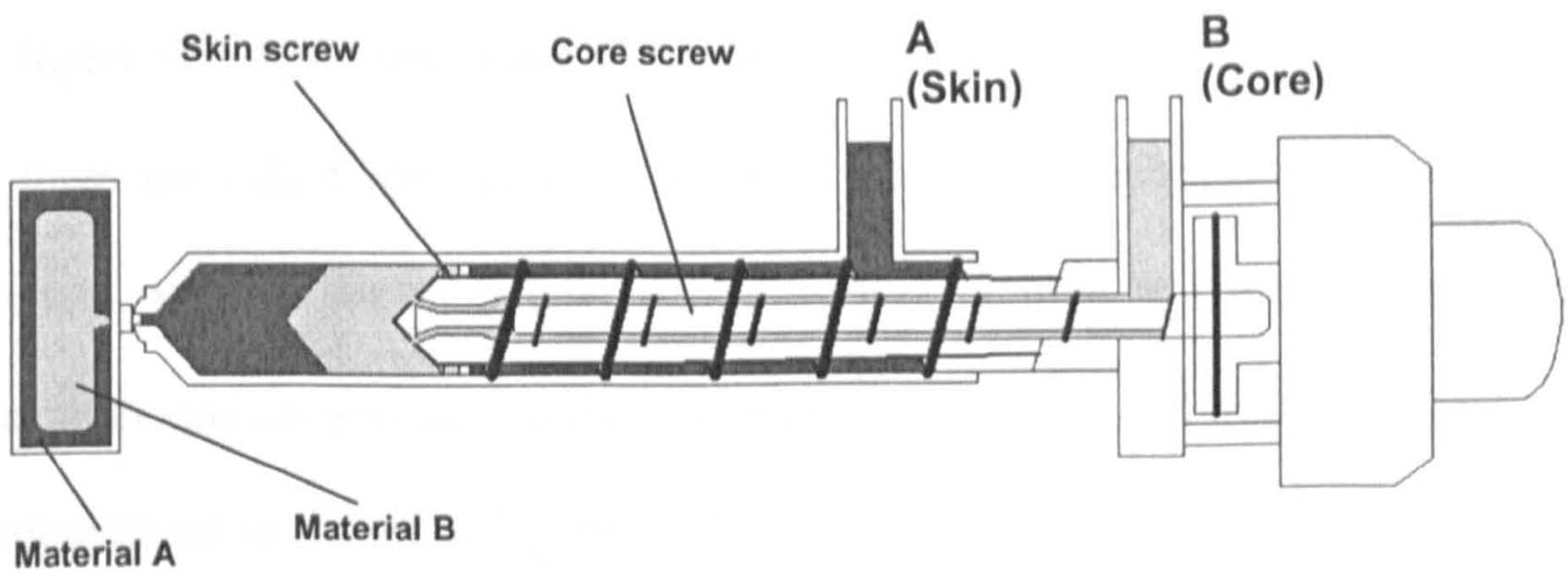

Figure 2.11 Twinshot co-injection system version I[18]

The second version of Twinshot combines the two screws into one as can be seen in Figure 2.12. The screw has two sections for separate the skin and core materials during metering. To start, the screw rotates to charge molten materials to the front of the barrel. Skin material or material A will reach the nozzle before core material or

material B, which is delivered to layer behind the skin through the skin screw. After that both materials are injected into the mould and form a sandwich moulding.

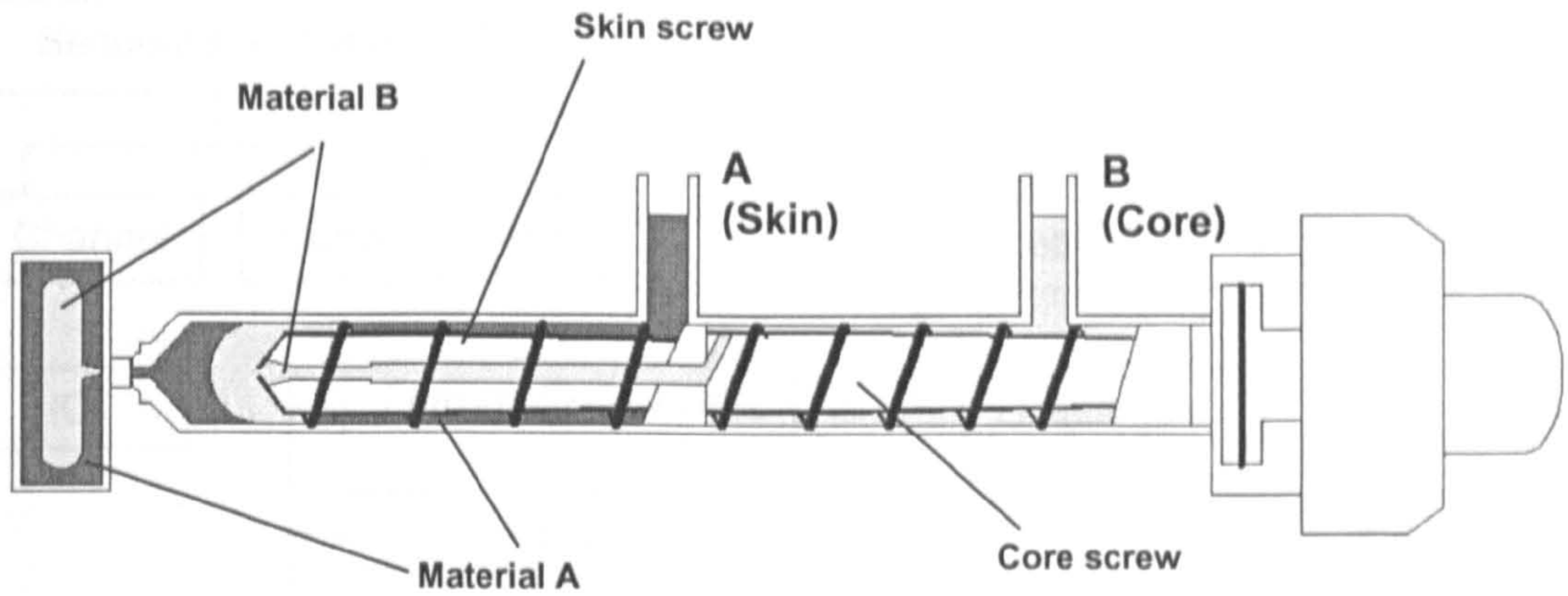

Figure 2.12 Twinshot co-injection system version II[18]

2.3 Sequential and Simultaneous co-injection moulding processes

The words 'Sequential' and 'Simultaneous' are used to define co-injection processes into two groups by looking at how materials are injected into mould. The machines that can inject skin and core materials orderly without any injection time overlap between them are called sequential co-injection while the machines that can inject materials into mould with an injection time overlap or both at the same time are called simultaneous co-injection. All of the techniques mentioned in the last section can be summarised as shown in Figure 2.13.

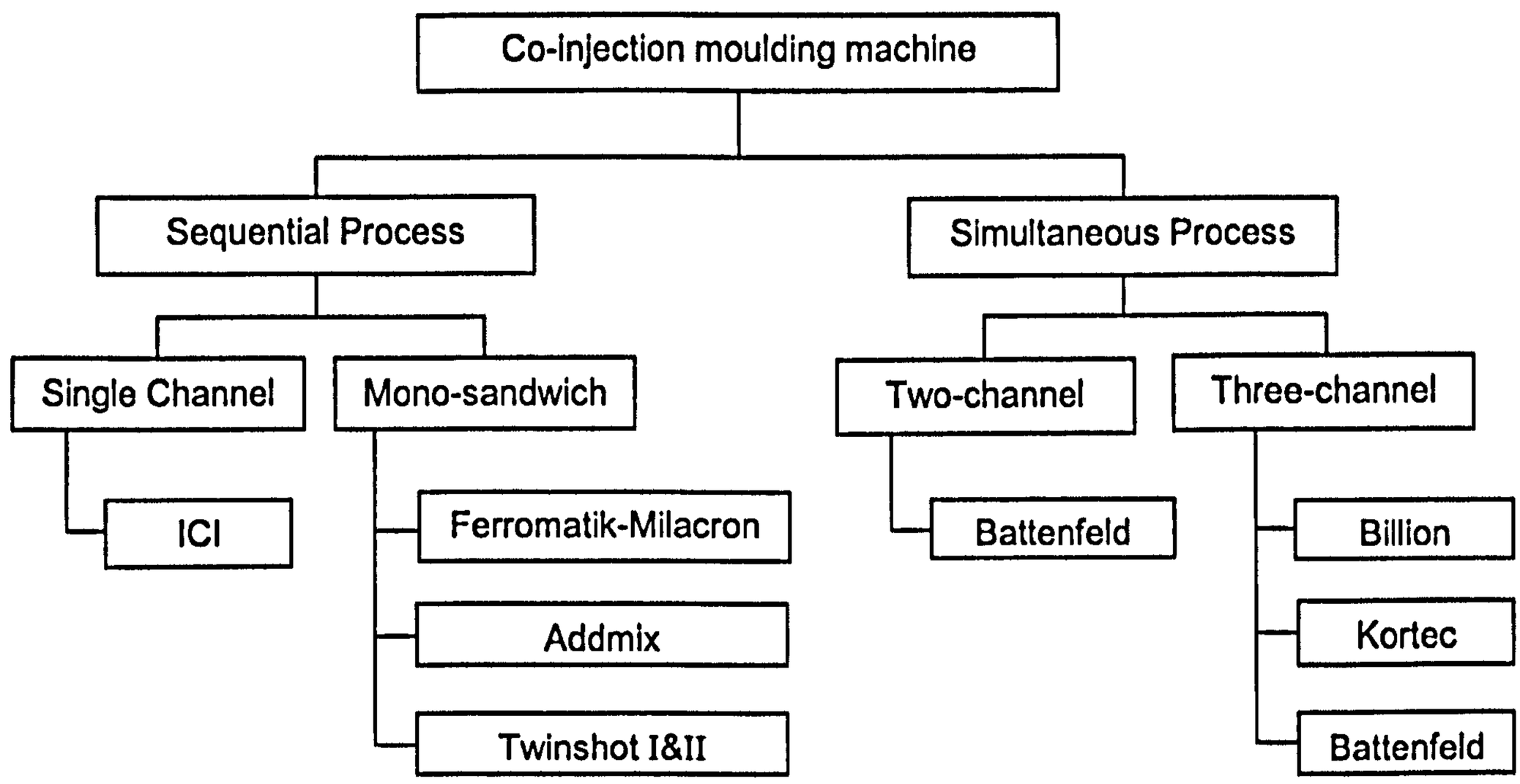

Figure 2.13 The different techniques for co-injection moulding process

2.3.1 The sequential co-injection moulding process of a single-channel moulding machine

The following diagram and table describe how a single-channel moulding machine of the ICI type works. This kind of machine has a major disadvantage of uneven distribution of core material and producing finished parts with gloss marks due to a sudden drop of injection pressure during switching materials between skin and core as already shown in Figure 2.3.

Table 2.1 Operating sequence of the single-channel moulding machine.[9,10]

Steps	Details
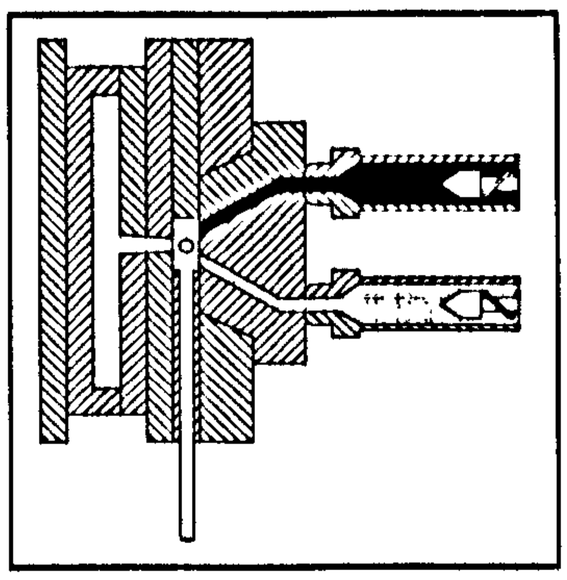 Step 1	The injection moulding cycle is started by hydraulically closing the mould. Skin and core screws rotate to charge the materials while the valve is fully closed.
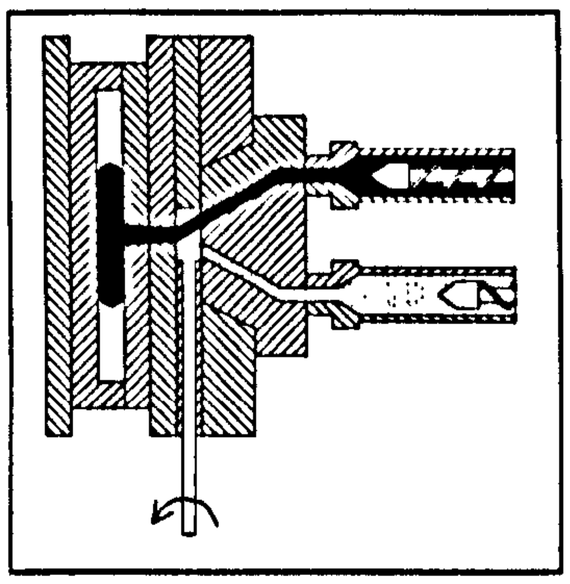 Step 2	The switching valve is opened to connect the first injection unit to the mould. Some of skin polymer is then injected.
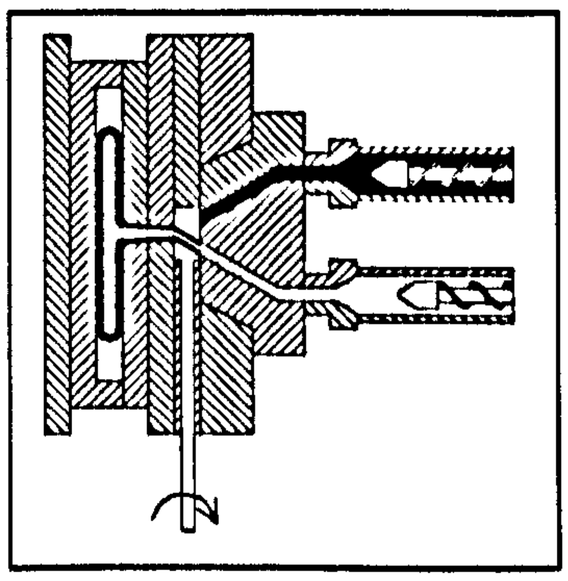 Step 3	After getting adequate skin melt, the valve is opened for the second injection unit to inject core material. During the injection, skin melt is being pushed outward.

Table 2.1 Operating sequence of the single-channel moulding machine (continue).[9,10]

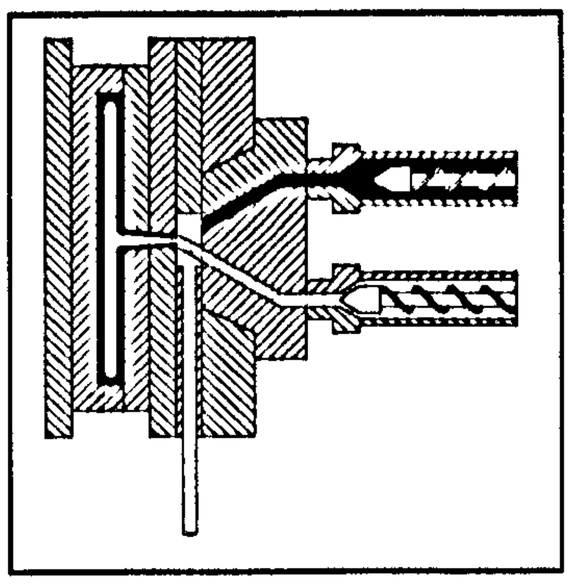 Step 4	The core material is injected until the mould is full. Pressure from the second injection unit is used to pack the mould to ensure a good surface finish.
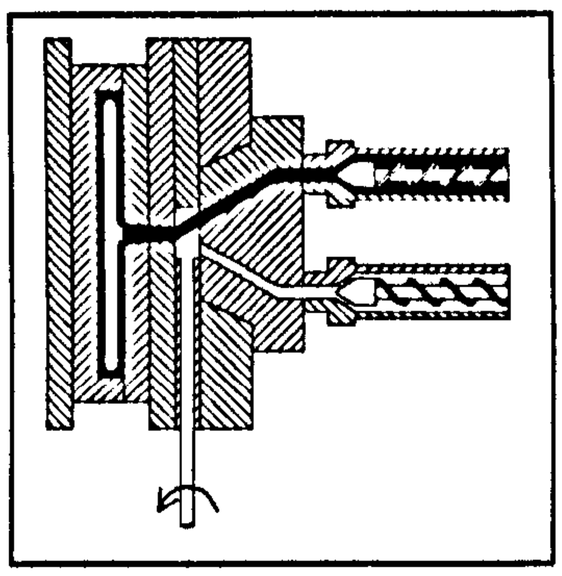 Step 5	The valve is switched to the first injection unit for the second time. The skin melt is injected again to repack the mould and conceal core polymer inside the skin. This also helps to clear the sprue and valve of core polymer in order to prepare for the next moulding cycle.
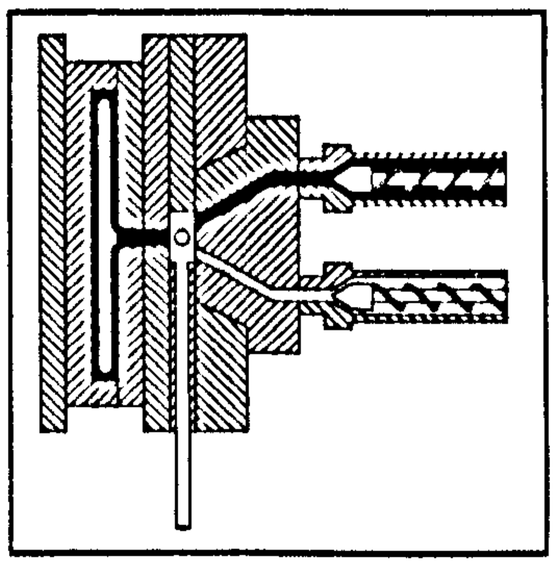 Step 6	The valve is closed. The applied clamp force is still held until the moulding is cooled down and solidified. During that, the screws rotate back to recharge the skin and core materials. At the end of cooling cycle, the mould is opened to eject the finished part then the machine is ready for the next moulding cycle.

2.3.2 The sequential co-injection moulding process of a mono-sandwich moulding machine

The mono-sandwich moulding process is described by Table 2.2. This technique is classed as a sequential injection moulding process as the single channel technique. However, the operating details are different. In this case no gloss mark is seen. It is because both skin and core materials are injected from the same barrel. A short overlap injection time of the materials prevents the melt flow front from temporary stopping. Consequently, smooth pressure (as shown in Figure 2.14) is developed inside mould cavity as is occurred in the simultaneous injection moulding process.

Table 2.2 Operating sequence of the mono-sandwich moulding machine[15,19].

Steps	Details
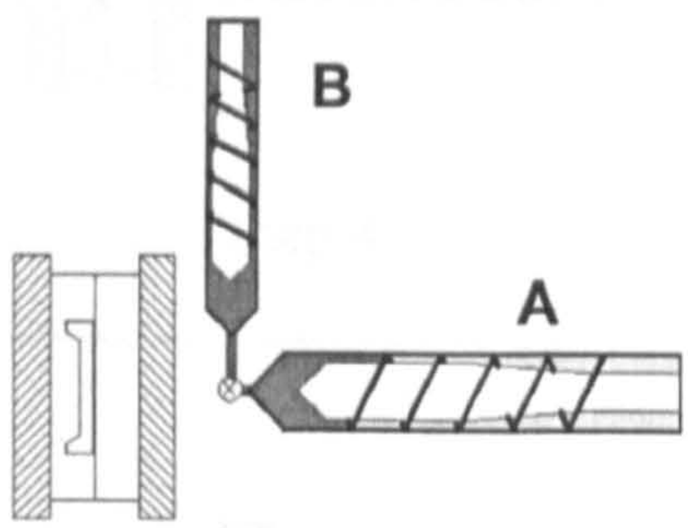 Step 1	The cycle is started when the mould is closed hydraulically. A required amount of skin material, which is plasticised in the auxiliary extruder B is injected into the main injection unit A. Pressure from skin melt inside the main barrel will push the screw backward.
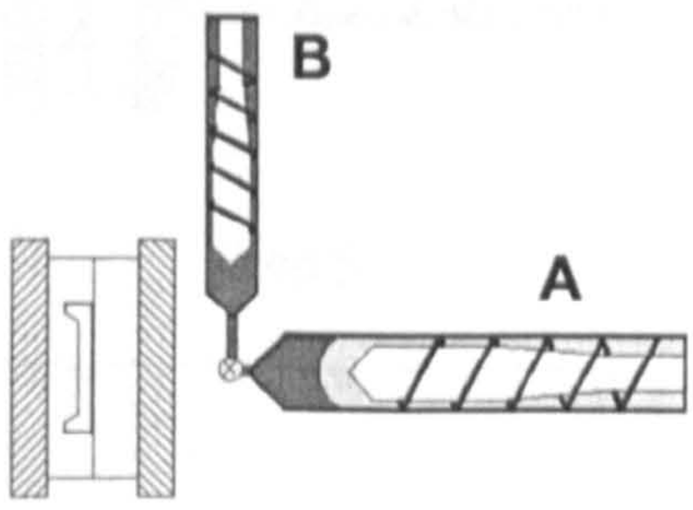 Step 2	The main screw then rotates to charge core material to the front and sit behind the skin material.

Table 2.2 Operating sequence of the mono-sandwich moulding machine (continue) [15,19].

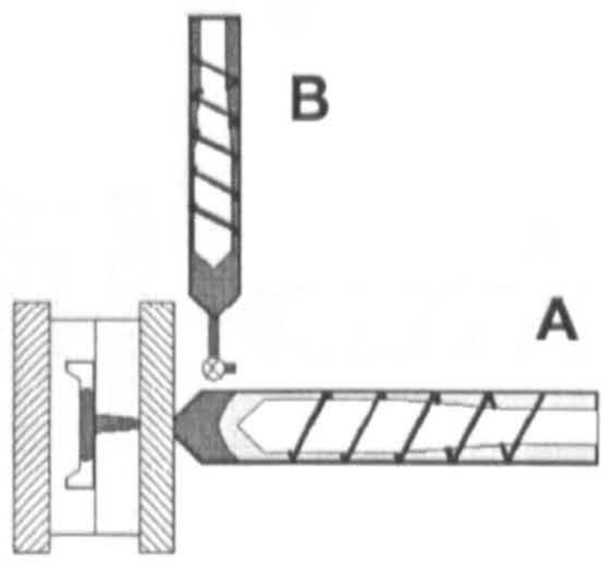 Step 3	After getting enough skin and core melts, the extruder B is driven up to provide space for the main injection unit to move forward and connects to the mould. The machine then injects both skin and core materials into the mould cavity.
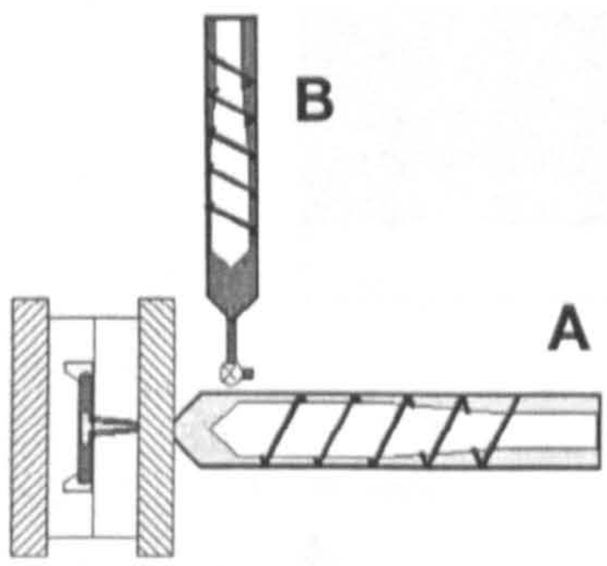 Step 4	Once the skin material touches the mould wall, it forms a thin frozen layer. The screw continues injecting more core material into the mould. The core melt pushes the skin outward and forms a sandwich moulding.
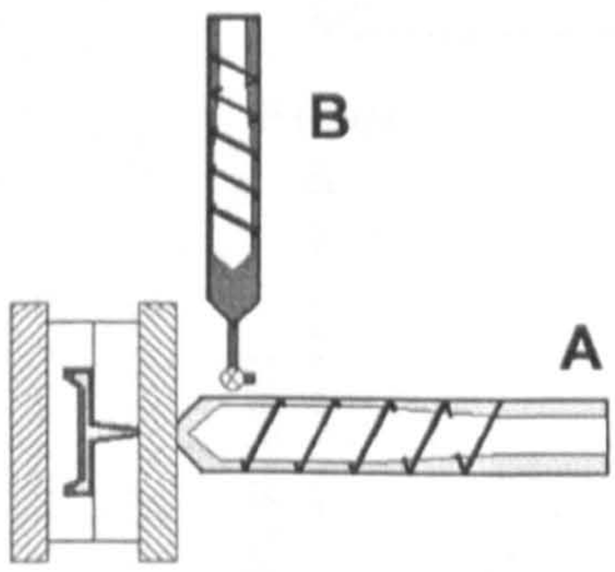 Step 5	The main injection unit discharges some more core melt in order to fill and pack the mould. After finishing injection cycle, the main unit A retracts.

Table 2.2 Operating sequence of the mono-sandwich moulding machine (continue)[15,19].

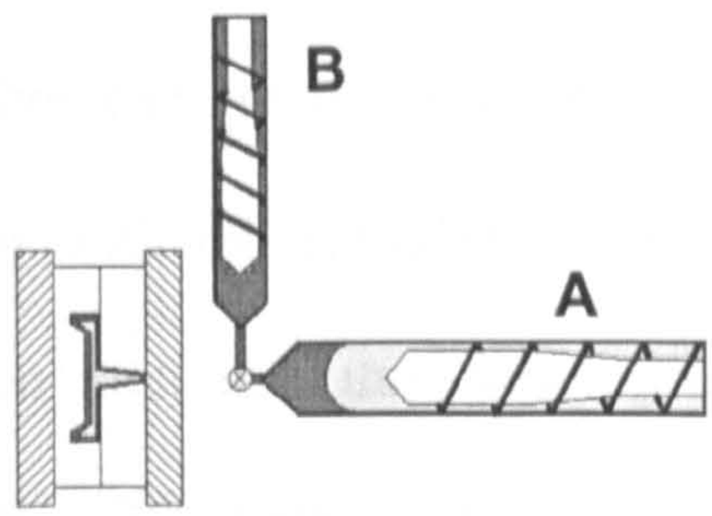 Step 6	While the moulding is left to cool down in the mould, the extruder B is recharged with skin material and then moves down to connect with the main unit A to start the new moulding cycle.

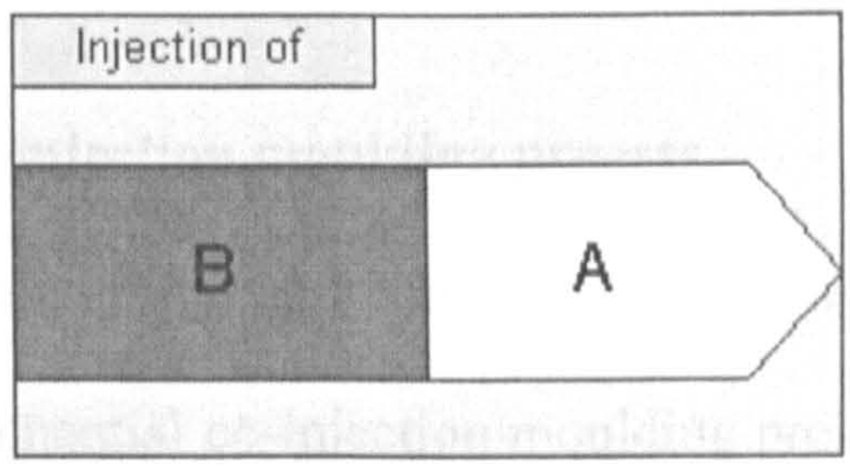

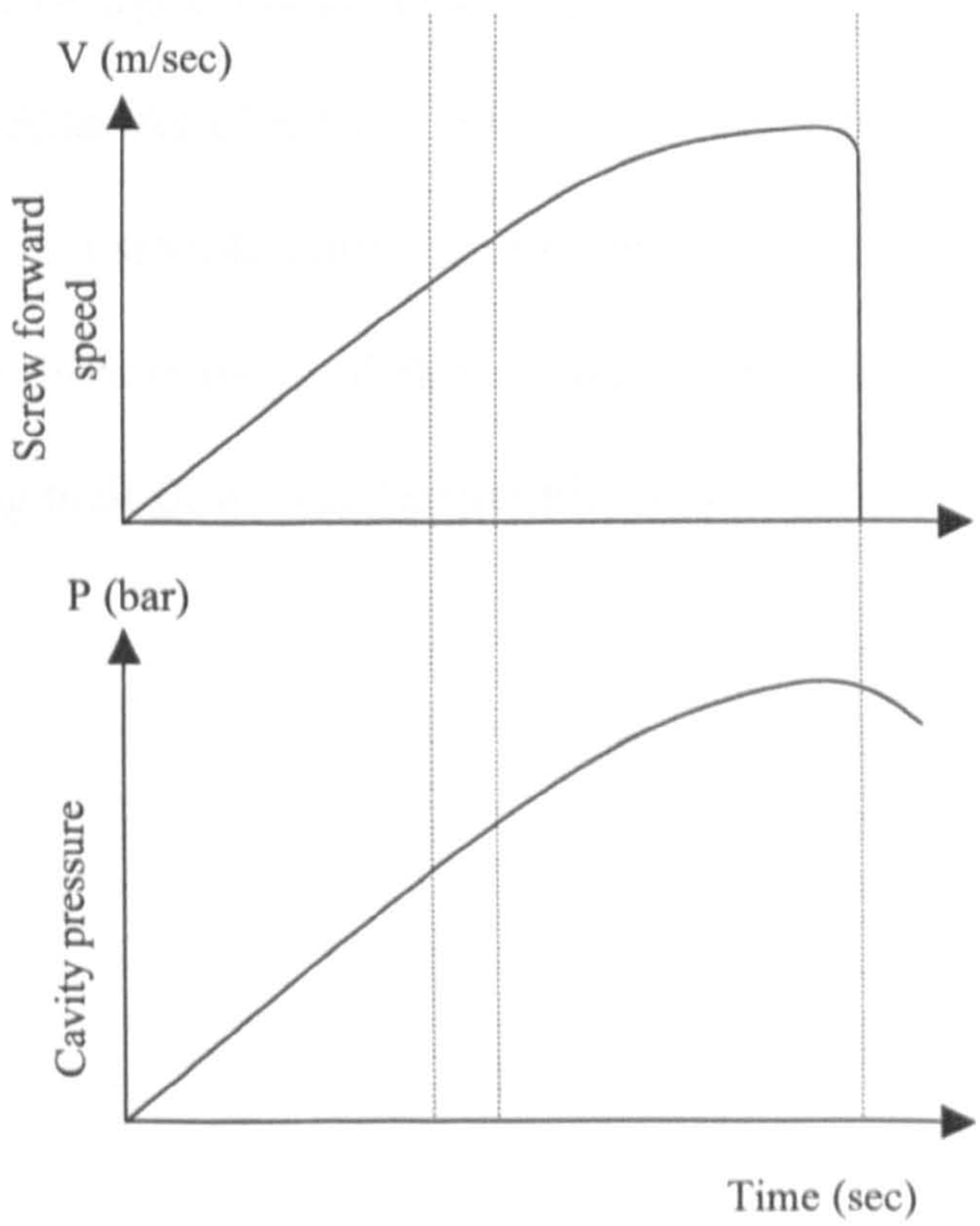

Figure 2.14 Principle mould filling diagram of the mono-sandwich co-injection moulding process

Because core material is used last to pack mouldings, sandwich parts produced from this process normally reveal the core material at the sprue end. This is unsatisfactory if very high quality surface is needed. Alternatively, an accumulator with a flow control valve can be installed alongside the extruder. This valve connects the accumulator with the extruder and the mould cavity. After the extruder finishes feeding skin melt into the main injection unit, some of the melt is fed to the accumulator. This material will be used to pack the mould via the sprue after required amount of core material is injected and the injection unit is retracting (at the end of step 5 in Table 2.2).

2.3.3 Simultaneous co-injection moulding process

More complicated nozzle design and computer control were developed to eliminate the limitation of the sequential co-injection moulding process. The following are the operating sequence of the simultaneous co-injection machine of Battenfeld and the mould filling principle. As illustrated by Table 2.3 and Figure 2.5, cavity pressure can be maintained in a smooth curve. The screws and shut-off nozzles are designed to function so that there is material flow to the cavity throughout the mould filling cycle, thus avoiding melt flow from temporarily stopping.

Table 2.3 Operating sequence of the simultaneous co-injection moulding machine[16]

Steps	Details
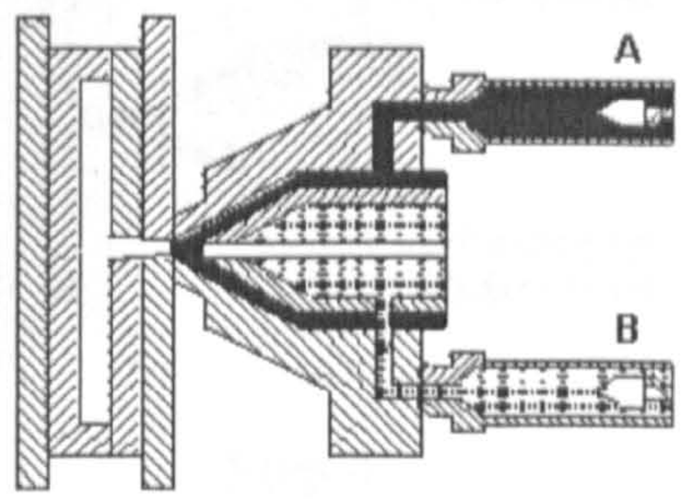 Step 1	The mould is closed and hydraulic clamp force is applied to start a moulding cycle. Main injection units A and B are charged with skin and core melts respectively and the moved forward to face the mould sprue.
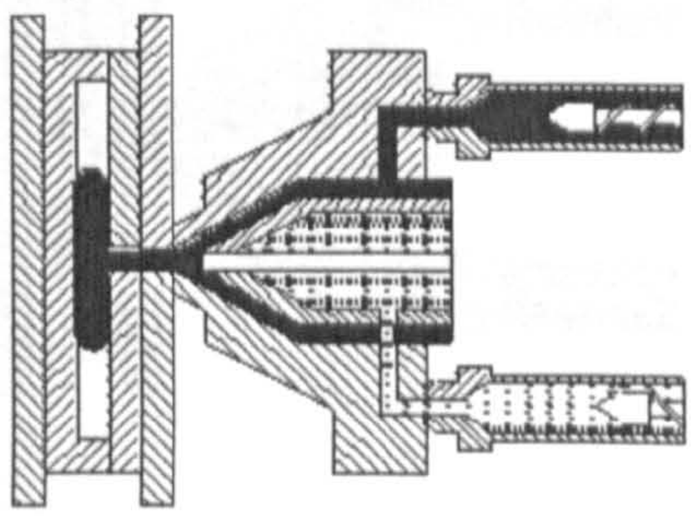 Step 2	The shut-off nozzle A opens and the screw A injects some skin melt into the mould. The shut-off nozzle B still closes.
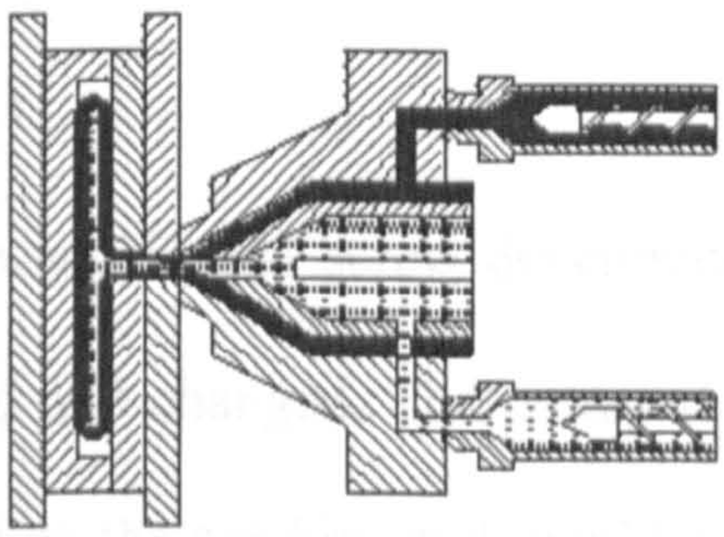 Step 3	When the screw A reaches the setting switching point for starting injection B, the shut-off nozzle B opens and the screw B starts injecting some core melt. Note that during this, skin melt is still flowing. The process continues until both screws reach the setting stop points.

Table 2.3 Operating sequence of the simultaneous co-injection moulding machine (continue) [16]

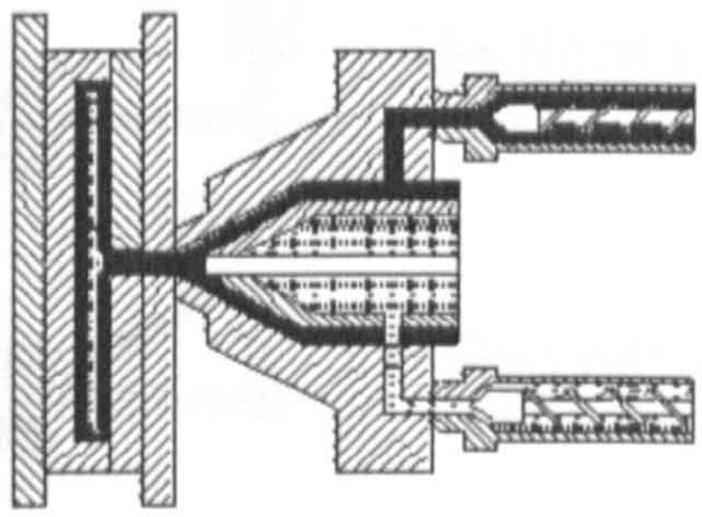 Step 4	While the shut-off A is still opening, the shut-off nozzle B closes. Screw A injects some more material and hold it for a few seconds in order to pack the mould and to ensure that the core material is concealed completely inside.
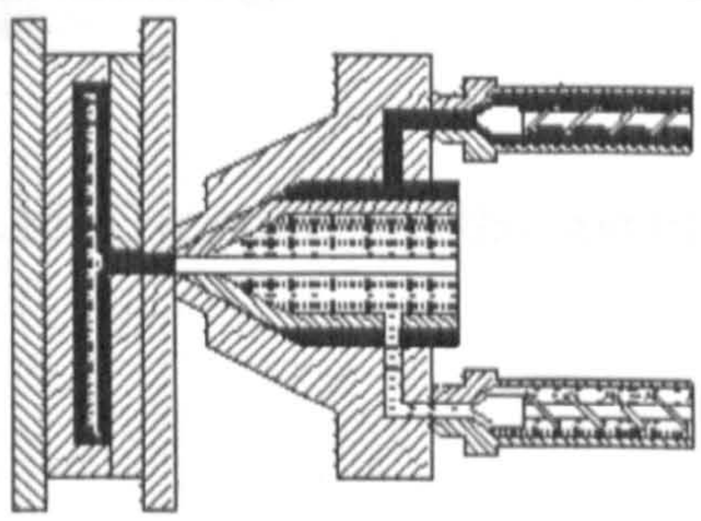 Step 5	The shut-off nozzle A closes and the cooling cycle starts. The injection unit is recharged with new skin and core materials for the next injection cycle.

2.4 Different machine structures and injection unit arrangement [11,20,21]

Alongside nozzle and screw development, the machine construction has also been redesigned and changed. The potential arrangement of the injection units, which is dependent on the machine and mould designs and available space of the plant, can be as illustrated in Figure 2.15.

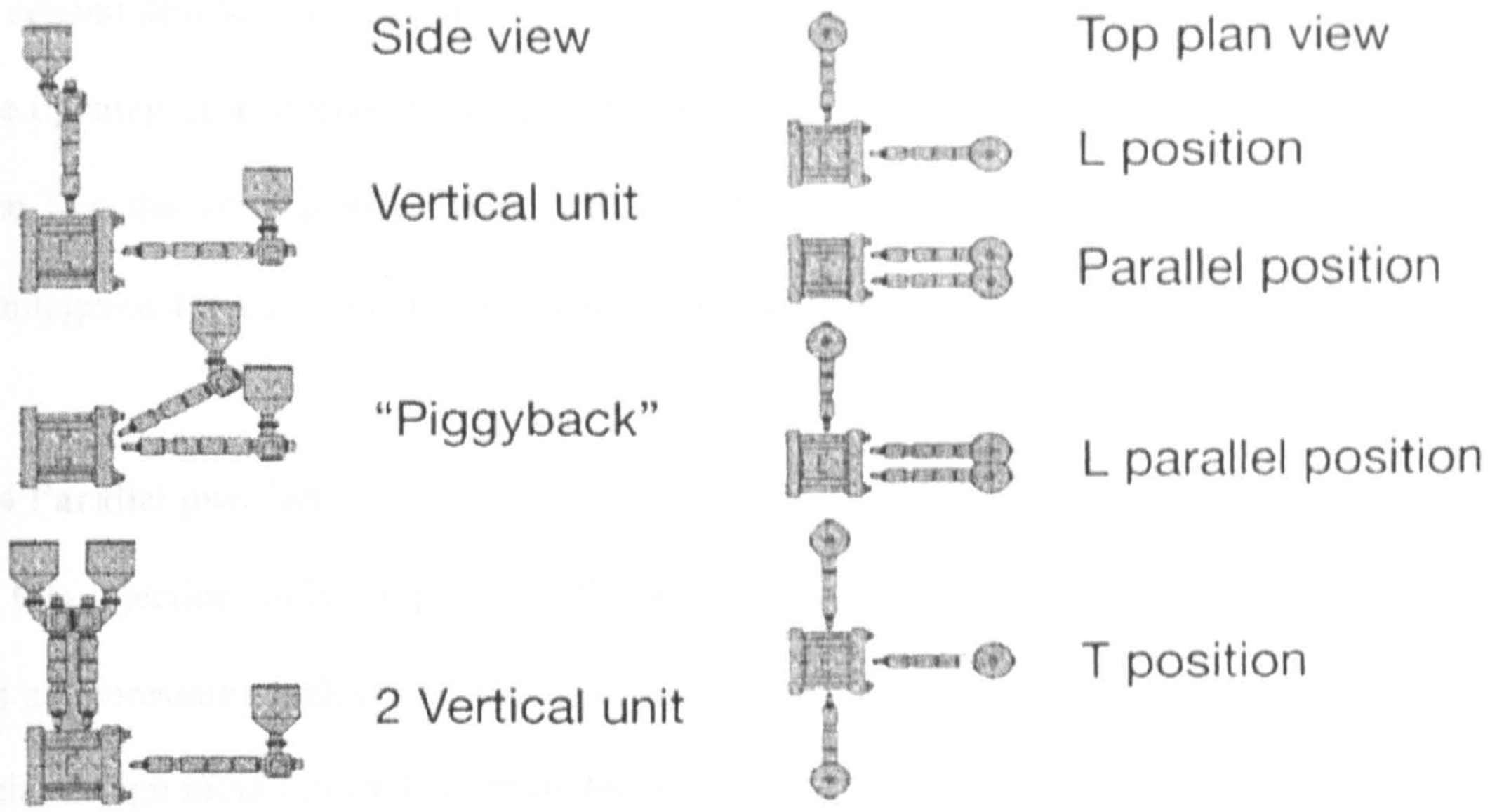

Figure 2.15 Overview of the available standard arrangements of the injection unit[21]

2.4.1 Vertical injection unit

The second injection unit is mounted on the top, over the fixed platen. For mould changing, the injection unit can be slid back to stand behind the platen. Although this unit is the most space saving and frequently used arrangement, the disadvantages of the vertical unit is it needs high hall height.

2.4.2 L position

The second unit lies as a 90° angle to the first unit but in a different direction from the Vertical unit design, as both barrels are lined horizontally. This design is an alternative to a low hall height requirement of the vertical design.

2.4.3 Piggyback

The second unit may also be arranged at an angle from above and inject through the same opening or a second opening in the fixed platen. This arrangement saves floor space like the vertical unit design but requires less hall height. It is particularly advantageous for a second injection unit much smaller than the first.

2.4.4 Parallel position

The two injection units are parallel. This design does not need a very high hall and does not consume much space. This is different from the other designs, which need a special design mould or tool channels for leading materials into the mould in order to make a sandwich part. The nozzle is placed in front of and connects both injection barrels and controls the flow of materials. The disadvantage of this unit is it has a limited range of temperature difference between two barrels. Since the barrels are parallel and installed on the same carriage, too much difference of temperature can cause a misalignment problem due to unequal expansion of the injection unit. As a result, the materials chosen should have the same range of operating temperature.

With the standard unit arrangement in Figure 2.15, the maximum of six component plastics can be achievable as presented by Ferromatik Milacron in Figure 2.16[21]. Four injection units can be arranged vertically and one unit at an angle of 45°. The mould design requires central injection and two injection points on the top of the fixed platen as well as three injection points on the top of the moving platen.

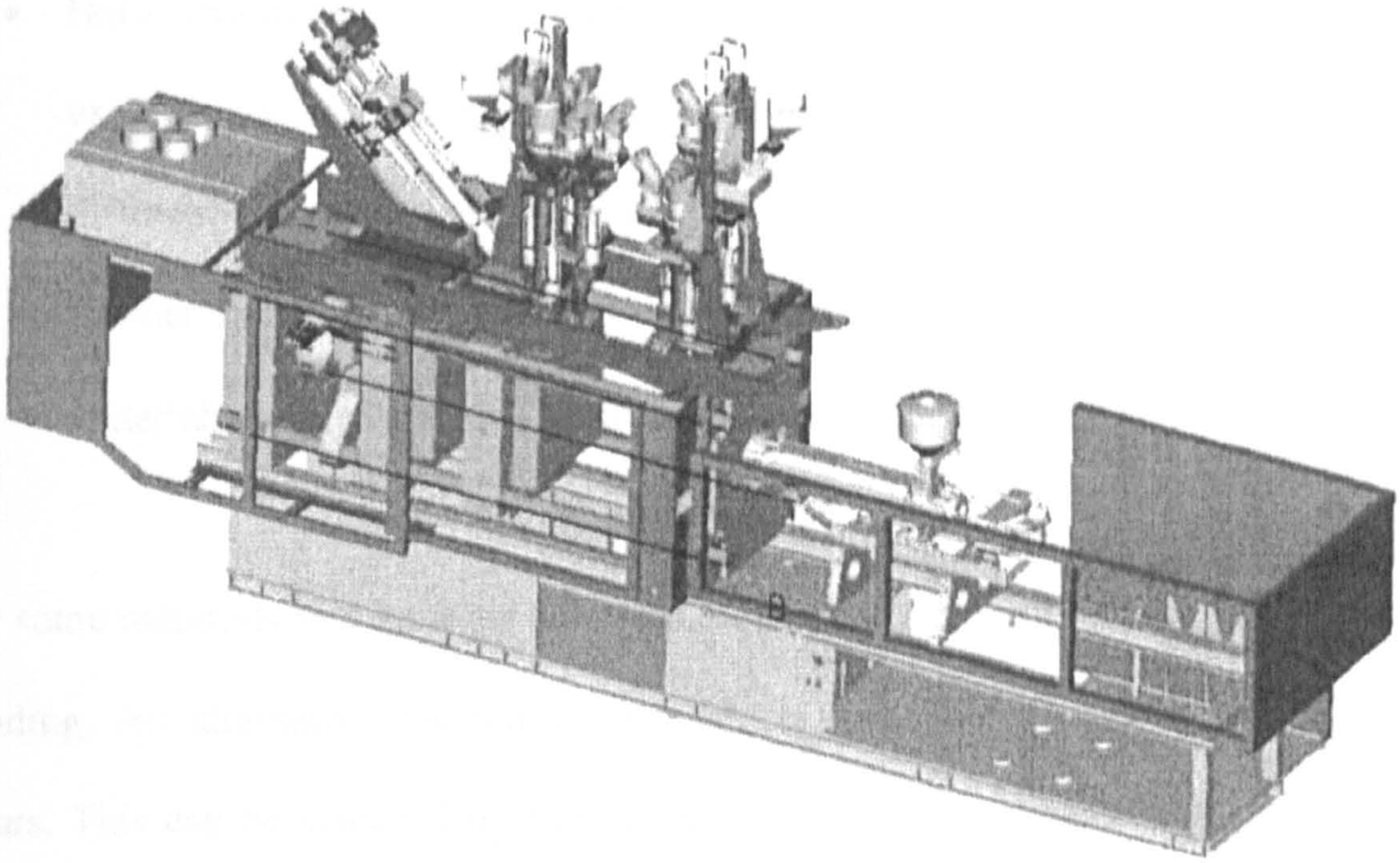

Figure 2.16 Design of a six-component injection moulding machine of Ferromatik Milacron[21]

2.5 Criteria of selecting raw materials[2,3]

The selection of materials depends on the properties required for the finished parts. However, when two materials are involved in the process, some rules have to be followed. It is necessary to consider how well the skin and core layers of those selected materials stick to each other. The following are a guide to good adhesion mouldings:

- The materials offer some degree of bonding at the interface. It is important that the finished part is looked like it is made of a sole material. If the part is exposed to a mechanical load, the skin layer should not be detached from the core layer easily.

- Both materials have approximately the same shrinkage and thermal expansion value. The parts produced from a couple of materials with a large difference in shrinkage value might have sink marks, voids and warpage. Further more, it will lower the interfacial bond strength even though the materials themselves have some adhesion.

For some materials that have no adhesion, compatibiliser may be added to promote bonding. An alternative method is to produce mechanical interlock between the layers. This can be achieved by very high injection speed, which causes mixing of the materials at the interface. [22]

Tables of compatible and incompatible thermoplastic material combinations have been produced[3,23]. An example is shown in Table 2.4. Note that the adhesion properties of materials listed in the table are for some exact grades only. It excludes the materials that are filled with fibre reinforcements and compatibilisers. Those fillers may affect the mould shrinkage and thermal expansion and thus the bond strength.

Table 2.4 Compatible and incompatible thermoplastic material combinations[3,23]

	ABS	ASA	EVA	PA6	PA66	PBT	PC	PE-HD	PE-LD	PET	PMMA	POM	PP	PPO.mod.	PS-GP	PS-HI	PVAC	PVC-W	SAN	TPU
ABS	+	+	+			+	+	-	-	+	+	-	-	-	*	*		+	+	+
ASA	+	+	+			+	+	-	-	+	+	-	-	-	*	-		+	+	+
EVA	+	+	+					+	+				+		+	+			+	
PA6				+	+	*	*	*	*			-	*	-	-	-			+	+
PA66				+	+	*	*	*	*			-	-	-	-	-			+	+
PBT	+	+		*	*	+	+	-	-	+	-	-	-	-	-	-		+	+	+
PC	+	+		*	*	+	+	-	-	+		-	-	-	-	-			+	+
PE-HD	-	-	+	*	*	-	-	+	+	-	*	*	-	-	-	-		-	-	-
PE-LD	-	-	+	*	*	-	-	+	+	-	*	*	+	-	*	-		-	-	-
PET	+	+				+	+	-	-	+	-	-		-	-	-				+
PMMA	+	+				-		*	*	-	+		*	-	-	-		+	+	
POM	-	-		-	-	-	-	*	*	-		+	-	-	-	-			-	
PP	-	-	+	*	-	-	-	-	+		*	-	+	-	-	-		-	-	-
PPO.mod.	-	-		-	-	-	-	-	-	-	-	-	-	+	+	+		-	*	-
PS-GP	*	*	+	-	-	-	-	-	*	-	-	-	-	+	+	+		-	-	-
PS-HI	*	-	+	-	-	-	-	-	-	-	-	-	-	+	+	+		-	-	-
PVAC																	+			
PVC-W	+	+				+		-	-		+		-	-	-	-		+	+	+
SAN	+	+	+	+	+	+	+	-	-		+	-	-	*	-	-		+	+	+
TPU	+	+		+	+	+	+	-	-	+			-	-	-	-		+	+	+

(-) : No adhesion, (*) : Poor adhesion, (+) : Good adhesion

2.6 Applications of sandwich moulding

The unique characteristic of sandwich moulding is it can combine two different required properties of skin and core materials together. This gives designers the flexibility to decide and choose the right materials for the right job. Presently, thermoplastics are widely used. Some examples will now follow. [3,24]

2.6.1 In-mould painting plastic

Natural colour polymer as the core enclosed by coloured polymer. The core material can be a commodity material for a lower cost or an engineering material if it needs to be a high strength part. For this application, the painting process can be eliminated as the completed coloured part is obtained directly from the machine.

2.6.2 Reinforced mouldings

For the part that needs a high impact strength, a glass filled material can be applied for the core layer. Its rough surface can be concealed for an improved surface finish by using a smooth or soft touch surface. Coloured polymer can also be applied as the skin layer.

2.6.3 Electromagnetic Interference (EMI) shielding

Shielding or conductive fillers such as carbon black, aluminium flakes and stainless steel fibres are added to the core and coated by colour and/or for the desired surface finish. This can be applied for computer, electronic equipment and some automotive parts.

2.6.4 Recycle material application

Unpredictable property material from the scrap yard can be mixed with a pure one and then injected as the core material. Another pure or virgin material is used as skin. This reduces the cost of production and is environmentally friendly.

2.6.5 Foam core of a very thick part

A limitation of the thermoplastic injection moulding process is that it is unable to produce a very thick part (more than 4 mm) without shrinkage, warping, high internal stress, and sinking. Foaming agent added to the material is used to reduce the problem and helps in reducing the part weight. However, foaming causes unwanted finishing. Again, a painted or smooth layer can be applied outside to enclose the foam.

2.7 Previous studies in co-injection moulding process

Some of the studies dealing with co-injection moulding since it was invented are listed in this section. The works can be divided into experimental and simulation. It can be noted that most of them are based on thermoplastic materials and almost all of them are related to the one-channel technique.

2.7.1 Experiment works

In the first few years since the co-injection technology was invented, research work focussed on the effect of material flow property on mould filling. White and Dee[25] studied sequential mould filling of polystyrene and polyethylene in a thin rectangular cavity. A special mould (1/2 inch x 2 inch x 4 inch) consisting of two aluminium-clamping blocks with thick glass windows was designed for visualisation by high-speed photography. It was found that the skin material should have a much lower viscosity than the core to achieve a good sandwich moulding.

Later White and Lee[26] studied simultaneous mould filling by using a modified rheometer. Instead of a capillary die, they installed a small nozzle to the barrel end. The rectangular mould with glass windows was used again for visual observation. To prepare for the test, two polymer rods were sliced in half and inserted to the rheometer barrel. Heat was applied to bring them to a molten state, and then the melts were pushed by the rheometer plunger through Dee's special nozzle design. A skin-core melt was formed and injected into the mould. They found that the lower viscosity melt would encapsulate the higher one and the sandwich moulding was achieved. The smaller the viscosity difference between skin and core was, the more difficult it was to control the process.

With the idea of concealing one plastic inside another, a new method of recycling plastics was possible. Donovan et al [27] structured a machine called two-shot injection moulding. They installed the second injection unit perpendicular to the first and connected them with a special nozzle similar to the two-channel nozzle. Virgin and recycled acrylonitrile-butadiene-styrene (ABS) compounds were sequentially injected into five different moulds; an end-gated, two-cavity, rectangular plaque mould, a centre-gated disc mould, two telephone housings with different thickness and a telephone handle. With the scrap material, around 50 percent of the part volume could be moulded in the plaque mould and up to around 60 percent was successful in the disc mould. For the more complicated shapes like telephone housings, the scrap polymer was about 40 percent, which would be increased if the cavity filling were well balanced.

The results from the plaque and disc mould were also compared with a conventional (single shot) mould filling simulation. Skin thickness was sectioned and measured by an optical comparator attached to a microscope. In general, there was a good agreement between the experiment and simulation.

Continuing the work on the mould and apparatus designed by White and Dee and White and Lee, Young et al.[28] took a more detailed look at the influence of differences in rheological behaviour of the melts on the phase distribution in sequential injection moulding. Six different materials including two polystyrenes, two high-density polyethylenes, a low-density polyethylene and a polypropylene were used as six different viscosity materials and injected into the rectangular, centre gate mould. The viscosity ratio, i.e. the ratio of the core viscosity to that of the skin

viscosity was compared to the phase distribution. The results of their research narrowed down the viscosity window for sequential co-injection. They found that the best uniformity of skin and core thickness occurred when the ratio of zero shear viscosities was 1.5 to 2.0. By using excessive quantities of skin material, the burst-through or breakthrough of core material could be reduced in cases where the core viscosity was lower than skin and a more uniform phase distribution could be achieved.

Somnuk and Smith[2] investigated a different moulding type from above. They studied the simultaneous co-injection moulding process by using Battenfeld's two-channel nozzle unit. Four grades of polypropylene with different viscosities were used and injected into end-gated rectangular plaque moulds. A mould with cavity dimension of 195 x 138 x 3 mm was used for the first case study. A specially designed glass-window mould with cavity dimension of 100 x 75 x 4 mm was used for the second case in order to do a visual study of filling with a high-speed camera. By adjusting the volume proportions of materials and the injection speed, it was shown that the materials with ratio of viscosities (skin/core) between 0.82 and 1.83, measured at a shear rate of 10^3 second^{-1}, could be successfully moulded with the most uniform core distributions and the amount of core material that could be concealed was around 55 to 60 percent. The length of simultaneous phase could be increased from 5 to 20 percent up to 95 percent of the setting for the skin-metering stroke. Too low a core viscosity and too high skin viscosity could cause breakthrough. If the core viscosity was lower than skin, more skin material was needed to conceal the core inside. However, in this case, the core distribution was more uniform.

Derdouri et al.[29] focussed on other factors, which are skin/core ratio, material melting temperature, injection speed and mould temperature. These factors could also influence the mould filling and skin/core forming apart from the viscosity. They used a co-injection moulding machine from Engel to inject acrylonitrile-butadiene-styrene (ABS) and polycarbonate (PC) into a 76 x 164 x 7 mm rectangular plaque mould. This mould is unusually thick compared to general moulds used in injection moulding. Better skin/core ratio can be obtained but sink marks and voids are also likely to happen on the moulding surface. The skin/core volume ratio was varied from 85 down to 25 percent. With the changing of material melting temperature, injection speed and mould temperature, the maximum flow length of both skin and core were plotted. The experiment concluded that at 5-25 mm/s injection speed, breakthrough of the core through the skin was a direct function of the skin/core ratio and was an effect more sensitive to the mould temperature than to the melt temperature. Viscosity ratio also had an important effect on the onset of breakthrough and more skin was needed to conceal core material. When the viscosity ratio was close to 1, the injection speed had a small effect.

Many studies have focussed on how various parameters affect to the skin and core formation, but Seldén[30] looked at a different problem, the chemical compatibility of two materials. In his work, he coupled non-compatible polyamide 6 (PA6) and polyethylene (PP) by Ferromatik's mono-sandwich injection moulding. Different percentage values of compatibiliser were added to the polypropylene. The interfacial bond strength between those materials was measured by peel tests. He then measured the mechanical strength of finished parts by impact and flexural tests. From the result, he suggested that non-compatible materials, like PA and PP, could be made to

form a strong interfacial bond by adding a relatively low amount of a suitable compatibiliser. For a tough skin and a brittle core, high impact strength was achieved only if the interfacial strength is sufficiently high. Viscous fingering, which was a common type of interfacial instability, was found especially in the 0 percent compatibiliser specimens, but also in mouldings with a higher percentage of compatibiliser. It was noted that those unmodified PA/PP sandwich specimens also had relatively high strength. This was due to the mechanical interlocking between the interface layers caused by interfacial instability.

Later, Rungseesantivanon[16] studied factors affecting adhesion of polymers in simultaneous co-injection. Polyamide 6 and polypropylene with and without 10 percent of compatibiliser were injected through a two-channel nozzle of a Battenfeld co-injection moulding machine into a square plaque mould. Impact and peel tests were done to measure the interfacial strength between skin and core layers. It was found that compatibiliser, skin layer thickness and simultaneous injection time were the major factors to affect skin and core adhesion of incompatible materials. The compatibiliser promoted chemical bonding between the materials. However suitable conditions like a greater thickness of skin layer and a longer simultaneous injection time were necessary to produce good bonding between skin and core. This was possible by varying setting parameters such as melt temperature, tool temperature, injection speed, length of simultaneous phase and the metering stroke ratio of the skin and core.

Since compatibilisers tend to be expensive, the number of chemical sites available at the interface limits the final bond strength. Co-injection moulding of non-compatible

materials without adding any compatibilisers was proposed by Goodship and Kirwan[22]. It was intended to control the level of turbulent flow where the interfacial instabilities occurred, which promoted mechanical interlocks between the layers. This occurred without any effects to the surface and skin-core distribution. In the research, six different materials consisting of polycarbonate, poly (methyl methacrylate), nylon 12, polypropylene, polystyrene and high-density polyethylene were used and machine speed was varied in order to find the boundary between laminar and turbulent flow. The results were compared with mouldings that had compatibilisers added. It was concluded that interfacial instabilities were achieved by control of injection speeds. This method was advantageous to the compatibiliser added mouldings as there was no surface distortion or halo effect at the layer interface. Even though compatibiliser technology offered possibilities for future multi-material products, the lack of interfacial mixing with resultant surface defects and the cost itself meant that a system that could induce interfacial mixing would be an attractive alternative.

2.7.2 Simulation works

It was not until around 20 years after co-injection had been invented that the first simulation of sequential co-injection moulding process was published. Based on conventional injection moulding, Turng and Wang[31] of AC Technology applied the basic theory, Hele-Shaw flow of inelastic, non-Newtonian fluids under non-isothermal conditions to their simulation. A numerical analysis using a hybrid Finite element/Finite different/Control-volume numerical scheme had been developed. Residence time, which is the duration that a particular material element had spent in the cavity since it entered the cavity, was a major difference used for the calculation.

The simulations were done in three cases by varying skin and core viscosity ratio from less than 1 to more than 1. Then the results were compared with C-shape plates, which were made by injection moulding of two polypropylene resins. Spatial distribution of skin and core, injection pressure and clamp forced were predicted. It was concluded that the analysis agreed fairly well with the experimental data.

The concept of a residual time approach was also used to simulate the core and skin melt front advancement by Chen et al[32]. In this case, two complicated moulds, a plate mould with three different thickness regions and one with a block inserted to form weld line and an asymmetric melt flow, were designed to conduct the process studies. Transparent and green coloured poly methyl methacrylate (PMMA) resins were injected and the results were compared with the analysis. The simulated results on the material distribution from the plate mould showed a reasonable agreement with the experiments. However the results from the mould with inserts showed slight differences. It suggested that more investigations should have been done in both cases.

This work was followed by Schlatter et al[33]. Experiments and simulation studies on the co-injection of polystyrenes were performed in order to test the influence of processing parameters on the interface location and on the pressure in a centre gated, 90-mm radius disk mould. The temperature was varied between 200°C to 260 °C. Skin and core thickness were observed. The experimental results showed that the thickness of the layer would be greater if its viscosity was higher. When changing skin or core temperatures and flow rates, the thickness of each layer was also changed. This was because increasing those factors resulted in a decreasing of the

viscosity. The influence of flow rates was larger than that of the temperature due to the larger shear thinning effect. Consequently, it was used as the main factor in the thermo-mechanical model simulation. In the case of the disk mould, a numerical and experimental comparison of the influence of the flow rate on the interface location showed a good agreement. A trial was done on a more complex geometry like a tape distributor mould. It was also proved that this simulation model could work very well with this industrial case.

Although the simultaneous co-injection moulding was invented only a few years after the sequential moulding, none of the simulation works were focussed on the simultaneous moulding technique. Lee et al.[34] presented the first simulation of simultaneous sandwich injection moulding based on the Hele-Shaw approximation. The results were compared with the experiments done on two injection moulding machines with a two-channel nozzle and a visualised rectangular mould assembled. The materials used were high-density polyethylene (HDPE), low-density polyethylene (LDPE) and polystyrene (PS). Many factors such as material temperatures, injection rate and length of simultaneous were varied. The analysis gave fairly good results. However, it needed further investigation with regard to more complex geometries.

2.8 Related works on thermoset co-injection moulding

At present, the only published work related to the injection of two thermoset materials together is by the author[35]. The first conference paper of the co-injection moulding of different types of material, thermoset and thermoplastic and thermoset and rubber was presented by Hunold[36] in 2001. The first sandwich moulding was a combination of a phenolic skin and a polyethylene core. The result was a panhandle consisting of approximate 50 percent phenolic and 50 percent polyethylene. It was demoulded at a temperature of 160°C while leaving the polyethylene in liquid state. The curing time was reduced from 70 seconds to 30 seconds due to the high core temperature. However, because the polyethylene was still liquid, the phenolic skin layer must have been strong enough to fulfil the part strength requirements during demoulding. The author suggested that further work had to be done to find or develop appropriate compounds, mould and machine technology.

It is not only plastic material that can be used to aid thermoset injection moulding, compressed air can also be used to replace the core component. Nunnery of Bulk Molding Compounds Inc. (BMCI) presented the first thermoset gas-assist injection moulding at the 13th International Molding in February 2003.[37] The mould cavity is first completely filled with BMC and packed. After a delay to allow the film layer to set up against the mould wall, the gas pin, which is located as far as possible from the gate, is activated and pushes soft uncured material from the centre of the part back to the barrel. Using this method, it was claimed that cycle time was reduced and material usage was lowered to one third or one half.

2.9 Conclusions

This chapter contained a literature review on the co-injection technology since it was invented and explains all different techniques to produce a sandwich component.

The experimental research published shows that the co-injection moulding process has been shown to work successfully. A wide range of compatible materials can be used with this technology by varying the machine parameters. Furthermore, the recent works have shown that non-compatible materials such as nylon and polypropylene are also possible to use if adding a compatibiliser and having suitable machine settings.

The simulation works on co-injection moulding have been gradually developed and are successful to a degree. Prediction of mould filling of a simple mould is accurate but the more complicated ones need further study.

The first processing of thermosets in combinations with thermoplastic or rubber in the co-injection moulding process was reported recently. However, there were some heat related problems during the experiments, which required more investigation.

Despite the fact that a lot of research work in co-injection moulding has been done, the research has concentrated on thermoplastic materials only. The thermoset co-injection moulding is a very novel process, which was influenced by the thermoplastic sandwich injection moulding idea. Similar to thermoplastics, the viscosity of the material and machine condition setting, such as injection time and injection speed can be expected to be the factors affecting mould filling and the

sandwich formation. However, the most important factor that needs more consideration is the system temperature since it affects directly to the thermoset cross-linking networks and hence, the change of material flowability.

Chapter 3

Thermosetting plastics and mouldings

3.1 Definition

Plastics can be divided into two types, thermoplastics, and thermosets.[38] Their varied characteristics are due to dissimilar structures, which are suitable for different functions of work. With the more linear molecules of thermoplastics, they tend to be more flexible than thermosets. This polymer can be softened and turned to a viscous fluid at high temperatures and solidified at a lower temperature. The process can be reversed many times, which is completely different in the case of thermosetting materials.

Tony Whelan and John Goff gave the definition of thermoset in Molding of Thermoset Plastics[39] that "*a thermosetting plastic or a thermoset is material which once shaped by heat and pressure is incapable of being re-processed by further applications of heat and pressure*". This is because during moulding the molecular chains of thermosets form linkages between each other by means of a chemical reaction, which is called cross-linking. The strong and complicated network of thermosets prevents the chains from moving or slippage when heat and pressure are applied. As a result, plastic parts made by thermosetting material are rigid and hard but brittle.

As well as thermoplastics, thermosets can be classified broadly referring to their physical properties as general purpose, engineering and specialty plastics. General purpose or commodities thermosets are characterised by their average mechanical properties, higher expansion co-efficient, lower temperature resistance and lower production cost. Engineering thermosets have better properties so they are more durable and more expensive. Specialty thermosets offer one or more highly specific or unusual property. They are very expensive and produced in a small quantity. Table 3.1 shows a classification of different thermosets into those three groups. Details of their properties and application can be found in many reference works that exist.[23,38-40]

Table 3.1 Classification of thermosetting materials

Classification	Thermosetting Plastics
General Purpose	Phenolics, Aminos, Polyesters
Engineering	Epoxy, Polyurethane
Specialty	Silicones, Allyls, High-temperature Thermosets

This chapter will be focussed on the general characteristics of thermosetting materials that have been used in the standard injection moulding process. Resin or liquid thermosets will not be included as they are beyond the scope of this research. Processes involved in shaping and moulding this kind of material will be explained briefly including their advantages and disadvantages. Some examples of products made of thermosets are listed and thermoset recycling is described in the last section.

3.2 Cross-linking and Curing

The major difference of thermosets and thermoplastics is that the process of moulding thermosets cannot be reversed. Once some heat and pressure are applied to a raw thermoset, its molecular chains will start chemical reactions among the others. This will form cross-linked networks, which hold all the chains as a single structure as illustrated in Figure 3.1 (a). The arrows in the figure show connections among chains. The network polymer is very strong as if more heat and pressure are applied, the molecular chains are relatively rigid and the plastic part remains in a solid state. This is unlike thermoplastic materials, whose chains stay in a group with no inter-chain connection. Extra heat and pressure cause the molecular chains to become loose and move, thus turning the plastic into a viscous liquid and then back to solid state again after it is cooled.

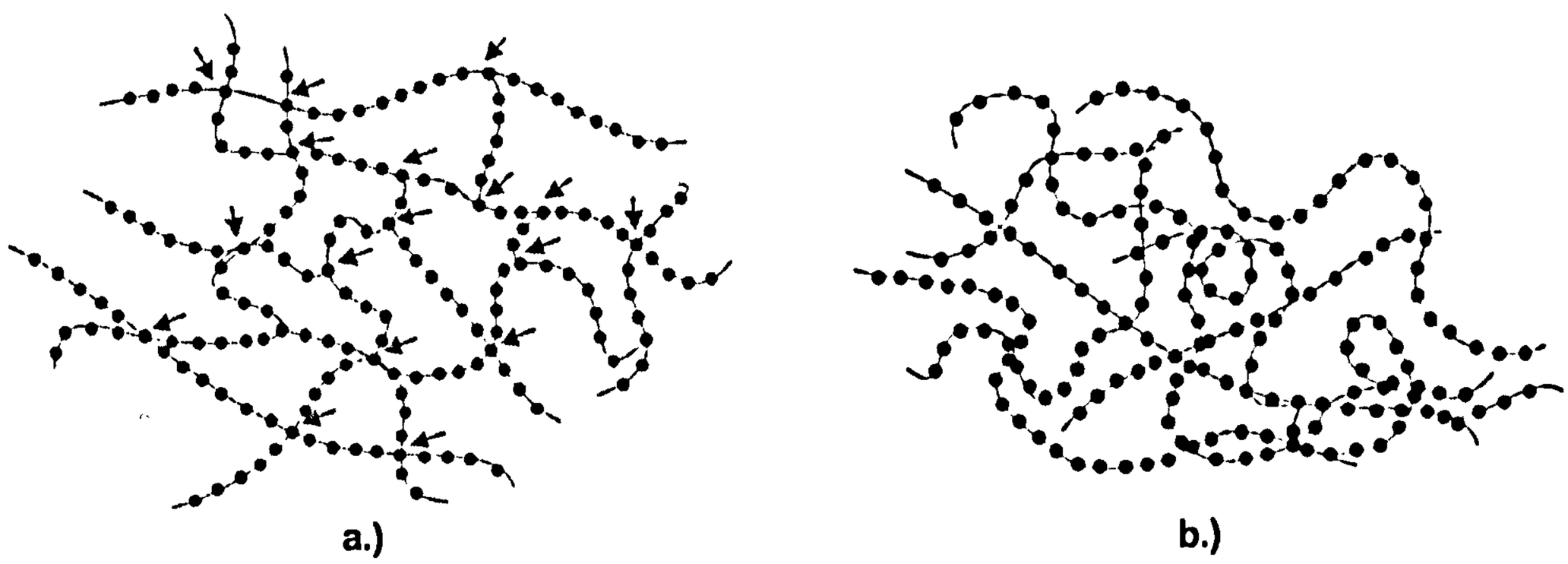

Figure 3.1 The simplify 2D model of
a.) Cross-linked network polymer b.) Thermoplastic polymer

The network structure of a cross-linked thermosetting plastic results in high heat resistance and high impact properties. A thermoset part will remain unchanged under

an application of heat until it is raised to a certain level that can destroy the chemical linkages. At this point, the part is decomposing.

By looking at how the plastic is changed during the cross-linking process, Figure 3.2 shows the relationship of viscosity and time when applying heat to a thermoset. As the heat has two effects on the material here, melting it down and activating the cross-linking reaction, the viscosity-time curve is a combination of those effects. The curve starts at the first point, t_0, where the material is heated at a constant temperature. After a certain time, the viscosity will drop to η_1, which is the lowest viscosity point. It then rises up as the molecular weight increases due to the cross-linking effect and continues to increase as the cross-linked network grows through time to a point where the liquid turns to gel. This point is called gel point or more commonly gel time (t_{gel}). Beyond this, the viscosity is going to infinity, which means the melt is completely solidified.

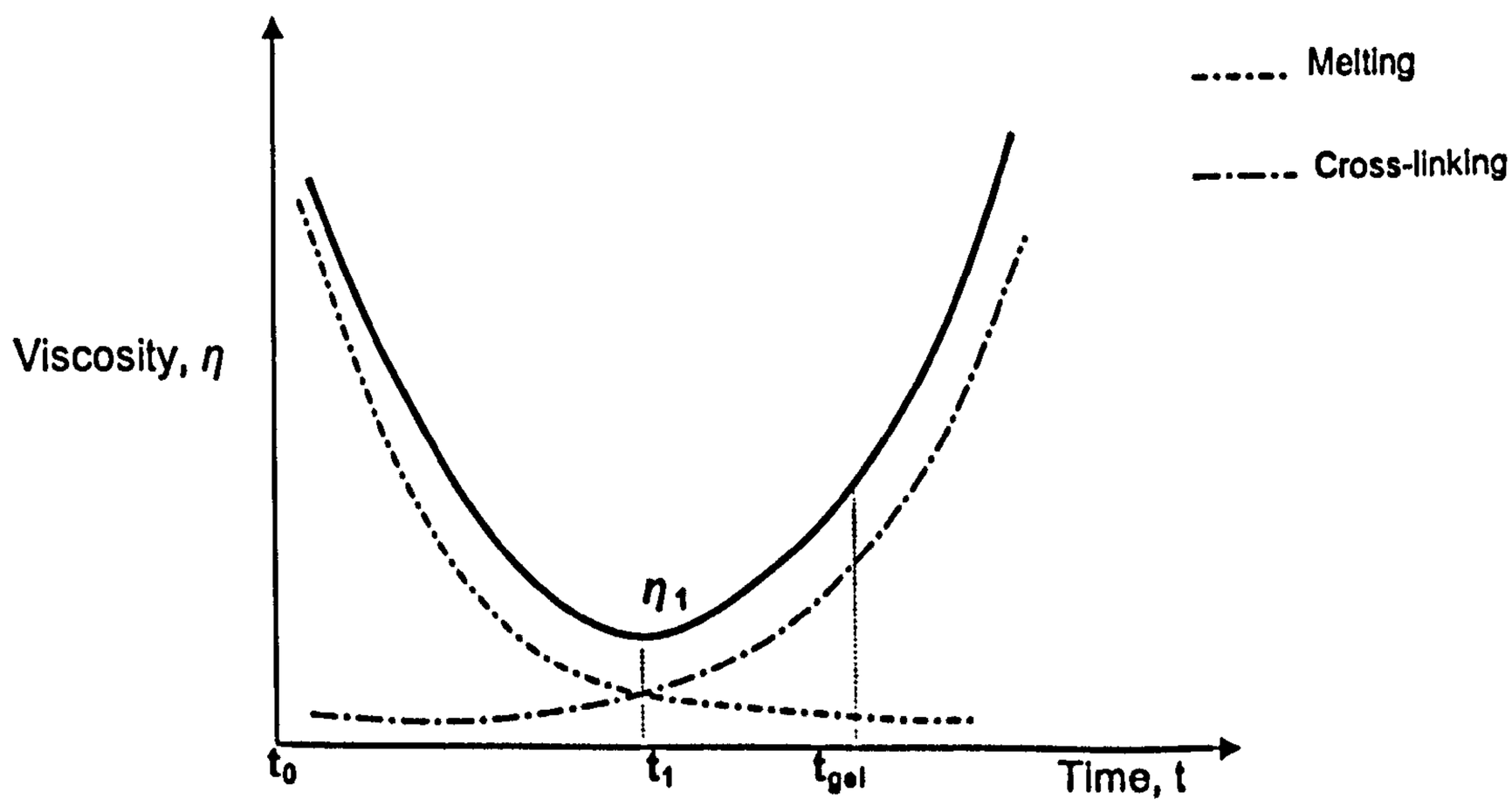

Figure 3.2 Viscosity and time of a thermoset at a constant temperature

Increasing the constant temperature has consequences in decreasing of gel time as shown in Figure 3.3. Figure 3.4 shows that the higher the temperature not only does it speeds up the curing rate but also reduces the material viscosity, i.e. the material is easier flowing.

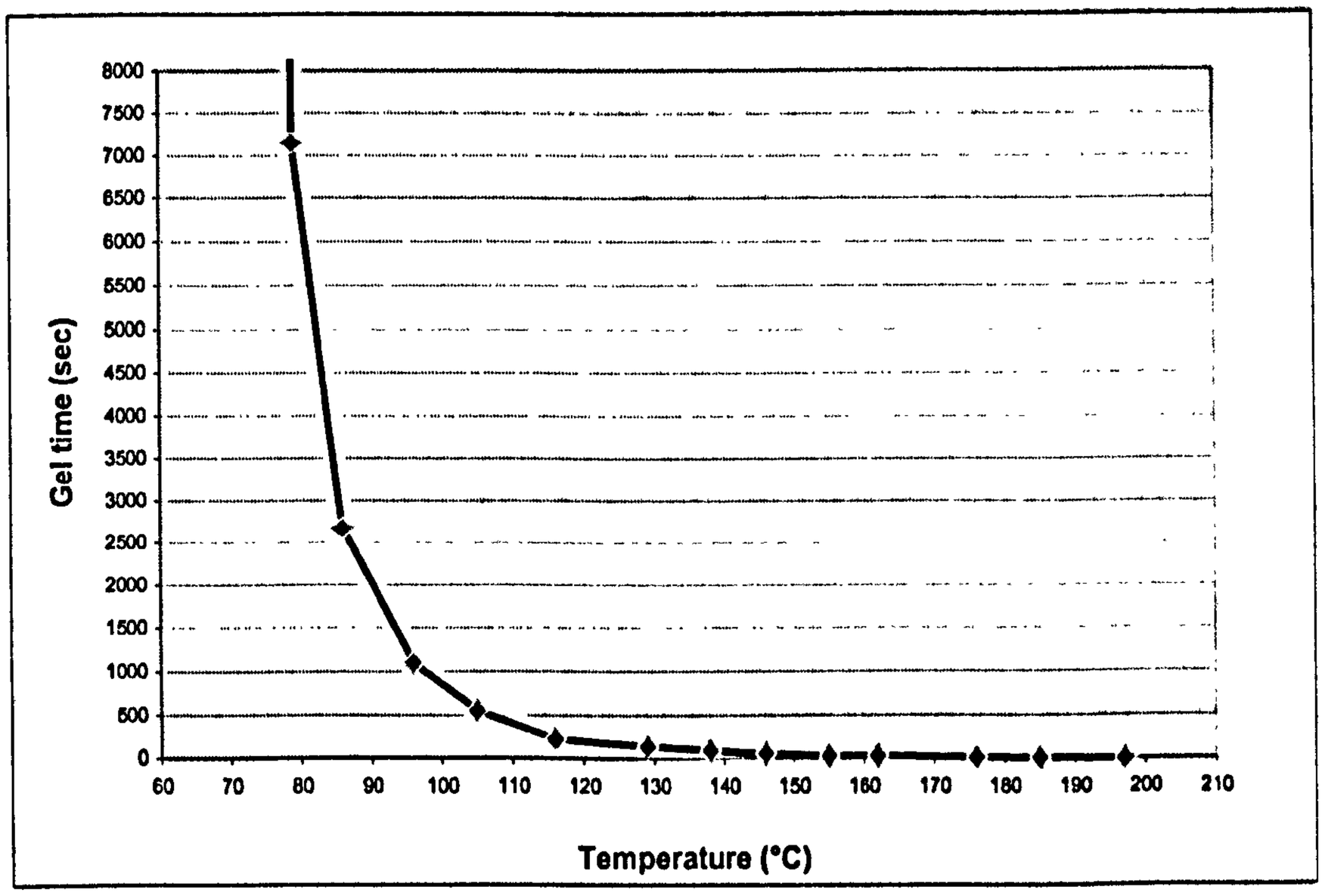

Figure 3.3 Effect of temperature on gel time of a thermoset polyester

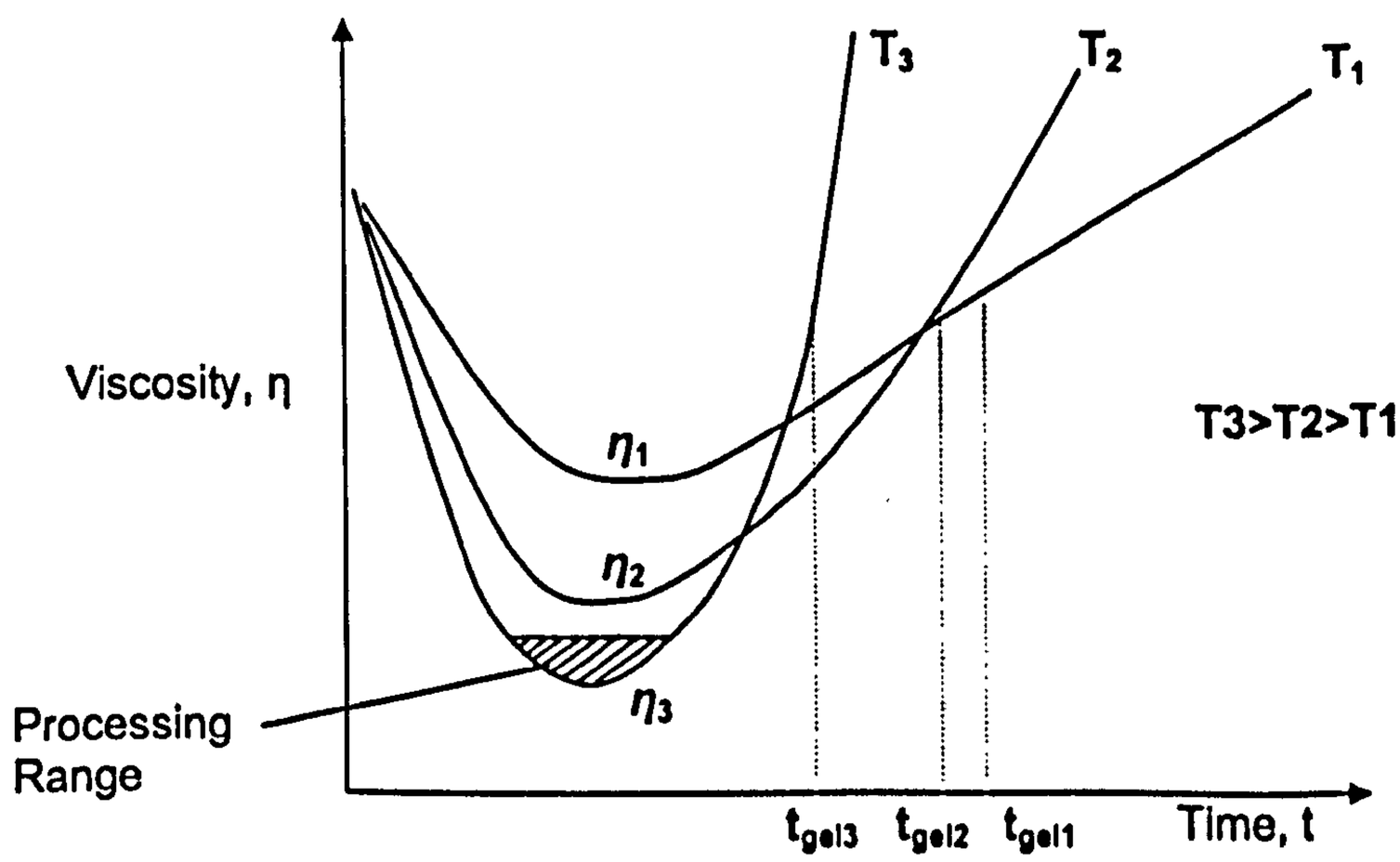

Figure 3.4 Effect of temperature on viscosity and time of a thermoset

It is very important to consider the gel time of any materials used in plastic production as it implies the critical point where the material starts to solidify and block the whole system. Obviously, it is recommended that the maximum duration of the molten material that can stay in the machine-feeding unit should be lower than the solidification time and certainly depends on the processing viscosity. To roughly find this point, usually a wooden probe has a sufficient enough accuracy (±0.5 minute)[38]. This method was used to find gel times of a thermosetting powder coating as shown in Figure 3.3.

Viscosity of material increases sharply to infinity after the gel time. This means, at that point, the thermosetting part is solid enough to be taken off from the mould and is ready to be used or sent to the next process. However the moulding is only partly cured there. The formation of internal bonds is still going on after the moulding cycle by using the internal heat generated from the cross-linking reaction. This process needs much more time than the machine setting curing time and results in dimensional changes and shrinkage after moulding. To investigate the part, it is recommended to wait until its dimension is stable, i.e. 48 hours for some grades of DMC (dough moulding compound) and melamine formaldehyde. [39]

3.3 Flow behaviour of thermoset

Generally, when injection moulding thermosets, the moulding engineer is always looking for a compound that has long flowing characteristics and fast final curing in the mould. Flow behaviour of the plasticised thermosets is a very critical aspect of processing. To understand the flowing of thermosets, it is worthwhile to start by looking at the basic fluid behaviour.

3.3.1 Rheological behaviour[41]

Consider a viscous liquid under a simple shear between 2 parallel plates, separated by a gap thickness h as illustrated in Figure 3.5. One of the plates is displaced with respected to the other at a velocity U by a force F.

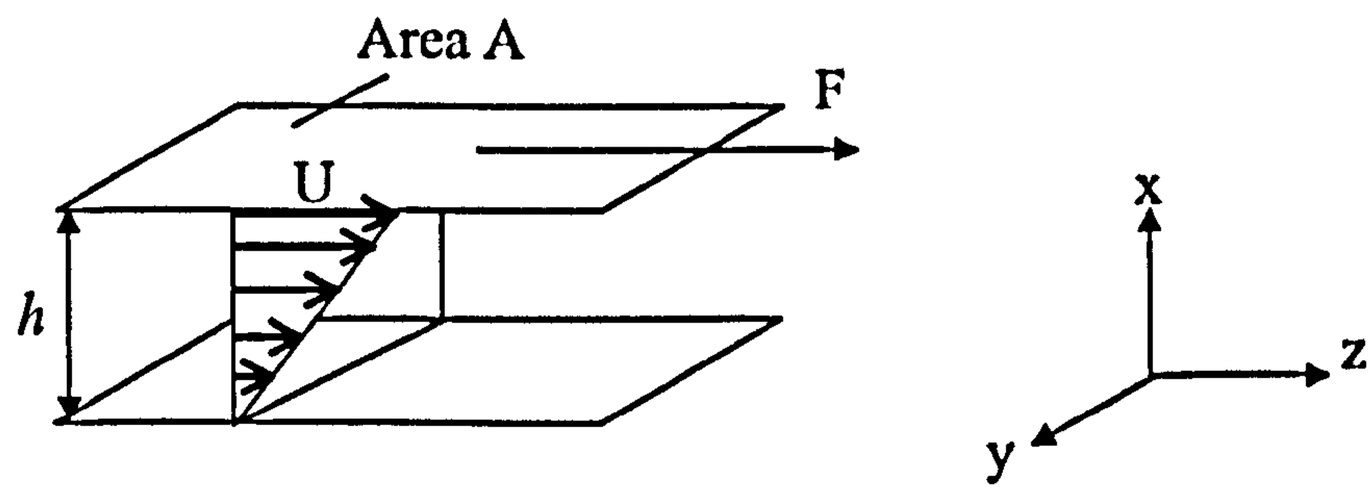

Figure 3.5 Simple shear experiment

The shear rate $\dot{\gamma}$ and stress τ are given by

$$\dot{\gamma} = U / h \tag{3.1}$$

and

$$\tau = F / A \tag{3.2}$$

When a stress is applied to a viscous fluid, the fluid will continue to deform until the applied stress is removed. In the case of a Newtonian fluid, Newton defined the relationship of the applied stress and shear rate by the following equation.

$$\tau = \eta \dot{\gamma} \tag{3.3}$$

where η is a constant called Newtonian viscosity.

The Newtonian viscosity η is a proportion of shear stress and the rate of deformation. This value is a property of the fluid and can be used to tell how easy the fluid can flow. It is always constant. Only temperature and pressure have an effect to the value.

The majority of polymers do not demonstrate the Newtonian behaviour. The most common case for polymers is their viscosity decreases with increasing shear rate. The behaviour is called pseudoplastic or shear thinning. The less common case is in the opposite way. The viscosity increases with increasing shear rate, which is called dilatant or shear thickening. Some materials that exhibit this behaviour are wet sand or wet cornstarch. Commercially, Silly Putty™ from Dow Corning® Corporation is a good sample of a dilatant polymer. These characteristics are illustrated in Figure 3.6.

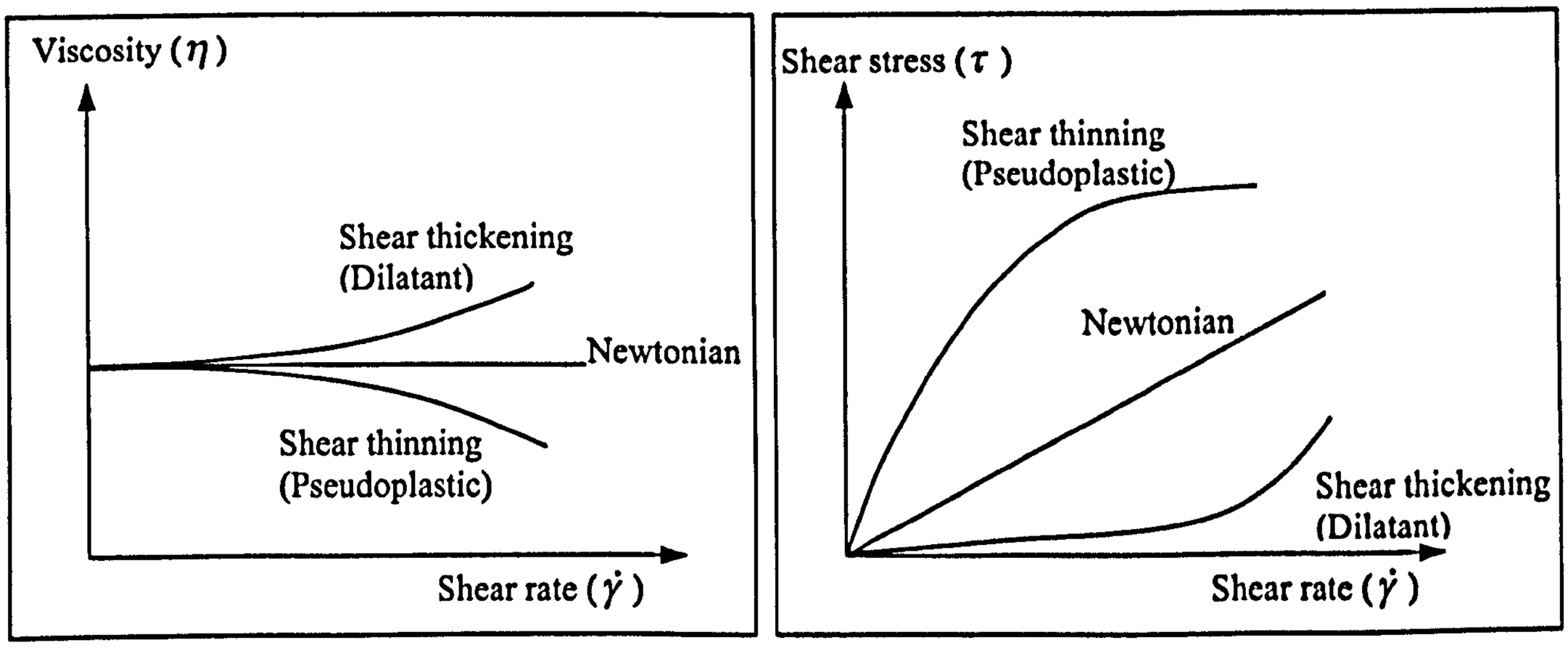

Figure 3.6 The characteristic behaviour of Newtonian and non-Newtonian fluid[40,42]

As shown in Figure 3.6, the viscosity of polymers, which are classed as non-Newtonian fluids, is dependent on the shear rate. The viscosity η in Equation 3.1 can be rewritten as a function of shear rate as in the following equation.

$$\tau = \eta(\dot{\gamma})\dot{\gamma} \tag{3.4}$$

There are many various empirical and theoretical works have been done in order to explain the flow of non-Newtonian polymers. A simple power law expression is suggested and is shown here.

$$\tau = \eta_0 \dot{\gamma}^n \tag{3.5}$$

where η_0 is a constant zero shear viscosity and n is a power law index, which depend on the polymer and temperature. For a pseudoplastic melt, n lies between 0 and 1 ($0<n<1$). From Equation 3.1.5, the viscosity of a polymer can be written as

$$\eta = \eta_0 \dot{\gamma}^{n-1} \tag{3.6}$$

Although Equation 3.6 is simple and can explain the flow quite well, it does not properly predict limiting zero shear viscosity.

This can be achieved by adding more parameters, one of the most popular viscosity models is the Bird-Carreau expression, which is

$$\frac{\eta - \eta_\alpha}{\eta_0 - \eta_\alpha} = [1 + (\lambda \dot{\gamma})^2]^{\frac{n-1}{2}} \tag{3.7}$$

where λ is a time constant and η_α is a constant viscosity at very high shear rate. Since η_α is usually small compared to other quantities, this equation can be reduced to

$$\eta = \eta_0[1+(\lambda\dot{\gamma})^2]^{\frac{n-1}{2}} \tag{3.8}$$

Another popular viscosity model is the modified Cross expression.

$$\eta = \frac{\eta_0(T)}{1+\left[\frac{\eta_0\dot{\gamma}}{\tau^*}\right]^{1-n}} \tag{3.9}$$

with

$$\eta_0(T) = A\exp[T_b/T] \tag{3.10}$$

where η_0 is the temperature dependent zero shear viscosity.

τ^* is shear stress of resin at which shear-thinning behaviour begins to manifest itself.

T_b is temperature sensitivity factor.

A is resin-dependent constant.

The Cross model includes four material constants (η_0, τ^*, A, T_b), which are dependent of temperature. However under injection moulding conditions, pressure is another factor that needs to be considered. The Cross model, therefore, has been developed by the C-Mold Company and used as a filling stage model for the simulation programme[43]. Equation 3.9 and 3.10 are replaced by the Cross-Exp model as shown in Equation 3.11 and 3.12.

$$\eta = \frac{\eta_0(T,p)}{1+\left[\frac{\eta_0\dot{\gamma}}{\tau^*}\right]^{1-n}} \tag{3.11}$$

with

$$\eta_0(T,p) = A\exp[T_b/T].\exp(\beta p) \tag{3.12}$$

where β characterises the pressure dependence of η_0

3.3.2 Rheological behaviour of thermoset

The mathematical models mentioned in the last section can be used to explain the flowing behaviour of thermoplastic polymers quite well. Nevertheless, to explain the flowing of thermoset, another factor that has to be considered is its complicated curing reaction, which leads to the increasing of viscosity with an increasing of time during curing. The basic Equation 3.4 is expanded by the dependence of viscosity on the cross-linking reaction as following.

$$\eta = \eta_0 f(\dot{\gamma})g(T)h(\alpha) \tag{3.13}$$

where η_0 is zero shear viscosity, $f(\dot{\gamma})$ is the function of shear rate dependence, $g(T)$ is the function of temperature dependence and $h(\alpha)$ is the function of cross-linking reaction.

Using the power law from Equation 3.6, temperature dependence according to Arrhenius law (Equation 3.14) and the Catro and Macosko model[44] for dependence on degree of cross-linking (Equation 3.15), the following equation is

widely successfully used in many simulation work and commercial computer software packages for moulding process simulation.[40,45,46]

$$\ln\eta(T) = C + \left[\frac{\Delta E_\eta}{RT}\right] \tag{3.14}$$

$$\eta(\alpha) = \left[\frac{\alpha_g}{\alpha_g - \alpha}\right]^{A+B\alpha} \tag{3.15}$$

$$\eta(\dot{\gamma}, T, \alpha) = \eta_0 \dot{\gamma}^{n-1} \exp\left[\frac{\Delta E_\eta}{RT}\right] \cdot \left[\frac{\alpha_g}{\alpha_g - \alpha}\right]^{A+B\alpha} \tag{3.16}$$

where η_0 is the temperature dependent zero shear viscosity.

$\dot{\gamma}$ is shear rate.

n is the power law index lies between 0 and 1.

ΔE_η is the activation energy of reaction.

R is the gas constant ($8.314 JK^{-1}mol^{-1}$).

T is temperature.

α_g is the degree of completeness of curing reaction at the gel point.

α is degree of cross-linking.

A, B, C are model parameters.

At high shear rates it is more accurate to develop the Cross model to predict the viscosity of thermosets. Moldflow Company proposed the viscosity model as in Equation 3.17. This model has been used in the thermoset mould filling module of MoldFlow Plastic Insight, a simulation software package.[47]

$$\eta = \frac{\eta_0(T)}{1+\left[\frac{\eta_0\dot{\gamma}}{\tau^*}\right]^{1-n}}\left(\frac{\alpha_g}{\alpha_g-\alpha}\right)^{A+B\alpha} \tag{3.17}$$

with $$\eta_0(T) = A\exp[T_b/T] \tag{3.18}$$

There are further research works that have been done in order to develop the viscosity model of thermoset melts, which are very complex and not mentioned here[48-50] as the subject is beyond the objective of this thesis. However the equations discussed here are adequate for representing the difference between thermoplastic and thermoset flow.

3.3.3 Flow effects of thermoset in the mould[40]

Consider three types of polymer melts flow in the mould as shown in Figure 3.7, type A shows the flowing of a Newtonian fluid, type B shows the flowing of typical polymer melts or non-Newtonian behaviour and type C show the plug flow behaviour, which is common in very high fibre filled polymer melts.

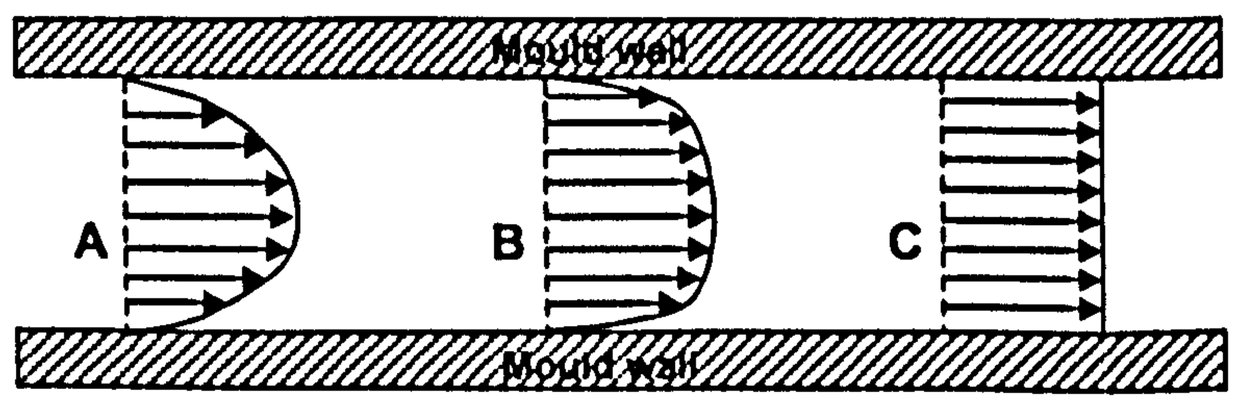

Figure 3.7 Flowing of fluid in the mould; A: Newtonian fluid, B: non-Newtonian fluid and C: high fibre-filled polymer melt

Consider the non-Newtonian fluid (Type B), it can be seen from the figure that the movement of the melt at the position closer to the wall is slower than the centre. Some molecular relaxation may occur when the movement ceases, causing the polymer to return to its disorderly molecular arrangement. In this flow-front, velocity difference is reduced as a result of fibre fill. Type C is the extreme case, which can represent the flow of a thermoset BMC as a result of high fibre content and cross-linking.

The next flowing behaviour that needs to be focussed on is the cross section of the classic fountain flow of polymer in the mould as shown in Figure 3.8. This figure shows the effect of the temperature difference between the mould wall and the polymer melts to the flow of the polymers. Generally when the plasticised plastic is injected into the mould, it will flow as the same pattern as flowing type B in Figure 3.7. In fact, the mould walls have a very different temperature compared to the melt temperature, i.e. much lower temperature in the thermoplastic case and much higher temperature in thermoset case. The temperature difference affects the melt solidification at the closest area to the wall and results in the fountain flow pattern. When fibrous fillers are presented, their fibre orientation is heavily influenced by this effect. This is shown in Figure 3.9.

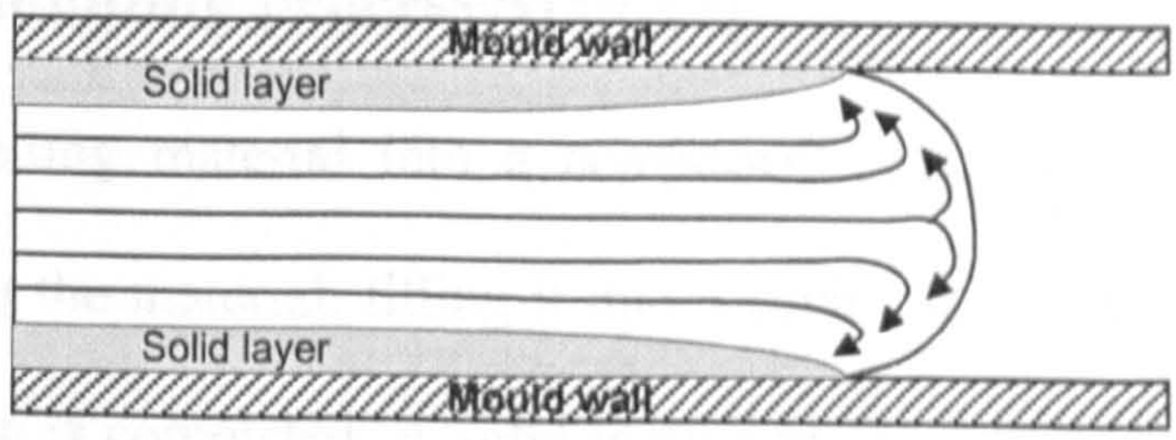

Figure 3.8 The fountain flow pattern of polymer in the mould

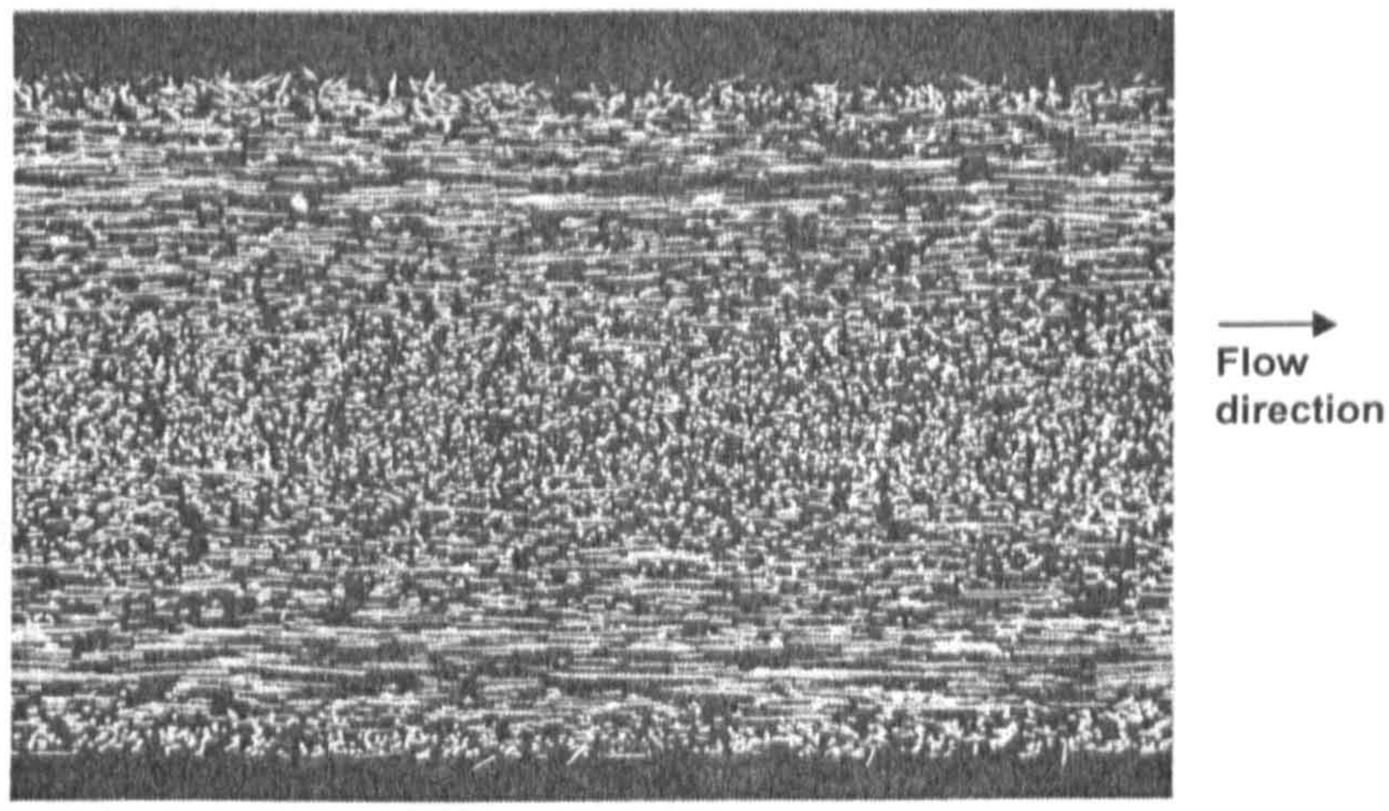

Figure 3.9 The fountain flow affects the short fibre orientation of a glass-filled polypropylene, showing the short fibre oriented parallel to the flow direction.[51]

It is important to note that there is a significant difference between thermoplastics and thermosets in this aspect. When thermoplastic melts flow into the cold mould, they are losing a large amount of heat, especially near the mould wall. This causes the viscosity to increase. Then the melt forms solid layers near the walls. For thermosets, the hot walls cause the viscosity to reduce first so that the material is flowing easier and this is followed by an increasing of viscosity due to the cross-linking effect. Consequently, the solidified layers of thermosets tend to be much thinner and the fountain flow effect is less than with thermoplastic.

3.4 Thermoset moulding processes[39,40]

Shaping a thermosetting material into a component requires processes with the capability of melting the material, filling it into a cavity and heating it up until the cross-linking reaction is completed. A solid moulding shaped like the cavity is then obtained. The processes that can do the work are normally known as compression

moulding, transfer moulding and injection moulding processes. Each of them has the same concept but is different in details, which will be described briefly here. For the injection moulding of thermosets, a more detailed explanation is provided in the next chapter.

3.4.1 Compression moulding

The compression moulding machine is designed to operate vertically. It consists of two halves of mould; one is fixed to the machine base and another is able to open and close in order to apply some pressure onto the raw materials. To start the process, both mould halves are heated up to a curing temperature. Then the stationary halve is filled with some thermoset by hand. The upper halve moves down to press the material. Heat and pressure from both halves turn the solid material to a viscous liquid. The plastic melt is left to cure in the mould while the excess material is forced out between the flash lands. Figure 3.10 shows an operation diagram of the compression moulding process.

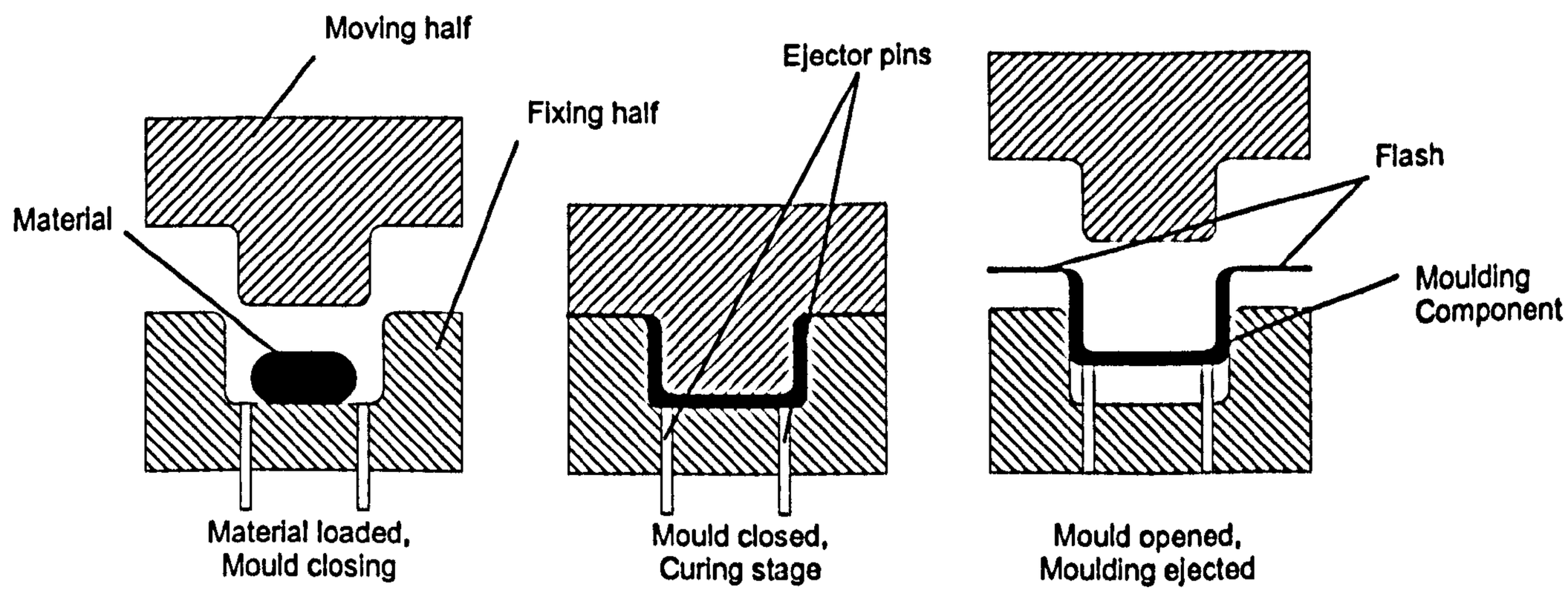

Figure 3.10 Diagram of compression moulding operations

3.4.2 Transfer moulding

In this process, similarly to compression moulding, the mould halves are heated up to a curing temperature before the process starts. However, instead of putting dry moulding compound in an opened mould, raw thermoset is heated up first to a point of plasticity and then hydraulically forced into the mould, which is already closed and clamped. After a sufficient time, the cured moulding and the feed runner are removed together. The process is also said to be one-shot injection moulding. Figure 3.11 shows a simplified diagram of a transfer moulding machine.

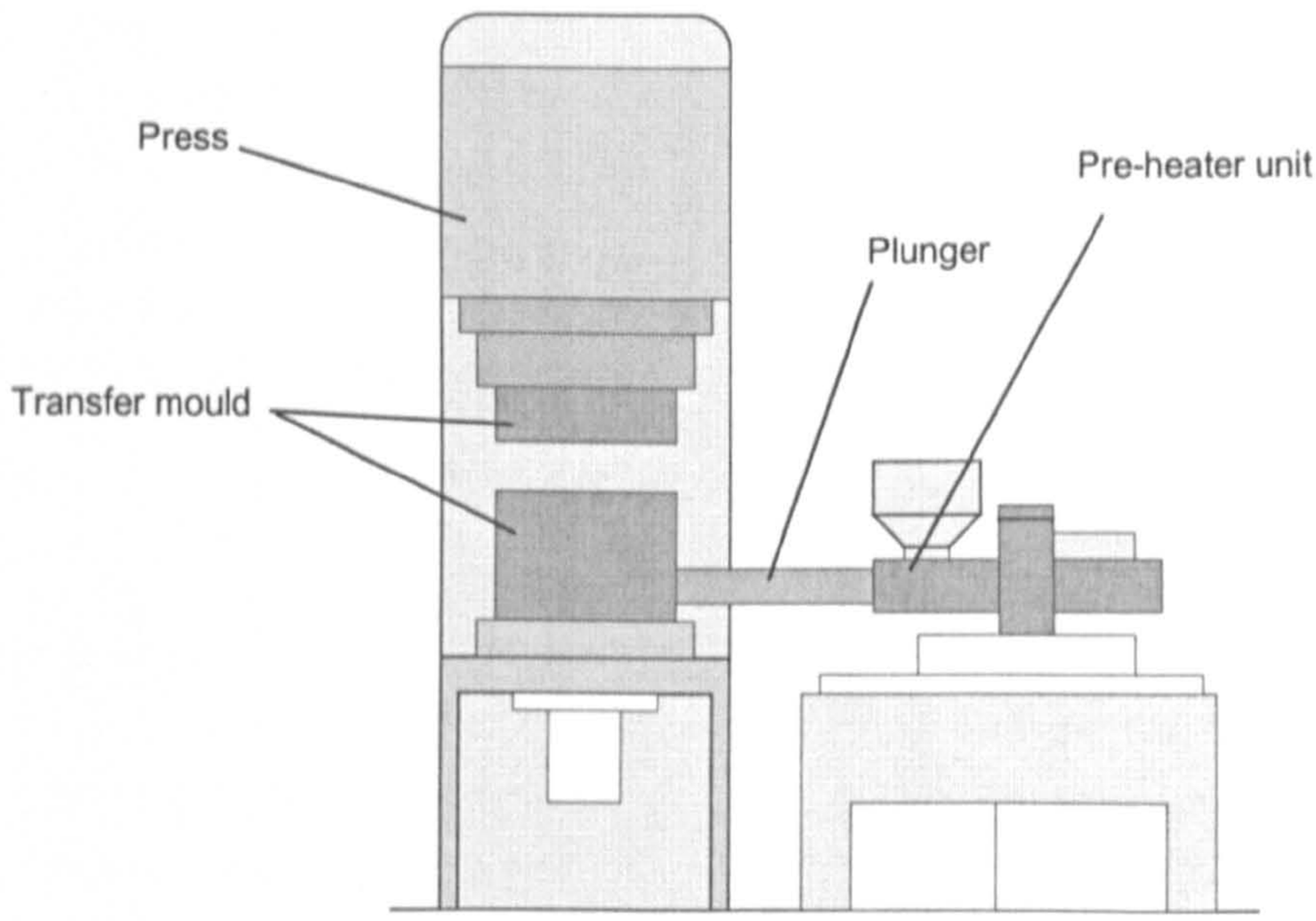

Figure 3.11 Simplified diagram of a transfer moulding machine

3.4.3 Injection moulding

Basically the machine is similar to a thermoplastic injection moulding machine, which consists of a reciprocating screw injection unit and a clamped mould. Thermoset compound is fed through a feeding hopper in the case of a dry material or a stuffer in the case of putty like compound like BMC (bulk moulding compound). To produce a component, the reciprocating screw is rotated and moved back to give

space for the molten material to accumulate at the front of the screw. It is heat generated from the heater and screw rotating that turns the material into melting plastic. The mould that has been heated is hydraulically closed and clamped then the melt is injected into the mould by the screw moving forward. Again, the moulding is left to cure inside and ejected when the cycle is finished.

The advantages and disadvantages of those three thermoset moulding processes are listed in Table 3.2.

Table 3.2 Advantages and disadvantages of different thermoset moulding methods

Advantages	Disadvantages
Compression moulding	
1. Can mould heavily reinforced material 2. Best method for mouldings with large surface area related to thickness 3. Minimum fibre breakage 4. Capital equipment costs are less than the transfer and injection mouldings 5. Simple to understand and control	1. Labour intensive, with more material handling involved 2. Material losses due to the need for flash allowance and general wastage 3. Requires secondary operation for flash removal 4. Difficult to mould round delicate inserts or pins as high pressure from cold material can damage to them
Transfer moulding	
1. Improved labour utilisation compared with compression moulding 2. Shorter cures compared with compression moulding 3. Good control of part and flash thickness 4. Suitable for moulding with inserts	1. More skill in term of process control is required 2. Mould is often more complex and costly 3. Cannot use as a wide range of compounds as with compression moulding 4. Greater risk of distortion and directionality of mechanical properties 5. Care is required to minimise weld lines 6. Material losses in central feed system
Injection moulding	
1. Process offers automatic operation 2. Rapid cycle times result from a substantial reduction in cure time 3. Good control of dimension and flash thickness 4. Good part-to-part consistency 5. Can mould with thin sections	1. Skill required for setting up and controlling the process 2. More complex machine and mould 3. Process is not tolerant to stop-start conditions of operations 4. More fibre orientation and degradation than compression moulding 5. Care is required to minimise weld lines 6. Loss of material in sprue and runner

3.5 Thermoset components

Thermoset products possess unrivalled thermal resistance, stiffness, creep resistance, dimension stability and chemical resistance in relation to other organic polymer families as a result of their cross-linked structure. They offer an excellent combination of electrical properties, especially resistance to high voltage electrical tracking. More importantly, these properties are provided by families of materials, which generally are relatively inexpensive when compared with thermoplastics offering the same thermal, mechanical, chemical and electrical performances.[40] The component made of thermosets can be found in the following applications.

3.5.1 Automotive industry[52-54]

Compared to the traditional metal parts, which are heavier and more expensive than plastics, plastics give cars better fuel mileage and design flexibility to achieve more styling and aerodynamic designs as well as lower production cost, required properties and better dent resistance. Car manufacturing uses both thermoplastic and thermoset materials in different functions, dependent on their basic properties. The cross-linking structure of thermoset materials makes them strong and able to tolerate severe conditions such as high heat, UV and chemical substance concentration so that it is more suitable to use as under bonnet parts, body panels and structural components, while thermoplastic has been used as trim or interior parts where high strength is not an issue.

Some engineering thermoplastic grades such as reinforced nylons are also widely used under bonnet as well as BMC. However, they are generally more costly when measured on a cost per unit volume basis[53].

3.5.1.1 Exterior

As plastics allow engineers to have greater freedom in styling, building and placing components, a new look of modern car, which can be produced at a lower cost, is not impossible. From the front to the back of a car almost every part can be made of a non-metal material, either thermosets, thermoplastics, elastomers or a blend of those. Some parts that are made of thermosets are,

- Body panels and bonnets; BMC, SMC, RIM-urethane or unsaturated polyester with glass filled are used.
- Bumpers and fascias are made of unsaturated polyester and polyurethane or blending of those with thermoplastics. Glass fibre reinforced is often included in the component for added strength and rigidity.
- Trims, which are important parts designed for exterior's operative and aesthetic purposes. This includes mirror housings, door handles, side trims and radiator grills. They can be made of polyurethane and unsaturated polyester.
- Headlamp reflectors and headlamps and tail lamp housings: Theses are made by injection moulding, the part is made of BMC, SMC or unsaturated polyester. The reflectors are coated with high-reflected material to make it look like metal.

3.5.1.2 Interior

Because of their strength and high environmental resistance, thermosets are mainly used in semi-structural applications and non-appearance parts so that not many of them are found inside the car. Especially in a component where aesthetic appeal, comfort and practicality have a great impact on a customer's decision.

Thermoplastics, which are available in a greater variety of colours and are easier to process, are often more suitable. However, thermosets are used in the following parts.

- Instrument panels, door handles and central console; by reaction injection moulding (RIM), these parts can be made of polyurethane.
- Window frame; Injection moulding of unsaturated polyester was used in a Renault's car model 4.
- Steering wheel; the material has been used is RIM urethane.
- Interior trims; also made of RIM polyurethane.

3.5.1.3 Under bonnet applications

High heat, electrical and chemical resistances are required in this area. Thermoset is used to make many parts under bonnet as well as glass-filled nylon (thermoplastic polyamide). The main materials used here are BMC or SMC. Some examples are

- Engine cover
- Valve cover
- Oil pan
- Rocker arm covers
- Fuel tank heat shield
- Intake manifold, etc.

3.5.2 Electronic industry[55]

Again, as thermosets provide very good heat resistance and electrical performance, they can be used for switches and covers, circuit breakers and fuse carriers.

3.5.3 Housing for domestic appliance, business machine and kitchen ware[55]

The following thermoset components are produced:

- Toaster, sandwich toaster, irons and cooker handle, microwave oven and dishwasher.
- Photocopy machine, fax machine, telephone, computer case and etc.
- Plates, glass, bow and kitchen tools

3.5.4 Fuel cell Technology

One potential growth area for thermosets could be in Fuel cells. A Fuel cell is the result of the concept of converting hydrogen gas into electricity by a reaction called the electro chemical reaction. Figure 3.12 shows the diagram of a fuel cell stack.

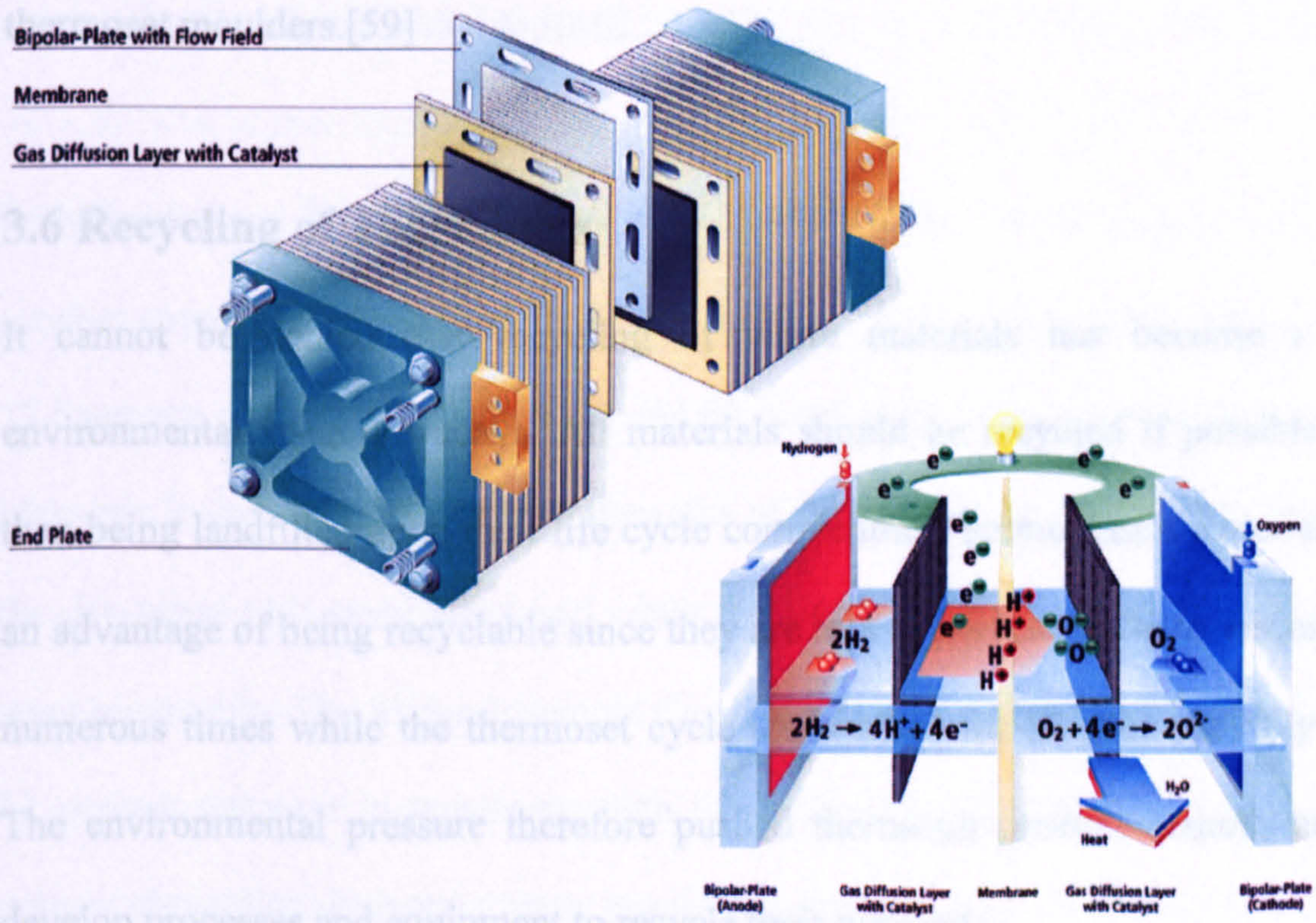

Figure 3.12 Diagram of a fuel cell stack[56,57]

One fuel cell stack consists of many fuel cells arranged in series. Bipolar plates between each cell are used to electrically connect the cells together and used as the flow channels for hydrogen and oxygen, which are the essential inputs for the fuel cells. They can be made of a thin structure of machined graphite composite or moulded graphite composite. All of the current generated from the electrochemical reaction is collected by the end plates, which are placed at the both ends of the stack. Generally, a fuel cell stack consists of more than 400 cells arranged in series in order to provide an adequate power for a system.[58]

It was estimated that this new technology would be launched commercially during 2002 and utilised in automotive sector by year 2005. The requirement of high heat resistance, high chemical resistance and easy-to-produce components, with a reliable tolerance for producing the bipolar and end plates then give a good opportunity for thermoset moulders.[59]

3.6 Recycling of Thermosets

It cannot be denied that recycling of waste materials has become a major environmental issue nowadays. All materials should be recycled if possible rather than being landfilled upon their life cycle completion. Thermoplastic materials have an advantage of being recyclable since they are reversible from solid to viscous fluid numerous times while the thermoset cycle stops when the plastics are fully cured. The environmental pressure therefore pushed thermoset product manufacturers to develop processes and equipment to recycle their materials.

Two potential techniques for recycling thermosets are (i) regrinding used thermoset and mixing the recyclate filler with a virgin material and (ii) chemical degradation and pyrolysis of thermoset composites to regenerate basic organic and inorganic raw material to reuse. The first technique is more acceptable in industry because of its lower processing cost and the lack of pyrolysis facilities. The regrind technique has been further expanded to recover only glass fibres by combustion of the polymer in a fluidised bed[5,7].

Perterson and Nilsson[4] evaluated strength of products added with reground SMC scrap. The tests showed that using standard process equipment it was possible to mix10-30 percent recyclate and new BMC and SMC. Improved flexural strength with slightly reduced flexural modulus was achieved for SMC containing 10 percent reground material but overall mechanical properties decreased when 30 percent reground material was added to BMC.

Dzeskiewicz and Ralston[6] proposed that particle size of recyclate filler affected to product strength. They carried out dry blended test and compounded tests of 8.6 and 17.5 percent of two particle sizes, 32 and 60 mesh, reground material with 20 percent glass reinforce BMC. The overall strengths of the material (of both mesh sizes) from the dry blend tests were decreased while the results of the compound tests showed were acceptable. The 32-mesh sample showed 33 percent decrease in elongation and 13 percent decrease in tensile strength while the 60-mesh sample showed only 2 percent elongation drop and greater tensile strength of 1.05 percent.

Gruskiewicz and Butler[5] looked at the feasibility of recycling thermosets in industry in terms of technical and economic aspects. Many recycled products from thermosets had been used and developed in the automotive industry. For example, SMC containing recyclate filler was being used commercially on non-Class A body panels and interior parts and BMC with recyclate filler had been developed for forward lighting applications. Many mouldings utilising recyclate filler had been tested and found to meet the requirement of Federal Motor Vehicle Safety Standard for forward lighting applications. Similar work with Thick Moulding Compound (TMC®) for engine valve cover application showed success with recyclate filler of 25 percent of the total product weight. The tensile strength was found to be equivalent to virgin TMC but the flexural strength dropped to 75 percent of that of the virgin TMC.

Although the recycling of thermoset is technically feasible, the cost of the recycling process was higher than producing parts from virgin material due to the lack of an infrastructure to recover thermoset components for reprocessing.

In Europe, a SMC and BMC recycling project, ERCOM, was established by the German Federal government in partnership with a group of major raw material suppliers in order to recycle SMC and BMC components from motor vehicles to a standardised recyclate. Used thermoset components or waste are sent to the ERCOM plant from part manufacturers, while parts from dismantled cars come from a companion project PRAVDA. The plant had a capacity of 6000 tons per year in 1991 and was targeted that the recyclate throughput from the plant would be 10000 tonnes

per year[4,40]. Unfortunately the process was not economically viable and the activities had been discontinued.[60]

In 2003, the European Trade Association, the GPRMC (Groupement européen des Plastiques Renforcés / Matériaux Composites) and the key European fibre reinforced plastic suppliers introduced a *'European Composite Recycling Concept'* in order to fund the high investment needed to develop, validate and promote new recycling solutions for fibre reinforced thermosets and thermoplastics. The concept was that fibre reinforced plastic suppliers across Europe would financially participate in the development of a standardised composite waste management solution for the plastic waste. Funding would be used to launch R&D programs to study new and improved ways of collecting and recycling the plastics, as well as seeking out and developing new markets for recyclate. The target date for the launch of the European Composite Recycling Concept was the end of 2003.[61]

3.7 Conclusions

This chapter introduced the basic characteristics of thermoset materials and explains the differences of the material from thermoplastics in terms of cross-linking and curing. Flow and cure of thermosets are the important properties that should be considered in any plastic processing. The changes of temperature applied to the material affect directly to those properties as can be seen in a decreasing of the material's gel time with an increasing of the applied temperature. It is a significant parameter that implies the critical point where the material starts to solidify and block the whole system.

Viscosity of a polymer is used to define the polymer flow and can be described by many viscosity models. The function of the cross-linking reaction is added to the model used for thermoplastics when describing the flow of thermoset materials.

When a polymer flows into the mould that has a very different temperature from the polymer melt, frozen layers near the mould walls are formed and results in the fountain flow pattern. When moulding with a fibre-filled material, this flow pattern influences the fibre orientation of the material in the mould.

The flowing and skin-core formation of thermoplastics, when sandwich injection moulding, are also affected by the fountain flow effect. In the case of thermoset, the fountain flow effect is less, as the solidified layers of thermosets tend to be much thinner. It is likely that the skin-core formation of thermoset sandwich components will differ from the thermoplastic sandwich mouldings.

Thermoset moulding processes, which are compression, transfer and injection moulding, were briefly explained. Each process has advantages and disadvantages over each other. Choosing a suitable process is dependent on the moulding components that are produced.

The usage of thermoset material in the automotive industry, including exterior, interior and under bonnet, and the new fuel cell technology offers a good opportunity for thermosets in the market. However, the fact that thermosets are more difficult to recycle than thermoplastics and the recycling process is costly, can slow down the market growth of thermosets.

Recycling thermosets by regrinding used thermoset and mixing with a virgin material is more acceptable than the chemical and pyrolysis technique in industry because of its lower processing cost. Many researchers showed that the strength of the products added with reground materials were acceptable. The components made of recycled thermosets were used commercially as a non-Class A body panel and interior parts. However, the cost of the recycling process was too high and needed more development in collecting used plastics and recycling methods.

The new thermoset co-injection moulding can be an alternative way of producing thermoset components from reground materials. It can improve the surface quality of the component, which will expand their usage and applications.

Chapter 4

Thermoset Co-Injection Moulding

4.1 Introduction

Co-injection moulding of thermosetting material is a new technology combining the technology of thermoset injection and thermoplastic co-injection mouldings. It has been invented to make thermoset sandwich parts. The concept is to inject two thermosetting plastic melts into a mould simultaneously or sequentially by a two-barrel thermoset injection moulding machine equipped with a prototype manifold system for working as the novel thermoset co-injection moulding machine. This process is different from the ordinary thermoplastic co-injection since material temperature and time are the most significant factors. Thermosetting materials need sufficient heat to melt and activate the cross-linking and a certain amount of time for the reaction to be completed so that a solid moulding is obtained. In other words, the injection units and mould tools need to be carefully temperature controlled with a suitable processing time, i.e. the time that the material can be left in the system without causing a blockage. It should be noted that the material is not only influenced by the setting temperatures, but is also affected by frictional heat being generated during injection. A high screw rotation, fast injection rate and high back pressure can cause the frictional heat in the system to rise. This should be clearly understood before setting up the machine. A general guide to the effects of various stages of injection moulding thermosets on the material temperature is shown in Figure 4.1.

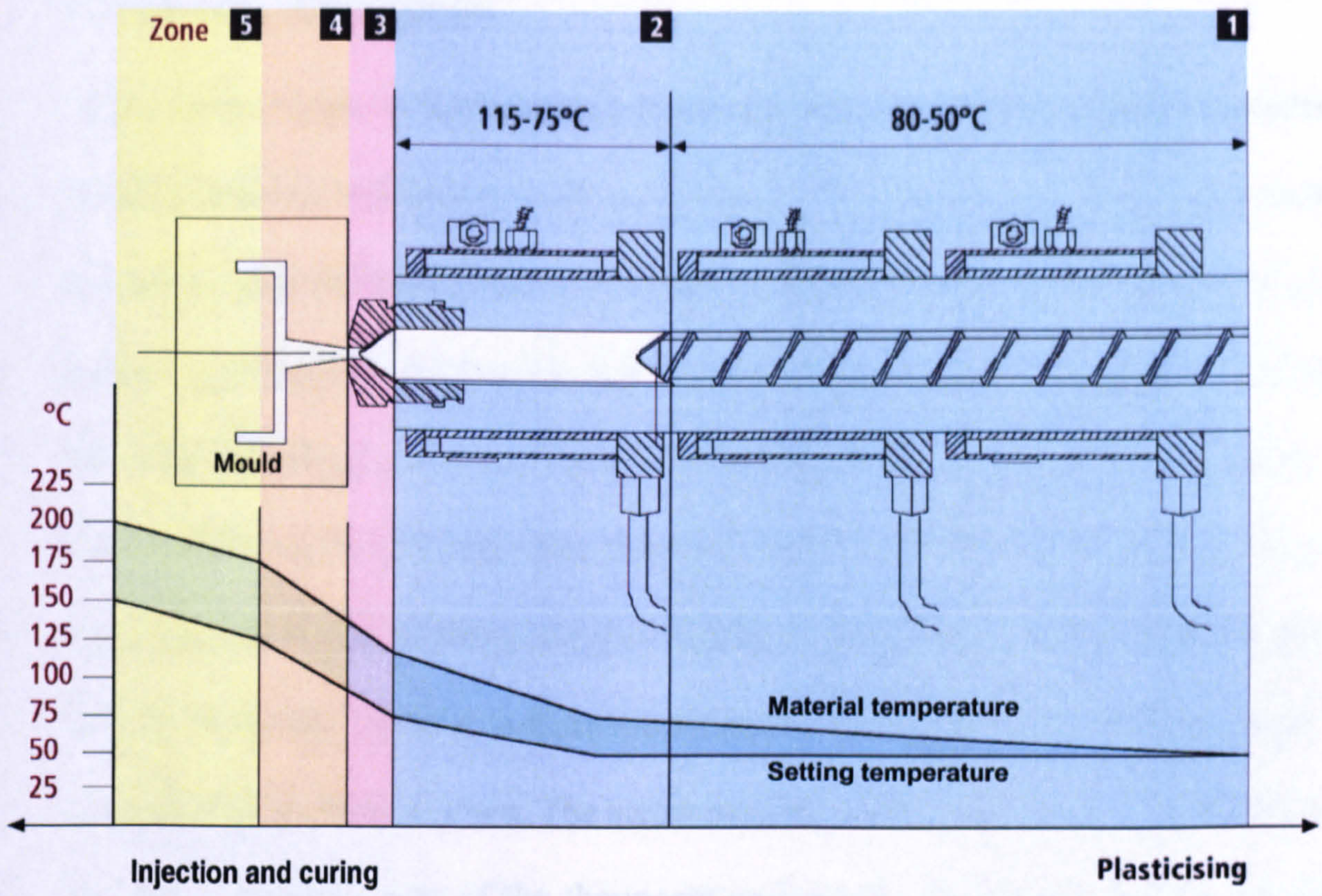

Zone 1	Pre-heating zone	Effect of screw geometry, rotational speed, back-pressure and cylinder temperature control
Zone 2	Plasticising zone	
Zone 3	Friction dependent upon injection capacity (injection pressure and injection speed) and nozzle bore	
Zone 4	Friction caused by sprue and gate cross section	
Zone 5	Effect of mould heating an curing	

Figure 4.1 Effects of various stages of thermoset injection moulding[62]

4.2 Process description

There are two types of thermosetting materials used in thermoset injection moulding, granular material and bulk or putty compounds. The granular materials, for example, phenolics, urea-formaldehydes and melamine-formaldehydes are suitable for typical gravity feed hoppers, the same type that is used in thermoplastic injection moulding. The bulk moulding compound (BMC) or an unsaturated styrene-modified polyester, is fed differently, as its putty-like character results in difficulty in flowing through the machine's throat. Feeding is carried out by a stuffer unit, which is installed at the back of the barrel, in order to force the material to the back of the injection screw by hydraulically pushing it down. The screw rotating delivers the material to the front of the barrel. General parts of the thermoset co-injection moulding machine specially built for this research from Battenfeld are illustrated in Figure 4.2.

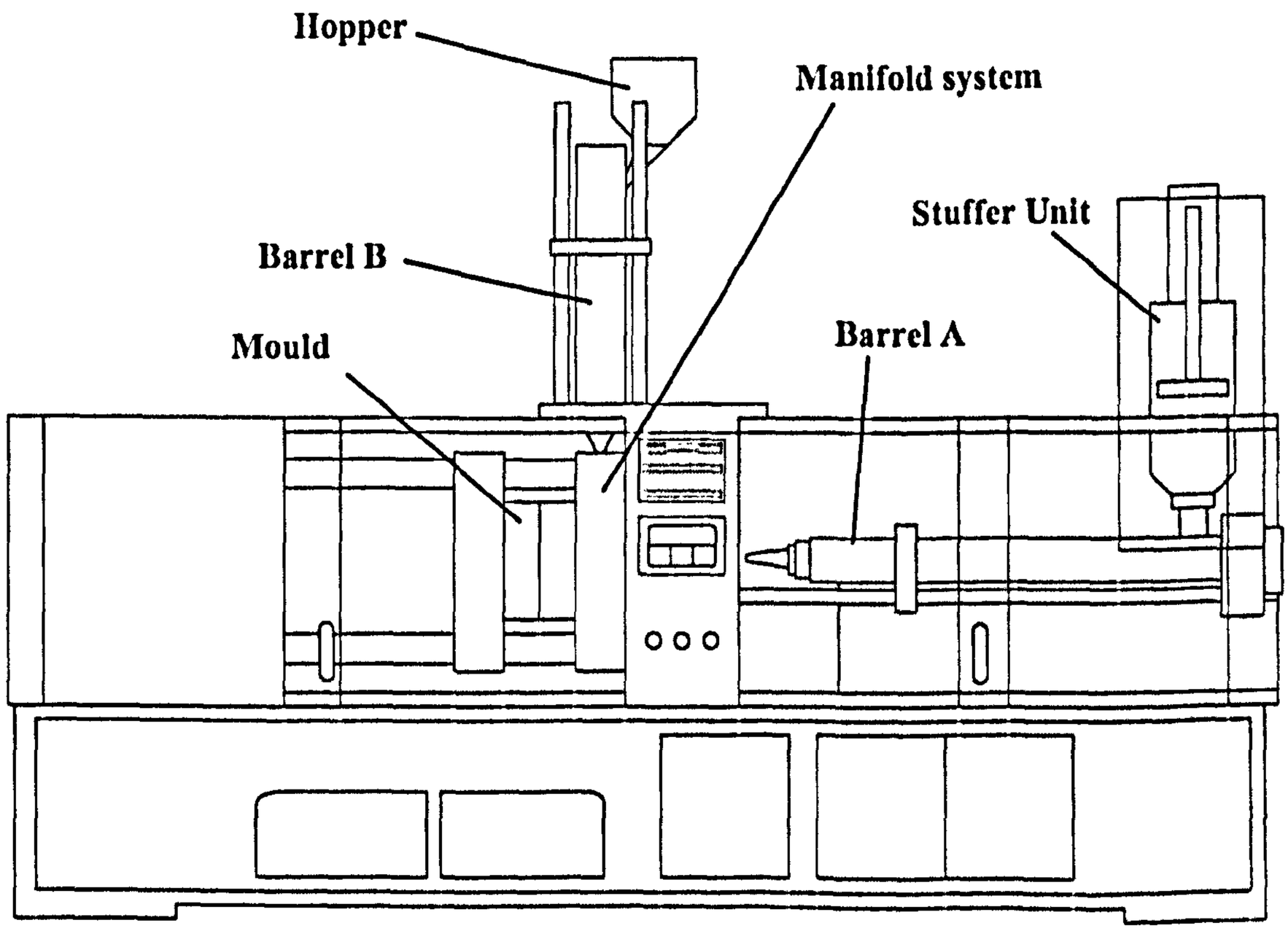

Figure 4.2 Diagram of the thermosetting co-injection moulding machine

Similar to the thermoplastic co-injection moulding process, the injection cycle is started when the mould is closed hydraulically and clamp force is applied. This force needs to be high enough to keep the mould closed against the maximum injection and cavity pressure so that during the injection and holding phases, no material leaks from the mould and causes flashing. However, the clamp force should not be too high as to exceed the mould's strength. The machine then injects skin and core melts from the barrels through the manifold and into the mould that has been heated up to the moulding or curing temperature. The injection sequence, and injection time are dependent on the material types and the mould geometry. It is also necessary to apply holding pressure to pack the moulding in order to maintain the cavity pressure to ensure that no sink marks and voids are presented on the surface of the component.

After the required amount of materials is injected into the hot mould, the melts are left there until the internal cross-linking networks are strong enough for the plastic to maintain the moulding shape. During this time, the barrel A and B, as shown in Figure 4.2, are charged with the new materials, which have been fed from a stuffer unit and a gravity feed hopper respectively. At the end of the curing phase, the mould is opened and then the component is ejected from the mould. Note that the cross-linking reaction has been started since the material was beginning to melt in the barrels, but at a very slow rate. Most of the reaction happens inside the mould and still continues going on, but more slowly even after the part is ejected. The operating sequence of the thermoset co-injection moulding will be shown later in Table 4.1. Figure 4.3 shows the moulding cycle diagram of the co-injection moulding of thermoset.

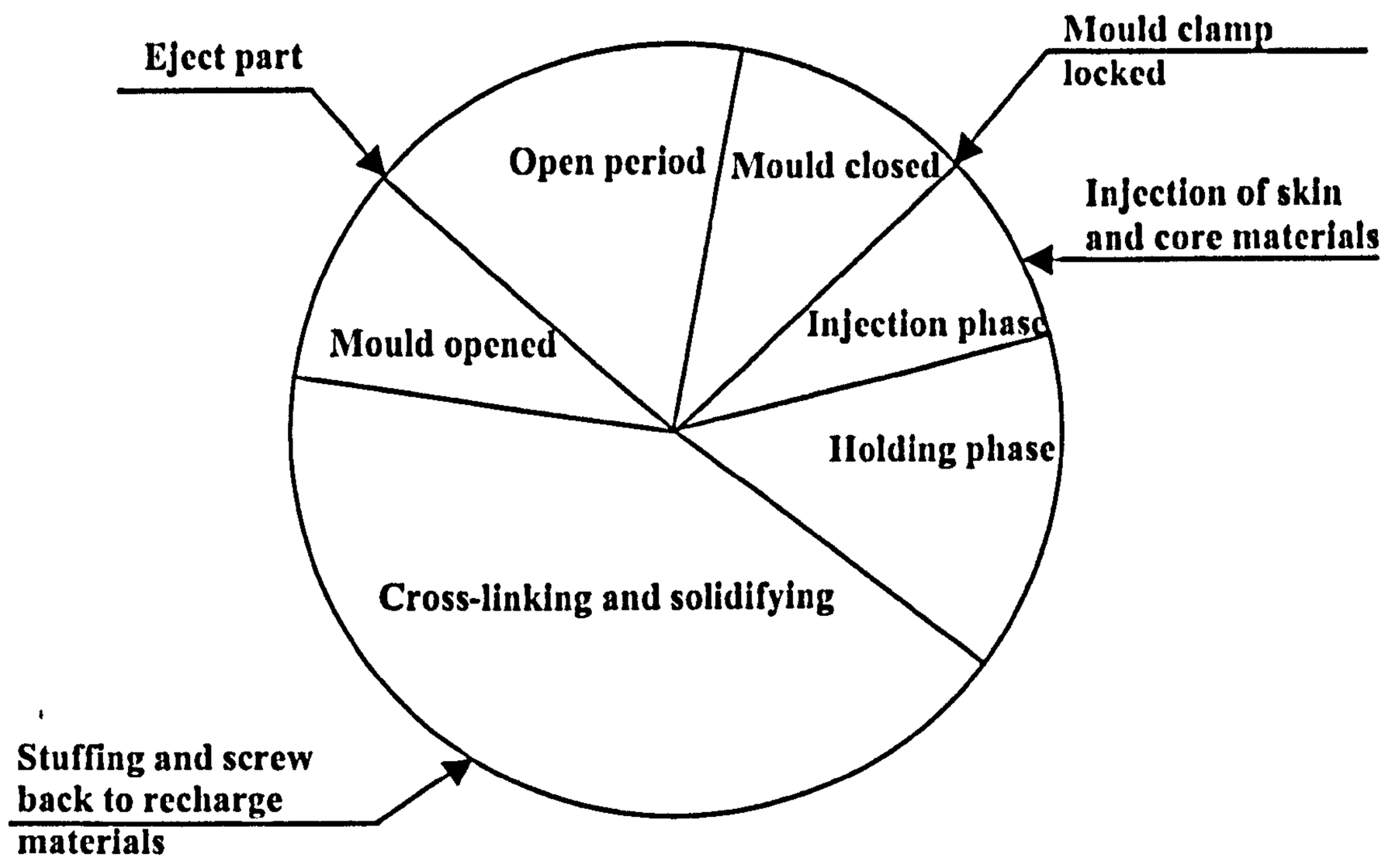

Figure 4.3 Moulding cycle of thermoset co-injection moulding

4.3 Thermoset co-injection moulding machine

As shown previously, the procedure of co-injection moulding of thermosets is similar to that of thermoplastics. The main objectives are to melt the polymers, inject them into the mould, leave the melts to solidify and then eject the part. However as the basic characteristics of thermosets are not the same as thermoplastics, the machine has to be modified in some details.

4.3.1 Feeding unit

The co-injection moulding machine consists of two main feeding units for feeding skin and core materials. Designs of the units are different and depend on the materials being used. For the existing machine, the top injection unit has a simple

gravity feed hopper, which is suitable for any granular compounds, whereas the horizontal barrel is a little more complicated.

Bulk moulding compound (BMC), which is also known as dough moulding compound (DMC) is a modified reinforced thermoset polyester that needs a special feeding method. The material is like a dough at room temperature and so is very difficult to feed into the barrel. The stuffer unit as shown in Figure 4.4 has been used to do the job. The basic idea is to have a piston that can force or pressurise the material, which has been fed by hand, down from the hopper through the throat and to the back of the injection screw. The system is hydraulically controlled so that at the throat, a pressure transducer is installed to get the pressure reading for moulding in automatic mode.

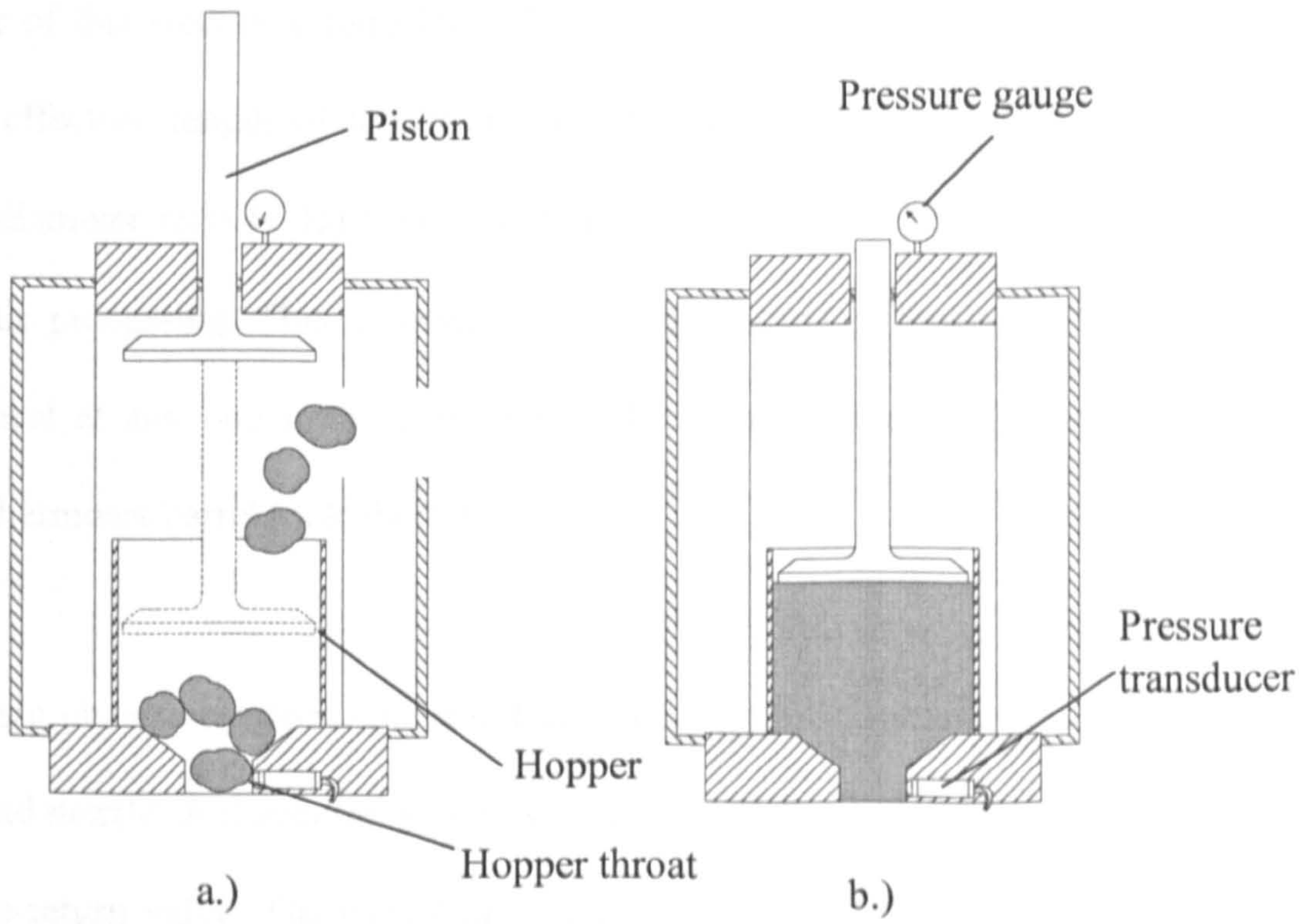

Figure 4.4 Stuffer unit;

a.) Loading BMC into hopper and b.) Fully loaded hopper

4.3.2 Barrel, screw and nozzle[23,51,63]

From the stuffer and the hopper, the materials are fed to plasticise in the injection unit, which consists of a rotating screw installed in a barrel. This is where the material temperature is brought up to its start melting point. Heating is achieved by hot water jackets around the whole barrel. As the heat control of thermosets is very critical during plasticising, this is a more effective way to smoothly control the barrel temperature than by the heater bands used in thermoplastic moulding. Furthermore, the water jackets can be used as a cooling device to remove excess heat when the barrel is overheated. This is to ensure that the barrel temperatures are always within the setting range. This will be discussed in more detail in section 4.5.2.

Normally the barrel contains two zones of temperature control. The front zone near the nozzle is 1/3 of the effective length of the barrel (See Figure 4.5). Setting temperature of this zone is around 20-30 °C higher than the rear zone, which is the 2/3 of the effective length of the barrel near to the feeding unit. Standard barrel length per diameter ratio (L/D) is only 12:1 or 13:1, while it is more than 20:1 for thermoplastic processing. This is because a smaller amount of thermoset is allowed into the barrel at any one time in order to reduce the chance of pre-curing. This makes the thermoset barrel look shorter.

Another basic change between thermoset and thermoplastic moulding machines is the screw and nozzle. A thermoset screw is designed to have a blunt tip and normally with no non-return valve. The exception is for moulding BMC. In this case, a non-return valve is necessary to prevent the material flowing back to the barrel during injection moulding. The thermoset screw also has a smaller length per diameter

(L/D) ratio compared to a thermoplastic screw. Most of the screws have square pitch, i.e. the length of the screw flight is equal to the screw outside diameter and have low or no compression ratio. The compression ratio is calculated by taking the volume of the first flight of the screw where the material enters the barrel divided by the volume of the last full flight near the screw tip. A low compression ratio is required as the materials are very fluid in the barrel.

The nozzle for thermoset injection moulding is normally designed to be easy to take out in case of pre-curing in the barrel, so that it can be cleared quickly. This is also applied to the extended nozzle, which is used sometimes in order to reduce the sprue size. The characteristic of a typical thermoset screw and barrel are shown in Figure 4.5.

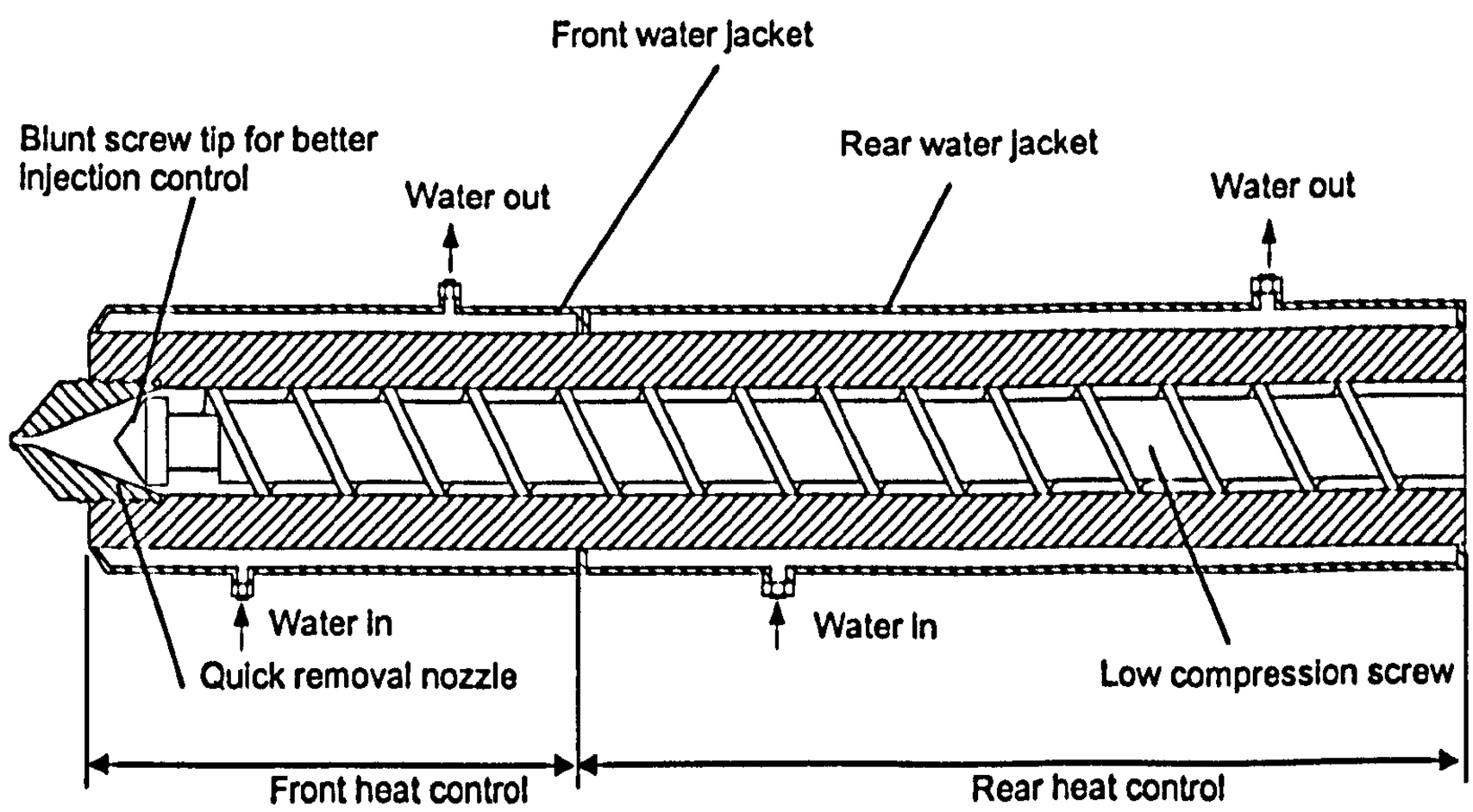

Figure 4.5 General characteristic of a thermoset screw and barrel[51]

In Figure 4.6, recommended tool steel grades for thermoset barrel systems are shown. A surface treatment, such as chromium plating, nickel plating or nitriding is

required, in order to improve the wear resistance of the parts where they contact directly to the plastic, as higher abrasion is more likely to occur there.

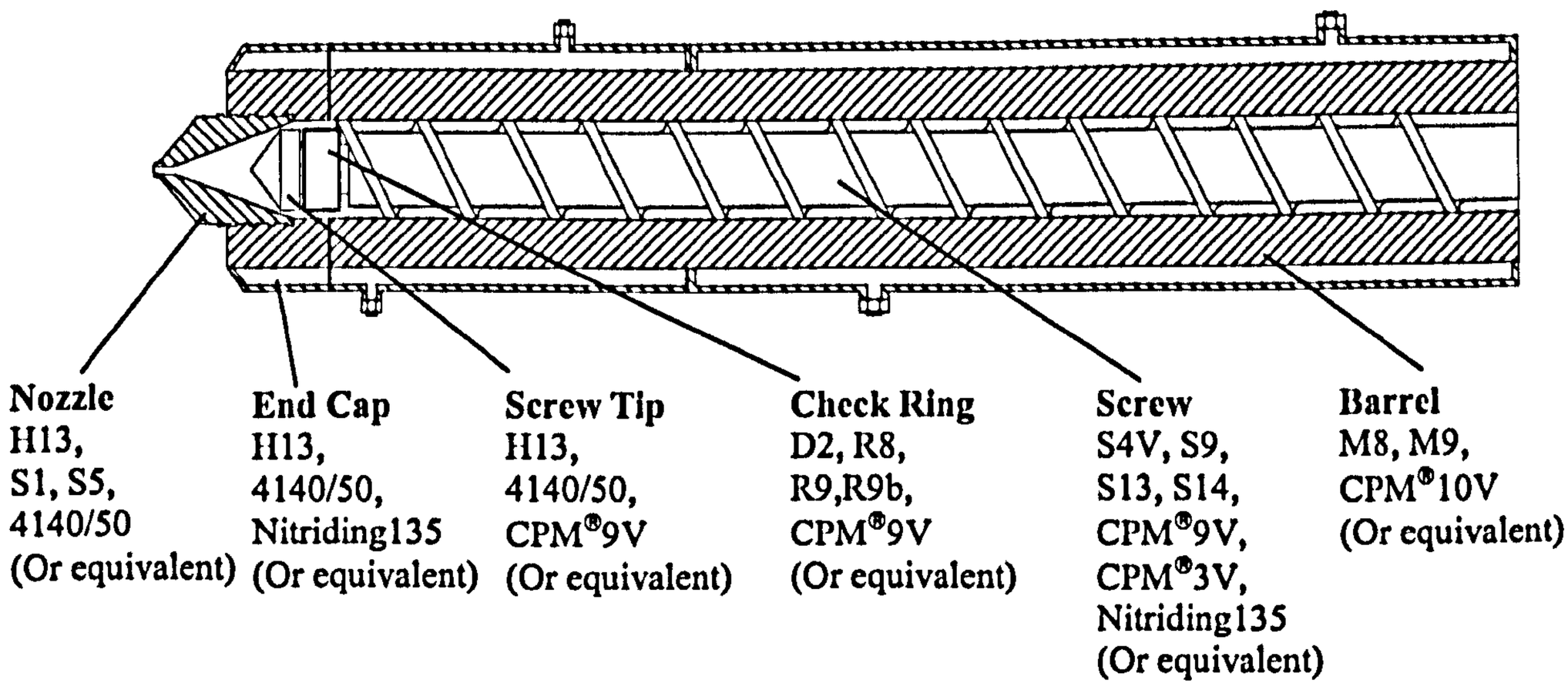

Figure 4.6 Recommended steel for thermoset barrel system showing AISI grades and CPM® grades[64]

4.4 The manifold system

In order to bring the two plasticised thermosets together and layer them as a sandwich moulding, a new manifold was designed internally at the International Automotive Research Centre, Warwick Manufacturing Group, University of Warwick, and is shown in Figure 4.7.

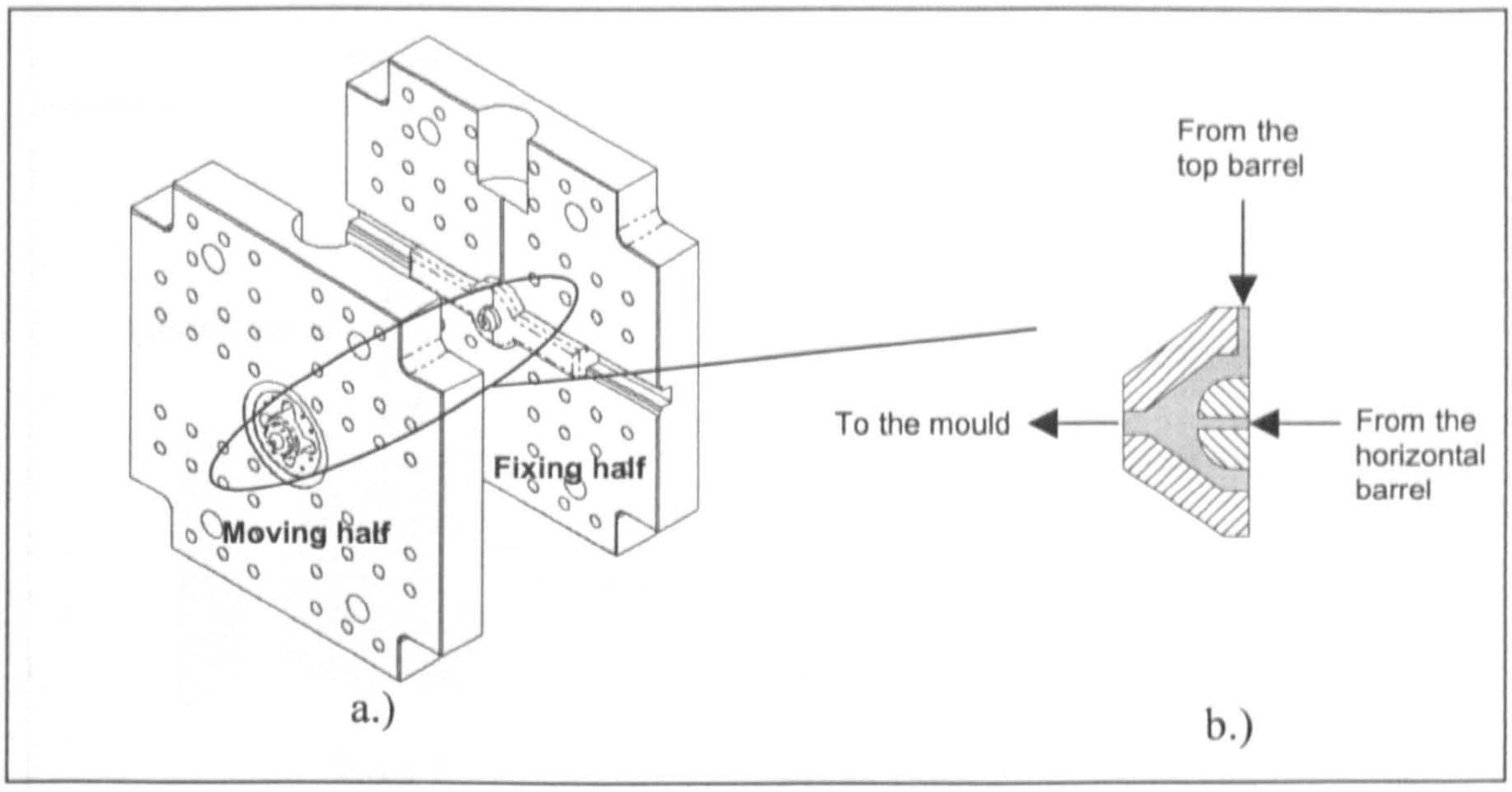

Figure 4.7 a.)The manifold for thermoset co-injection moulding machine. (The halves are placed between the injection unit and the heated mould.) and b.) The cross-section of the manifold nozzle

The system was installed between the machine injection unit and the mould. It consists of two halves, one is fixed to the machine and the other moves on the support of four tie bars. When the manifold is closed the system consists of two runners that bring two different materials from different directions (vertical and horizontal) to a central gate. This gate will lead the materials into the mould to form sandwich layers dependent on how the injection moulding machine has been set. Table 4.1 shows how the manifold system works when the machine is operating. More details of the manifold design will be described in Chapter 7.

Table 4.1 Operating sequence of thermoset co-injection moulding

Steps	Details
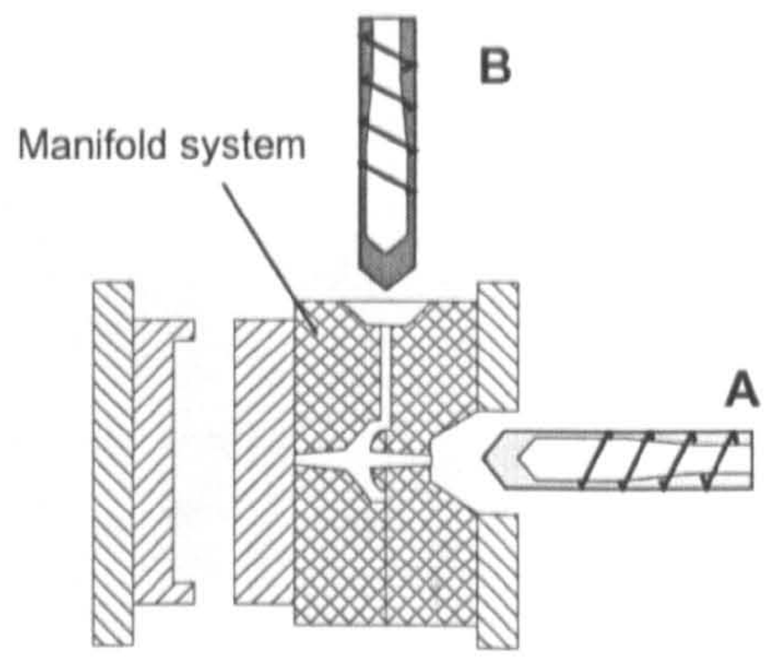 Step 1	To start the injection cycle, the manifold is hydraulically closed. Barrel A (core) and barrel B (skin) are charged with some molten thermoset plastics that is adequate to fully fill the mould.
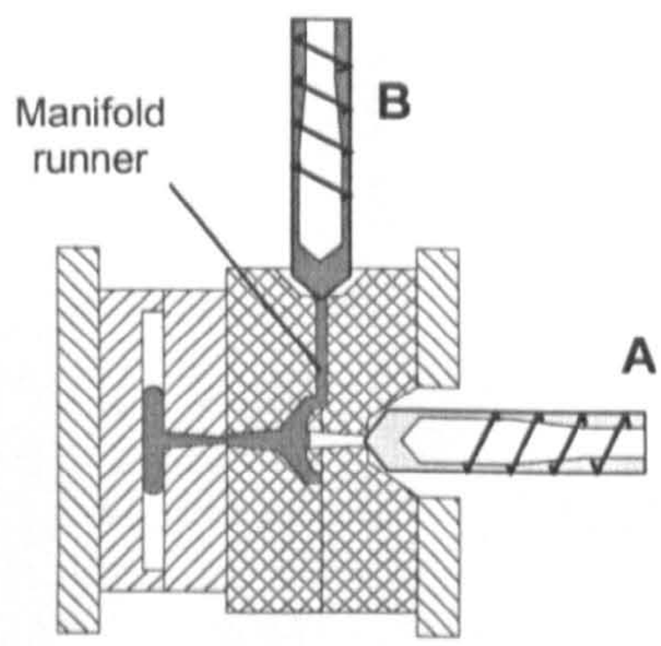 Step2	The mould is closed and clamp locked. Main injection units A and B move forward to face the manifold. Then some skin material is injected from the B barrel into the mould through the manifold runner.
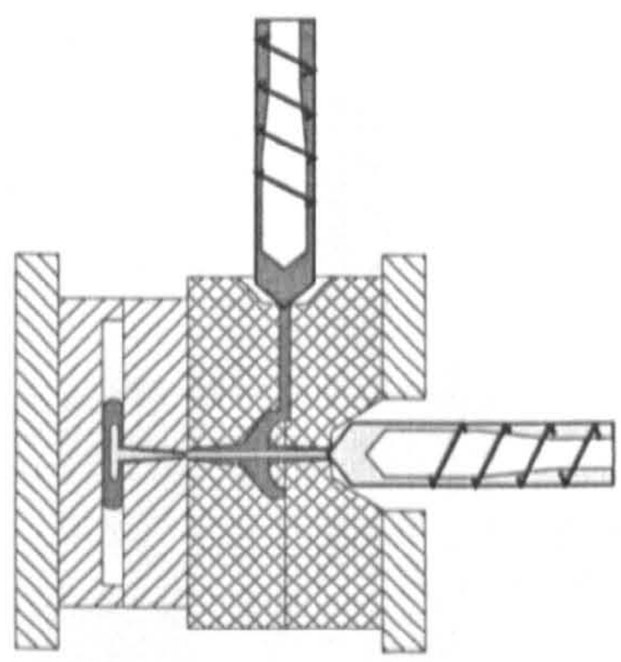 Step 3	After a small delay time, screw A, which is inside the injection unit A moves forward to inject some core material into the mould cavity.

Table 4.1 Operating sequence of thermoset co-injection moulding (continue)

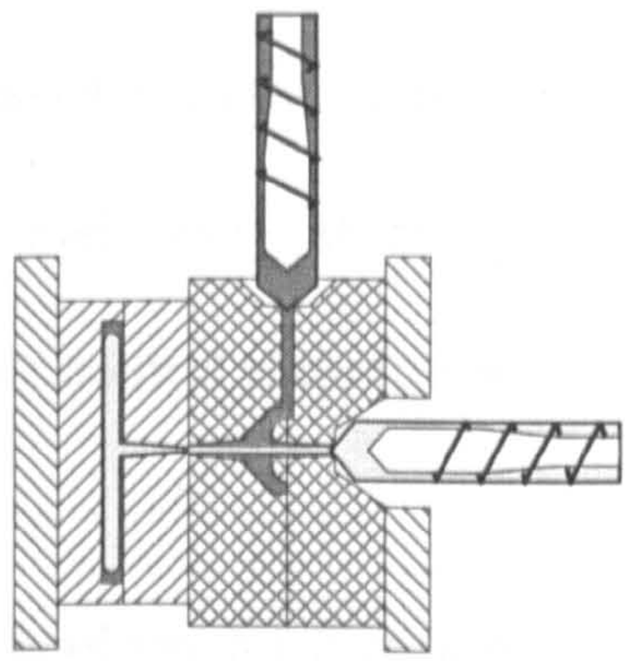 Step 4	The two injection units continue delivering the materials into the mould until the mould is filled by the pre-set amount. Injection of A then stops, while B keeps pushing material in by pressure during the holding phase. The curing cycle starts after this.
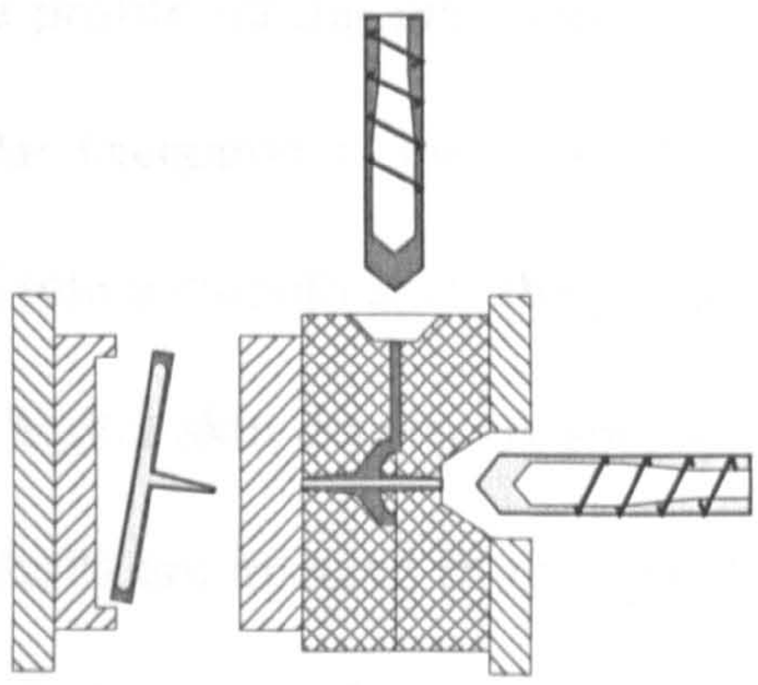 Step 5	Injection unit A and B are recharged with fresh materials and are retracted from the manifold during the curing cycle. After the curing time is reached, the mould is opened to release the component. The manifold is still closed.
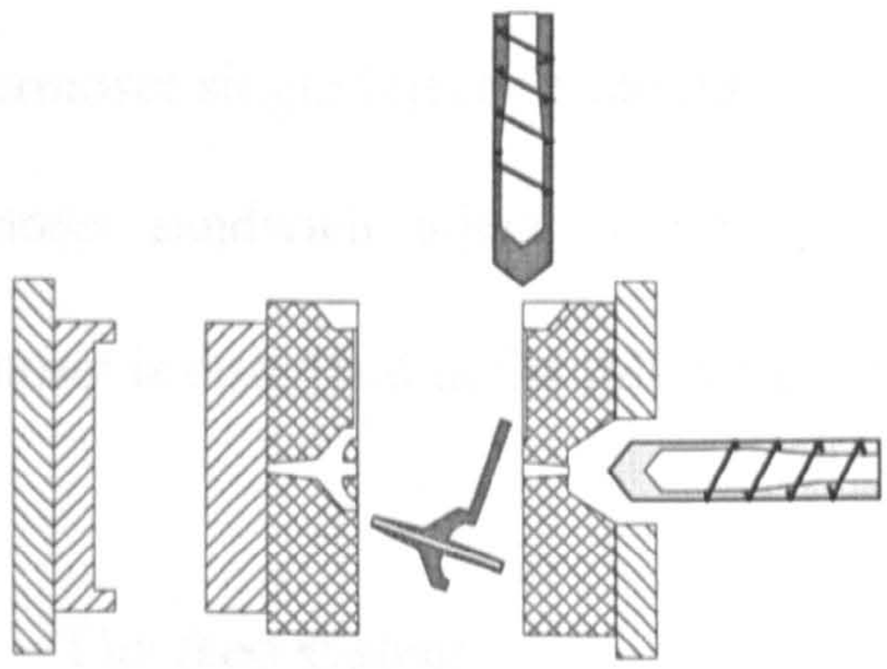 Step 6	The injection moulding repeats from step 1 to step 5 while the material in the manifold is controlled in a liquid state. At the end of the work, the manifold temperature is brought up to the melt's curing temperature. The component inside the manifold is cured and taken off by hand.

4.5 Thermoset Moulds[40,65]

Mould technology for thermosets is similar to thermoplastics. It still consists of the basic three parts; feed system, mould cavity and ejection system. However, the fact that thermoset materials need heat to activate the cross-linking reaction in order to shape the melt while thermoplastics need a lower temperature, leads to different temperature control techniques in the mould cavity.

Mould technology for thermoplastic sandwich injection moulding is the same as for conventional tooling, even though an extra material is injected in. The cavity pressure profile during injection is changed but the maximum pressure remains the same. An exception is the case of foam injection moulding when a foam core is injected into a smooth skin, the pressure may be increased due to the core expansion and the higher skin density. A special design of nozzle and channels are necessary if plastic melts are injected from separated nozzles, in order to layer the two materials from their barrels before they flow through the mould sprue. Generally, a single injection mould can be used for co-injection.

A thermoset single injection mould, therefore, was considered suitable for the novel thermoset sandwich injection moulding system. Fundamental mould design for thermoset is described in the following sections.

4.5.1 The feed system

The feed system generally comprises of sprue, runner and gate as shown in Figure 4.8. Especially wear-resistant steels or chrome plating and hard coated surfaces should be used to make the feed system for thermosetting injection moulding as the

materials are normally glass-fibre filled. The sprue is the first part that plastic flows through after the mould is closed and is where the machine nozzle applies some force in order to seal the mould off. This procedure puts a very high pressure onto the sprue surface so it is practical to use a sprue bush, which can be replaced when it is worn out.

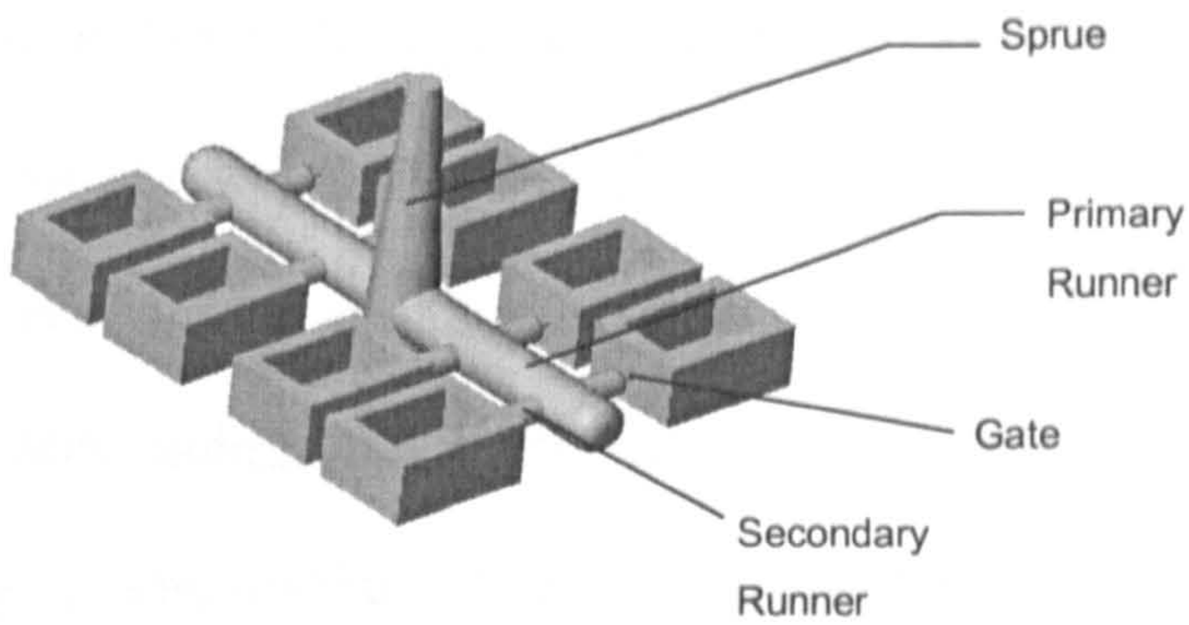

Figure 4.8 The feed system

The contact surface between sprue and nozzle is also important as it is used to seal the connection between them. Plane surfaces are rarely used, as they require higher pressure to seal than more general curved or spherical contacts. The two types of sprue are shown in Figure 4.9 and 4.10.

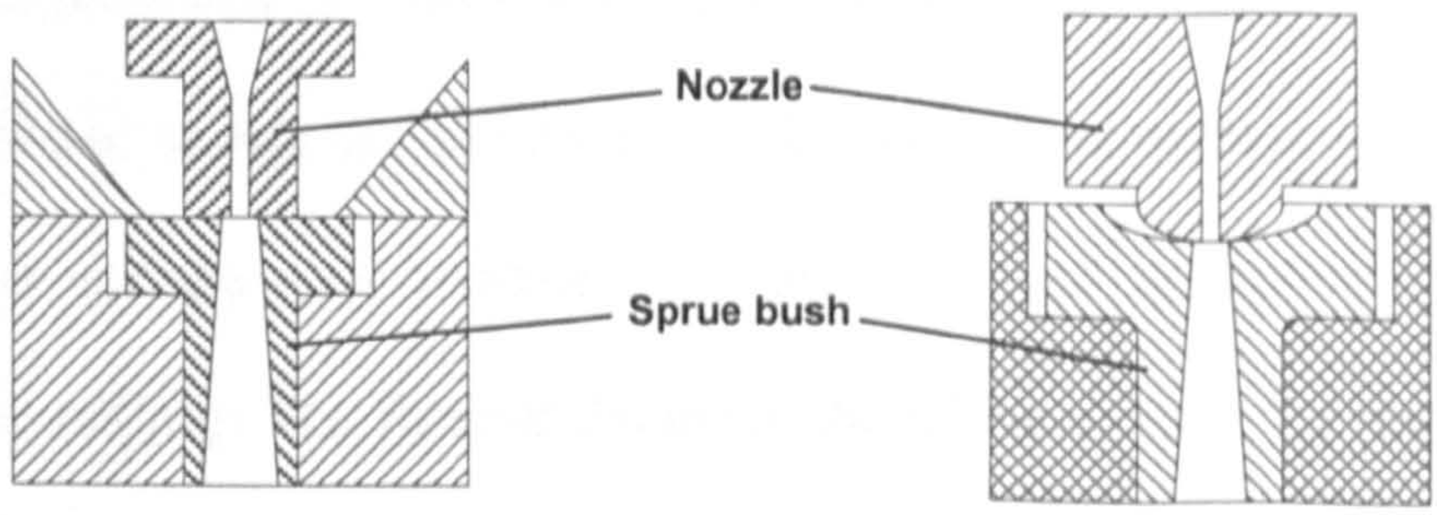

Figure 4.9 Plane surface sprue

Figure 4.10 Curved contact surface sprue

To get good sealing, spherical radius and orifice diameter of the sprue should be larger than those of the nozzle by at least 1 mm.

The dimension of the sprue is dependent on the dimension of the component and its cross-section thickness. The sprue must not freeze before any cross sections so that sufficient melt can flow into the mould and enough holding pressure can be applied. Normally the sprue has to be tapered around 1-2° to demould easily. Any sharp corners should be avoided to facilitate flowing. Furthermore, surface finish inside must be perfect to avoid the moulding attaching to the mould fixed half, which leads to difficulty in demoulding. In a multi-cavity mould, the sprue connects to a runner and demoulding is more difficult. A sprue puller installed in the moving half is used to help pull out the moulding and the sprue from the fixing half. More design details can be found in the many references available[23,65-68].

The runner is a connection part from the sprue. It leads the material into the mould cavity or distributes the material to fill all cavities in a multi-cavity mould. Similar to the sprue, it should be large enough not to freeze the material before it can fill all cavities, but at the same time should not be too large as to waste the material. The runner geometry can be many shapes, however it should have a small surface per volume ratio as shown in Figure 4.11 a.). Unfavourable runners as in Figure 4.11 b.) have larger surface over volume ratio and can lead to material freezing during injection moulding. The Runner diameter should be at least 1.5 mm more than the thickest cross-section of the moulding. Size of the runner is also determined from the material flow properties. The lower the viscosity of the material is, the longer and the

thinner runner that is permitted. A larger diameter runner promotes flowing of the material if a more viscous melt is injected.

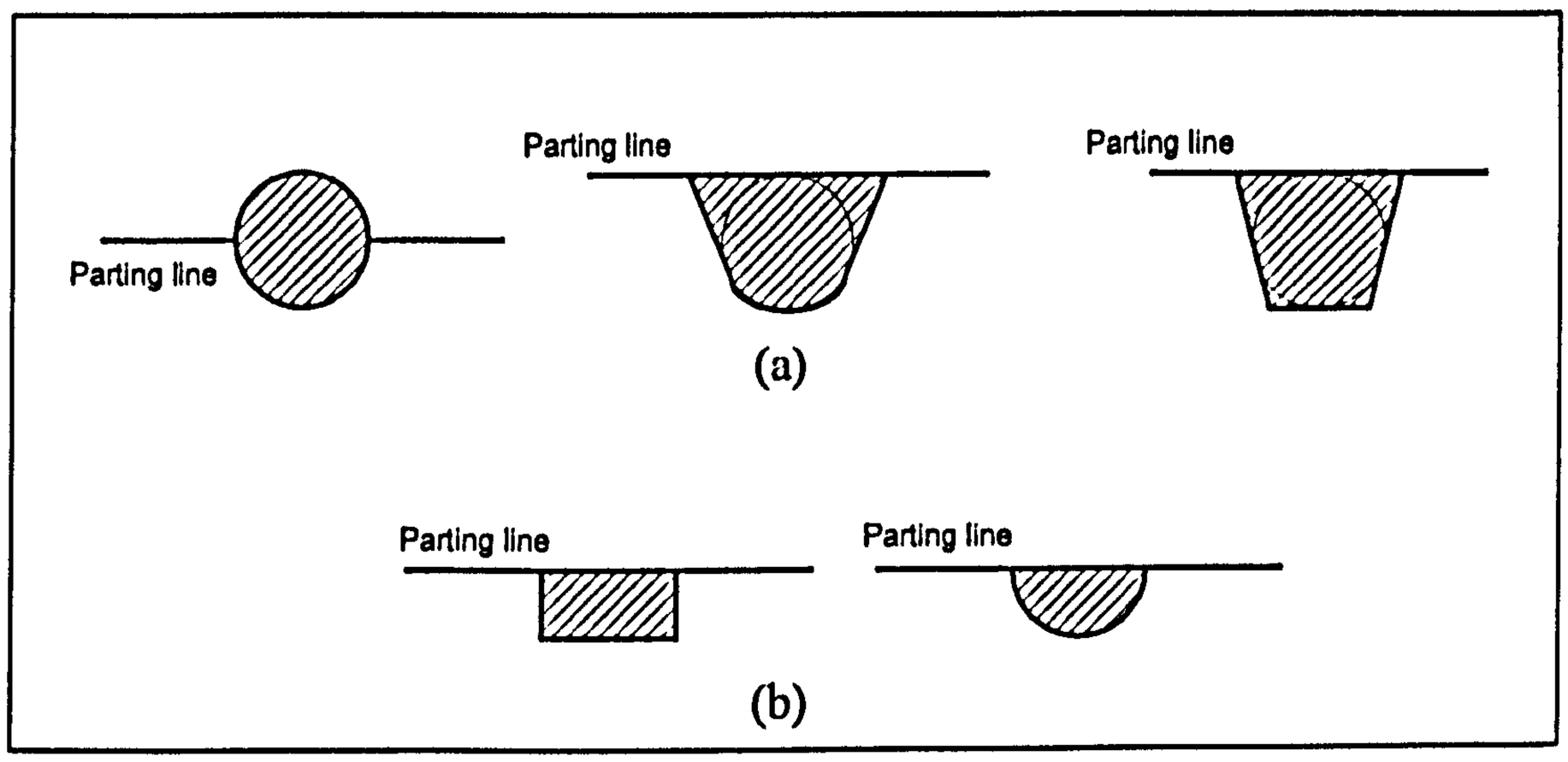

Figure 4.11 Cross sections for runners[65]

a.) Favourable Runners b.) Unfavourable Runners

The gate connects the cavity with the runner. It is usually the thinnest point of the mould. Different types of gate design are shown in Figure 4.12. Gate design for thermosetting materials follows the thermoplastic standard (the dimensions can be seen in 'How to make injection molds'[65]). However because the thermoset materials are normally filled with glass fibre, the gate thickness should be larger. Practically, with thermosetting materials having fine fillers, 0.25-0.50 mm is the minimum gate thickness than can be used. With coarse fillers, 0.75-1.0 mm is the minimum[40]. Too small a gate thickness causes excess heat production and then pre-curing problems.

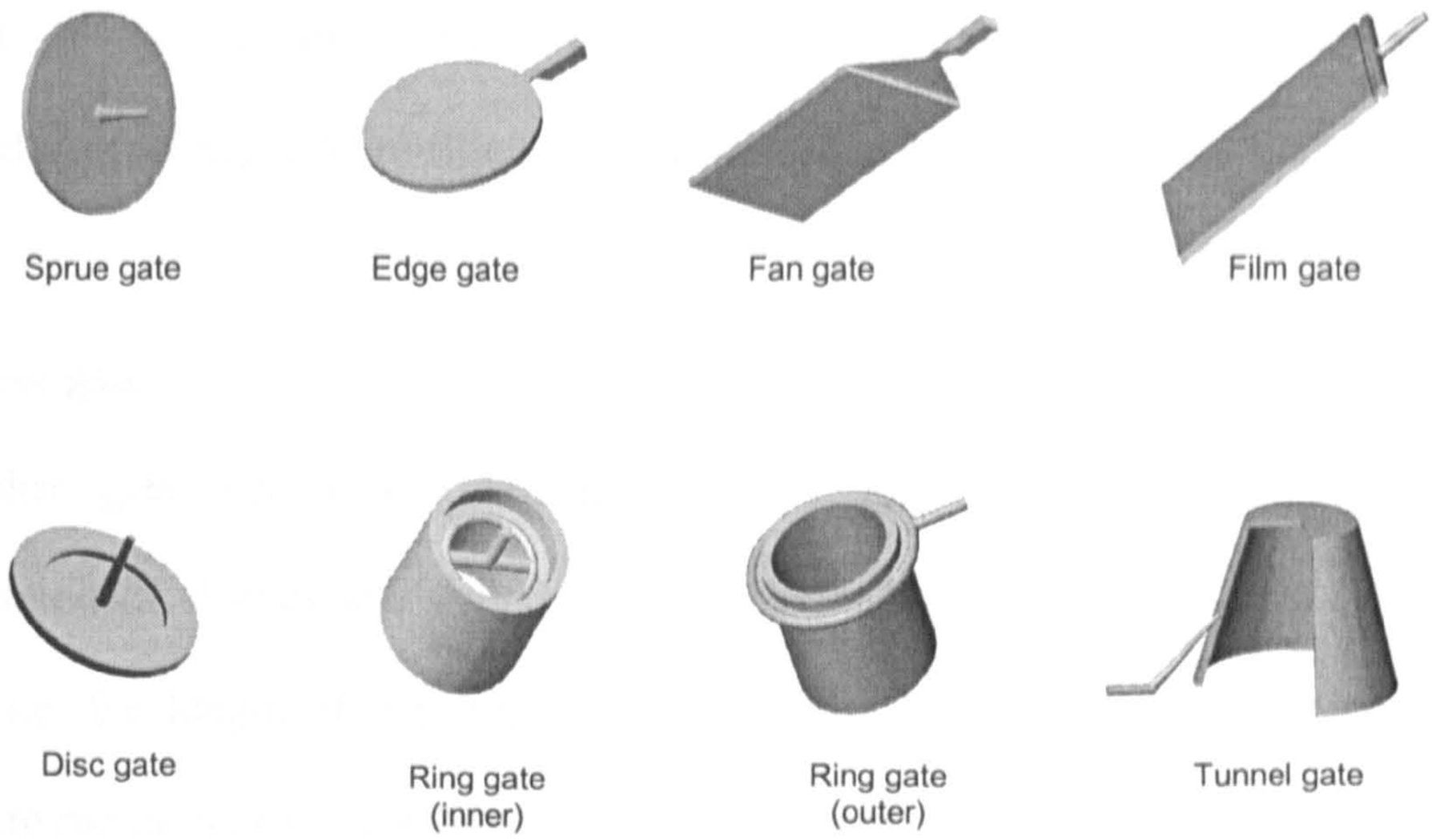

Figure 4.12 Different types of gate in used in injection moulding

- Sprue gate

The sprue gate is the oldest and simplest gate. It is normally used with high viscosity materials and positioned at the thickest section. It allows high holding pressure resulting in high quality and exact dimensioning. However, it needs a post-operation to remove the gate and leaves a visible gate mark on the component.

- Edge gate and fan gate

For multi-cavity moulds, the edge gate is often applied. The molten material is injected from the side of the mouldings. It is necessary to balance the runners so that all cavities are completely filled in the same time. Distortion may occur in each cavity due to the difference in mould pressure distribution. Applying a fan gate can reduce this problem since it gives parallel orientation of the material across the whole width and produces uniform shrinkage both in direction of flow and transverse. However, a longer gate mark will appear at one side of the component.

- Film gate

A film gate is normally used for a large flat area moulding similar to the fan gate. It is used particularly in fibre-filled material to reduce distortion.

- Disc gate

The disc gate, which is sometimes called a diaphragm gate, is used for the production of sleeves and cylindrical mouldings, which do not have a very long core, i.e. the length of the core over diameter is less than 5 ($L_{core}/D_{core} < 5$). A uniform moulding can be achieved without any strength loss and weld lines. A post-operation is needed to remove the gate.

- Ring gate

For cylindrical mouldings with a longer core, the ring gate is more suitable and helps to reduce distortion of the component. The ring gate can be used as both internal and external gate. The latter allows the use of multi-cavity moulding. Both of them produce two weld lines and need a post-operation for gate removal.

- Tunnel gate

A tunnel gate is the only gate that can be removed automatically at the time the part is ejected from the mould. It is used primarily for small parts in a multi-cavity mould and elastic material. Because of high-pressure losses, this gate is suitable for simple parts only.

4.5.2 Mould temperature control[40,68]

It is necessary for thermoset injection moulding that the moulds are temperature controlled and heated up to a moulding temperature before starting the process. The heat sources of the mould can be water, oil or electrically heating. The first two methods give more uniform mould temperature within ±3°C while the latter can vary as much as ±6°C. A more uniform temperature mould will fill easier and produces parts with less warpage and more dimensional stability.

A mould that is heated with steam or oil will have a more uniform mould temperature because the heat sources are maintained at a constant temperature. The electrically heated mould popularly uses cartridge heaters, with the heaters cycling on and off. When they are on, a great deal of heat is generated and must be distributed throughout the mould in a way that produces a uniform mould temperature. The amount of 1.25 kW for every 45 kg of mould steel or 0.25 to 0.5 Wcm^{-3} excluding ejector housing allows the mould to be heated to the moulding temperature within 1 to 2 hours. [40]

Thermocouples are necessary to monitor the mould temperature in electrical closed-loop controlled heating. A minimum of one thermocouple is required in each mould half. More should be installed for more accurate control of a larger mould.

Location of the thermocouples is also important. They should be located not too close to the cartridge heaters and cause the heaters to turn off before the mould reaches the setting temperature. Also, they should not be too far from the heater or too close to the mould surface, as the thermocouples will read the external

temperature resulting in an overheated mould. Practically, a distance of 32 to 38 mm from the cartridge heater and 38 to 51 mm inside the mould are suitable.

4.5.3 Ejection

After the moulding is cured, the mould then opens and the part has to be taken off before starting the next cycle. It will be difficult to get the component out of the hot mould if there is no ejector installed on it. The ejection system is usually actuated mechanically by the opening stroke of the moulding machine. Ejector pins will be pushed forward by an ejector bar and ejector plate, which are installed at the back of the moving half. Then the component is released from the mould. Number and positions of the ejector pins depend on the mould configuration as well as on the moulding material, as ejection can leave an objectionable mark or distort the part.[65] Some thermoset mouldings can be soft and flexible when the mould opens and easy to bend and break.

Some good ejector positions are shown in Figure 4.13. It was suggested the ejector pins should be located on the deepest points of ribs and bosses to prevent problems[68]. Another method that is also possible is to design the mould with an incline angle to facilitate moving (Figure 4.14). Size of the pins is dependent on the moulding. However, it is advised not to use pins smaller than 2.4 mm diameter and the holes for the ejector pins should be 0.025 mm larger than the pin for a depth of 13 to 16 mm to prevent material flowing down around the pin and then jamming.[68]

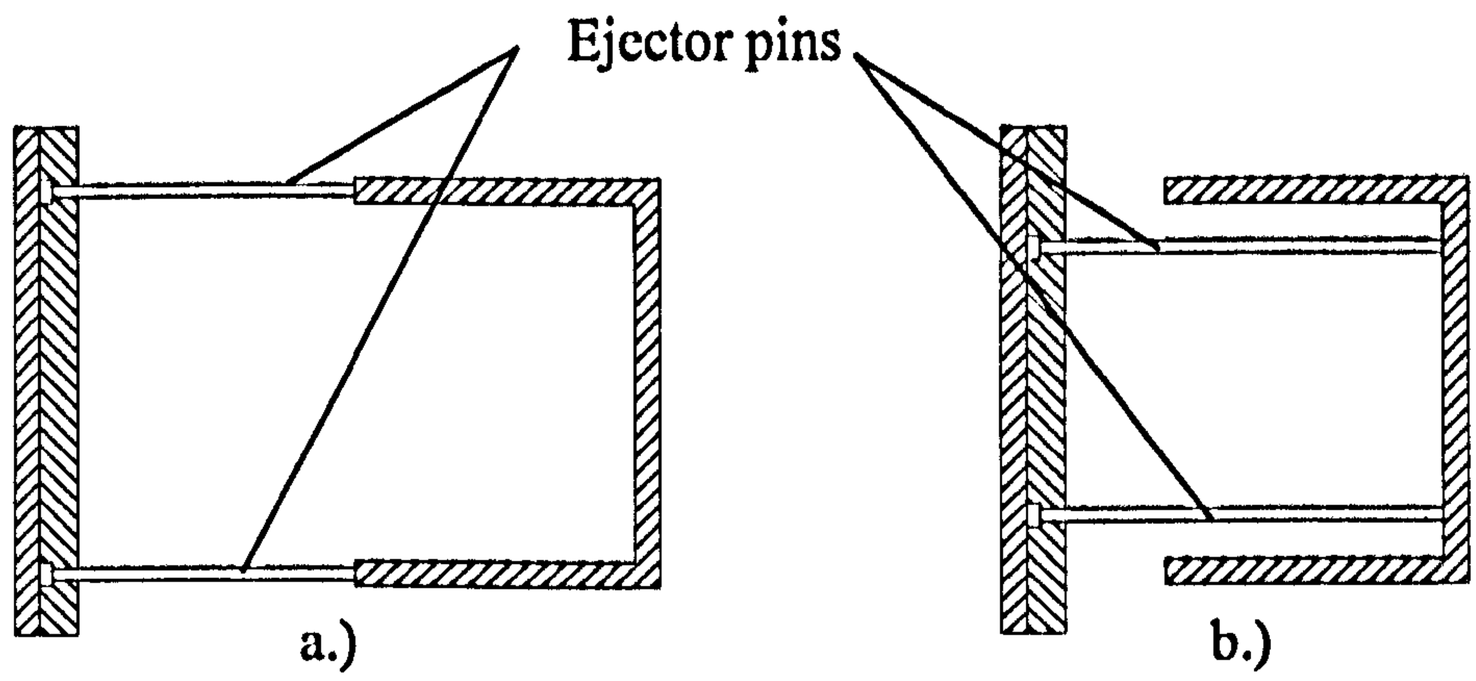

Figure 4.13 Ejector pin positions: a.) Good position and b.) Bad position[68]

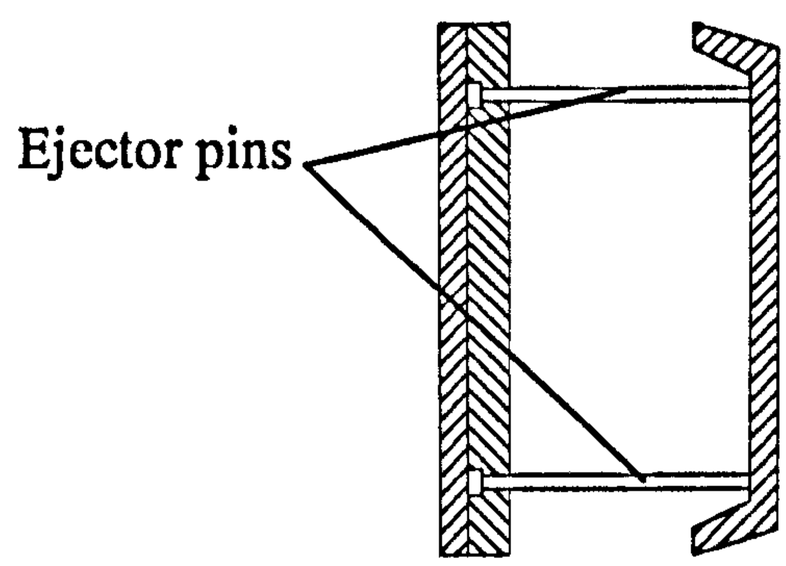

Figure 4.14 Acceptable ejector position with inclined angles to facilitate demoulding[47]

Another advantage of having ejector pins is venting. During injection, material is flowing into the mould and fills the cavity. Ideally, having air evacuation prior to injection should be the best aid to mould filling. However, the system is complicated and needs high maintenance. To get good filling, the mould has to have some holes where the air can escape from the mould. These can be placed at the parting line or at the back of the ejector pins.

4.6 Related works in thermoset injection moulding

Currently, there is no literature on the thermoset sandwich injection moulding except by the author[35]. However, the prior knowledge of the single injection moulding of thermoset is beneficial to the processing and improvement of the novel thermoset co-injection moulding system.

Karabut et al[69] studied the uniformity of the thermoset injection moulding process by looking at the effect of mould temperature on the size and the strength of moulding components. Phenolic powder was injected into a mould, which contained three different cavities, a bar, a dumb-bell shaped moulding and a disc. The mould temperature was varied at 150, 170 and 190°C while the other machine settings were constant. At each mould temperature, more than 10 samples were produced and measured for weight and dimensions. The results showed that at each mould temperature, there was a tendency for weight loss of the moulding from cycle to cycle due to heat formation in the barrel, which caused thermal expansion of the material. Because the mould was volumetrically filled, this resulted in moulding weight reduction. However, the density was found to remain unchanged since the material was compacted by the injection pressure during mould filling. The shrinkage of the mouldings increased with an increase in mould temperature. This was due to higher rates of mould filling and hardening of the material, with more degree of volatiles elimination and more complete curing of the material. A greater shrinkage was seen in the direction of moulding and followed the glass fibre flow as the same way as thermoplastics.

The effects of processing conditions on moulding quality; (a) visual appearance in terms of flow lines and surface finish, (b) moulding thickness and distortion, (c) heat distortion temperature and degree of cure, (d) flexural modulus and flexural strength and (e) weight of mouldings were studied and reported by Whisson and Paul[70]. Processing parameters, which were screw speed, back pressure, injection speed and injection pressure were varied and additional experiments were also performed at different levels of injection temperature, mould temperature and cure time. Plaque shaped Phenolics and Urea Formaldehyde components were observed. The results showed that optimum machine setting existed to produce mouldings of high gloss, minimum flow marks, minimum warpage, heat distortion point and maximum mechanical properties, although these were not necessarily identical for each property. However, most properties were approaching their optimum for machine settings that resulted in the minimum melt viscosity. The machine conditions for good gloss were those that produced a maximum flow rate, which was limited by the curing condition in the mould.

Mould temperature had been considered as one of the important factors that affected the cure of cross-linking materials. Temperature field and heat balance moulds for thermoset and rubber injection mouldings were investigated by Čatić et al[71]. They suggested that the heat required for the processing of these cross-linking materials was provided by heaters, exothermal reaction, friction and heat applied to the material in the heating chamber. There was also some heat loss to the environment during processing. The cyclic temperature change on the mould surface during injection is shown in Figure 4.15. This showed that the mould could not stay at a constant temperature due to the effect of melt temperature. It was also suggested that

the time to reach the minimum temperature at the cavity surface (t_k), which was influenced by the melt temperature would have to be carefully monitored.

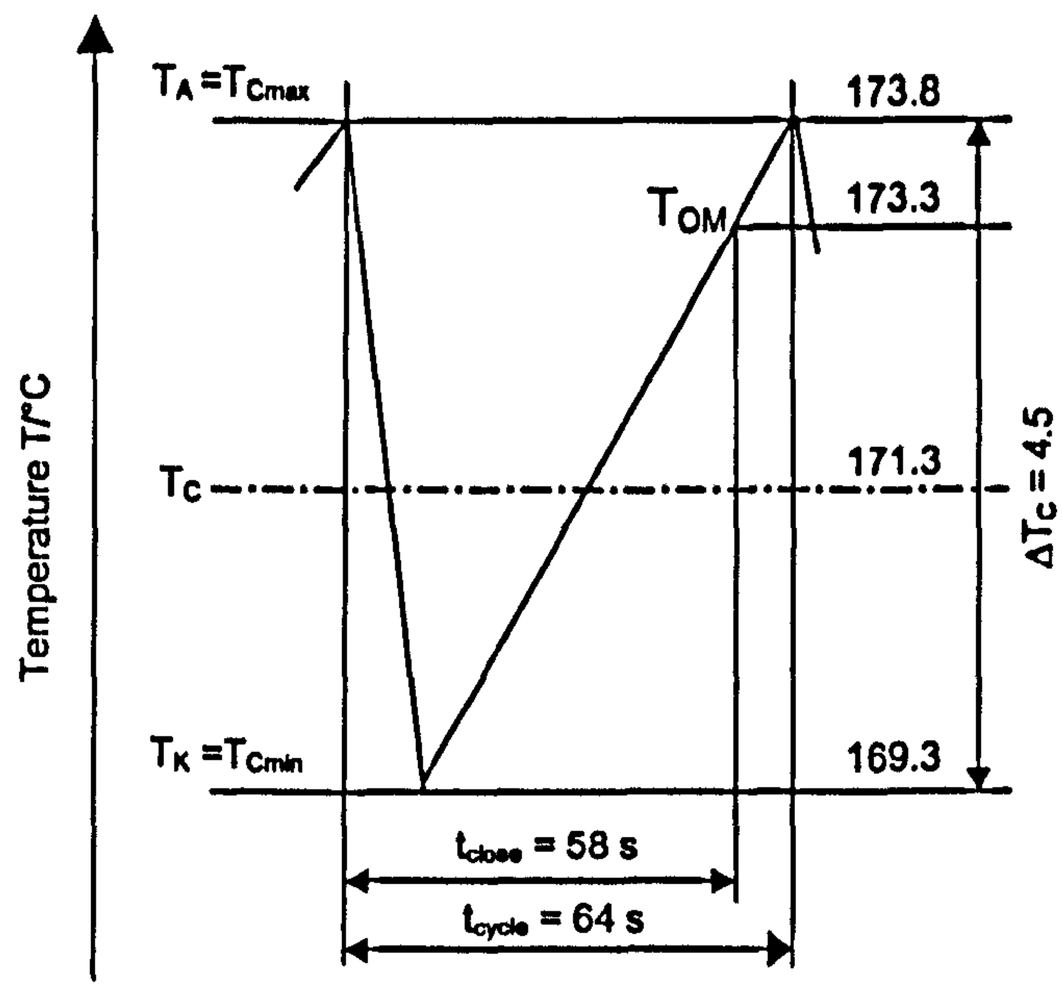

Figure 4.15 Cyclic temperature change on the mould surface during injection moulding of a thermoset when T_A = mould setting temperature, T_{OM} = temperature at the beginning of opening the mould, T_C = mean temperature of the mould surface, T_K = contact temperature. t_{close} = mould closing time and t_{cycle} = injection cycle time

Hadi et al[72] studied the effect of injection temperature on thermoset curing in order to reduce the curing times of thermosets. A 34-mm diameter and 7-mm thick disc mould with thermoset resin was first heated by immersing the mould in heated oil at a temperature varied from 22 to 110°C. These temperatures were called injection temperatures. Secondly, the pre-heated mould with resin was soaked in a second oil bath, which had a higher temperature of 146°C. This temperature was called the mould temperature. The material temperatures were recorded at the mid plane of the moulding and used to calculate the state of cure. Curing time at each injection temperature was examined from the time when the material reached the maximum state of cure. Effects of the injection temperature on the curing time were discussed. It was found that the curing cycle time was reduced when increasing the

temperature of injection, but that too high an injection temperature may have caused pre-curing in the system.

The curing times obtained from this experimental work may not be applicable to the injection moulding of the same material at the same injection temperatures even though it was claimed that this simulation of the injection process was an easy way to represent the real process. The material and the mould required some time to reach the injection and mould temperature when they were immersed into the hot oil bath. This is different from the real process in that the injection unit and the mould are already maintained at constant temperatures. The curing rate of the material in the real process will be very fast as it is injected into the hot mould, while in these experiments, the cross-linking started since the mould was immersed in the oil but the curing rate was gradually developed as a result of heat transferring from the oil through the mould and to the material. The actual curing time of this material can be higher or lower than the reported results. However, the effect of too high injection temperature on the material pre-curing should be considered. To prevent the pre-curing in the system, temperature of the tool before the material enters the mould, i.e. manifold temperature, should be controlled at temperature levels that only maintain the flow of materials.

The studies of thermoset recently focused on mathematical models of the material properties and cure behaviour, which is beyond the interest of this thesis. The details of the research can be found in many references.[48-50,73]

4.7 Conclusions

This chapter introduced the novel thermoset co-injection moulding machine and the prototype manifold system. The process description was also explained in detail.

General machine and mould design for thermosets, which had been used as a guide for designing the manifold system, were described. It was shown that there were some differences between thermoplastic and thermoset systems. Temperature control was the main reason as heat could affect the thermoset flowing and curing. The system needed a more effective way to control the temperature in the system than thermoplastics.

A single injection mould with a temperature control unit could be used with the thermoset co-injection moulding machine. The thermoset moulds followed the general design rules of making plastic injection moulds. However, when using the mould with fibre-filled thermosets, a larger gate and runner was required.

The literature on thermoset injection moulding was mainly focussed on the effects of machine parameters and mould temperature on component quality. Naturally, they concentrated on the parameters that controlled the material flow and cure in the mould. The material temperature and machine parameters will also be considered in this research in order to set the process window for the new thermoset co-injection moulding and develop the manifold system prototype.

During the injection moulding cycle, the mould temperature was reduced as a result of a lower temperature material being injected into the mould. The mould

temperature varies depending on the gate position, i.e. the low temperature region is near to the gate since it is the first place where the material enters the hot mould. Therefore, curing of the material there is slower than the position further in the mould. When co-injection moulding of two thermoset materials, the time of injection of the second material (core) into the first material (skin) should be considered since the skin may not have enough time to form an adequate layer.

Chapter 5

Material Experiments

5.1 Introduction

Prior to the test runs on the co-injection moulding machine, it was necessary to understand the materials' properties especially their flow and cure. The experiments on the thermoset co-injection moulding were therefore divided into two categories, material experiments and injection moulding experiments. In this chapter, the experiments on materials are described.

The materials used in this research were a general grade bulk moulding compound, BMC G7B 5580 from BIP Ltd and black thermoset polyester chips, Interpon PM-300011-F from Akzo Nobel. The BMC was a grey, putty-like, glass filled unsaturated polyester with a density of 1730 $Mg.m^{-3}$. This material is normally injection or compression moulded to produce engineering and electrical components. It was proposed to use this material as the core of the sandwich mouldings. Table 5.1 shows the composition of the material.

Table 5.1 Composition of BMC G7B 5580

Components	%weight	%volume
Glass-fibre (6 mm length)	15	12
Mineral filler (including mould release agent)	57	44
Resin and thermoplastic additive	28	44

Interpon is a dry unsaturated polyester consisting of a carbon black pigment and some other additives. Since the formulation is confidential, the composition of this material cannot be presented here. The same material in powder form is used as an in-mould paint to coat BMC in the compression moulding technology, as it provides more than 90% gloss when using with a finished chrome tool. The material density is 1250 $Mg.m^{-3}$. This material was used as a skin of the sandwich mouldings.

Interpon has been used with compression moulding but not with an injection moulding machine, so this material is new to the injection moulding process. It is therefore necessary to examine its properties in terms of the material gelation and flowability. These were determined by experiments on gel time, melt flow index and viscosity using a capillary rheometer. At the end of the tests, a processing window for Interpon could be established.

5.2 Gel test

Gel time of a cross-linking material is the time that the material changes its state from viscous liquid into gel. It is very important for all experiments and processes that involve this kind of material as it can show how fast the material reacts to the changing of temperature. For more accurate results, cone and plate or parallel plate rheometers are used for determining gel time of a thermoset material at a low shear rate. This method was tried at the National Metal and Materials technology centre, Thailand. However, there was a difficulty with premature curing of the materials during testing.

The method that was used in this research is more practical and is used in industry. Results from this test were less accurate than those from a cone and plate rheometer. However, they were considered to be sufficient enough for this project.

To prepare materials prior to the test, Interpon chips were crushed down to approximately 2-4 mm. This was the same size as the input material feed in the vertical barrel. BMC was injected through the horizontal nozzle before the test to reduce the fibre length down, so the material that was brought to the test would have similar conditions to the material that would enter the manifold during injection moulding. 5 grams of each material was weighed and put onto a hot plate. It was then levelled down to around 1 mm thickness.

Temperature of the plate was controlled and varied from 60-200°C. The gel time was measured from the time that material started to melt until it turned into gel, which was determined by a metal stick. Uncured material would show plastic behaviour and could be picked up without breakage. At the gel point, material temperature was measured by an infrared pyrometer, Impac Infratherm series 14. The results from this test would be used to determine the barrel and manifold temperatures. Figure 5.1 shows the gel time results of BMC and Interpon.

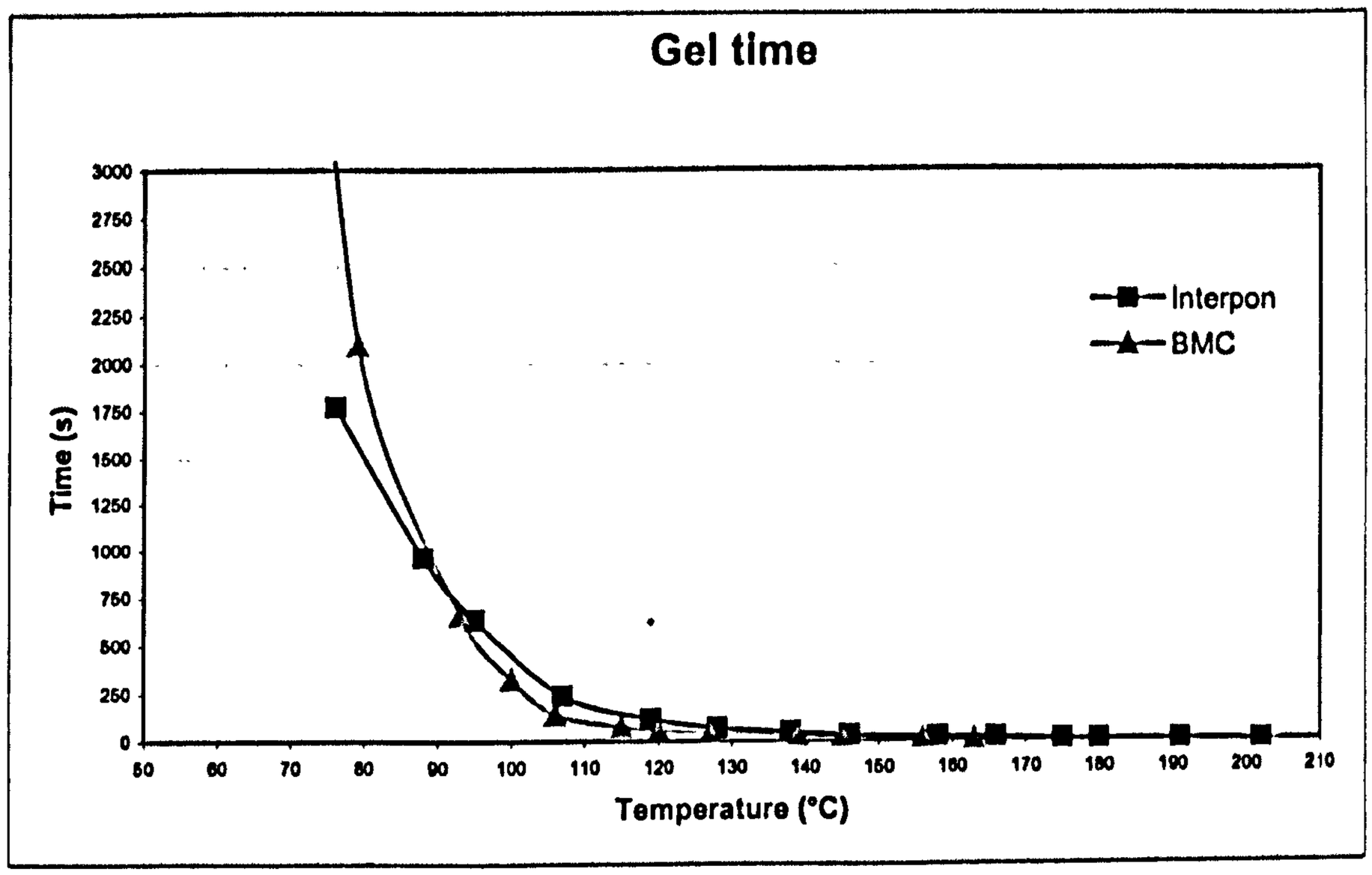

Figure 5.1 Gel time results of BMC and Interpon

Interpon started to melt at around 75°C. It can be seen that the gel time of Interpon decreased dramatically as the temperature increased. Similar results were obtained from BMC but at the faster decreasing rate.

At around 90°C, the gel time of both materials was around 800 seconds. This was considered to be sufficient for a test on a melt flow indexer and a capillary rheometer as the cycle time of both equipments; including charging material, pre-heating, testing and cleaning, was less than 12 minutes per test. The temperature of 90°C was then set to be the top limit for all experiments in order to prevent the material pre-curing in the equipment. The low limit of the temperature was set at 80°C, which was 5°C higher than the temperature that the material started to melt. This was to ensure that the material was not too viscous to flow through the die.

At a temperature higher than 90°C Interpon cured slower than BMC while the opposite occurred at the lower temperature. This can effect the sandwich formation of both materials when injecting them into the hot mould, which is normally at a temperature higher than 90°C. The Interpon skin needs more time to form a solid layer than the BMC core at that temperature. It is possible that the BMC core would breakthrough the skin and can be seen on the moulding surface.

5.3 Melt flow index test

A melt flow indexer is a simple machine used to determine the basic flow ability of a plastic material at a single low shear rate. The equipment shown in Figure 5.2 is a Ray-Ran 4MPCA melt flow indexer, which consisted of a computer controlled heated cylinder, 2.095 mm test die and a piston assembled with a load set. In normal operation, the tested plastic is loaded into the hot cylinder, which has been heated and controlled at the test temperature. The material in the cylinder is pre-heated for 420 seconds in order to balance the temperature of the melt. After that, the piston, which is installed with the load set on the top, moves down and presses the melt plastic through the die. Weight of the polymer melt in g/10 minutes is recorded.

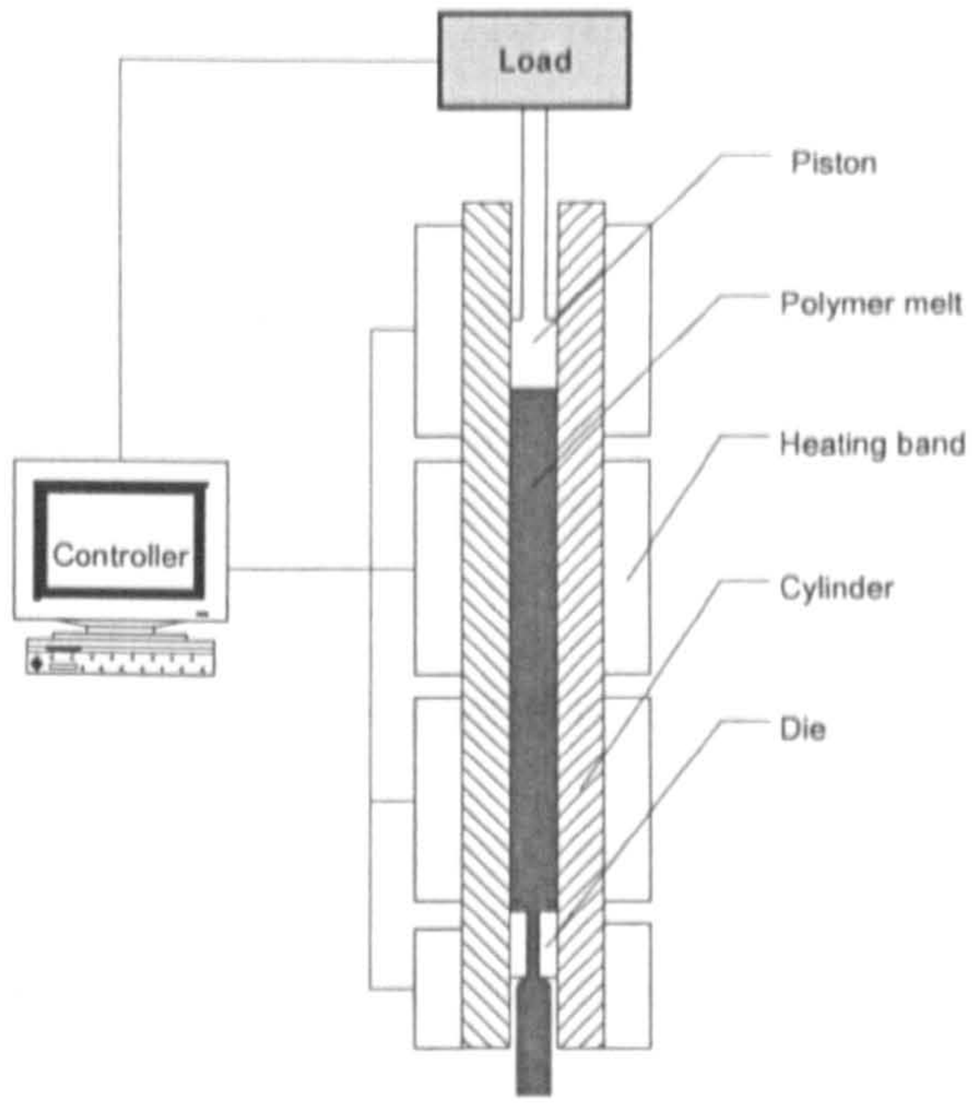

Figure 5.2 Melt flow indexer simplified diagram

The materials were prepared the same as they were in the gel time test. Interpon's melt flow indexes were determined from the melt flow indexer by setting three temperatures that were selected from the gel time test. At those temperatures, it had been found that the materials would be in a liquid state for what was considered a reasonable injection moulding processing time, which was assumed to be around 10 minutes for setting up the first injection cycle and less than 3 minutes for the following cycle.

By selecting a multi-slicing mode, the melt flow index value (MFI) was measured ten times at ten different points, giving an average MFI value and the standard deviation. Table 5.2 shows the effect of temperature on the material MFI value.

Table 5.2 Interpon melt flow indexes (g/10min) and standard deviation at three temperatures

Temp (°C)	MFI	STD
80	11.767	0.170
85	19.316	0.363
90	25.099	1.573

At higher temperature the materials tended to flow more easily as is shown by the higher MFI numbers, but the time they could stay in a liquid state was shorter as shown by an increase in the standard deviation value. This also means that the materials tended to cure more easily at the higher temperature. This is to be expected when considering the results from the gel test.

The standard deviation values showed how stable the Interpon was at each temperature. From the data shown in Table 5.2, the high standard deviation value of the melt flow indexes at 90°C is much higher than the rest. It shows that during the test, the melt flow index of the material in the cylinder varied more than those of the other temperatures as a result of cross-linking. This narrowed down the processing window from 80-90°C to 80-85°C.

The BMC that had been injected from the barrel was put into the cylinder and tested at 35°C. This temperature was the injection temperature that would be used in the injection moulding according to the material data sheet. The melt flow indexer was also set to multi-slicing mode in order to find the average MFI value of BMC.

During the test, the material could not flow through the die as the glass fibres blocked the die hole during the test. It was suggested that normally 4 to 6-mm

diameter dies are more suitable for the test of material that contained glass-fibres[74]. The melt flow indexer therefore could not be used to examine the MFI value of the BMC. In order to determine the flow ability of BMC and Interpon, it was decided to compare the viscosity data of BMC from the supplier to the viscosity of Interpon measured by a capillary rheometer.

5.4 Viscosity by capillary rheometer

A capillary rheometer is a tool for plastic rheology determination. Similar to the melt flow indexer, the concept is to push a plastic melt through a small diameter die (see Figure 5.3). Instead of measuring the material weight, the melt pressure differences between the die entrance and the exit are recorded. The result is the relationship between viscosity and shear rate as can be calculated by Equation 5.1-5.3.

$$\tau = \frac{r(\Delta P - P_0)}{2L} \tag{5.1}$$

$$\dot{\gamma} = \frac{4Q}{\pi r^3} \tag{5.2}$$

$$Q = \left(\frac{\pi}{4}\phi_b^2\right)v_b \tag{5.3}$$

r is die radius (mm),

L is die length (mm),

$\dot{\gamma}$ is shear rate (1/s),

Q is polymer melt flow rate (mm^3/s),

ϕ_b is cylinder diameter (mm) and

v_b is polymer melt velocity (mm/s).

The proportion of shear stress and shear rate is the polymer viscosity as described in chapter 3.

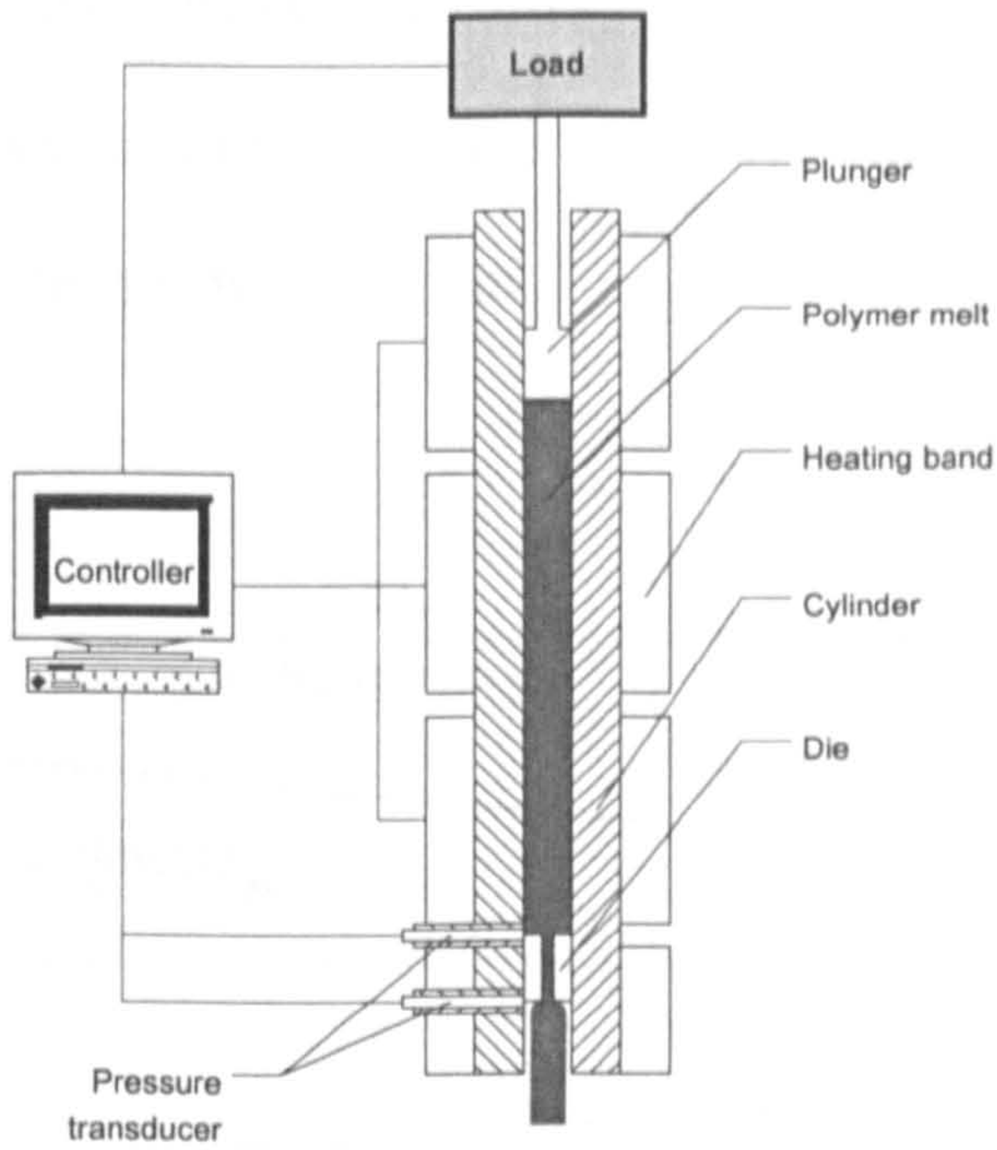

Figure 5.3 Capillary rheometer simplified diagram

The relationship of viscosity and shear rate of Interpon was determined by a Rosand Advanced Extrusion Capillary rheometer. This equipment can provide the polymer viscosity at a high shear rate (more than 10,000 1/s), which can occur during injection moulding. However, its 1mm-diameter die can be blocked when using a fibre-filled polymer like BMC. Therefore the relationship of viscosity and shear rate of BMC was acquired from the material supplier. The data were obtained by using a special designed in-line viscosity measurement developed by the National Physical Laboratory, UK[45,74].

The in-line viscosity measurement is an instrumented injection moulding machine nozzle fitted with a general injection moulding machine. It can be used as a normal

injection nozzle with a water temperature control unit connected to it in order to maintain the melt temperature in the nozzle. Two pressure transducers are inside the nozzle to measure the pressure differences between the two ends when the test material is injected from the injection barrel. These pressure differences will be used to calculate the material shear rate and viscosity. Figure 5.4 shows the nozzle geometry of the in-line measuring system.

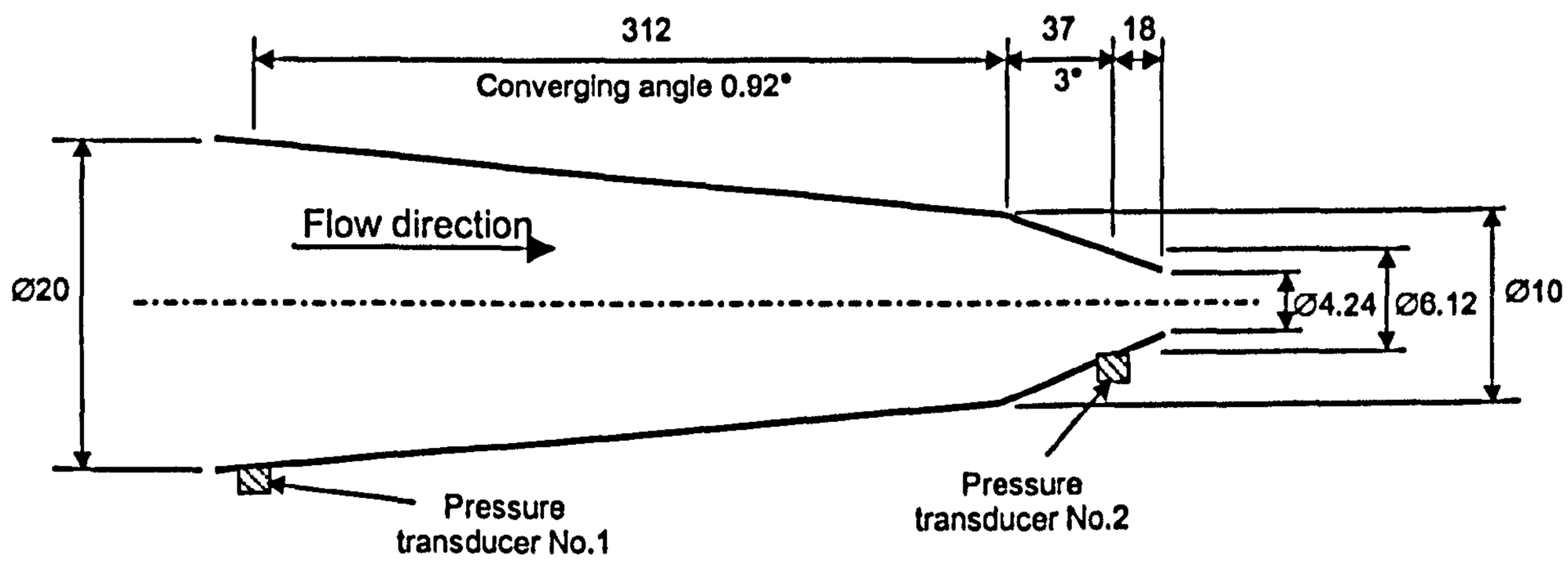

Figure 5.4 Diagram of the nozzle for the in-line measuring system[74].

It was claimed that there was reasonable agreement of shear viscosity value measured in-line on the moulding machine with value measured using the capillary rheometer[45]. In Figure 5.5, the viscosity of Interpon and BMC are compared in order to determine the difference in flow ability of both materials.

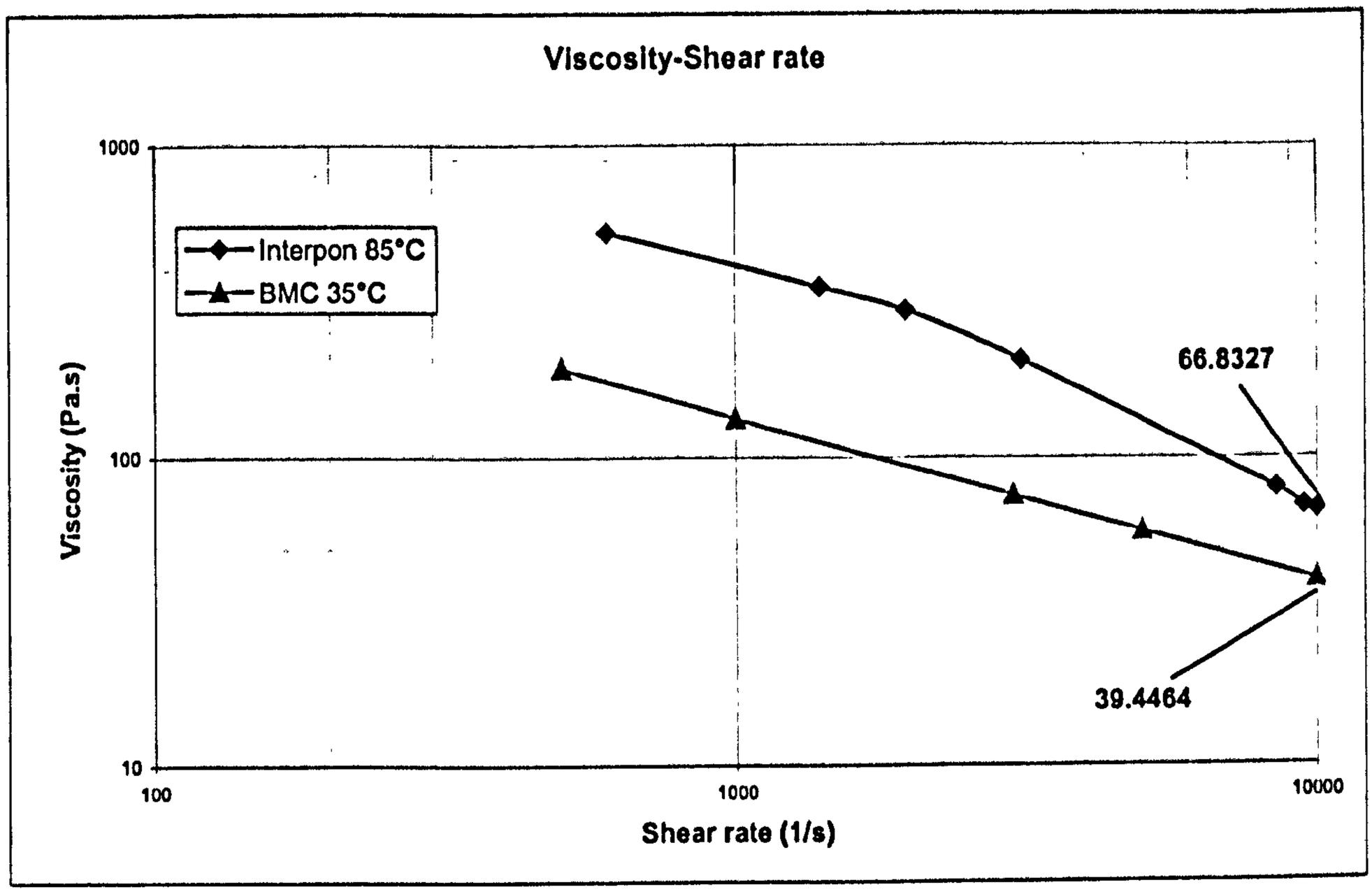

Figure 5.5 Relationship between viscosity and shear rate of BMC and Interpon

Figure 5.5 shows the comparison of BMC and Interpon viscosities at 35°C and 85°C respectively. 85°C was the maximum melt temperature of Interpon that was allowed in the injection moulding barrel while 35°C was the BMC's barrel temperature.

From Figure 5.4, the viscosity of BMC is lower than that of Interpon at any identical shear rate. Skin/core viscosity ratio is 1.69 at the shear rate of 10^4 s^{-1}, which is typical for injection moulding. If it is assumed that there is no curing reaction during injection cycle, this skin/core viscosity ratio can be compared to the results of thermoplastic sandwich injection moulding of the previous research. It was reported that at high skin/core ratio, the core material could penetrate to the skin easily and breakthrough was possible. For the thermoplastic case, this problem could be solved by starting injection of the core very late in the injection cycle or by doing sequential

injection moulding[2,16]. The material breakthrough is also possible when co-injecting Interpon and BMC due to the high viscosity ratio between both materials. The starting injection time of the BMC core into the Interpon skin should therefore be carefully considered. Sequential injection might be necessary in order to get a fully encapsulated sandwich moulding.

5.5 Conclusions

This chapter described the experiments on the materials that were carried out before the materials were used in the thermoset co-injection moulding machine. The experiments were designed to determine the materials' flow abilities and gel times, which could be used to optimise the initial temperature settings for the co-injection moulding machine.

The results from the gel time test and the melt flow indexer showed that the suitable temperature for processing Interpon was 80-85°C. In this temperature range, the materials could stay liquid at a low curing rate for a sufficient time to enable injection moulding.

The gel time test results of BMC and Interpon gave a cross over point at around 90°C. Beyond this point, Interpon cured slower than BMC. This could affect to the formation of the sandwich moulding when co-injecting both materials into the mould. The Interpon skin layer may have not cured enough when the BMC core was injected in so it is possible that the BMC core can breakthrough the skin and can be seen on the moulding surface.

Long fibres filled in BMC caused testing problems when the material was pressed through a small diameter die of the melt flow indexer. The fibres lock-jammed the die so it was unable to examine the viscosity of the BMC by the equipment. The viscosity data of BMC therefore were received from the material supplier.

In-line viscosity measurement is a special designed nozzle equipped with two pressure transducers. The nozzle attaches to a conventional injection moulding machine and measure the pressure differences of the material between the entrance and the exit of the nozzle when the material is injected from the barrel. This system was used to measure the viscosity of BMC that had been used in this research.

As it was claimed that the results from the in-line measurement agreed with the result from the capillary rheometer very well, the viscosity data of BMC then was compared with the viscosity of Interpon that was obtained by a capillary rheometer.

A high viscosity ratio between skin (Interpon) and core (BMC) materials at a shear rate of 10^4 s^{-1} suggested that the core material was easier to flow into the mould than the skin and was likely to break through the skin layer. This suggested sequential injection might be a solution in order to get a fully encapsulated sandwich moulding.

Chapter 6

Injection Moulding Experiments

Using test results from the material experiments in the last chapter, BMC and Interpon were injection moulded by using the novel thermoset co-injection moulding machine. The experiments were started with a single injection moulding of each material before moving onto the co-injection moulding. Specifications of the machine and tooling are described. The experiments involved in the novel thermoset sandwich injection moulding are explained in detail and discussed.

6.1 Machine and Tooling

A Battenfeld sandwich injection moulding machine, BA2000/630+630 equipped with the UNILOG 9000C control system had been especially designed and built for this project. It consisted of a horizontal stuffer-feed injection unit suitable for bulk moulding compounds and a vertical hopper-feed unit for granular materials. The specification of this machine is given in Table 6.1.

Table 6.1 Specification of BA2000/630+630 thermoset co-injection moulding machine

Injection Unit	Screw diameter	50 mm
	Maximum stroke	180 mm
	Maximum screw speed	280 rpm
	Maximum pressure	1767 bar
	Nozzle contact force	99 kN
	Nozzle stroke	400 mm
Clamping Unit	Clamping design	Hydraulic-double toggle clamping system
	Maximum clamping force	2000 kN
	Locking force	2200 kN
	Distance between tie bars	560x560 mm
	Mould height (adjustable)	200-520 mm
	Maximum daylight	450 mm
Ejector	Ejector force	67 kN
	Ejector maximum stroke	160 mm
Barrel heating control	Type	Water temperature controller
	Model	GWK teco200
	Maximum temperature	140°C
	Heating capacity	3 kW
	Cooling capacity at 15°C cooling water/80-130°C	8 kW

To join two thermoset materials together in order to form suitable layers for a sandwich moulding, a new manifold system had been installed to work as a gate channel where the two injected polymers met at the back of the mould sprue. Figure 6.1 shows the manifold system and how it connects to the mould and injection units.

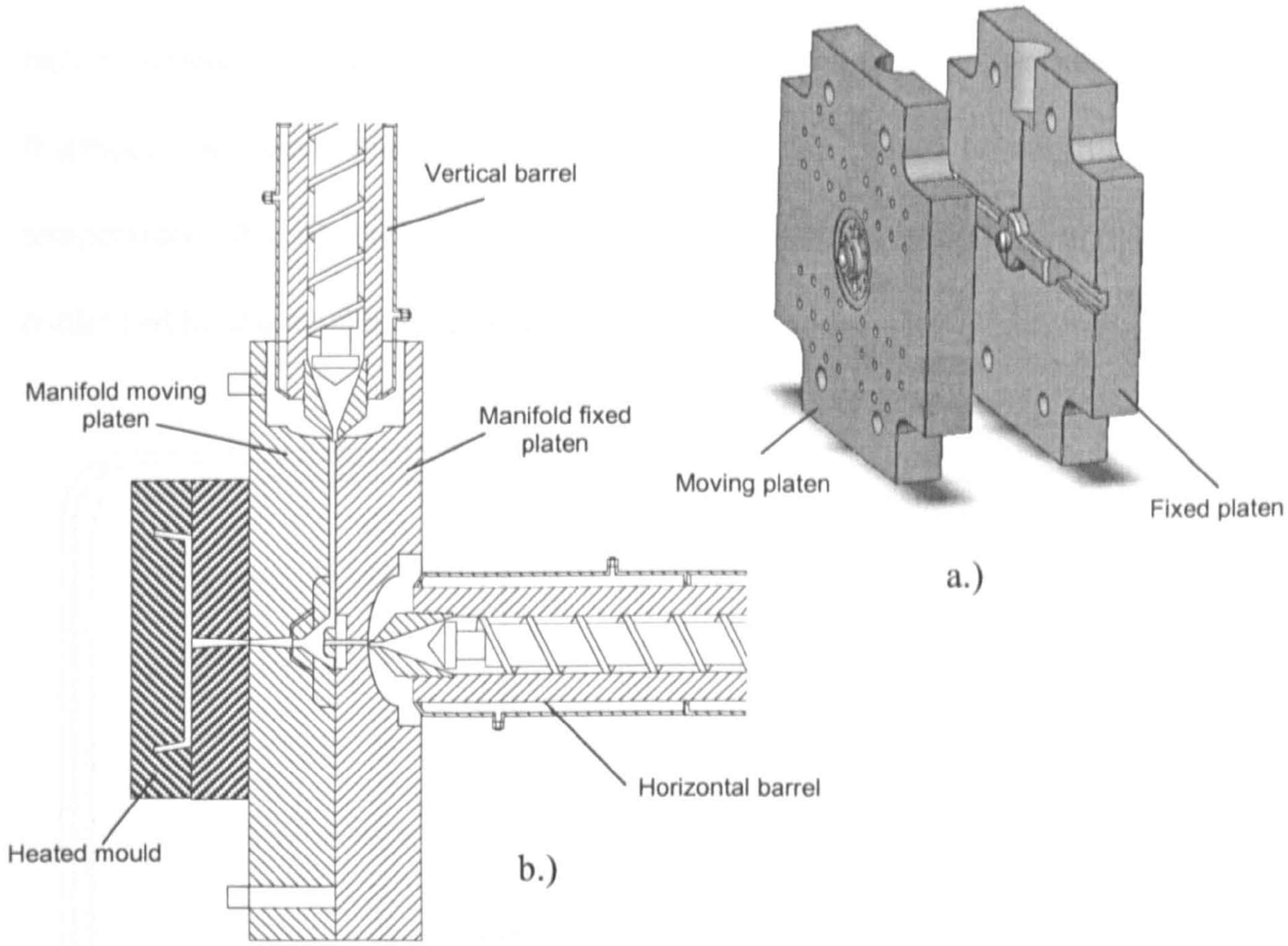

Figure 6.1 a.) The manifold system and b.) Cross-section of the manifold during injection moulding process

Inside each half of the manifold, PDE cartridge heaters and thermocouples had been installed and used to control the operating temperature. The temperature of the manifold is very important to maintain the flow ability of the thermosetting materials inside the manifold and must be carefully controlled to ensure that there is no pre-curing during injection. Details of heaters and thermocouple positions are in Chapter 7.

6.2 Mould

A central sprue, tray shape mould of dimension 312 x 242 x 2.5 mm was used in this experiment (see Figure 6.2). It provided a good flat surface with curves at its four

sides. For the thermoset injection moulding process, heat is necessary for the cross-linking reaction during curing. Another two sets of four cartridge heaters and two thermocouples were placed inside each half of the mould to control the mould temperature. All of the heaters, both in the manifold and in the mould, were controlled by the machine's control systems.

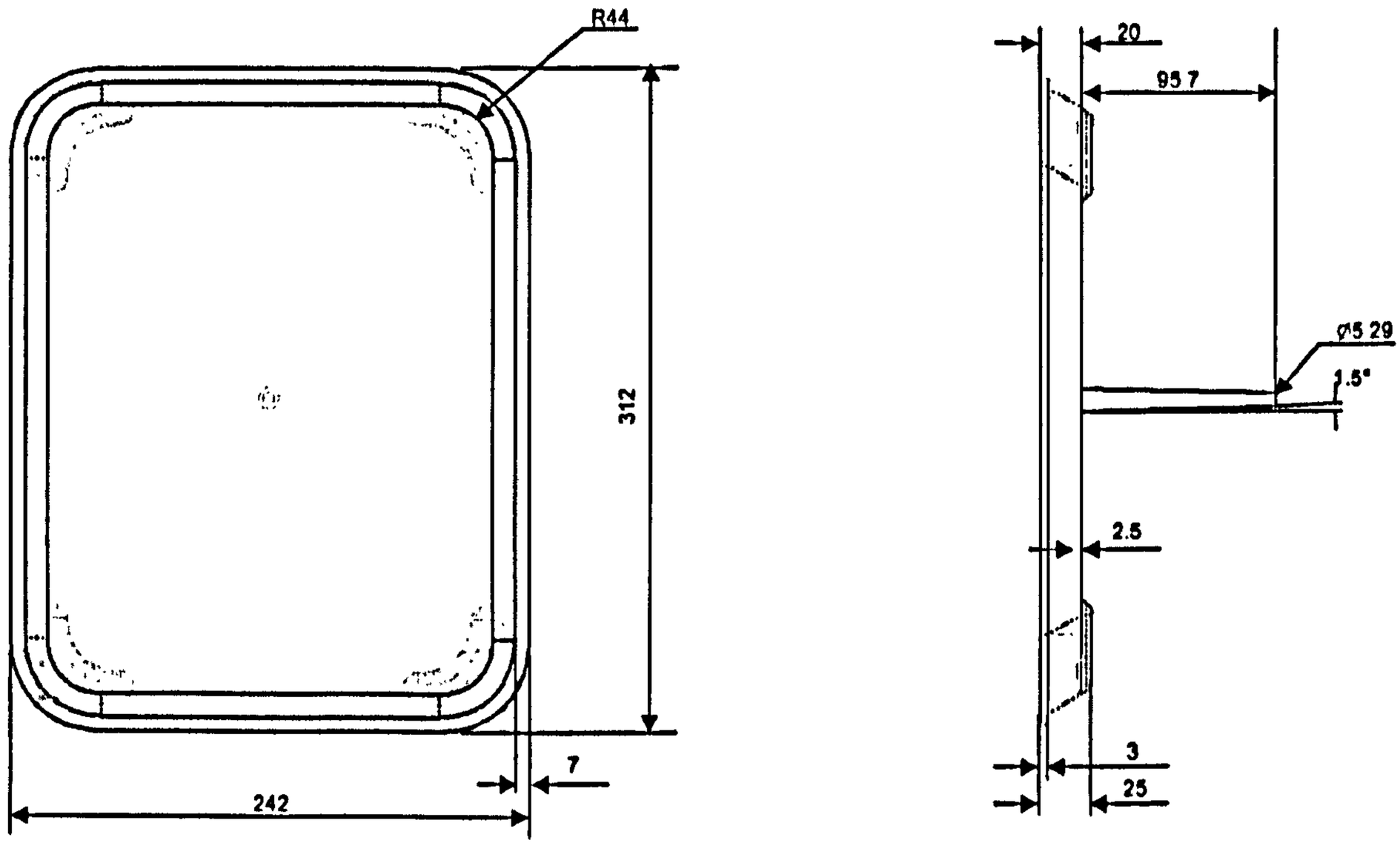

Figure 6.2 Front and side view of the tray moulding

6.3 Materials

A general grade bulk moulding compound, BMC G7B 5580 from BIP Ltd was used as a core material and a black powder coating, Interpon PM-300011-F from Akzo Nobel was used as a skin material.

6.4 Experiments

Each material was moulded separately prior to sandwich injection moulding to study the individual flow behaviour in the existing manifold system while changing some

temperature parameters. The information from the single injection mouldings was used to set up the sandwich injection moulding process.

6.4.1 Single injection of BMC moulding

BMC was moulded alone in order to set up a suitable sprue temperature window. The molten BMC was injected from the horizontal barrel through the manifold runner and then flowed into the mould, while the top runner of the manifold was blocked to prevent the material escaping from the system during injection. The machine condition setting supplied by the material supplier is given in Table 6.2.

Table 6.2 Machine condition settings for BMC injection moulding[75]

Settings	BMC G7B 5580
Barrel Temperature (°C)	35/35 (front/rear)
Screw Rotational Speed (rpm)	50
Back Pressure (bar)	0-3
Injection speed (mm/s)	80
Mould temperature (°C)	150 (145-160°C)[1]
Curing time (s)	60-90

Since BMC and Interpon would be moulded together later, the manifold temperature was set at a temperature that both of the two materials could flow through. The results from the gel time test in Chapter 5 suggested that the manifold temperature could be set at around 70-90°C. Therefore, 80°C was set as the manifold temperature. Throughout the process, the manifold was closed.

[1] Minimum and maximum mould temperature that can set. 150°C is a nominal setting.

Injection stroke and sprue temperature were varied until the moulding could be completed. The sprue temperature[2] was at 70°C for the start. This temperature was determined to be low enough to quickly remove some heat, which transferred to the material from the hot mould, but not too low as to cause a large temperature difference between the sprue and the manifold nozzle. The temperature was increased from 70°C to 90°C or until pre-curing of the material occurred in the sprue, which could be determined by obtaining a short shot moulding and the material in the mould sprue became solid. When finishing the whole process, the BMC inside the manifold was left to harden and then cleared out.

A full shot moulding could be made from injecting at a 130mm metering stroke when the sprue temperature was around 70-74°C, while a short shot happened at the higher temperature. Figure 6.3 shows a full shot moulding obtained from this experiment.

Figure 6.3 Front and back of a BMC full moulding

[2] The temperature is the outlet temperature of the cooling water.

6.4.2 Single injection of Interpon moulding

As mentioned previously, Interpon had never been used in the injection moulding process. Some experiments were needed to find the most suitable mould and manifold temperatures to match the settings of the BMC moulding so a process window could be set for co-injection moulding of these materials.

Table 6.3 is the machine settings for Interpon. Under these settings, the melt temperature was approximately 80-85°C, which was the optimum temperature selected from the gel time and the melt flow index test results in the last chapter. Water temperature around the sprue was controlled within 70 to 74°C, the same as the settings in the single injection of BMC. Within this range, the material could stay liquid more than 1500 seconds (see Figure 5.1 Gel time results from Chapter 5). However, the melt temperature in the sprue during injection was likely to be higher as it was influenced by the heat transferred back from the hot mould, which would be set at 140-150°C. Therefore, the material inside the manifold nozzle and mould sprue would need to be investigated during these experiments.

Curing time for moulding Interpon was set at 90 seconds, which was long enough to ensure that the material would be cured at the end of the curing cycle.

Table 6.3 Settings for single injection moulding of Interpon

Setting parameters	Setting values
Barrel temperature (°C)	80/60 (Front/Rear)
Screw rotational speed (rpm)	50
Back pressure (bar)	0
Injection speed (mm/sec)	80

6.4.2.1 Experiment I: Effect of mould temperature

The gel time results from Chapter 5 showed that at the temperature above 140°C, Interpon reacted to the heat very quickly. Any temperatures above this would be possible to use as a curing temperature or mould setting temperature.

The machine parameters were set as in Table 6.3 while the mould temperature was varied at 140, 150 and 160°C. Flows of the melts of these three mouldings were affected by the mould temperatures only, due to the same machine settings and the same conditions of the material in the manifold. The manifold temperature was controlled at 80°C. This was to maintain the temperature of the material when it was injected from the barrel, which was approximately 80-85°C. This temperature range was shown to be the temperature window for Interpon as described in the last chapter. Since different levels of heat applied to the material would affect its cross-linking and flowing, the curing of the melt inside the mould would be different. The results of this experiment would be determined by the moulding size. The mould temperature that gave a full short or the largest moulding would be considered as the optimum mould temperature for injection moulding using Interpon.

Figure 6.4-6.6 shows the mouldings of Interpon at different mould temperatures and Figure 6.7 shows the comparison of the three mouldings.

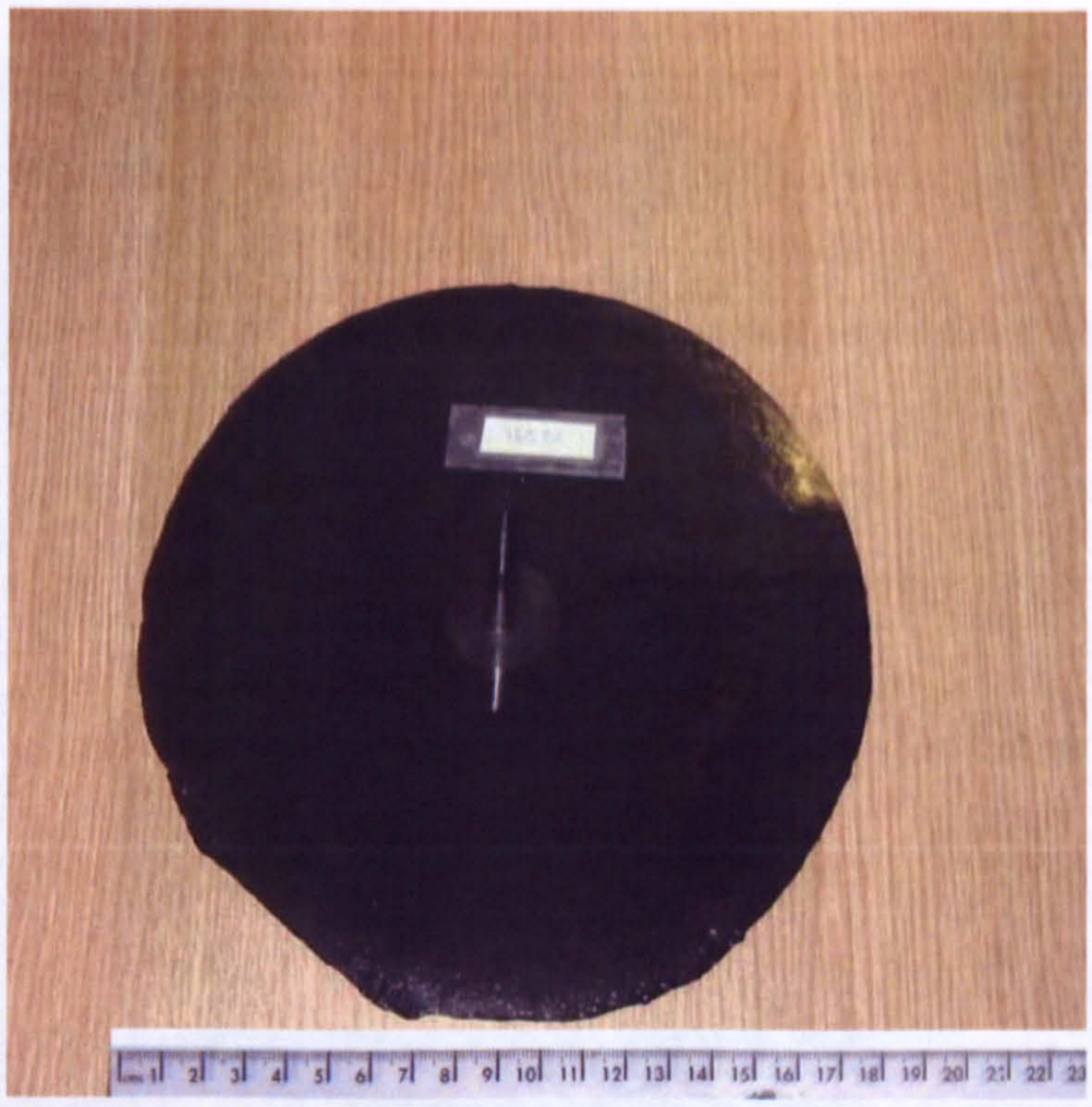

Figure 6.4 Interpon moulding at 140°C mould temperature

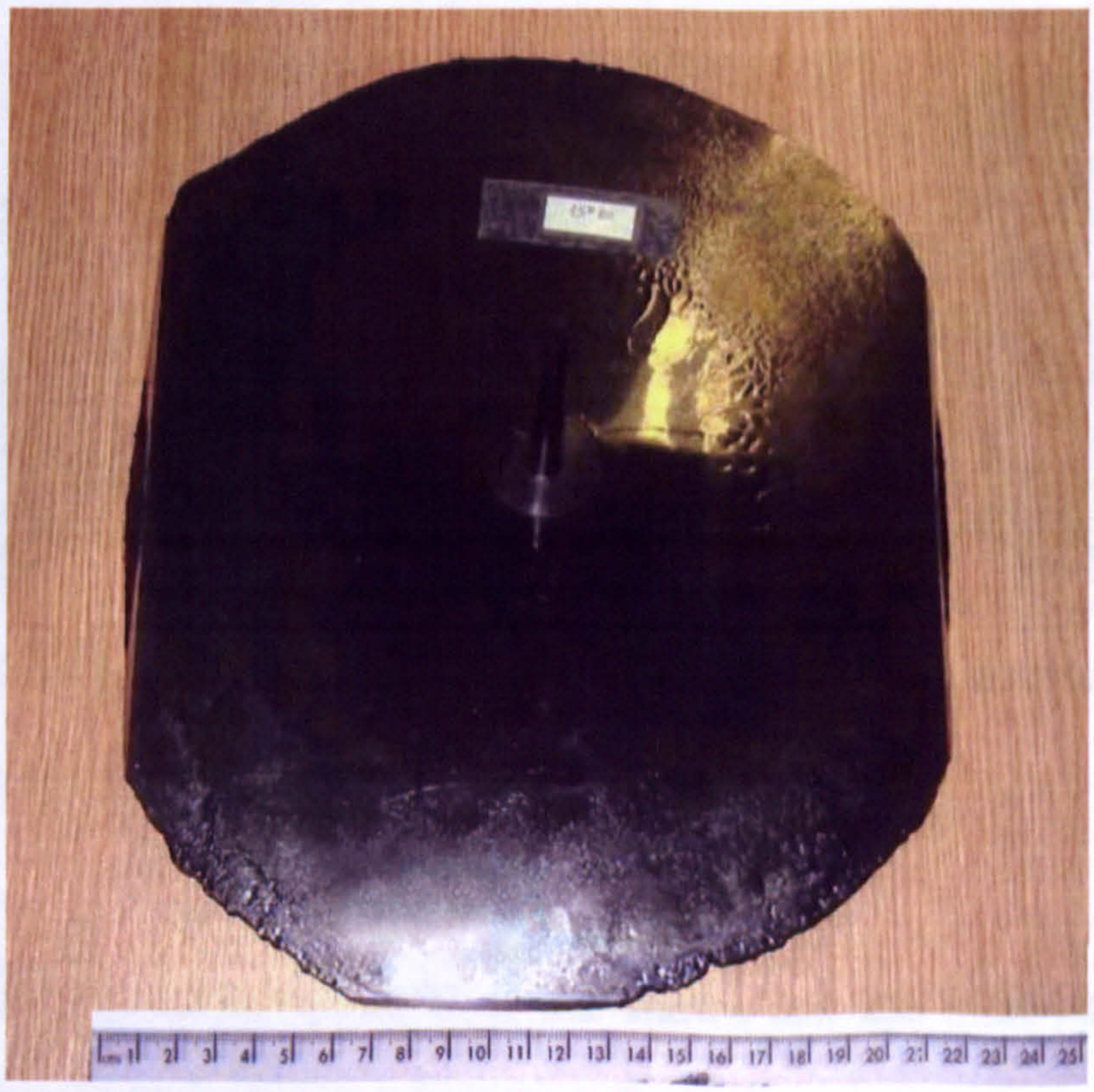

Figure 6.5 Interpon moulding at 150°C mould temperature

Figure 6.6 Interpon moulding at 160°C mould temperature

Figure 6.7 Comparing the three mouldings, 140, 150, 160°C mould temperature (start from the left)

At a low mould temperature of 140°C, it was shown that less material could flow into the mould than at higher temperatures of 150°C and 160°C. At the higher temperatures, the material flow front could go further into the mould because of its

lower viscosity and therefore, easier flowing. However the higher temperature also caused a higher cross-linking reaction rate and less time for the melt in a liquid state.

The effect of too high a mould temperature is shown by the result of moulding at 160°C. Although a similar moulding size was obtained from the 150°C mould temperature, the surface finish was different. At 160°C, the melt started to pre-cure during injection and left some flow marks on the back surface as shown in Figure 6.8 and 6.9.

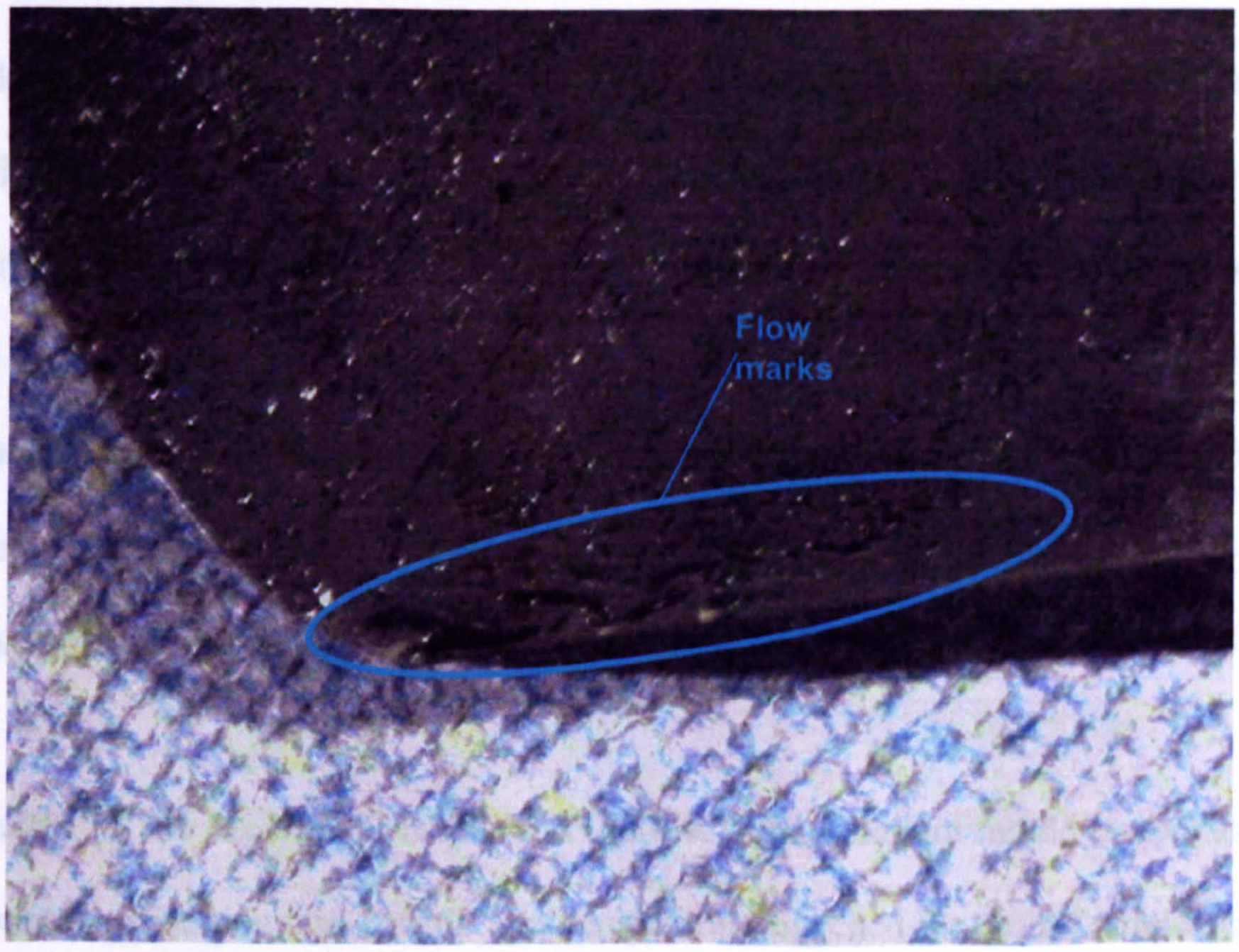

Figure 6.8 Some flow marks at the edge near the top of the moulding from Figure 6.6

Figure 6.9 Some flow marks at the other side near to the bottom of the moulding from Figure 6.6

Moulding Interpon by using this machine system presented a problem that was not found when moulding BMC solely. After a shot was made, it was not possible to continue the next shot like in BMC injection moulding. The system was blocked since the connection between the mould sprue and the manifold nozzle could not be broken. It was not possible to take the component out of the mould because of the opposite taper of the sprue and the nozzle. So, the mould and manifold had to be disassembled. This problem will be explained more in Chapter 7.

As shown by the experiment results in Figure 6.7, the optimum mould temperature for moulding Interpon was 150°C. This temperature matched the mould temperature of BMC so both materials could share the same mould temperature and curing time.

Nevertheless, a full moulding could not be achieved at 150°C since the material pre-cured before the mould could be fully filled. This could be because of unsuitable

manifold temperature. The effect of various manifold temperatures on the mould filling therefore was investigated and is explained in the next experiment.

6.4.2.2 Experiment II: Effect of manifold temperature

This experiment was designed to find a suitable manifold temperature for Interpon moulding. Even though 80°C was set for moulding BMC and Interpon in the previous experiment, this temperature might not be the optimum for the Interpon. As a result of the long and small vertical runner through which Interpon would be injected, internal shear friction could be higher than the horizontal runner of BMC; the result could be that the Interpon melt temperature could be increased by the shear friction effect. The cross-linking reaction caused by the increasing temperature would affect the Interpon curing and flowability.

From Experiment I, 150°C was found to be the optimum mould temperature, so it was chosen for this experiment, while the manifold temperature was varied from 65 to 90°C. After a moulding had been made, the manifold was opened in order to examine the material inside to see whether it was still viscous and still able to flow into the mould. The results were compared and the manifold temperature that gave the largest moulding would be considered as the manifold setting temperature. Figure 6.10-6.13 shows the results of this experiment and Figure 6.14 shows the comparison of all mouldings.

Figure 6.10 Interpon moulding at 65°C manifold temperature

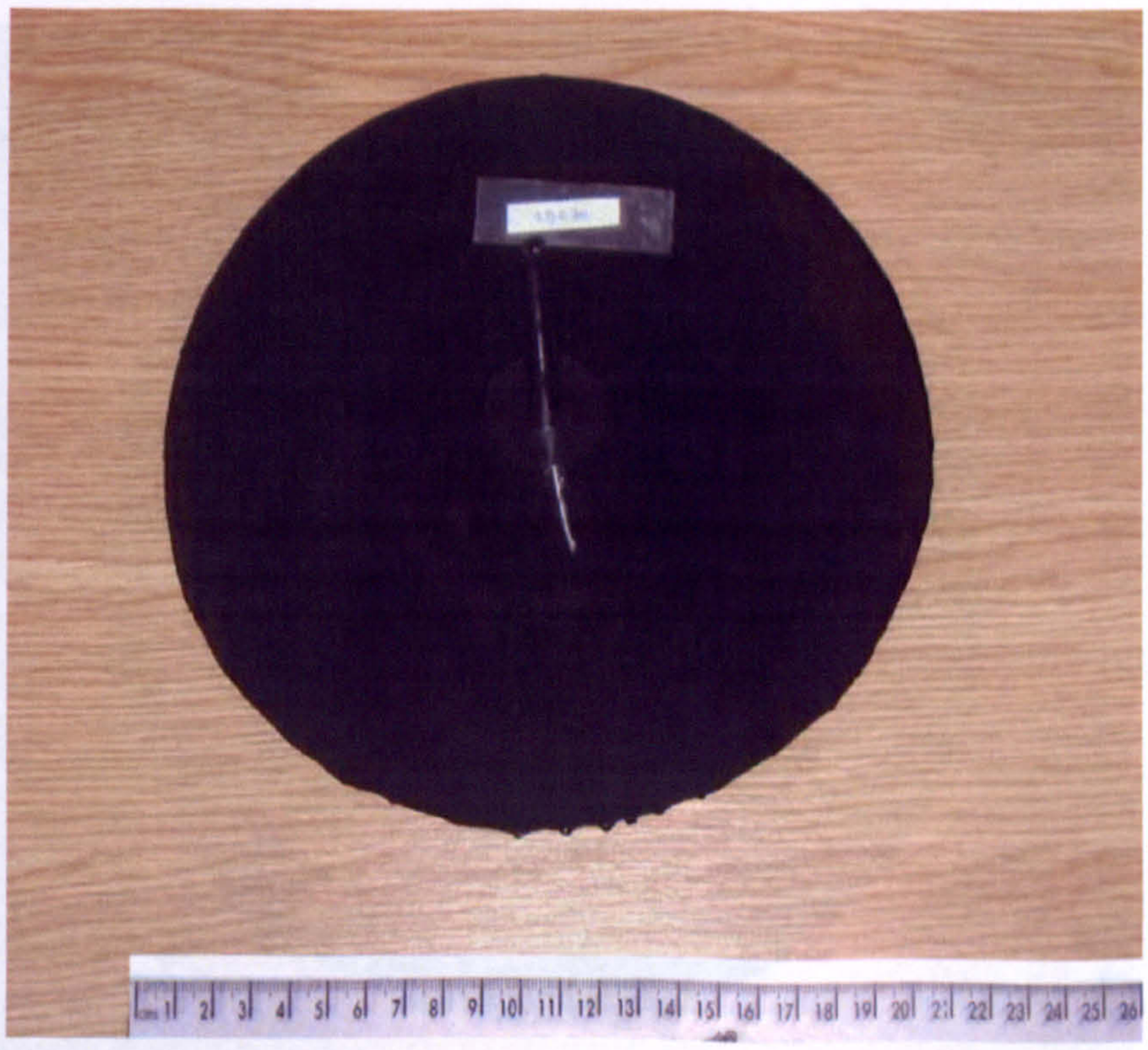

Figure 6.11 Interpon moulding at 70°C manifold temperature

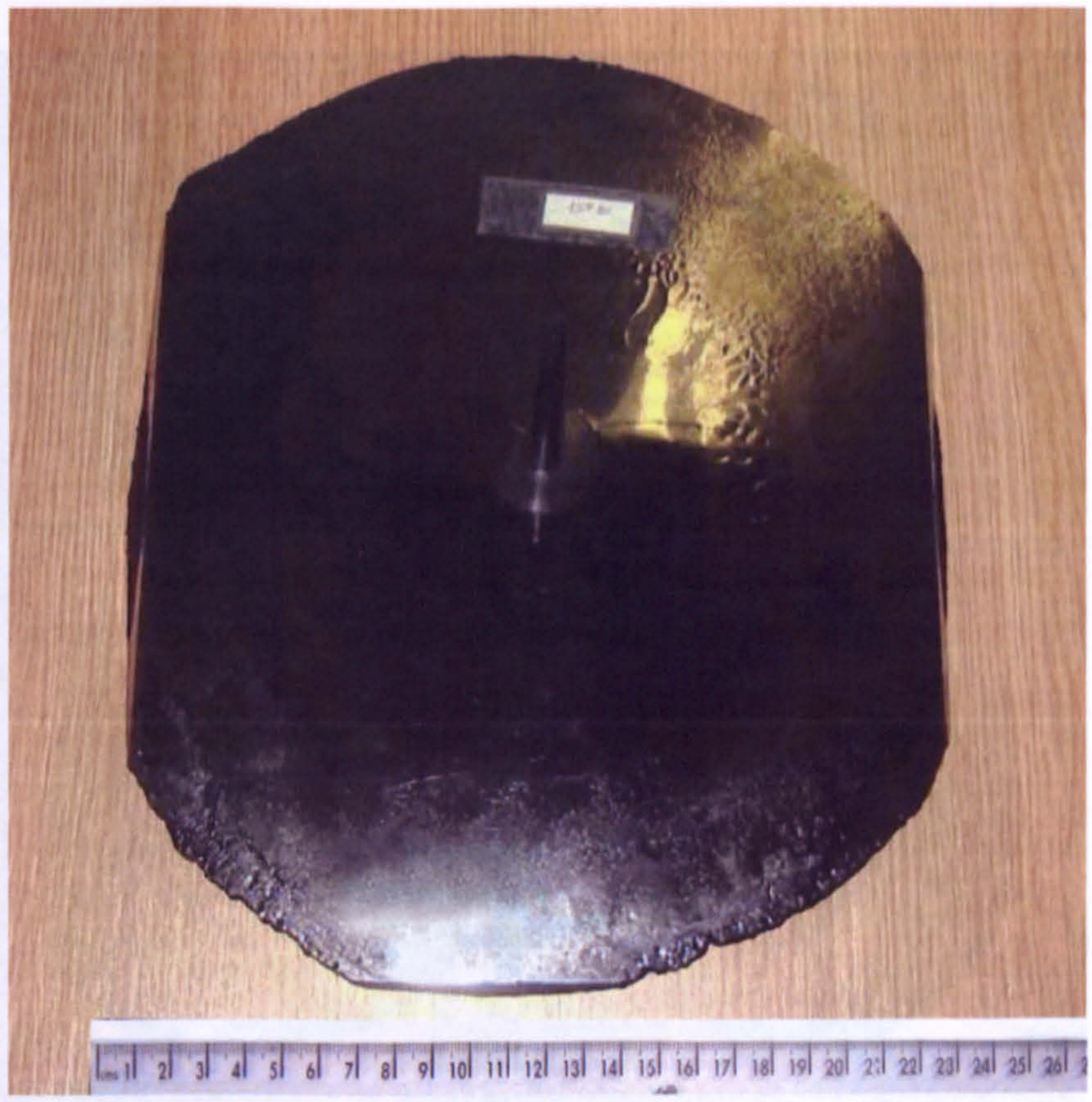

Figure 6.12 Interpon moulding at 80°C manifold temperature

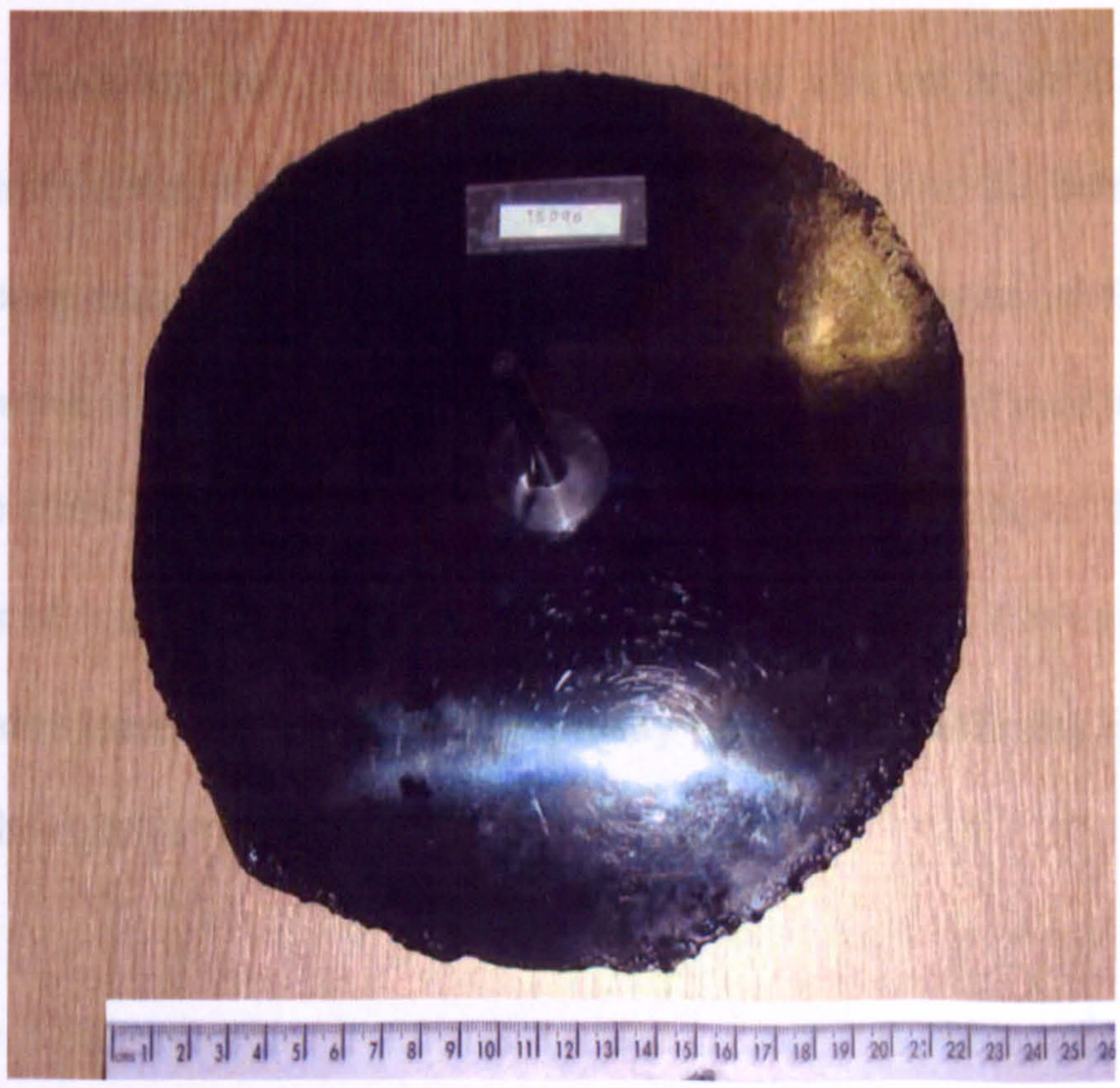

Figure 6.13 Interpon moulding at 90°C manifold temperature

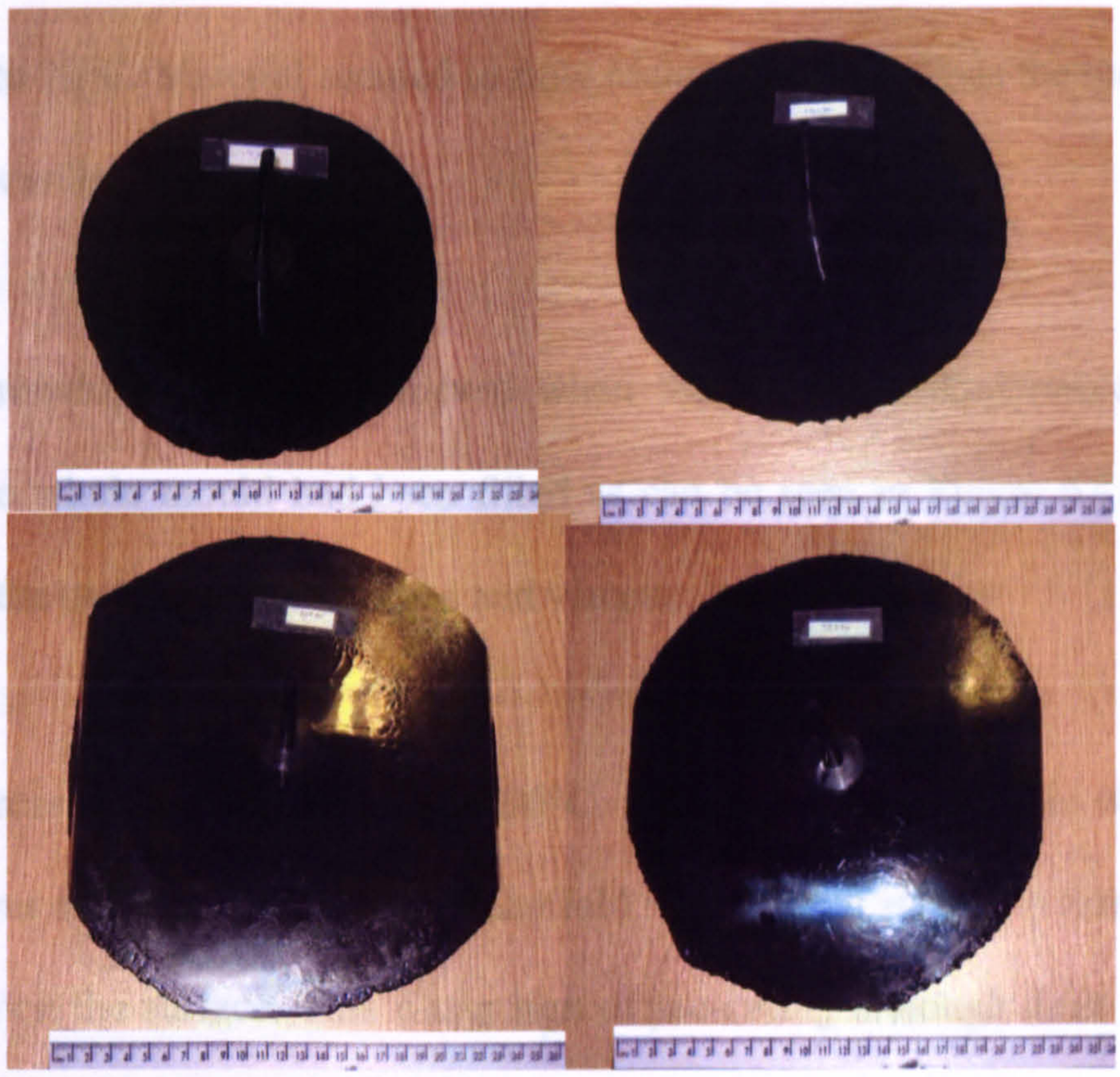

Figure 6.14 Comparison of Interpon mouldings at varied manifold temperature

(Top left: 65°C, Top right: 70°C, Bottom left: 80°C and Bottom right: 90°C)

The smallest moulding was made when the manifold was set at 65°C. The melt inside the manifold was much more viscous than the output from the barrel and was the most viscous among all four cases. This was because the material temperature was reduced when it flowed through the manifold. The reduction of melt temperature decreased the cross-linking rate, which was satisfactory since curing of the material before it entered into the mould would block the whole system. However, the low temperature also increased the material viscosity and caused difficulty in injecting the material through the manifold.

A larger and rounder moulding was obtained when the manifold temperature was increased to 70°C. Material seemed to flow easier than at 65°C, as the melt inside the manifold was less viscous.

The best mould filling was achieved when the manifold temperature was 80°C. Almost the whole mould had been filled as can be seen in Figure 6.12. Inside the manifold, the melt was still uncured and viscous.

When increasing the temperature to 90°C, a smaller moulding was obtained. The material was still viscous inside the manifold runner but it started to form a very thin black film on the surface. This was a sign of pre-curing although there was no flow mark found on the moulding component as seen in Figure 6.8 and 6.9. The pre-curing that occurred in the manifold system was also likely to cause a problem in the next shot.

In all four cases, the melts inside the manifold were still able to flow into the mould although each of their flow abilities in the mould were different. However, a full shot moulding could not be achieved from any of these settings. The melts inside the manifold nozzle where it connected to the mould sprue (see Figure 7.3) were then examined. It was found that the melt was most viscous inside the manifold nozzle tip when the manifold temperature was at 80°C and 90°C, while they were less viscous at the lower temperatures. Since the mould sprue was smaller than the nozzle diameter, there was a possibility that the melt could be frozen inside the sprue at all temperature settings as well.

From the two experiments, the optimum temperatures that gave the best filling were 80°C at the manifold and 150°C at the mould. Almost the whole mould could be filled under this condition. Adding BMC from the horizontal barrel could fill the rest of the mould and a full shot moulding was possible. Furthermore, these temperatures also matched the settings for moulding BMC, so they could be used as the manifold and mould temperature for the co-injection moulding of both materials. Pre-curing that was likely to happen inside the mould sprue could be reduced as the lower temperature of the BMC melt would reduce the Interpon melt temperature down and then slow the chemical reaction inside the manifold nozzle and mould sprue.

6.4.3 Sandwich injection moulding of Interpon and BMC

6.4.3.1 Initial experiments

The first thermoset sandwich injection moulding was made after the machine settings were obtained as described in section 6.4.1 and 6.4.2. The settings for the co-injection moulding of Interpon and BMC are shown in Table 6.4.

Table 6.4 Settings for sandwich injection moulding of Interpon and BMC

Settings/Material	**Interpon**	**BMC G7B 5580**
Barrel temperature (°C)	80/ 60 (front/rear)	35/ 35 (front/rear)
Screw rotational speed (rpm)	50	50
Back pressure (bar)	0	0-3
Injection speed (mm/sec)	80	80
Mould Temperature (°C)	150	
Curing time (s)	90	

The overall metering stroke was assumed to be equal to the value used in BMC single injection moulding, which was 130mm. 80 and 50 mm were set respectively as the initial skin and core metering strokes, which made approximately 60:40 percent skin/core ratio. This value was proven to be a good ratio for thermoplastic co-injection moulding.[2,16]

The switchover point was set at 8mm and the core delay time was 0.2 second, i.e. the core screw would start to inject BMC into the mould 0.2 second after the skin screw reached 8 mm. Figure 6.15 shows the injection diagram for this experiment.

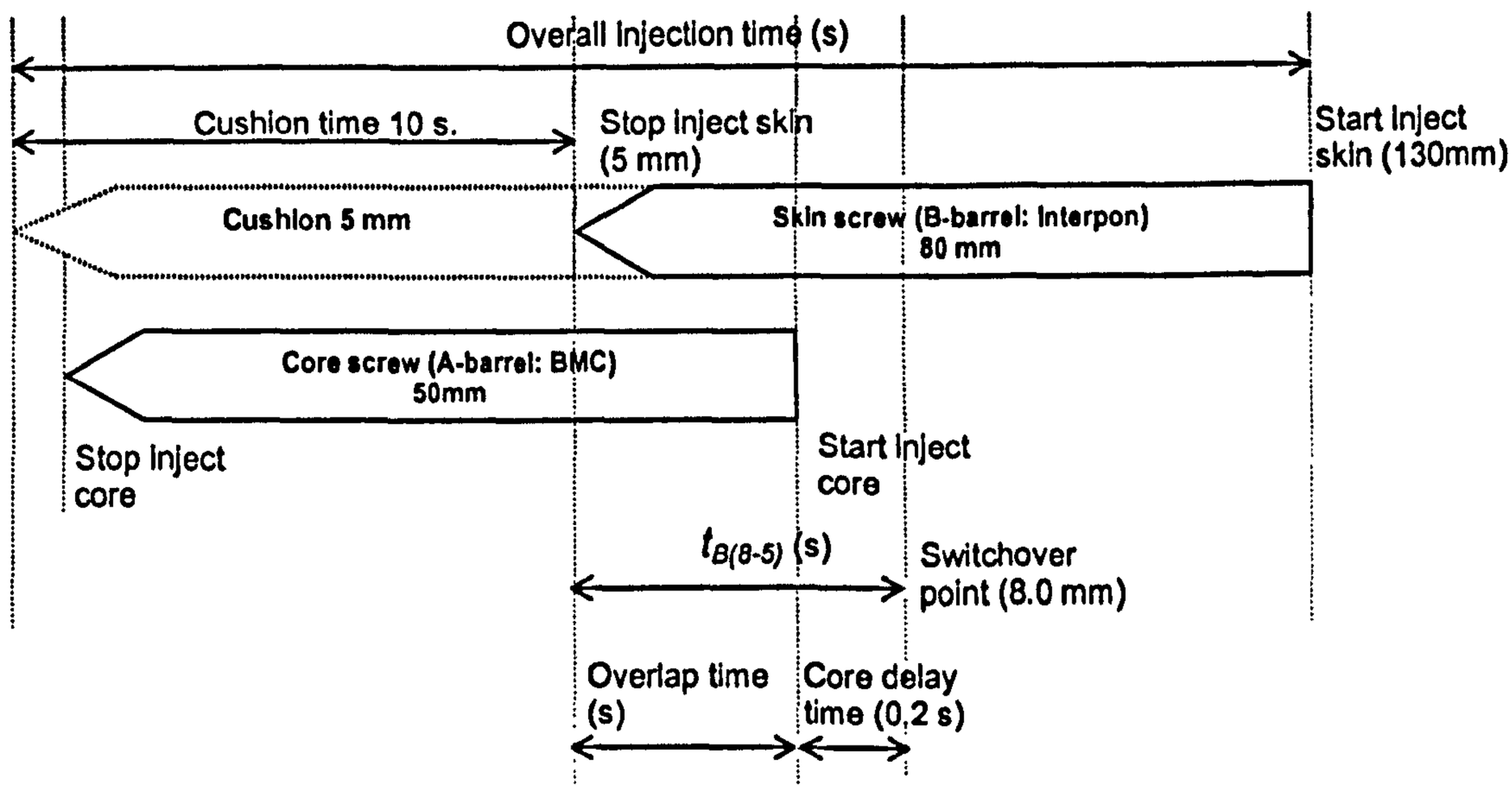

Figure 6.15 Diagram of injection sequence for sandwich injection moulding of BMC and Interpon (The figure is not in scale.)

As described in the last chapter, in order to get a fully encapsulated sandwich moulding, the machine parameters should have been set to perform sequential injection, i.e. no overlap time between skin and core injection. The injection settings shown in Figure 6.15 were used to calculate the overlap time. Figure 6.16 shows the

ideal injection velocity diagram of the skin screw (Interpon). The co-ordination in the figure shows the velocity of the screw when it reaches 8 mm, which was the setting switchover point.

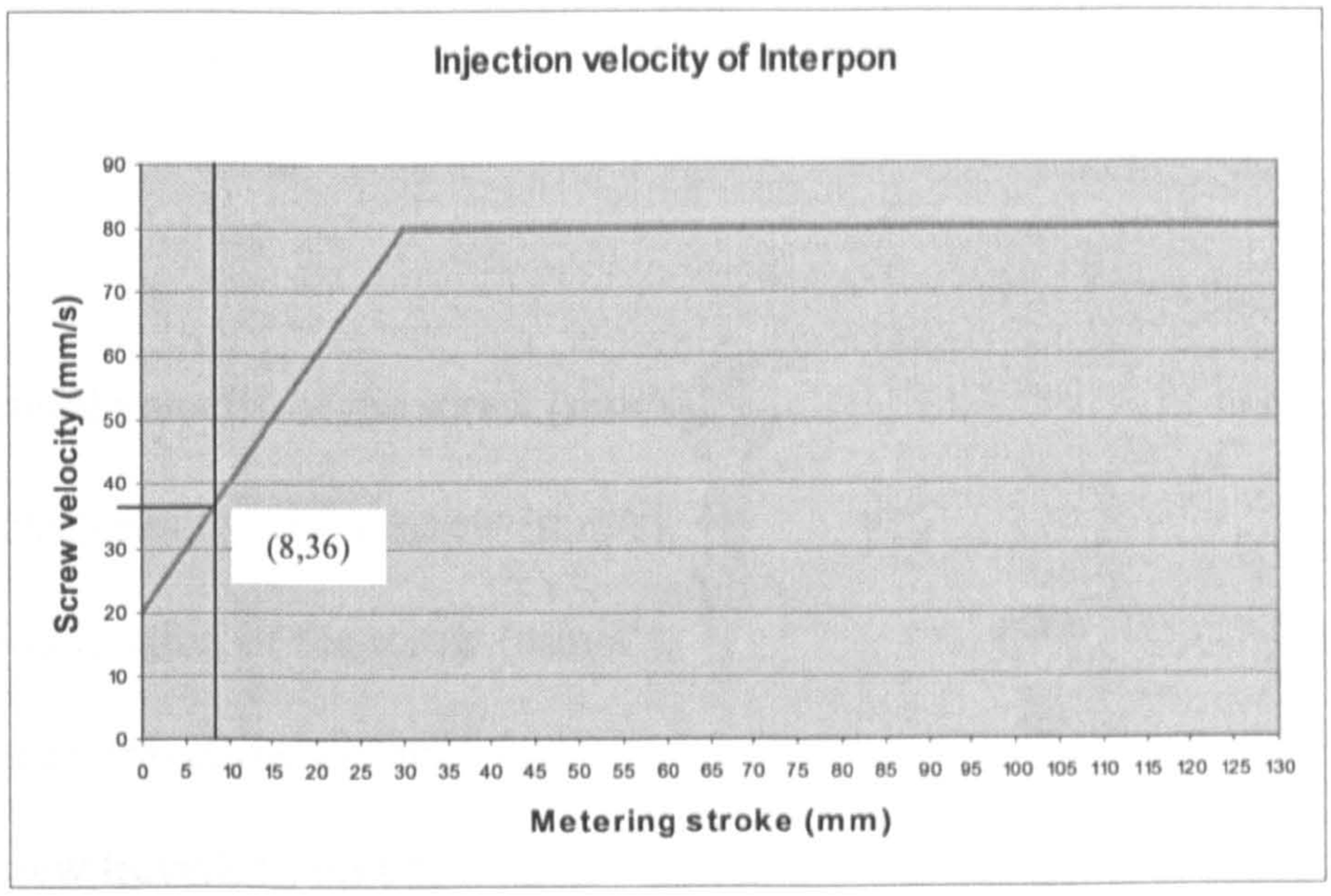

Figure 6.16 The injection velocity diagram of Interpon. The co-ordinate represents the screw velocity when it reaches 8-mm metering stroke

The time of simultaneous phase or overlap time in Figure 6.15 can be calculated by,

$$t_{ov} = t_{B(8\text{-}5mm)} - t_{delayA} \tag{6.1}$$

where,

t_{ov} is the overlap time (second),

$t_{B(8\text{-}5mm)}$ is the injection time of the skin screw when moving from 8-mm to 5-mm injection stroke (second) and

t_{delayA} is the core delay time (second).

t_{ov} will be negative when t_{delayA} is more than $t_{B(8\text{-}5mm)}$. This means the process is sequential co-injection moulding

The injection time of the skin when the screw moves from 8 mm to 5 mm and the overlap time can be calculated by

$$v = u + at \tag{6.2}$$

$$v^2 = u^2 + 2as \tag{6.3}$$

where

u is initial velocity of the screw (mm/s),

v is final velocity of the screw (mm/s),

a is acceleration of the screw (mm/s^2),

s is screw travelling distance (mm) and

t is screw travelling time (second).

The screw travelled from 8 mm to 5 mm, which made 3 mm as the screw travelling distance. The screw initial velocity was 36 mm/s when the screw travelled to 8-mm and the final screw velocity was 30 mm/s at 5-mm.

Using the Equation 6.2 and 6.3, the screw travelling time from 8 mm to 5 mm was 0.09 second, which is the $t_{B(8\text{-}5mm)}$ in Equation 6.1. Consequently, the overlap time of this setting was –0.11 second, which means the process was sequential co-injection moulding. For clarity, this time will be call '*Sequential time*' and represented in positive value.

The sandwich moulding of the two thermosets is shown in Figure 6.17 and 6.18. Despite the fact that there was no pre-curing in the manifold and the sprue, the mould was still not fully filled by these settings. The 130-mm metering stroke could

not be applied to the Interpon moulding material. This can be explained by the difference in volumetric expansion of the two materials inside the barrel. The Interpon melt at 80°C expanded more than the BMC melt at 35°C. Because the injection shot was measured by volume, and was pushed into the mould by injection pressure, a short shot could happen when injecting Interpon at the same stroke as BMC. In order to complete the moulding, a higher metering stroke was required.

Figure 6.17 Thermoset sandwich moulding from the setting in Table 6.3

Figure 6.18 Back view of the moulding from the setting in Table 6.3

It can be seen in Figure 6.17 and 6.18 that the Interpon could not wholly cover the BMC. At the front of the moulding, there was a break-through of the core material at the middle of the component opposite to the mould sprue as a result of a shear flow effect, while at the back BMC flowing lines appeared near to the edges. This showed that the film of the Interpon skin was very thin and soft so the BMC fibre could sweep out the skin material as can be seen by the white markings, which were indicative of fibre flow, in both Figure 6.17 and 6.18.

This initial experiment showed that the Interpon needed to form a more thick and rigid layer before the BMC was injected into the mould. Normally, this can be achieved by a higher mould temperature in order to increase the curing rate, or a longer curing time, to obtain more cross-linking networks produced between the

plastic chains. However, the results from the single injection moulding of Interpon showed that pre-curing inside the mould occurred at the higher mould temperature as could be seen on the moulding surface in Figure 6.8 and 6.9. It was decided to give more time for the skin to form a thicker layer by reducing the switchover position to 6 mm and increasing the time delay of injecting the BMC core.

6.4.3.2 Increasing core injection delay time and skin metering stroke

This experiment used the same settings as shown in Table 6.3. The injection delay time of injecting BMC (core material) was varied and increased to 1.5 seconds in order to give more time for the Interpon (skin material) to form a more rigid and thicker layer. More skin material was also injected to cover the core breaking through at the centre and to fill the rest of the mould. The results are shown in Figure 6.19 and 6.20.

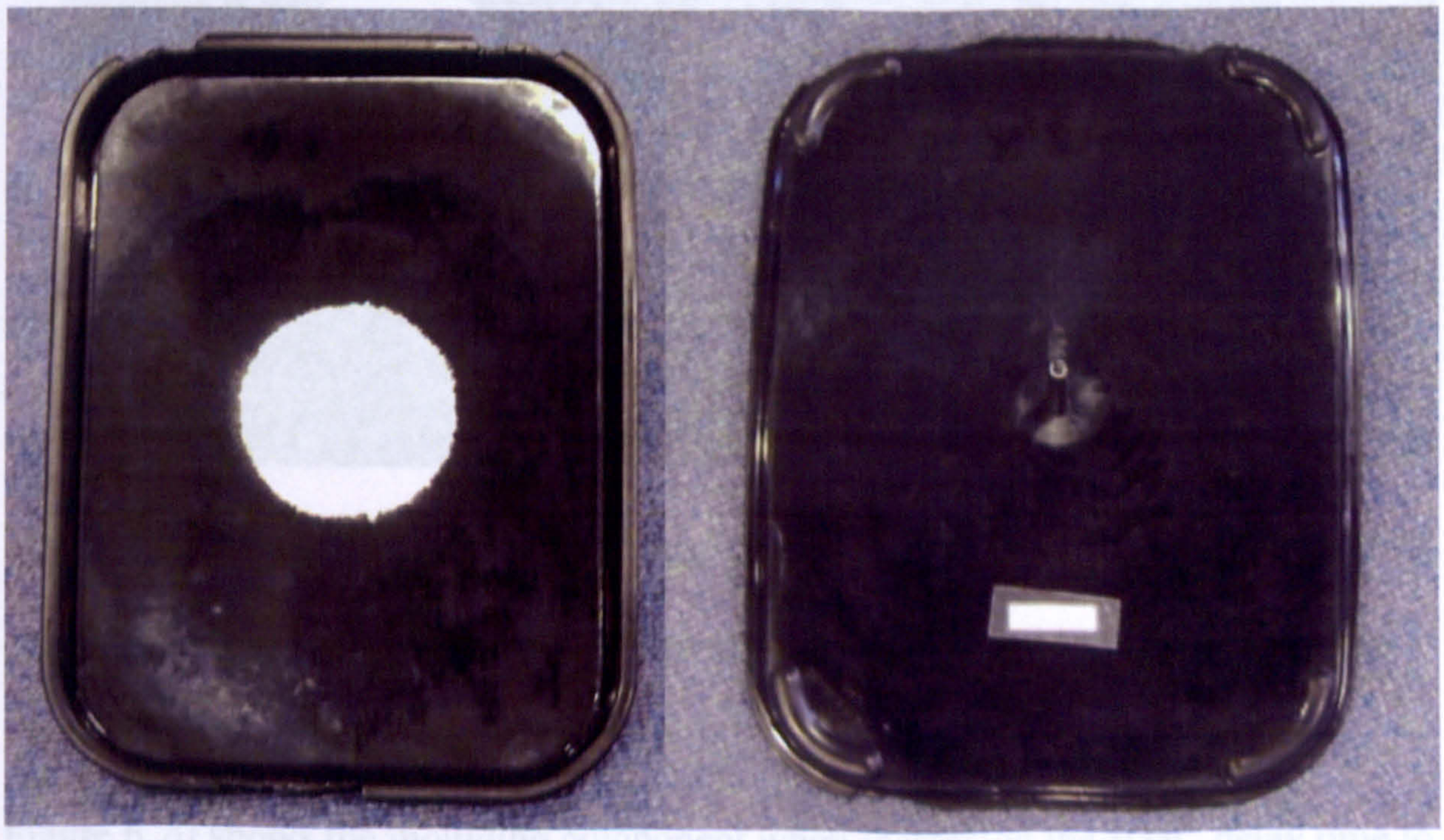

Figure 6.19 Front and back of the sandwich moulding of Interpon and BMC when using 0.5-second delay time, 6.0mm switchover point and 130:50 skin/core ratio

Figure 6.19 shows the moulding component when increasing BMC delay time to 0.5 second and reducing the switchover point to 6.0 mm. The skin metering stroke was increased to 130 mm while the core metering stroke was still at 50 mm. This made a 165 mm overall metering stroke for the sandwich moulding.

Break-through of the core still happened at the centre but not on the back of the moulding as shown in Figure 6.19. The core was completely covered in the rest of the moulding. Even though the overall metering stroke was increased from 130 to 180 mm, the mould was still not completely filled by this setting.

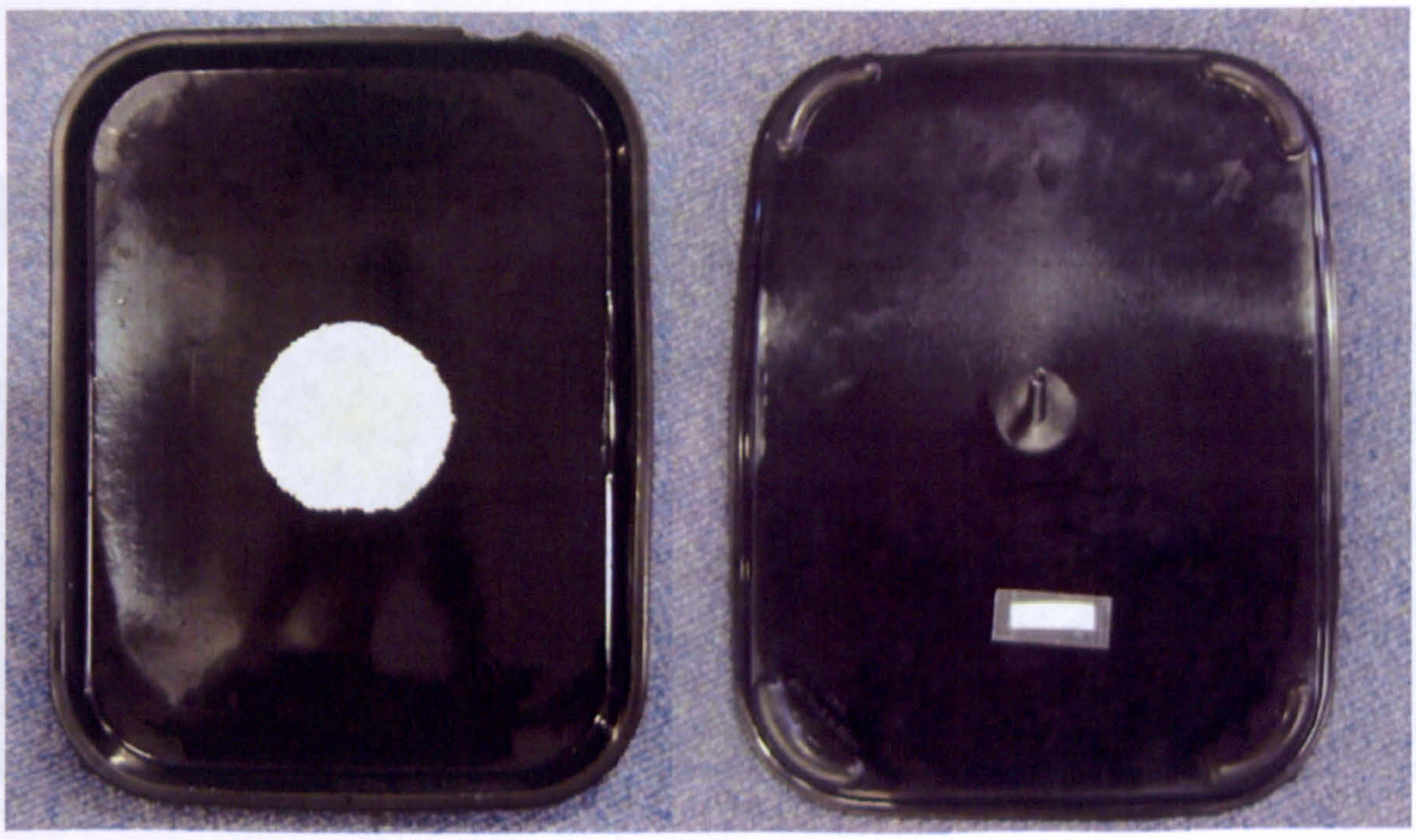

Figure 6.20 Front and back of the sandwich moulding of Interpon and BMC when using 1.5-second delay time, 6.0mm switch over point and 140:50 skin/core ratio

Figure 6.20 shows the moulding component when increasing the BMC delay time to 1.5 second and using the same switchover point at 6.0 mm. The skin metering stroke

was increased to 140 mm. The overall metering stroke for the sandwich moulding in this case was 190 mm.

Again, break-through of the core still happened at the centre of the moulding. No core break-through was found in the rest of the moulding. More Interpon was injected into the mould so in this case the mould was more fully filled than with previous settings.

Figure 6.21 is the comparison of the three sandwich mouldings that had been made using the novel co-injection moulding machine.

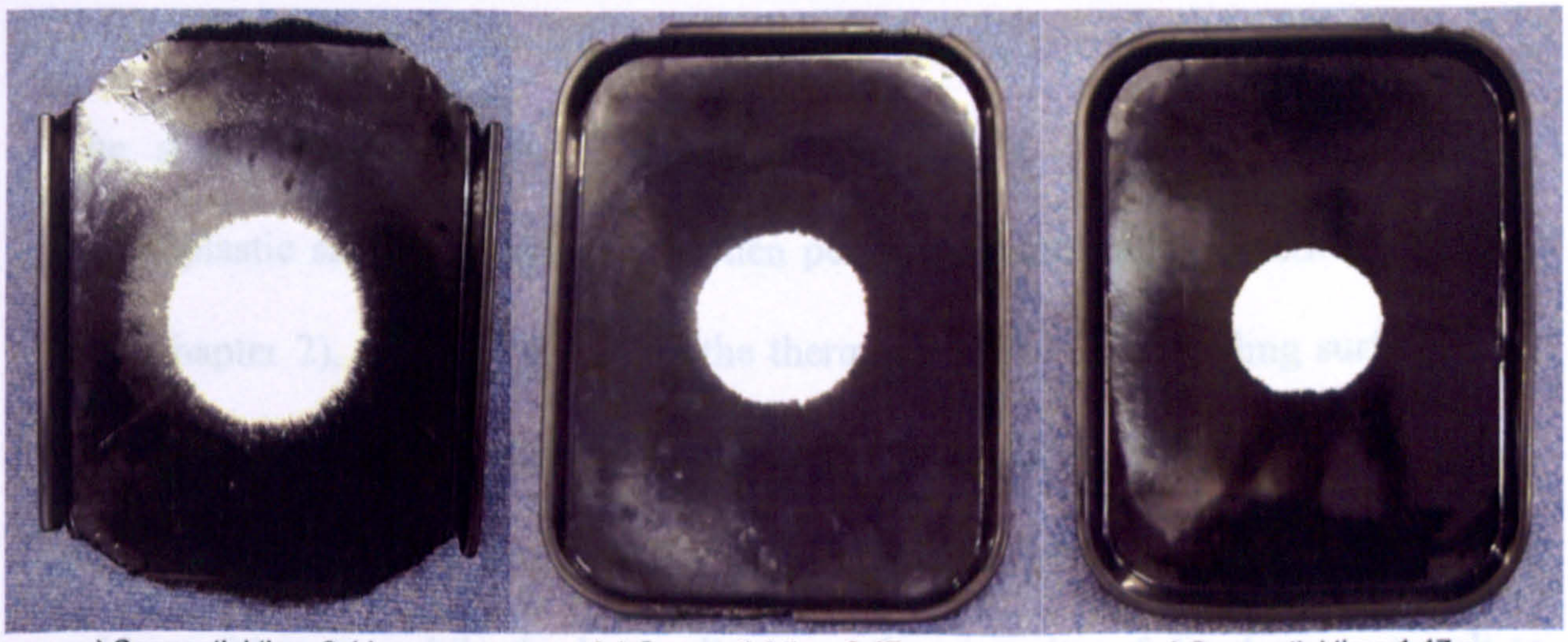

a.) Sequential time 0.11 s b.) Sequential time 0.47 s c.) Sequential time 1.47 s

Figure 6.21 Comparison of the three sandwich mouldings produced by the novel co-injection moulding machine

The effect of increasing core delay time and Interpon metering stroke can be seen in Figure 6.21. Moulding 6.21a was a result of 0.2-second core delay time, 8-mm switchover point and 130-mm overall metering stroke, moulding 6.21b was

produced when using 0.5-second core delay time, 6-mm switchover point and 165-mm overall metering stroke and moulding 6.21c was produced when using 1.5-second core delay time, 6-mm switchover point and 190-mm overall metering stroke. The numbers shown underneath each moulding are the sequential times, calculated by Equation 6.1-6.3.

It can be seen that a larger moulding could be produced when increasing the amount of skin material. The white circle shape in the moulding, which represented core break-though at the moulding centre, was smaller when increasing core delay time or the sequential time. Also, a sharper perimeter of the circle was found. This is because the skin was allowed to form a thicker and stronger layer, which was more difficult to be swept out by the core.

The shadow marks or gloss mark, which can be found on the surface of thermoplastic sandwich mouldings when performing sequential injection moulding (see Chapter 2), were not found on the thermoset sandwich moulding surface. This was because of the different behaviour of the materials when they are flowing into the mould. Thermoplastic melt will form a solid layer right away when it touches the cold mould walls, while the hot walls cause the viscosity of the thermoset melt to reduce before the cross-linking turns the viscous melt near to the mould wall into a solid layer. The flow-front of the thermoset melt was still viscous and not cured when the core was injected into the mould. However, if the core delay time was increased, it was also possible that the shadow mark could be presented on the moulding surface.

Figure 6.22 shows cross sections of the sandwich injection mouldings from Figure 6.21.

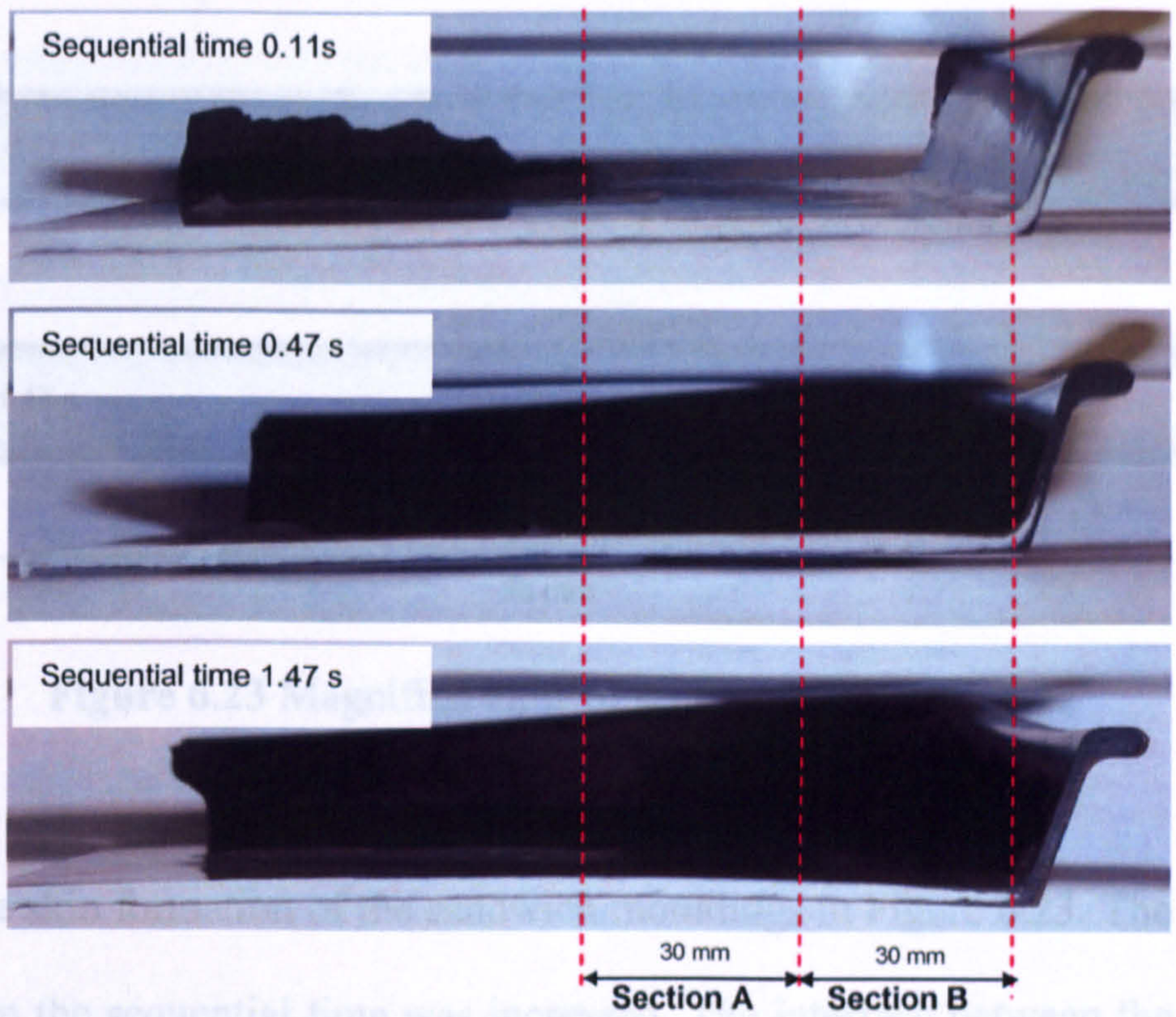

Figure 6.22 Cross sections of the sandwich injection mouldings; section A and section B are magnified and shown in Figure 6.23 and 6.24, respectively.

It can be seen from Figure 6.22 that the more sequential time or the more core delay time that was set, the less core penetration into skin was obtained. Increasing the core delay time not only gave more time for the skin to form a thicker layer but also increased the curing of the skin flow front. This resulted in a more viscous skin melt inside the mould, which made it more difficult for the core to penetrate into the skin. The close-up sections of each moulding are shown in Figure 6.23 and 6.24.

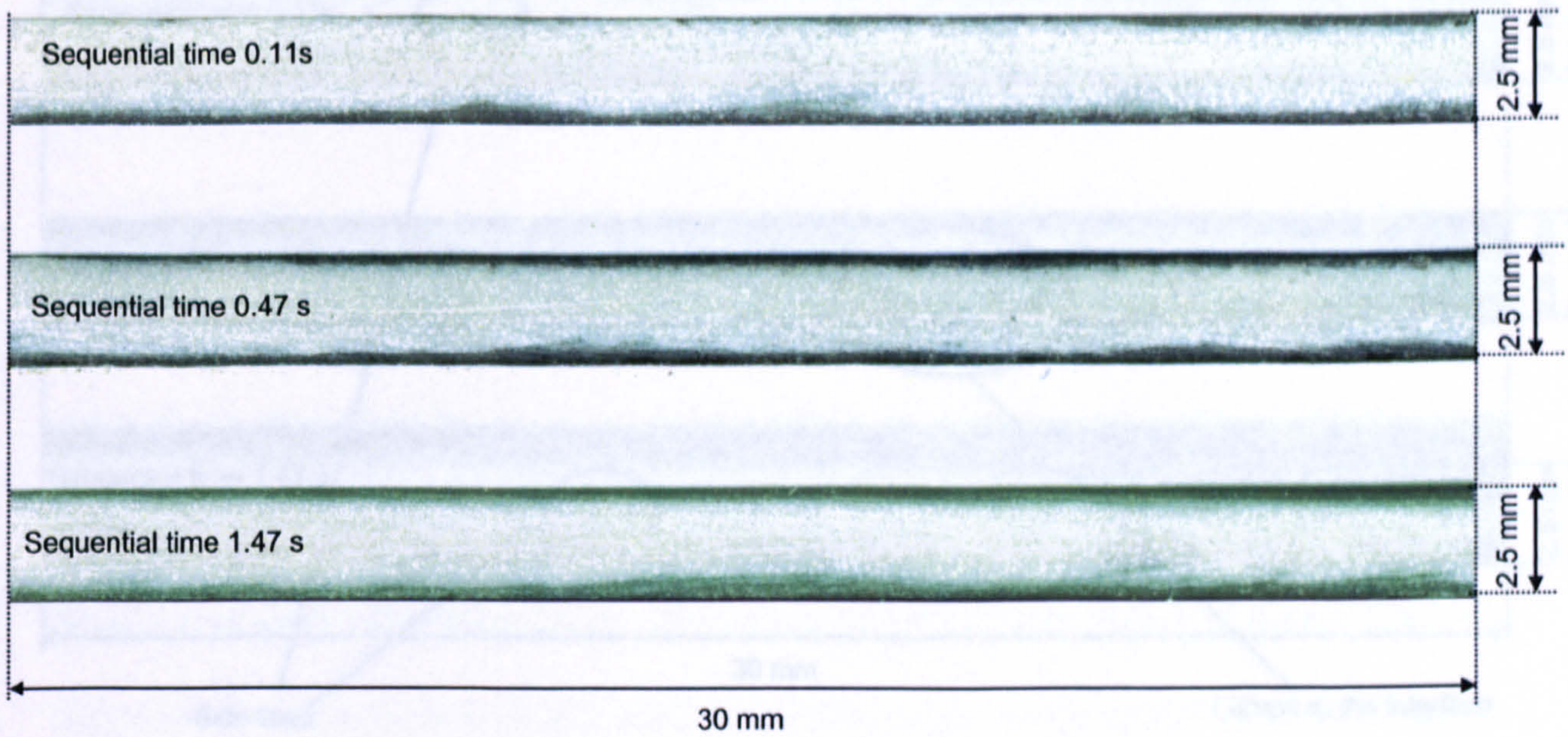

Figure 6.23 Magnified view of section A in Figure 6.22

Consider the skin formation of the sandwich mouldings in Figure 6.23. The skin was thicker when the sequential time was increased. The interface between the skin and core of the large sequential time was sharper and more defined showing that there was less material mixing between the skin and core layer during injection as the skin was more viscous when starting injection core.

The skin film was thickest when applying 1.47-second sequential time. A smaller break-through area as can be seen in Figure 6.21 and less core penetration as in Figure 6.22 show that the core volume was reduced although the same core amount was injected from the barrel. This means the core was packed in the mould and mould sprue during injection.

Figure 6.24 shows the magnification of section B from Figure 6.22. Non-uniform skin thickness can be seen here.

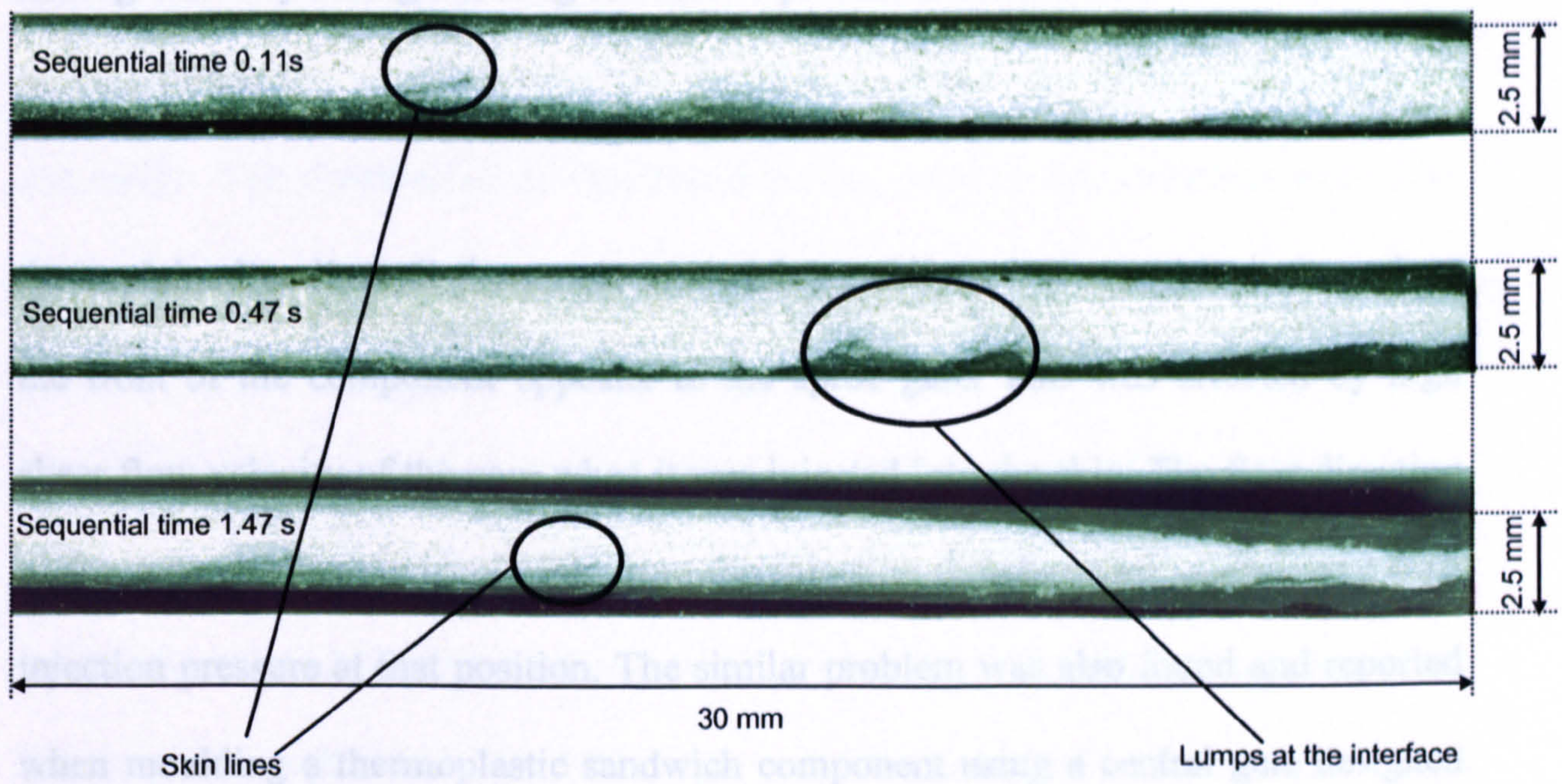

Figure 6.24 Magnified view of section B in Figure 6.22

The skin thickness was less uniform near to the moulding edge as a result of more curing there. The viscosity of the skin melt, which was pushed into the mould, became higher when it flowed further and more difficult for the core to penetrate into the skin. A parabolic flow shape in the core as a result of the fountain flow effect, which can be seen in thermoplastic sandwich mouldings as explained in Chapter 2, was also found in the thermoset case. This can be seen in Figure 6.24 when sequential time was 0.47s and 1.47 s. Lumps at the interface between the skin and core were found when the skin viscosity was too high and too difficult to be pushed further by the core as can be seen in Figure 6.24 at 0.47-second sequential time.

The sections showed more mixing between skin and core here as can be seen from some small skin lines in the core layer in Figure 6.24. Cross-linking between the layers started while the core was flowing into the skin. At some positions, the cross

linking was very strong enabling the core to pull some skin material with it as it was moving forward.

As explained earlier, all thermoset sandwich mouldings had core break-through at the front of the component opposite to the sprue gate. This was affected by high shear flow velocity of the core when it was injected into the skin. The flow direction of the core changed suddenly 90° from the injection direction and caused very high injection pressure at that position. The similar problem was also found and reported when moulding a thermoplastic sandwich component using a central gate designed mould[3]. However, the skin was only thinner at that position. To add additional skin layer there, the three-channel nozzle designed from Kortec provided the third channel for injecting more skin material into the mould. A diagram of this nozzle can be found in Figure 2.7, Chapter 2.

In the thermoset case, because of fibre abrasion and the higher density of BMC, the BMC core could sweep out the Interpon skin from the front of the component and leave a white circle at the centre. Even though more core delay time and more skin metering stroke were applied to the core injection, in order to increase the skin thickness and reduce the break-through problem, these parameters were not significant enough as the problem still persisted.

Another possible cause for the break-through was that the mould temperature was not consistent throughout the mould surface as a result of the lower temperature melt. The temperature of the surface around the mould sprue could be lower than the preset value, at 150°C in this experiment. Formation of the skin film at that area

required more time than the rest of the mould. During co-injection, the film may not have formed there when the core was flowing in, so the core could sweep the skin out easily. The distribution of the mould surface temperature therefore should be further investigated.

The sprue gate that had been used in this research was therefore considered not suitable for the co-injection moulding of a fibre-filled and a paint material since the sandwich area could be obtained only in some areas of the mould. A larger sandwich area would be achieved, if the BMC core could be controlled to flow in the mould more uniformly. This would reduce the abrasion between the core and the skin layer. Figure 6.25 shows the molecular flow of a thermoset material when moving the gate from the centre to an edge of the moulding. The gate type that offers the melt flow into the mould from the moulding edge is a side gate such as a fan gate and film gate.

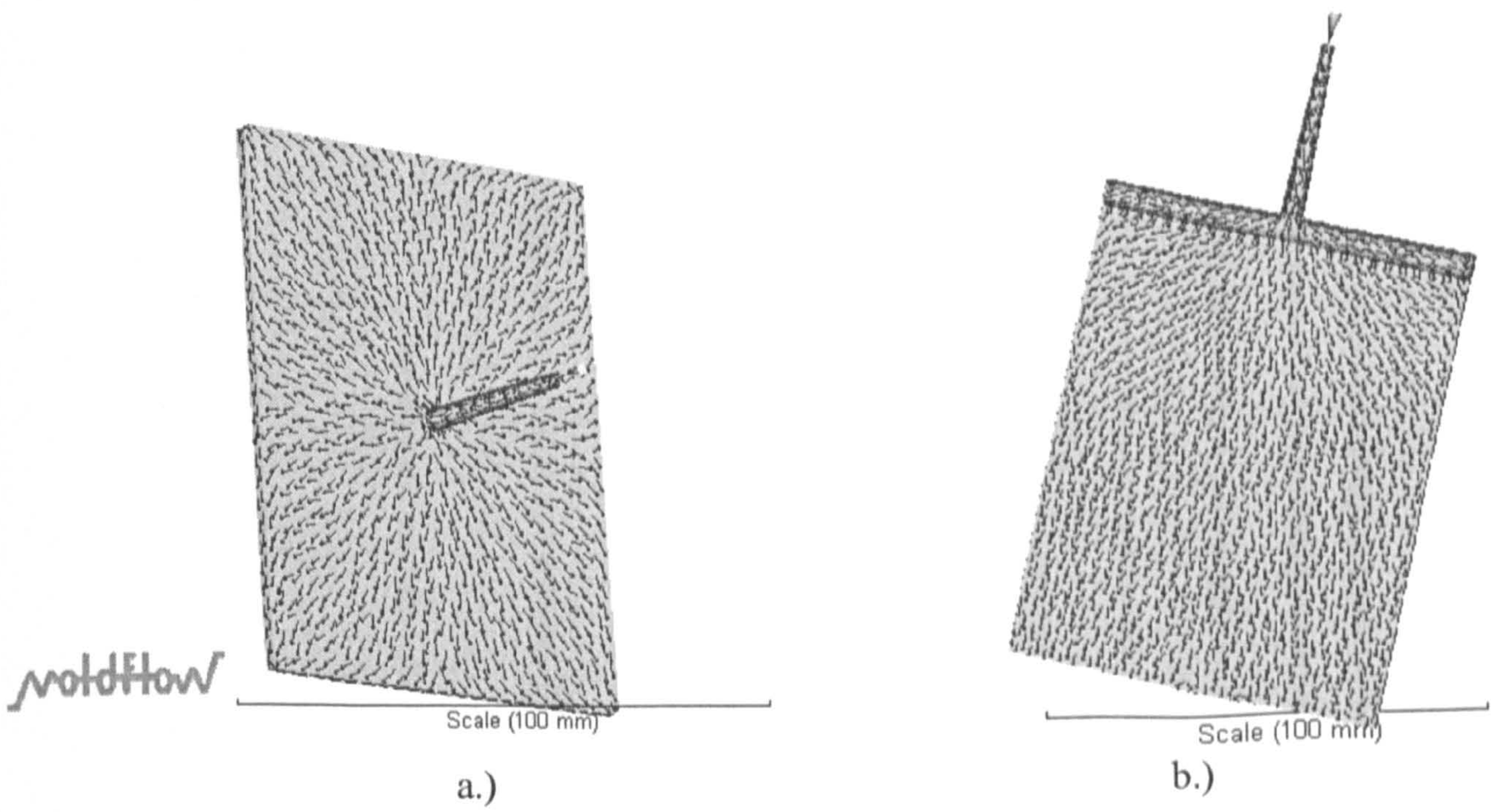

Figure 6.25 Molecular flow at the moulding skin when injecting a thermoset material from a.) Central sprue gate and b.) Side gate

The molecular flow of a thermoset when injecting the melt from a moulding edge was similar to the bottom half of the sprue gate moulding but had a larger area of good flow uniformity, which would result in a larger sandwich area. However, more shear stress and cavity pressure may occur and the melt might be cured before the mould could be completed. Therefore, the dimensions of the gate would need to be carefully considered.

Table 6.5 shows the summary of all injection moulding experiments.

Table 6.5 Summary of all injection moulding experiments

Trial No.	Describtion	Manifold temp.(°C)	Mould temp. (°C)	Delay time (s)	Metering stroke	Results	Demoulding
1	Single BMC moulding	60	150	N/A	130 mm	Good filling moulding	demoulding easily, can continueously mouding
2		70	150	N/A			
3		80	150	N/A			
4		90	150	N/A			
5	Single Interpon moulding	80	160	N/A	130 mm	Very small material injected, leaking at the top of manifold. Manifold required fixing.	Part stuck at the mould fixed half, process was not continueous. Mould was disessembled from the manifold for cleaning.
6		80	140	N/A	130 mm	Small moulding obtained, gate froze off.	
7		80	150	N/A	140 mm	Largest moulding obtained, gate froze off.	
8		80	160	N/A	140 mm	Similar size as no.6 but precuring at the flow front, gate froze off.	
9		65	150	N/A	140 mm	Small moulding similar to no.5, gate froze off.	
10		70	150	N/A	140 mm	Larger moulding than no.8, gate froze off.	
11		90	150	N/A	140 mm	Small moulding obtained, pre-curing in manifold.	
12	2K injection moulding	80	160	0	135 mm	Short shot, breakthrough at the centre, Interpon leaking at the top of manifold. The manifold required fixing.	
13	2K injection moulding	80	150	0.2	135 mm	Short shot, larger area of breakthrough at centre and some on the back, core penetraing into skin very well but very thin skin layer obtained.	
14	2K injection moulding	80	150	0.5	180 mm	Larger moulding than no.13 but short shot, smaller breakthrough at centre, no breakthrough on the back, less core penetration with thicker skin layer.	
15	2K injection moulding	80	150	1.5	190 mm	Largest 2K-moulding, almost fully filled, smallest breakthrough at center, no breakthrough on the back, least core penetration with thickest skin obtained.	

6.4.3.3 Roughness of the thermoset sandwich injection mouldings

In order to consider the effectiveness of the Interpon to paint BMC, the thermoset sandwich mouldings were cut and the roughness of the surface was measured as shown in Figure 6.26. Measuring was carried out on the front surface of the mouldings or the surface opposite to the sprue. This is because the best smooth surface could be achieved on this face as the result of high injection pressure, which was applied directly through the material onto the mould wall during injection.

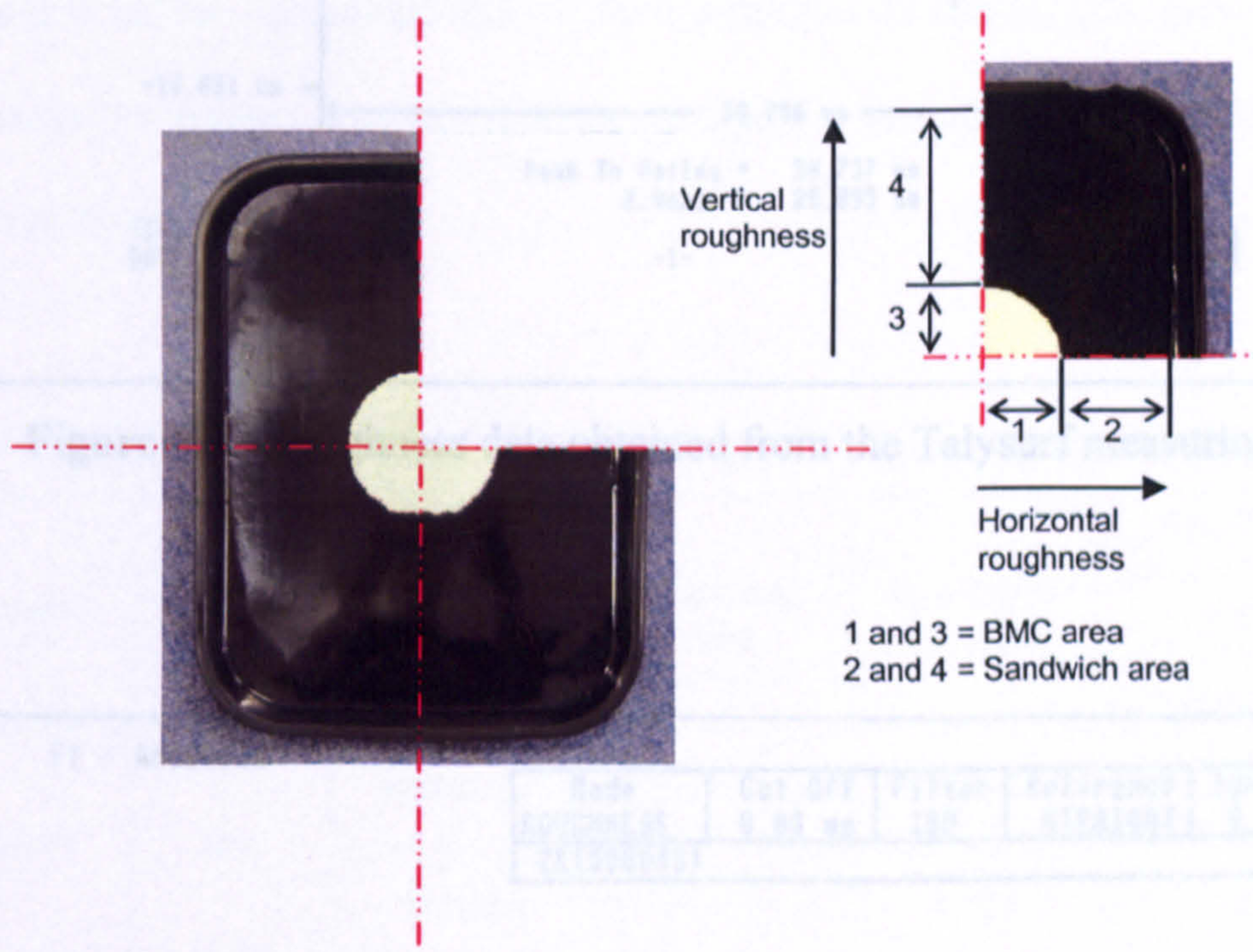

Figure 6.26 The cut sample used to measure roughness of the surface

The roughness of the moulding surface was measured by using Form Talysurf, a stylus instrument for assessment of component form, surface texture and dimensional data. A 8.0-mm cut size was used and a minimum of five profiles per sample were collected. Using these selections, the equipment would measure a 40-mm length of sample at a time. Curvature of the sample was determined during measurement and used as a mean value for computing the surface roughness. Figure

6.27 shows a graph obtained from the computed data. The roughness was reported in the separated text screen output and can be seen in Figure 6.28.

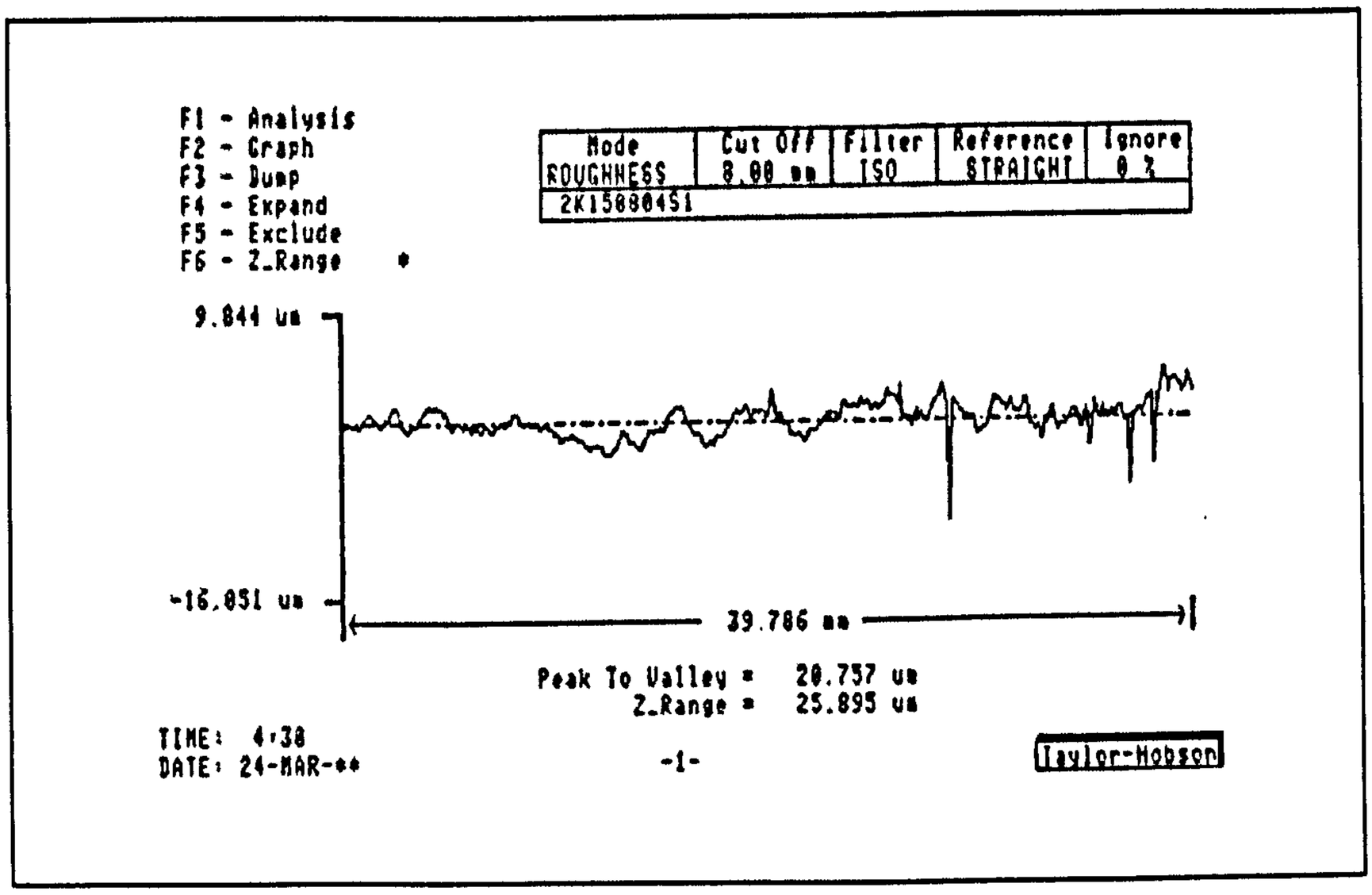

Figure 6.27 Roughness data obtained from the Talysurf measuring device

F1 - Analysis

Mode	Cut Off	Filter	Reference	Ignore
ROUGHNESS	8.00 mm	ISO	STRAIGHT	0 %
2K15080451				

Rtm	=	9.057 um	Lo	=	39.786 mm	Ra	=	1.093 um
Rpm	=	2.733 um	Rp	=	4.705 um	Rq	=	1.494 um
Ry	=	20.757 um	Rv	=	16.051 um	Rsk	=	-1.6
Rt1	=	2.522 um	Rt	=	20.757 um	Rku	=	18.5
Rt2	=	4.532 um				Delq	=	1.22 Deg
Rt3	=	5.272 um	SLOPE	=	2.17 Deg	Lamq	=	439.135 um
Rt4	=	12.203 um				S	=	497.954 um
Rt5	=	20.757 um				Sm	=	1.889 mm
						R3z	=	3.505 um
						R3y	=	6.119 um

TIME: 4:38
DATE: 24-MAR-**
-2-
Taylor-Hobson

Figure 6.28 Example of data output from surface profile

A wide range of the data output was available as can be seen in Figure 6.28. This included parameters such as surface roughness (R_a), the peak to valley height (R_t) and surface skew (R_{sk}). However, the parameter that is universally recognised and commonly used to represent the quality of surface finish is the surface roughness (R_a). Further details on the derivation of this parameter and other parameters can be found in the reference works provided[76,77].

Table 6.6 shows the surface roughness (R_a) of the sandwich mouldings, which was measured in the horizontal and vertical direction as shown in Figure 6.26. At each direction the sample was divided into two areas; including BMC break-through area and sandwich area.

Table 6.6 The roughness of the thermoset sandwich injection mouldings

Sample	Delay time (s)	Measuring direction **	Measuring area	Roughness Ra (μm)	Average roughness of each direction (μm)	Average roughness (μm)
15080*	N/A	Horizontal		1.491	1.419	1.400
		Vertical		1.388	1.388	
2K1508002	0.2	Horizontal	BMC	4.893	2.535	3.595
			Sandwich	2.712		
		Vertical	BMC	5.914	4.656	
			Sandwich	3.216		
2K1508005	0.5	Horizontal	BMC	1.532	1.620	3.185
			Sandwich	1.707		
		Vertical	BMC	7.462	4.750	
			Sandwich	2.039		
2K1508015	1.5	Horizontal	BMC	1.274	1.184	1.520
			Sandwich	1.093		
		Vertical	BMC	2.481	1.857	
			Sandwich	1.233		

*15080 – Single injection moulding of Interpon when using 150°C mould temperature and 80°C manifold temperature
**See Figure 6.26

From Table 6.6, it can be seen that most of the roughness measured at the BMC area was higher than the value measured at the sandwich area as a result of the glass fibre in the material. The surface was improved when covering the BMC with an unfilled material, Interpon in this case, as can be seen from the roughness of the sandwich areas.

The average roughness of the sandwich mouldings was reduced or a better surface finish was obtained when increasing skin amount and core delay time. This is clearly shown by the average roughness results of the 2K1508005 and 2K1505015 sample. When increasing the Interpon metering stroke but using the same injection speed, more injection time was needed to deliver the material into the mould, in other words, the more time the material needed to stay in the mould. The melt flow front would penetrate further in the mould cavity but the viscosity was also increasing due to the cross-linking reaction. Injection of core started after a delay time, which allowed the skin to form a film or cure layer near to the mould wall. When applying more core delay time, the film became thicker as it had more time to build more cross-linking networks between molecules. The higher cured layer of the Interpon near to the mould wall and at the flow front would perform as a shell when the core melt was injected into the mould. The more viscous shell would flow slower and be more packed by the core injection, which resulted in a better surface smoothness at the sandwich area. The best result from this experiment was when injecting the core at 1.5-second delay at the highest overall metering stroke of 190 mm (2K1505015).

The roughness of the BMC area was also improved when injecting more material into the mould and increasing the core delay time due to the same reason explained

above. When the skin became more viscous, it was more difficult for the core to penetrate so the BMC melt was packed by the new BMC melt from the injection unit.

The roughness results measured in the vertical direction were more than those in horizontal direction since the materials could reach the two sides of the mould in horizontal direction before the top and the bottom. The melts then were packed there more than in the vertical direction. It was not only the surface finish of the sandwich area that was improved, but the surface of BMC area was also better. The horizontal roughness of the BMC area was surprisingly reduced from 4.893μm (sample 2K1508002) to 1.532μm (sample 2K1508005) and 1.274μm (sample 2K1508015) when more material was injected into the mould. This shows that under a sufficient packing pressure of injection moulding, a good surface finish moulding can be produced from a fibre-filled thermoset material like BMC. In order to get a good surface finish all over the moulding surface, more material was needed to fully fill the mould.

The roughness of the sample 2K1508015 was close to the value measured from the Interpon moulding (sample 15080). However, the surface of the Interpon moulding could not be considered as the best finish as a result of short shot moulding and insufficient packing pressure. The component will be much smoother if the mould is completely filled and packed.

6.5 Conclusions

This chapter contained the results of the experiments that were described in the last chapter. The initial material test results were used to set up the process parameters of the novel thermoset co-injection moulding machine in order to produce a sandwich moulding of Interpon and BMC.

Prior to the co-injection moulding, single injection experiments on each material were performed. Suitable mould temperature, manifold temperature and sprue temperatures were obtained.

Single injection moulding of Interpon was found to be more difficult than BMC. The reason for this was because Interpon was injected through a more complicated runner of the manifold system. Frictional heat during injection affected the material flow and cure and caused demoulding problems, which will be further explained later in Chapter 7.

A complete Interpon moulding produced by the novel thermoset co-injection system could not be achieved. Pre-curing of the material occurred around the manifold nozzle and mould sprue resulting in short shot moulding. Injecting BMC into the Interpon in the co-injection moulding process helped to push in the Interpon melt and reduce the melt temperature down, so a complete moulding could be achieved.

Sequential co-injection moulding was set for producing sandwich components of Interpon and BMC. Interpon was injected into the mould first and after an amount of delay time, BMC followed. This time was called 'Sequential time'.

A short shot was the result in the initial experiments, even though the overall metering stroke was the same as the setting used for moulding a complete BMC component. This was because the heat expansion of Interpon in the barrel was more than that of BMC. A greater metering stroke was required for Interpon in order to complete the mould.

Another major problem that was found in the co-injection moulding of Interpon and BMC was break-through of the core on the moulding surface, especially at the position opposite to the sprue gate. This showed that the skin film was very thin and soft when BMC was flowing into the mould. An increased sequential time and more Interpon were applied in the following experiments in order to cover the BMC layer.

Break-through of the core at the position opposite to the sprue gate may come from too low a mould surface temperature at that area. The distribution of the mould surface temperature therefore should be further investigated.

The BMC core could be covered by the Interpon skin in the rest of the moulding except the central area opposite to the sprue gate. This gate design was considered not suitable for the co-injection moulding of Interpon and BMC. A side gate such as fan gate and film gate could be a solution for this.

Curing of the skin layer was important to the skin and core formation of a thermoset sandwich moulding. Sections of the sandwich components showed a thicker skin layer when applying more sequential time and skin amount. However, less core penetration also occurred as a result of more curing skin.

Cross-links of Interpon and BMC were developing throughout the injection cycle. Thicker skin was found near to the edge of the moulding as a result of more skin curing. At the same area, more mixing between skin and core layer was also found since the cross-linking between both materials was developing during injection.

The surface finish of the sandwich mouldings was determined by measuring the roughness of the surface. The results showed the possibility of obtaining a good surface finish moulding when applying enough material and pressure into the mould. The co-injection moulding might be an alternative method for coating or painting a fibre-filled thermoset material in the automotive industry. However, the moulding technique needs more improvement in order to achieve production of Class-A surface components.

Chapter 7

Manifold system design and improvement

7.1 Introduction

The original manifold system had been designed using a general design concept for injection mould and tools internally at the International Automotive Research Centre, University of Warwick. Two manifold systems were built in order to use with the 3K-thermoplastic injection moulding machine (see Figure 2.9) and the thermoset co-injection moulding machine. At the time of starting this project, the manifold prototype for the thermoset moulding machine was used for initial single injection moulding experiments. It was found that thermoset material injected from the vertical barrel froze off inside the manifold runner because of too low a temperature there. Also, a leakage was found on the plates at the top of the manifold system where it was connected to the vertical nozzle, which caused a massive drop of injection pressure and resulted in only small amounts of the material being injected into the system. By increasing the spherical radius of the manifold plates, better sealing was obtained and the leakage problem was solved. Sets of cartridge heaters and thermocouples were added to control the manifold temperature and to maintain the material flow during injection moulding. This modified manifold was then used for all injection moulding experiments in this research. However, short shot and pre-curing of material were found during injection moulding as mentioned in Chapter 6.

This chapter describes how the modified manifold system can be improved by looking at the problems that occurred during injection moulding. The first part of the chapter explains the functions of each component assembled in the existing manifold system and the second part discusses the new design of manifold system. Both existing manifold and new manifold system have been analysed using Moldflow Plastic Insight®, an injection moulding simulation package, and are discussed in the next chapter.

7.2 The existing manifold system

7.2.1 Design concept

The existing manifold system had been built based on a general design for thermoplastic sandwich injection moulds and tools. It comprised of two halves, one was fixed on the machine and another one was able to move in order to remove excess sprue and runner after the moulding process was finished. Figure 7.1 shows the side view and the isometric view of the existing manifold system.

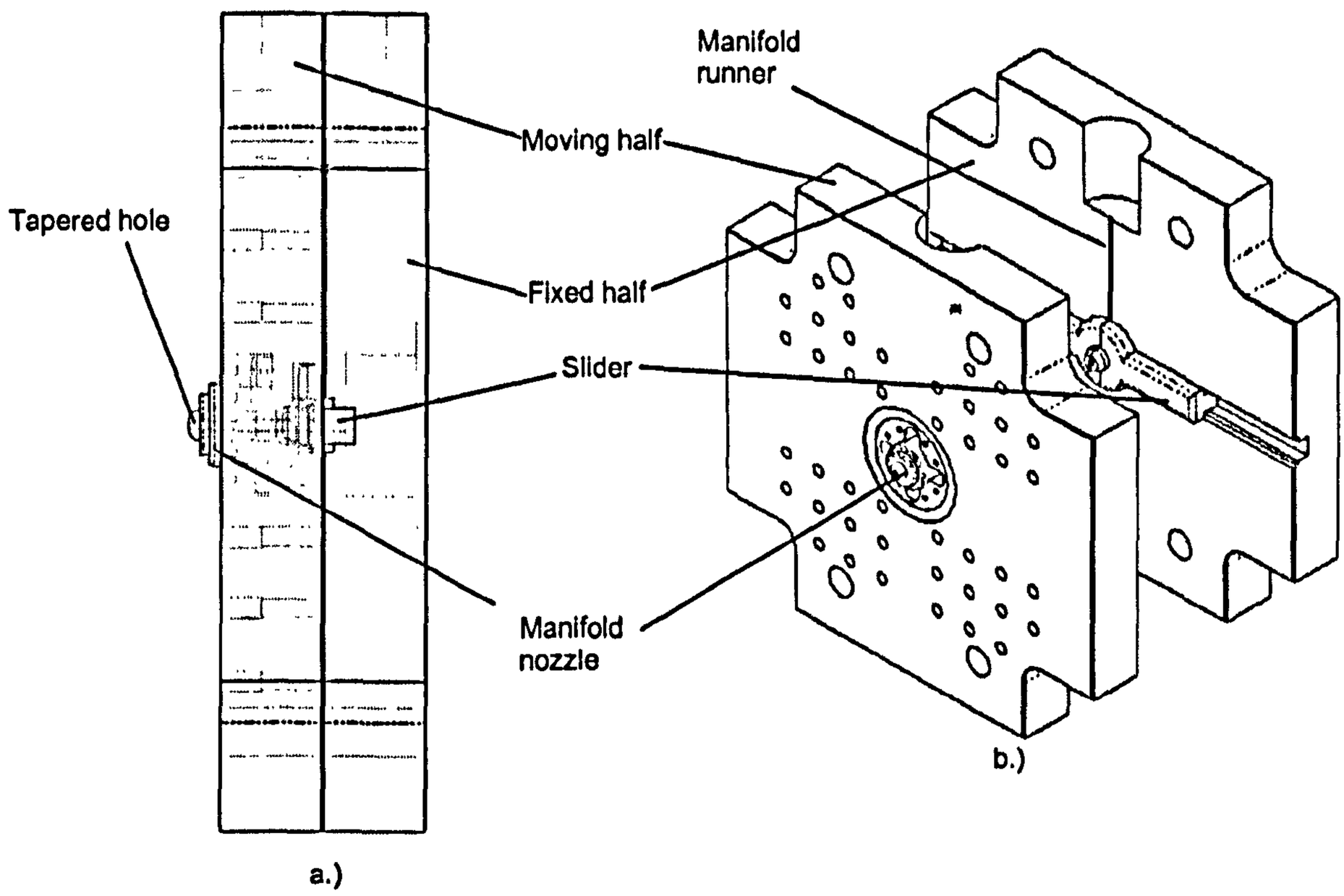

Figure 7.1 The existing manifold system a.) Side view and b.) Isometric view

The manifold moving platen consisted of a movable nozzle in the middle, which was able to move forward when the manifold was closed and backward when the manifold was opened. This was achieved by the forces from a set of springs assembled in front of the nozzle. At the closed position, this nozzle was pushed against the mould sprue. There was a 6 mm-diameter half-circle slot drilled on the back of the platen, starting from the top of the manifold to the back of the manifold nozzle. The same slot was also drilled on the front of the fixed platen. When both halves were closed, those slots would form a vertical runner. This was used to lead the skin material from the vertical barrel into the mould.

There were two sliders installed on the manifold fixed platen, which would push the manifold nozzle forward against the mould sprue when the manifold system was

closed and clamped. When finishing an injection moulding, the manifold would open and the connection between the mould sprue and the nozzle would be parted as the nozzle went backward. Solid plastic inside the system would be captured within the slider onto the fixed platen. This included the plastic inside the manifold nozzle, which would be pulled out from the tapered hole. The sliders were then opened by hand and so the whole plastic part in the manifold could be pulled out.

To keep the melt in the processing temperature range, PDE cartridge heaters from KIT electrics and type-J thermocouples were installed in both halves of the manifold. The operating temperature could be as high as 500°C however not more than 90°C was used in the experiments due to the material properties. Figure 7.2 shows the positions of all cartridge heaters and the thermocouples in the manifold. The numbers in the figure represent the thermocouple positions and the letters represent the sets of the cartridge heaters.

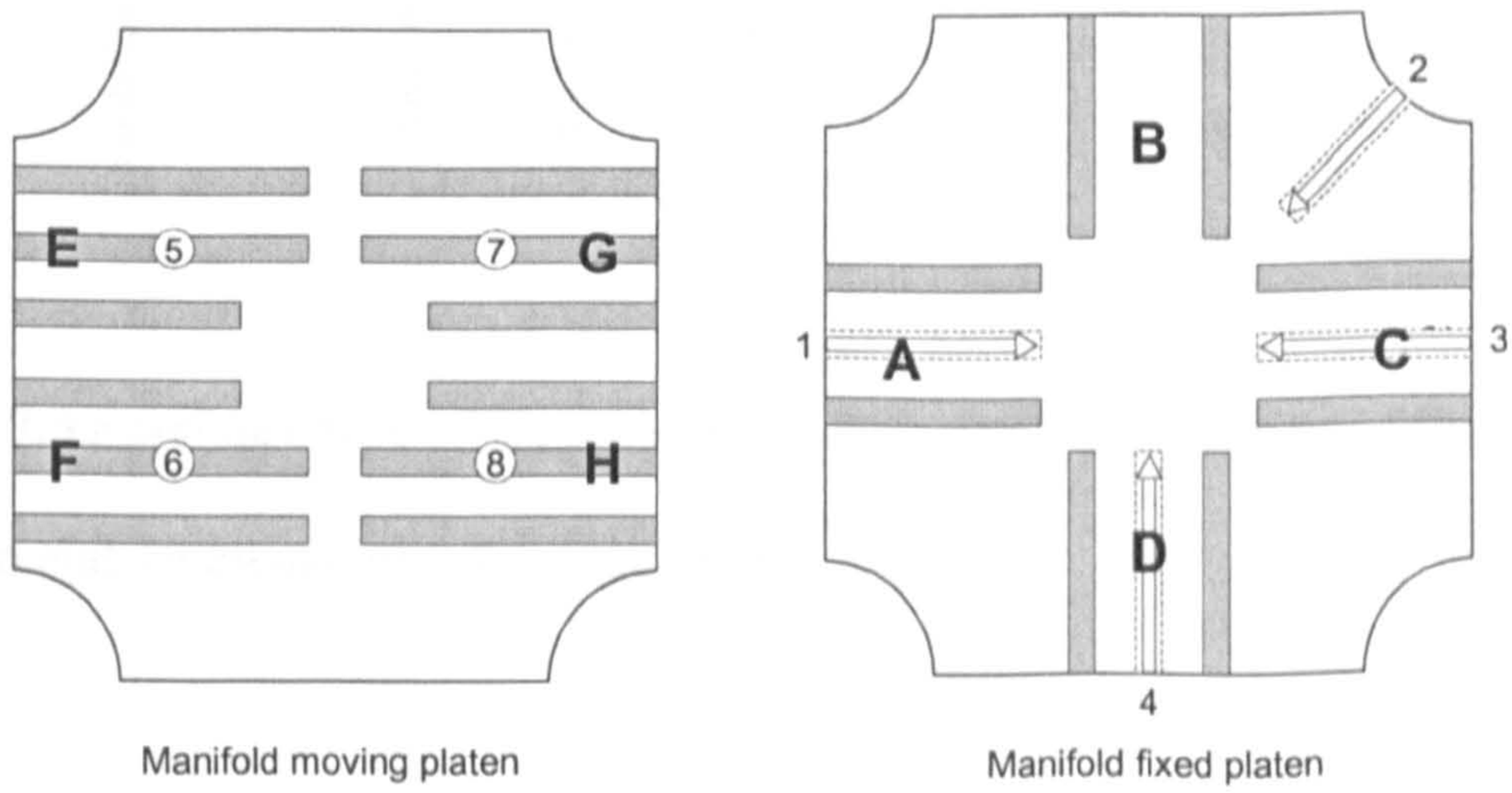

Figure 7.2 Positions of cartridge heaters and thermocouples in moving and fixed platens of the existing manifold system, where heaters thermocouples

7.2.2 Problems during injection moulding

As described in chapter 6, there were some problems during single injection moulding of Interpon and sandwich injection moulding. Full shot moulding could not be achieved when injecting Interpon alone, which was caused from material being frozen-off inside the mould sprue and manifold runner. Also, the mouldings from single and sandwich moulding sometimes jammed inside the mould fixed half since the plastic inside the mould sprue and the manifold nozzle could not be broken off. These problems were analysed and the possible causes are shown in Figure 7.3.

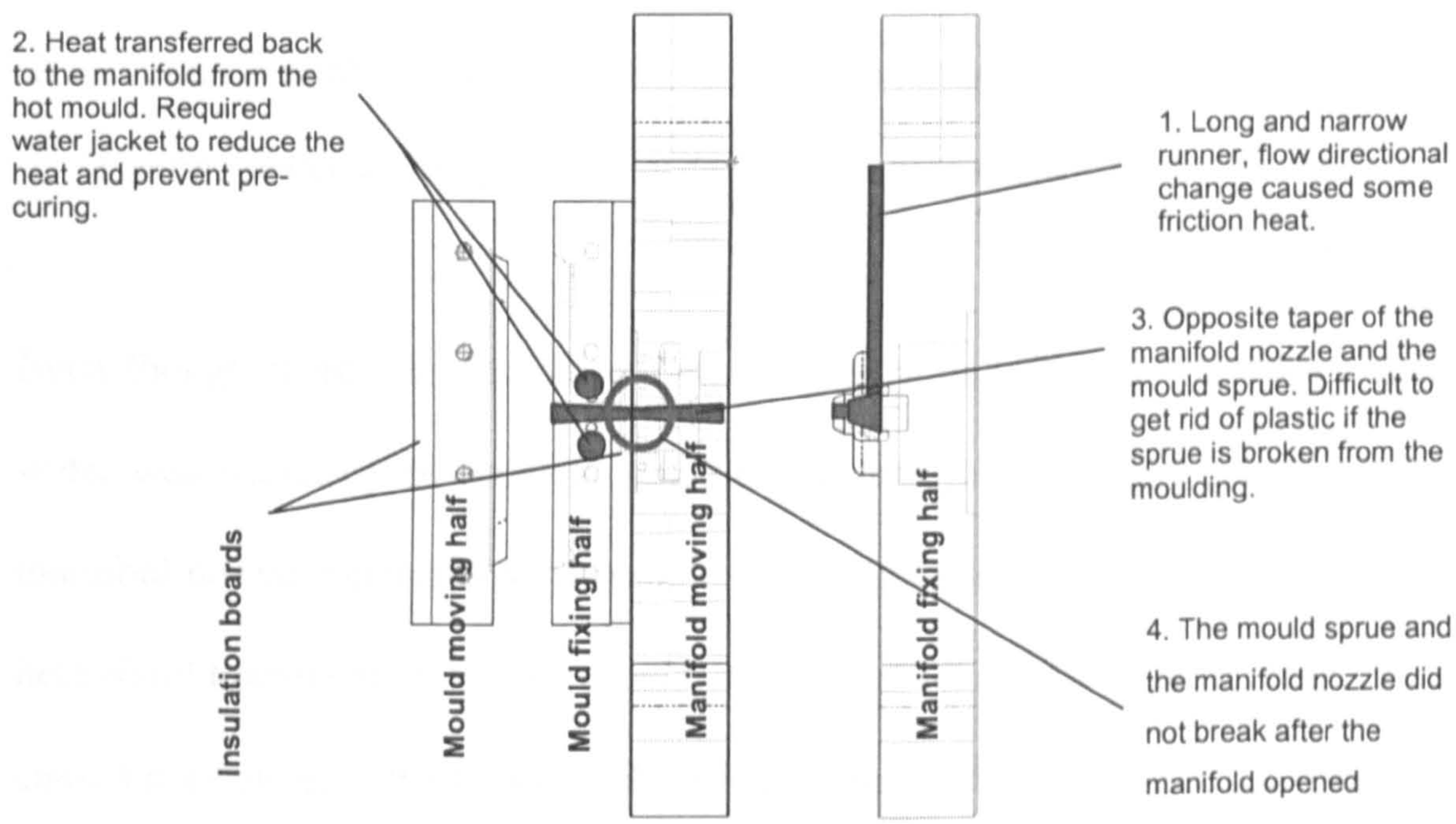

Figure 7.3 Possible cause of the problems during single injection moulding of Interpon and sandwich injection moulding

1. *Long and narrow runner with flow directional change during injection moulding.*

High shear friction occurred when the material was injected through the long and small runner of the manifold, especially where the flow direction changed. This was not practical for a highly viscous material. Increasing injection speed to overcome material pre-curing due to the cross-linking reaction inside the manifold was difficult as the higher injection speed promoted the increasing of the shear friction.

2. *Heat transferred back to the manifold moving platen from the hot mould. Cooling water was required in order to prevent pre-curing.*

Even though there was insulation between the mould and the manifold, cooling water was necessary in order to separate the manifold from the mould since the manifold nozzle connected to the mould sprue throughout injection moulding. Some heat could transfer from the hot mould, which was set at 150°C, to the manifold and caused pre-curing of the plastic melt inside the manifold nozzle. Setting temperature of the cooling water was also important as it could affect the sprue curing and sprue breaking at the end of the moulding cycle.

3. *Opposite tapers of the mould sprue and the manifold nozzle*

Normally, a tapered sprue is used to accommodate demoulding. This manifold was also designed to have a tapered hole inside the nozzle so the plastic could be removed easily from the nozzle. This hole was positioned against the mould sprue,

which had an opposite tapered direction. When a short shot happened or a plastic component in the mould was not cured enough, the sprue was likely to break from the component and become trapped inside the mould fixed half. The only way to get rid of the plastic sprue was to dissemble the mould from the manifold.

4. *Sprue did not break at the end of the injection moulding cycle.*

This problem happened when moulding Interpon in both single injection and co-injection moulding. In order to break the mould sprue from the manifold nozzle, the plastic inside the sprue must be hardened or cured enough but not too cured to degrade the melt inside the nozzle, which will be used for the next shot. Hence, the material around the connection between the sprue and nozzle was still soft at the end of the injection cycle. Practically, due to the elastic characteristic of Interpon and too short a distance between the mould sprue and the manifold nozzle, the sprue only stretched out when the nozzle moved back and was too elastic to break at the end of the mould sprue. Consequently, the whole system was blocked and the component could not be taken out of the mould until the whole system was cooled down to the room temperature.

7.3 New manifold system design concept

A new manifold system was designed based on the same manifold structure but which improved some parts in order to solve the problems that were explained in the last section. Following are the design parameters that were considered for designing the new manifold.

- The new manifold system could be installed on the thermoset co-injection moulding machine without machine modification.
- The manifold could be easily disassembled for cleaning.
- It would be equipped with a temperature controlled system to maintain the material flow during injection moulding.
- The new manifold nozzle would be able to be disconnected from the mould at the end of the injection cycle in order to reduce heat transferring from the hot mould.
- Minimise the shear friction in the system.

Figure 7.4 shows the side view and the isometric view of the new manifold that has been designed following the parameters above and using simulation results from Moldflow simulations, which will be explained in the next Chapter.

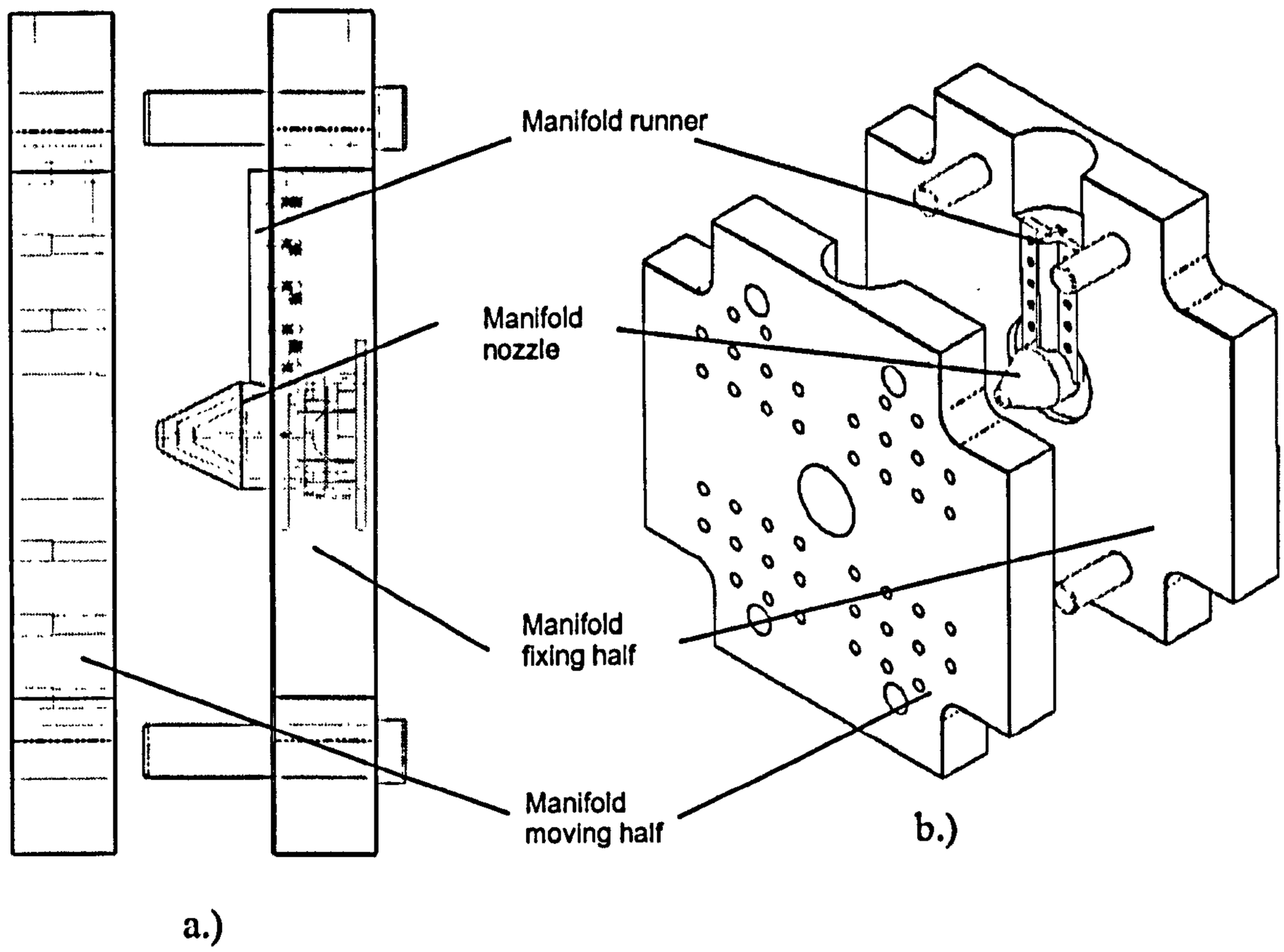

Figure 7.4 The new manifold system a.) Side view and b.) Isometric view

The manifold nozzle is moved from the manifold moving platen to installation in the fixed platen. The moving platen is now having only a plain hole in the middle and is used for installing the mould fixed half only. This new nozzle will be able to move forward to connect to the mould sprue by a pushing force from the horizontal injection unit during injection moulding and move backward by a spring set installed inside the manifold fixed platen when the injection unit retracts. The nozzle and the sprue then separate. This helps to reduce heat transfer from the mould to the melt inside the nozzle. As a result, the cooling water unit as installed in the existing design manifold is unnecessary. Another advantage of this new nozzle is there is no opposite taper hole at the back of the mould sprue so that it gets rid of the blockage problem and the moulding can be taken out easily. Table 7.1 shows the operating sequence of the new manifold system.

Table 7.1 Operating sequence of the new manifold system

Steps	Details
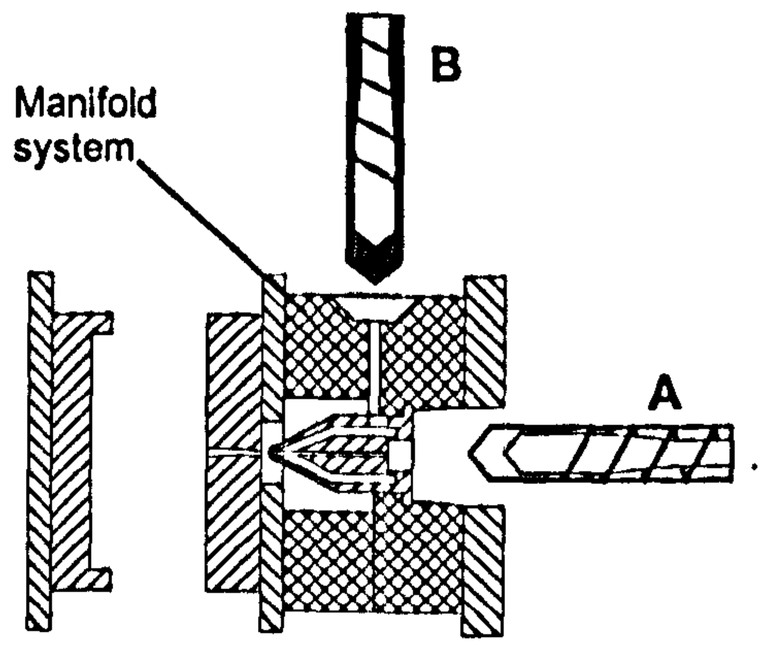 Step 1	To start the injection cycle, the manifold is hydraulically closed. Core barrel A and Skin barrel B are charged with some molten thermoset plastic that is adequate to fully fill the mould.
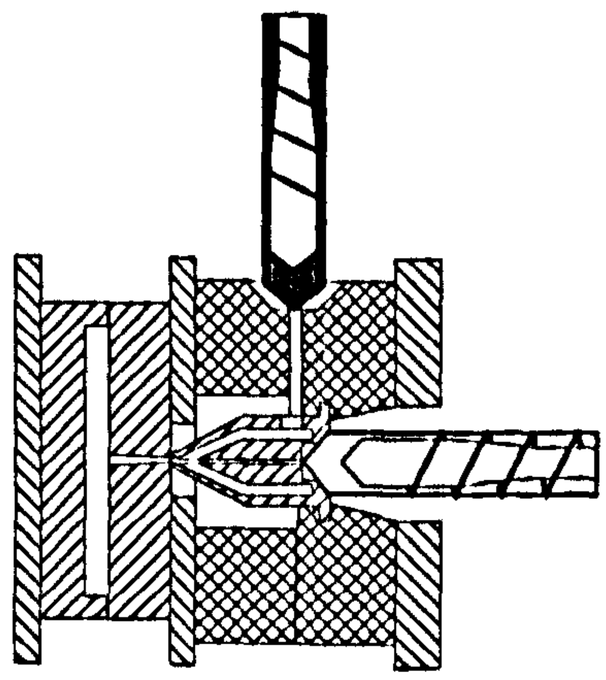 Step2	The mould is closed and clamp locked. Main injection A and B move forward to face the manifold. The manifold nozzle is pushed forward to against the mould sprue by the A-barrel.
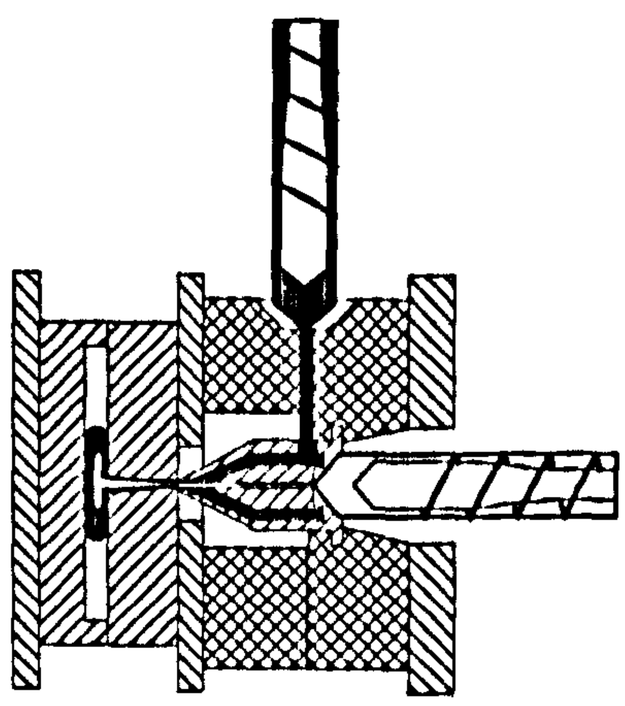 Step 3	Some skin material is injected from injection unit B. After a small delay time, screw A, which is inside the injection unit A moves forward to inject some core material into the mould cavity.

Table 7.1 Operating sequence of the new manifold system (continue)

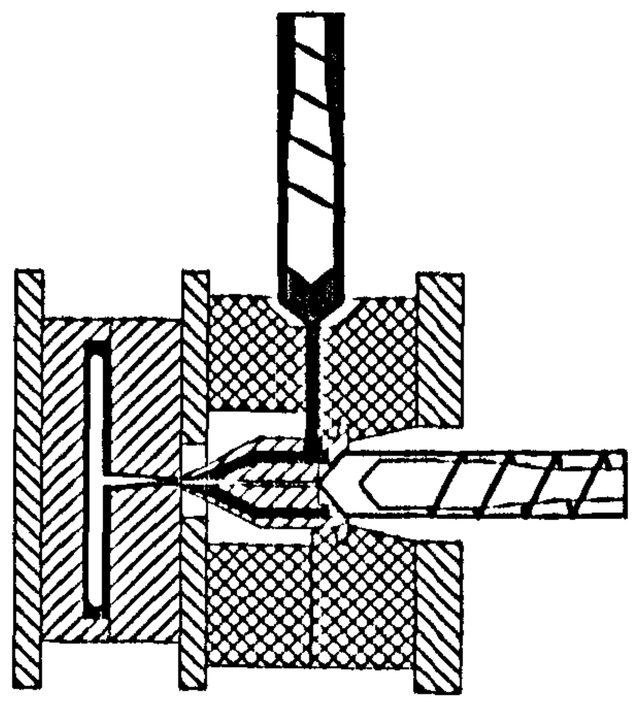 Step 4	The two injection units continue delivering the materials into the mould until the mould is fully filled. The screw A then stops while B keeps pushing some material in by pressure in holding phase. The curing cycle follows.
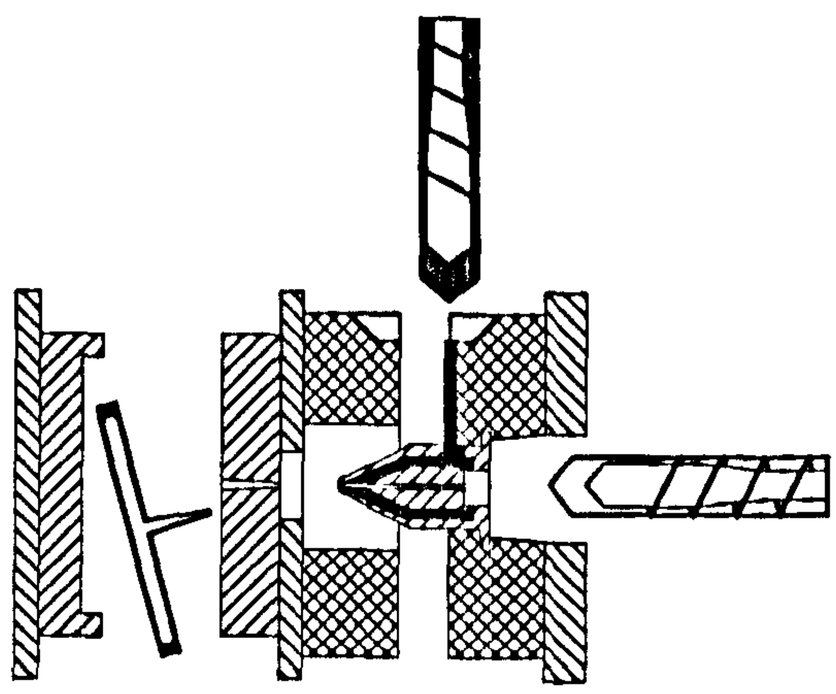 Step 5	Injection unit A and B are recharged with fresh materials and retract from the manifold during the curing cycle. The manifold nozzle moves backward. After the curing time is reached, the mould and manifold open to release the component. Step 1 to 5 is repeated again for the next injection cycle.

The nozzle is fitted inside the manifold between two rings so that it can be removed from the front and the backsides. On the fixed platen, a set of inserts will be screwed in to function as a new manifold runner with a larger diameter. All of the components are designed for easy disassembly, so the parts can be cleaned easily

when pre-curing and blockage occur. Figure 7.5 shows a close up view of the new nozzle.

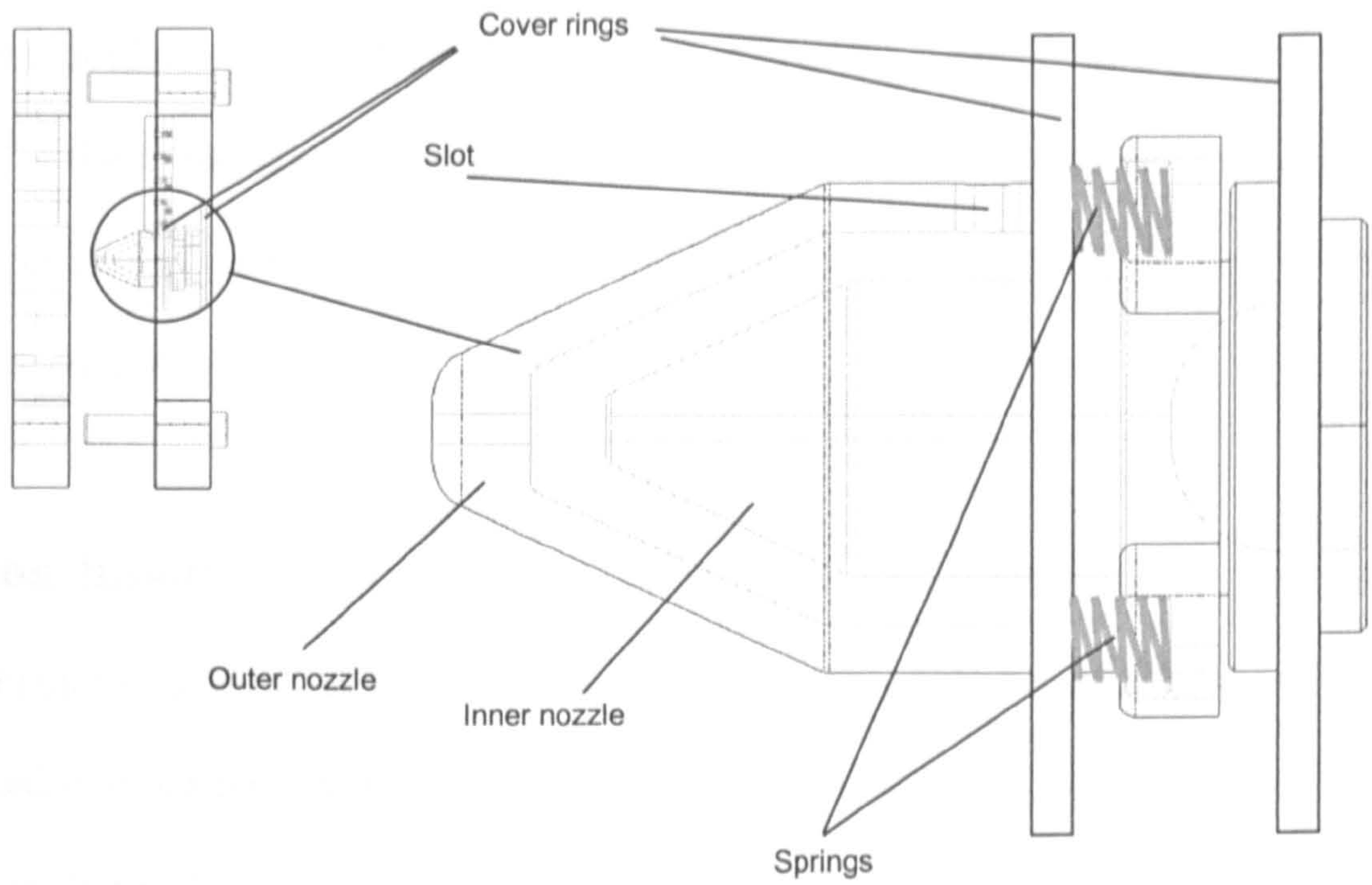

Figure 7.5 Close-up view of the new nozzle design

The new nozzle comprises a smaller inner nozzle screw fitted in an outer nozzle for skin and core material, respectively. The skin melt will flow from the vertical runner through a hole on the top of the outer manifold, while the core melt will flow through the inner nozzle. After finishing the whole injection moulding process, one of the rings can be taken off to release the nozzle from the manifold and then the inner nozzle can be unscrewed from the outer nozzle to clear out the trapped materials inside.

The manifold platens will be installed with sets of cartridge heaters and thermocouples to maintain the manifold temperature in order to keep the material

flowing during injection. Insulation boards at the back of the platens are necessary to increase the heaters' efficiency and reduce the heating time.

This manifold system will be compared with the existing one in terms of flow and cure of a thermoset material in the system by using a simulation software package and explained in next chapter. Full assembly and part drawings of this new system can be seen in Appendix I.

7.4 Conclusions

This chapter identified the problems occurring with the existing manifold system that was used in this research. These problems resulted in the ability to produce only one injection shot in the machine before the need to stop for cleaning.

A new manifold concept, which was designed to improve the existing manifold system, was proposed and explained. It was proposed that this design could solve the problems of the existing manifold system so the moulding cycle could be continued without having to stop the machine for cleaning. However, it needed more experiments to prove the design. The system will now be compared with the existing manifold by using a simulation software package. This will be further explained in the next chapter.

Chapter 8

Thermoset Injection Moulding Simulation

8.1 Introduction

Together with the injection moulding operation itself, plastic injection moulding simulation helps moulders to understand the mechanism of shaping plastic from the beginning of injecting material into the mould until a finished part is acquired. This is very useful for product development as a lot of information can be gained before doing the real work on the machine in terms of mould design and process design, i.e., it gives sufficient information for making and improving prototype mould tools and provides useful results for machine condition settings. Consequently, trial and error experiments can be reduced to a few tests and hence, reduction of overall product development time and cost.

Moldflow Plastic Insight® is a simulation software package for plastic injection moulding. The software version 4.1 offers a Reactive moulding module, which is designed for simulation of thermoset and rubber single injection moulding, reaction injection moulding (RIM), structural reaction injection moulding (SRIM) and resin transfer moulding (RTM). The analysis module generates results from the calculations of many input parameters such as material melt temperature, mould temperature, viscosity and gelation using the reactive viscosity model (Equation 8.1 and 8.2) and Kamal's reaction kinetic equations (Equation 8.3 to 8.5).

$$\eta(\alpha,T,\dot{\gamma}) = \frac{\eta_0(T)}{1+\left(\frac{\eta_0(T)\dot{\gamma}}{\tau^*}\right)^{1-n}}\left(\frac{\alpha_g}{\alpha_g-\alpha}\right)^{(C_1+C_2\alpha)} \tag{8.1}$$

$$\eta_0(T) = B\exp(T_b/T) \tag{8.2}$$

where η is the viscosity (Pa.sec)

$\dot{\gamma}$ is the shear rate (1/sec)

T is the temperature (deg.K)

α is the conversion or degree of cure (0-1)

n,τ^*,B,T_b,C_1,C_2 and α_g are data fitted coefficient, which is constant dependent on material.

$$\frac{d\alpha}{dt} = (K_1 + K_2\alpha^m)(1-\alpha)^n \tag{8.3}$$

$$K_1 = A_1 e^{(-E_1/T)} \tag{8.4}$$

$$K_2 = A_2 e^{(-E_2/T)} \tag{8.5}$$

where m, n, A_1, A_2, E_1 and E_2 are constant parameters.

As it was described in chapter 3 and 4, heat has been considered as a very important parameter in thermoset processing. The temperature of the material inside the mould can therefore be a useful guide to determine the process and settings. This simulation programme had been used to help the study relating to flow and cure of a thermoset in the manifold system and the mould under different injection parameters by investigating the changes of the material temperatures inside the mould. Since there

was no material in the database that exactly matched the material that was used in the experiment, general grade thermoset polyester without fibre fill was selected for the simulations. The results then could not be used to explain the flow behaviour of the materials, which were used in the experiments, in the manifold system. However, they could help to point out the problems that would happen when injecting a thermoset through the manifold in general.

The first part of simulation considered the whole system including the existing manifold runner and the moulding as a plastic component in order to study how the material would flow through the whole system when the tool temperature was changed from a low level to a high level. At each temperature, the injection speeds were also varied from a very fast injection time of 1 second to a very low injection time of 5 seconds.

The second part of the simulation considered filling and curing of the tray mould alone, at different mould temperatures varied from 80 to 140°C and different injection speeds from 1 to 5 second. It was assumed in this case that there was no effect from the manifold on the material flow so the melt temperature was constant at 80°C before injection into the mould.

The new manifold system explained in last chapter was designed and analysed using Moldflow® with the same set of condition settings as the existing system. The final part of the chapter shows the simulation results of this new system. Examples of Moldflow simulation screen outputs can be seen in Appendix II.

8.2 Moldflow® simulation of the existing manifold system and the tray

In order to study the effect of the runner on mould filling, in this simulation, the existing manifold and the tray mould were considered as a single mould, which could produce a tray and a manifold runner as a single plastic component. By doing this, flowing of the material from the injection nozzle through the manifold runner into the mould could be determined. However, the temperature set for the system had to be lower than the actual mould temperature for this material, which is normally at 140-180°C. The simulation could not represent the post process qualities of the moulding components such as the percentage of cure, warping and shrinkage ratio.

The meshing solid model is shown in Figure 8.1. A thermoset polyester was injected from the vertical direction as illustrated by an arrow. Points on the figure show different positions on the moulding that would be used to represent the melt temperatures, which will be discussed in section 8.2.2.

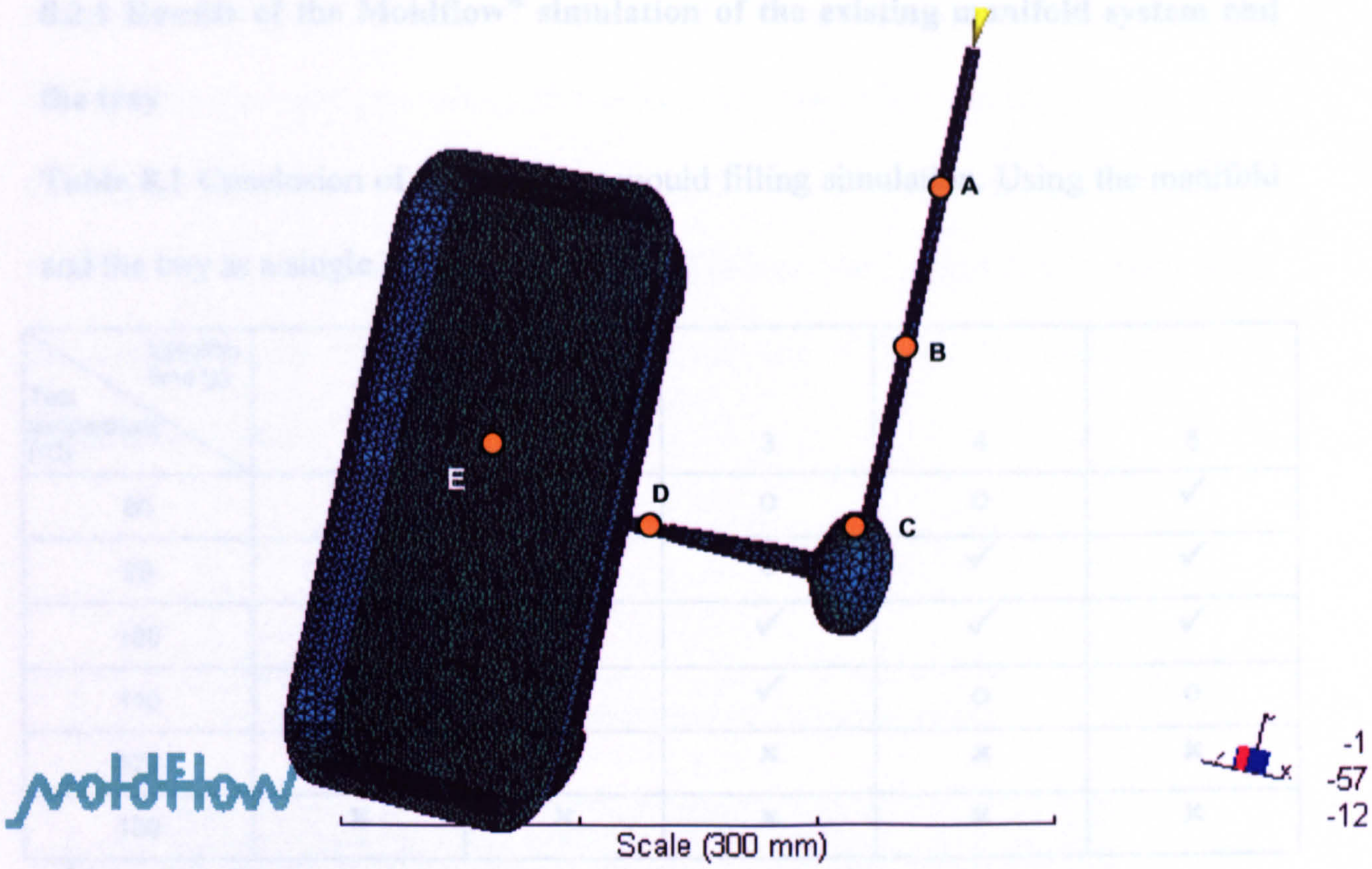

Figure 8.1 The meshing model of the tray and the existing manifold runner

The input tool temperature was varied from 80 to 130°C. At each temperature, injection times were changed from 1 to 5 seconds. Table 8.1 shows the conclusion of the filling simulations.

Since a cross-linking reaction is exothermic, the changing of material temperature is an indicator to predict the curing and is therefore, related to the material flow ability in the mould. During injection, material temperatures at different positions of the tools were recorded.

8.2.1 Results of the Moldflow® simulation of the existing manifold system and the tray

Table 8.1 Conclusion of the polyester mould filling simulation. Using the manifold and the tray as a single mould.

Tool temperature (°C) \ Injection time (s)	1	2	3	4	5
80	o	o	o	o	✓
90	o	o	o	✓	✓
100	o	✓	✓	✓	✓
110	o	✓	✓	o	o
120	✓	o	✗	✗	✗
130	✗	✗	✗	✗	✗

✓ Complete filling obtained without pre-curing reported.

o Complete filling but pre-curing was reported.

✗ Cannot complete filling. Short shot and pre-curing was reported.

From the simulation results in Table 8.1, it was shown that the mould could be fully filled when it was set at 80-120°C, however, pre-curing was reported at some injection times. Although the simulation showed that the material pre-cured in the cases when injection time was 2 seconds and mould temperature was at 80, 90 and 120°C, the causes of pre-curing at the low temperature of 80°C and 90°C were different from the high temperature of 120°C. Figures 8.2-8.4 show the melt temperature of the material in the mould at different positions as shown in Figure 8.1. These three graphs show completely different temperature distributions. At low temperature (Figure 8.2), the temperature gaps between each position were uneven compared to those at high temperature (Figure 8.4), meaning that as the melt flowed through each position in the manifold and the mould, some heat was generated in the

system. This was caused by shear friction of a flowing viscous material and resulted in some hot spots and pre-curing. This effect was small when compared to the effect of using a high mould temperature, which led to high cross-linking rate of the whole material inside the mould and the manifold. The moulding at low temperature could be completed but the material was viscous and difficult to inject into this complicated system.

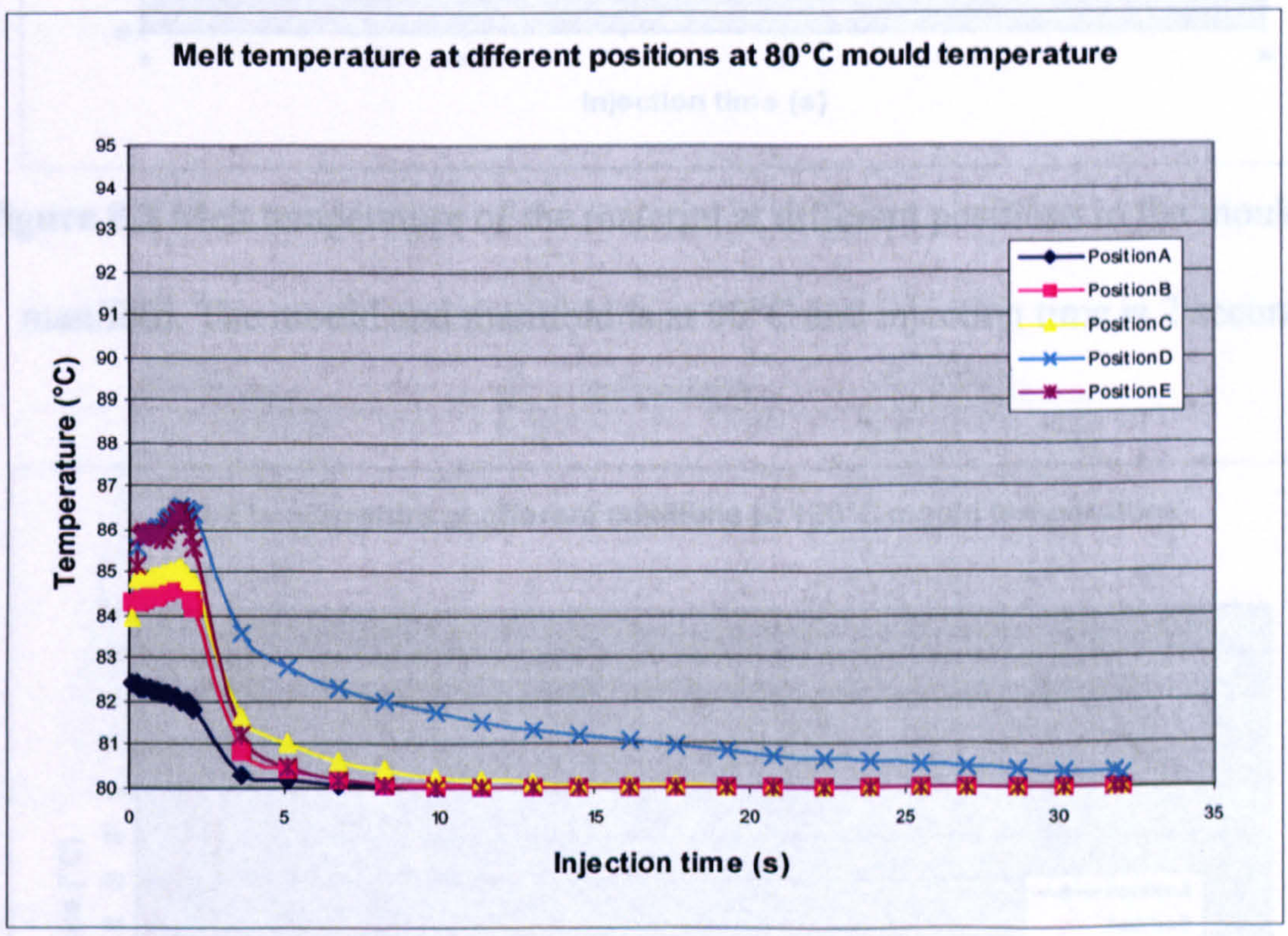

Figure 8.2 Melt temperature of the material at different positions in the mould and manifold. The mould and manifold is at 80°C and injection time is 2 seconds.

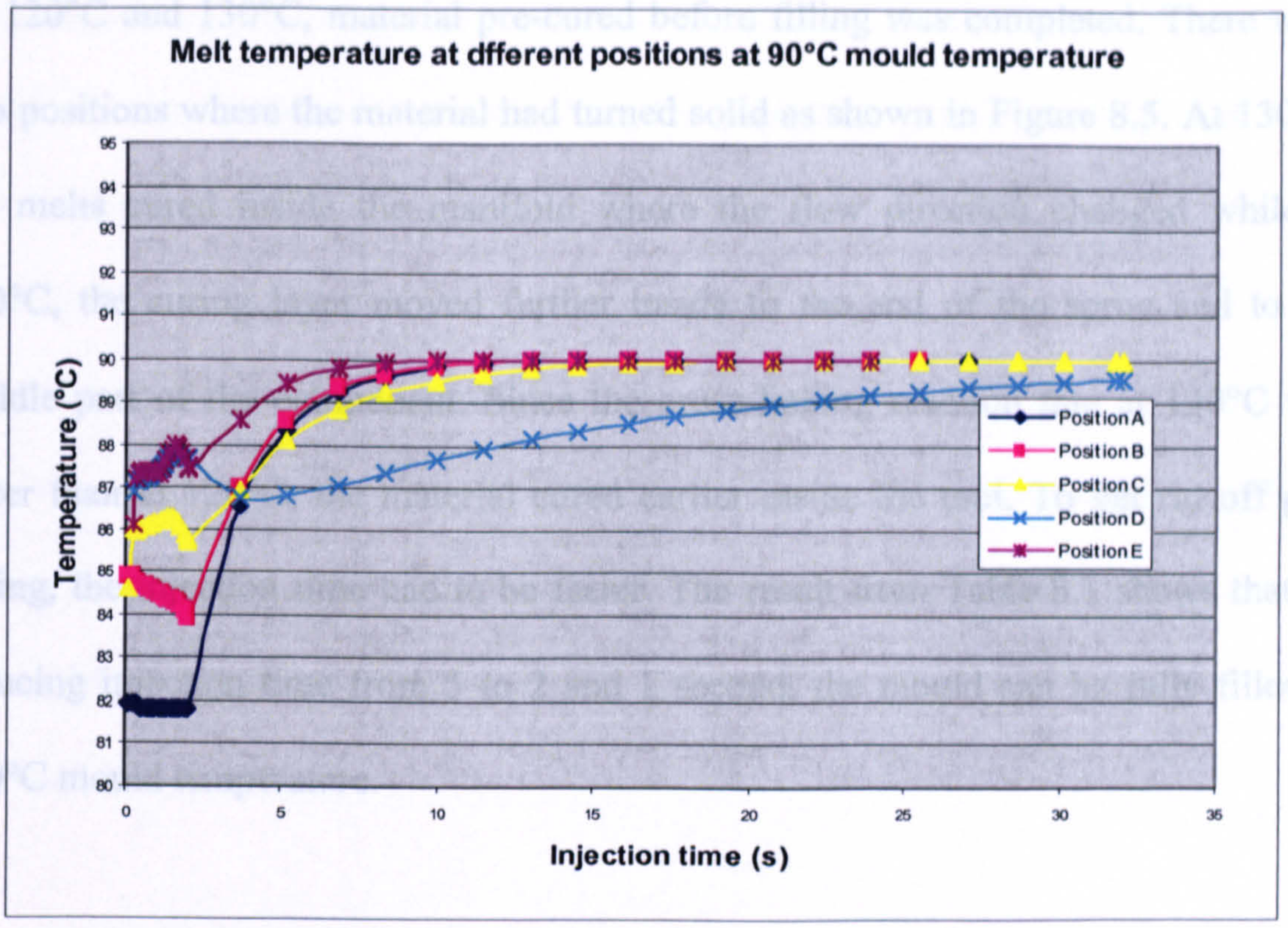

Figure 8.3 Melt temperature of the material at different positions in the mould and manifold. The mould and manifold is at 90°C and injection time is 2 seconds.

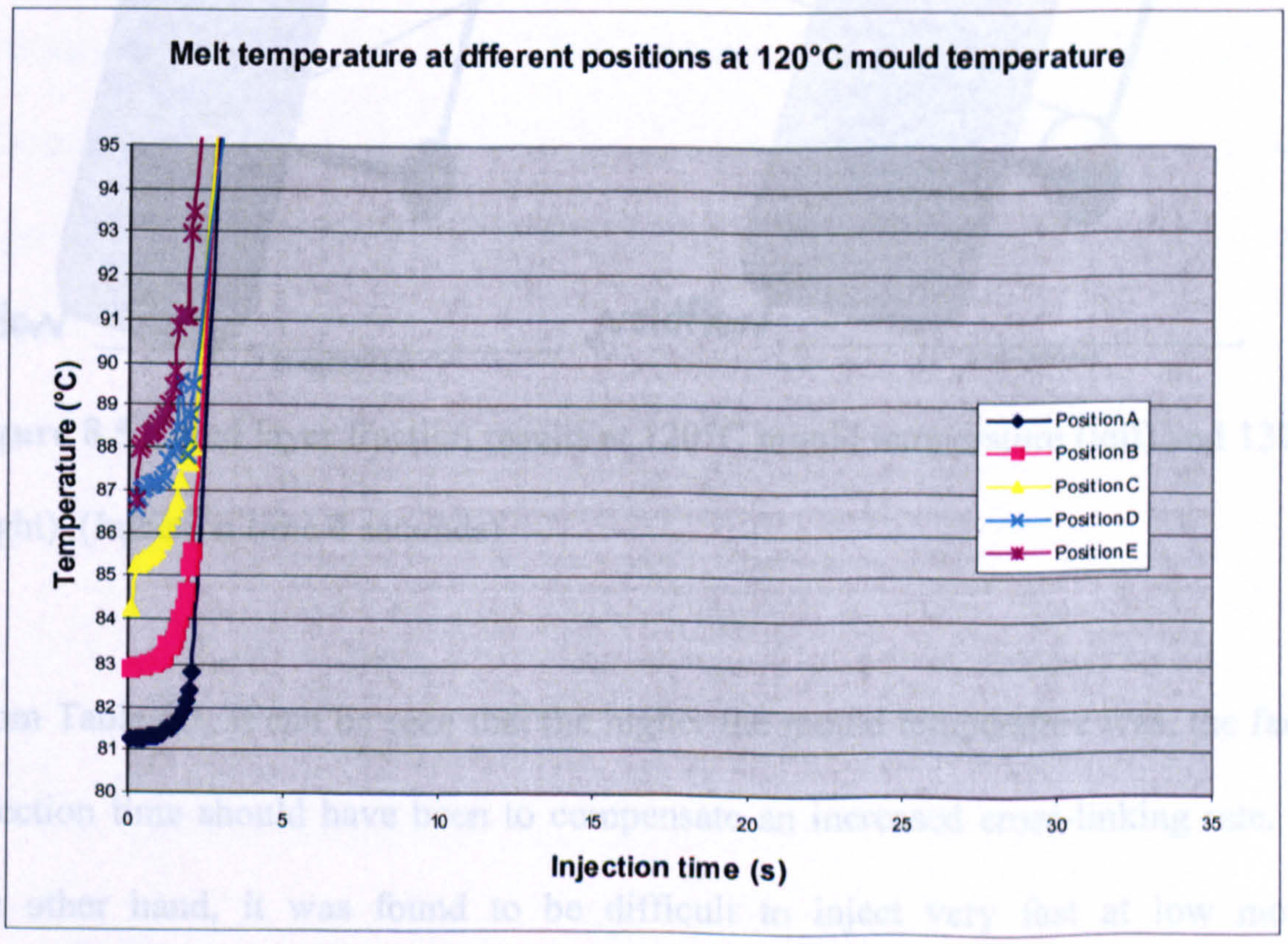

Figure 8.4 Melt temperature of the material at different positions in the mould and manifold. The mould and manifold is at 120°C and injection time is 2 seconds.

At 120°C and 130°C, material pre-cured before filling was completed. There were two positions where the material had turned solid as shown in Figure 8.5. At 130°C, the melts cured inside the manifold where the flow direction changed while at 120°C, the curing layer moved further inside to the end of the sprue and to the middle part of the component. Since the cross-linking reaction rate at 130°C was faster than at 120°C, the material cured earlier inside the tool. To get rid off pre-curing, the injection time had to be faster. The result from Table 8.1 shows that by reducing injection time from 5 to 2 and 1 second, the mould can be fully filled at 120°C mould temperature.

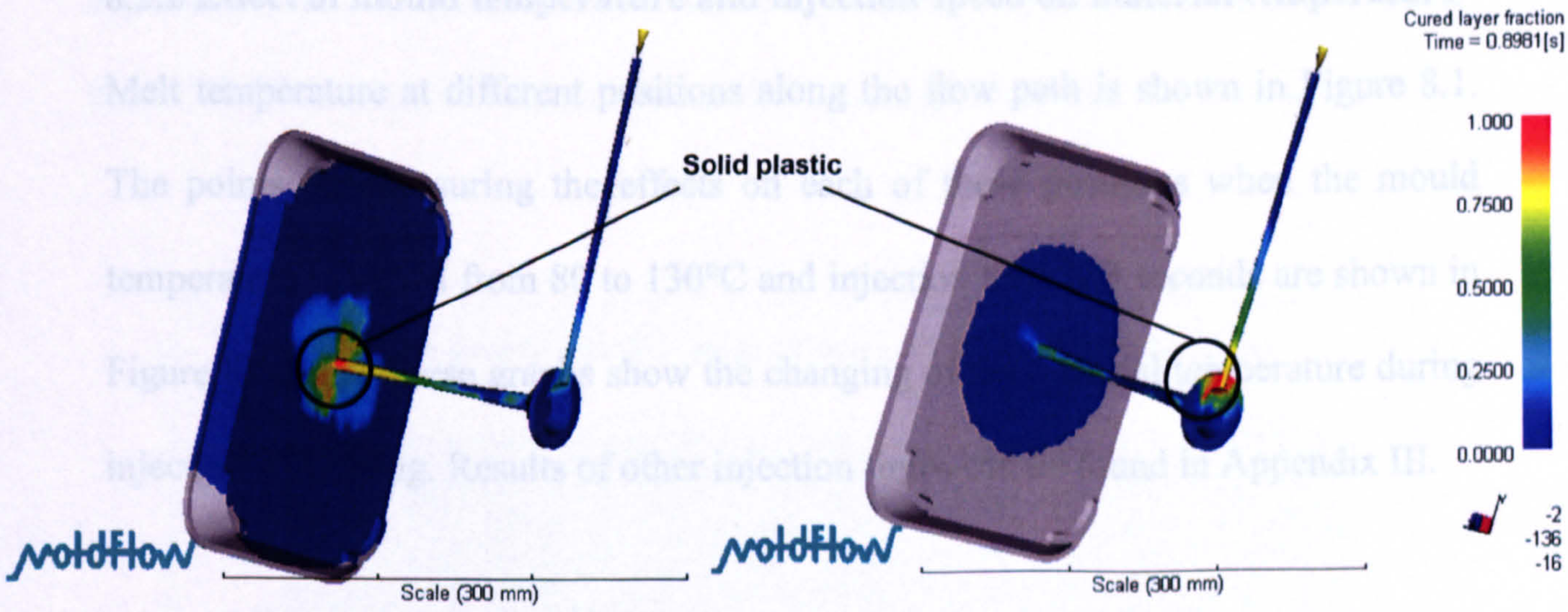

Figure 8.5 Cured layer fraction results at 120°C mould temperature (left) and 130°C (right) (Injection time 4 seconds)

From Table 8.1, it can be seen that the higher the mould temperature was, the faster injection time should have been to compensate an increased cross-linking rate. On the other hand, it was found to be difficult to inject very fast at low mould temperatures due to the material's high viscosity and hence, high inertia and hot spots could occur during injection.

The inertia did not have much affect when injecting slowly as can be seen from Table 8.1. At 5-second injection time, the moulding could be completed at 80-100°C. Furthermore, the temperature window was larger if the injection time was slower. For example, 120°C mould temperature was the optimum for a 1 second injection time, 100-110°C were the optimum temperatures of 2 and 3 second, 90-100°C were the optimum temperatures of 4 second and 80-100°C were the optimum temperatures of 5 second injection time. It should be noted that in this case, too high a mould temperature could cause pre-curing before all of the material could be injected into the mould.

8.2.2 Effect of mould temperature and injection speed on material temperature

Melt temperature at different positions along the flow path is shown in Figure 8.1. The points for measuring the effects on each of these positions when the mould temperature is varied from 80 to 130°C and injection time is 3 seconds are shown in Figure 8.6-8.11. These graphs show the changing of the material temperature during injection and curing. Results of other injection times can be found in Appendix III.

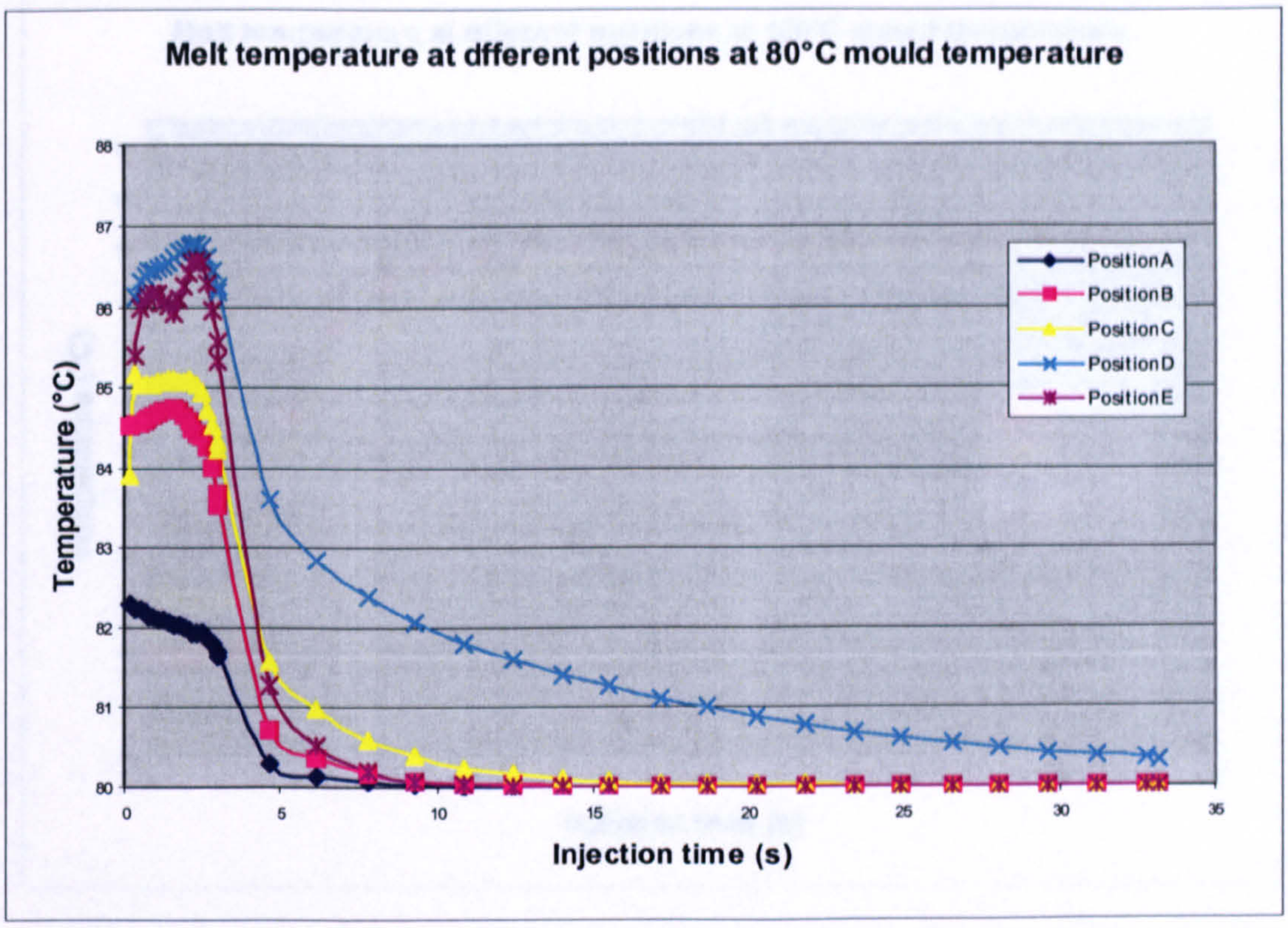

Figure 8.6 Melt temperature of the material at different positions in the mould and manifold. The mould and manifold is at 80°C and injection time is 3 seconds.

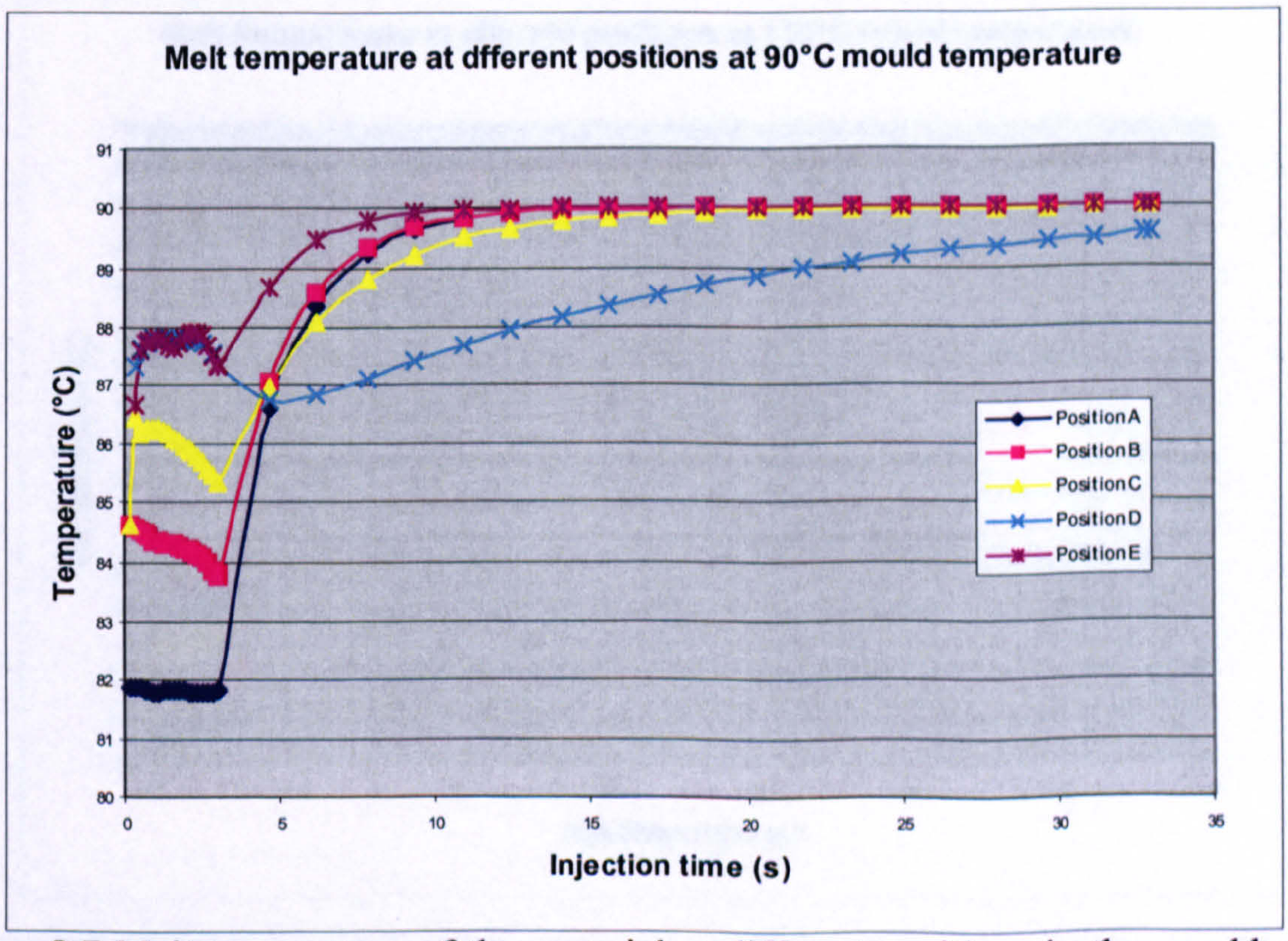

Figure 8.7 Melt temperature of the material at different positions in the mould and manifold. The mould and manifold is at 90°C and injection time is 3 seconds.

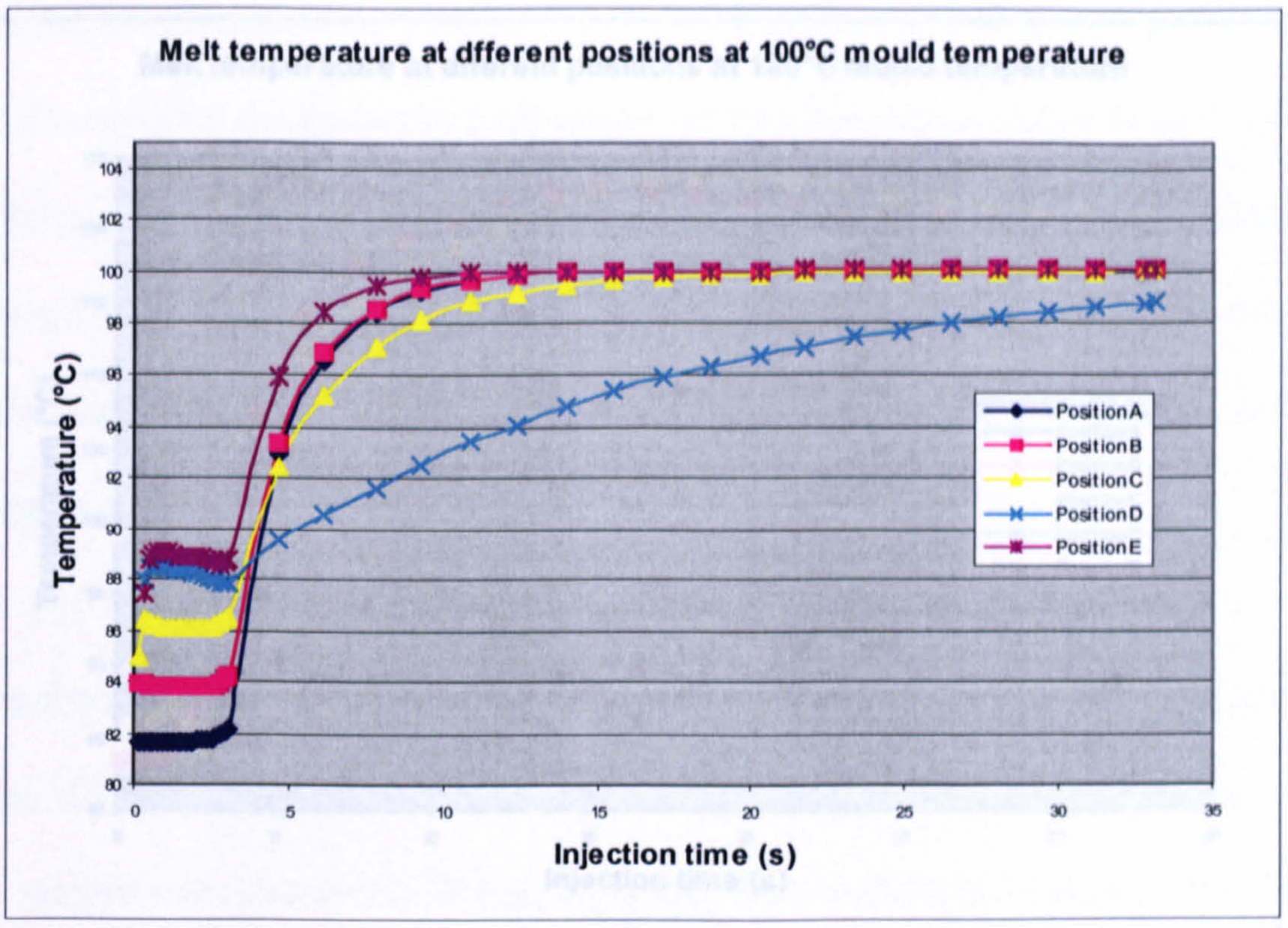

Figure 8.8 Melt temperature of the material at different positions in the mould and manifold. The mould and manifold is at 100°C and injection time is 3 seconds.

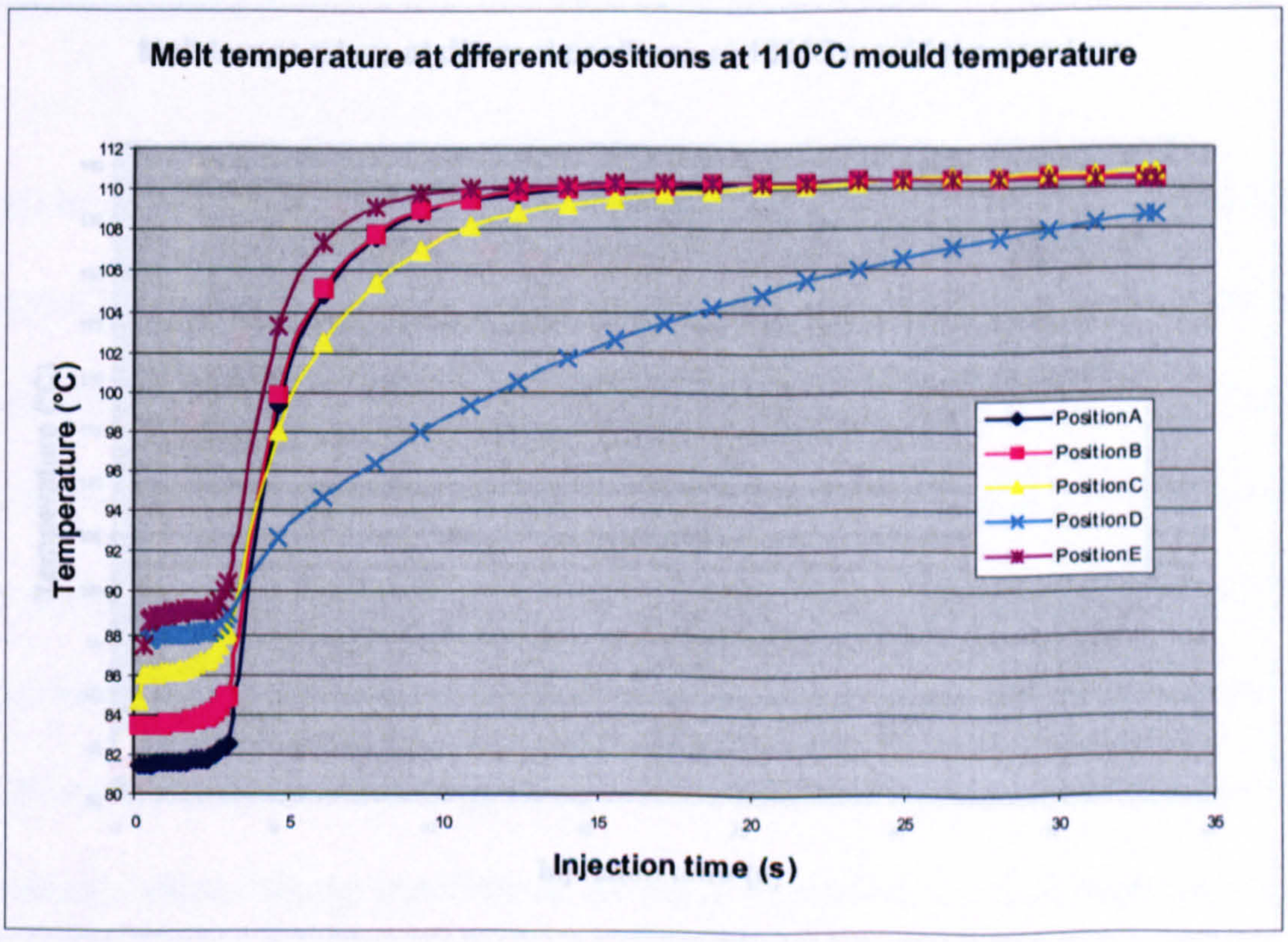

Figure 8.9 Melt temperature of the material at different positions in the mould and manifold. The mould and manifold is at 110°C and injection time is 3 seconds.

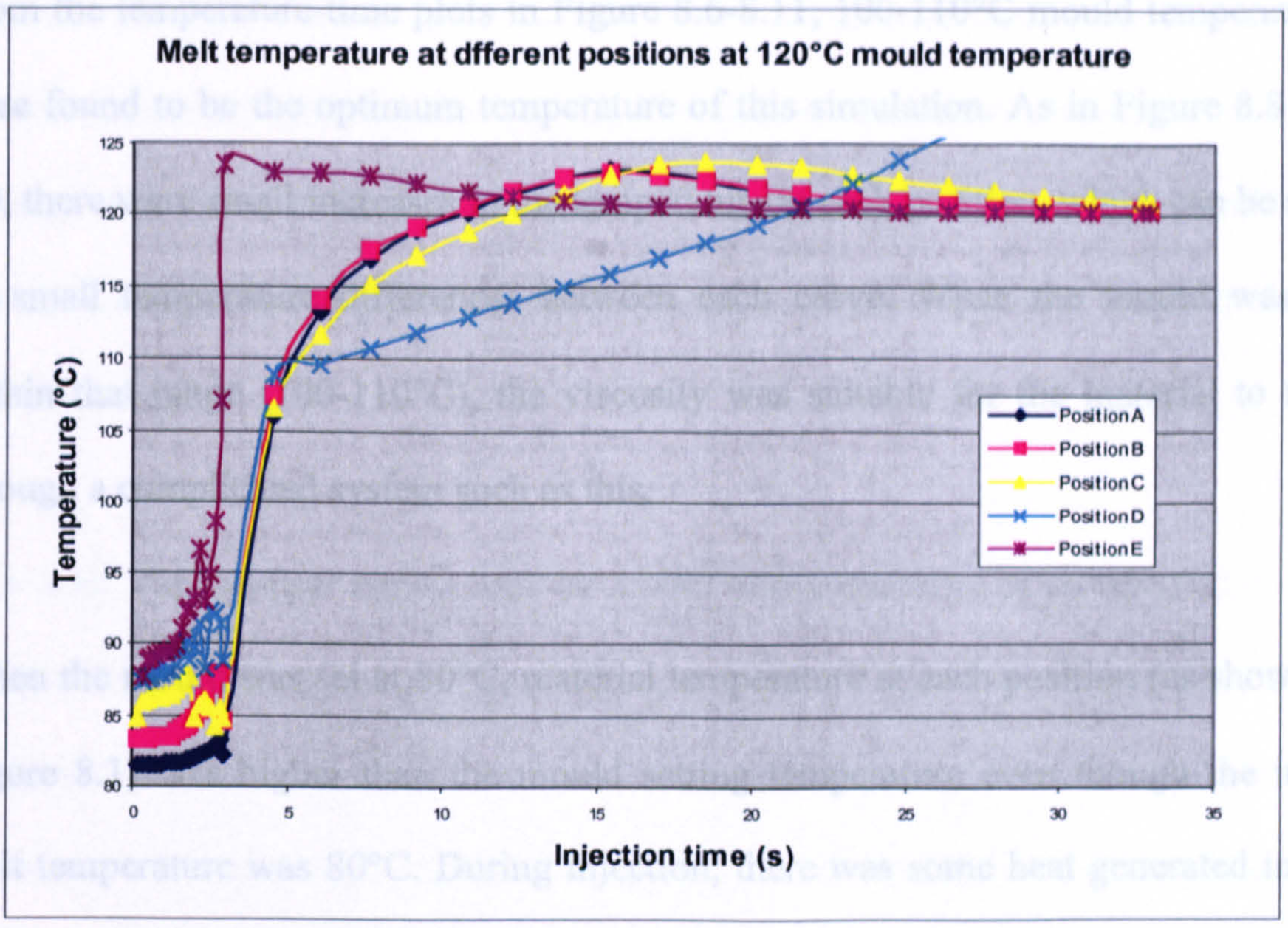

Figure 8.10 Melt temperature of the material at different positions in the mould and manifold. The mould and manifold is at 120°C and injection time is 3 seconds.

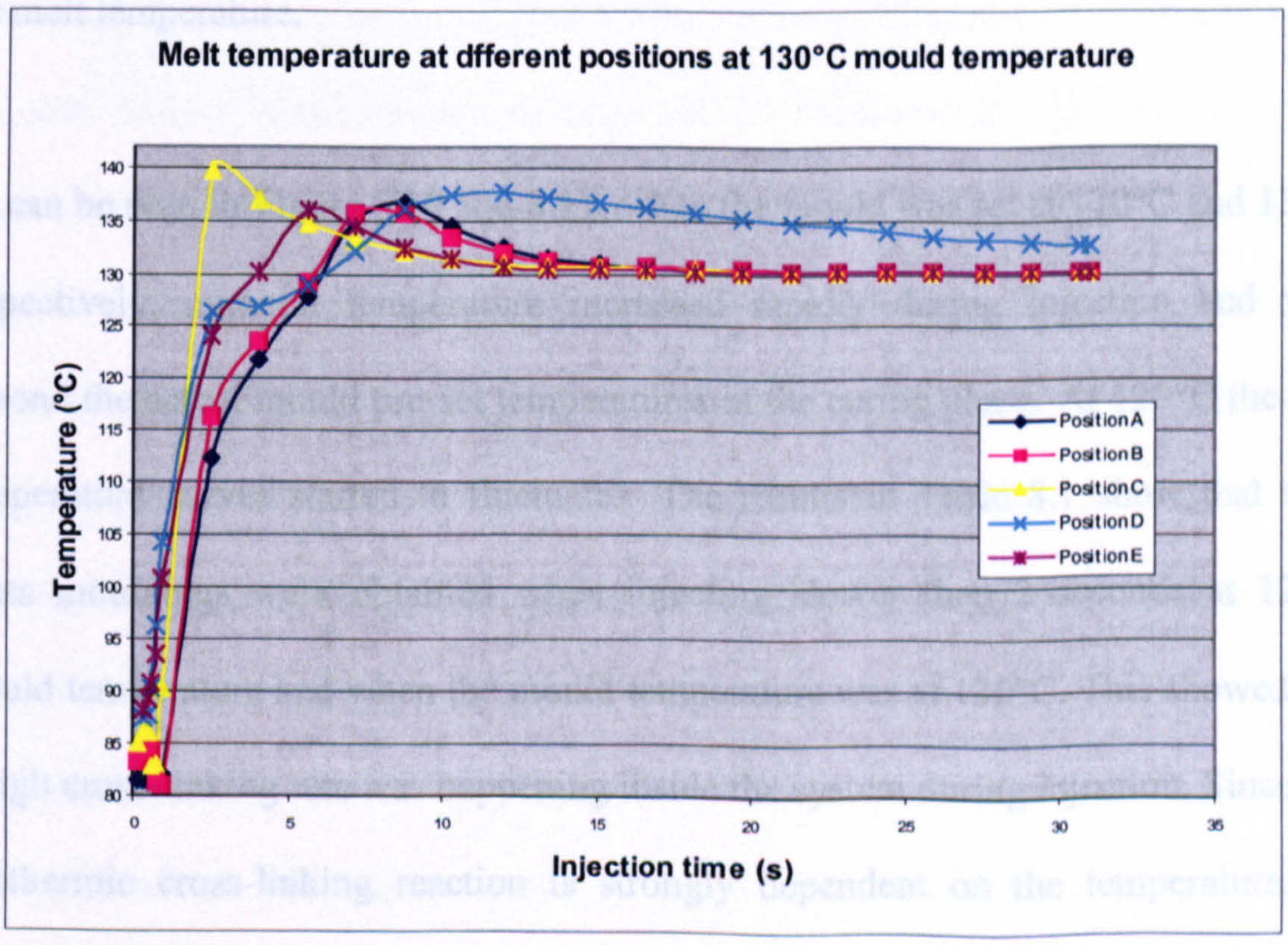

Figure 8.11 Melt temperature of the material at different positions in the mould and manifold. The mould and manifold is at 130°C and injection time is 3 seconds.

From the temperature-time plots in Figure 8.6-8.11, 100-110°C mould temperatures were found to be the optimum temperature of this simulation. As in Figure 8.8 and 8.9, there were small increases in the temperature at each position, which can be seen by small temperature differences between each curve. When the mould was set within that range (100-110°C), the viscosity was suitable for the material to flow through a complicated system such as this.

When the mould was set at 80°C, material temperature at each position (as shown in Figure 8.1) was higher than the mould setting temperature even though the input melt temperature was 80°C. During injection, there was some heat generated in the system, which was caused by heat transfer from the mould wall, the cross-linking reaction and shear friction. When a viscous material flows through a complicated mould system like this, friction could be the main factor that caused the increasing of the melt temperature.

As can be seen in Figure 8.10 and 8.11, when the mould was set at 120°C and 130°C respectively, material temperature increased rapidly during injection and went beyond the actual mould pre-set temperatures in the curing phase. At 120°C the melt temperature curves started to fluctuate. The results in Table 8.1 show that short shots mouldings were obtained when injecting slower than 2 seconds at 120°C mould temperature and when the mould temperature was at 130°C. This showed that a high cross-linking rate was happening inside the system during injection. Since this exothermic cross-linking reaction is strongly dependent on the temperature, the higher the mould temperature that was set, the higher the reaction rate would be, and the more heat that was generated. Ideally, the cross-linking should start in the mould

after the whole mould is fully filled or in the curing phase. However, in practice, the reaction starts on applying heat to the material in the barrel. All of the machine settings that affect to the system and material temperatures must be controlled to ensure that the reaction rate is very slow during mould filling and is very fast during mould curing.

The melt temperature curves can be useful for prediction of material flow and gelation in a mould system. A good filling case can be seen from Figure 8.8-8.9. As explained previously, smooth curves can be seen from the temperature and time plots, and the melt temperature at each position is almost constant during injection. The effect of chemical reaction and shear friction, which led to an increasing in temperature, was very low here.

A drop-down curve (as seen in Figure 8.6-8.7) occurs when the mould temperature is too low. Only a small amount of heat can be transferred to the melt. The melt temperature lowers when fresh material is flowing into the mould. Even though the temperature is low at the start and the material has almost no chance of pre-curing, the problem will occur when the viscous melt flows further in. The melt temperature increases due to frictional heat, which is caused by the high viscosity material flowing in the system. This will increase the reaction rate during mould filling.

A fluctuating curve as shown in Figure 8.10-8.11 happens when there is pre-curing during injection. This often results in short shot moulding. A close-up figure showing the effect of the mould temperature on the melt temperature is shown in Figure 8.12. The high peaks of the fluctuation curve represent the high melt

temperature due to high cross-linking rate. These show when the material viscosity is high due to pre-curing and the melt flow starts to slow down. When more fresh material flows into the mould, it pushes the high temperature melt further in so the temperature at that position decreases as shown by the low peaks of the fluctuation curve.

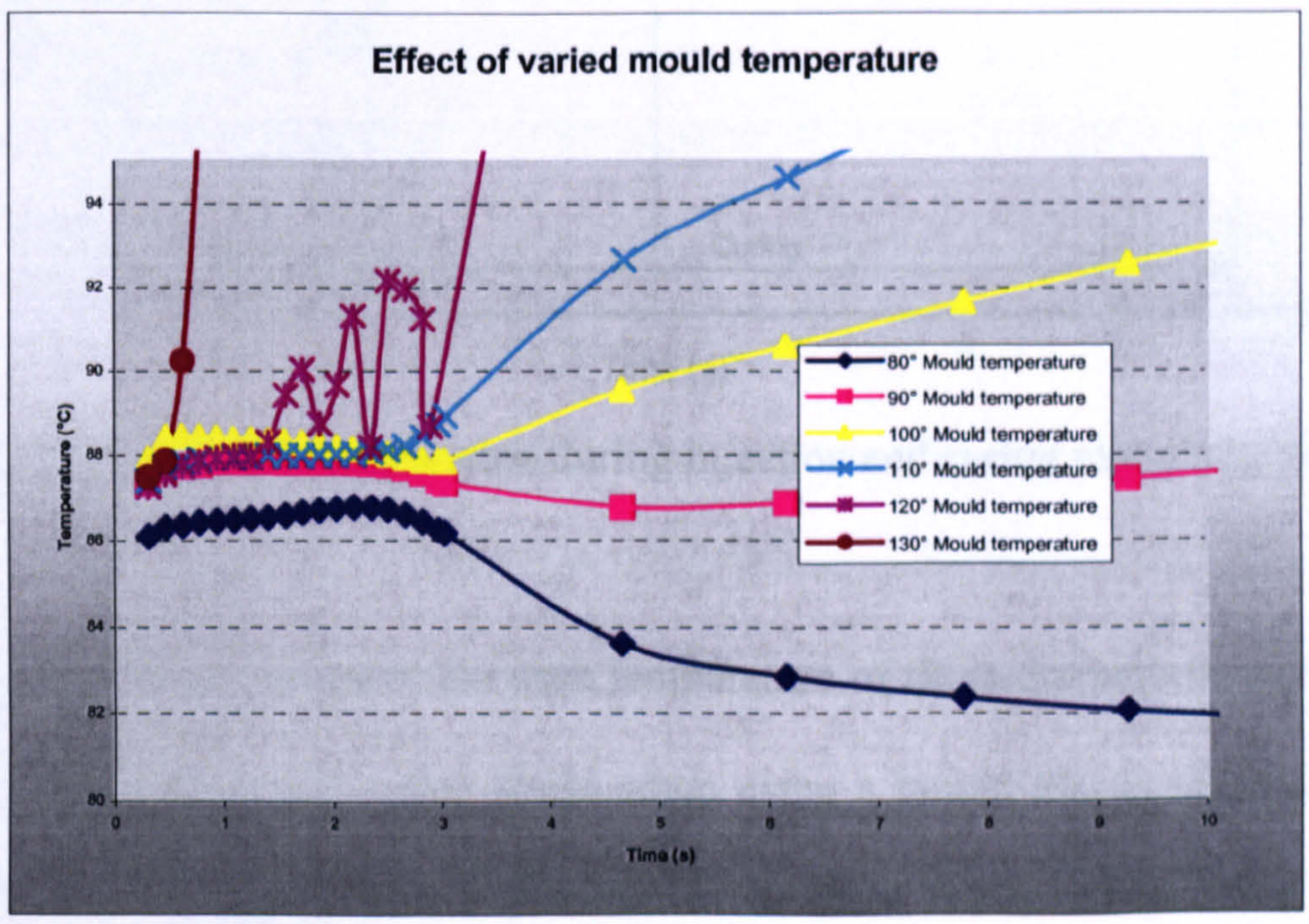

Figure 8.12 Time and temperature curve of a thermoset polyester in the sprue end when varying mould temperature. Injection time is 3 second.

The injection time-temperature curves can be redrawn as shown in Figure 8.13. This figure represents the temperature-time curve shapes of good and bad mould fillings when the mould is completely filled.

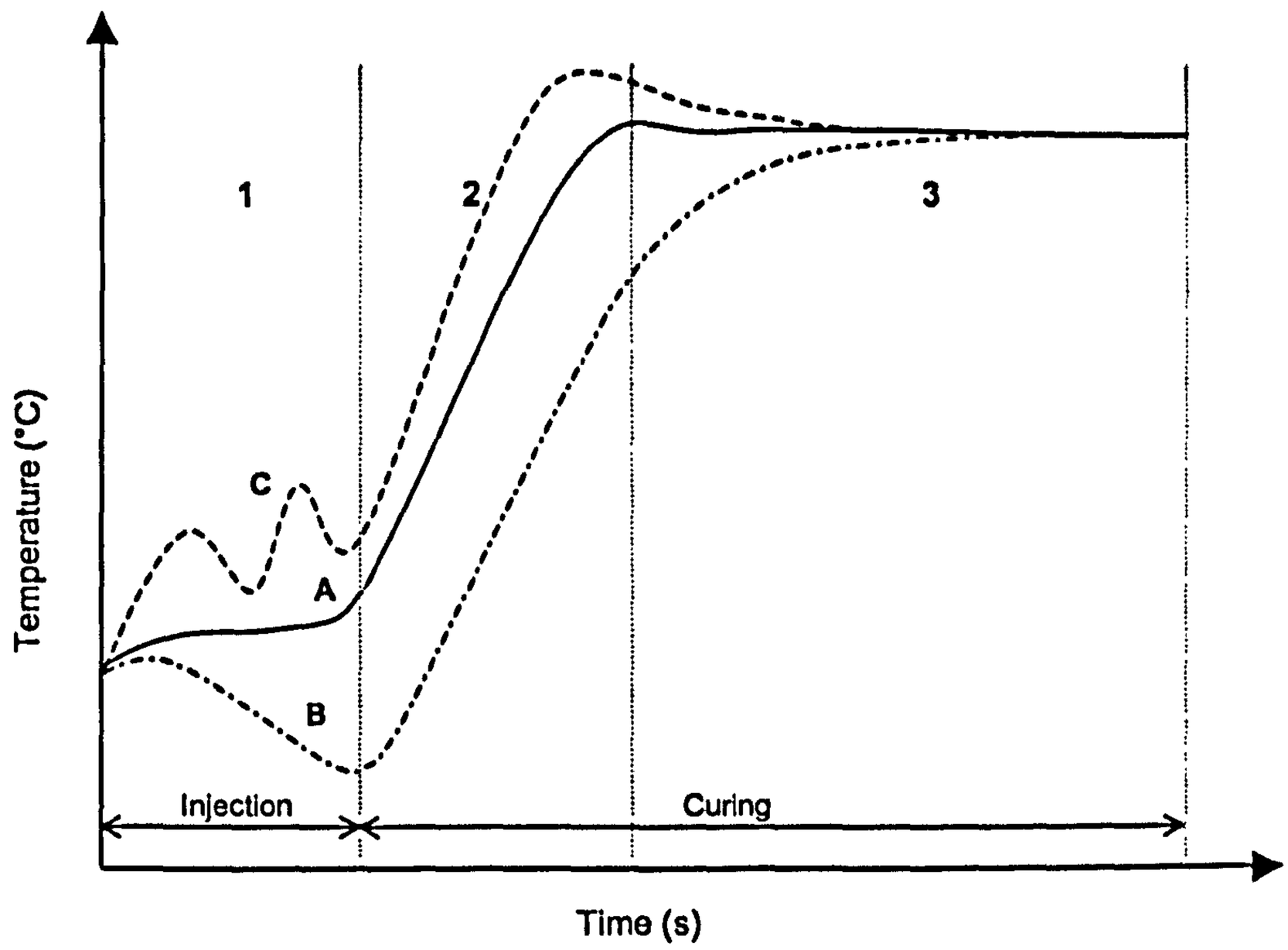

Figure 8.13 The melt temperature during injection and curing phase of a thermoset

These three curves represent the melt temperature of three thermosets, A, B and C, during the injection and curing phase when using a mould that is set at a constant temperature. The graph area is divided in to three zones, where zone 1 is the injection phase or mould filling and zone 2 and 3 are curing phase or mould curing.

In zone 1, material is being injected into the mould. The heat in the system, which is determined by an increasing of temperature, is affected by,

- Material temperature
- Mould temperature
- Shear friction
- Cross-linking reaction

The shape of the curves depends on the weight that each factor has on the material. For curve A, the material A is being injected at a suitable mould temperature. A small amount of heat is generated as can be seen by an almost constant temperature curve in zone 1. The main factors that affect the changing of the melt temperature are heat transfer from the mould and the lower temperature material from the barrel. Shear friction and cross-linking have a very small effect here.

The mould temperature is too low for material B as can be seen from the shape of curve B. The melt temperature is reducing because the lower temperature material from the barrel is flowing into the mould. There is almost no effect from the cross-linking reaction. However, shear friction starts to build up some heat due to the high viscosity material when it is at low temperature. The friction will effect to the increasing of the melt temperature when it flow further in the mould.

Curve C shows that the mould temperature is too high for the material C. Material is very low in viscosity so there is low shear friction during injection. Heat transfer from the mould wall and the fresh material affect the melt temperature but not as much as the effect from the exothermic cross-linking reaction. The melt temperature of material C is higher than the rest. Since the reaction rate is high, there is a chance of pre-curing at some parts of the mould and results in flow marks on the surface.

In zone 2, the mould is fully filled and no more material is injected in. This is when the cross-linking network should start to form and turns the melt into a solid component. Heat generation in this zone is from

- Mould temperature
- Cross-linking reaction

All materials show a rapid increase in the melt temperature. The heat transfer from the mould to the material is at the same rate in each curve but each material reacts to the heat differently. A very high cross-linking rate occurs with material C, so there is a lot of heat generating during curing, which is shown by a very fast increasing rate of temperature and a large overshoot temperature from the mould setting temperature. A good curing curve is shown by material A when the reaction rate is moderate and a smaller overshoot happens at the end of zone 2.

The curve of material B shows a very slow cross-linking rate due to too low mould temperature. The material temperature is increasing slowly and cannot reach the mould setting temperature at the end of zone 2.

In zone 3, cross-linking is continued. The temperatures of material A, B and C are equal to the mould temperature, which is controlled by a heat control system. Moulding components can be achieved at the end of this zone from material A and C. However, the material B, which has the slowest cross-linking rate and needs more time for curing among the three materials, might not cure enough for demoulding by the end of zone 3.

8.3 Moldflow® simulation of the tray

The complicated runner of the manifold system was omitted from this simulation, in order to look at material flow into the mould without any effect from the manifold system. This time, the injection point was changed from the vertical to horizontal direction. Similar to the simulation in section 8.1, the injection time was varied from 1 to 5 seconds with the temperature changed from 80 up to 140°C. The meshing model and the results are shown in Figure 8.14 and Table 8.2, respectively.

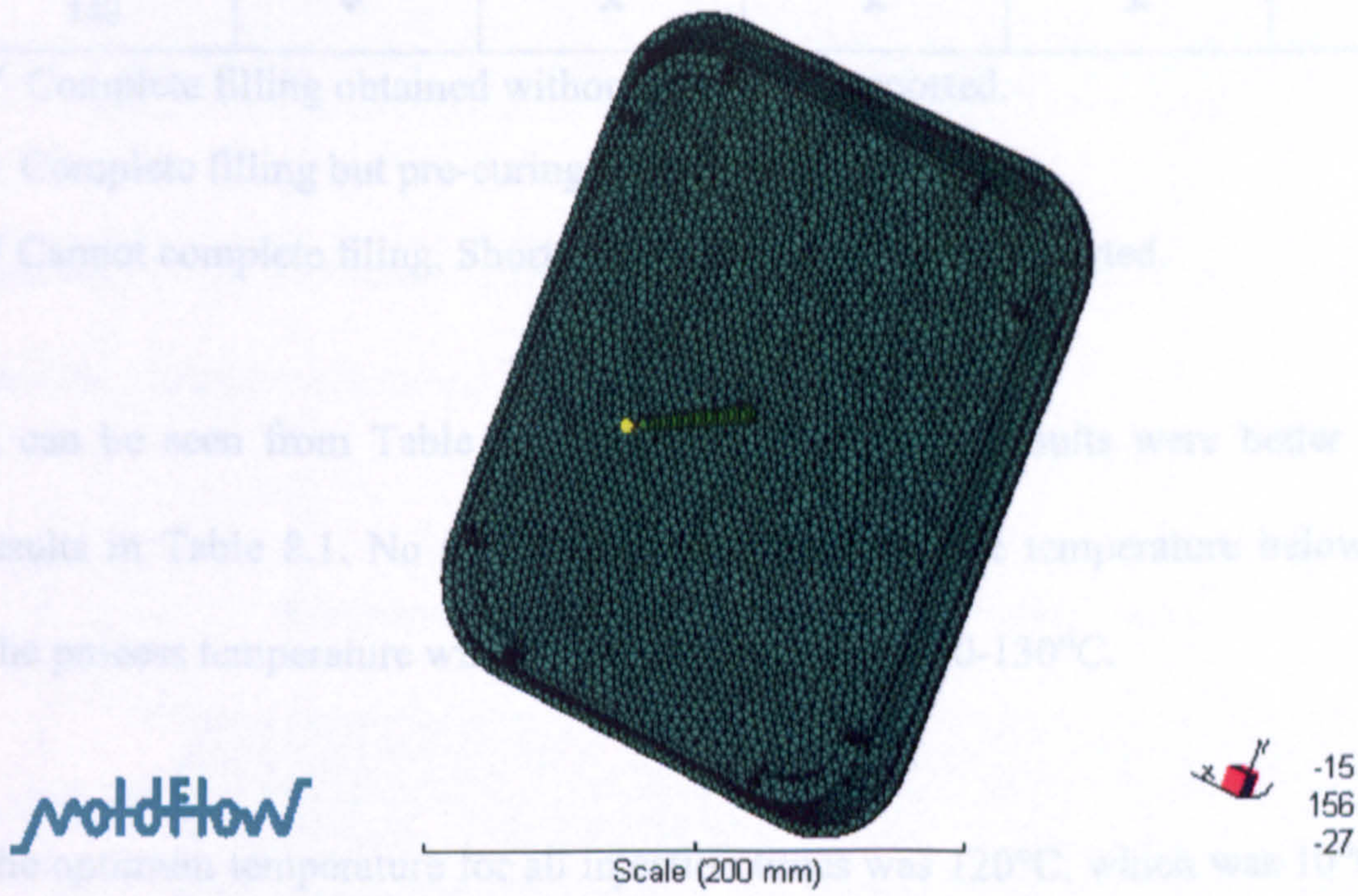

Figure 8.14 Fusion model of the tray

Table 8.2 Conclusion of polyester mould filling simulation of the tray mould

Mould temperature (°C) \ Injection time (s)	1	2	3	4	5
80	✓	✓	✓	✓	✓
90	✓	✓	✓	✓	✓
100	✓	✓	✓	✓	✓
110	✓	✓	✓	✓	✓
120	✓	✓	✓	✓	✓
130	✓	✓	o	×	×
140	✓	×	×	×	×

✓ Complete filling obtained without pre-curing reported.

o Complete filling but pre-curing was reported.

× Cannot complete filing. Short shot and pre-curing was reported.

It can be seen from Table 8.2 that the mould filling results were better than the results in Table 8.1. No pre-curing was reported at the temperature below 130°C. The process temperature window for this mould was 80-130°C.

The optimum temperature for all injection times was 120°C, which was 10°C higher than the top limit of the optimum temperatures when there was the manifold attached to the mould (100-110°C). This means that at least 10°C reduction of the system temperature was needed in order to balance between the material flow and cure inside the manifold system. In other words, this temperature difference was used to compensate the system's heat generation. Figure 8.15 and 8.16 show the melt temperatures in the sprue end when the mould was attached with and without the manifold system. The mould temperatures of both cases were set at 120°C. It can be seen that more smooth curves were reported when the manifold was removed.

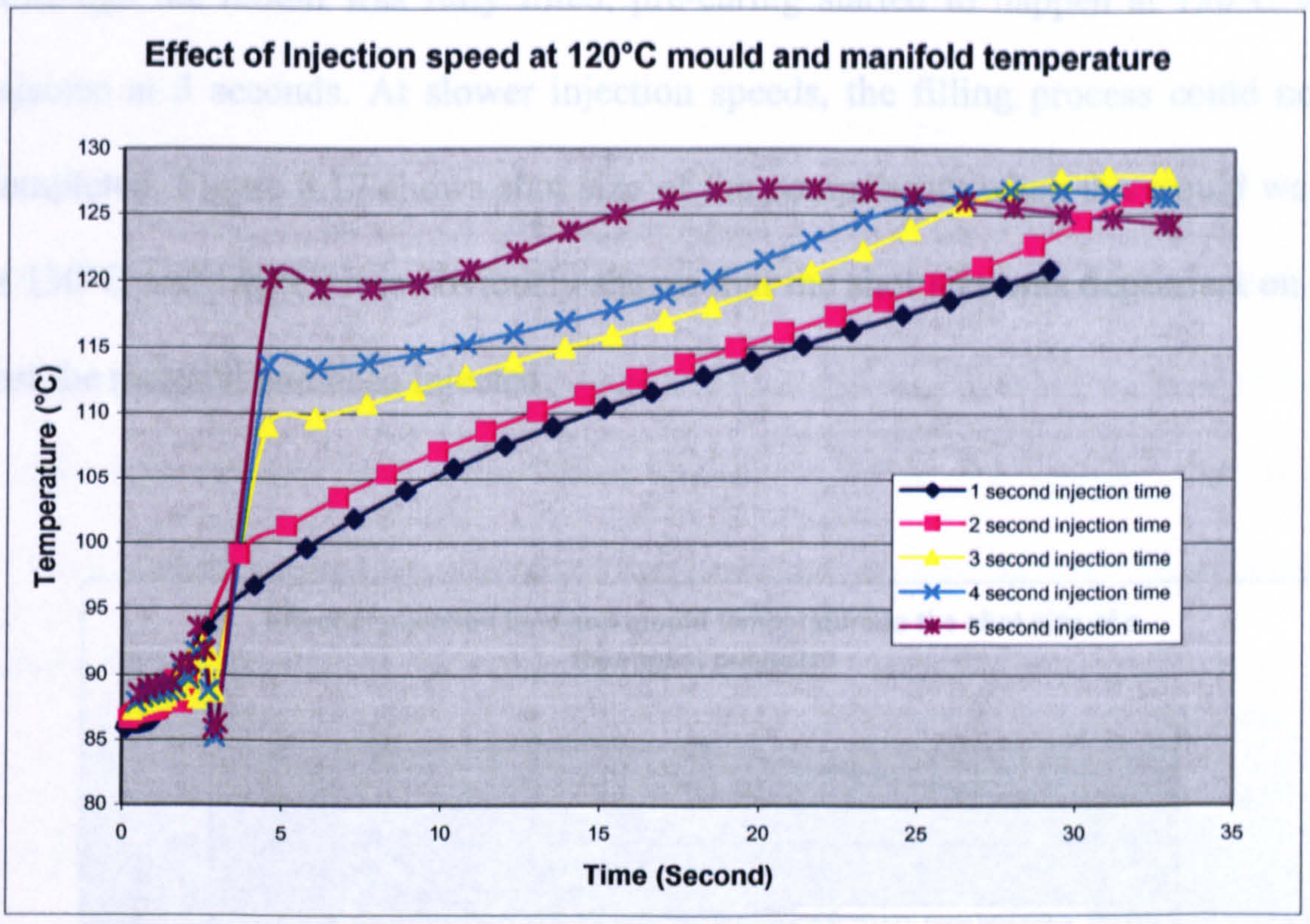

Figure 8.15 The melt temperatures at the mould sprue end at varied injection time when the manifold and mould were set at 120°C

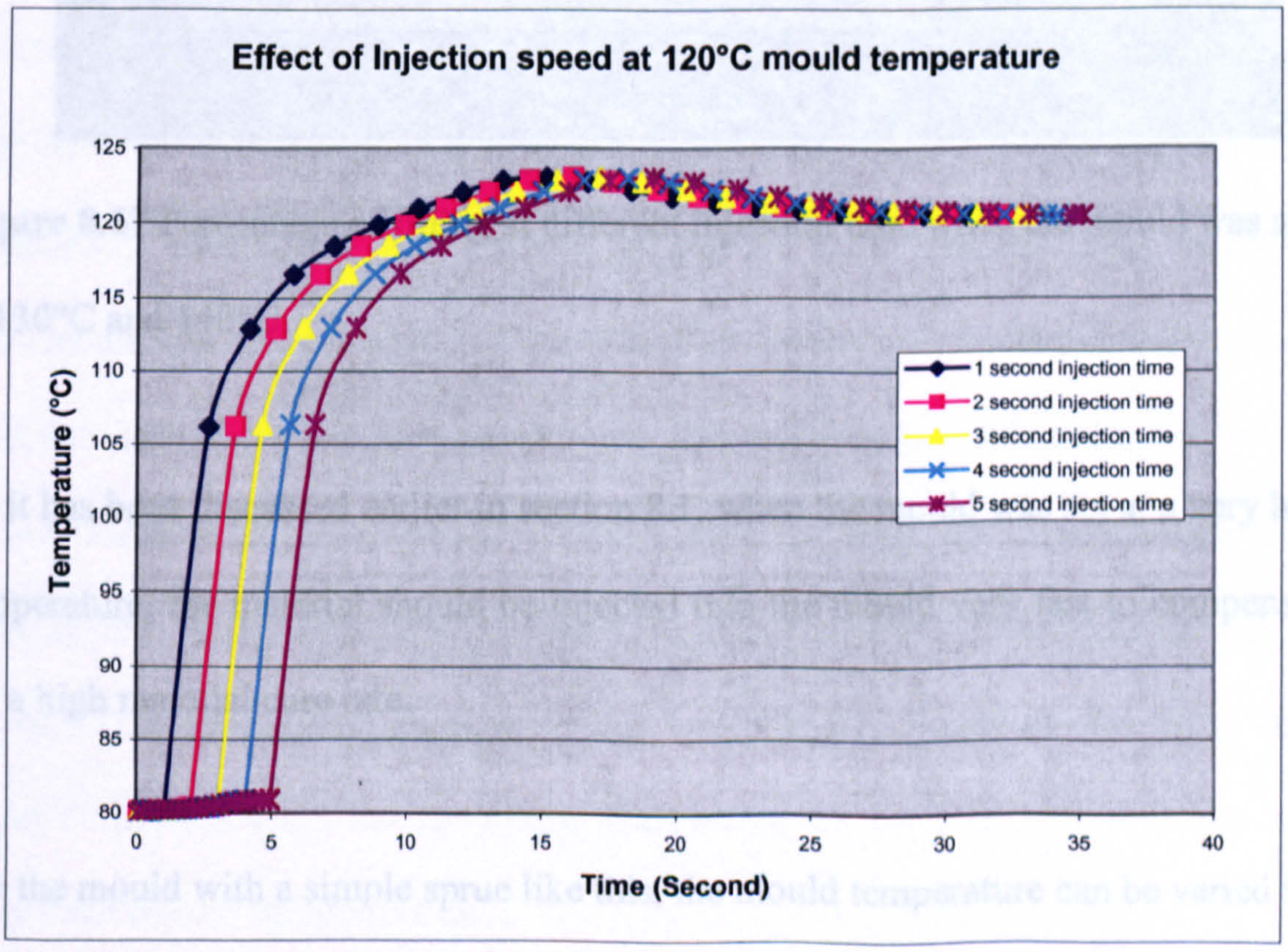

Figure 8.16 The melt temperatures at the mould sprue end at varied injection time when the mould was set at 120°C

Although the mould was fully filled, pre-curing started to happen at 130°C when injected at 3 seconds. At slower injection speeds, the filling process could not be completed. Figure 8.17 shows shot size of the components when the mould was set at 130°C and 140°C. It is obviously shown that the shot size was dependent on how fast the material had been injected.

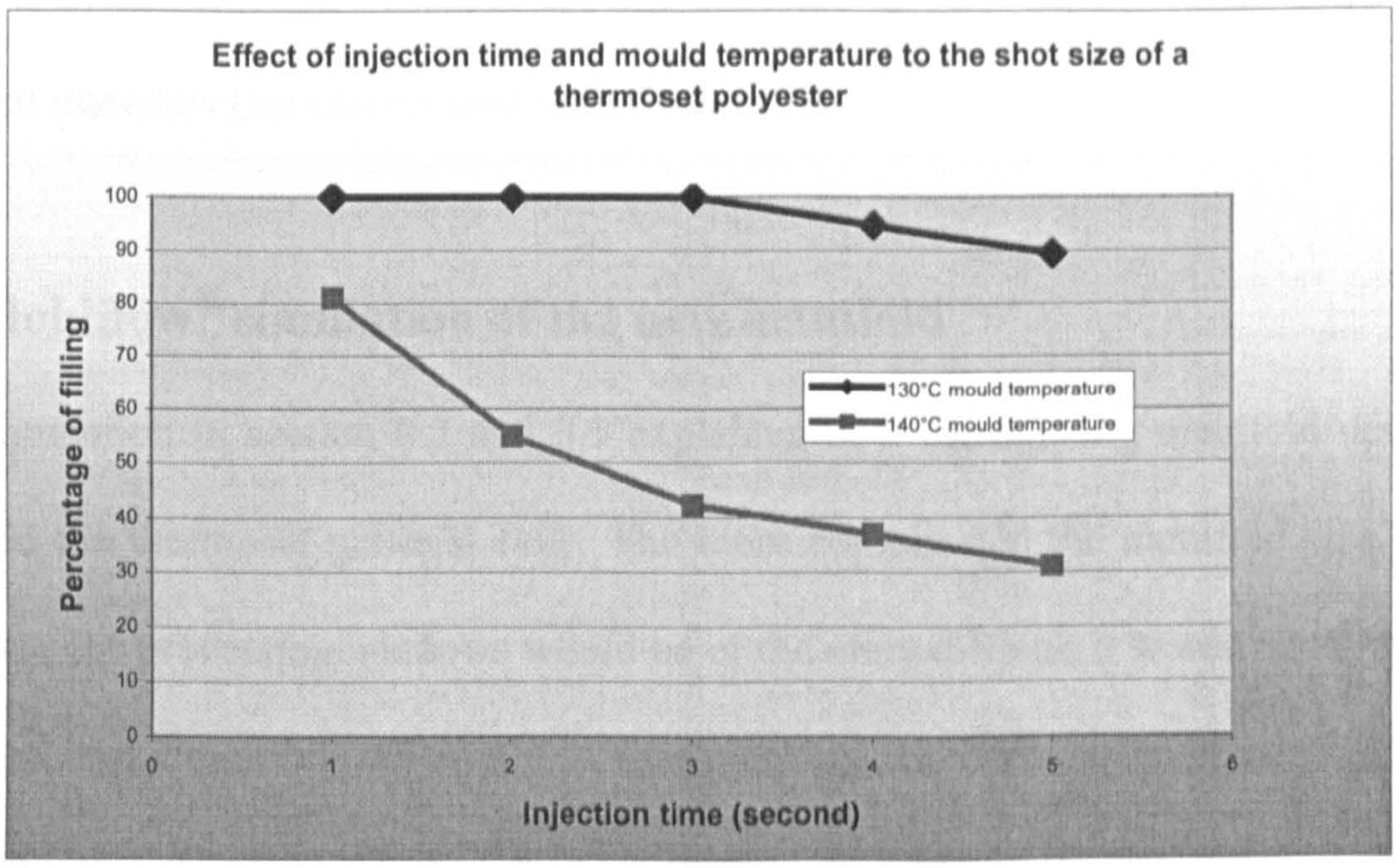

Figure 8.17 Percentage of filling at different injection time when the mould was set at 130°C and 140°C

As it has been discussed earlier in section 8.1, when the mould was set at a very high temperature, the material should be injected into the mould very fast to compensate for a high material cure rate.

For the mould with a simple sprue like this, the mould temperature can be varied in a wide range from a low to high temperature. The injection time is the only parameter to consider when the mould is set at a high temperature. However, when the mould is

connected to a more complicated runner as in the existing manifold system, it is important to consider the internal shear friction in the system since it will advance the material cross-linking rate and causes pre-curing. The manifold system temperature cannot be too low because it will increase the material viscosity and reduce the melt flowability. Also, the melt cannot be injected very fast at any temperature since it will cause more shear friction in the system. The process window of the existing manifold system therefore is very narrow. This limits the types of materials that can be used with the machine.

8.4 Moldflow® simulation of the new manifold

The simulation in section 8.2 and 8.3 explained how the existing manifold design affected the thermoset material flow. The more complicated the manifold was, the narrower the processing windows would be or the more difficult it would be to inject a thermoset material into the mould. A new manifold had been designed based on the problems that occurred during the experiments (see Chapter 7) and analysed using Moldflow® simulation. As shown by Figure 8.18, outputs from numerous simulations had been used to aid the designed dimensions, which were continually modified until a good result was obtained. The simulation in this section shows the mould filling of the final design manifold under the same condition settings as the existing one. Figure 8.20 shows the meshing model of the new manifold system and the tray. The simulation results are given by Table 8.3. Points on the figure show different positions on the moulding that would be used to represent the melt temperatures later in this section.

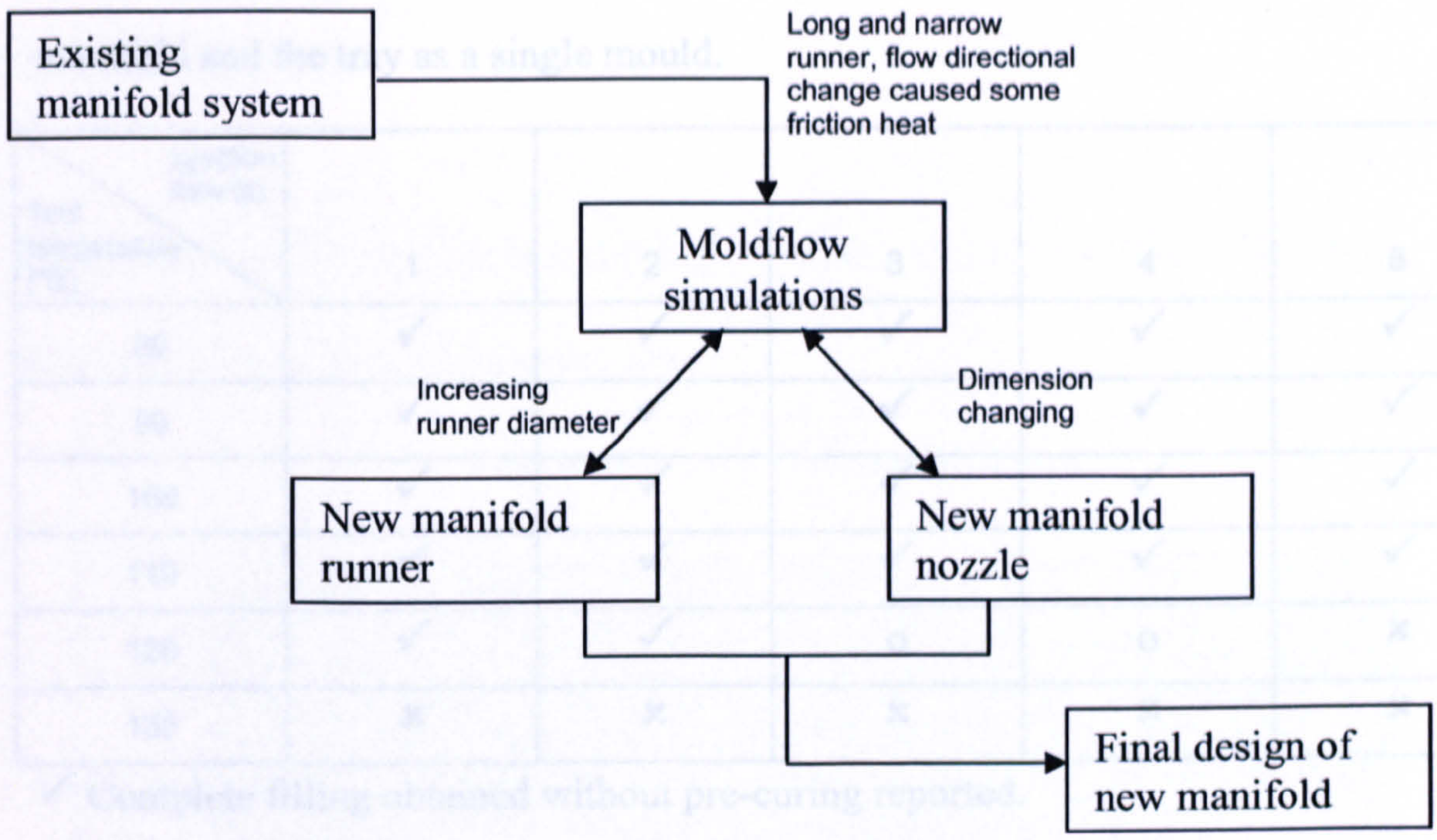

Figure 8.18 Process of designing the new manifold system

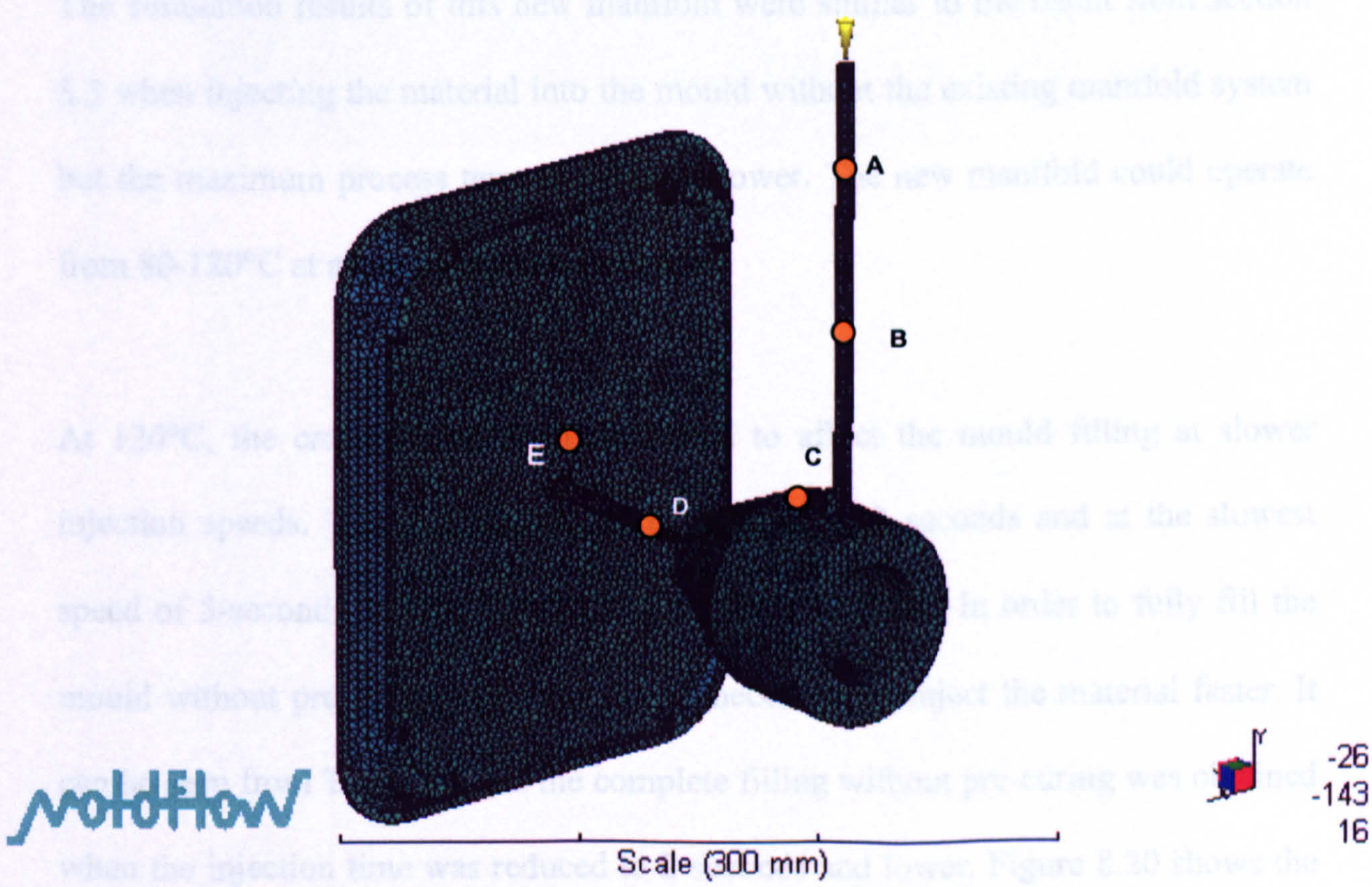

Figure 8.19 Meshing model of the new design manifold and the tray mould

Table 8.3 Conclusion of polyester mould filling simulation. Using the new designed manifold and the tray as a single mould.

Tool temperature (°C) \ Injection time (s)	1	2	3	4	5
80	✓	✓	✓	✓	✓
90	✓	✓	✓	✓	✓
100	✓	✓	✓	✓	✓
110	✓	✓	✓	✓	✓
120	✓	✓	o	o	×
130	×	×	×	×	×

✓ Complete filling obtained without pre-curing reported.

o Complete filling but pre-curing was reported.

× Cannot complete filing. Short shot and pre-curing was reported.

The simulation results of this new manifold were similar to the result from section 8.3 when injecting the material into the mould without the existing manifold system but the maximum process temperature was lower. The new manifold could operate from 80-120°C at almost all injection times.

At 120°C, the cross-linking reaction started to affect the mould filling at slower injection speeds. The material started to pre-cure at 3 seconds and at the slowest speed of 5-seconds, mould filling could not be completed. In order to fully fill the mould without pre-curing occurred, it was necessary to inject the material faster. It can be seen from Table 8.3 that the complete filling without pre-curing was obtained when the injection time was reduced to 2 seconds and lower. Figure 8.20 shows the changes of material temperature at different positions inside the manifold and the

mould when then mould was set at 120°C and the injection time was varied from 1 second to 5 second.

Figure 8.20 Melt temperature at different positions of 120°C mould temperature

Figure 8.20 a.) 1-second injection time

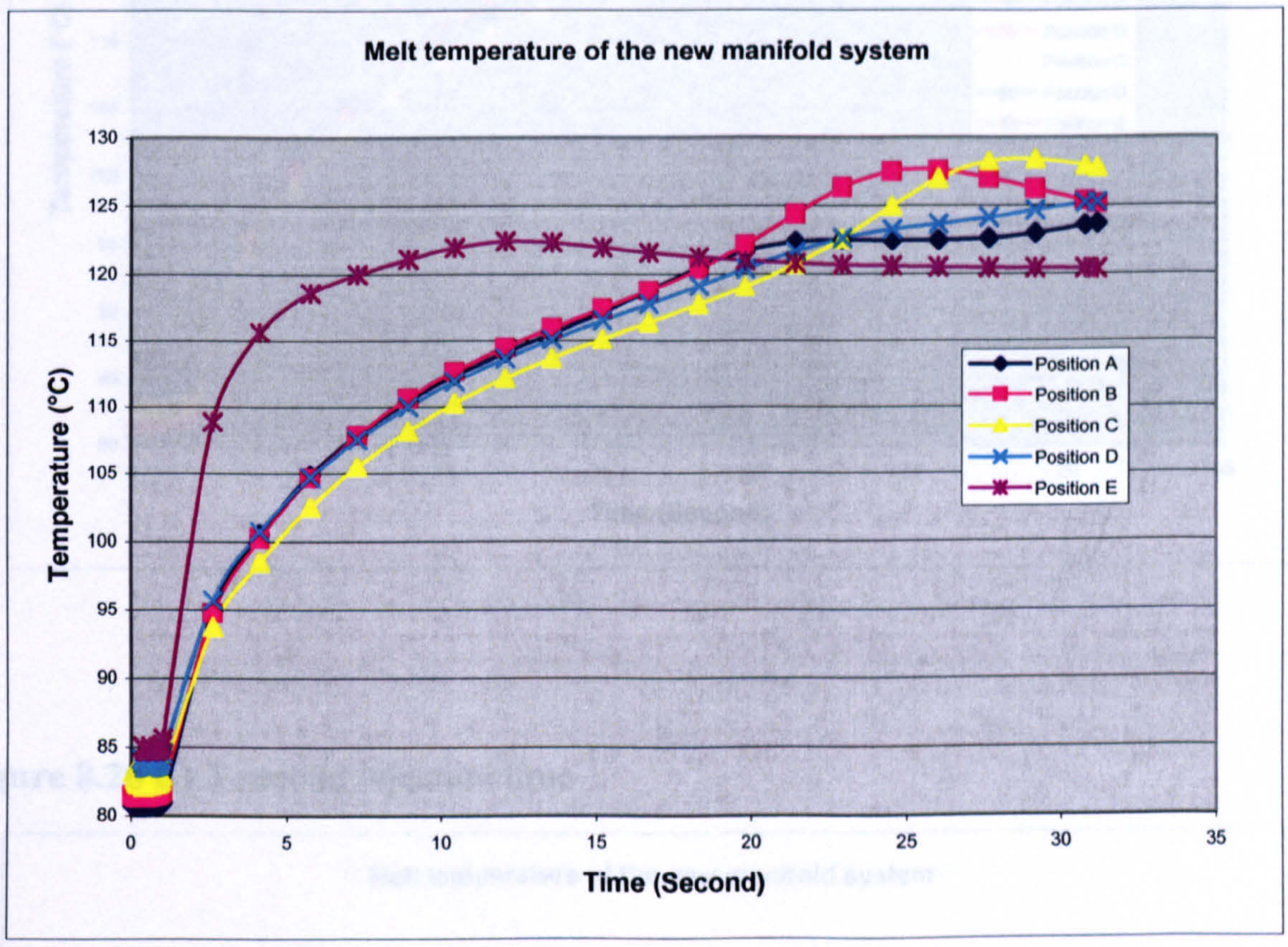

Figure 8.20 b.) 2-second injection time

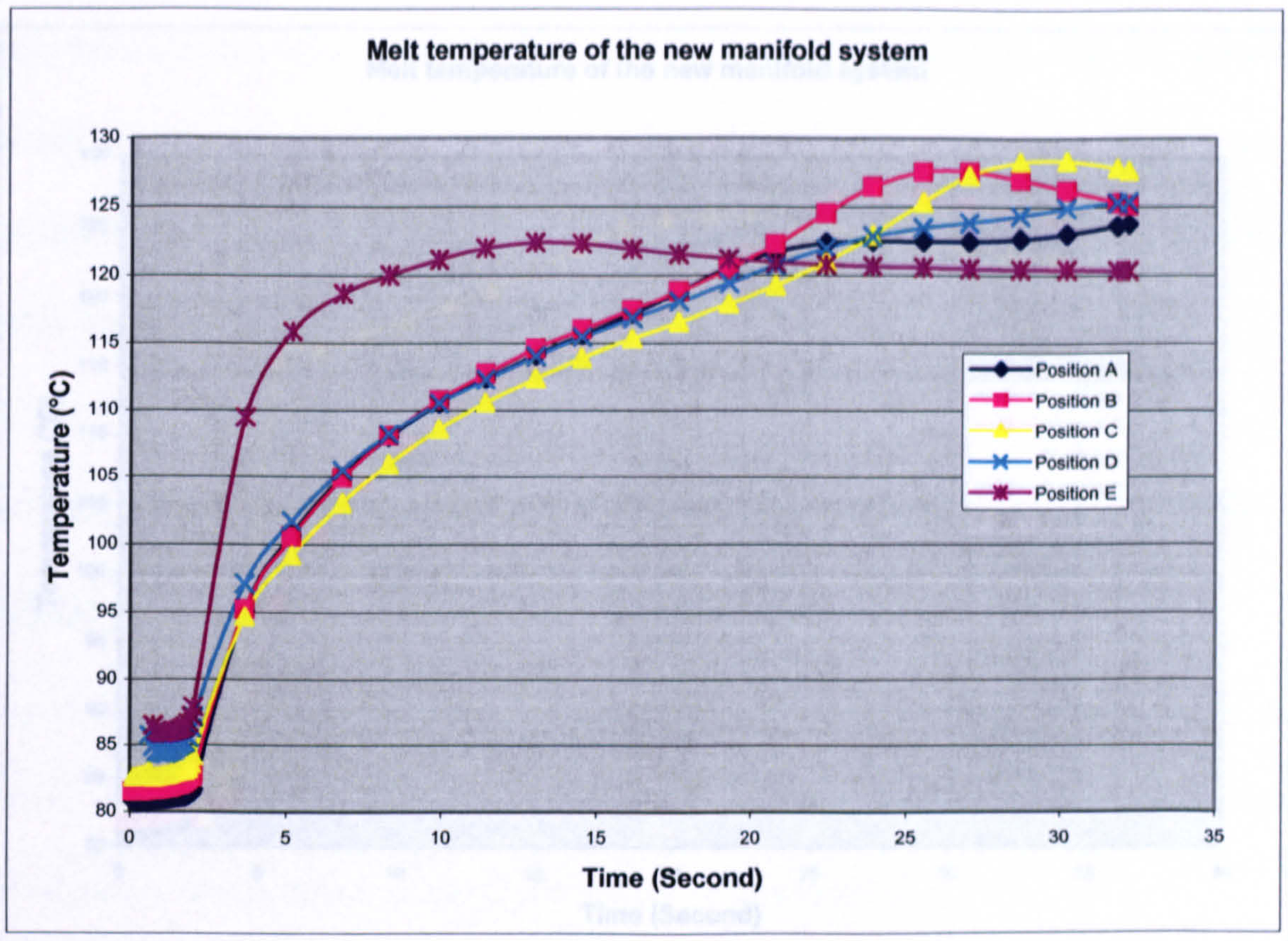

Figure 8.20 c.) 3-second injection time

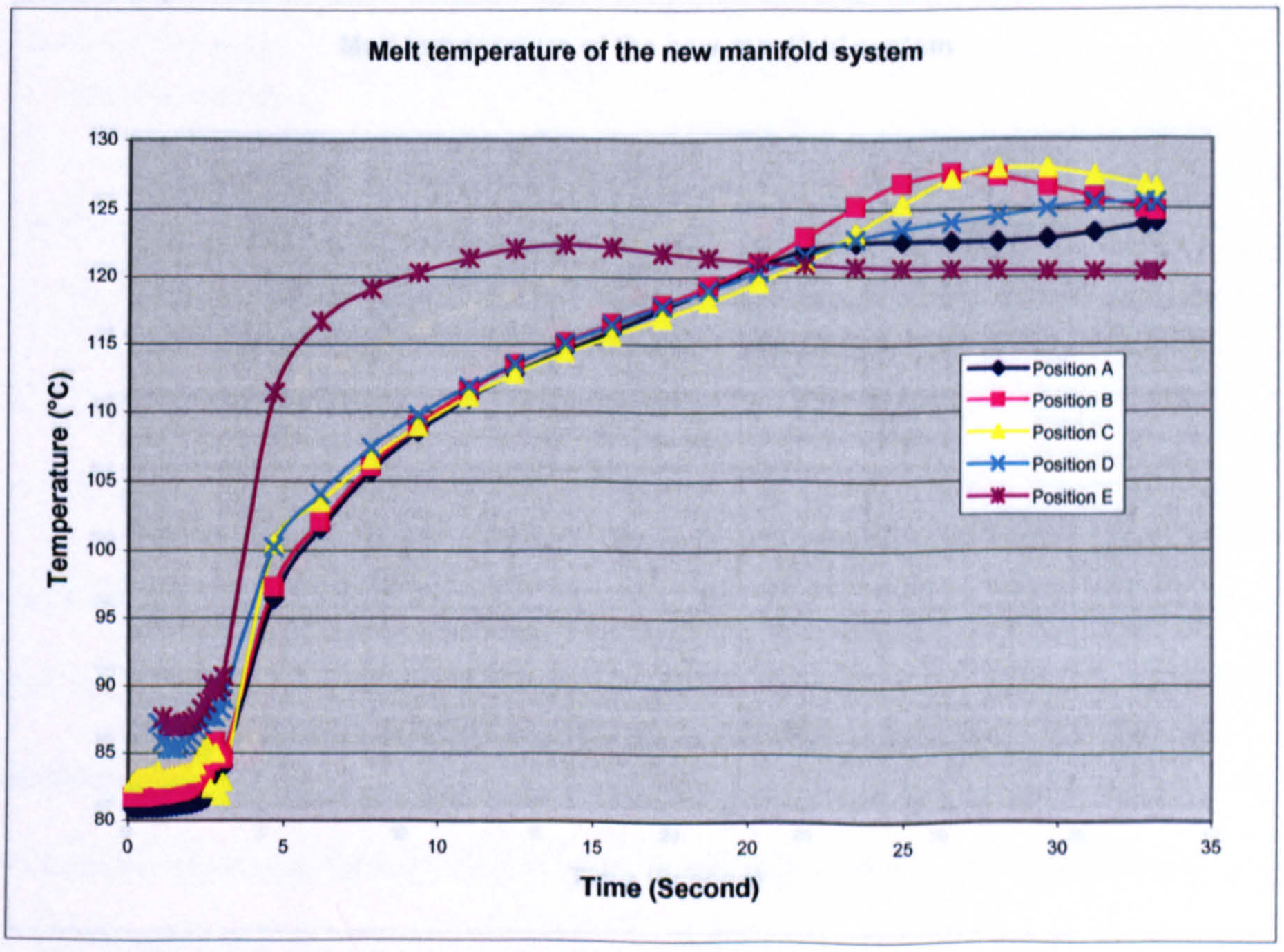

Figure 8.20 d.) 4-second injection time

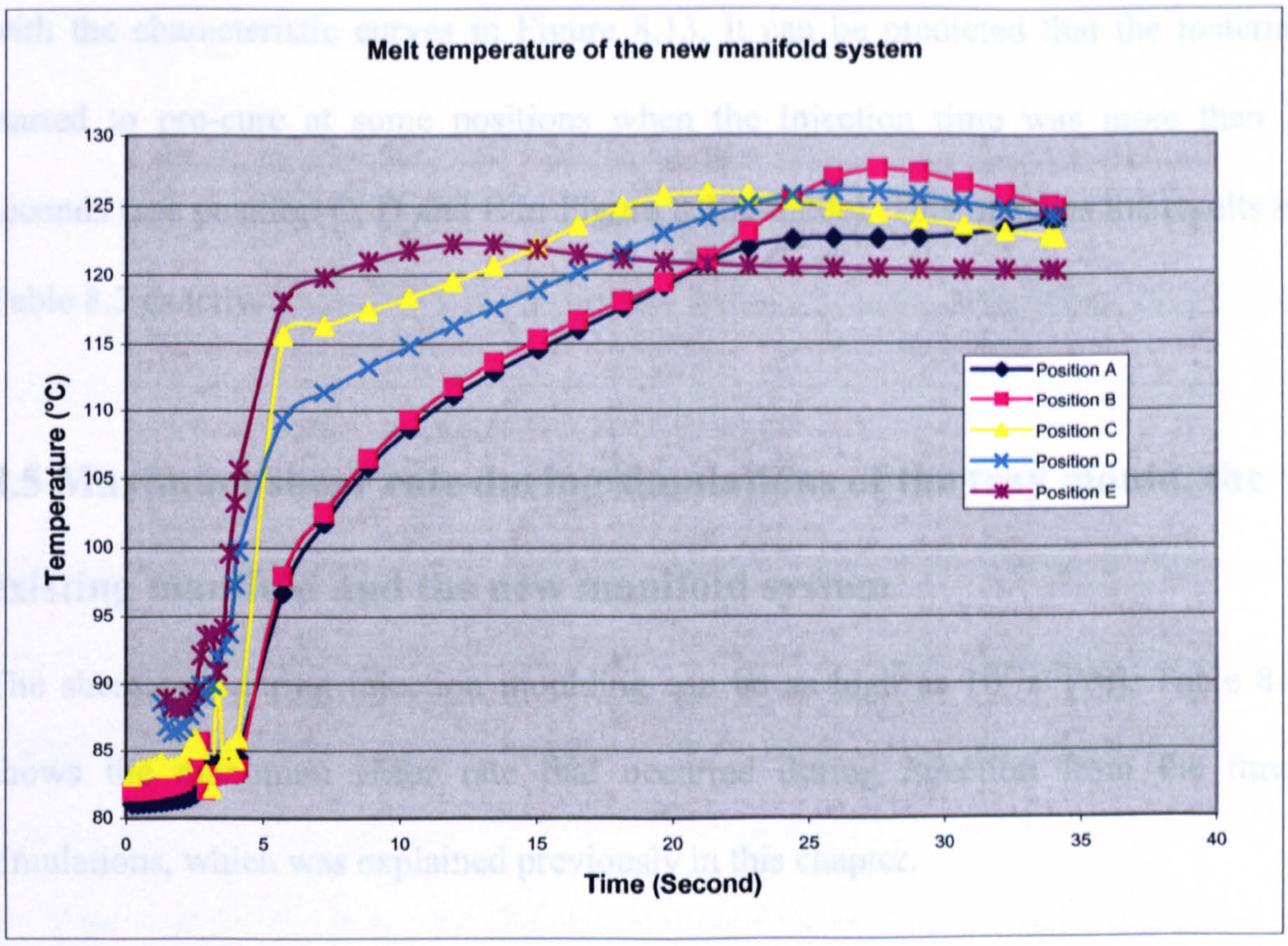

Figure 8.20 e.) 5-second injection time

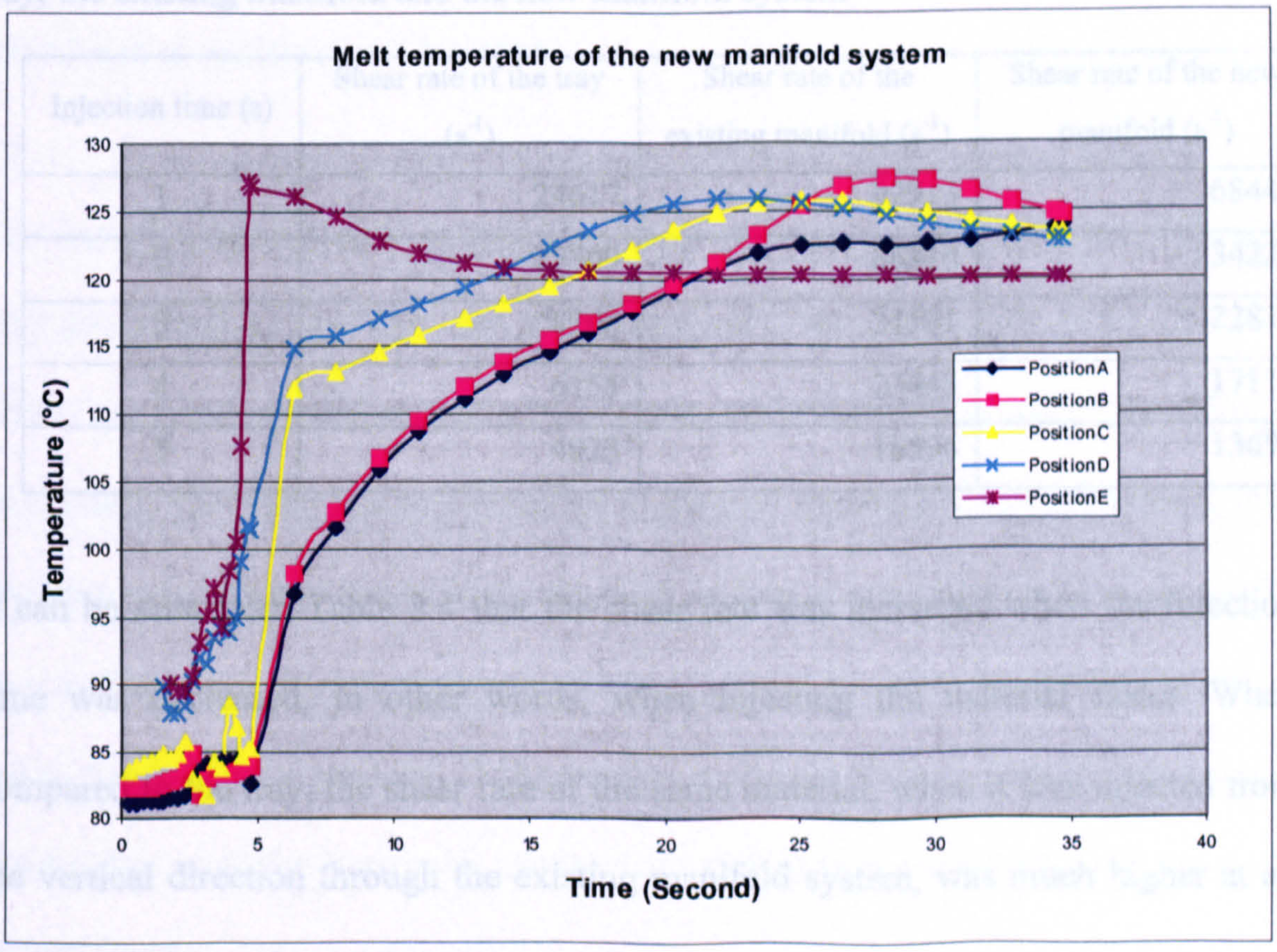

Looking at the melt temperature-time curves in Figure 8.20 and comparing them with the characteristic curves in Figure 8.13, it can be predicted that the material started to pre-cure at some positions when the injection time was more than 3 seconds (see position C, D and E in Figure 8.20c-8.20e). This matches the results in Table 8.3 exactly.

8.5 Maximum shear rate during simulations of the tray mould, the existing manifold and the new manifold system

The shear rate during injection moulding can be as high as 10^5 s^{-1}[78]. Table 8.4 shows the maximum shear rate that occurred during injection from the three simulations, which was explained previously in this chapter.

Table 8.4 The maximum shear rate during injection moulding simulations of the tray, the existing manifold and the new manifold system

Injection time (s)	Shear rate of the tray (s^{-1})	Shear rate of the existing manifold (s^{-1})	Shear rate of the new manifold (s^{-1})
1	24617	92913	68448
2	12309	46810	34224
3	8206	31501	22816
4	6155	23443	17112
5	4923	18596	13690

It can be seen from Table 8.4 that the shear rate was increased when the injection time was decreased, in other words, when injecting the material faster. When compared to the tray, the shear rate of the same material, when it was injected from the vertical direction through the existing manifold system, was much higher at all

injection times. This also clearly represents that this system was more difficult to flow through than the tray mould.

Normally, high shear rates in the system result in less polymer viscosity. When injecting two materials from both vertical and horizontal directions, the vertical injected material will be affected by a high shear rate due to the long and complicated runner of the manifold, while the horizontal injected material will be affected by a lower shear rate. The real viscosity ratio of the materials during co-injection moulding therefore cannot be considered at a single shear rate as it was in Figure 5.5, Chapter 5. Since the real viscosity of Interpon that was injected from the vertical direction was less than the value shown in the graph and the BMC may have not flowed at 10^4 $^{s-1}$ shear rate, the skin and core viscosity ratio would be less. The core could be injected earlier with no break-through at the edge of the moulding. However, the time for the skin to form an adequate layer also needed to be considered as explained in Chapter 6.

Flowing of a thermoset at a very high shear rate can cause pre-curing. Reducing injection speed to decrease the shear rate may also cause the same problem. Therefore, a less complicated system is more appropriate for injection moulding of thermosets. The shear rate that occurred in the new manifold system was lower than the shear rate value in the existing manifold system at any injection time, as can be seen in Table 8.4. However, it was still higher than the value in the tray mould. A better result will be achieved if the vertical runner is shorter. This means a major design change of the horizontal carriage in order to move the vertical barrel much further down.

8.6 Conclusions

This chapter presented the mould filling simulations of the existing manifold system and the new manifold system. Since there is no simulation software for co-injection of thermoset existing presently, thermoset single injection moulding simulation was used to help to understand the flow and cure of a thermoset material. The simulation results of the existing and new manifold system were compared and discussed.

The existing manifold system was shown to have a narrow process window, as there were many parameters involved during injection. It might not be suitable for using with some materials and limits the usage of the machine.

By considering the melt temperature-time curve of a thermoset at different positions in the mould during mould filling, the material pre-curing can be predicted.

The tray mould represents a simulation of a simple geometry mould without any effect from the manifold system. The results showed that this mould could operate at a wider range than a complicated mould like the existing manifold. Only injection time was a factor to consider when moulding at high temperature.

The new manifold system was proved to be an improvement over the existing one with the results of a simulation software package. This design expands the process window and feasibility of using the new system with more types of thermosetting materials. It may help improve the flowing of Interpon and reduce the short shot problem that always occurred when performing single injection of the material through the existing manifold. However, practical experiments are necessary in order

to prove the simulation results and the existing manifold could not be remachined with the scope of this project time scale.

The shear rate of a thermoset, which flowed through the manifold system, was much higher in vertical direction than horizontal direction. This would affect the flow of materials into the mould during co-injection moulding since the viscosities of the materials were changed. The viscosity ratio of the two materials, therefore, should be considered at a real shear rate of each material.

Moldflow® single injection moulding results will be not 100% accurate for prediction of thermoset co-injection and so the results of the manifold design cannot be considered to be conclusive. This is because when injecting two materials by co-injection through the same system, the melt temperatures at different positions inside the mould and manifold will differ from the results of the single injection moulding due to more complicated heat transferring between each material and between the system and the materials. Heat generation in each material during injection is also dependent on the material temperature, curing characteristics and amount of material that is injected into the mould. One material may be injected at a lower temperature than another, which will reduce the melt temperature of the latter material and hence, its curing rate. Even though the simulation results of the single injection moulding of the latter material show pre-curing and short shot, a complete filling is possible. In the opposite way, the high temperature melt of one material may raise the melt temperature and curing rate of another material. As a result, a short shot is also possible. Results from the single injection moulding simulation, therefore, may be

useful for predicting the pre-curing during injection of two materials that have similar input melt temperature, mould temperature and curing rate.

Chapter 9

Conclusions

The feasibility of making a thermoset sandwich moulding component by using the novel thermoset co-injection moulding machine was studied in this research. In order to achieve this, a knowledge of thermoset materials, the injection moulding of thermosets and the successful thermoplastic co-injection process were very important and were used for designing the experiments and improving the manifold system.

Prior to the experiment on the thermoset co-injection moulding machine, experimental works focussed on the cure and flow characteristics of two thermoset polyester materials, Interpon and BMC, at different temperatures. Temperature and time of applying heat to a thermoset material were investigated thoroughly as they are the main factors affecting the cross-linking and curing of that material. The viscosity of the material also increased when it was in an advanced cure state. The experiments on the material characteristics gave a temperature window setting for moulding these materials on the co-injection moulding machine.

The single injection of Interpon and BMC experiments gave more settings parameters for moulding these materials by using the newly designed thermoset co-injection moulding system. Novel thermoset sandwich moulding components were produced and investigated. The results can be summarised as following.

- Core break-through was likely to happen when co-injecting a glass filled material as the sandwich core, both at the position opposite to the sprue and at some positions on the moulding surface. The break-through on the moulding surface was likely to happen when injecting the core too early before the unreinforced polyester skin material could form a rigid film. Increasing the sequential time gave more time for the skin to form a thicker film and it was able to cover the core material.

- Core break-through occurred at the position opposite to the mould sprue, due to the lower temperature of the mould surface where fresh material from the barrel was entering into the mould and this was followed by very high shear pressure of the core on the uncured skin during injection. Applying more sequential time to the process could not solve the problem. The existing central sprue gate was considered to be not suitable for the co-injection moulding of thermosets.

- The skin was thicker when more sequential time was applied to the process. However, less core penetration was found due to the more viscous skin.

- Thickness of the skin was not uniform throughout the moulding section. This was similar to thermoplastic sandwich mouldings.

- Surface finish of the sandwich moulding was determined by their roughness. It was found that the more skin material that was injected into the mould, the

more the moulding was packed and the better surface finish could be obtained.

- The roughness results showed the possibility of obtaining a good surface finished moulding when applying enough material and pressure to the mould. The thermoset co-injection moulding might be an alterative method for coating and painting a moulding of fibre-filled material.

- The existing manifold was found to be not suitable for delivery of the materials from the injection units. The runner was too complicated, which caused pre-curing and blockage during injection moulding.

- The new manifold was designed and validated using a simulation software package from Moldflow®. The simulation results showed that this new design was proved to be an improvement of the existing manifold.

Recommendation for the future work

This work has provided useful information for improving the innovative co-injection moulding system for thermosets. The problems during co-injection moulding were listed and the suggestions on solving those problems have been made. The following future works are recommended in order to improve the existing thermoset co-injection moulding system.

- The newly designed manifold system that was suggested in Chapter 7 should be built and put it into a practical experiment.

- The machine configuration could be altered to enable a shorter runner for the vertical injection.

- Since the sprue gate can cause core break-through, a side gate, such as a fan gate or a film gate, should be applied to the mould in order to increase the sandwich area.

- The temperature distribution on the mould surface should be investigated in order to get a temperature figure and a suitable time for injecting core material. This can be done by applying some thermocouples inside the mould platens and recording the temperature profile during injection.

- After getting a reliable system, applying the system to other thermoset materials and determining the machine capability and the material compatibility.

References

[1] G.F.Smith and R.A.Easterlow, *New method for manufacturing painted components,* Plastics, Rubber and Composites Processing and Applications, vol. 25, pp. 115-119, 1996.

[2] P.Somnuk and G.F.Smith, *Experiment Study of Simultaneous Co-injection Moulding Process*, ANTEC '95, Boston USA, pp. 760-764, 1995.

[3] R.Sélden, *Sandwich Injection Moulding of Thermoplastics-A Literature Survey*, Journal of Injection Moulding Technology, vol. 1, no. 4, pp. 189-203, Dec 1997.

[4] J.Petterson and P.Nilsson, *Recycling of SMC and BMC in Standard Process Equipment*, of Thermoplastic Composite Materials, vol. 7, pp. 56-63, Jan 1994.

[5] M.Gruskiewicz and K.Butler, *Meeting the Challenge of Thermoset Recycling Under-the-Hood Application*, Advances in Automotive Plastic Components and Technology, pp. 23-29, 1995.

[6] L.A.Dzeskiewicz and J.D.Ralston, *Evaluation of Regrind in Thermoset Application,* ANTEC'94, San Francisco USA, pp. 931-934, 1994.

[7] J.R.Kennerley, N.J.Fenwick, S.J.Pickering and C.D.Rudd, *The Properties of Glass Fibres Recycled From the Thermal Processing of Scrap Thermoset Composites,* ANTEC '96, Indianapolis USA, pp. 890-894, 1996.

[8] G.Brewer, *Processing Structural Foam,* The Society of Plastics Industry, Inc., pp. 80-85, 1986.

[9] D D.F.Oxley and D.J.H.Sandiford, *Sandwich Moulding*, Plastics & Polymers, vol. 39, pp. 288-292, Aug 1971.

[10] D.J.H.Sandiford and D.F.Oxley, *Serving Up a New Plastic Sandwich,* SPE Journal, vol. 27, pp. 38-42, Sep 1971.

[11] V Goodship, J C Love, *Multi-Material Injection Moulding,* Rapra Technology Ltd., Nov 2002.

[12] Battenfeld GmbH, *Battenfeld 's Operating Instructions for BMT-1100/2x300 Co-injection Moulding Machine*, 1998.

[13] Richard Wood. *Automotive Engineering Plastics*, Pentech Press, 1991.

[14] Kortec, *Three-Layer Nozzle Injection Technology*, www.kortec.com, accessed 28 July 2002.

[15] Jaroschek Christoph; Sreger Reinhard; Nesch Wolfgang; Gehring Alexander; Bourdon Karlheinz., *Apparatus for sandwich injection moulding*, EP0692359, 22 Aug 1995.

[16] W Rungseesantivanon, *Factors Affecting adhesion of polymers during Coinjection*, PhD Thesis, University of Warwick Coventry UK, Dec 2000.

[17] Addmix Ltd. (London, U. K), *Addmix Publications*, www.addmix.co.uk/Publications/Publications.html, accessed 4 March 2004.

[18] Twinshot Technologies, *Twinshot*, www.twinshot.com, accessed 3 March 2004.

[19] Milacron Plastics Technologies Group, *Mono-Sandwich*, http://plastics.milacron.com/monosand.htm, accessed 1 October 2002.

[20] Battenfeld Ltd., *Injection unit arrangement*, www.sms-k.com/SMS-Einstieg/default.html, accessed 1 March 2004.

[21] M.J.Dassow, *Prepared for All Situations Technology Leadership by Mult-component Technology*, Kunststoffe Plast Europe, vol. 92, pp. 43-45, Sep 2002.

[22] V.Goodship and K.Kirwan, *Interfacial Instabilities in Multimaterial Co-injection Mouldings*, Plastics, Rubber and Composites, vol. 30, pp. 11-15, 2001.

[23] Donald V Rosato and Dominic V Rosato, *Injection Moulding Handbook*, Chapman & Hall, 1995.

[24] P Somnuk, *Experimental Study of Simultaneous Co-Injection Moulding Process*, PhD Thesis, University of Warwick Coventry UK, April 1995.

[25] J.L.White and H.B.Dee, *Flow Visualisation for Injection Molding of Polyethylene and Polystyrene Melts*, Polymer Engineering and Science, vol. 14, pp. 212, 1974.

[26] J J.LWhite and B.L.Lee, *An Experiment Study of Sandwich Injection Moulding of Two Polymer Melts Using Simultaneous Injection*, Polymer Engineering and Science, vol. 15, pp. 481, Jul 1975.

[27] R.C.Donovan, K.S.Rabe, W.K.Mammel and H.A.Lord, *Recycle Plastics by Two-Shot Moulding*, Polymer Engineering and Science, vol. 15, no. 11, pp. 774-780, Nov 1975.

[28] S.S.Young, J.L.White, E.S.Clark and Y.Oyanagi, *A Basic Experimental Study of Sandwich Injection Molding With Sequential Injection*, SPE ANTEC'80, New York USA, pp. 163-165, 1980.

[29] A.Derdouri, A.Garcia-Réjon, K.T.Nguyen and Y.Simard, *Effect of the Skin/Core Ratio on the Flow Behaviour During Co-injection Moulding*, SPE ANTEC'99, New York USA, pp. 481-484, 1999.

[30] R.Sélden , *Co-injection Moulding: Compatibilization of Polyamide-Polypropylene Sandwich Structures,* Journal of Injection Moulding Technology, vol. 2, no. 4, pp.166-175, Dec 1998.

[31] L.S.Turng, V.W.Wang and K.K.Wang, *Numerical Simulation of The Co-injection Moulding Process,* ASME (Heat and Mass Transfer in Solidification Processing), vol. 25, pp. 113-119, 1991.

[32] S.C.Chen, K.F.Hsu, K.S.Hsu and M.C.Jeng, *Numerical Simulations and Experimental Studies of the Co-injection Molding Process*, SPE ANTEC'93, New Orleans USA, pp. 82-86, 1993.

[33] G.Schlatter, J.F.Agassant, A.Davidoff and M.Vincent, *An Unsteady Multifluid Flow Model: Application to Sandwich Injection Molding Process,* Polymer Engineering and Science, vol. 39, pp. 78-88, Jan 1999.

[34] D.J.Lee, A.I.Isayev and J.L.White, *Simultaneous Sanwich Injection Moulding: Simulation and Experiment,* ANTEC '98, Atlanta USA, pp. 346-350, 1998.

[35] S.Kiatmanaroj, V. Goodship and G. F. Smith, *Sandwich Injection Moulding of Thermosetting Materials. Part I: Initial Experiments,* Progress in Rubber, Plastics and Recycling Technology, vol. 20, no. 3, pp. 171-186, 2004.

[36] Dietrich Hunold, *New and Better Products by Combining Thermosetting Rubber and Thermoplastic Materials in Injection Moulding*, SPE Thermoset Topical Conference: Thermoset Technology for The Molder, Research Triangle Park, NC, 12-14 Mar 2001.

[37] M.Knight, *Gas Assist Works for Thermosets & Smaller Parts, Too,* Plastic Technology, vol. 49, pp. 65-68, May 2003.

[38] Sidney H Goodman, *Handbook of Thermoset Plastics*, Noyes Publications, 1998.

[39] Tony Whelan and John Goff. *Molding of Thermosetting Plastics*,Van Nostrand Reinhold, 1990.

[40] J.F.Monk. *Thermosetting Plastics: Moulding Material and Processes*, Addison Wesley Longman, 1997.

[41] J.-F.Agassant, P. Avenas J. Ph. Sergent and P. J. Carreau, *Polymer Processing Principles and Modeling*, Hanser Publishers, 1991.

[42] J.A. Brydson, *Plastics Materials*, 7th Ed., Butterworth-Heinemann Ltd., 1999.

[43] AC Technology, *C-Mold Reference Manual*, Advanced CAE Technology, Inc., 1996.

[44] J. M. Castro and C. W. Macosko , *Studies of Mold Filllng and Curing in the Reaction Injection Molding (RIM) Process*, AIChE Journal, vol. 28, pp. 250-260, Mar 1982.

[45] M.Rides, *In-line Measurement of Shear Viscosity Using an Injection Moulding Machine*, National Physical Laboratory, 1993.

[46] K.T.Nguyen, K.K.Kabanemi and D.M.Gao, *Simulation of the Injection Molding of Thermosetting Polymers,* ANTEC '95, Boston USA, pp. 868-873, 1995.

[47] Moldflow Corporation, *Plastic Insight 4.1 Reference Manual.* 2004.

[48] Richard Theriault, Tim A. Osswald and Linards Stradins, *Properties of Thermosetting Polymers During Cure,* ANTEC '97, Toronto USA, pp. 766-773, 1997.

[49] Hung-Tzu Chiu, Cheng-Hsien Wu and L. James Lee, *Flow Modeling of Thermoset Injection Molding*, ANTEC '96, Indianapolis USA, pp. 910-916, 1996.

[50] Kimberly J. Bailey, Nikki L. McDowell, Hussan Mahfaz, Trevis Bogetti, Xaoguang Huang and John W. Gillespie, Jr., *Cure Behavior of Thick-Section Thermoset Composites*, ANTEC '98, Atlanta USA, pp. 725-729, 1998.

[51] N.G.McCrum, C.P.Buckley and C.P.Bucknall, *Principles of Polymer Engineering*, Oxford University Press, 1999.

[52] Material Department, Queen Mary University of London, *MAT 604 Material Selection,* www.materials.qmul.ac.uk/mat604/2001/selection.htm, accessed 2 March 2004.

[53] L.R.Nunnery, J., *BMC vs. Nylon Engine covers,* SPE Thermoset Topical Conference: Thermoset Technology for The Molder, Research Triangle Park, NC, 12-14 Mar 2001.

[54] American Plastics Council, *Plastic applications in cars,* www.plastics-car.com/index.html, accessed 6 March 2004.

[55] European Alliance for SMC, *SMC/BMC Design for success*, www.smc-alliance.com/success.pdf, accessed 18 July 2002.

[56] Power Technology, *Contractor Images*, www.power-technology.com/contractor_images/ticonia/2_fuel_cell.jpg, accessed 8 March 2004.

[57] Power Technology, *Contractor Images*, www.power-technology.com/contractor_images/ticonia/3_fuel_cell.jpg, accessed 8 March 2004.

[58] K Kinoshita, *Electrochemical uses of carbon,* http://electrochem.cwru.edu/ed/encycl/art_c01_carcon.htm, accessed 8 March 2004.

[59] M.Imbrogno, *Thermoset in Fuel Cell Market,* SPE Thermoset Topical Conference: Thermoset Technology for The Molder, Research Triangle Park, NC, 12-14 Mar 2001.

[60] CompositN, *The Future Use of Composites in Transport,* www.compositn.net, accessed 10 March 2004.

[61] GPRMC Press Releases, *European Composite Recycling Concept,* www.gprmc.be/PressReleases.htm, accessed 10 March 2004.

[62] V.Goodship, *Arburg Practical Guide for injection moulding,* Rapra Technology Ltd., 2004.

[63] Plastics Engineering Company, *Section 5 - Injection Unit Design Tips,* www.plenco.com/plenco_processing_guide/sect05.pdf, accessed 24 October 2003.

[64] Crucible Materials Corporation, *Crucible Mold&Tool Steels for Plastics,* www.crucibleservice.com/plastics.cfm, accessed 4 March 2004.

[65] Menges and Mohren, *How to Make Injection Molds,* Hanser Publishers, 1993.

[66] Ralph E Wright, *Injection/Transfer Molding of Thermosetting Plastics,* Hanser Publishers, 1995.

[67] Klaus Stoeckhert, *Mold-Making Handbook For the Plastics Engineer,* SPE/Hanser Publishers, 1983.

[68] Plastics Engineering Company, *Section 6 - Thermoset Injection Mold Design Tips,* www.plenco.com/plenco_processing_guide/sect06.pdf, accessed 24 October 2003.

[69] B.G.Karabut, A.D.Sokolov and Yu.I.Shchigel'skii, *Uniformity in Thermoset Injection Moulding,* Soviet Plastics English Translation of Plasticheski, pp. 20-24, 1972.

[70] R.R.Whisson and K.T.Paul, *Thermoset Injection Moulding Part 3.Effects of Processing Conditions on Mouldings,* RAPRA Member Journal, vol. 2, pp. 121-125, May 1974.

[71] I.Čatić, M.Šercer and P.Raos, *Temperature Field and Heat Balance of Moulds for Injection Moulding of Thermosets and Rubbers,* Plastics and Rubber Processing and Applications, vol. 5, pp. 375-378, 1985.

[72] H.Hadi, K.Azzar, A.El Brouzi, R Granger and J.M.Vergnaud, *Injection Moulding of Thermoset. Effect of the Temperature of Injection,* European Polymer Journal, vol. 29, pp. 575-583, 1993.

[73] John Viego, Richard P.Theriault and Tim A.Osswald, *3-D Simulation of Thick Thermoset Components,* ANTEC 2000, Orlando USA, pp. 849-853, 2000.

[74] M.Rides, *Rheological Measurement Methods for Fibre Filled Plastics*, National Physical Laboratory, 1994.

[75] BIP Limited, *Product Data Beetle BMC Type G7B 5580*, Jan 2001.

[76] D.J.Whitehouse, *Handbook of Surface Metrology*, Institute of Physics, 1994.

[77] M.A.dagnall, *Exploring Surface Texture*, Rank Taylor Hobson, 1986.

[78] F.N.Cogswell. *Polymer Melt Rheology: A guide for Industrial Practice*, Woodhead publishing limited, 1996.

Appendix I

Drawings of the new manifold system

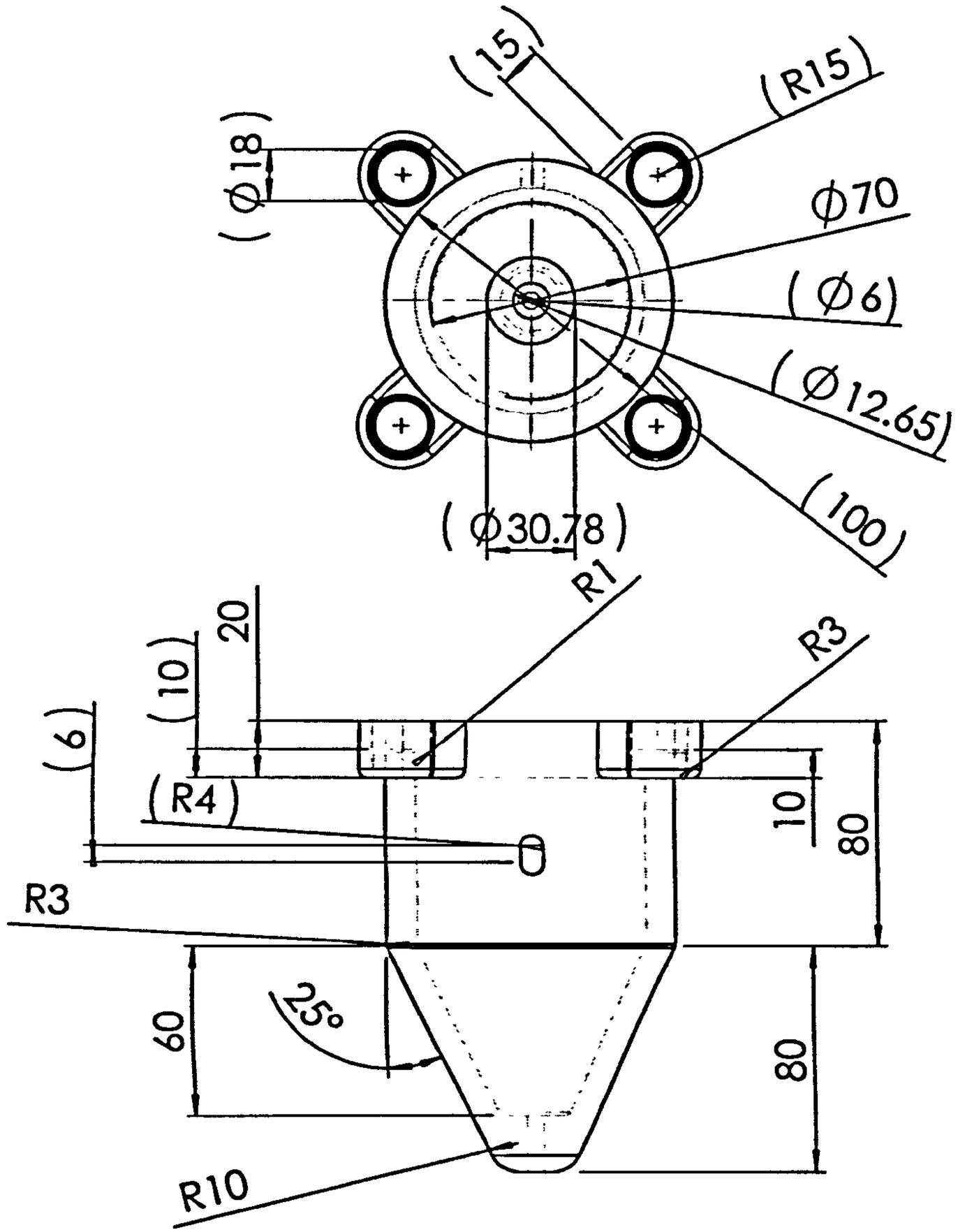

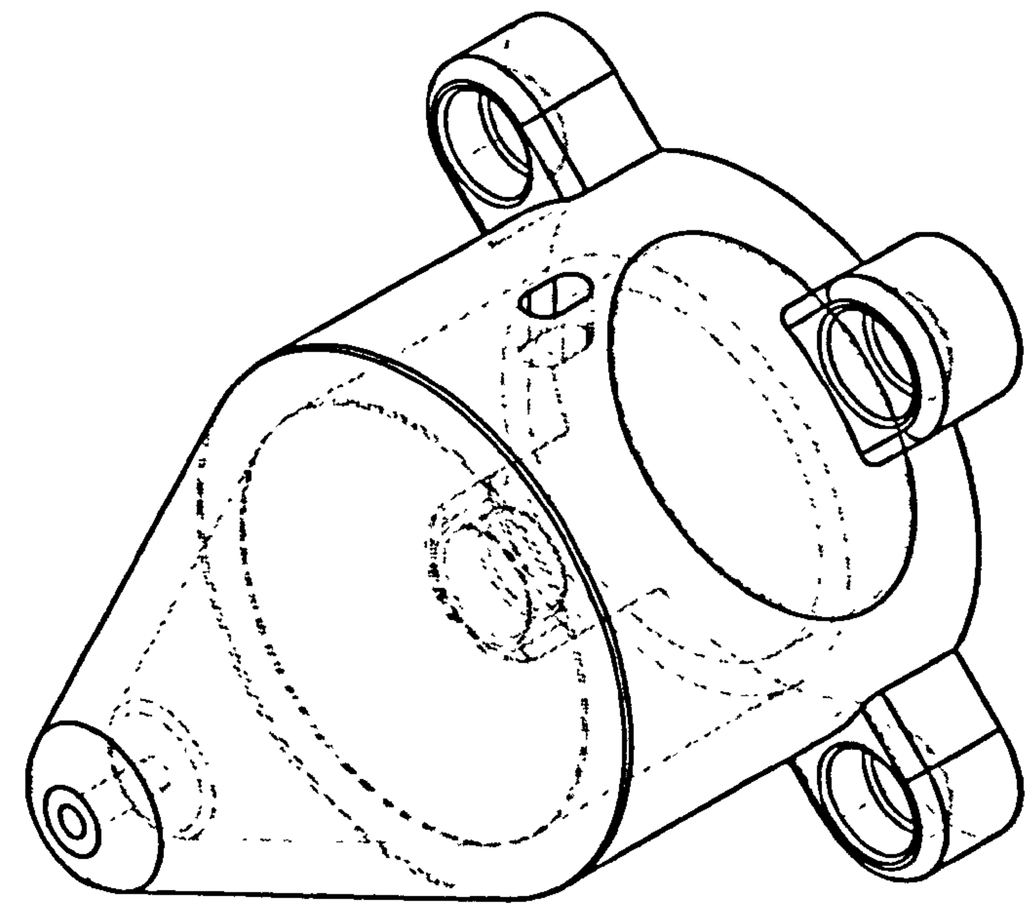

NOTE: This drawing is a private and confidential communication and the property of the University of Warwick. It must not be copied or loaned without the written consent of the University and must be returned immediately on completion of tender or contract

THIRD ANGLE PROJECTION

M/C AT 'F'
GRIND AT 'G'
GENERAL TOLERANCE :
I.S.O. LIMITS & FITS

University of Warwick

Department of Engineering

PROJECT TITLE **Thermoset sandwich injection moulding**

DRAW	SK
DATE	08/04/04
CHECK	
PROJECT No.	

Outer nozzle

SHEET 1 OF 1 SCALE 1:3

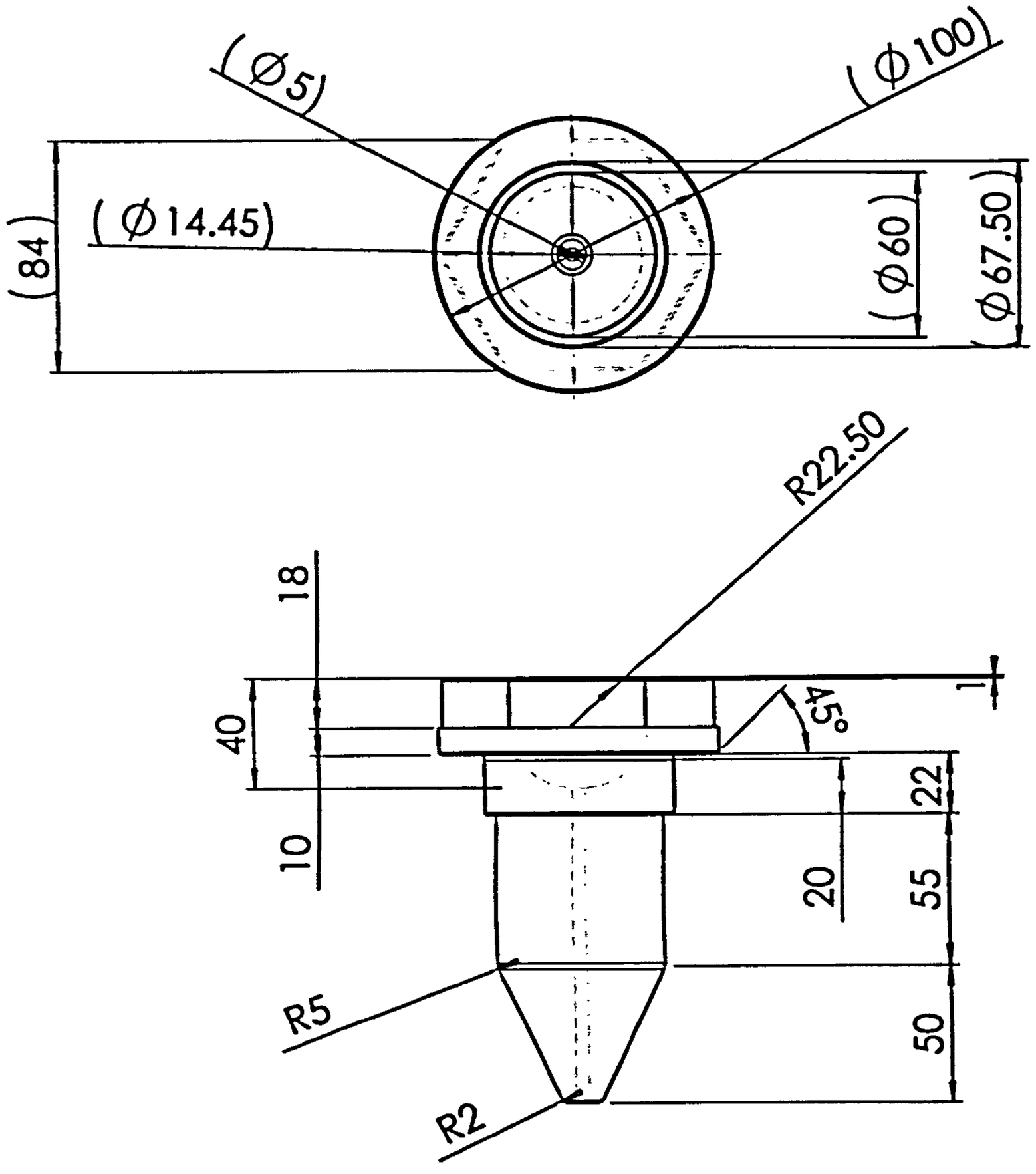

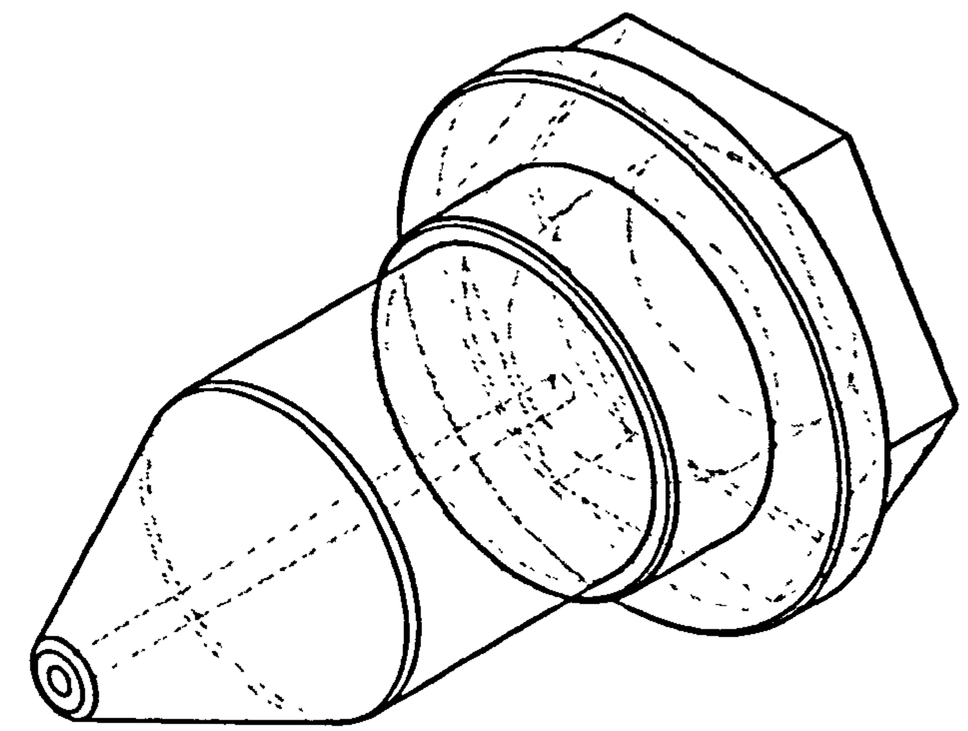

University of Warwick

Department of Engineering

PROJECT TITLE **Thermoset sandwich injection moulding**

THIRD ANGLE PROJECTION

M/C AT 'Y'
GRIND AT 'G'
GENERAL TOLERANCE :
I.S.O. LIMITS & FITS

DRAW	SK
DATE	08/04/04
CHECK	
PROJECT No.	

Inner nozzle

SHEET 1 OF 1 SCALE 1:3

NOTE: This drawing is a private and confidential communication and the property of the University of Warwick. It must not be copied or loaned without the written consent of the University and must be returned immediately on completion of tender or contract

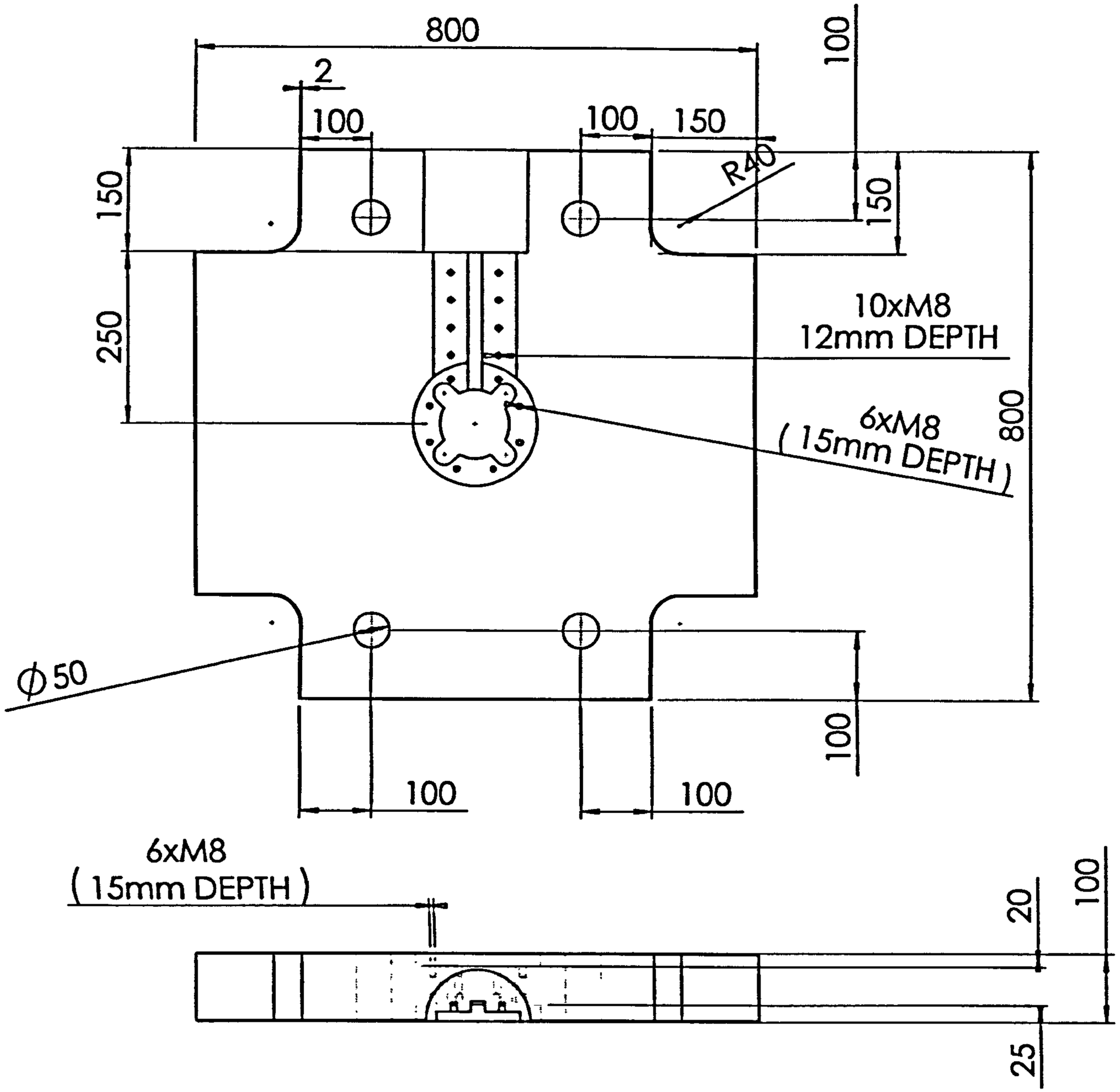

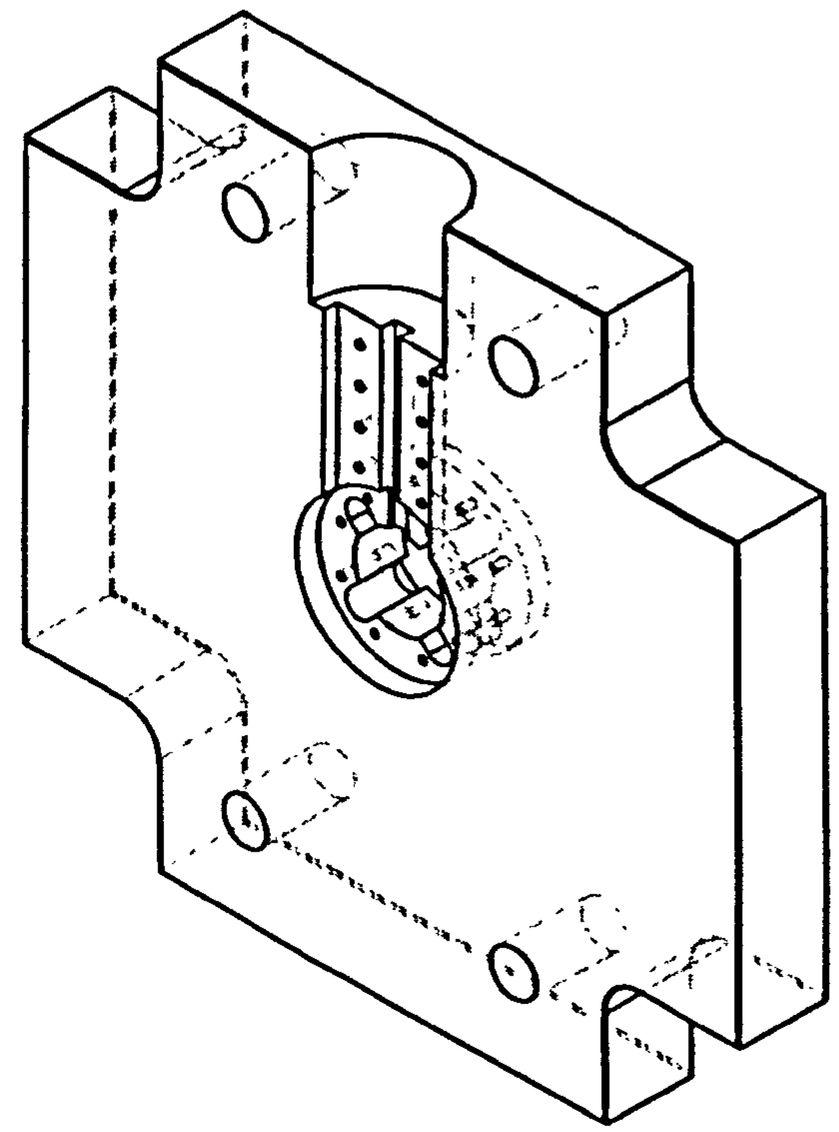

THIRD ANGLE PROJECTION

M/C AT Y

GRIND AT 'G'

GENERAL TOLERANCE :

I.S.O. LIMITS & FITS

NOTE: This drawing is a private and confidential communication and the property of the University of Warwick. It must not be copied or loaned without the written consent of the University and must be returned immediately on completion of tender or contract

University of Warwick

Department of Engineering

PROJECT TITLE **Thermoset sandwich injection moulding**

DRAW	SK	Fixed platen
DATE	08/04/04	
CHECK		
PROJECT No.		SHEET 1 OF 1 SCALE 1:5

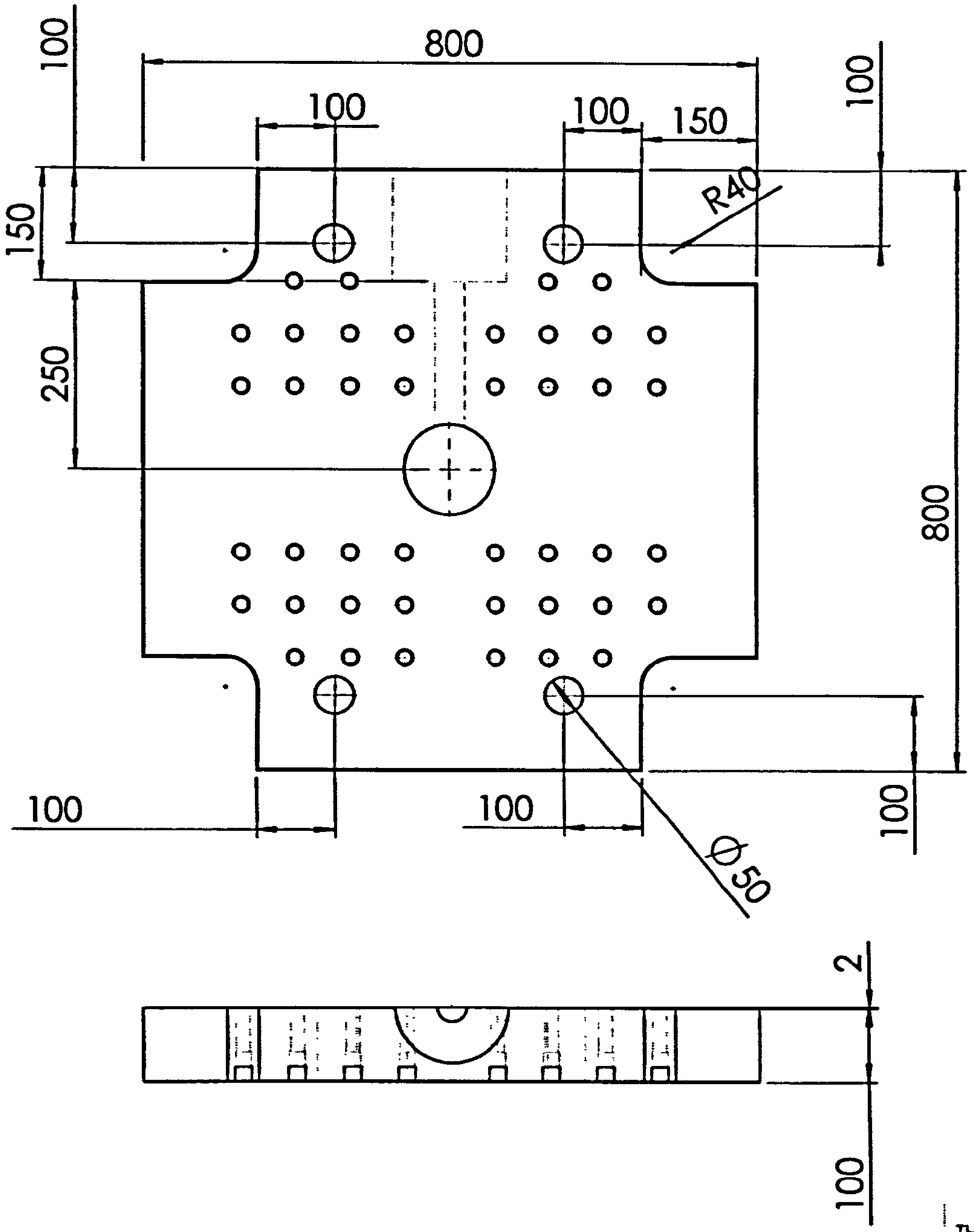

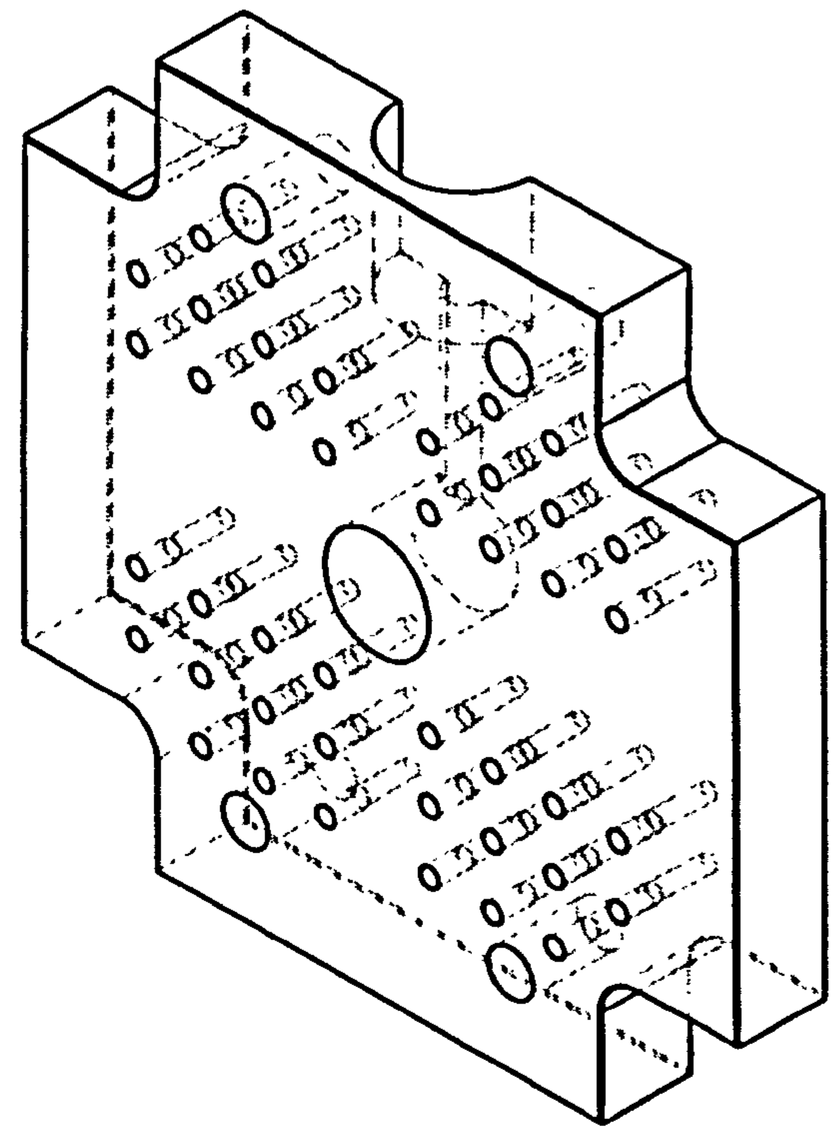

NOTE: This drawing is a private and confidential communication and the property of the University of Warwick. It must not be copied or loaned without the written consent of the University and must be returned immediately on completion of tender or contract

THIRD ANGLE PROJECTION

M/C AT 'Y'
GRIND AT 'G'
GENERAL TOLERANCE :
I.S.O. LIMITS & FITS

University of Warwick

Department of Engineering

PROJECT TITLE **Thermoset sandwich injection molding**

DRAW	SK	Moving platen
DATE	08/04/04	
CHECK		
PROJECT No.		SHEET 1 OF 1 — SCALE 1:5

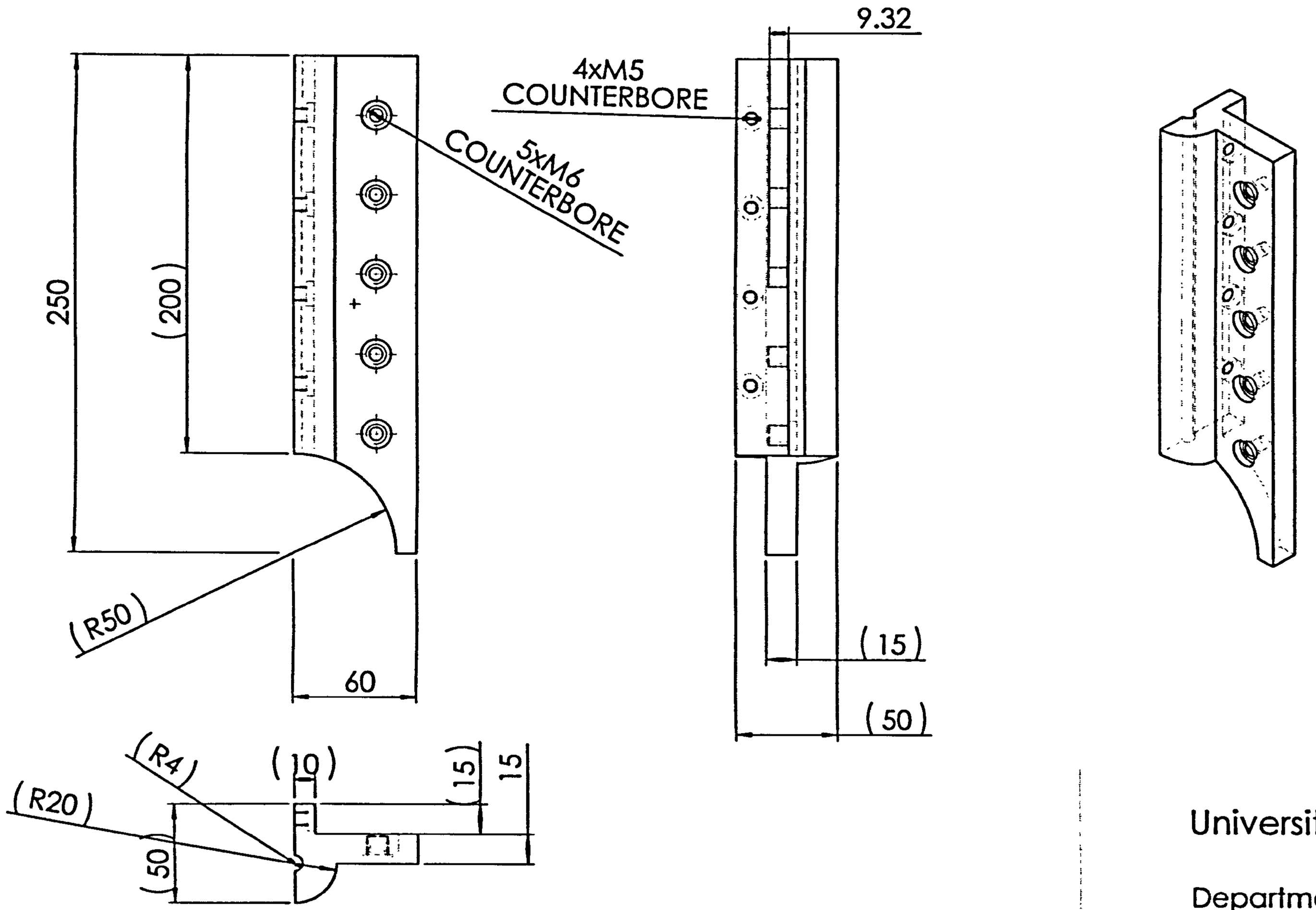

NOTE: This drawing is a private and confidential communication and the property of the University of Warwick. It must not be copied or loaned without the written consent of the University and must be returned immediately on completion of tender or contract

THIRD ANGLE PROJECTION

M/C AT Y

GRIND AT 'G'

GENERAL TOLERANCE :

I.S.O. LIMITS & FITS

University of Warwick

Department of Engineering

PROJECT TITLE **Thermoset sandwich injection moulding**

DRAW	SK
DATE	08/04/04
CHECK	
PROJECT No.	

Right insert

SHEET 1 OF 1

SCALE 1:3

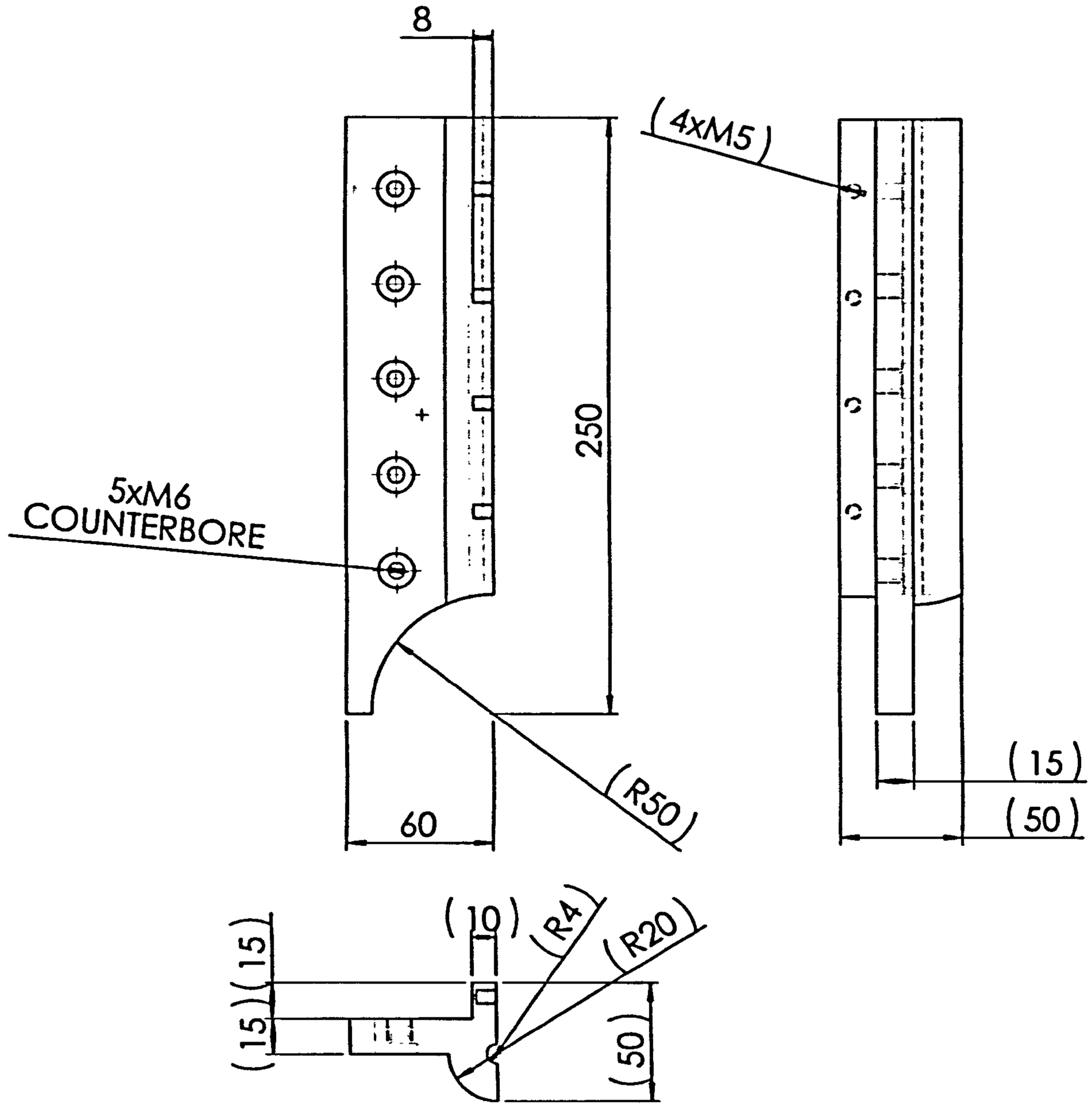

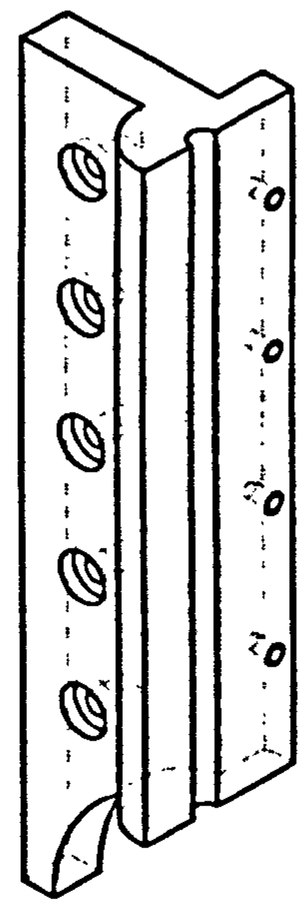

University of Warwick

Department of Engineering

PROJECT TITLE **Thermoset sandwich injection moulding**

DRAW	SK	Left insert
DATE	08/04/04	
CHECK		
PROJECT No.		SHEET 1 OF 1 — SCALE 1:3

THIRD ANGLE PROJECTION

M/C AT 'Y'
GRIND AT 'G'
GENERAL TOLERANCE :
I.S.O. LIMITS & FITS

NOTE: This drawing is a private and confidential communication and the property of the University of Warwick. It must not be copied or loaned without the written consent of the University and must be returned immediately on completion of tender or contract

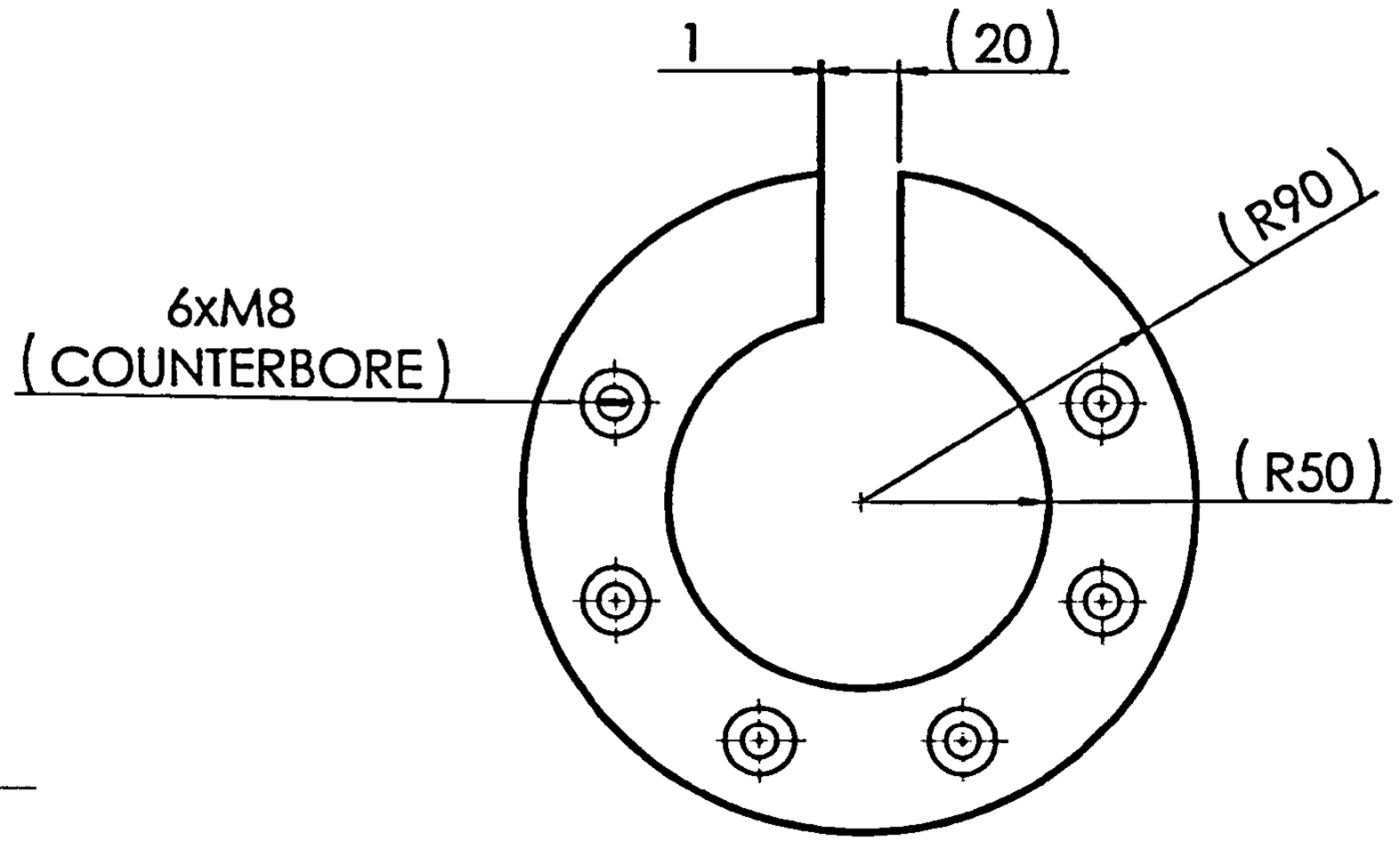

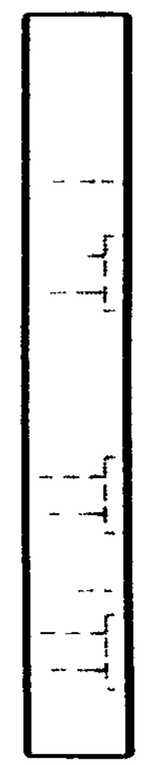

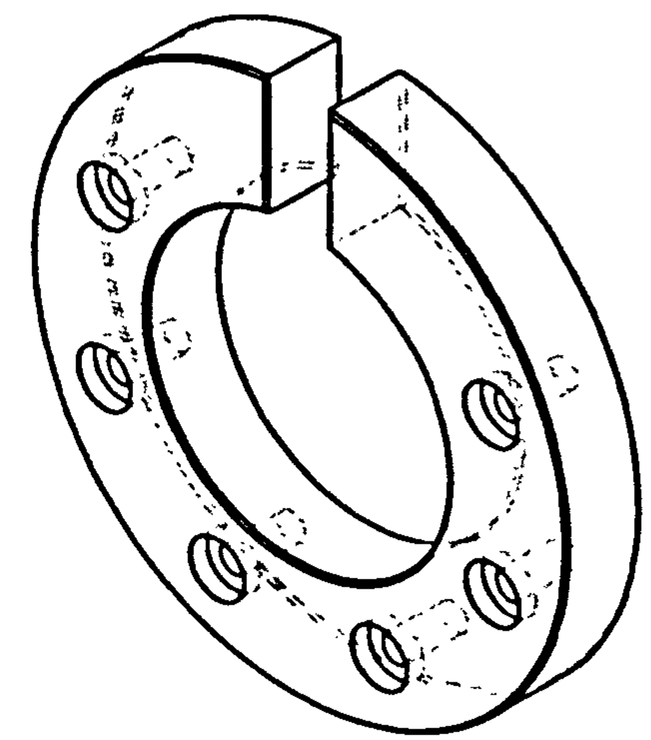

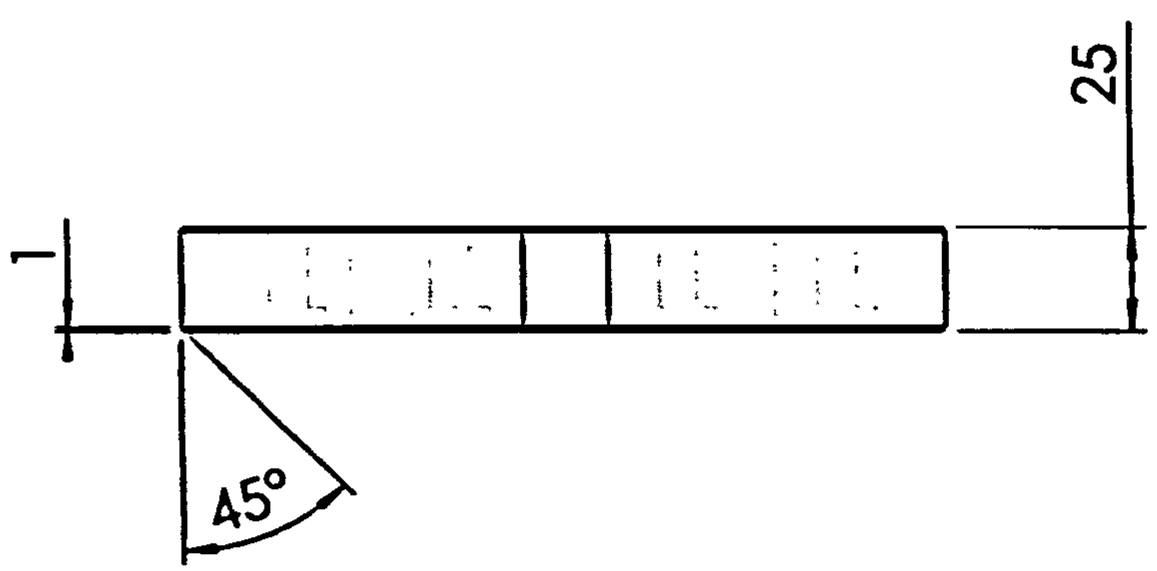

NOTE: This drawing is a private and confidential communication and the property of the University of Warwick. It must not be copied or loaned without the written consent of the University and must be returned immediately on completion of tender or contract

THIRD ANGLE PROJECTION

M/C AT Y
GRIND AT 'G'
GENERAL TOLERANCE :
I.S.O. LIMITS & FITS

University of Warwick

Department of Engineering

PROJECT TITLE **Thermoset sandwich injection moulding**

DRAW	SK
DATE	08/04/04
CHECK	
PROJECT No.	

Front ring

SHEET 1 OF 1 SCALE 1:3

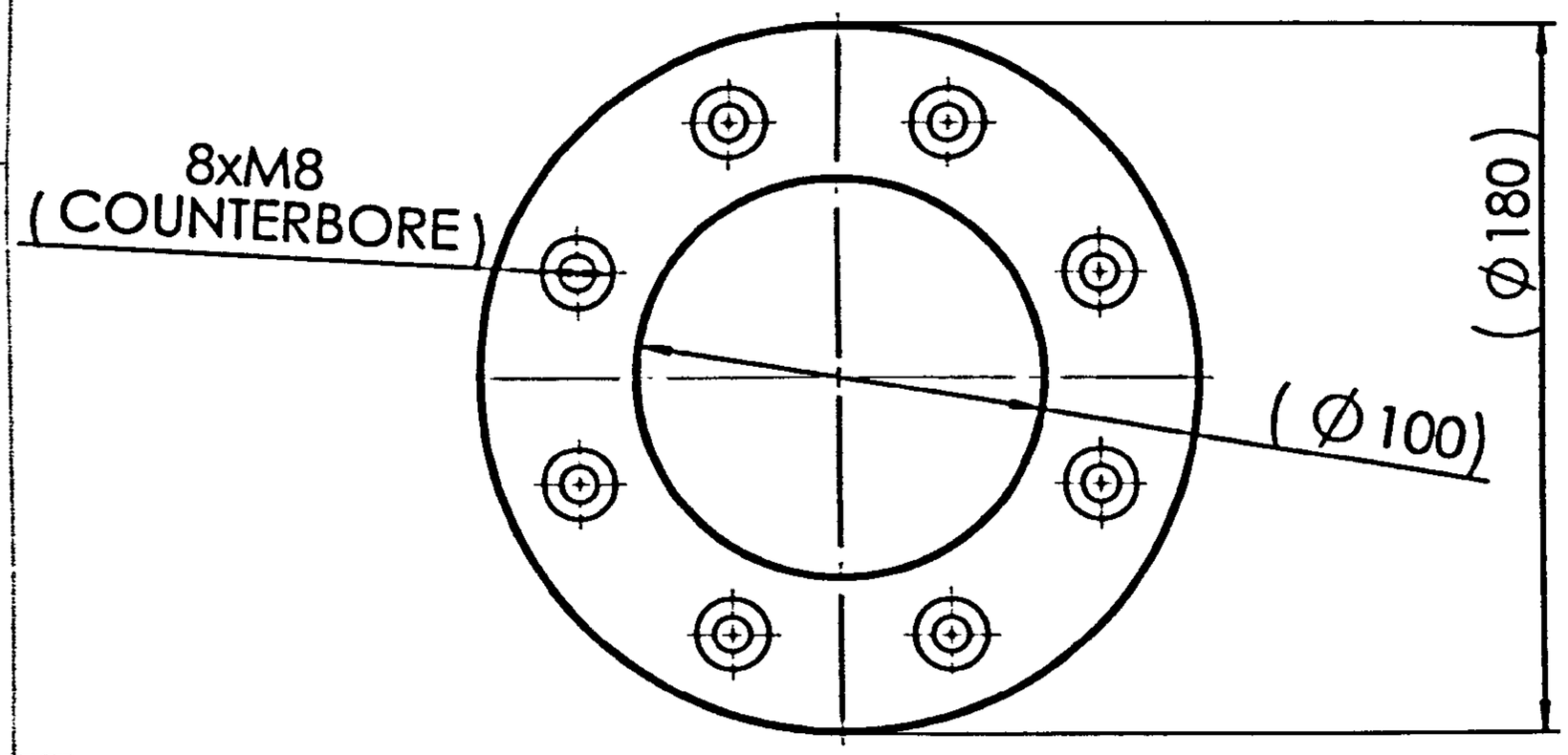

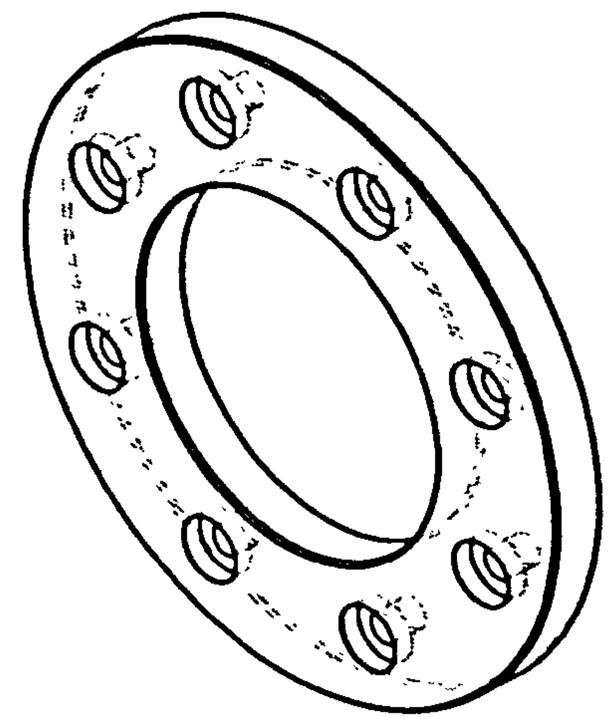

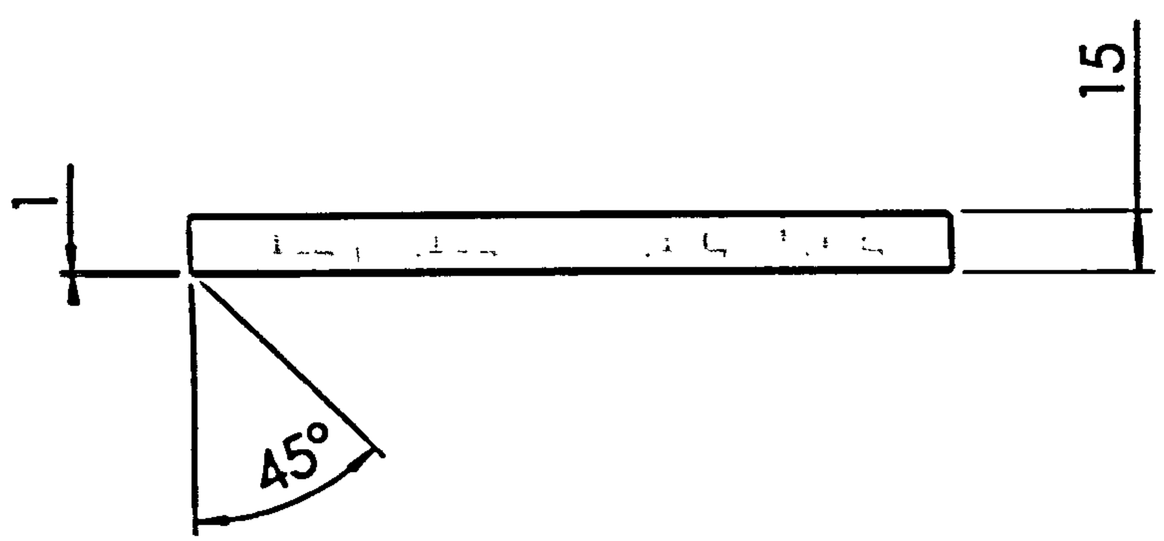

NOTE: This drawing is a private and confidential communication and the property of the University of Warwick. It must not be copied or loaned without the written consent of the University and must be returned immediately on completion of tender or contract

THIRD ANGLE PROJECTION

M/C AT 'F'
GRIND AT 'G'
GENERAL TOLERANCE :
I.S.O. LIMITS & FITS

University of Warwick

Department of Engineering

PROJECT TITLE **Thermoset sandwich injection moulding**

DRAW	SK	Back ring
DATE	08/04/04	
CHECK		
PROJECT No.		SHEET 1 OF 1 SCALE 1:3

Appendix II

Examples of Moldflow® simulation screen outputs

The existing manifold system

Mould temperature 80°C, Injection time 1 second

Copyright Moldflow Corporation and Moldflow Pty. Ltd. All Rights Reserved.
(C)2000 2001 2002 2003
This product may be covered by
US patent 6,096,088 ,
Australian Patent No. 721978 ,
and foreign patents and pending applications

Thermoset Flow Analysis

Version: mpi410 (Build 03203)

Analysis commenced at Mon Feb 09 11:04:13 2004
Processing fusion mesh...
... finished processing fusion mesh
Date : FEB-09-2004
Time : 11:04:47
Reading input data...
Processing fusion mesh...
... finished processing fusion mesh
Processing fusion mesh...
... finished processing fusion mesh
File name : 237nofillet801~2
Reading solver parameters...
Reading material data...
Reading process settings...
Reading finite element mesh...
Finished reading input data

Optimizing node and element numbering...
... finished optimizing node and element numbering

Summary of analysis inputs :

Solver parameters :

No. of laminae across thickness = 12
No. of results at constant intervals = 20
No. of profiled results at constant intervals = 0
Flow rate convergence tolerance = 0.5000 %
Melt temperature convergence tolerance = 0.2000 C
Conversion convergence tolerance = 0.2000 %
Mold-melt heat transfer coefficient = 2.5000E+04 W/m^2-C
Heat transfer coeff. between pot and pellet (side) = 5000.0000 W/m^2-C
Heat transfer coeff. between pot and pellet (bot.) = 5000.0000 W/m^2-C
Maximum no. of flow rate iterations = 125
Maximum no. of melt-temp and conversion iterations = 100

Material data :

Polymer :

Constant polymer density
RHO = 1.6240 g/cm^3

Specific heat (Cp) = 852.0000 J/kg-C

Thermal conductivity = 0.8500 W/m-C

Reactive polymer viscosity I

$$ETA = ETAm*\left(\frac{ALFAgel}{ALFAgel-ALFA}\right)(C1+C2*ALFA) \quad \text{if } ALFA < ALFAgel$$

$$ETA = \text{infinity} \quad \text{if } ALFA > ALFAgel$$

$$\text{where } ETAm = \frac{ETAo}{1 + (ETAo*GAMMA/TAUS)^{(1-n)}}$$

ETAo = B * EXP(Tb/T)
n = 0.0835
TAUS = 2.7200E+04 Pa
B = 2920.0000 Pa-s
Tb = 5880.0000 K
C1 = 0.1790
C2 = 102.0000

N-th order kinetics with induction time
Total heat of reaction (H)
where H = 2.9000E+04 J/kg
Isothermal induction time
Tind = B1 * EXP(B2/T)
where B1 = 0.0000 s
B2 = 0.0000 K
Isothermal curing kinetics
d(ALFA)/dt = (K1+K2*ALFA^EM)*(1-ALFA)^EN
where K1 = A1 * EXP(- E1/T)
K2 = A2 * EXP(- E2/T)
EM = 0.5660
EN = 2.9950
A1 = 0.0000 1/s
A2 = 5.1800E+25 1/s
E1 = 6.4540 K
E2 = 2.3900E+04 K
Gelation conversion (ALFAgel) = 0.0500

Process settings :

Machine parameters :

Maximum injection pressure = 1.7500E+02 MPa

Conditions at the Pot (pre-conditioning) :

Pellet diameter = 12.0000 mm
Pellet length = 20.0000 mm
Transfer pot temperature = 80.0000 C
Delay time in the pot = 5.0000 s

Process parameters :

Fill time = 1.0000 s
Curing time = 30.0000 s
Melt temperature = 80.0000 C
Inlet melt conversion = 0.0000
Melt temperature after preconditioning = 80.0000 C
Melt conversion after preconditioning = 0.0000
Mold temperature = 80.00 C
Ambient temperature = 25.0000 C
Velocity/pressure switch-over by % volume = 99.0000 %
Ram speed profile (rel):

% stroke	% ram speed
0.0000	100.0000

```
     56.0000        75.0000
     88.0000        50.0000
    100.0000        25.0000

Model details :

  Total number of nodes                    =    10492
  Total number of injection location nodes        =       1
    The injection location node labels are:
                                   10628
  Total number of elements                 =    20976
    Number of part elements                =    20976
    Number of sprue/runner/gate elements         =       0
    Number of connector elements                 =       0
 NOTE: The parting plane has not been specified. The global XY plane will be
      used instead.
  Parting plane normal                 (dx) =    0.0000
                                       (dy) =    0.0000
                                       (dz) =    1.0000
  Average aspect ratio of triangle elements        =    1.8487
  Maximum aspect ratio of triangle elements        =    5.9607
  Element number with maximum aspect ratio         =      2490
  Minimum aspect ratio of triangle elements        =    1.1548
  Element number with minimum aspect ratio         =     10774
  Total volume                             =  329.3560 cm^3
    Volume filled initially                =    0.0000 cm^3
    Volume to be filled                    =  329.3560 cm^3
      Part volume to be filled             =  329.3560 cm^3
      Sprue/runner/gate volume to be filled        =    0.0000 cm^3
Initializing variables...
... finished initializing variables
  Filling phase:   Status: V  = Velocity control
                   P  = Pressure control
                   V/P= Velocity/pressure switch-over
|-------------------------------------------------------|
| Time  | Volume|  Pressure   | Clamp force|Flow rate|Status |
| (s)   | (%)   |   (MPa)     | (tonne)    |(cm^3/s) |       |
|-------------------------------------------------------|
| 0.00 | 0.01 |      0.43 |      0.00 | 479.91 |  V  |
| 0.05 | 7.49 |     37.67 |      3.72 | 462.89 |  V  |

** WARNING ** Local hot spot encountered.  Material gelation may occur.
| 0.10 | 14.96 |     49.90 |      9.70 | 446.53 |  V  |

** WARNING ** Local hot spot encountered.  Material gelation may occur.

| 0.16 | 22.06 |     52.85 |     13.21 | 431.33 |  V  |.

** WARNING ** Local hot spot encountered.  Material gelation may occur.
| 0.21 | 28.89 |     54.66 |     16.98 | 416.73 |  V  |

** WARNING ** Local hot spot encountered.  Material gelation may occur.
| 0.26 | 35.31 |     56.01 |     20.95 | 402.95 |  V  |

** WARNING ** Local hot spot encountered.  Material gelation may occur..
| 0.31 | 41.56 |     57.14 |     25.23 | 389.61 |  V  |

** WARNING ** Local hot spot encountered.  Material gelation may occur.

| 0.37 | 48.05 |     58.08 |     29.69 | 375.66 |  V  |

** WARNING ** Local hot spot encountered.  Material gelation may occur.
| 0.42 | 53.82 |     58.71 |     33.34 | 363.28 |  V  |

** WARNING ** Local hot spot encountered.  Material gelation may occur.
| 0.47 | 59.44 |     59.18 |     36.93 | 345.79 |  V  |

** WARNING ** Local hot spot encountered.  Material gelation may occur.
| 0.52 | 65.04 |     59.53 |     40.37 | 324.92 |  V  |

** WARNING ** Local hot spot encountered.  Material gelation may occur.

| 0.57 | 69.78 |     60.03 |     44.92 | 307.22 |  V  |
```

** WARNING ** Local hot spot encountered. Material gelation may occur.
| 0.63 | 74.62 | 60.56 | 50.18 | 289.11 | V |
** WARNING ** Local hot spot encountered. Material gelation may occur.
| 0.73 | 83.53 | 61.21 | 58.63 | 255.72 | V |

** WARNING ** Local hot spot encountered. Material gelation may occur.
| 0.78 | 87.61 | 61.45 | 62.55 | 240.56 | V |

** WARNING ** Local hot spot encountered. Material gelation may occur.
| 0.83 | 91.14 | 61.18 | 65.46 | 207.79 | V |

** WARNING ** Local hot spot encountered. Material gelation may occur.
| 0.89 | 94.27 | 61.11 | 70.49 | 176.63 | V |

** WARNING ** Local hot spot encountered. Material gelation may occur.

** WARNING ** Local hot spot encountered. Material gelation may occur.
0.94	96.89	61.23	76.84	150.53	V
0.99	99.05				V/P
0.99	99.05	61.38	83.83	128.35	P
1.01	100.00	61.39	88.04	128.35	P

SYNERGY Reactive Molding 4.1 summary report of analysis.

Date : FEB09-04
Time : 11:05:59
Name : 237nofillet801~2

Filling phase results summary :

Maximum injection pressure (at 0.783 s) = 61.4534 MPa
Melt temperature after preconditioning = 80.0000 C
Melt conversion after preconditioning = 0.0000

End of filling phase results summary :

Time at the end of filling = 1.0102 s
Injection pressure = 61.3931 MPa
Injection pressure - extrapolated = 61.3571 MPa
Total weight = 529.4920 g
Maximum Clamp force - during filling = 88.0365 tonne
Clamp force - estimated = 511.6909 tonne

Filling phase results summary for the part :

Bulk temperature - maximum (at 0.989 s) = 91.9890 C
Bulk temperature - 95th percentile (at 0.886 s) = 85.5790 C
Bulk temperature - 5th percentile (at 1.010 s) = 82.2650 C
Bulk temperature - minimum (at 1.010 s) = 80.0000 C
Bulk conversion - maximum (at 1.010 s) = 0.0002
Bulk conversion - 95th percentile (at 1.010 s) = 1.1947E-06

Wall shear stress - maximum (at 0.105 s) = 0.2494 MPa
Wall shear stress - 95th percentile (at 0.105 s) = 0.1836 MPa

Shear rate - maximum (at 0.105 s) = 9.2877E+04 1/s
Shear rate - 95th percentile (at 0.105 s) = 3734.2100 1/s
Melt front area - average = 22.2520 cm^2
Melt front area - RMS deviation = 9.9326 cm^2
Melt front velocity = 36.5678 cm/s
Melt front velocity - RMS deviation = 91.7194 cm/s

End of filling phase results summary for the part :

Total part weight = 529.4920 g

Bulk temperature - maximum = 91.9260 C
Bulk temperature - 95th percentile = 85.4200 C
Bulk temperature - 5th percentile = 82.2650 C
Bulk temperature - minimum = 80.0000 C
Bulk temperature - average = 83.1840 C
Bulk temperature - RMS deviation = 0.9801 C
Bulk conversion - maximum = 0.0002

Bulk conversion - 95th percentile = 1.1947E-06
Bulk conversion - average = 4.1658E-07
Bulk conversion - RMS deviation = 0.0000

Wall shear stress - maximum = 0.2221 MPa
Wall shear stress - 95th percentile = 0.1672 MPa
Wall shear stress - average = 0.1406 MPa
Wall shear stress - RMS deviation = 0.0279 MPa

Shear rate - maximum = 2.4147E+04 1/s
Shear rate - 95th percentile = 924.3220 1/s
Shear rate - average = 347.2310 1/s
Shear rate - RMS deviation = 1094.4900 1/s

Curing phase:

Time (s)	Status
2.64	Curing phase
4.14	Curing phase
5.76	Curing phase
7.26	Curing phase
8.89	Curing phase
10.39	Curing phase
12.01	Curing phase
13.51	Curing phase
15.14	Curing phase
16.64	Curing phase
18.26	Curing phase
19.76	Curing phase
21.39	Curing phase
22.89	Curing phase
24.51	Curing phase
26.01	Curing phase
27.64	Curing phase
29.14	Curing phase
30.76	Curing phase
31.01	Curing phase

Preparing output data...
Finished preparing output data

SYNERGY Reactive Molding
has completed successfully.

Processing fusion mesh...
... finished processing fusion mesh
Weld line/air trap analysis completed

Preparing output data...
Finished preparing output data

SYNERGY Weld-line and air trap
has completed successfully.

Execution time
Analysis commenced at Mon Feb 09 11:04:13 2004
Analysis completed at Mon Feb 09 12:56:12 2004
CPU time used 6718.61 s

Mould temperature 120°C, Injection time 1 second

Copyright Moldflow Corporation and Moldflow Pty. Ltd. All Rights Reserved.
(C)2000 2001 2002 2003
This product may be covered by
US patent 6,096,088 ,
Australian Patent No. 721978 ,
and foreign patents and pending applications

Thermoset Flow Analysis

Version: mpi410 (Build 03203)

Analysis commenced at Mon Feb 02 15:44:33 2004
Processing fusion mesh...
... finished processing fusion mesh
Date : FEB-02-2004
Time : 15:45:08
Reading input data...
Processing fusion mesh...
... finished processing fusion mesh
Processing fusion mesh...
... finished processing fusion mesh
File name : 237nofillet1201~1
Reading solver parameters...
Reading material data...
Reading process settings...
Reading finite element mesh...
Finished reading input data

Optimizing node and element numbering...
... finished optimizing node and element numbering

Filling phase: Status: V = Velocity control
P = Pressure control
V/P= Velocity/pressure switch-over

Time (s)	Volume (%)	Pressure (MPa)	Clamp force (tonne)	Flow rate (cm^3/s)	Status
0.00	0.01	0.38	0.00	479.91	V
0.05	7.54	35.65	3.59	462.86	V
0.10	15.02	46.77	9.09	446.54	V
0.16	22.18	49.33	12.23	431.16	V
0.21	28.82	50.90	15.53	416.91	V
0.26	35.29	52.10	19.06	403.09	V
0.31	41.91	53.15	23.10	388.87	V
0.37	48.09	53.94	26.86	375.75	V
0.42	53.87	54.50	30.12	363.35	V
0.47	59.53	54.90	33.29	345.59	V
0.52	65.12	55.19	36.28	324.72	V
0.57	69.92	55.66	40.51	306.75	V
0.63	74.77	56.10	45.00	288.62	V
0.68	79.39	56.42	48.92	271.38	V
0.73	83.78	56.68	52.63	254.80	V
0.78	87.51	56.89	55.73	241.00	V
0.83	91.07	56.65	58.34	208.52	V
0.88	94.20	56.58	62.79	177.32	V
0.94	96.82	56.66	68.29	151.29	V
0.99	99.03			V/P	
0.99	99.13	56.74	74.69	126.95	P
1.01	100.00	56.75	77.83	126.95	P

SYNERGY Reactive Molding 4.1 summary report of analysis.

Date : FEB02-04
Time : 15:46:21
Name : 237nofillet1201~1

Filling phase results summary :

Maximum injection pressure (at 0.781 s) = 56.8938 MPa
Melt temperature after preconditioning = 80.0000 C
Melt conversion after preconditioning = 0.0000

End of filling phase results summary :

Time at the end of filling = 1.0089 s
Injection pressure = 56.7453 MPa
Injection pressure - extrapolated = 56.7453 MPa
Total weight = 529.4920 g
Maximum Clamp force - during filling = 77.8341 tonne
Clamp force - estimated = 472.9088 tonne

Filling phase results summary for the part :

Bulk temperature - maximum (at 0.626 s) = 106.0130 C
Bulk temperature - 95th percentile (at 1.009 s) = 99.6800 C
Bulk temperature - 5th percentile (at 0.104 s) = 84.4370 C
Bulk temperature - minimum (at 1.009 s) = 80.0000 C
Bulk conversion - maximum (at 1.009 s) = 0.2066
Bulk conversion - 95th percentile (at 1.009 s) = 0.0002

Wall shear stress - maximum (at 0.104 s) = 0.2374 MPa
Wall shear stress - 95th percentile (at 0.104 s) = 0.1701 MPa

Shear rate - maximum (at 0.104 s) = 9.2015E+04 1/s
Shear rate - 95th percentile (at 0.104 s) = 3599.8401 1/s
Melt front area - average = 22.3023 cm^2
Melt front area - RMS deviation = 9.9682 cm^2
Melt front velocity = 36.3033 cm/s
Melt front velocity - RMS deviation = 90.7840 cm/s

End of filling phase results summary for the part :

Total part weight = 529.4920 g

Bulk temperature - maximum = 104.9000 C
Bulk temperature - 95th percentile = 99.6800 C
Bulk temperature - 5th percentile = 87.0500 C
Bulk temperature - minimum = 80.0000 C
Bulk temperature - average = 95.5790 C
Bulk temperature - RMS deviation = 4.1179 C
Bulk conversion - maximum = 0.2066
Bulk conversion - 95th percentile = 0.0002
Bulk conversion - average = 7.3321E-05
Bulk conversion - RMS deviation = 0.0007

Wall shear stress - maximum = 0.2115 MPa
Wall shear stress - 95th percentile = 0.1544 MPa
Wall shear stress - average = 0.1257 MPa
Wall shear stress - RMS deviation = 0.0256 MPa

Shear rate - maximum = 2.3766E+04 1/s
Shear rate - 95th percentile = 945.0590 1/s
Shear rate - average = 353.0540 1/s
Shear rate - RMS deviation = 1106.9399 1/s

Curing phase:

Time (s)	Status
2.63	Curing phase
4.13	Curing phase
5.76	Curing phase
7.26	Curing phase
8.88	Curing phase
10.38	Curing phase
12.01	Curing phase
13.51	Curing phase
15.13	Curing phase
16.63	Curing phase
18.26	Curing phase
19.76	Curing phase
21.38	Curing phase
22.88	Curing phase
24.51	Curing phase
26.01	Curing phase
27.63	Curing phase
29.13	Curing phase
30.76	Curing phase
31.13	Curing phase

Preparing output data...
Finished preparing output data

SYNERGY Reactive Molding

has completed successfully.

Processing fusion mesh...
... finished processing fusion mesh
Weld line/air trap analysis completed

Preparing output data...
Finished preparing output data

SYNERGY Weld-line and air trap
has completed successfully.

Execution time
Analysis commenced at Mon Feb 02 15:44:33 2004
Analysis completed at Mon Feb 02 16:08:35 2004
CPU time used 1440.89 s

Mould temperature 130°C, Injection time 1 second

Copyright Moldflow Corporation and Moldflow Pty. Ltd. All Rights Reserved.
(C)2000 2001 2002 2003
This product may be covered by
US patent 6,096,088 ,
Australian Patent No. 721978 ,
and foreign patents and pending applications

Thermoset Flow Analysis

Version: mpi410 (Build 03203)

Analysis commenced at Tue Feb 03 09:55:27 2004
Processing fusion mesh...
... finished processing fusion mesh
Date : FEB-03-2004
Time : 09:56:02
Reading input data...
Processing fusion mesh...
... finished processing fusion mesh
Processing fusion mesh...
... finished processing fusion mesh
File name : 237nofillet1301~1
Reading solver parameters...
Reading material data...
Reading process settings...
Reading finite element mesh...
Finished reading input data

Optimizing node and element numbering...
... finished optimizing node and element numbering

Filling phase: Status: V = Velocity control
P = Pressure control
V/P= Velocity/pressure switch-over

Time (s)	Volume (%)	Pressure (MPa)	Clamp force (tonne)	Flow rate (cm^3/s)	Status
0.00	0.01	0.37	0.00	479.92	V
0.05	7.48	34.70	3.42	463.01	V
0.10	14.88	45.82	8.87	446.87	V
0.16	21.92	48.40	11.95	431.78	V
0.21	28.79	50.01	15.26	416.99	V
0.26	35.28	51.24	18.71	403.10	V
0.31	41.53	52.38	22.47	389.76	V
0.36	47.63	53.46	26.26	376.72	V

** WARNING ** Local hot spot encountered. Material gelation may occur.

** WARNING ** Local hot spot encountered. Material gelation may occur.

| 0.42 | 53.82 | 54.56 | 29.84 | 363.42 | V |
| 0.47 | 59.50 | 55.67 | 33.24 | 345.65 | V |

** WARNING ** Local hot spot encountered. Material gelation may occur.
| 0.52 | 64.68 | 56.39 | 36.22 | 326.33 | V |

** WARNING ** Local hot spot encountered. Material gelation may occur.
| 0.58 | 69.97 | 61.10 | 42.73 | 306.49 | V |

** WARNING ** Local hot spot encountered. Material gelation may occur.
| 0.62 | 74.48 | 65.94 | 48.76 | 289.61 | V |

WARNING ** Local hot spot encountered. Material gelation may occur.
| 0.68 | 79.11 | 74.81 | 57.08 | 272.15 | V |

** WARNING ** Local hot spot encountered. Material gelation may occur.
| 0.73 | 83.55 | 97.39 | 73.38 | 255.34 | V |

** WARNING ** Local hot spot encountered. Material gelation may occur.
| 0.75 | 84.79 | 175.00 | 75.41 | 255.34 | M.M.P |

****

** SHORT SHOT ** Insufficient injection pressure.

****

SYNERGY Reactive Molding 4.1 summary report of analysis.

Date : FEB03-04
Time : 09:57:15
Name : 237nofillet1301~1

Filling phase results summary :

Maximum injection pressure (at 0.746 s) = 175.0000 MPa
Melt temperature after preconditioning = 80.0000 C
Melt conversion after preconditioning = 0.0000

End of filling phase results summary :

Time at the end of filling = 0.7464 s
Injection pressure = 175.0000 MPa
Injection pressure - extrapolated = 78.0601 MPa

****

** SHORT SHOT ** Insufficient injection pressure.

****

Maximum Clamp force - during filling = 36.9351 tonne
Clamp force - estimated = 581.3771 tonne

Filling phase results summary for the part :

Bulk temperature - maximum (at 0.746 s) = 135.2210 C
Bulk temperature - 95th percentile (at 0.746 s) = 111.9670 C
Bulk temperature - 5th percentile (at 0.677 s) = 83.1320 C
Bulk temperature - minimum (at 0.746 s) = 80.0000 C
Bulk conversion - maximum (at 0.746 s) = 0.2504
Bulk conversion - 95th percentile (at 0.746 s) = 0.0089

Wall shear stress - maximum (at 0.746 s) = 7.9688 MPa
Wall shear stress - 95th percentile (at 0.731 s) = 0.3522 MPa

Shear rate - maximum (at 0.731 s) = 1.6113E+05 1/s
Shear rate - 95th percentile (at 0.731 s) = 9924.9600 1/s
Melt front area - average = 23.1075 cm^2
Melt front area - RMS deviation = 10.2532 cm^2
Melt front velocity = 46.0332 cm/s
Melt front velocity - RMS deviation = 105.7000 cm/s

End of filling phase results summary for the part :

Total part weight = 455.5530 g

Bulk temperature - maximum = 135.2210 C
Bulk temperature - 95th percentile = 111.9670 C
Bulk temperature - 5th percentile = 83.4830 C
Bulk temperature - minimum = 80.0000 C
Bulk temperature - average = 95.6780 C
Bulk temperature - RMS deviation = 8.0336 C
Bulk conversion - maximum = 0.2504
Bulk conversion - 95th percentile = 0.0089
Bulk conversion - average = 0.0013
Bulk conversion - RMS deviation = 0.0039

Wall shear stress - maximum = 7.9688 MPa
Wall shear stress - 95th percentile = 0.0007 MPa
Wall shear stress - average = 0.0248 MPa
Wall shear stress - RMS deviation = 0.3176 MPa

Shear rate - maximum = 0.0005 1/s
Shear rate - 95th percentile = 6.3591E-05 1/s
Shear rate - average = 1.2792E-05 1/s
Shear rate - RMS deviation = 4.6423E-05 1/s

Curing phase:

Time (s)	Status
2.37	Curing phase
3.87	Curing phase
5.50	Curing phase
7.00	Curing phase
8.62	Curing phase
10.12	Curing phase
11.75	Curing phase
13.25	Curing phase
14.87	Curing phase
16.37	Curing phase
18.00	Curing phase
19.50	Curing phase
21.12	Curing phase
22.62	Curing phase
24.25	Curing phase
25.75	Curing phase
27.37	Curing phase
28.87	Curing phase
30.50	Curing phase
30.75	Curing phase

Preparing output data...
Finished preparing output data

SYNERGY Reactive Molding
has completed successfully.

Processing fusion mesh...
... finished processing fusion mesh
Weld line/air trap analysis completed

Preparing output data...
Finished preparing output data

SYNERGY Weld-line and air trap
has completed successfully.

Execution time
Analysis commenced at Tue Feb 03 09:55:27 2004
Analysis completed at Tue Feb 03 10:44:41 2004
CPU time used 2954.06 s

The tray mould

Mould temperature 80°C, Injection time 1 second

Copyright Moldflow Corporation and Moldflow Pty. Ltd. All Rights Reserved.
(C)2000 2001 2002 2003
This product may be covered by
US patent 6,096,088 ,
Australian Patent No. 721978 ,
and foreign patents and pending applications

Thermoset Flow Analysis

Version: mpi410 (Build 03203)

Analysis commenced at Thu Feb 19 09:20:29 2004
Processing fusion mesh...
... finished processing fusion mesh
Date : FEB-19-2004
Time : 09:20:54
Reading input data...
Processing fusion mesh...
... finished processing fusion mesh
Processing fusion mesh...
... finished processing fusion mesh
File name : traynofillet801~1
Reading solver parameters...
Reading material data...
Reading process settings...
Reading finite element mesh...
Finished reading input data

Optimizing node and element numbering...
... finished optimizing node and element numbering

Summary of analysis inputs :

Solver parameters :

No. of laminae across thickness = 12
No. of results at constant intervals = 20
No. of profiled results at constant intervals = 0
Flow rate convergence tolerance = 0.5000 %
Melt temperature convergence tolerance = 0.2000 C
Conversion convergence tolerance = 0.2000 %
Mold-melt heat transfer coefficient = 2.5000E+04 W/m^2-C
Heat transfer coeff. between pot and pellet (side) = 5000.0000 W/m^2-C
Heat transfer coeff. between pot and pellet (bot.) = 5000.0000 W/m^2-C
Maximum no. of flow rate iterations = 125
Maximum no. of melt-temp and conversion iterations = 100

Material data :

Polymer :

Constant polymer density
RHO = 1.6240 g/cm^3

Specific heat (Cp) = 852.0000 J/kg-C

Thermal conductivity = 0.8500 W/m-C

Reactive polymer viscosity I

$$ETA = ETAm*\left(\frac{ALFAgel}{ALFAgel-ALFA}\right)^{(C1+C2*ALFA)} \quad \text{if } ALFA < ALFAgel$$

$$ETA = Infinity \quad \text{if } ALFA > ALFAgel$$

$$\text{where } ETAm = \frac{ETAo}{1 + (ETAo*GAMMA/TAUS)^{(1-n)}}$$

ETAo = B * EXP(Tb/T)
n = 0.0835
TAUS = 2.7200E+04 Pa
B = 2920.0000 Pa-s
Tb = 5880.0000 K
C1 = 0.1790
C2 = 102.0000

N-th order kinetics with induction time
Total heat of reaction (H)
where H = 2.9000E+04 J/kg
Isothermal induction time
Tind = B1 * EXP(B2/T)
where B1 = 0.0000 s
B2 = 0.0000 K
Isothermal curing kinetics
d(ALFA)/dt = (K1+K2*ALFA^EM)*(1-ALFA)^EN
where K1 = A1 * EXP(- E1/T)
K2 = A2 * EXP(- E2/T)
EM = 0.5660
EN = 2.9950
A1 = 0.0000 1/s
A2 = 5.1800E+25 1/s
E1 = 6.4540 K
E2 = 2.3900E+04 K
Gelation conversion (ALFAgel) = 0.0500

Process settings :

Machine parameters :

Maximum injection pressure = 1.7500E+02 MPa

Conditions at the Pot (pre-conditioning) :

Pellet diameter = 12.0000 mm
Pellet length = 20.0000 mm
Transfer pot temperature = 80.0000 C
Delay time in the pot = 5.0000 s

Process parameters :

Fill time = 1.0000 s
Curing time = 30.0000 s
Melt temperature = 80.0000 C
Inlet melt conversion = 0.0000
Melt temperature after preconditioning = 80.0000 C
Melt conversion after preconditioning = 0.0000
Mold temperature = 80.00 C
Ambient temperature = 25.0000 C
Velocity/pressure switch-over by % volume = 99.0000 %
Ram speed profile (rel):

% stroke	% ram speed
0.0000	100.0000
56.0000	75.0000
88.0000	50.0000
100.0000	25.0000

Model details :

Total number of nodes = 8379
Total number of injection location nodes = 1
The injection location node labels are:

8415

Total number of elements = 16734
Number of part elements = 16714
Number of sprue/runner/gate elements = 20
Number of connector elements = 0

NOTE: The parting plane has not been specified. The global XY plane will be used instead.

Parting plane normal (dx) = 0.0000
(dy) = 0.0000
(dz) = 1.0000

Average aspect ratio of triangle elements = 1.6619
Maximum aspect ratio of triangle elements = 5.9907
Element number with maximum aspect ratio = 16709
Minimum aspect ratio of triangle elements = 1.1569
Element number with minimum aspect ratio = 11025
Total volume = 265.2940 cm^3
Volume filled initially = 0.0000 cm^3
Volume to be filled = 265.2940 cm^3
Part volume to be filled = 256.0010 cm^3
Sprue/runner/gate volume to be filled = 9.2934 cm^3

Initializing variables...
... finished initializing variables

Filling phase: Status: V = Velocity control
P = Pressure control
V/P= Velocity/pressure switch-over

Time (s)	Volume (%)	Pressure (MPa)	Clamp force (tonne)	Flow rate (cm^3/s)	Status
0.01	1.78	0.86	0.00	385.21	V
0.05	7.63	15.77	0.86	374.74	V
0.10	14.83	19.19	3.68	362.20	V
0.16	21.87	21.56	7.57	349.95	V
0.21	28.70	23.31	11.84	338.10	V
0.26	35.37	24.82	16.65	326.52	V
0.32	41.88	25.94	21.12	315.24	V
0.37	48.05	26.73	24.91	304.54	V
0.42	54.08	27.33	28.23	294.09	V
0.47	59.41	27.97	31.94	280.43	V
0.52	64.85	28.73	36.72	263.93	V
0.58	70.34	29.51	41.99	247.32	V
0.63	74.99	30.09	46.31	233.21	V
0.68	79.88	30.54	50.13	218.41	V
0.73	84.01	30.89	53.37	205.90	V
0.78	88.10	31.33	57.30	193.02	V
0.84	91.77	31.47	60.72	163.36	V
0.89	94.67	31.60	63.83	139.93	V
0.94	97.19	31.92	68.43	119.60	V
0.98	99.03			V/P	
0.99	99.36	33.34	100.76	95.28	P
1.00	100.00	33.34	102.67	95.28	P

SYNERGY Reactive Molding 4.1 summary report of analysis.

Date : FEB19-04
Time : 09:21:42
Name : traynofillet801~1

Filling phase results summary :

Maximum injection pressure (at 1.003 s) = 33.3449 MPa
Melt temperature after preconditioning = 80.0000 C
Melt conversion after preconditioning = 0.0000

End of filling phase results summary :

Time at the end of filling = 1.0034 s
Injection pressure = 33.3449 MPa
Injection pressure - extrapolated = 32.5056 MPa
Total weight = 428.4160 g
Maximum Clamp force - during filling = 100.0826 tonne
Clamp force - estimated = 247.2371 tonne

Filling phase results summary for the part :

Bulk temperature - maximum (at 0.469 s) = 82.2460 C
Bulk temperature - 95th percentile (at 0.469 s) = 82.1250 C
Bulk temperature - 5th percentile (at 1.003 s) = 81.1280 C
Bulk temperature - minimum (at 1.003 s) = 80.9490 C
Bulk conversion - maximum (at 1.003 s) = 9.3491E-10
Bulk conversion - 95th percentile (at 1.003 s) = 8.6793E-10

Wall shear stress - maximum (at 0.104 s) = 0.2169 MPa
Wall shear stress - 95th percentile (at 0.104 s) = 0.1839 MPa

Shear rate - maximum (at 0.104 s) = 1.7271E+04 1/s
Shear rate - 95th percentile (at 0.104 s) = 1501.3300 1/s
Melt front area - average = 21.3154 cm^2
Melt front area - RMS deviation = 7.6270 cm^2
Melt front velocity = 16.0951 cm/s
Melt front velocity - RMS deviation = 24.3485 cm/s

End of filling phase results summary for the part :

Total part weight = 413.3240 g

Bulk temperature - maximum = 82.0160 C
Bulk temperature - 95th percentile = 81.7740 C
Bulk temperature - 5th percentile = 81.1280 C
Bulk temperature - minimum = 80.9490 C
Bulk temperature - average = 81.4420 C
Bulk temperature - RMS deviation = 0.1955 C
Bulk conversion - maximum = 9.3491E-10
Bulk conversion - 95th percentile = 8.6793E-10
Bulk conversion - average = 6.8073E-10
Bulk conversion - RMS deviation = 0.0000

Wall shear stress - maximum = 0.1978 MPa
Wall shear stress - 95th percentile = 0.1702 MPa
Wall shear stress - average = 0.1072 MPa
Wall shear stress - RMS deviation = 0.0540 MPa

Shear rate - maximum = 5195.7598 1/s
Shear rate - 95th percentile = 554.9850 1/s
Shear rate - average = 140.4780 1/s
Shear rate - RMS deviation = 263.1750 1/s

Filling phase results summary for the runner system :

Bulk temperature - maximum (at 0.104 s) = 82.3130 C
Bulk temperature - 95th percentile (at 0.104 s) = 82.2260 C
Bulk temperature - 5th percentile (at 1.003 s) = 80.0000 C
Bulk temperature - minimum (at 1.003 s) = 80.0000 C
Bulk conversion - maximum (at 1.003 s) = 4.9927E-10
Bulk conversion - 95th percentile (at 1.003 s) = 4.9927E-10

Wall shear stress - maximum (at 0.104 s) = 0.2092 MPa
Wall shear stress - 95th percentile (at 0.104 s) = 0.2018 MPa

Shear rate - maximum (at 0.104 s) = 7615.5801 1/s
Shear rate - 95th percentile (at 0.104 s) = 5112.0400 1/s
Melt front area - average = 1.1199 cm^2
Melt front area - RMS deviation = 0.3689 cm^2
Melt front velocity = 371.3340 cm/s
Melt front velocity - RMS deviation = 91.8262 cm/s

End of filling phase results summary for the runner system :

Total sprue/runner/gate weight = 15.0925 g
Bulk temperature - maximum = 81.9430 C
Bulk temperature - 95th percentile = 81.8590 C
Bulk temperature - 5th percentile = 80.0000 C
Bulk temperature - minimum = 80.0000 C
Bulk temperature - average = 80.7470 C
Bulk temperature - RMS deviation = 0.6904 C
Bulk conversion - maximum = 4.9927E-10
Bulk conversion - 95th percentile = 4.9927E-10
Bulk conversion - average = 4.8775E-10
Bulk conversion - RMS deviation = 0.0000

Wall shear stress - maximum = 0.1844 MPa
Wall shear stress - 95th percentile = 0.1780 MPa
Wall shear stress - average = 0.1732 MPa
Wall shear stress - RMS deviation = 0.0069 MPa

Shear rate - maximum = 1723.3101 1/s
Shear rate - 95th percentile = 1158.6400 1/s
Shear rate - average = 953.1660 1/s
Shear rate - RMS deviation = 342.1040 1/s

Curing phase:

Time (s)	Status
2.63	Curing phase
4.13	Curing phase
5.75	Curing phase
7.25	Curing phase
8.88	Curing phase
10.38	Curing phase
12.00	Curing phase
13.50	Curing phase
15.13	Curing phase
16.63	Curing phase
18.25	Curing phase
19.75	Curing phase
21.38	Curing phase
22.88	Curing phase
24.50	Curing phase
26.00	Curing phase
27.63	Curing phase
29.13	Curing phase
30.75	Curing phase
31.00	Curing phase

Preparing output data...
Finished preparing output data

SYNERGY Reactive Molding
has completed successfully.

Processing fusion mesh...
... finished processing fusion mesh
Weld line/air trap analysis completed

Preparing output data...
Finished preparing output data

SYNERGY Weld-line and air trap
has completed successfully.
Execution time
Analysis commenced at Thu Feb 19 09:20:29 2004
Analysis completed at Thu Feb 19 09:31:32 2004
CPU time used 662.16 s

Mould temperature 140°C, Injection time 1 second

Copyright Moldflow Corporation and Moldflow Pty. Ltd. All Rights Reserved.
(C)2000 2001 2002 2003
This product may be covered by
US patent 6,096,088 ,
Australian Patent No. 721978 ,
and foreign patents and pending applications

Thermoset Flow Analysis

Version: mpi410 (Build 03203)

Analysis commenced at Thu Feb 19 11:50:38 2004
Processing fusion mesh...
... finished processing fusion mesh
Date : FEB-19-2004
Time : 11:51:01
Reading input data...
Processing fusion mesh...
... finished processing fusion mesh
Processing fusion mesh...
... finished processing fusion mesh
File name : traynofillet1401~1
Reading solver parameters...
Reading material data...
Reading process settings...
Reading finite element mesh...
Finished reading input data

Optimizing node and element numbering...
... finished optimizing node and element numbering
Filling phase: Status: V = Velocity control
P = Pressure control
V/P= Velocity/pressure switch-over

Time (s)	Volume (%)	Pressure (MPa)	Clamp force (tonne)	Flow rate (cm^3/s)	Status
0.01	1.78	0.72	0.00	385.21	V
0.05	7.57	14.01	0.75	374.88	V
0.10	14.83	16.96	3.17	362.24	V
0.16	21.91	19.59	6.51	349.93	V
0.21	28.75	22.52	10.34	338.03	V
0.26	35.45	24.10	14.93	326.40	V
0.31	41.59	24.96	18.93	315.75	V
0.36	47.69	25.76	22.57	305.18	V
0.42	53.69	27.71	26.15	294.77	V

** WARNING ** Local hot spot encountered. Material gelation may occur.
| 0.47 | 59.67 | 30.77 | 30.60 | 279.59 | V |

** WARNING ** Local hot spot encountered. Material gelation may occur.
| 0.52 | 64.84 | 32.50 | 35.98 | 263.90 | V |

** WARNING ** Local hot spot encountered. Material gelation may occur.
| 0.57 | 70.01 | 37.41 | 42.90 | 248.19 | V |

** Local hot spot encountered. Material gelation may occur.

** WARNING ** Local hot spot encountered. Material gelation may occur.
| 0.63 | 75.29 | 47.24 | 50.23 | 232.08 | V |

** Local hot spot encountered. Material gelation may occur.

** WARNING ** Local hot spot encountered. Material gelation may occur.
| 0.68 | 79.88 | 76.64 | 54.59 | 217.82 | V |

** WARNING ** Local hot spot encountered. Material gelation may occur.
| 0.69 | 80.92 | 175.00 | 3.40 | 217.82 | M.M.P |

****

** SHORT SHOT ** Insufficient injection pressure.

****

SYNERGY Reactive Molding 4.1 summary report of analysis.

Date : FEB19-04
Time : 11:51:49
Name : traynofillet1401~1

Filling phase results summary :

Maximum injection pressure (at 0.693 s) = 175.0000 MPa

Melt temperature after preconditioning = 80.0000 C
Melt conversion after preconditioning = 0.0000

End of filling phase results summary :

Time at the end of filling = 0.6933 s
Injection pressure = 175.0000 MPa
Injection pressure - extrapolated = 50.7631 MPa

****

** SHORT SHOT ** Insufficient injection pressure.

****

Maximum Clamp force - during filling = 17.1526 tonne
Clamp force - estimated = 345.3360 tonne

Filling phase results summary for the part :

Bulk temperature - maximum (at 0.693 s) = 131.6040 C
Bulk temperature - 95th percentile (at 0.681 s) = 111.6060 C
Bulk temperature - 5th percentile (at 0.104 s) = 85.2520 C
Bulk temperature - minimum (at 0.417 s) = 80.5100 C
Bulk conversion - maximum (at 0.693 s) = 0.0262
Bulk conversion - 95th percentile (at 0.693 s) = 0.0066

Wall shear stress - maximum (at 0.693 s) = 1.0631 MPa
Wall shear stress - 95th percentile (at 0.681 s) = 0.2843 MPa

Shear rate - maximum (at 0.681 s) = 3.5184E+05 1/s
Shear rate - 95th percentile (at 0.681 s) = 2206.6001 1/s
Melt front area - average = 22.7403 cm^2
Melt front area - RMS deviation = 7.4058 cm^2
Melt front velocity = 18.7680 cm/s
Melt front velocity - RMS deviation = 28.9059 cm/s

End of filling phase results summary for the part :

Total part weight = 337.7960 g

Bulk temperature - maximum = 131.6040 C
Bulk temperature - 95th percentile = 110.4070 C
Bulk temperature - 5th percentile = 96.7130 C
Bulk temperature - minimum = 84.6090 C
Bulk temperature - average = 101.5250 C
Bulk temperature - RMS deviation = 4.9496 C
Bulk conversion - maximum = 0.0262
Bulk conversion - 95th percentile = 0.0066
Bulk conversion - average = 0.0012
Bulk conversion - RMS deviation = 0.0031

Wall shear stress - maximum = 1.0631 MPa
Wall shear stress - 95th percentile = 0.0001 MPa
Wall shear stress - average = 0.0045 MPa
Wall shear stress - RMS deviation = 0.0431 MPa

Shear rate - maximum = 4.2785E-05 1/s
Shear rate - 95th percentile = 1.4398E-07 1/s
Shear rate - average = 1.8868E-07 1/s
Shear rate - RMS deviation = 1.6814E-06 1/s

Filling phase results summary for the runner system :

Bulk temperature - maximum (at 0.693 s) = 120.4010 C
Bulk temperature - 95th percentile (at 0.693 s) = 119.3330 C
Bulk temperature - 5th percentile (at 0.693 s) = 80.0000 C
Bulk temperature - minimum (at 0.693 s) = 80.0000 C
Bulk conversion - maximum (at 0.693 s) = 0.0262
Bulk conversion - 95th percentile (at 0.693 s) = 0.0262

Wall shear stress - maximum (at 0.681 s) = 0.2736 MPa
Wall shear stress - 95th percentile (at 0.681 s) = 0.2613 MPa

Shear rate - maximum (at 0.681 s) = 2.2089E+05 1/s

Shear rate - 95th percentile (at 0.681 s) = 2.1069E+05 1/s
Melt front area - average = 1.0707 cm^2
Melt front area - RMS deviation = 0.3083 cm^2
Melt front velocity = 380.6980 cm/s
Melt front velocity - RMS deviation = 82.5449 cm/s

End of filling phase results summary for the runner system :

Total sprue/runner/gate weight = 15.0925 g
Bulk temperature - maximum = 120.4010 C
Bulk temperature - 95th percentile = 119.3330 C
Bulk temperature - 5th percentile = 80.0000 C
Bulk temperature - minimum = 80.0000 C
Bulk temperature - average = 84.5690 C
Bulk temperature - RMS deviation = 10.0727 C
Bulk conversion - maximum = 0.0262
Bulk conversion - 95th percentile = 0.0262
Bulk conversion - average = 0.0166
Bulk conversion - RMS deviation = 0.0123

Wall shear stress - maximum = 0.0349 MPa
Wall shear stress - 95th percentile = 0.0349 MPa
Wall shear stress - average = 0.0075 MPa
Wall shear stress - RMS deviation = 0.0143 MPa

Shear rate - maximum = 1.9201E-06 1/s
Shear rate - 95th percentile = 1.9201E-06 1/s
Shear rate - average = 7.4877E-07 1/s
Shear rate - RMS deviation = 7.3816E-07 1/s
Curing phase:

Time (s)	Status
2.32	Curing phase
3.82	Curing phase
5.44	Curing phase
6.94	Curing phase
8.57	Curing phase
10.07	Curing phase
11.69	Curing phase
13.19	Curing phase
14.82	Curing phase
16.32	Curing phase
17.94	Curing phase
19.44	Curing phase
21.07	Curing phase
22.57	Curing phase
24.19	Curing phase
25.69	Curing phase
27.32	Curing phase
28.82	Curing phase
30.44	Curing phase
30.82	Curing phase

Preparing output data...
Finished preparing output data

SYNERGY Reactive Molding
has completed successfully.

Processing fusion mesh...
... finished processing fusion mesh
Weld line/air trap analysis completed

Preparing output data...
Finished preparing output data

SYNERGY Weld-line and air trap
has completed successfully.

Execution time
Analysis commenced at Thu Feb 19 11:50:38 2004
Analysis completed at Thu Feb 19 12:14:16 2004
CPU time used 1417.22 s

The new manifold system

Mould temperature 80°C, Injection time 1 second

Copyright Moldflow Corporation and Moldflow Pty. Ltd. All Rights Reserved.
(C)2000 2001 2002 2003
This product may be covered by
US patent 6,096,088 ,
Australian Patent No. 721978 ,
and foreign patents and pending applications

Thermoset Flow Analysis

Version: mpi410 (Build 03203)

Analysis commenced at Mon Feb 23 16:35:08 2004
Processing fusion mesh...
... finished processing fusion mesh
Date : FEB-23-2004
Time : 16:36:04
Reading input data...
Processing fusion mesh...
... finished processing fusion mesh
Processing fusion mesh...
... finished processing fusion mesh
File name : traynewmanifold801~1
Reading solver parameters...
Reading material data...
Reading process settings...
Reading finite element mesh...
Finished reading input data

Optimizing node and element numbering...
... finished optimizing node and element numbering

Summary of analysis inputs :

Solver parameters :

No. of laminae across thickness = 12
No. of results at constant intervals = 20
No. of profiled results at constant intervals = 0
Flow rate convergence tolerance = 0.5000 %
Melt temperature convergence tolerance = 0.2000 C
Conversion convergence tolerance = 0.2000 %
Mold-melt heat transfer coefficient = 2.5000E+04 W/m^2-C
Heat transfer coeff. between pot and pellet (side) = 5000.0000 W/m^2-C
Heat transfer coeff. between pot and pellet (bot.) = 5000.0000 W/m^2-C
Maximum no. of flow rate iterations = 125
Maximum no. of melt-temp and conversion iterations = 100

Material data :

Polymer :

Constant polymer density
RHO = 1.6240 g/cm^3

Specific heat (Cp) = 852.0000 J/kg-C

Thermal conductivity = 0.8500 W/m-C

Reactive polymer viscosity I

$$ETA = ETAm*\left(\frac{ALFAgel}{(C1+C2*ALFA)}\right) \quad \text{if } ALFA < ALFAgel$$

ALFAgel-ALFA
ETA = Infinity If ALFA > ALFAgel

$$\text{where } ETAm = \frac{ETAo}{1 + (ETAo*GAMMA/TAUS)^{(1-n)}}$$

ETAo = B * EXP(Tb/T)
n = 0.0835
TAUS = 2.7200E+04 Pa
B = 2920.0000 Pa-s
Tb = 5880.0000 K
C1 = 0.1790
C2 = 102.0000

N-th order kinetics with induction time
Total heat of reaction (H)
where H = 2.9000E+04 J/kg
Isothermal induction time
Tind = B1 * EXP(B2/T)
where B1 = 0.0000 s
B2 = 0.0000 K
Isothermal curing kinetics
d(ALFA)/dt = (K1+K2*ALFA^EM)*(1-ALFA)^EN
where K1 = A1 * EXP(- E1/T)
K2 = A2 * EXP(- E2/T)
EM = 0.5660
EN = 2.9950
A1 = 0.0000 1/s
A2 = 5.1800E+25 1/s
E1 = 6.4540 K
E2 = 2.3900E+04 K
Gelation conversion (ALFAgel) = 0.0500

Process settings :

Machine parameters :

Maximum injection pressure = 1.7500E+02 MPa

Conditions at the Pot (pre-conditioning) :

Pellet diameter = 12.0000 mm
Pellet length = 20.0000 mm
Transfer pot temperature = 80.0000 C
Delay time in the pot = 5.0000 s

Process parameters :

Fill time = 1.0000 s
Curing time = 30.0000 s
Melt temperature = 80.0000 C
Inlet melt conversion = 0.0000
Melt temperature after preconditioning = 80.0000 C
Melt conversion after preconditioning = 0.0000
Mold temperature = 80.00 C
Ambient temperature = 25.0000 C
Velocity/pressure switch-over by % volume = 99.0000 %
Ram speed profile (rel):

% stroke	% ram speed
0.0000	100.0000
56.0000	75.0000
88.0000	50.0000
100.0000	25.0000

Model details :

Total number of nodes = 11769
Total number of injection location nodes = 1
The injection location node labels are:
6961
Total number of elements = 23534

Number of part elements = 23534
Number of sprue/runner/gate elements = 0
Number of connector elements = 0
NOTE: The parting plane has not been specified. The global XY plane will be used instead.
Parting plane normal (dx) = 0.0000
(dy) = 0.0000
(dz) = 1.0000
Average aspect ratio of triangle elements = 1.7292
Maximum aspect ratio of triangle elements = 5.9831
Element number with maximum aspect ratio = 18958
Minimum aspect ratio of triangle elements = 1.1562
Element number with minimum aspect ratio = 19748
Total volume = 814.6840 cm^3
Volume filled initially = 0.0000 cm^3
Volume to be filled = 814.6840 cm^3
Part volume to be filled = 814.6840 cm^3
Sprue/runner/gate volume to be filled = 0.0000 cm^3
Initializing variables...
... finished initializing variables
Filling phase: Status: V = Velocity control
P = Pressure control
V/P= Velocity/pressure switch-over

Time (s)	Volume (%)	Pressure (MPa)	Clamp force (tonne)	Flow rate (cm^3/s)	Status
0.00	0.02	0.35	0.00	763.95	V
0.05	7.64	19.46	1.91	737.18	V
0.10	14.97	20.89	2.38	712.20	V
0.16	22.10	21.84	2.84	687.81	V
0.21	28.83	22.59	3.33	664.94	V
0.26	35.39	23.34	3.97	642.48	V
0.31	41.57	27.56	9.38	621.28	V
0.36	47.79	36.06	19.95	599.89	V
0.42	53.72	38.77	26.74	579.50	V
0.47	59.51	40.73	33.93	550.96	V
0.52	64.70	42.09	40.62	519.93	V
0.57	69.89	43.01	46.51	488.84	V
0.63	74.80	43.75	51.91	459.74	V
0.68	79.06	44.63	58.74	434.37	V
0.73	83.44	45.52	66.65	408.25	V
0.78	87.52	46.01	71.89	383.91	V
0.83	91.10	45.95	75.11	331.70	V
0.89	94.23	45.83	77.89	282.19	V
0.94	96.76	46.21	84.97	241.96	V
0.99	99.00	46.88	94.82	206.45	V
0.99	99.09			V/P	
1.01	100.00	46.81	101.80	206.45	P

SYNERGY Reactive Molding 4.1 summary report of analysis.

Date : FEB23-04
Time : 16:37:56
Name : traynewmanifold801~1

Filling phase results summary :

Maximum injection pressure (at 0.988 s) = 46.8800 MPa
Melt temperature after preconditioning = 80.0000 C
Melt conversion after preconditioning = 0.0000

End of filling phase results summary :

Time at the end of filling = 1.0150 s
Injection pressure = 46.8068 MPa
Injection pressure - extrapolated = 46.6064 MPa
Total weight = 842.9230 g
Maximum Clamp force - during filling = 101.3608 tonne
Clamp force - estimated = 414.9824 tonne

Filling phase results summary for the part :

Bulk temperature - maximum (at 0.417 s) = 85.3240 C

Bulk temperature - 95th percentile (at 0.470 s) = 84.9030 C
Bulk temperature - 5th percentile (at 1.015 s) = 81.6070 C
Bulk temperature - minimum (at 1.015 s) = 80.0000 C
Bulk conversion - maximum (at 1.015 s) = 1.0990E-06
Bulk conversion - 95th percentile (at 1.015 s) = 4.5500E-07

Wall shear stress - maximum (at 0.312 s) = 0.2481 MPa
Wall shear stress - 95th percentile (at 0.365 s) = 0.1879 MPa

Shear rate - maximum (at 0.105 s) = 4.3752E+04 1/s
Shear rate - 95th percentile (at 0.365 s) = 3598.5500 1/s
Melt front area - average = 23.1627 cm^2
Melt front area - RMS deviation = 9.4199 cm^2
Melt front velocity = 40.2749 cm/s
Melt front velocity - RMS deviation = 78.6645 cm/s

End of filling phase results summary for the part :

Total part weight = 842.9230 g

Bulk temperature - maximum = 85.2040 C
Bulk temperature - 95th percentile = 84.3020 C
Bulk temperature - 5th percentile = 81.6070 C
Bulk temperature - minimum = 80.0000 C
Bulk temperature - average = 82.8650 C
Bulk temperature - RMS deviation = 0.8709 C
Bulk conversion - maximum = 1.0990E-06
Bulk conversion - 95th percentile = 4.5500E-07
Bulk conversion - average = 1.9014E-07
Bulk conversion - RMS deviation = 0.0000

Wall shear stress - maximum = 0.2136 MPa
Wall shear stress - 95th percentile = 0.1705 MPa
Wall shear stress - average = 0.1213 MPa
Wall shear stress - RMS deviation = 0.0461 MPa

Shear rate - maximum = 1.0770E+04 1/s
Shear rate - 95th percentile = 970.4640 1/s
Shear rate - average = 237.9020 1/s
Shear rate - RMS deviation = 578.1210 1/s

Curing phase:

Time (s)	Status
2.64	Curing phase
4.14	Curing phase
5.76	Curing phase
7.26	Curing phase
8.89	Curing phase
10.39	Curing phase
12.02	Curing phase
13.52	Curing phase
15.14	Curing phase
16.64	Curing phase
18.26	Curing phase
19.76	Curing phase
21.39	Curing phase
22.89	Curing phase
24.51	Curing phase
26.01	Curing phase
27.64	Curing phase
29.14	Curing phase
30.76	Curing phase
31.14	Curing phase

Preparing output data...
Finished preparing output data

SYNERGY Reactive Molding
has completed successfully.

Processing fusion mesh...
... finished processing fusion mesh

Weld line/air trap analysis completed

Preparing output data...
Finished preparing output data

SYNERGY Weld-line and air trap
has completed successfully.

Execution time
Analysis commenced at Mon Feb 23 16:35:08 2004
Analysis completed at Mon Feb 23 17:05:09 2004
CPU time used 1800.08 s

Mould temperature 130°C, Injection time 1 second

Copyright Moldflow Corporation and Moldflow Pty. Ltd. All Rights Reserved.
(C)2000 2001 2002 2003
This product may be covered by
US patent 6,096,088 ,
Australian Patent No. 721978 ,
and foreign patents and pending applications

Thermoset Flow Analysis

Version: mpi410 (Build 03203)

Analysis commenced at Sat Feb 21 11:00:09 2004
Processing fusion mesh...
... finished processing fusion mesh
Date : FEB-21-2004
Time : 11:01:06
Reading input data...
Processing fusion mesh...
... finished processing fusion mesh
Processing fusion mesh...
... finished processing fusion mesh
File name : traynewmanifold1301~1
Reading solver parameters...
Reading material data...
Reading process settings...
Reading finite element mesh...
Finished reading input data

Optimizing node and element numbering...
... finished optimizing node and element numbering

Filling phase: Status: V = Velocity control
P = Pressure control
V/P= Velocity/pressure switch-over

Time (s)	Volume (%)	Pressure (MPa)	Clamp force (tonne)	Flow rate (cm^3/s)	Status
0.00	0.02	0.30	0.00	763.95	V
0.05	7.64	17.74	1.76	737.23	V
0.11	15.01	18.97	2.18	712.11	V
0.16	21.95	19.81	2.59	688.42	V
0.21	28.71	20.50	3.02	665.30	V
0.26	35.33	21.21	3.59	642.77	V
0.31	41.58	25.15	8.53	621.39	V
0.36	47.80	33.11	18.26	599.86	V
0.42	53.76	35.76	24.38	579.64	V
0.47	59.34	37.74	30.50	551.93	V
0.52	64.82	39.51	36.77	519.27	V
0.57	69.77	40.92	41.85	489.66	V
0.63	74.68	42.12	46.68	460.56	V

| 0.68 | 79.04 | 42.42 | 52.50 | 434.55 | V |

** WARNING ** Local hot spot encountered. Material gelation may occur.
| 0.73 | 83.48 | 47.05 | 62.13 | 407.99 | V |

** WARNING ** Local hot spot encountered. Material gelation may occur.
| 0.78 | 87.30 | 52.13 | 69.76 | 385.06 | V |

** WARNING ** Local hot spot encountered. Material gelation may occur.
| 0.83 | 90.94 | 59.39 | 76.36 | 334.19 | V |

** WARNING ** Local hot spot encountered. Material gelation may occur.
| 0.88 | 94.12 | 75.15 | 86.44 | 283.49 | V |

** WARNING ** Local hot spot encountered. Material gelation may occur.
| 0.90 | 95.05 | 175.00 | 31.49 | 283.49 | M.M.P |

****

** SHORT SHOT ** Insufficient injection pressure.

****

SYNERGY Reactive Molding 4.1 summary report of analysis.

Date : FEB21-04
Time : 11:03:05
Name : traynewmanifold1301~1

Filling phase results summary :

Maximum injection pressure (at 0.902 s) = 175.0000 MPa
Melt temperature after preconditioning = 80.0000 C
Melt conversion after preconditioning = 0.0000

End of filling phase results summary :

Time at the end of filling = 0.9022 s
Injection pressure = 175.0000 MPa
Injection pressure - extrapolated = 58.6109 MPa

****

** SHORT SHOT ** Insufficient injection pressure.

****

Maximum Clamp force - during filling = 31.7629 tonne
Clamp force - estimated = 496.8821 tonne

Filling phase results summary for the part :

Bulk temperature - maximum (at 0.902 s) = 136.4640 C
Bulk temperature - 95th percentile (at 0.902 s) = 101.0440 C
Bulk temperature - 5th percentile (at 0.312 s) = 81.6000 C
Bulk temperature - minimum (at 0.902 s) = 80.0000 C
Bulk conversion - maximum (at 0.902 s) = 0.0296
Bulk conversion - 95th percentile (at 0.902 s) = 0.0050

Wall shear stress - maximum (at 0.902 s) = 10.7223 MPa
Wall shear stress - 95th percentile (at 0.885 s) = 0.2362 MPa

Shear rate - maximum (at 0.885 s) = 2.5559E+05 1/s
Shear rate - 95th percentile (at 0.885 s) = 3627.2500 1/s
Melt front area - average = 24.2693 cm^2
Melt front area - RMS deviation = 9.2634 cm^2
Melt front velocity = 43.1286 cm/s
Melt front velocity - RMS deviation = 83.0354 cm/s

End of filling phase results summary for the part :

Total part weight	= 807.4300 g
Bulk temperature - maximum	= 136.4640 C
Bulk temperature - 95th percentile	= 101.0440 C
Bulk temperature - 5th percentile	= 83.3790 C
Bulk temperature - minimum	= 80.0000 C
Bulk temperature - average	= 90.5230 C
Bulk temperature - RMS deviation	= 6.4479 C
Bulk conversion - maximum	= 0.0296
Bulk conversion - 95th percentile	= 0.0050
Bulk conversion - average	= 0.0009
Bulk conversion - RMS deviation	= 0.0029
Wall shear stress - maximum	= 10.7223 MPa
Wall shear stress - 95th percentile	= 0.0009 MPa
Wall shear stress - average	= 0.0309 MPa
Wall shear stress - RMS deviation	= 0.3772 MPa
Shear rate - maximum	= 0.0086 1/s
Shear rate - 95th percentile	= 7.6091E-05 1/s
Shear rate - average	= 2.1473E-05 1/s
Shear rate - RMS deviation	= 0.0002 1/s

Curing phase:

Time (s)	Status
2.53	Curing phase
4.03	Curing phase
5.65	Curing phase
7.15	Curing phase
8.78	Curing phase
10.28	Curing phase
11.90	Curing phase
13.40	Curing phase
15.03	Curing phase
16.53	Curing phase
18.15	Curing phase
19.65	Curing phase
21.28	Curing phase
22.78	Curing phase
24.40	Curing phase
25.90	Curing phase
27.53	Curing phase
29.03	Curing phase
30.65	Curing phase
30.90	Curing phase

Preparing output data...
Finished preparing output data

SYNERGY Reactive Molding
has completed successfully.

Processing fusion mesh...
... finished processing fusion mesh
Weld line/air trap analysis completed

Preparing output data...
Finished preparing output data

SYNERGY Weld-line and air trap
has completed successfully.

Execution time

Analysis commenced at	Sat Feb 21 11:00:09 2004
Analysis completed at	Sat Feb 21 12:10:51 2004
CPU time used	4241.23 s

Appendix III

Moldflow® simulation results Injection time-Melt temperature plots of the existing manifold system and the tray moulding

Figure App3.1 Injection time-melt temperature plot at 1-second injection time and mould temperatures is varied from 80 to 130°C

Figure App3.1 a.) Mould temperature 80°C

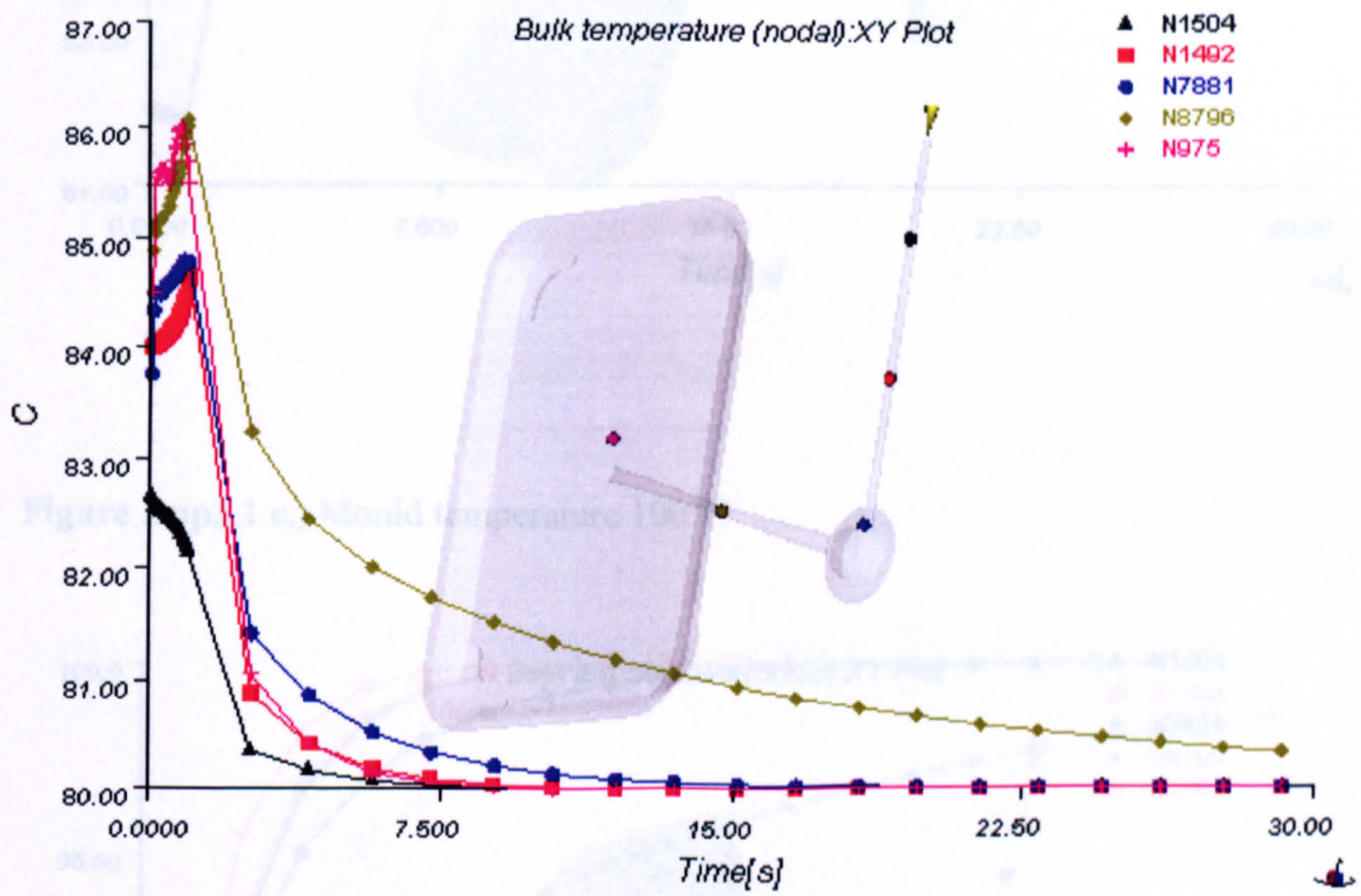

Figure App3.1 b.) Mould temperature 90°C

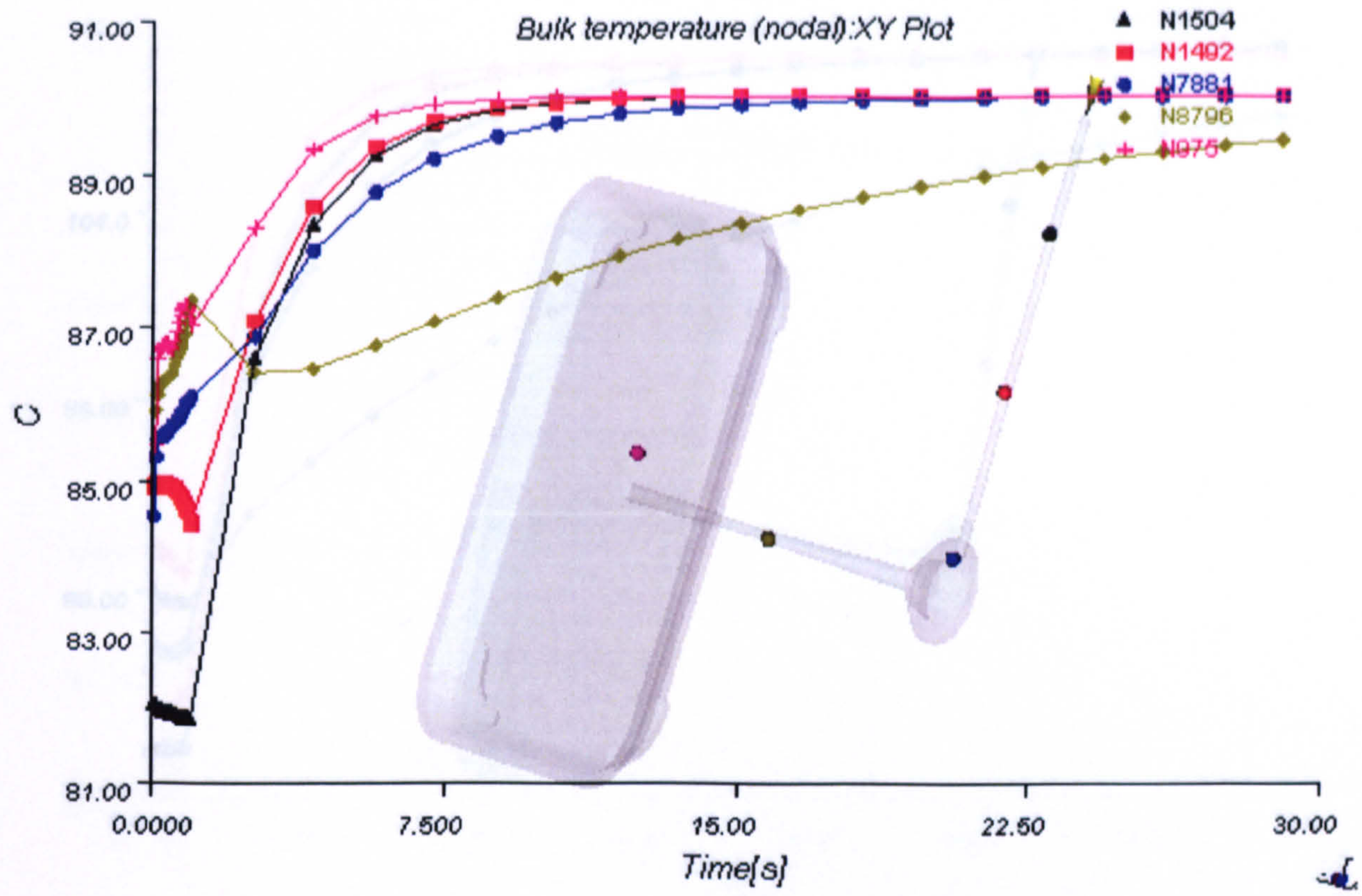

Figure App3.1 c.) Mould temperature 100°C

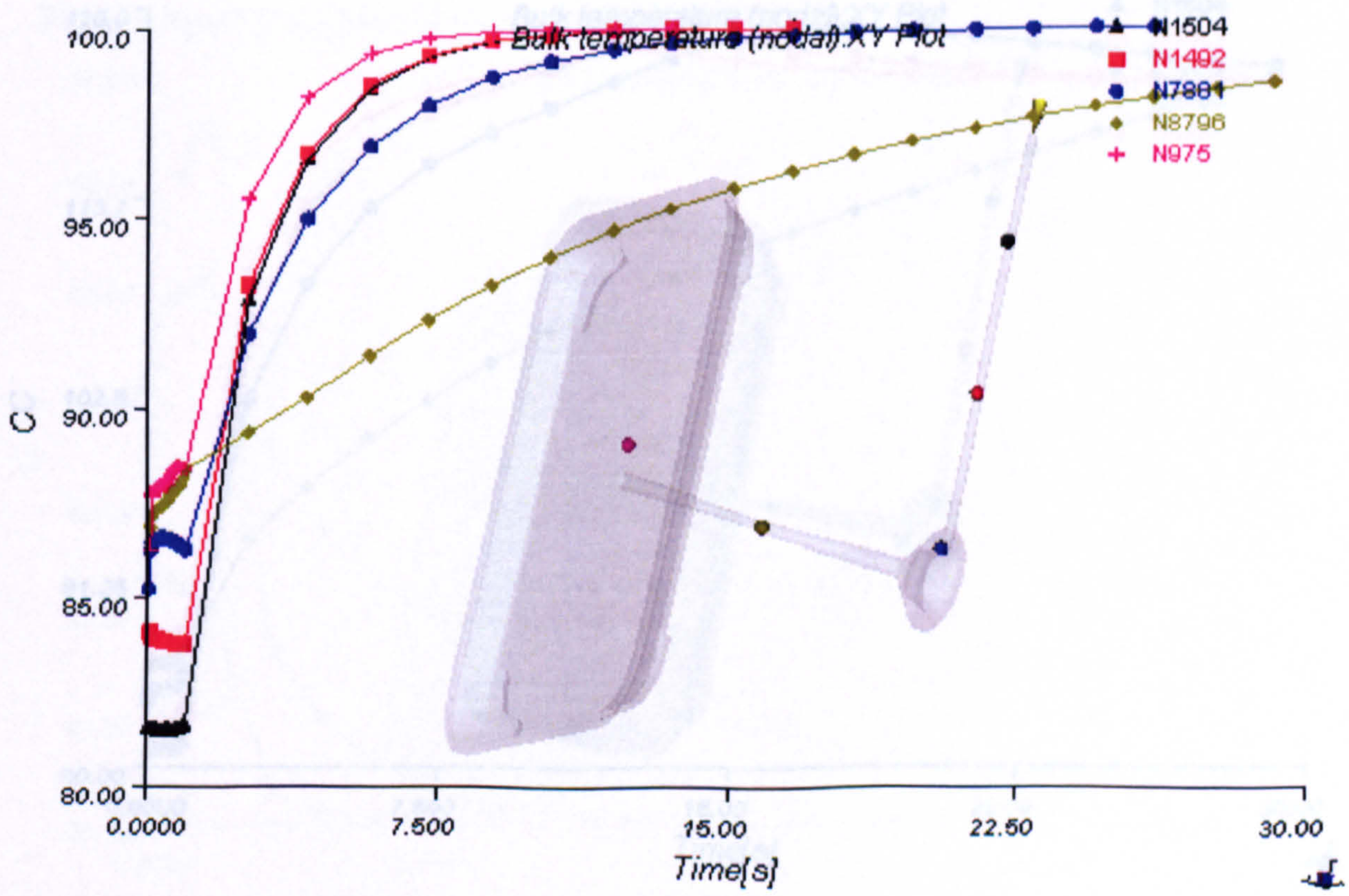

Figure App3.1 d.) Mould temperature 110°C

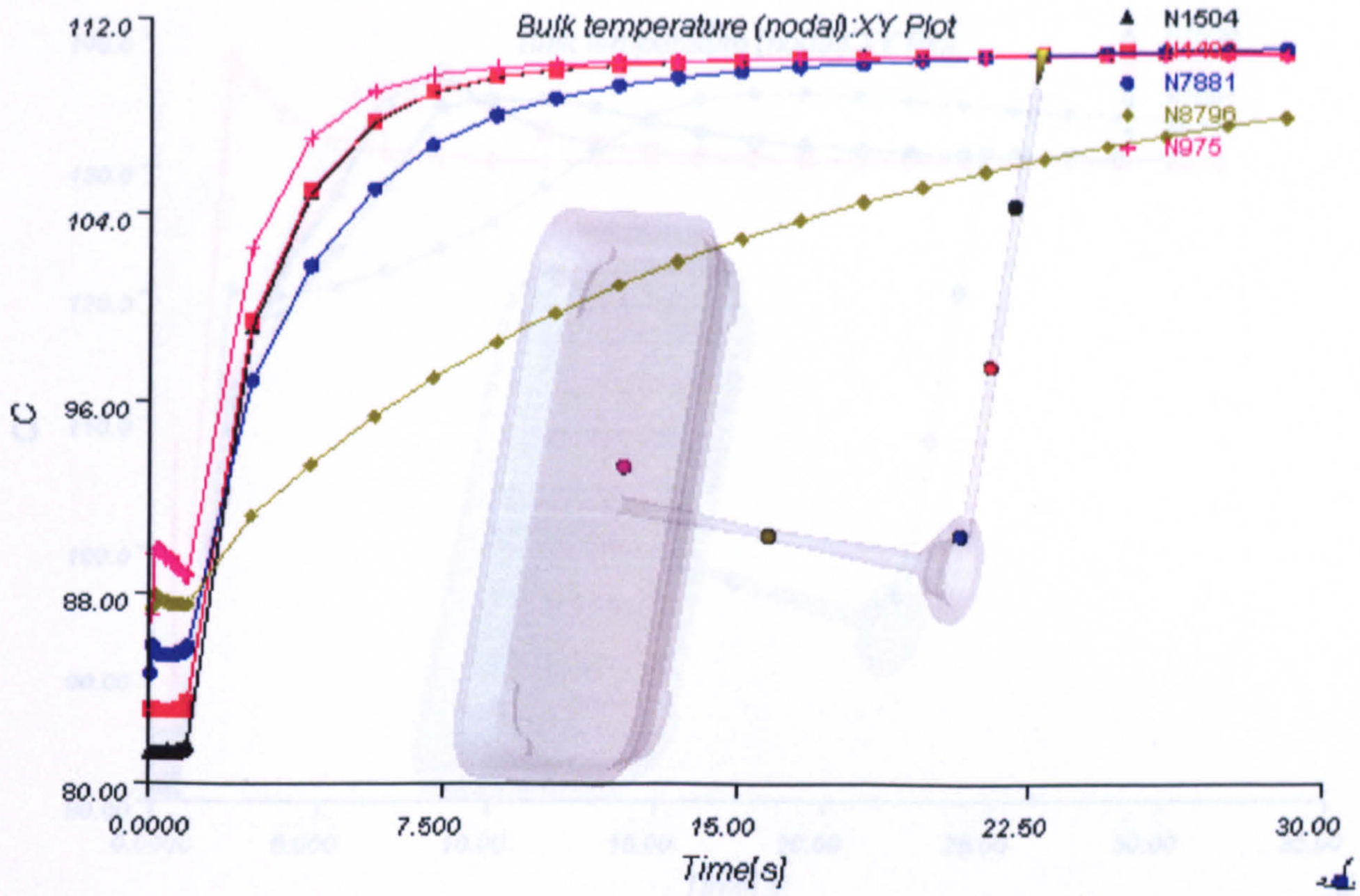

Figure App3.1 e.) Mould temperature 120°C

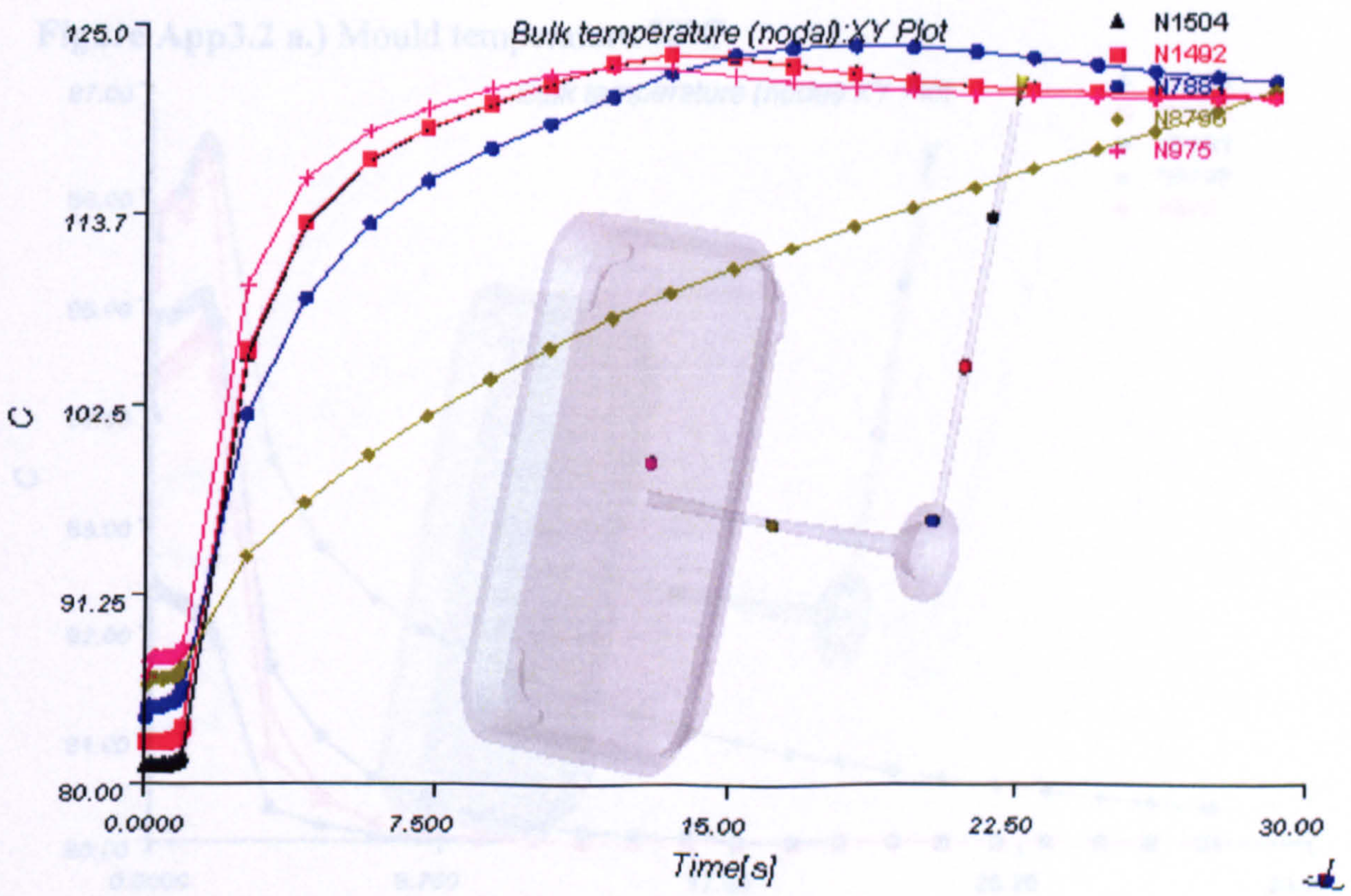

Figure App3.1 f.) Mould temperature 130°C

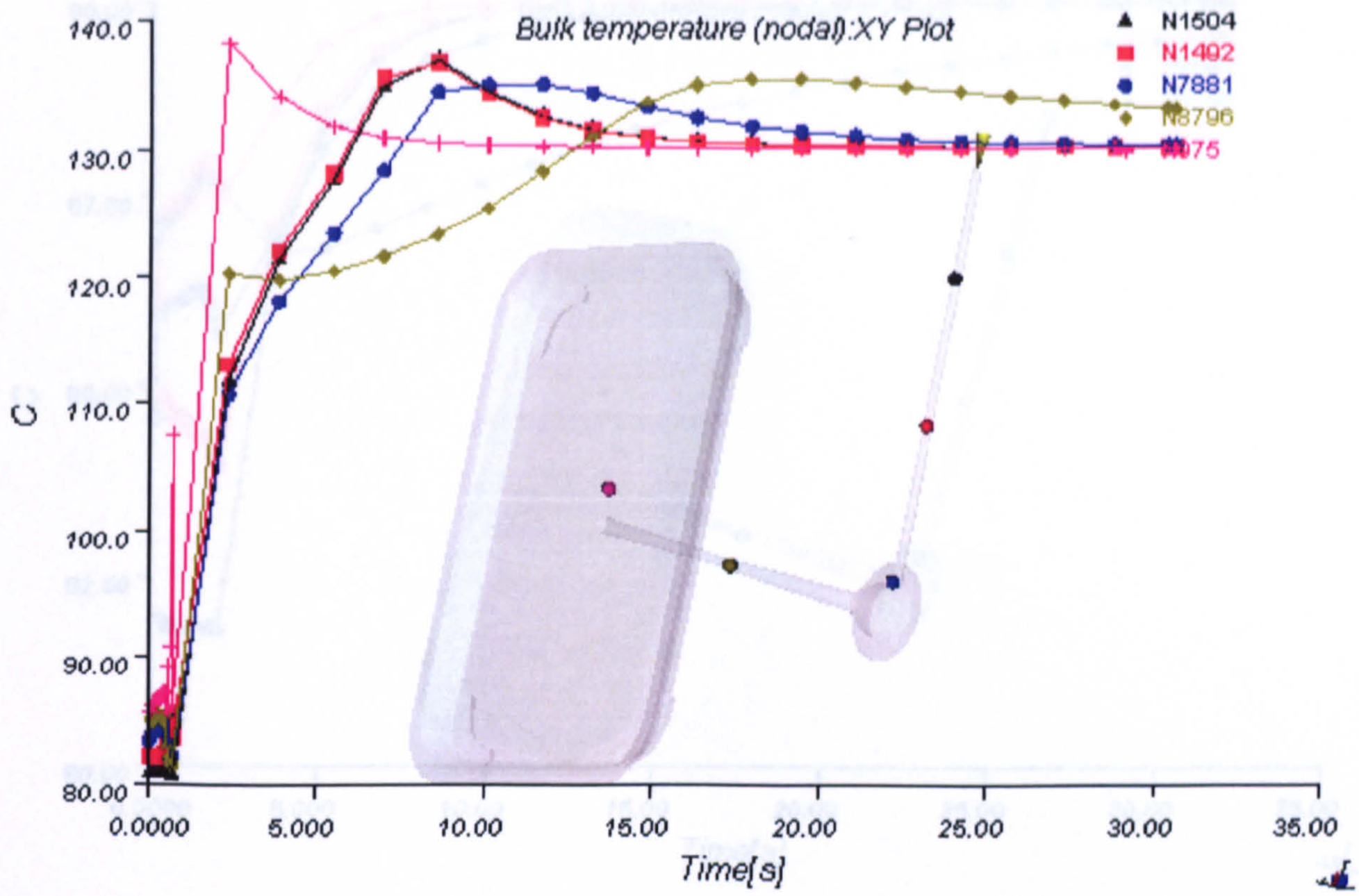

Figure App3.2 Injection time-melt temperature plot at 2-second injection time and mould temperatures is varied from 80 to 130°C

Figure App3.2 a.) Mould temperature 80°C

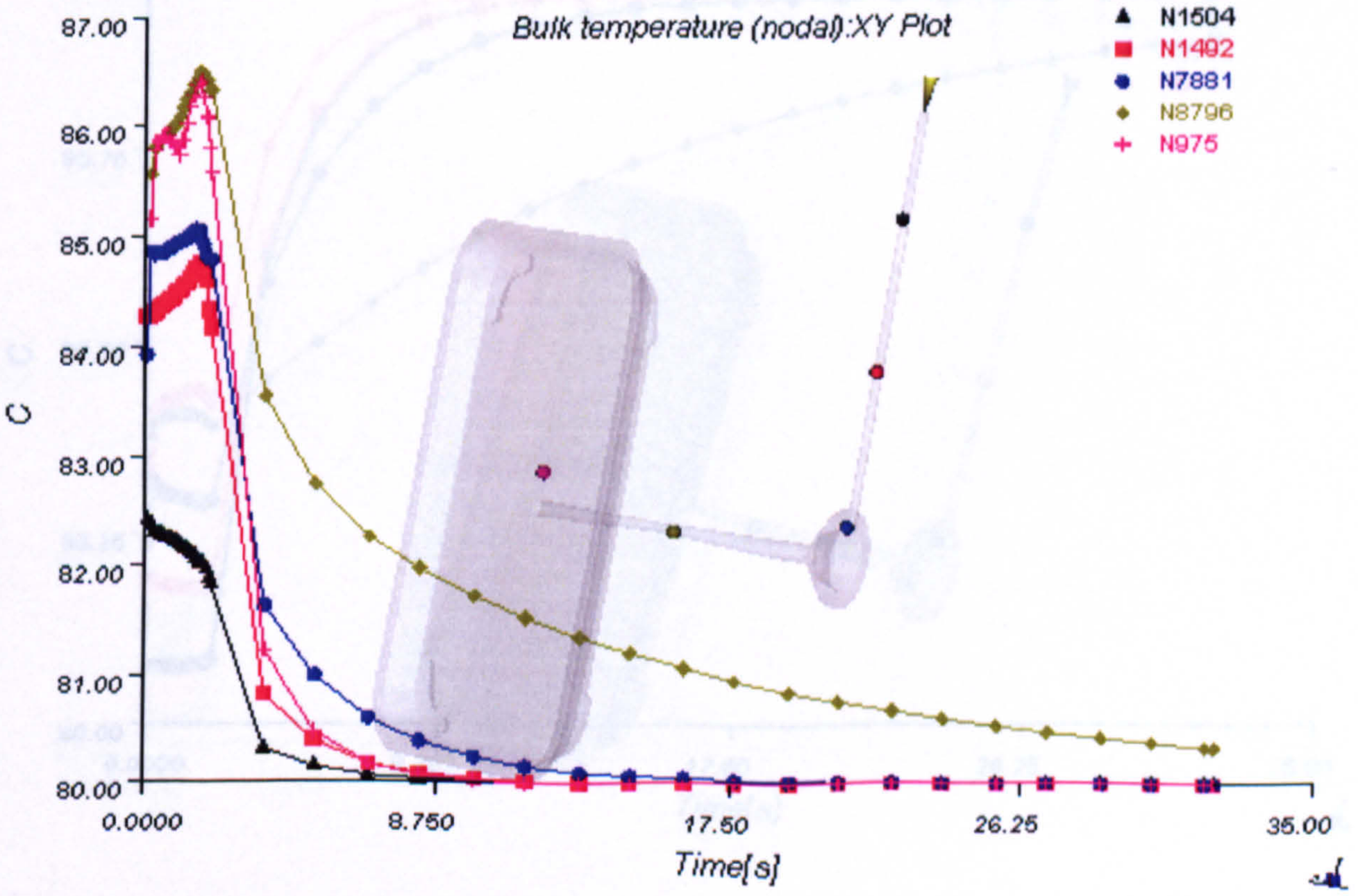

Figure App3.2 b.) Mould temperature 90°C

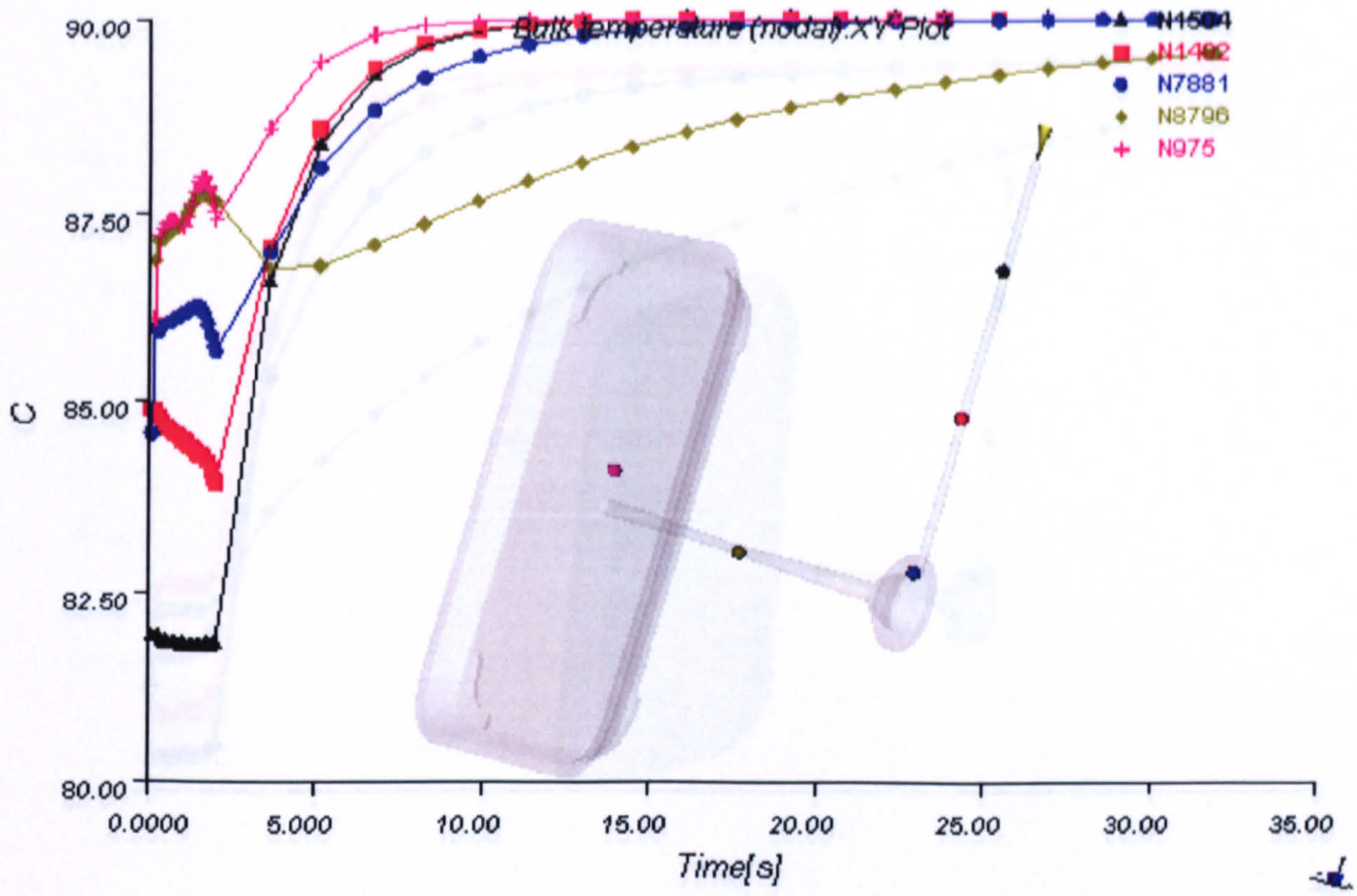

Figure App3.2 c.) Mould temperature 100°C

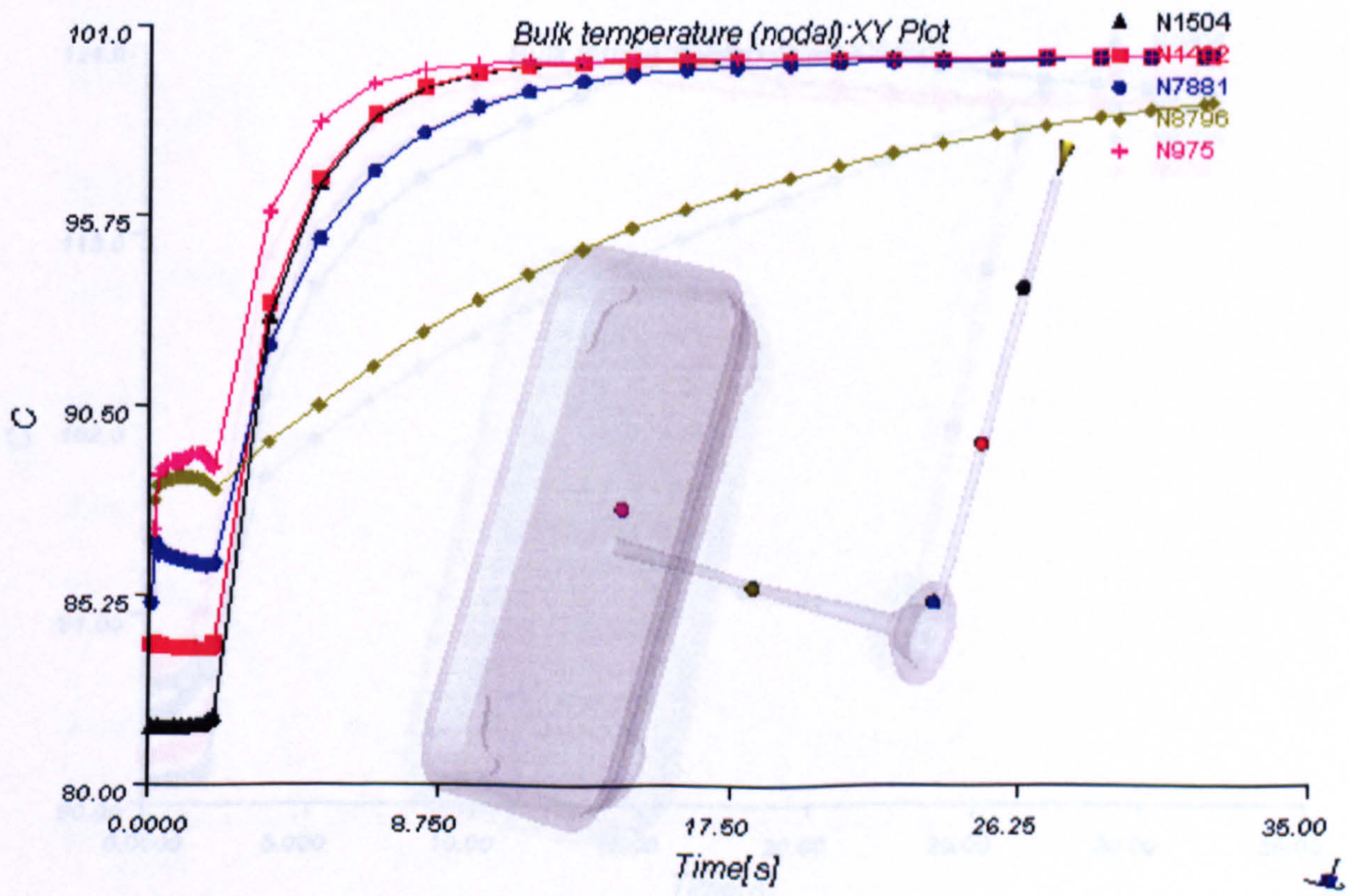

Figure App3.2 d.) Mould temperature 110°C

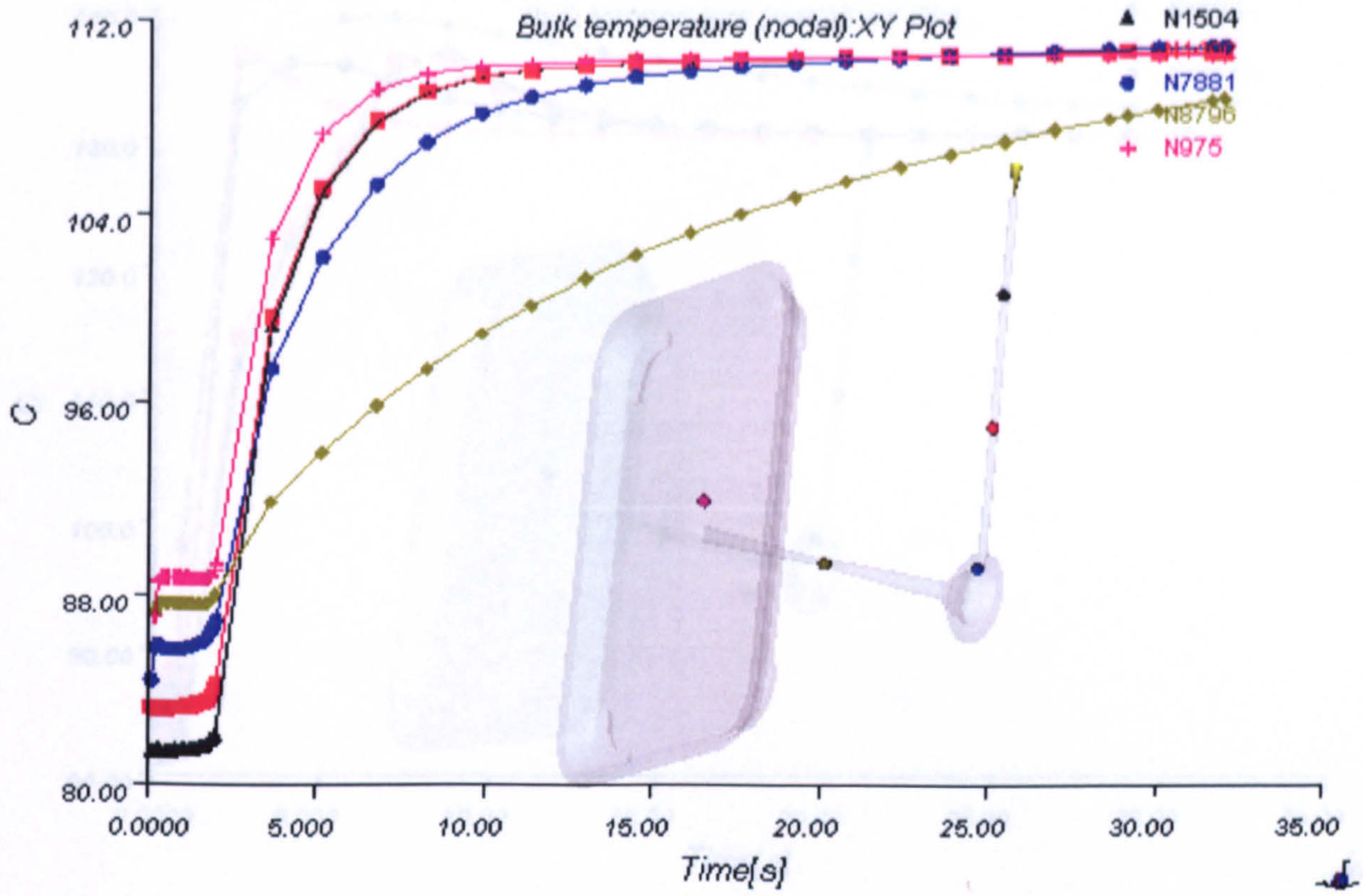

Figure App3.2 e.) Mould temperature 120°C

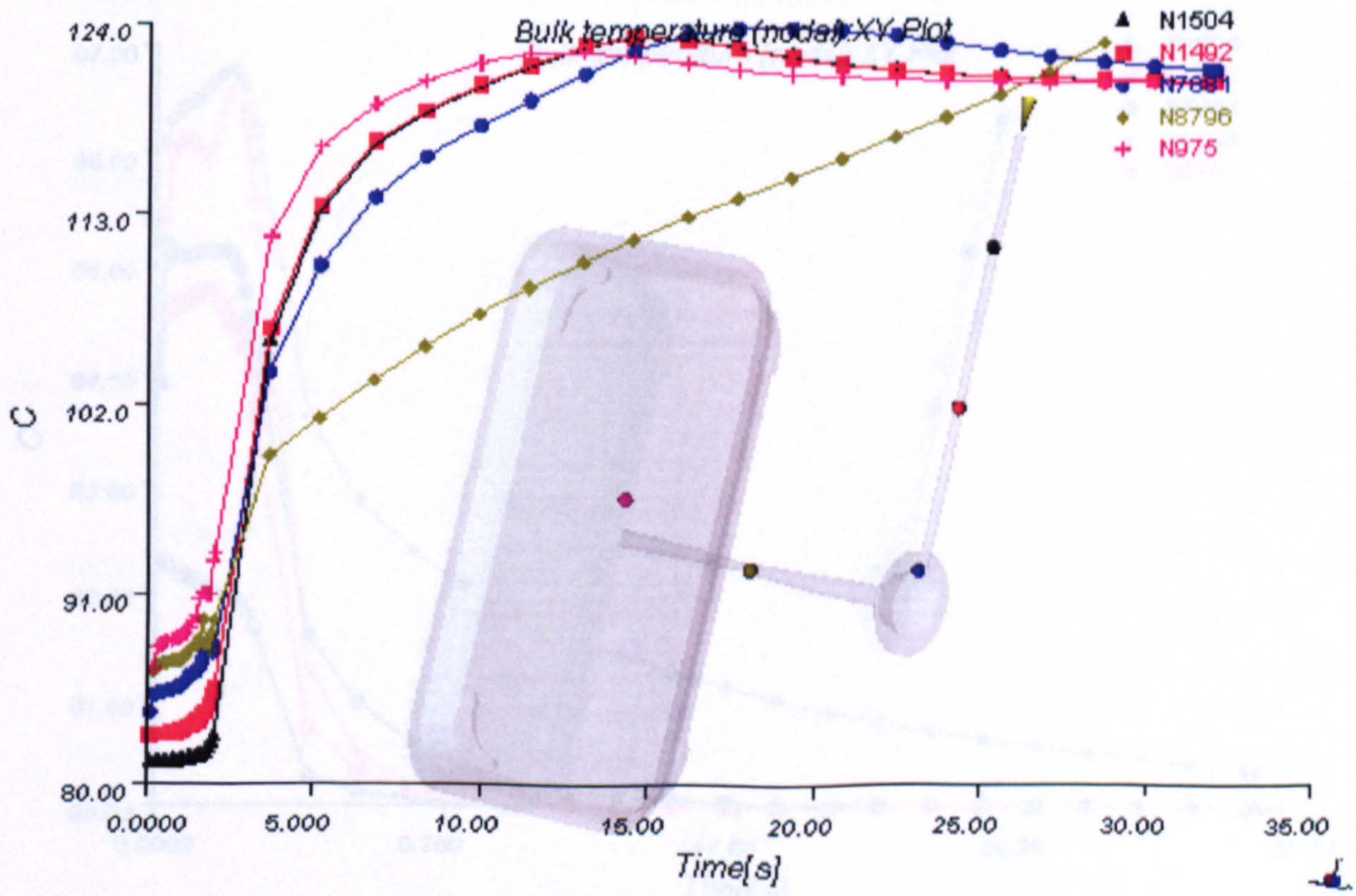

Figure App3.2 f.) Mould temperature 130°C

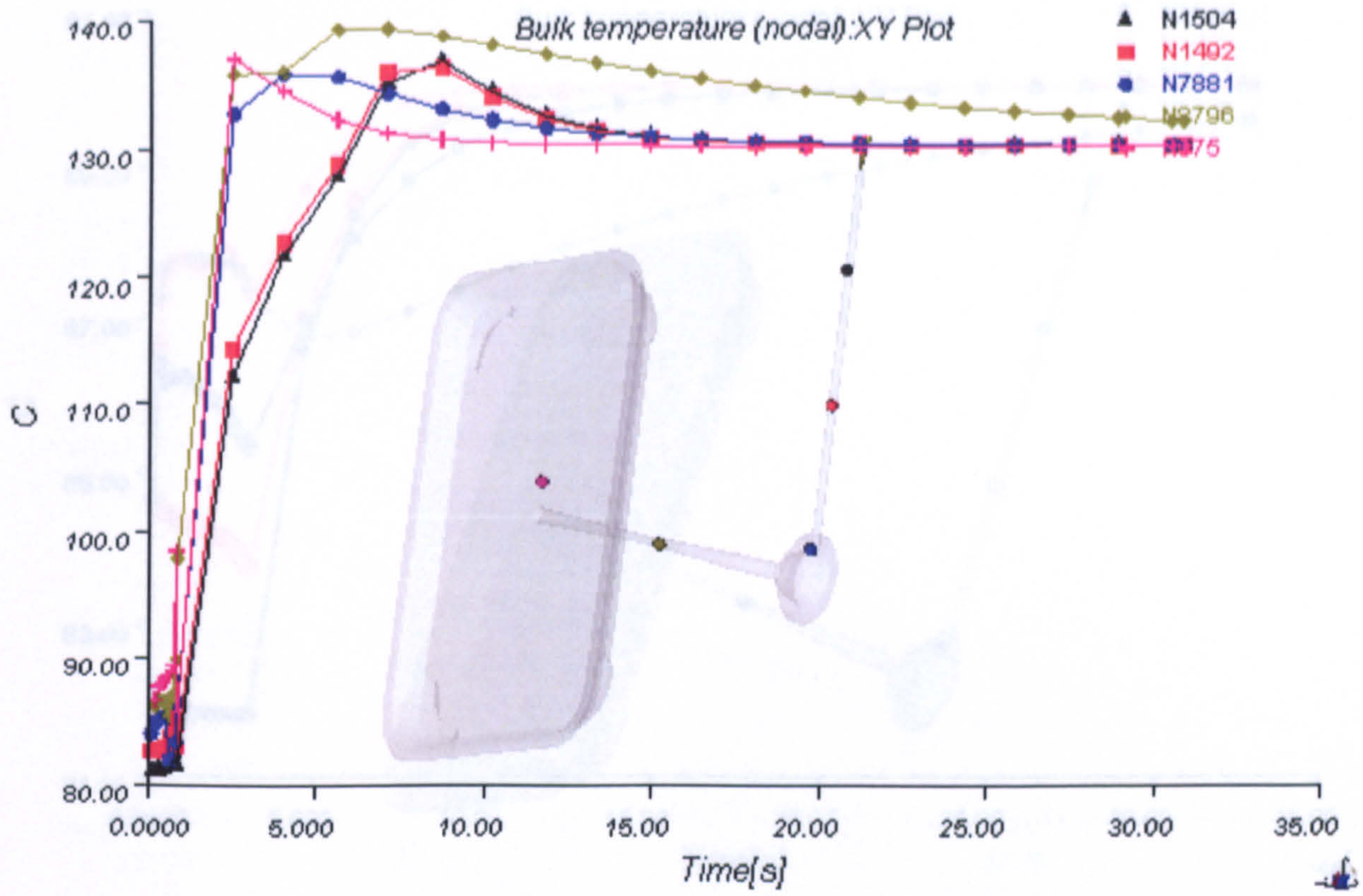

Figure App3.3 Injection time-melt temperature plot at 3-second injection time and mould temperatures is varied from 80 to 130°C

Figure App3.3 a.) Mould temperature 80°C

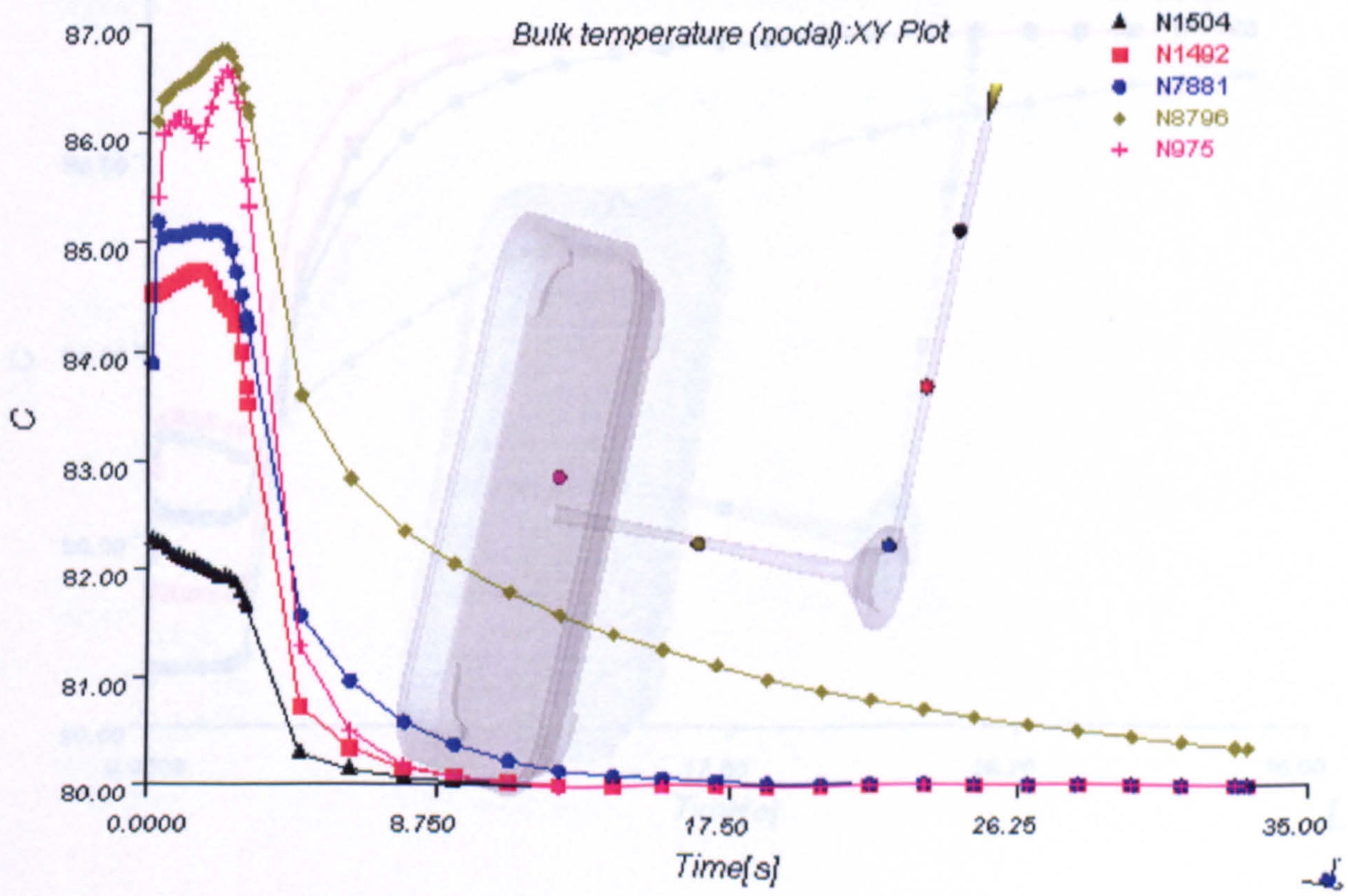

Figure App3.3 b.) Mould temperature 90°C

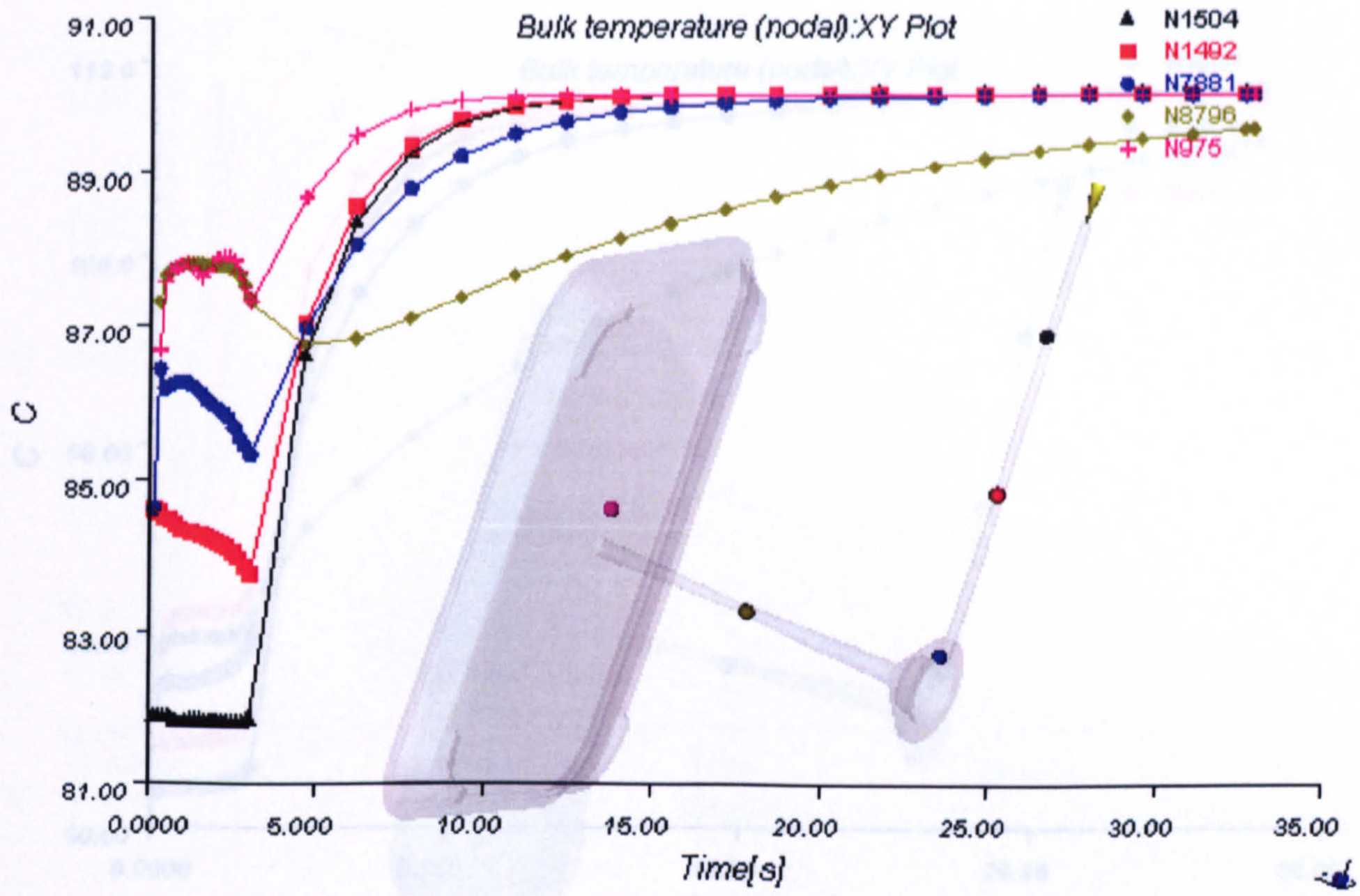

Figure App3.3 c.) Mould temperature 100°C

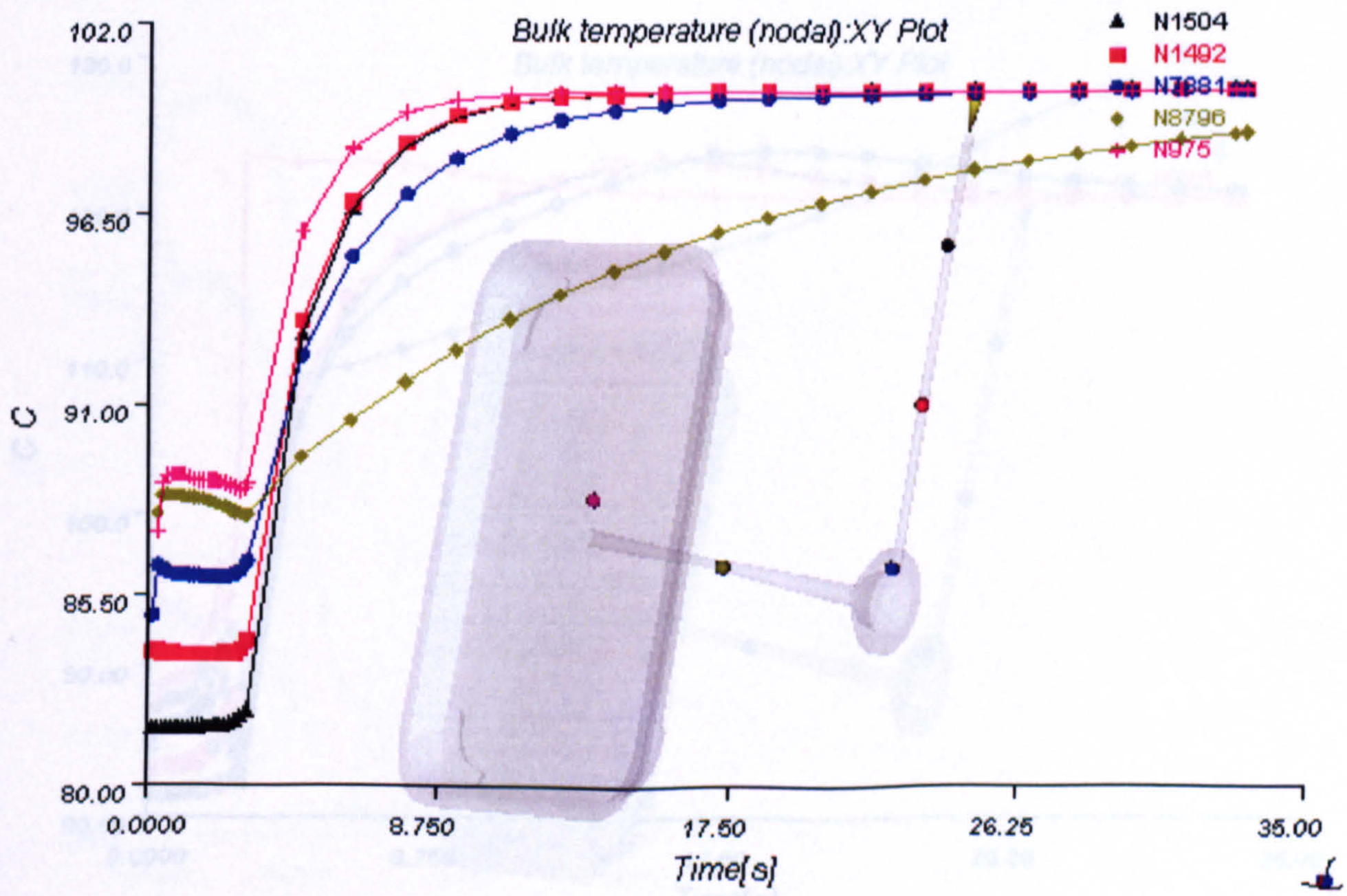

Figure App3.3 d.) Mould temperature 110°C

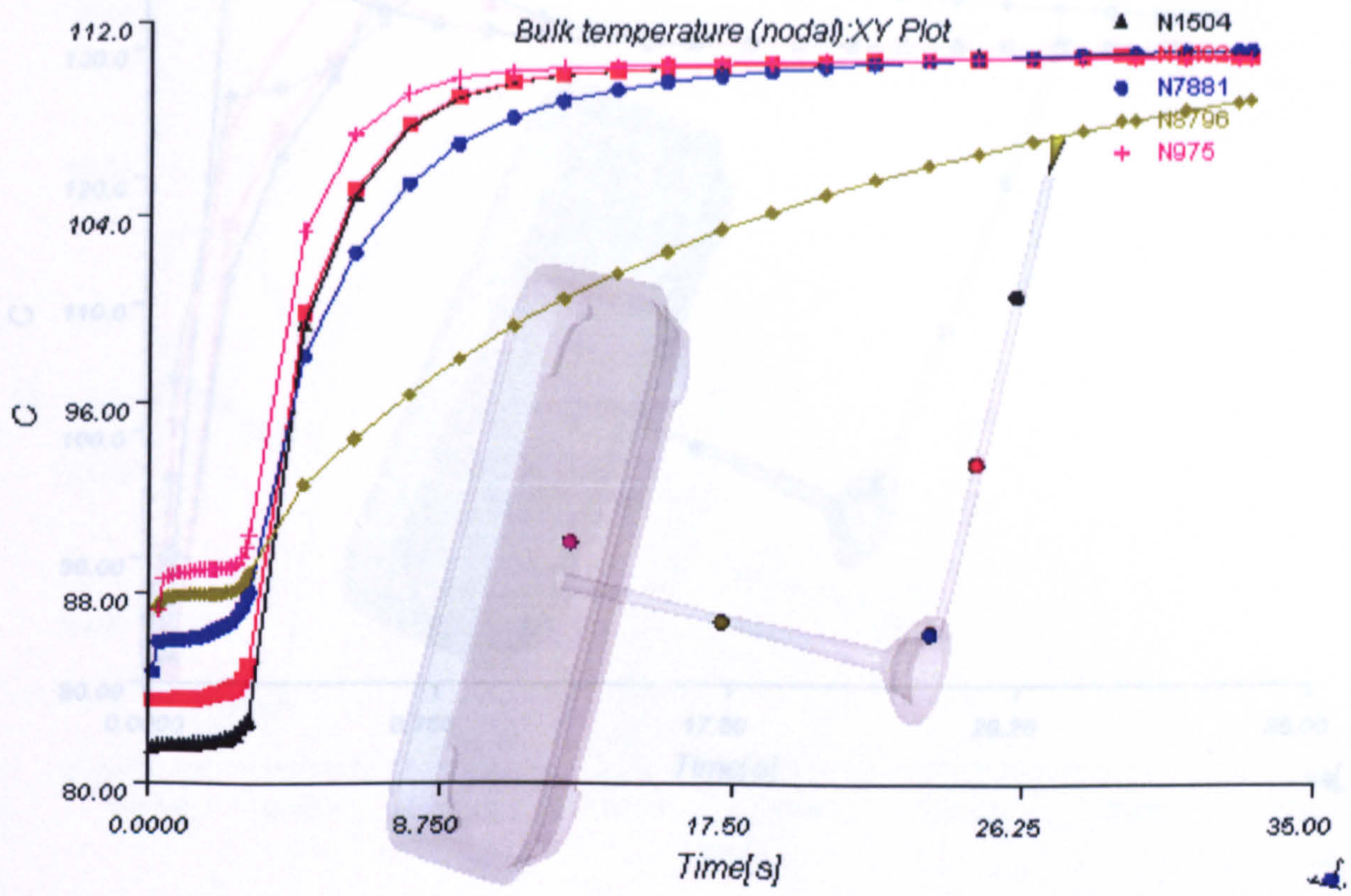

Figure App3.3 e.) Mould temperature 120°C

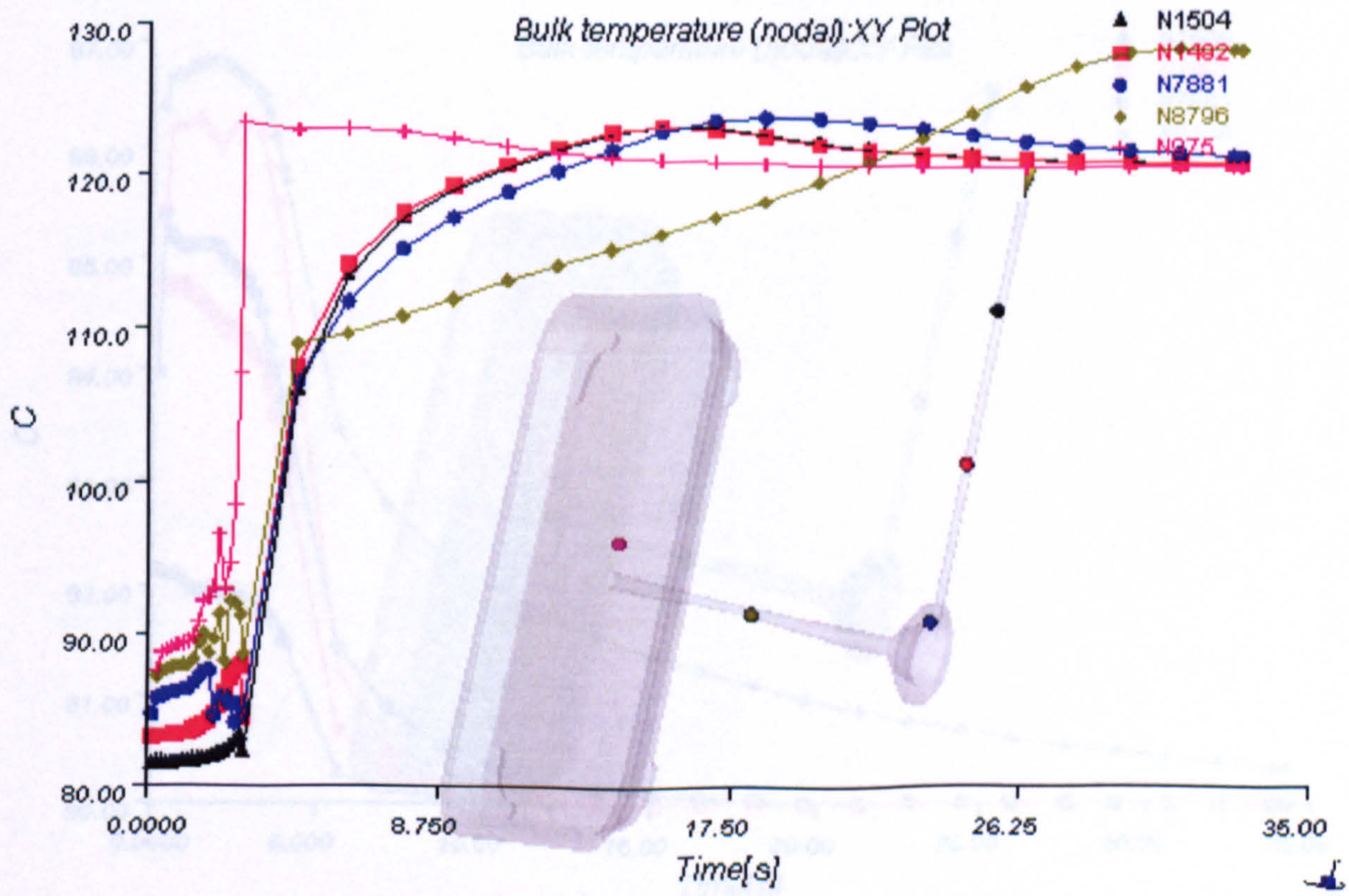

Figure App3.3 f.) Mould temperature 130°C

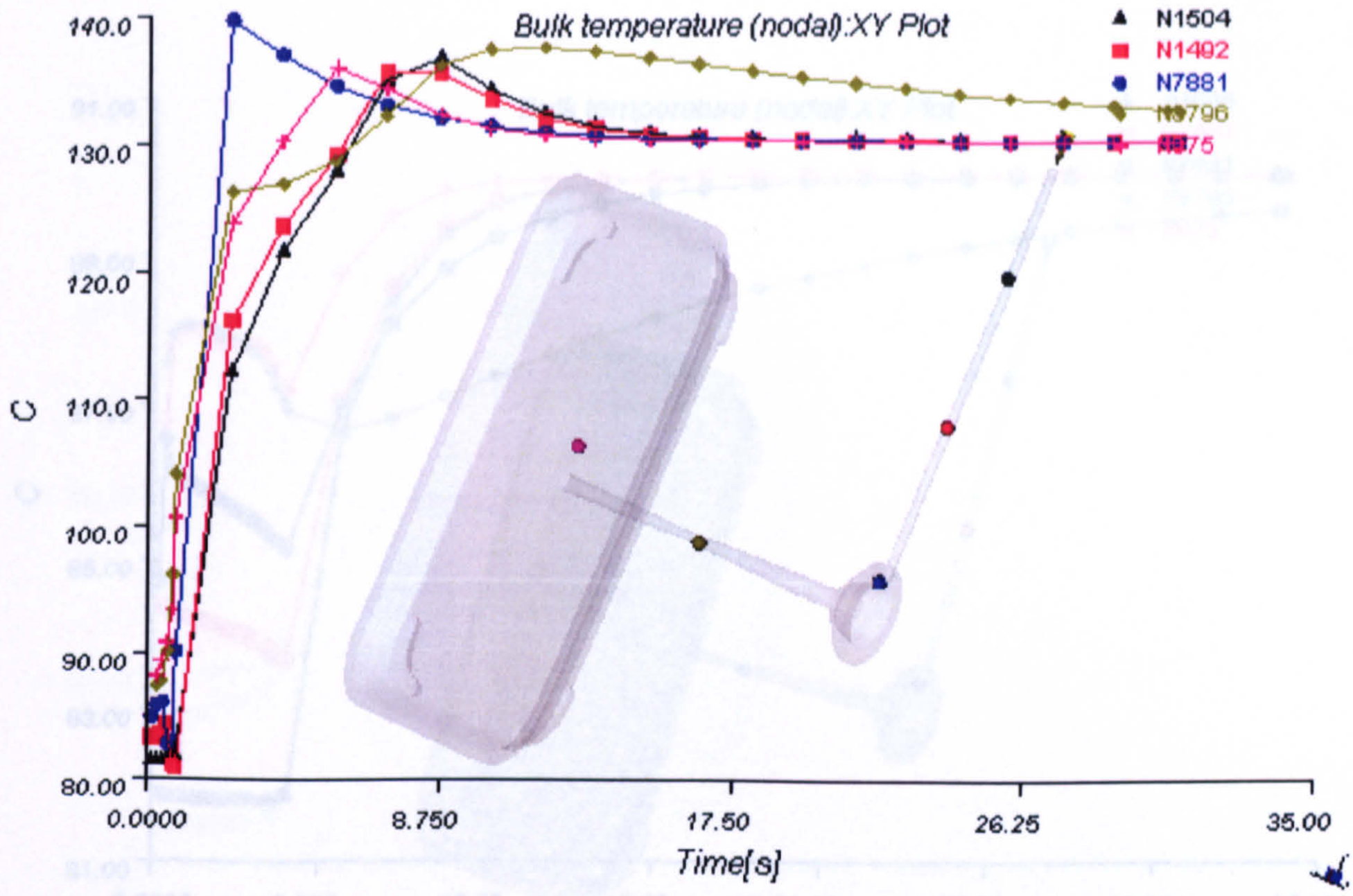

Figure App3.4 Injection time-melt temperature plot at 4-second injection time and mould temperatures is varied from 80 to 130°C

Figure App3.4 a.) Mould temperature 80°C

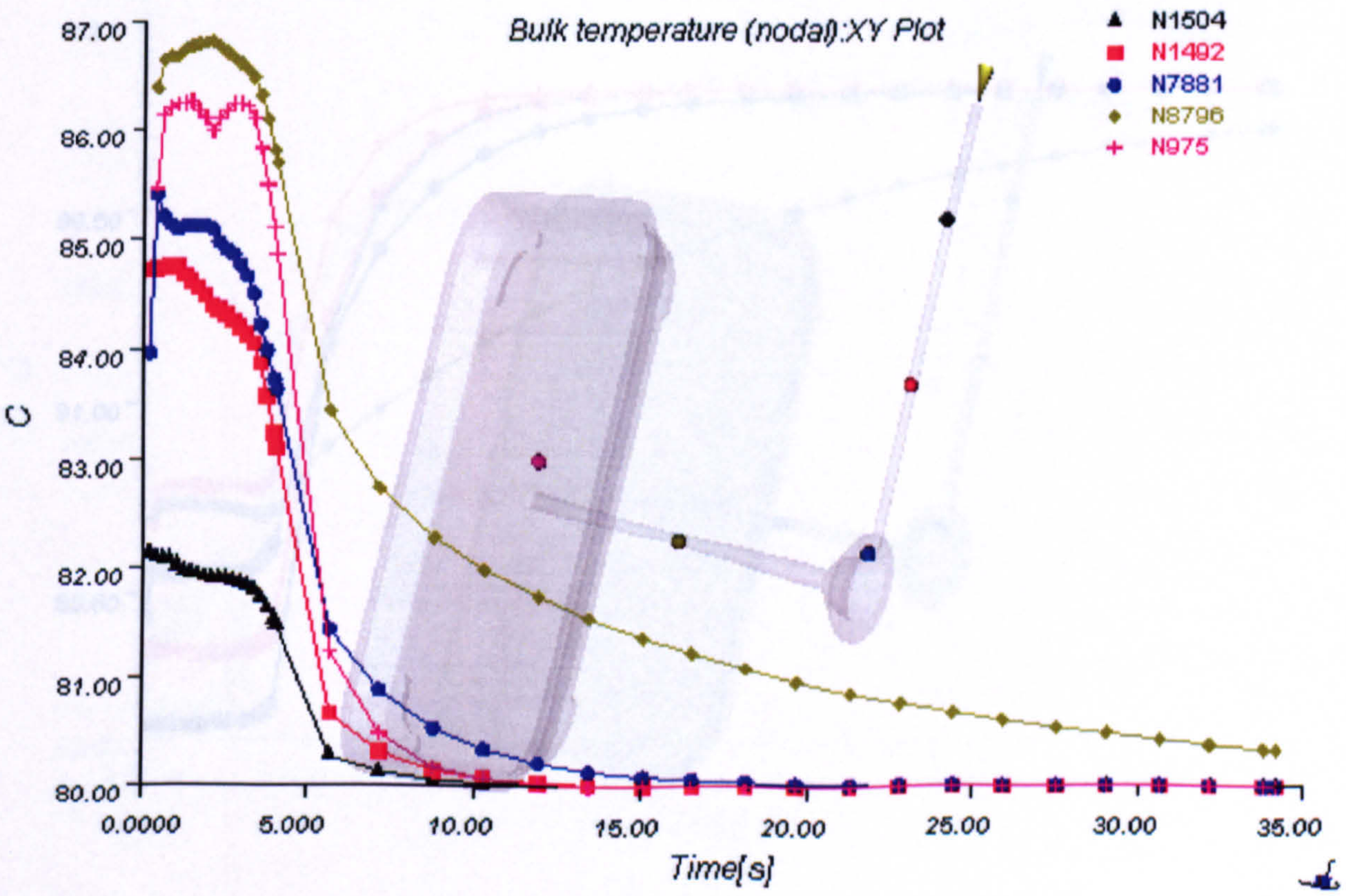

Figure App3.4 b.) Mould temperature 90°C

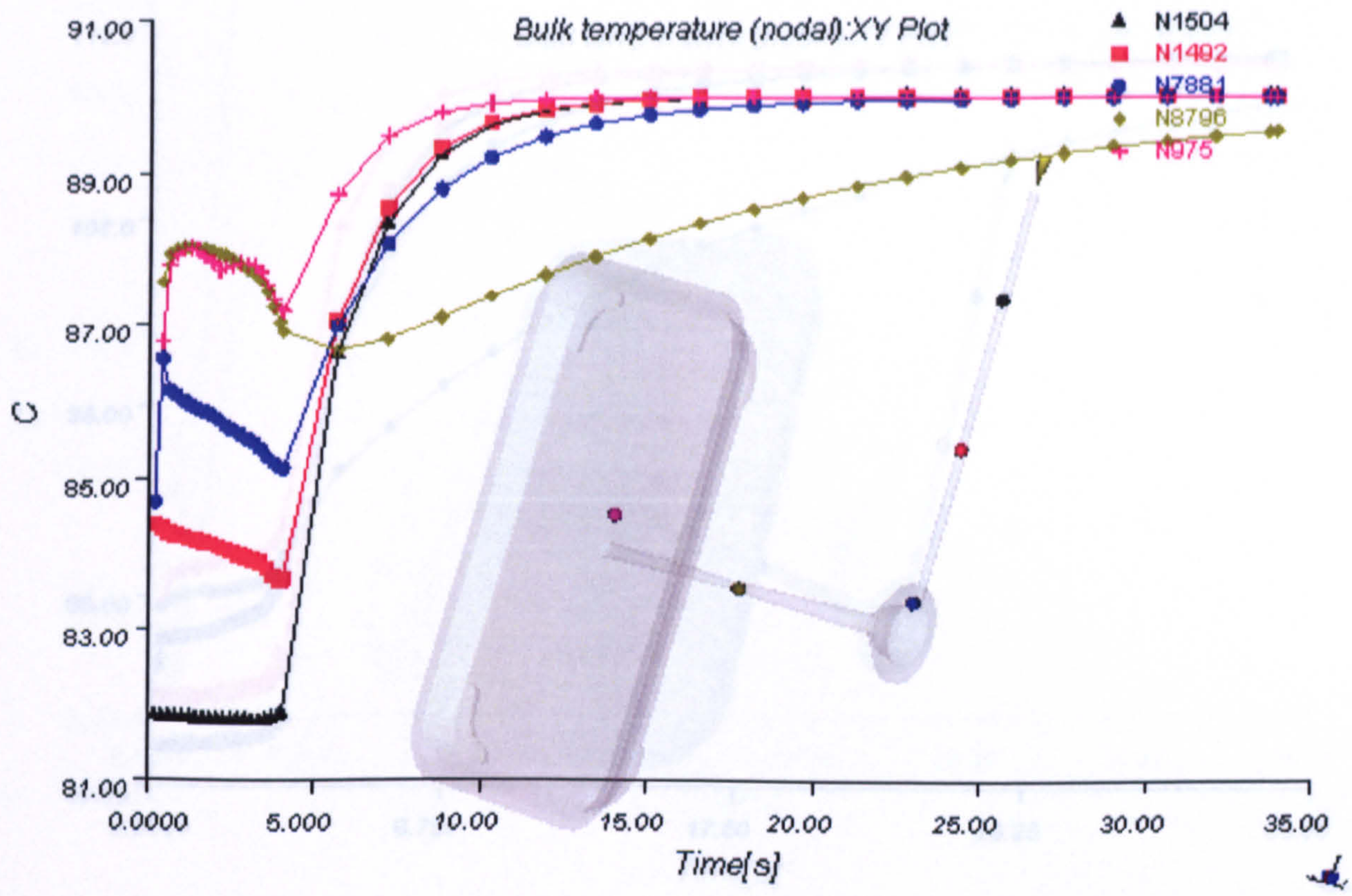

Figure App3.4 c.) Mould temperature 100°C

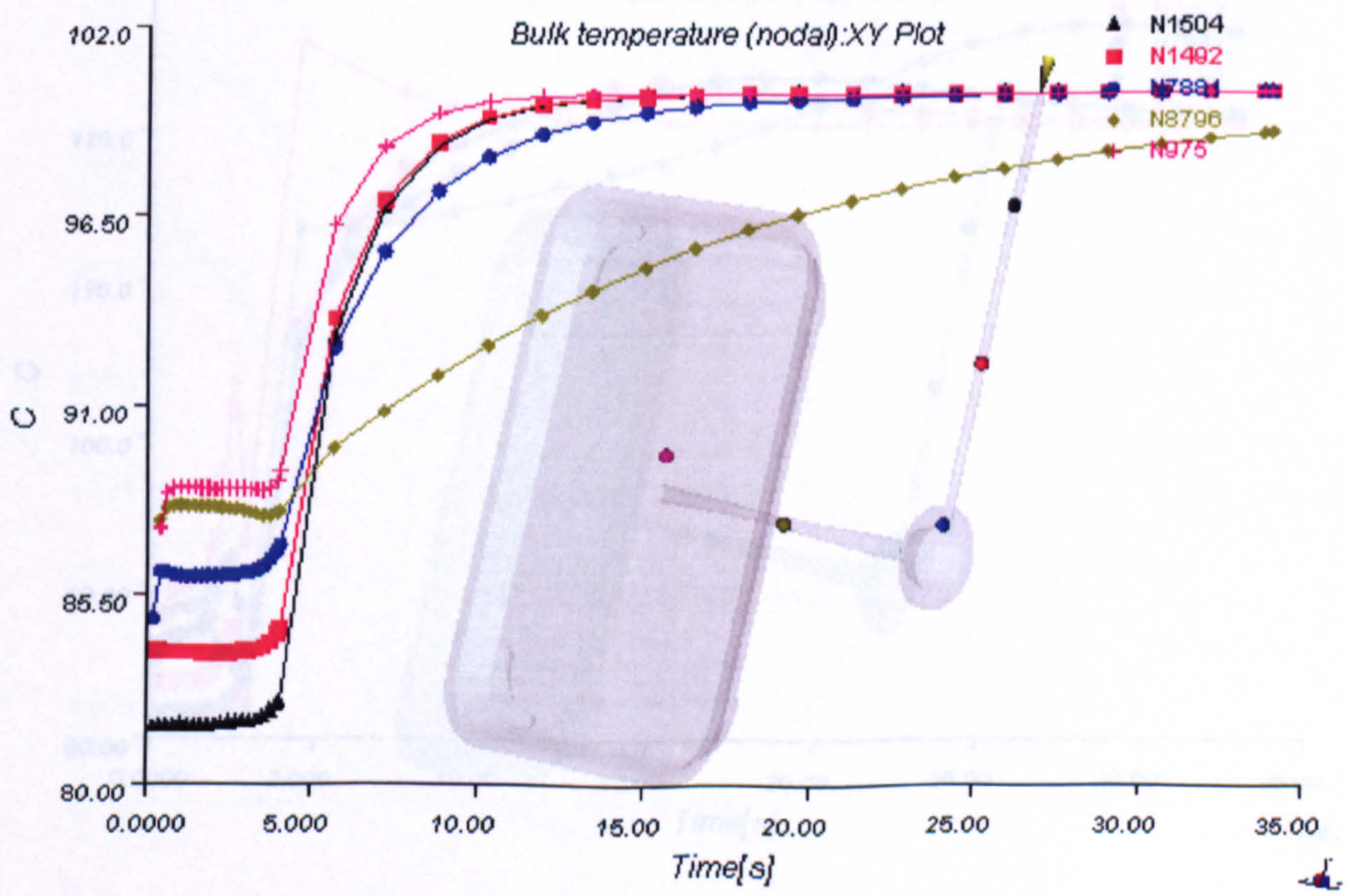

Figure App3.4 d.) Mould temperature 110°C

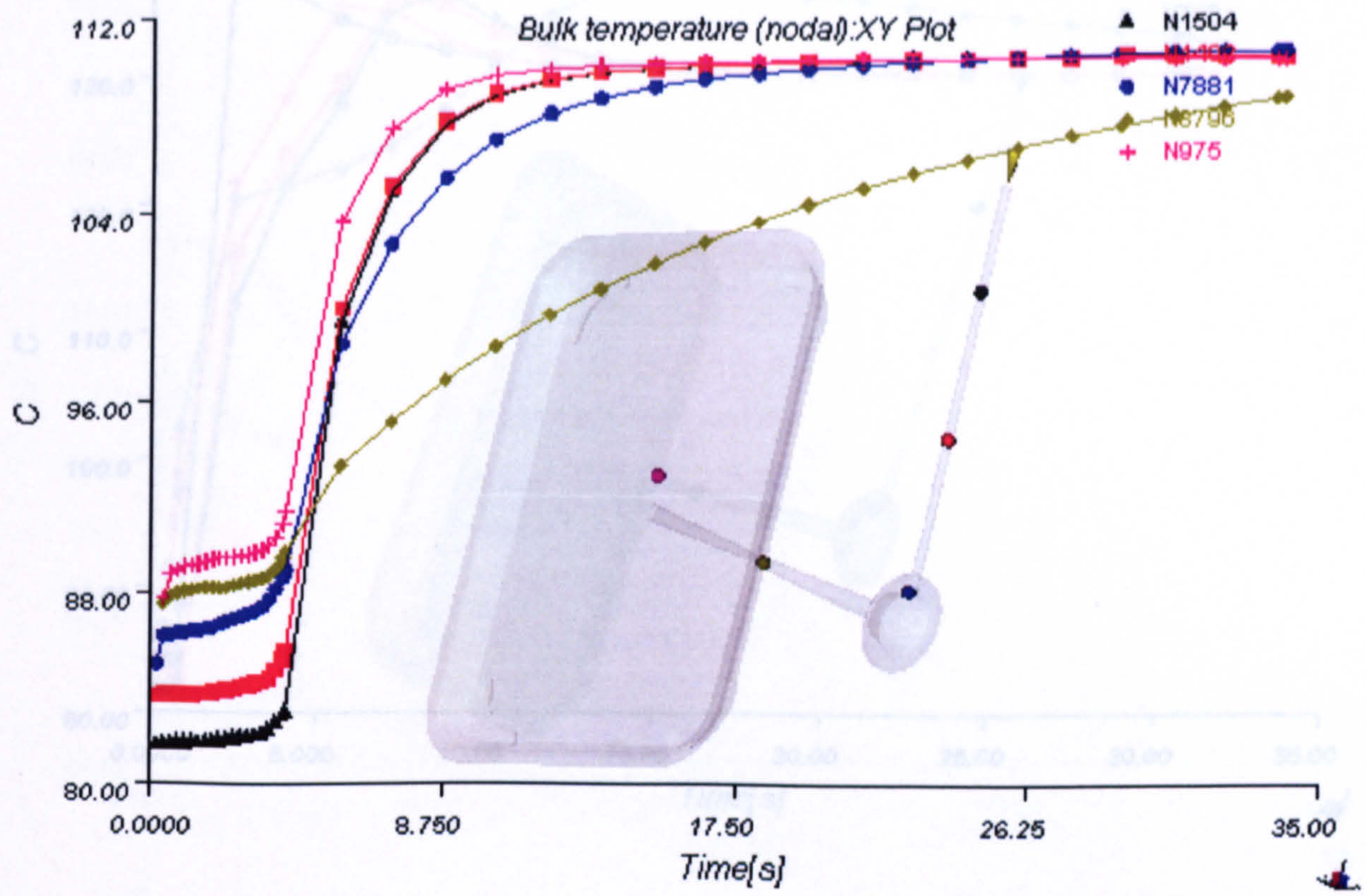

Figure App3.4 e.) Mould temperature 120°C

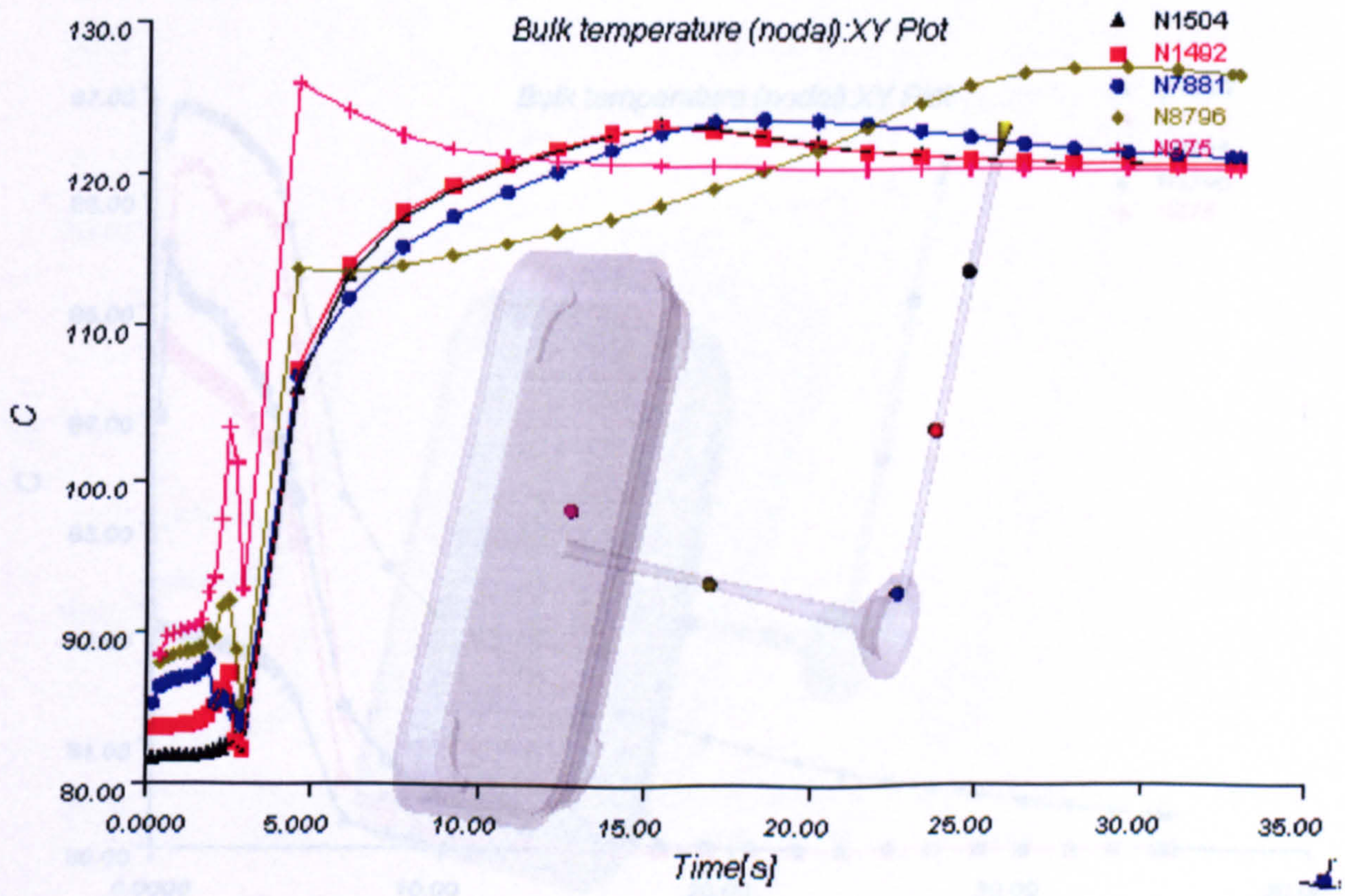

Figure App3.4 f.) Mould temperature 130°C

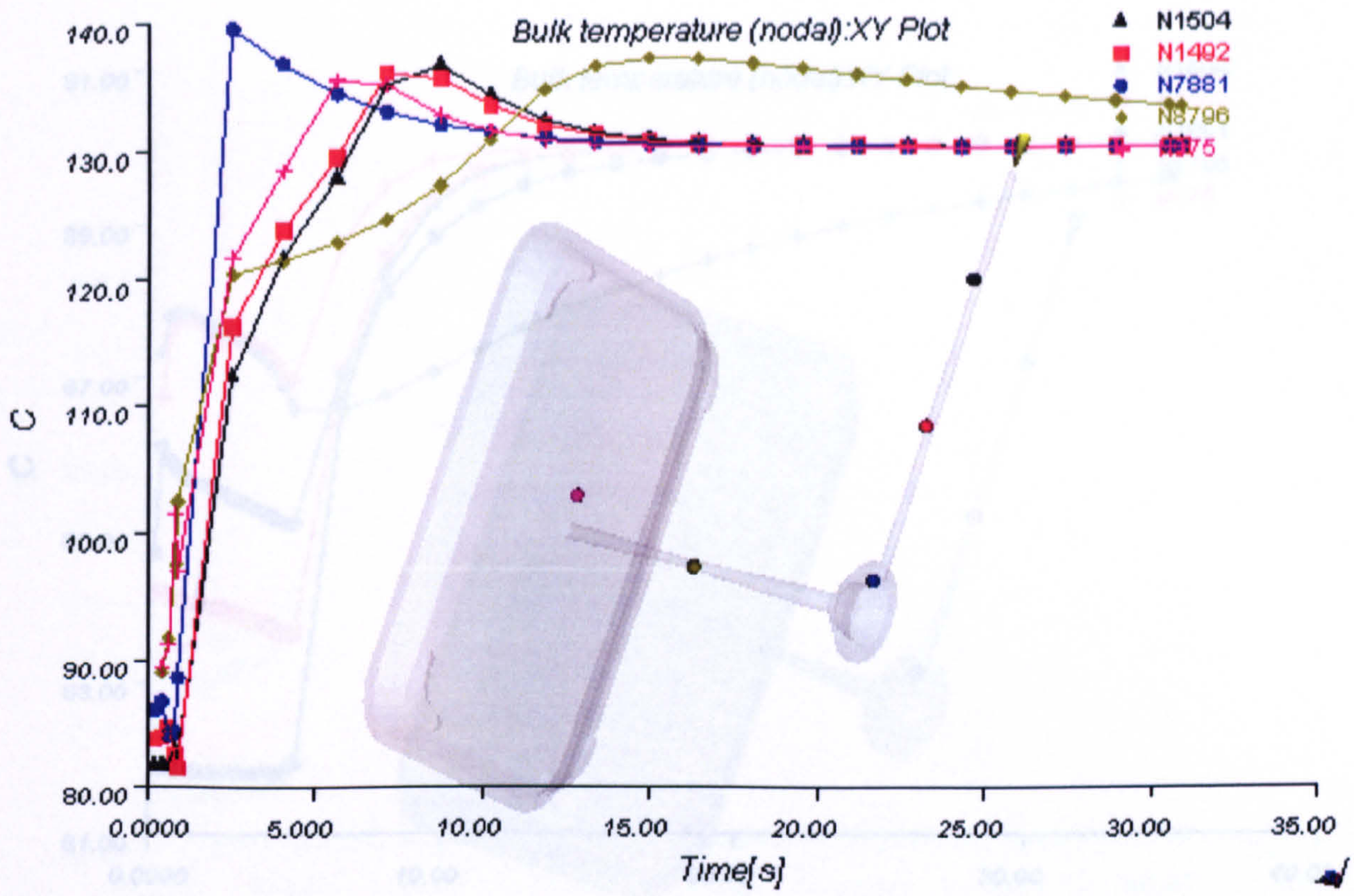

Figure App3.5 Injection time-melt temperature plot at 5-second injection time and mould temperatures is varied from 80 to 130°C

Figure App3.5 a.) Mould temperature 80°C

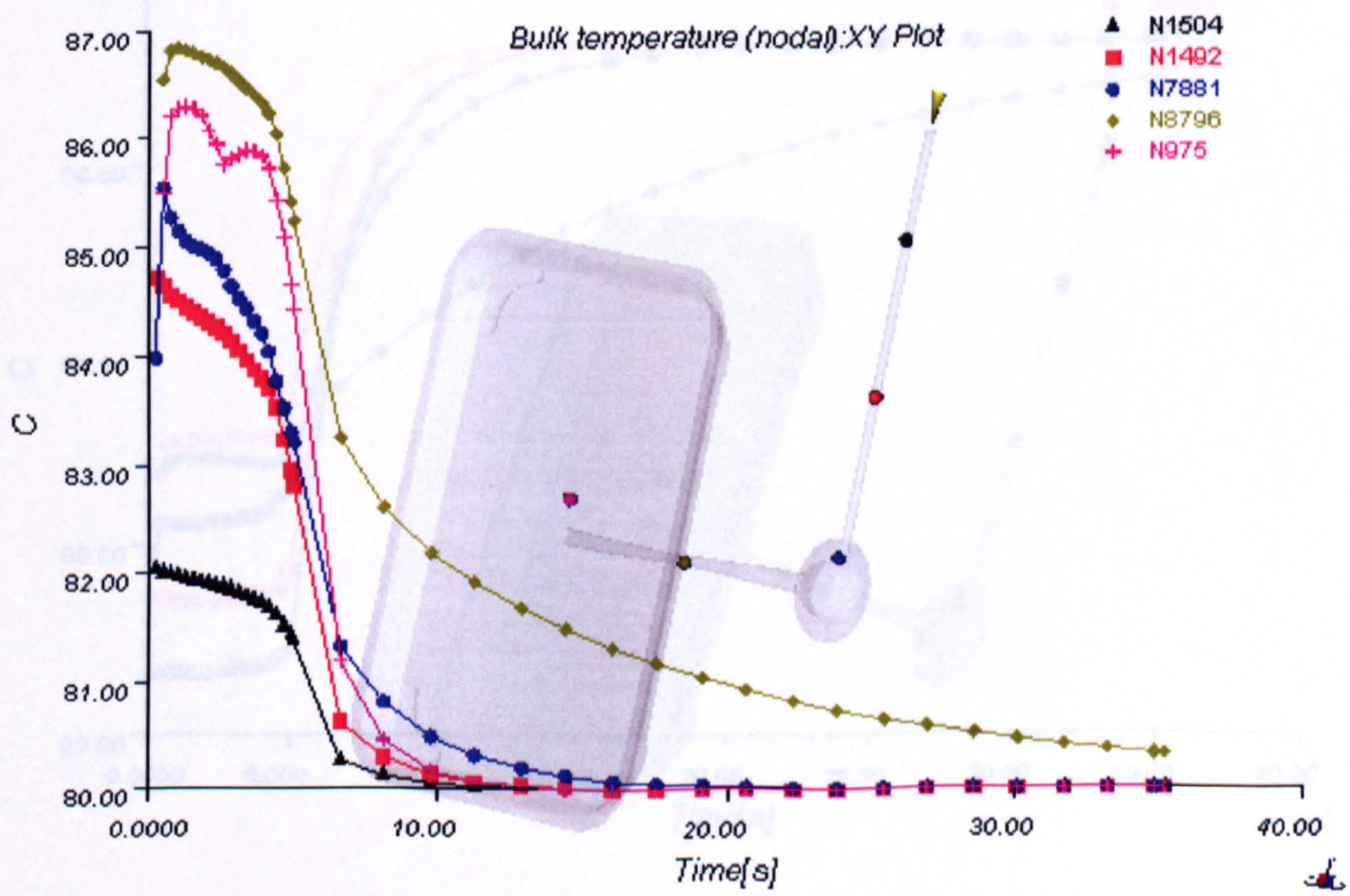

Figure App3.5 b.) Mould temperature 90°C

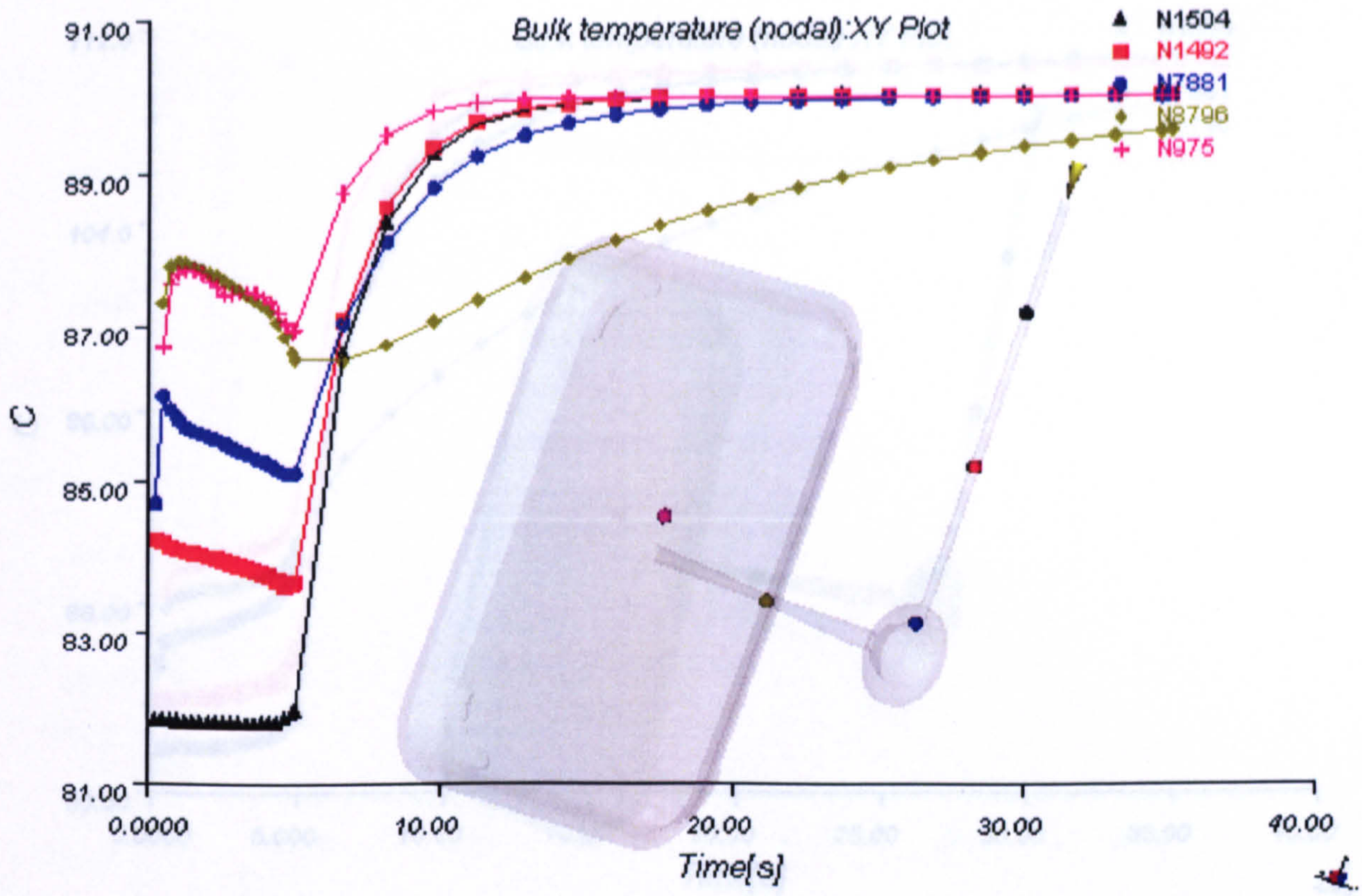

Figure App3.5 c.) Mould temperature 100°C

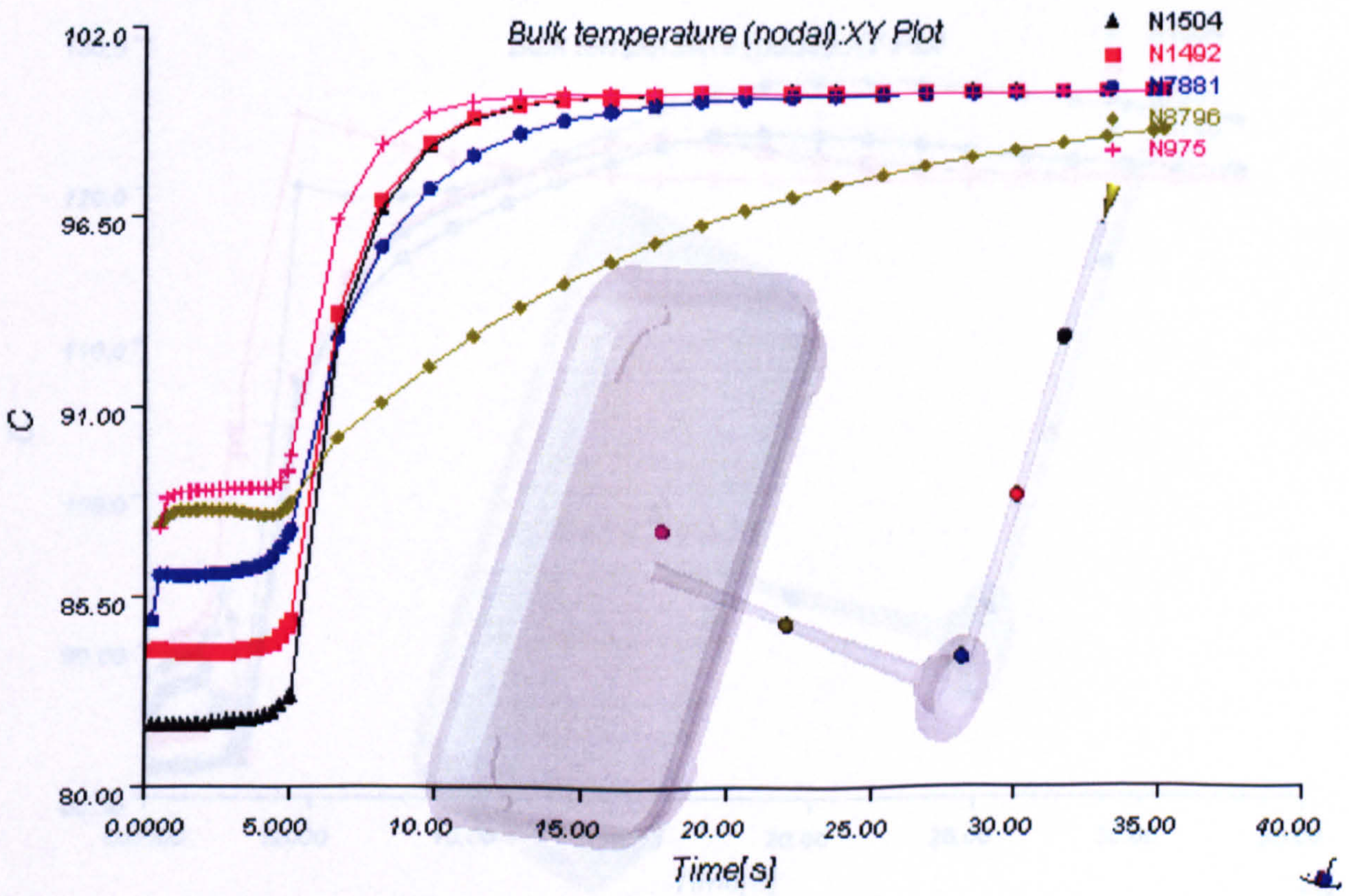

Figure App3.5 d.) Mould temperature 110°C

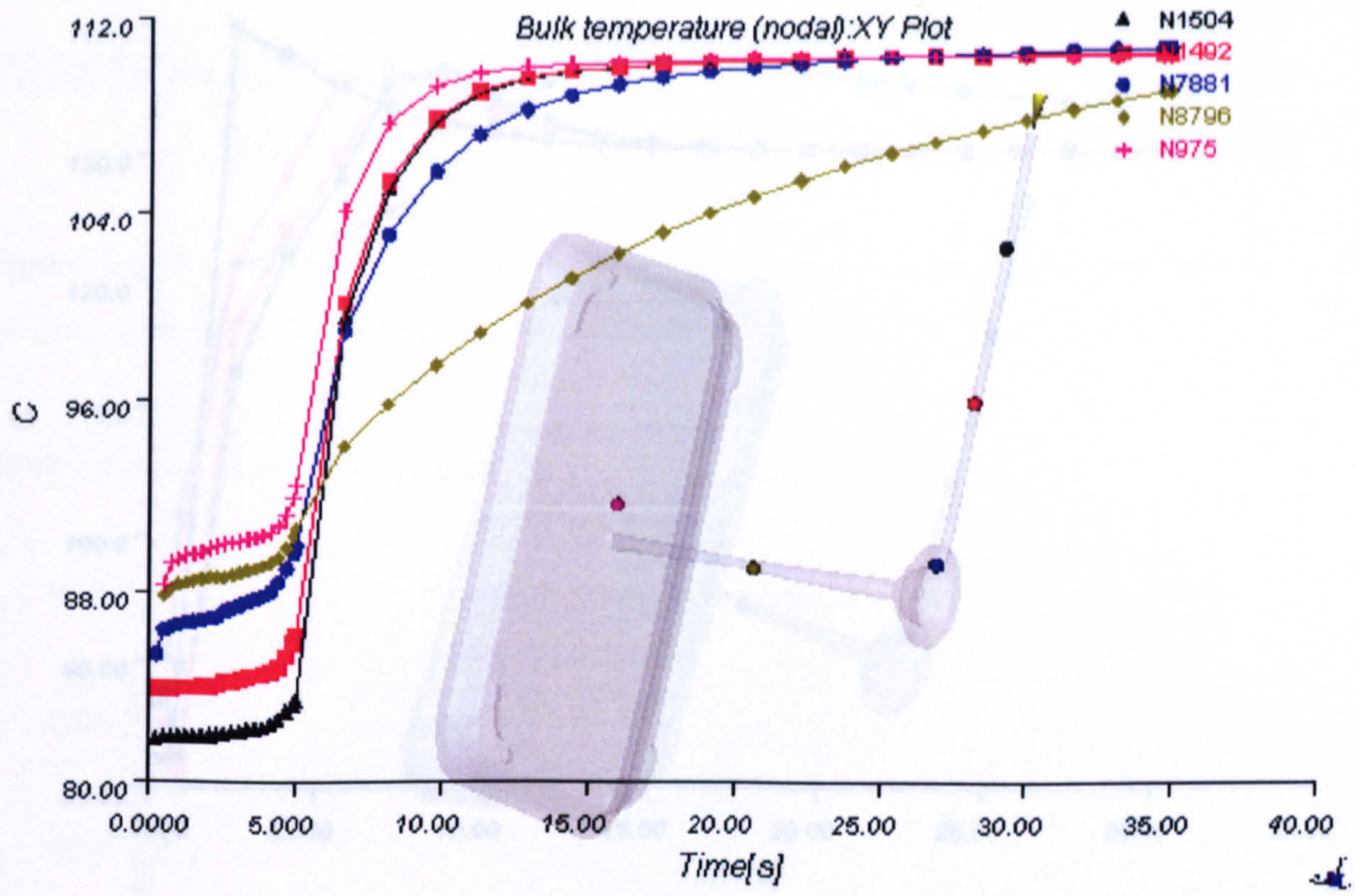

Figure App3.5 e.) Mould temperature 120°C

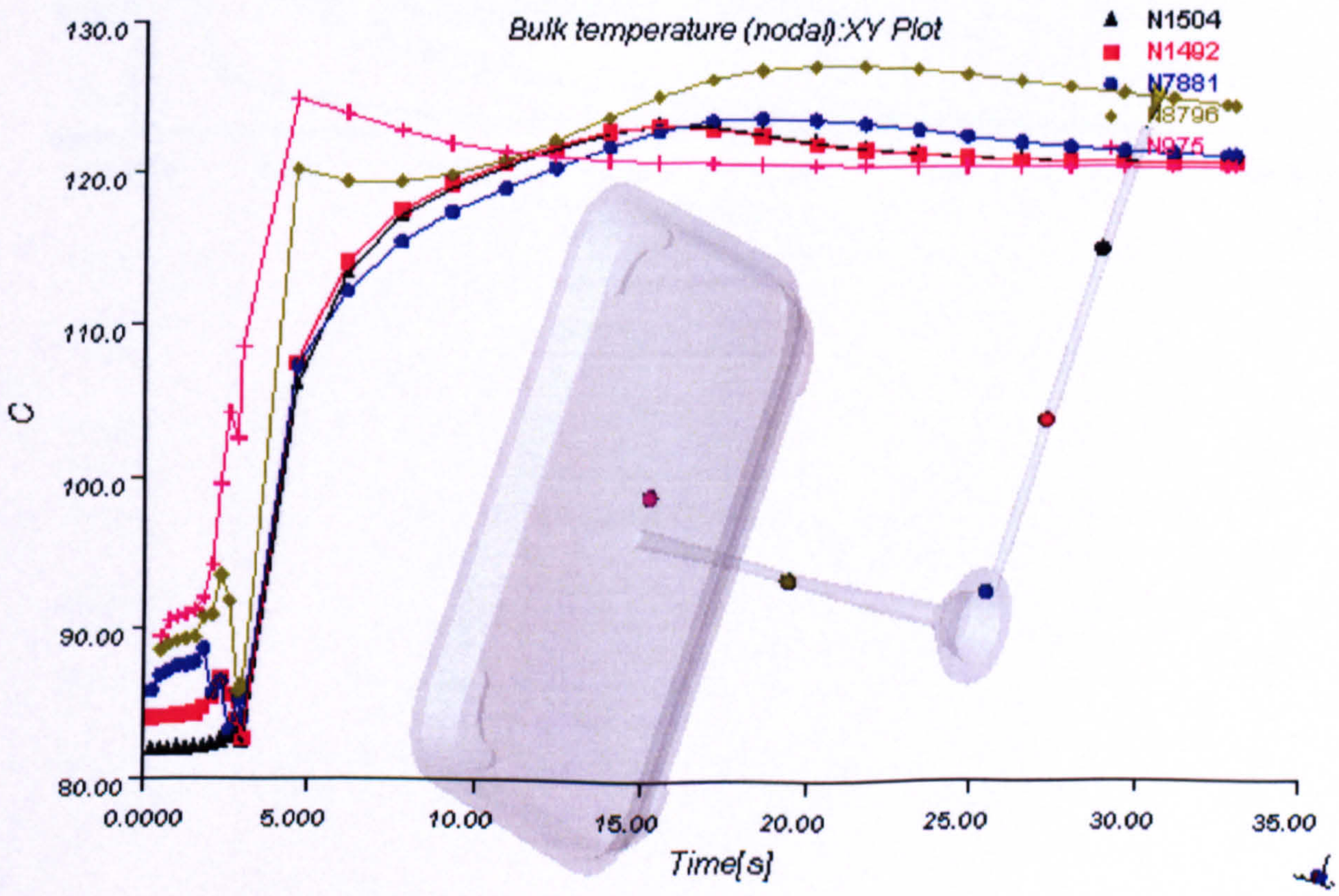

Figure App3.5 f.) Mould temperature 130°C

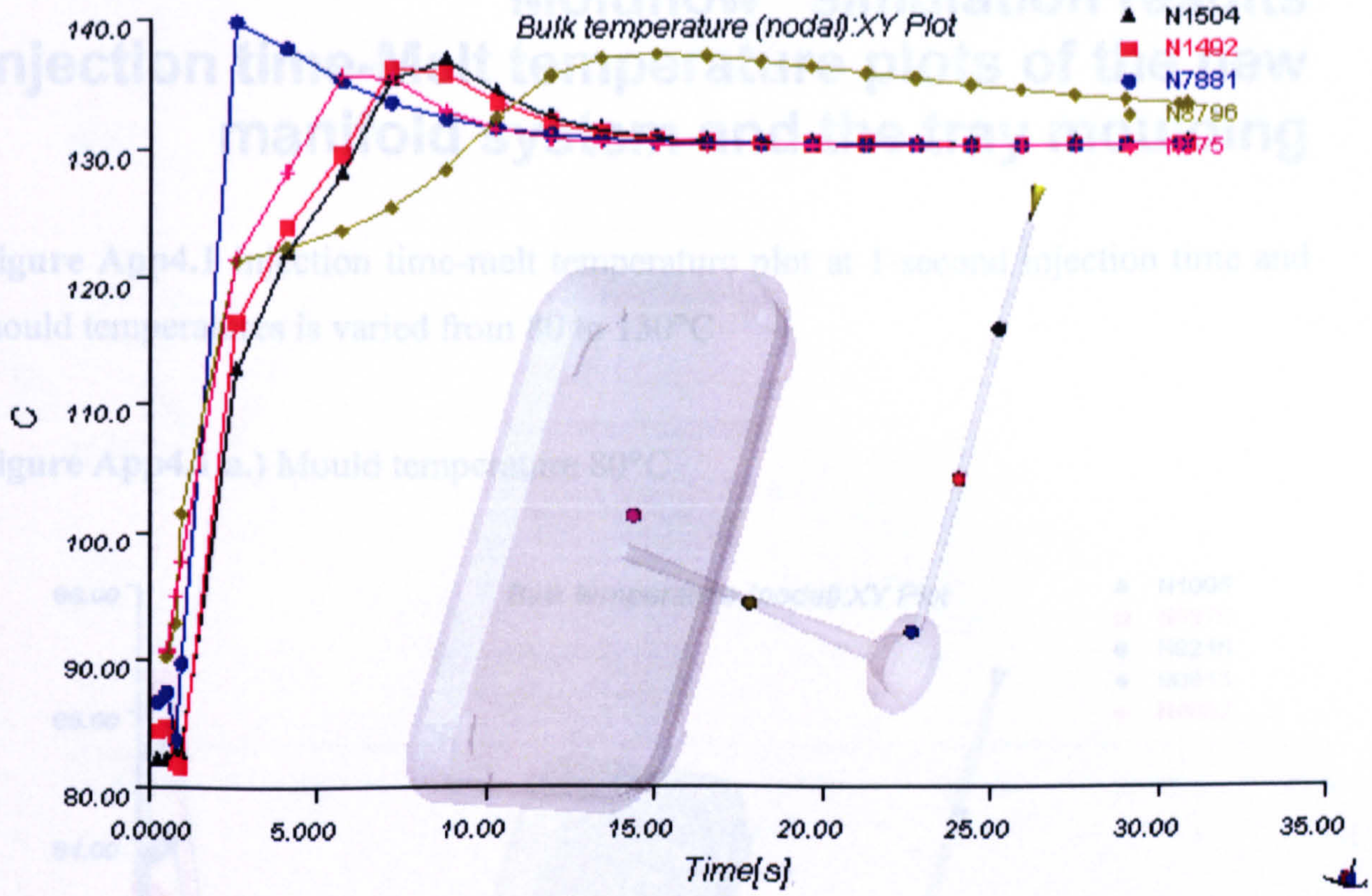

Appendix IV

Moldflow® simulation results Injection time-Melt temperature plots of the new manifold system and the tray moulding

Figure App4.1 Injection time-melt temperature plot at 1-second injection time and mould temperatures is varied from 80 to 130°C

Figure App4.1 a.) Mould temperature 80°C

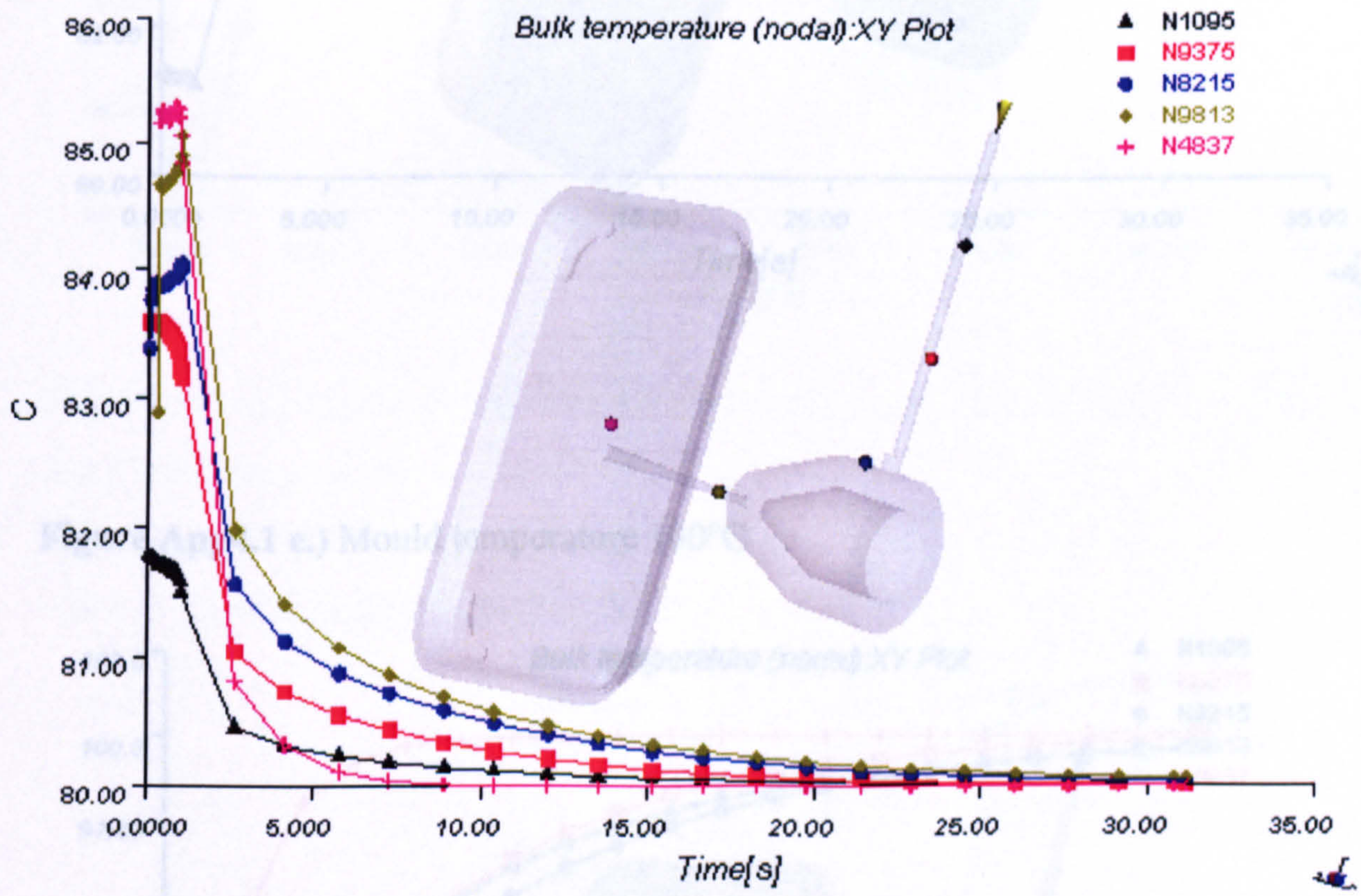

Figure App4.1 b.) Mould temperature 90°C

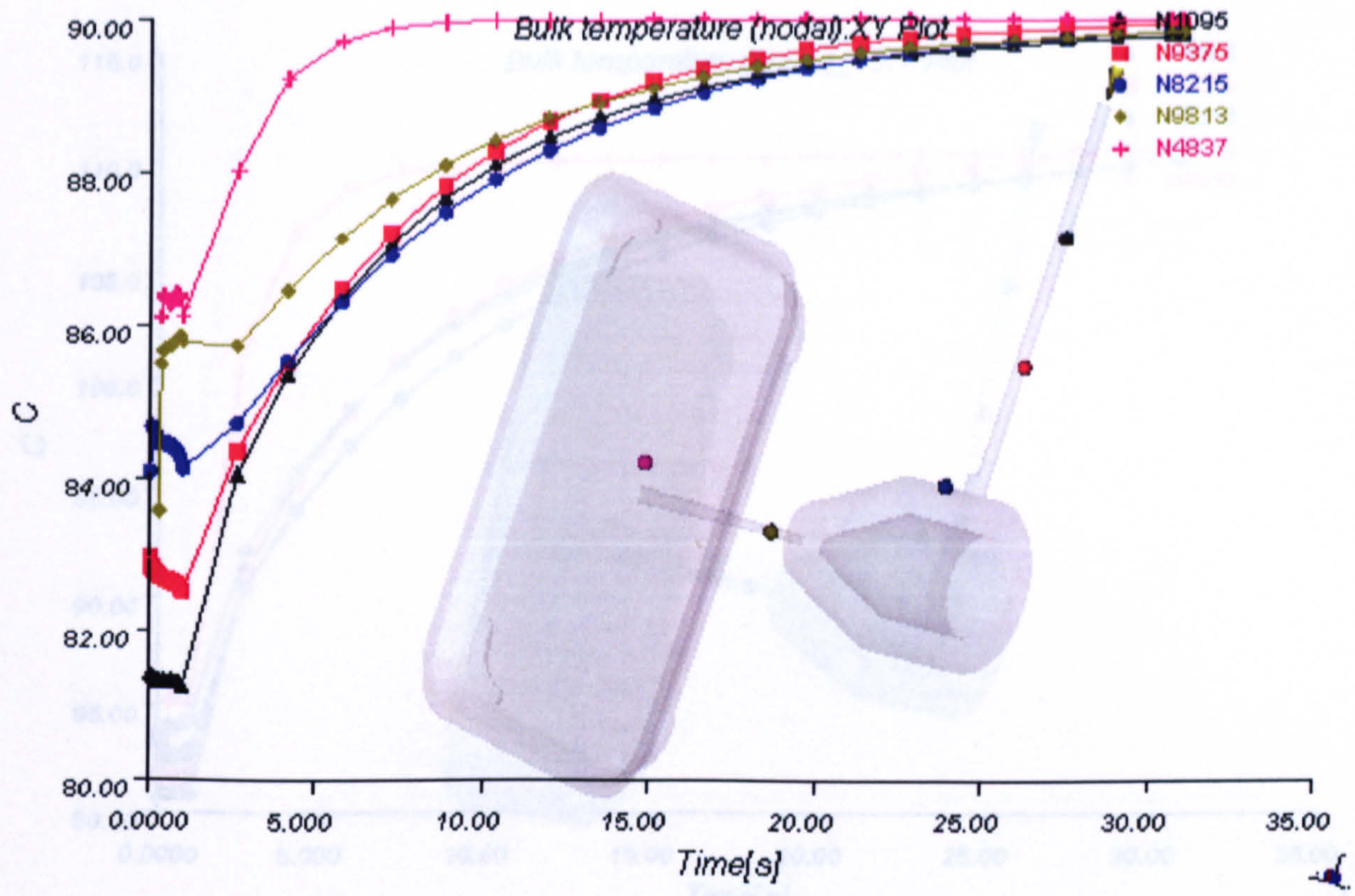

Figure App4.1 c.) Mould temperature 100°C

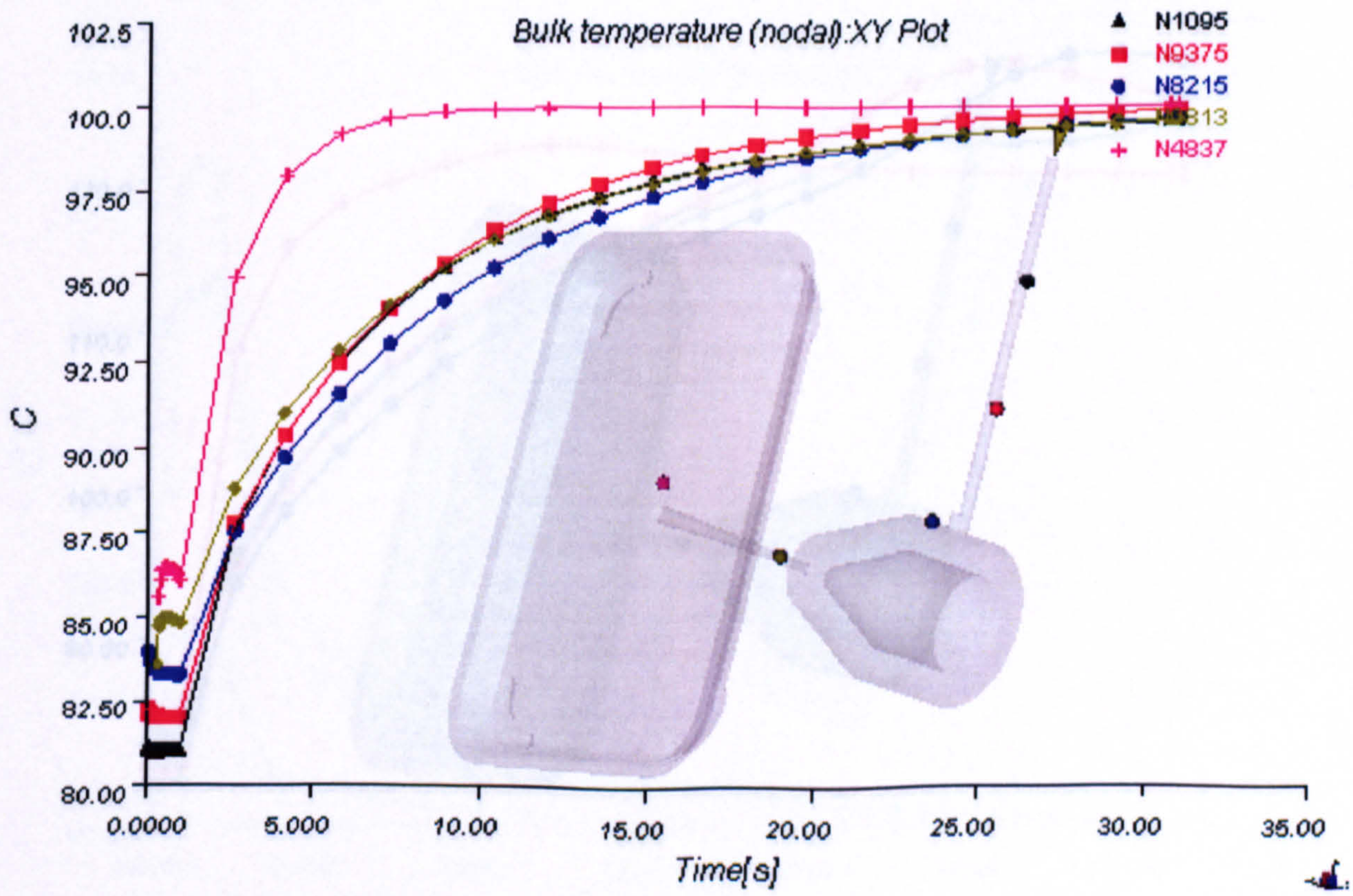

Figure App4.1 d.) Mould temperature 110°C

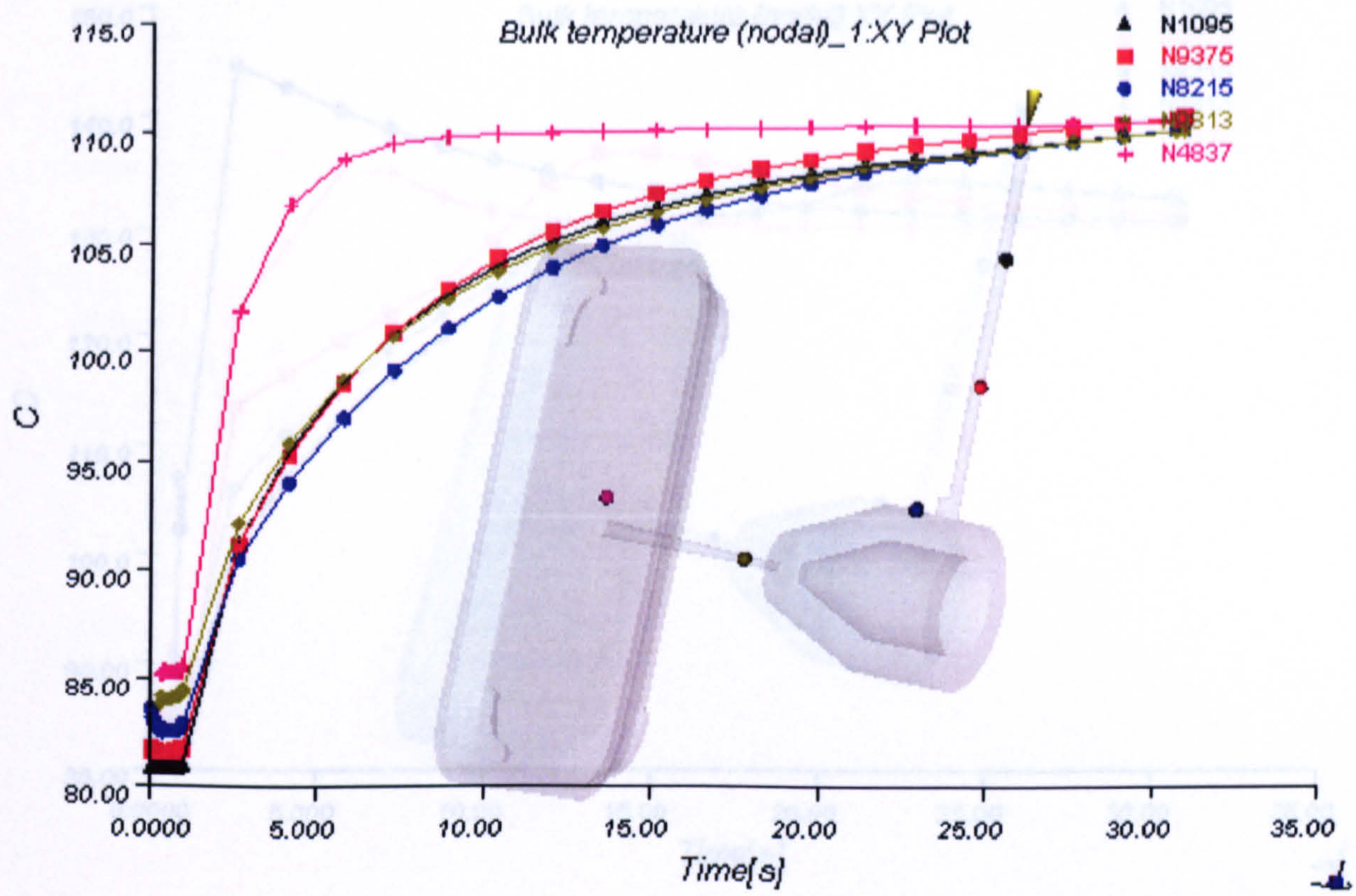

Figure App4.1 e.) Mould temperature 120°C

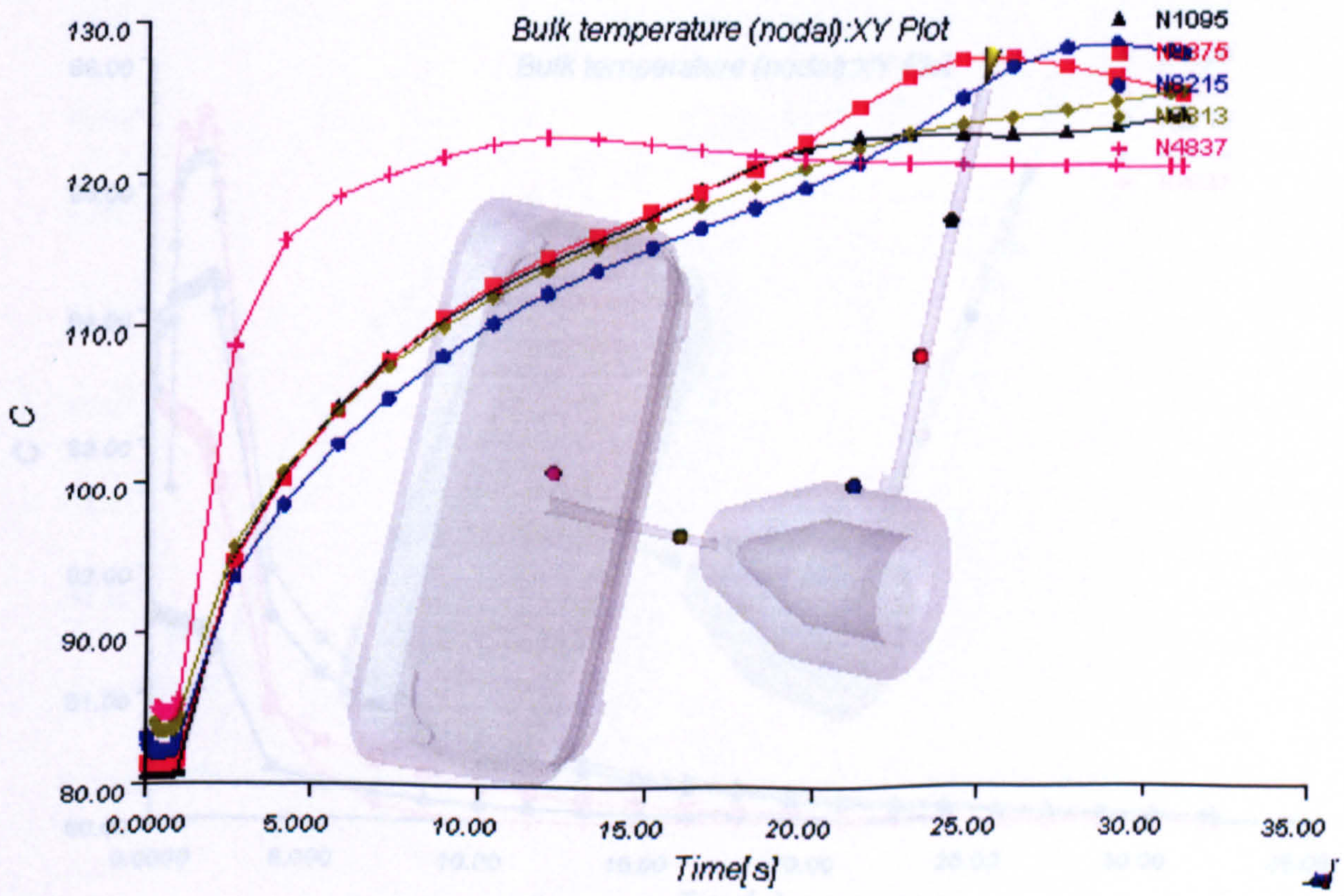

Figure App4.1 f.) Mould temperature 130°C

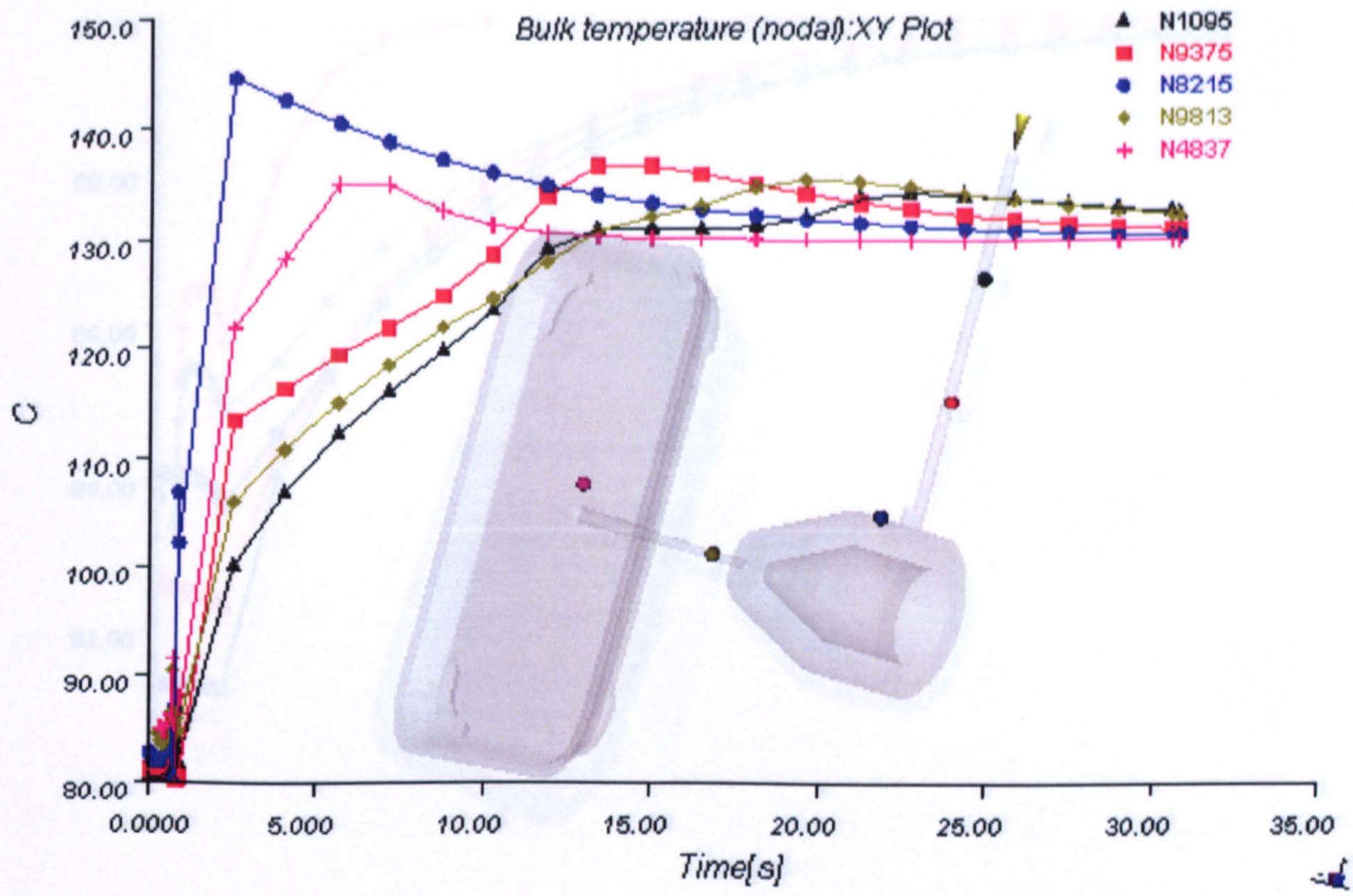

Figure App4.2 Injection time-melt temperature plot at 2-second injection time and mould temperatures is varied from 80 to 130°C

Figure App4.2 a.) Mould temperature 80°C

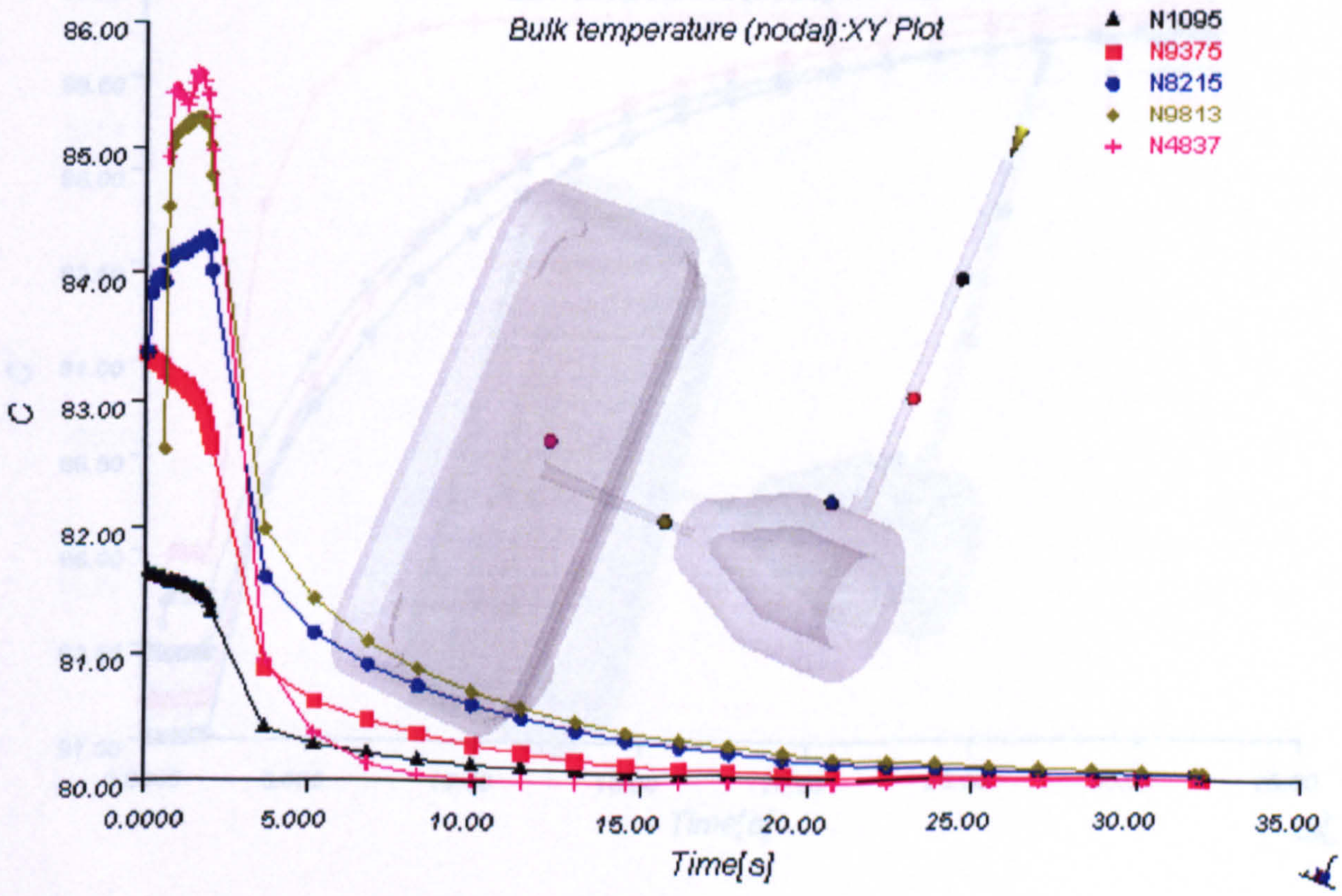

Figure App4.2 b.) Mould temperature 90°C

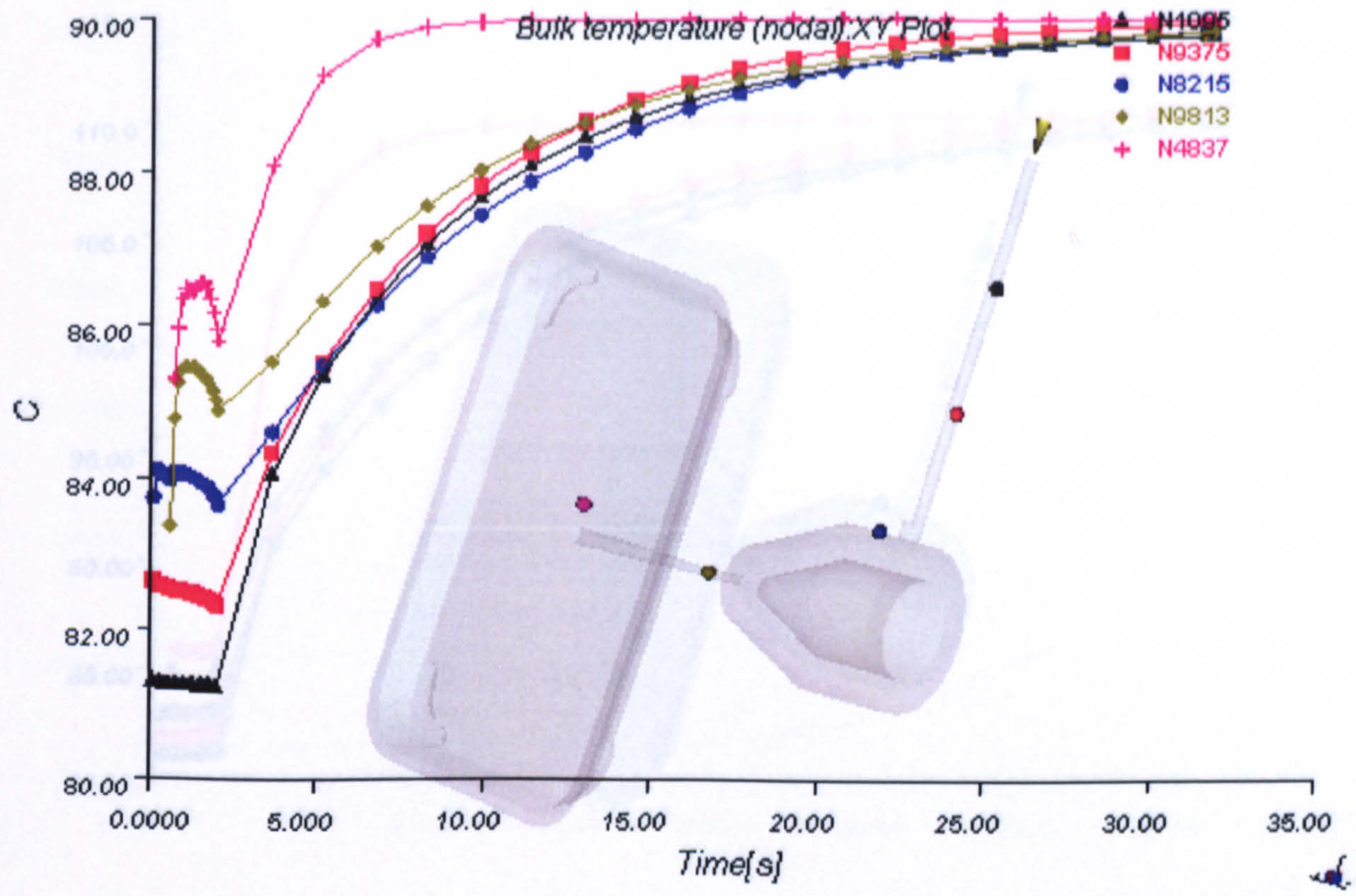

Figure App4.2 c.) Mould temperature 100°C

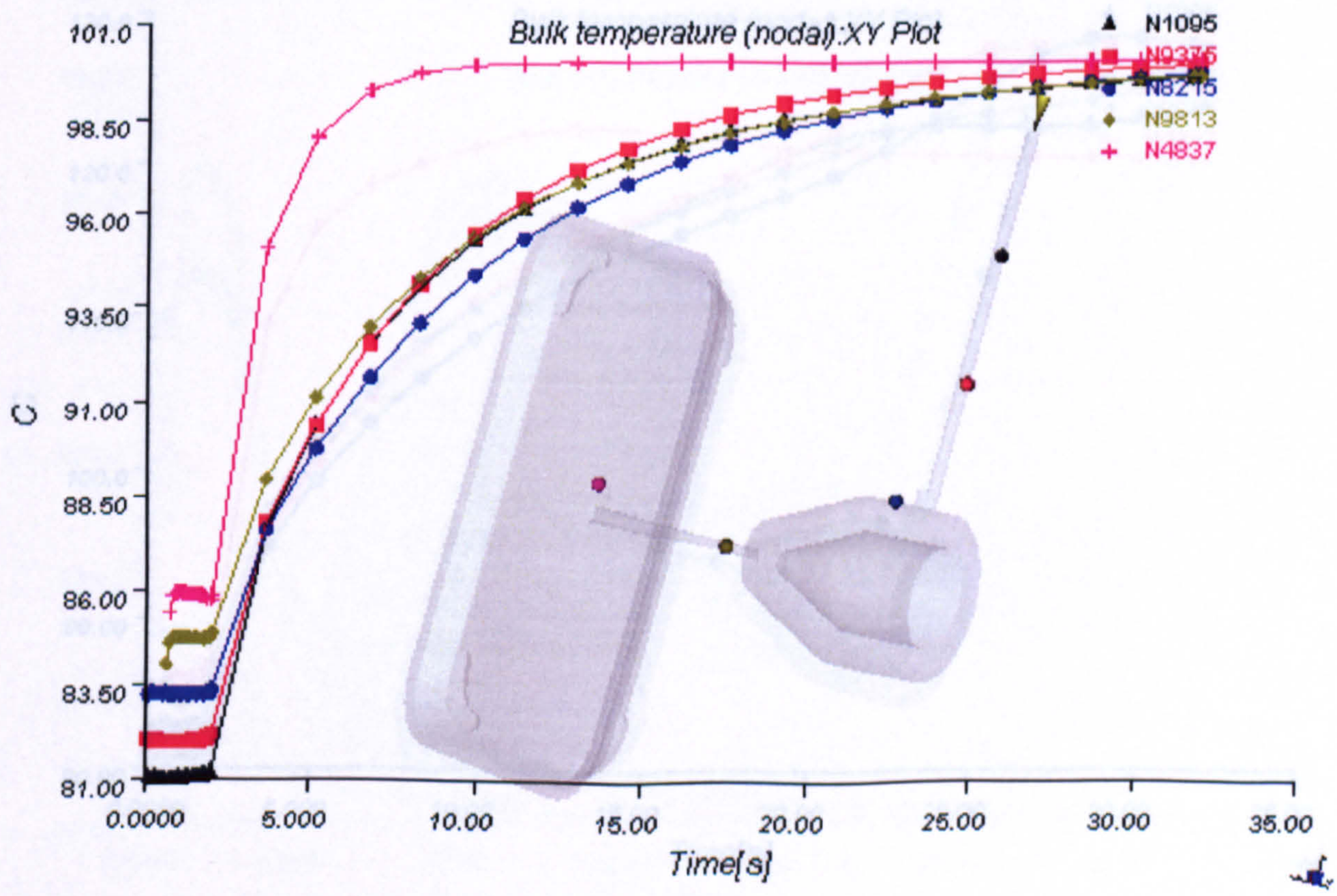

Figure App4.2 d.) Mould temperature 110°C

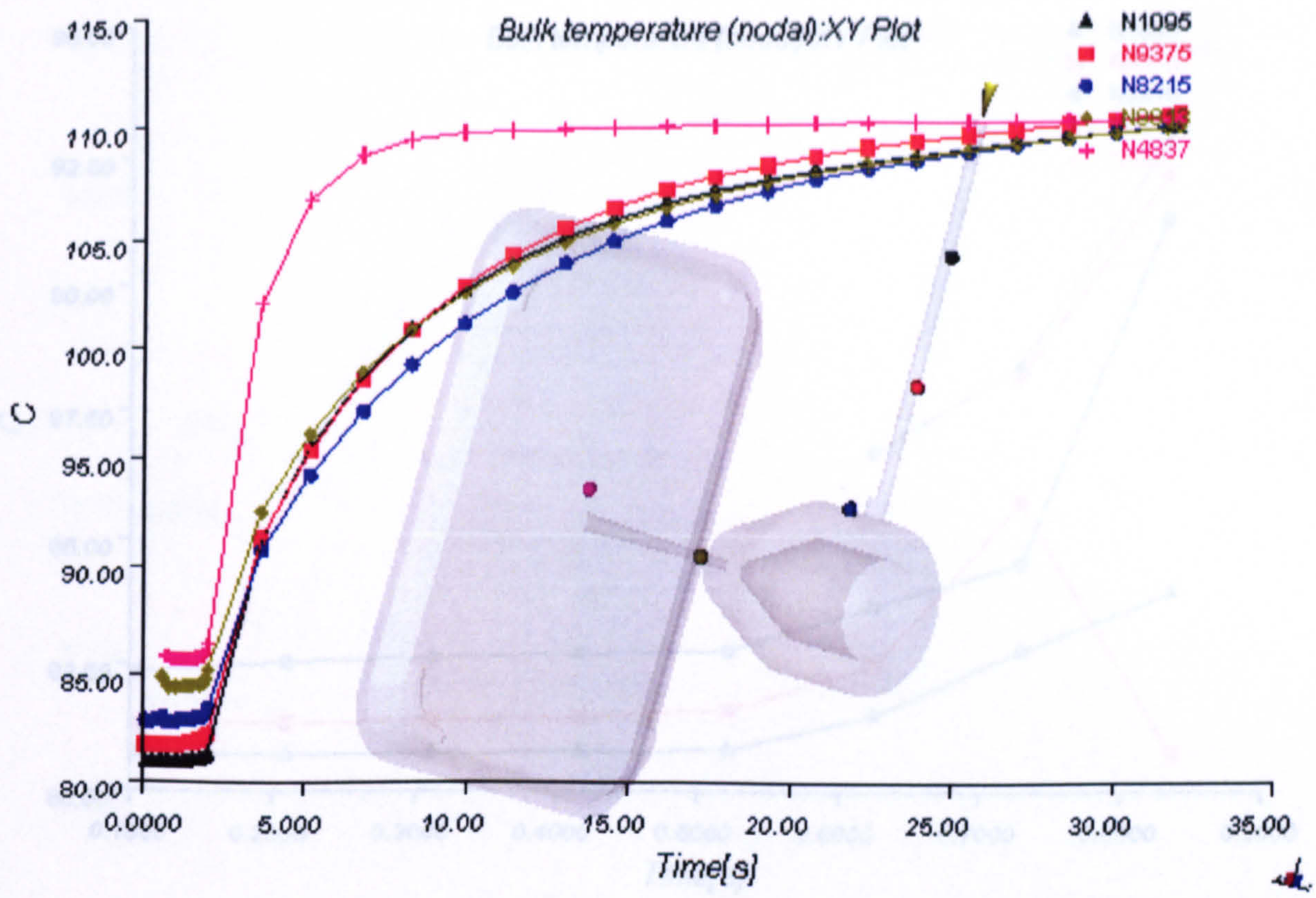

Figure App4.2 e.) Mould temperature 120°C

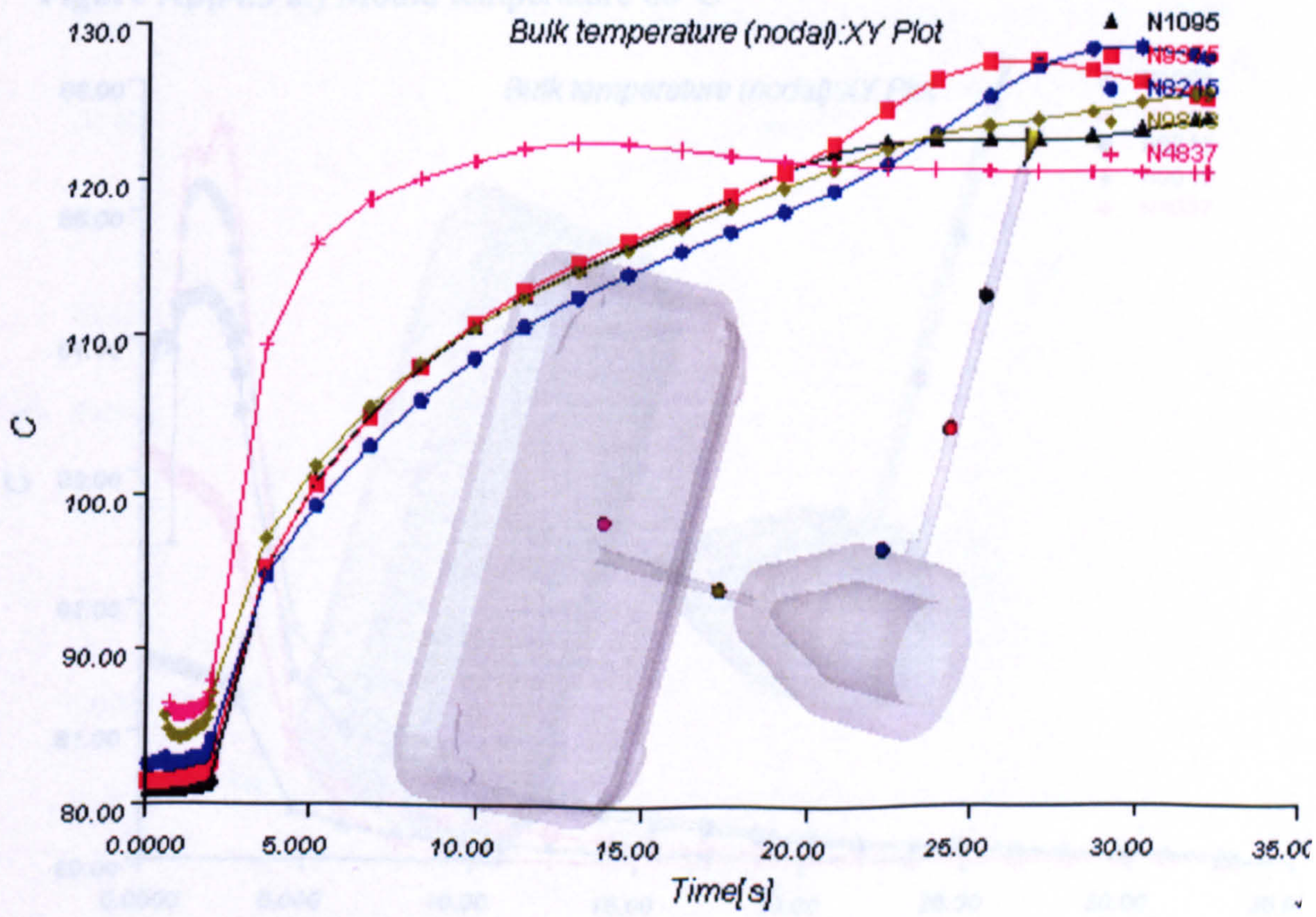

Figure App4.2 d.) Mould temperature 110°C

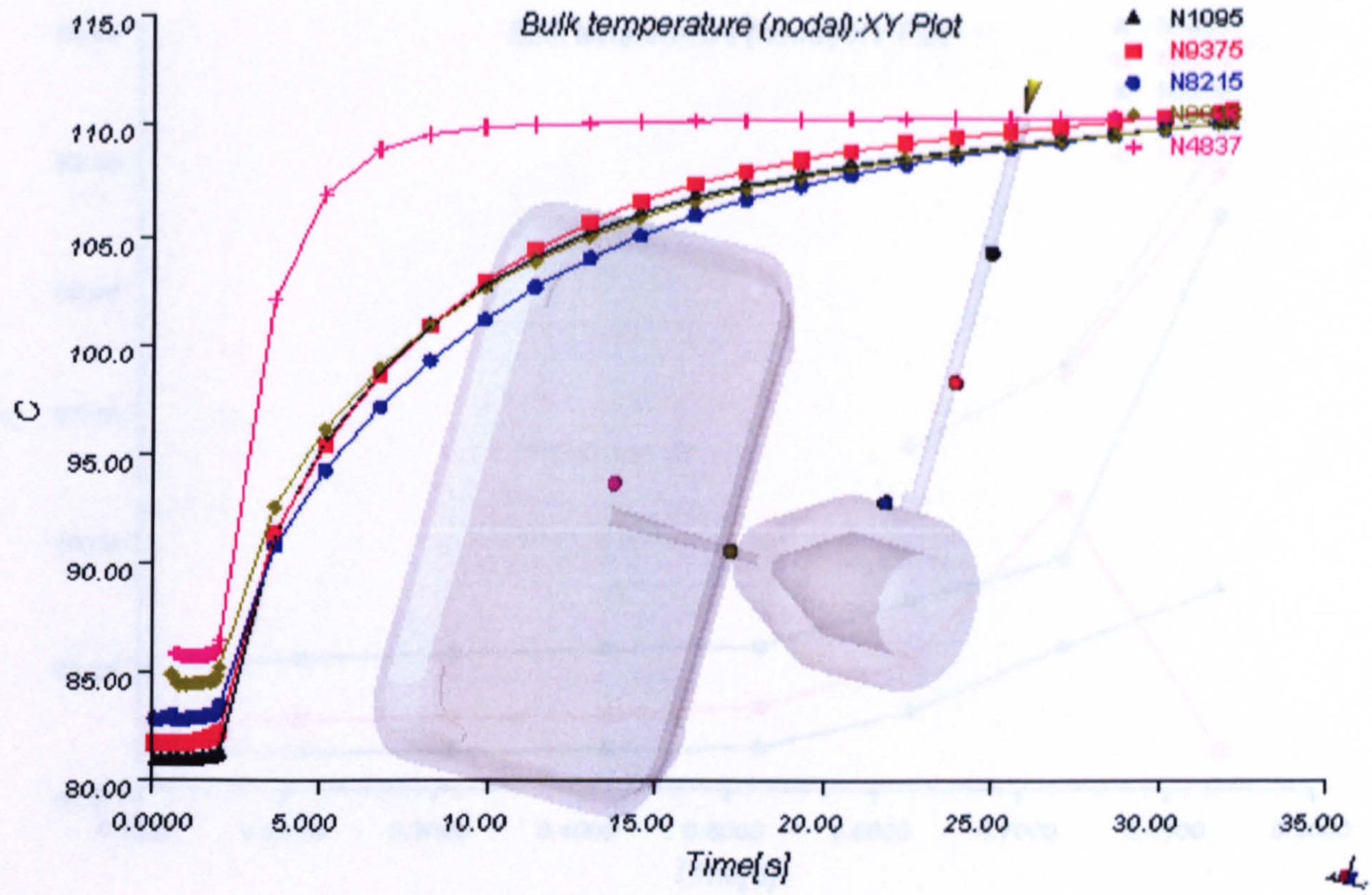

Figure App4.2 e.) Mould temperature 120°C

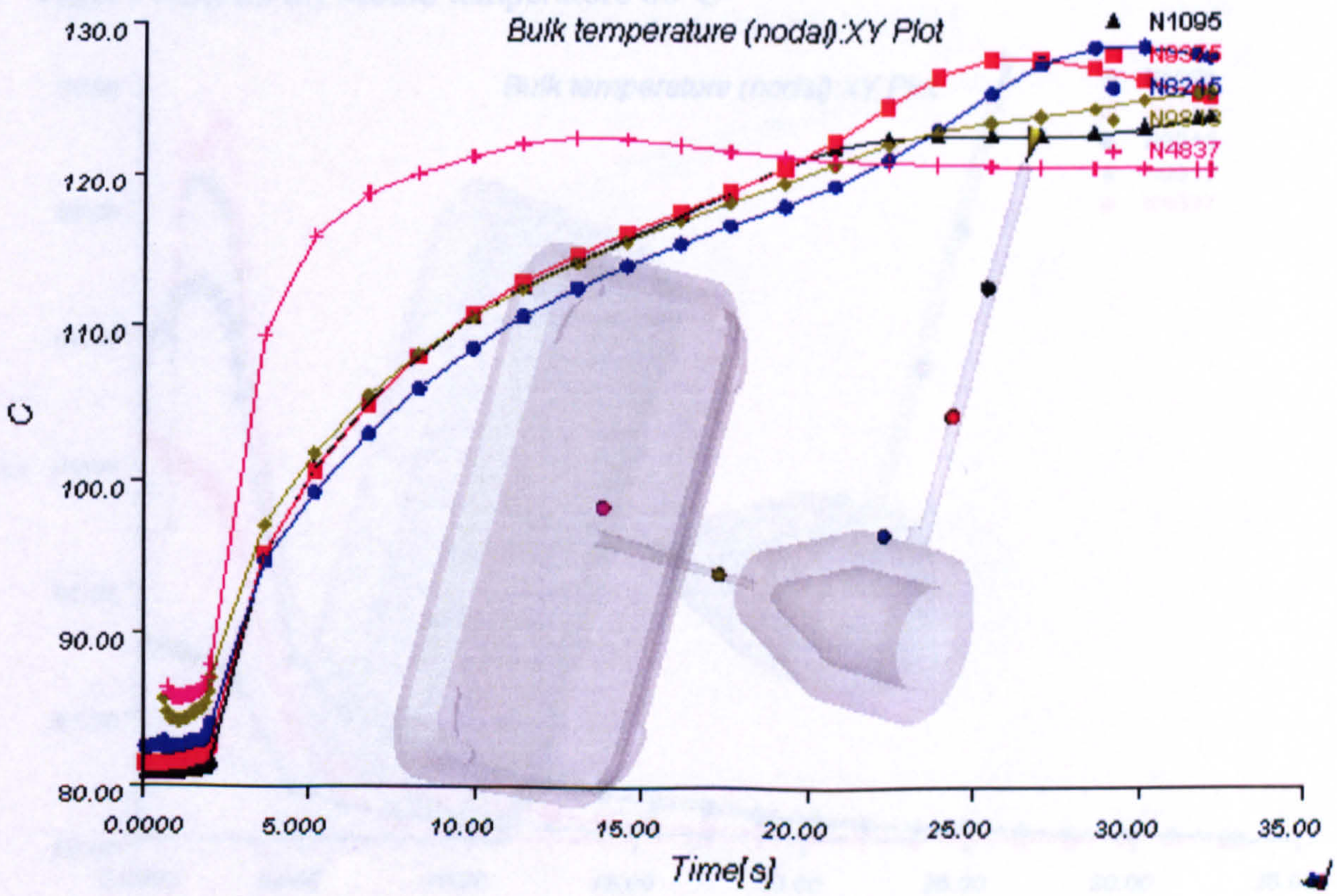

Figure App4.2 f.) Mould temperature 130°C

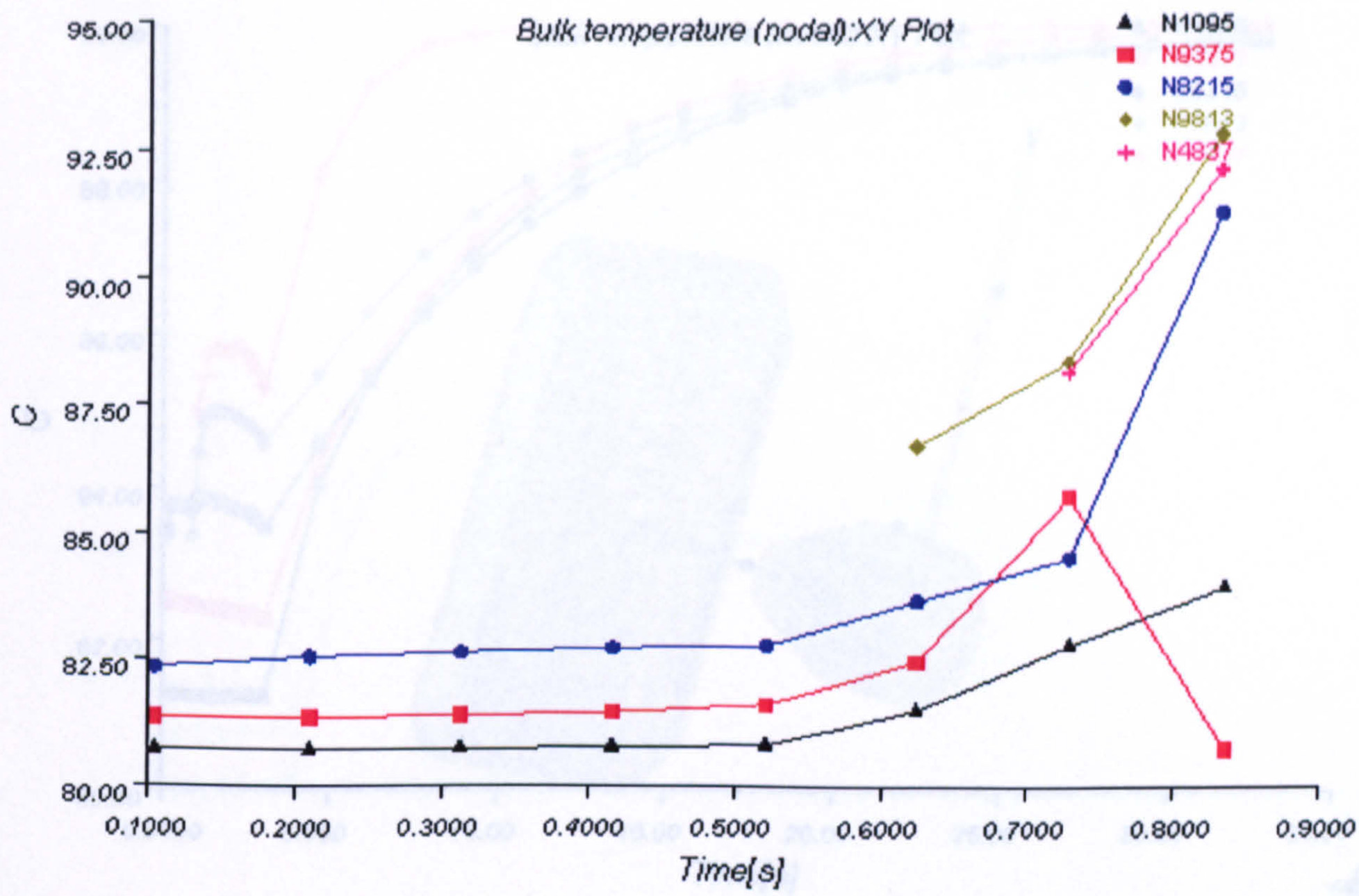

Figure App4.3 Injection time-melt temperature plot at 3-second injection time and mould temperatures is varied from 80 to 130°C

Figure App4.3 a.) Mould temperature 80°C

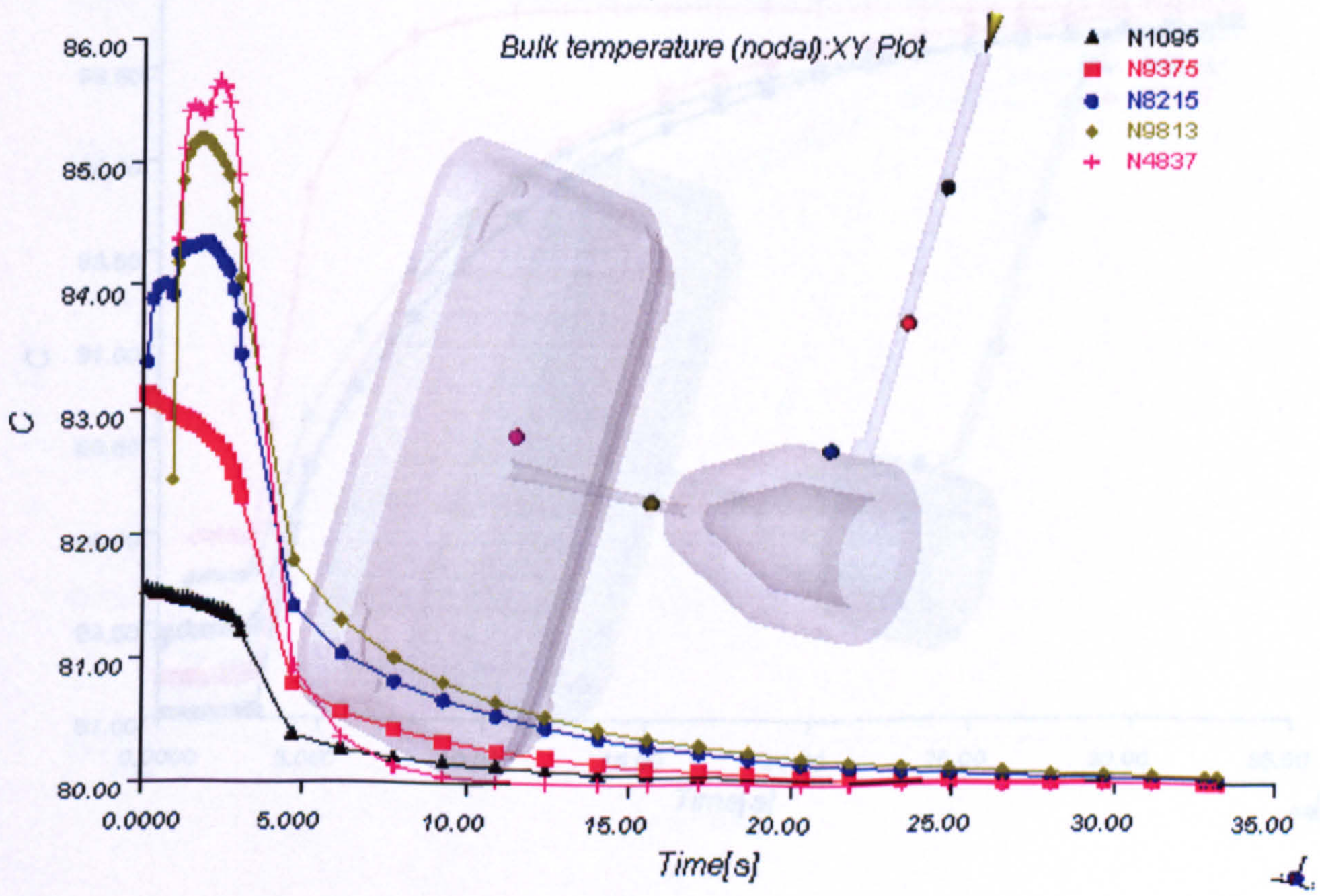

Figure App4.3 b.) Mould temperature 90°C

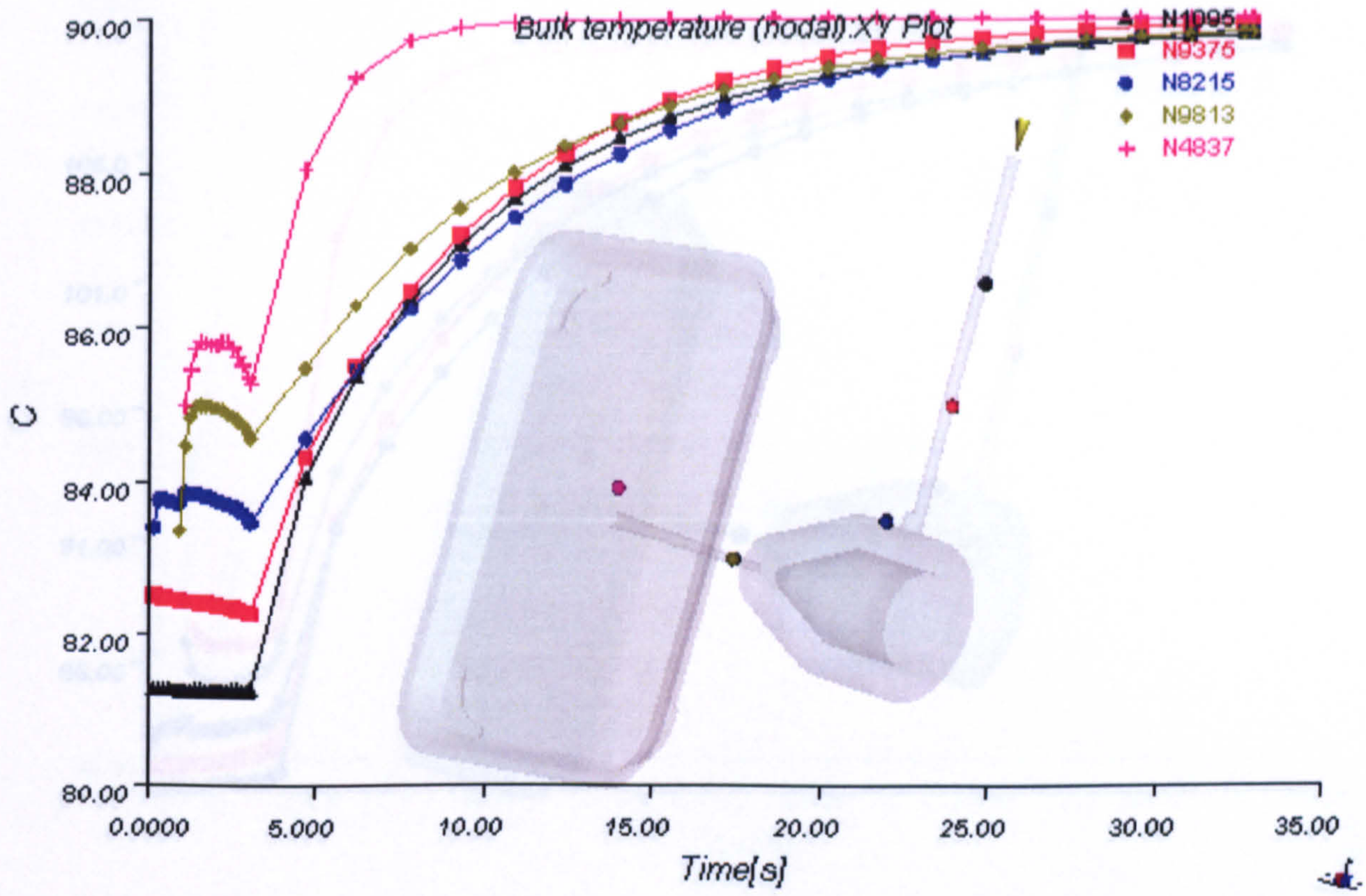

Figure App4.3 c.) Mould temperature 100°C

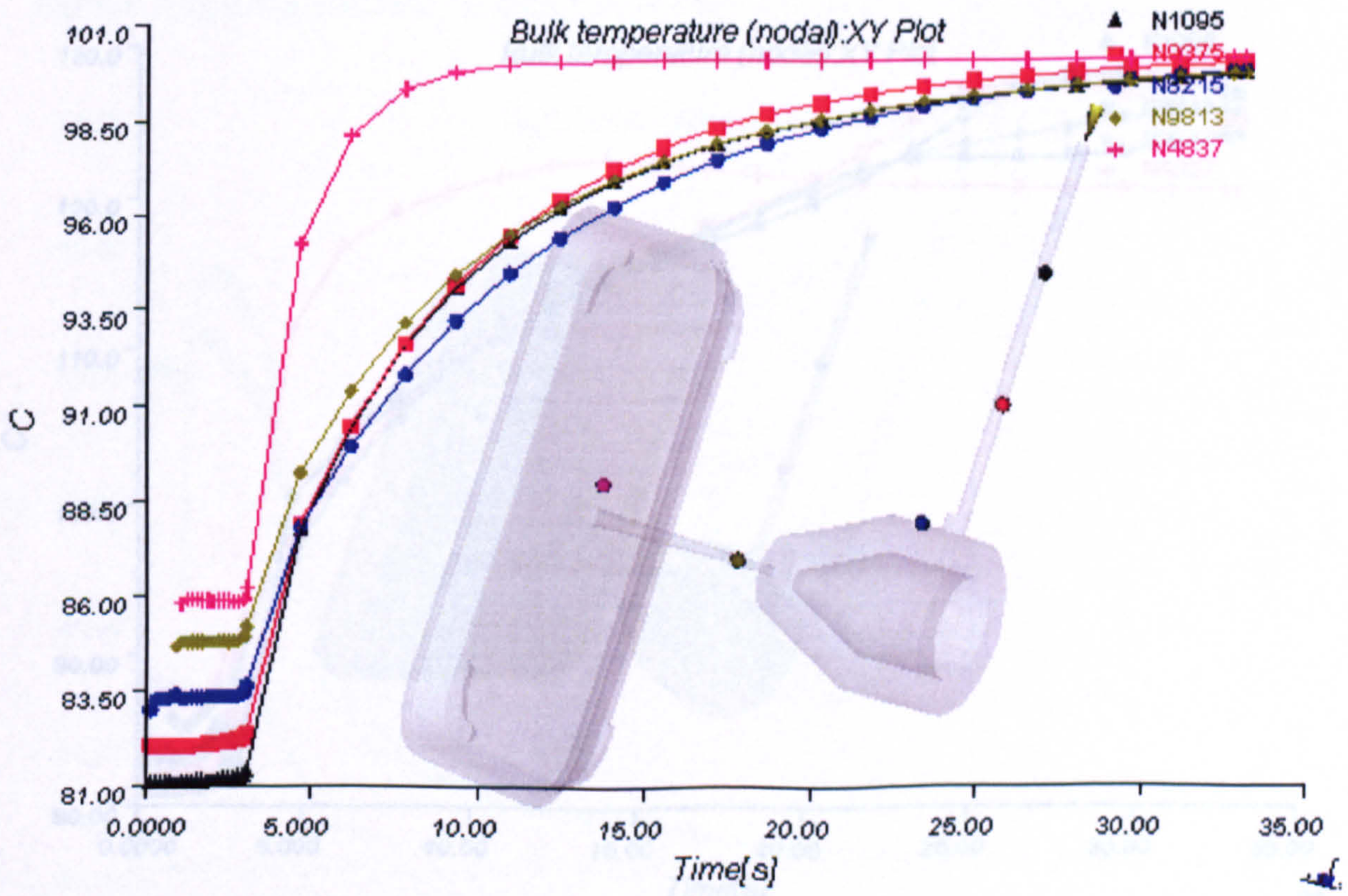

Figure App4.3 d.) Mould temperature 110°C

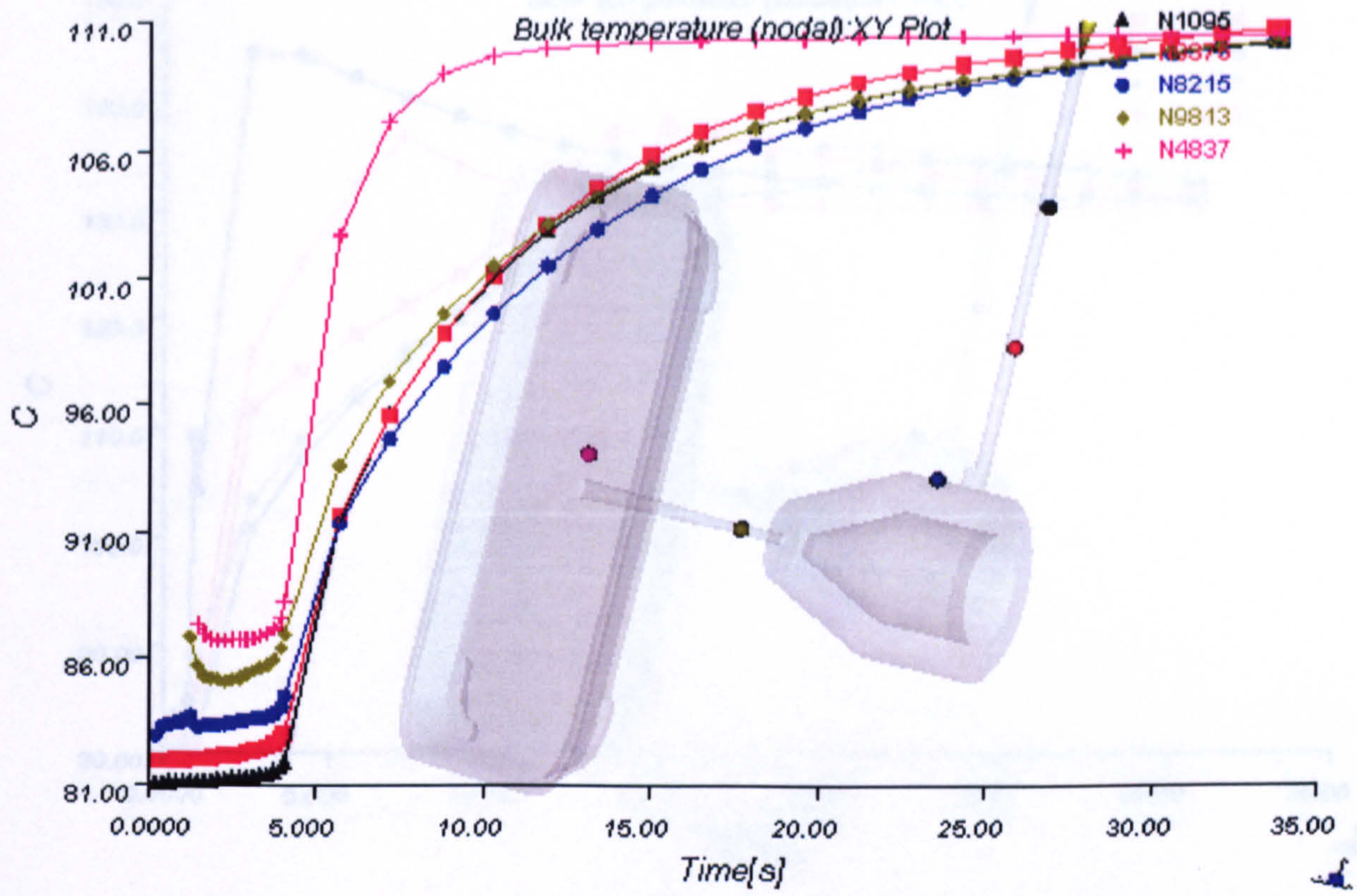

Figure App4.3 e.) Mould temperature 120°C

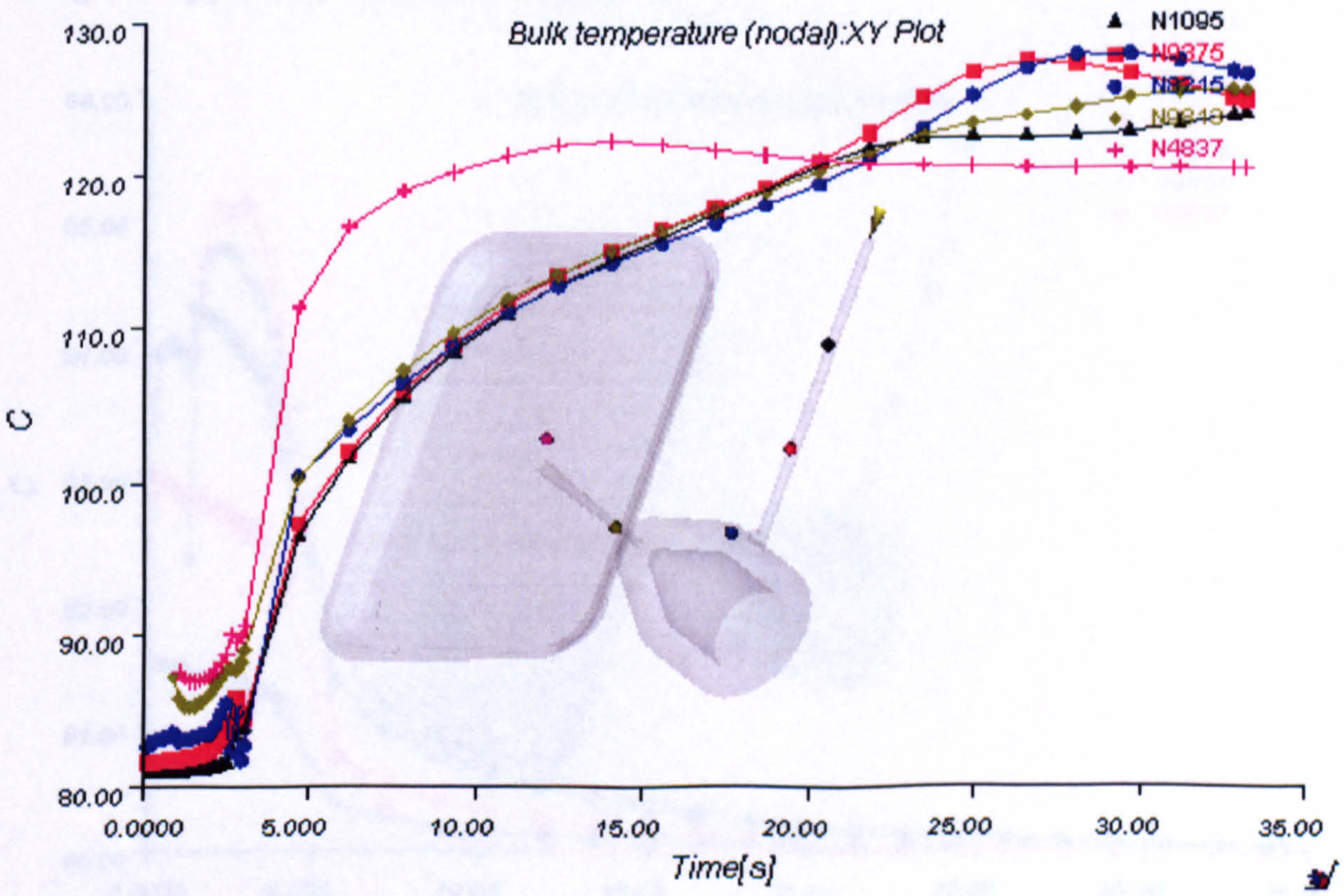

Figure App4.3 f.) Mould temperature 130°C

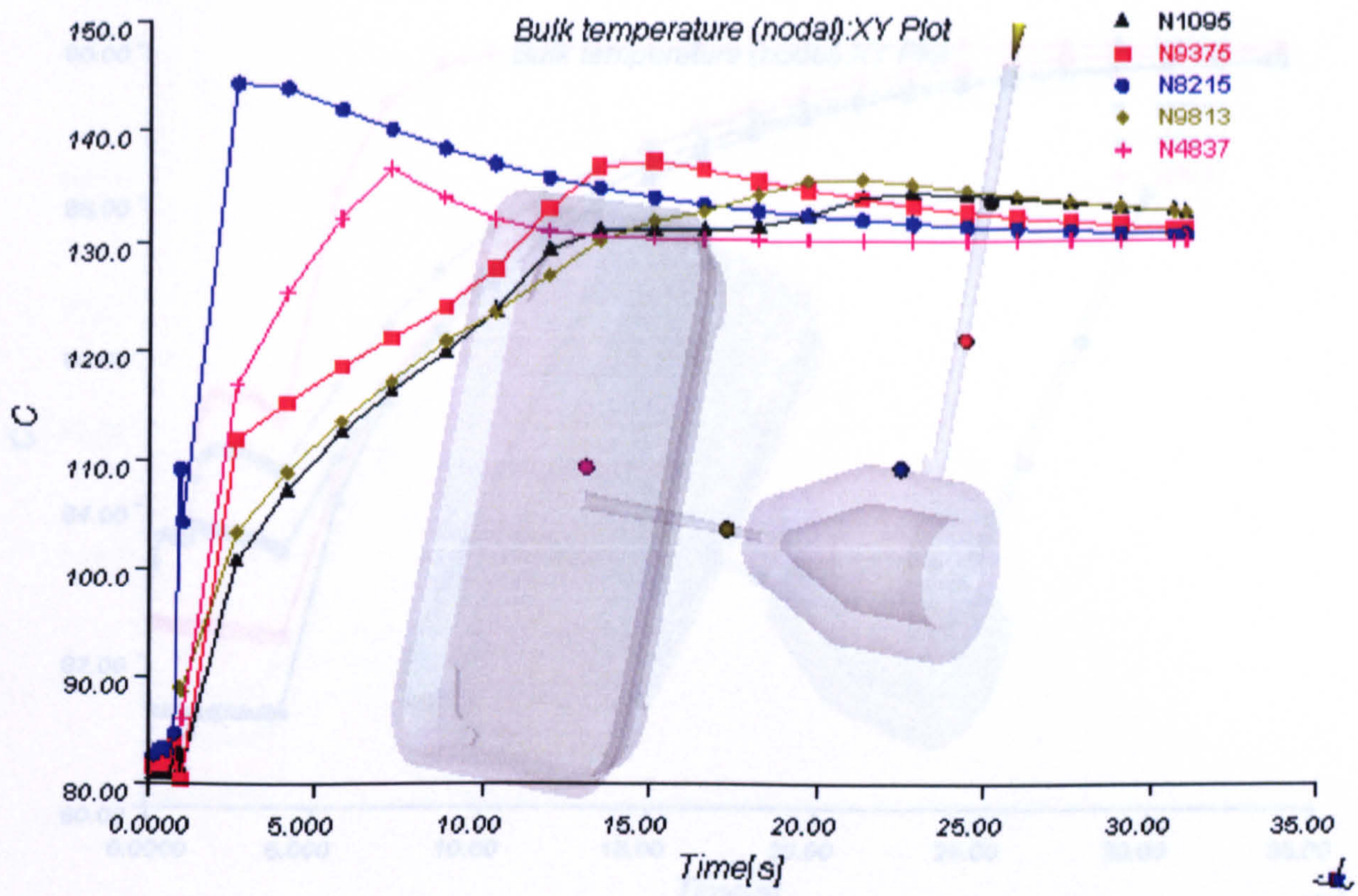

Figure App4.4 Injection time-melt temperature plot at 4-second injection time and mould temperatures is varied from 80 to 130°C

Figure App4.4 a.) Mould temperature 80°C

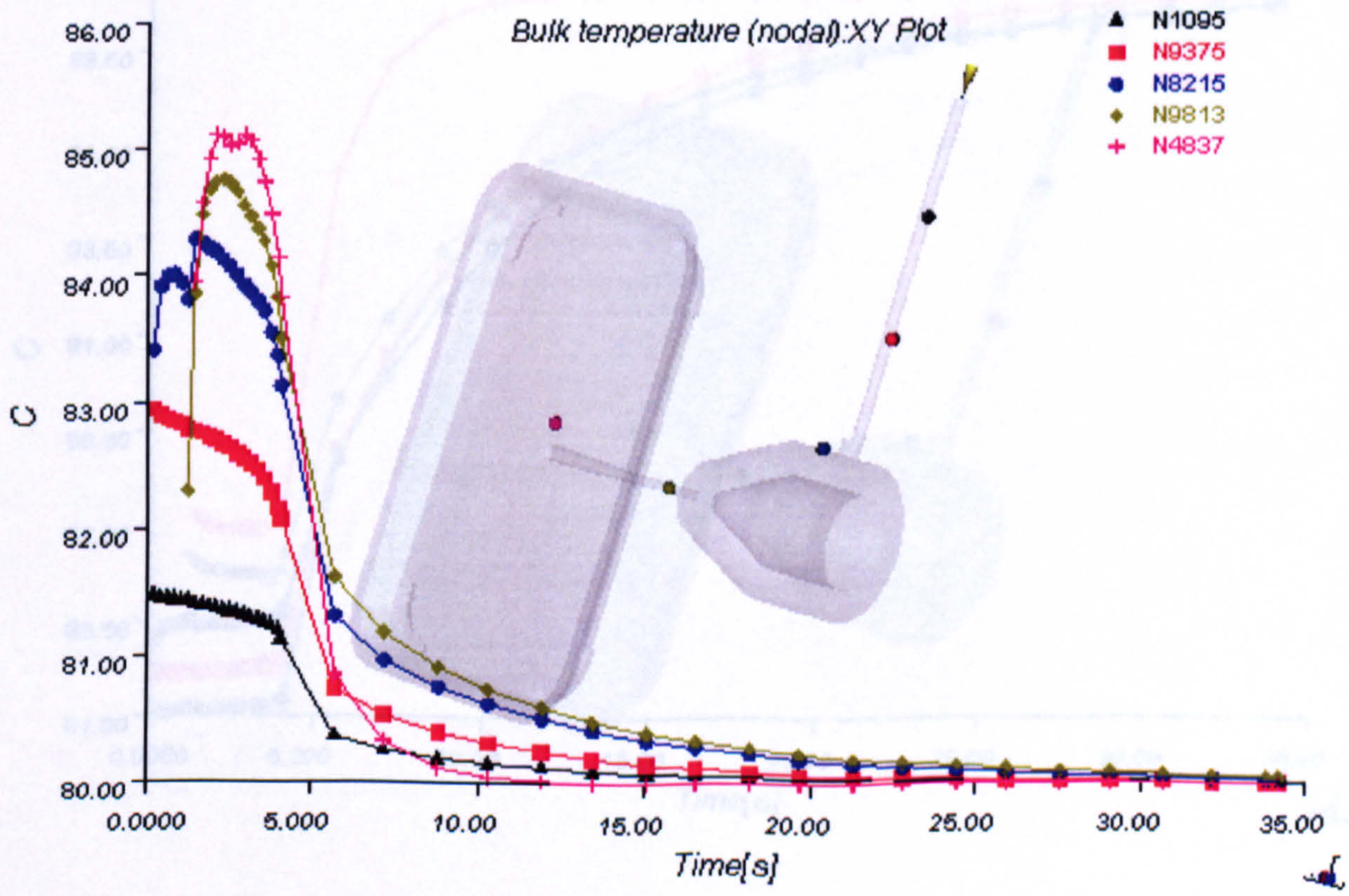

Figure App4.4 b.) Mould temperature 90°C

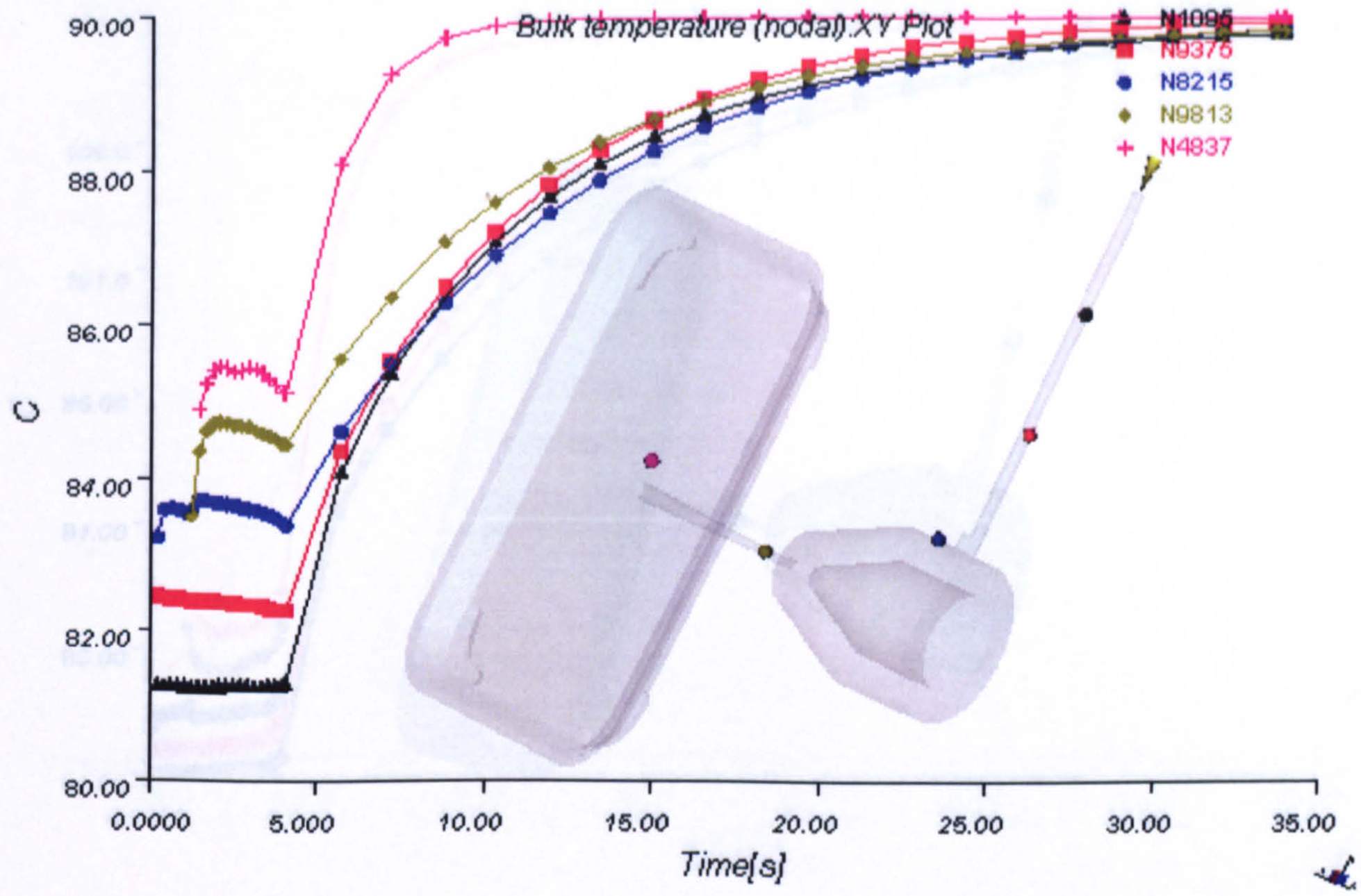

Figure App4.4 c.) Mould temperature 100°C

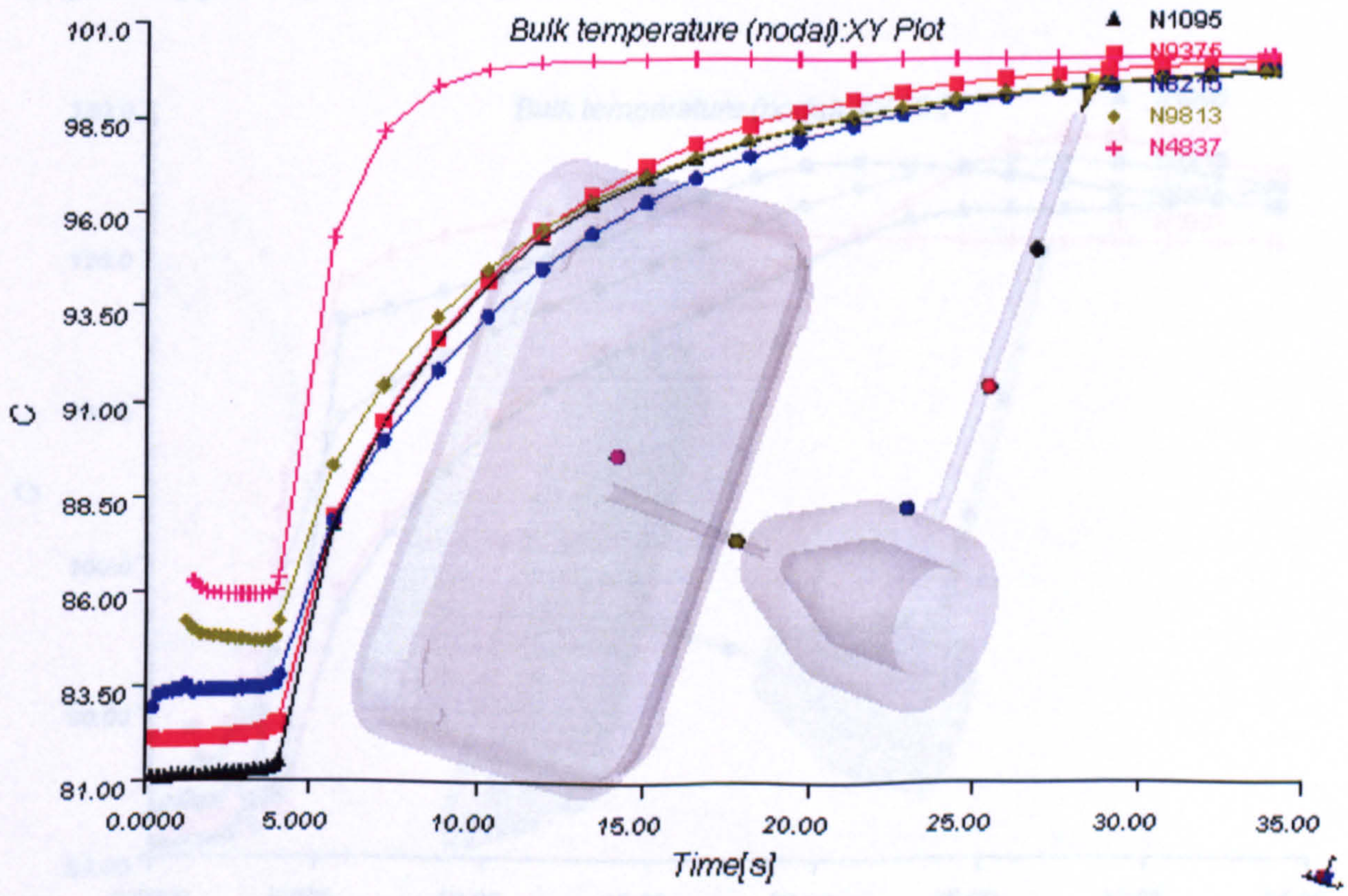

Figure App4.4 d.) Mould temperature 110°C

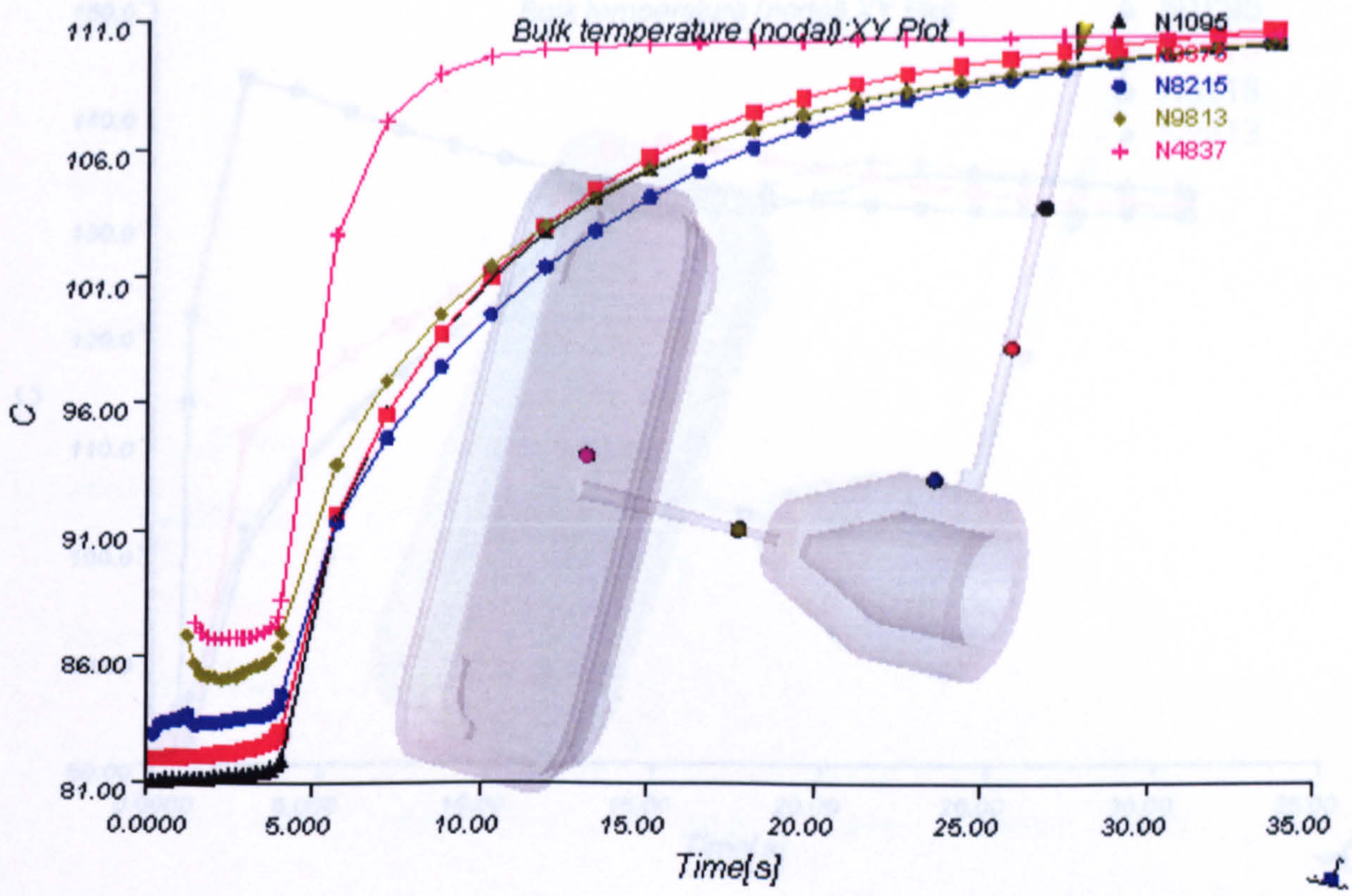

Figure App4.4 e.) Mould temperature 120°C

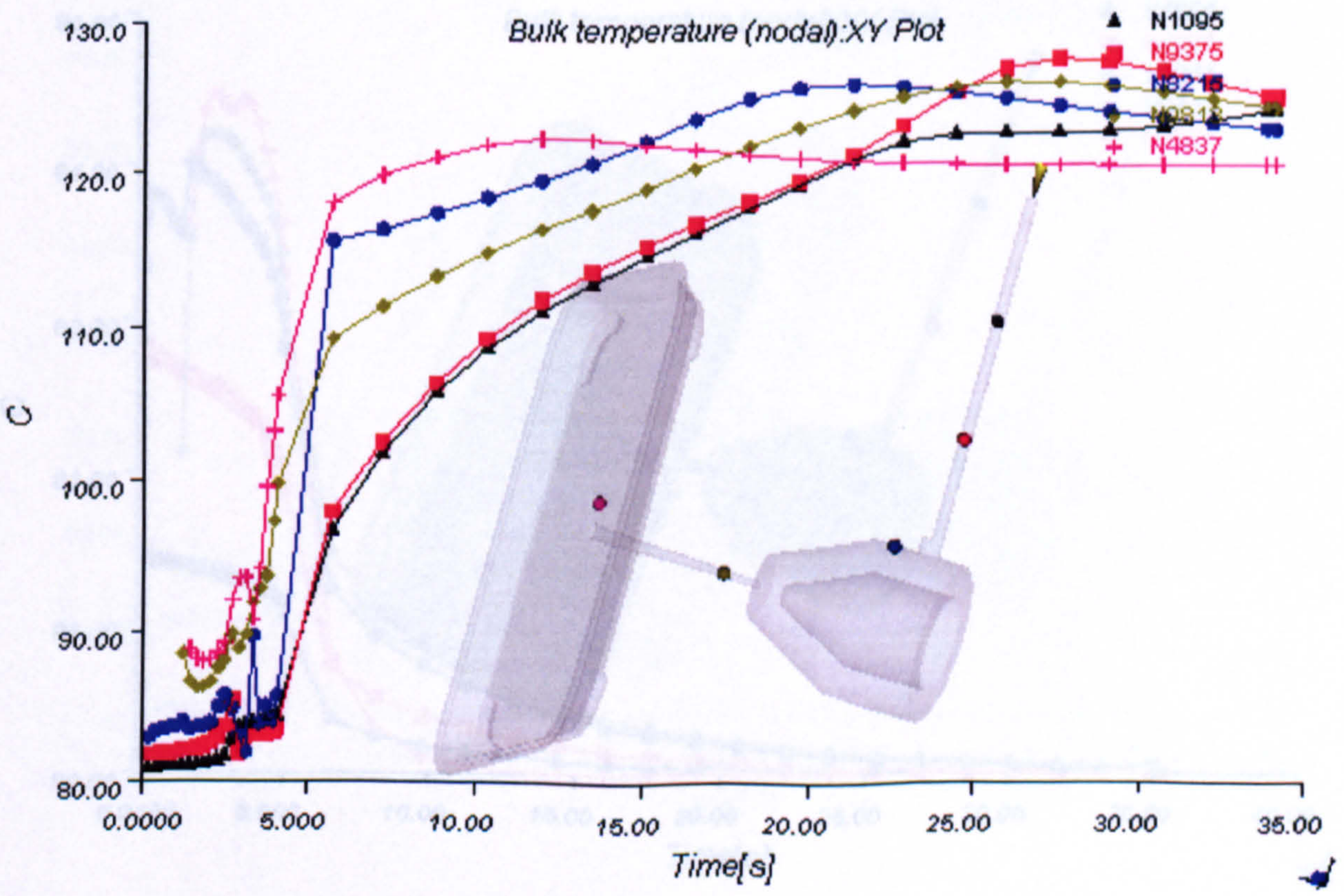

Figure App4.4 f.) Mould temperature 130°C

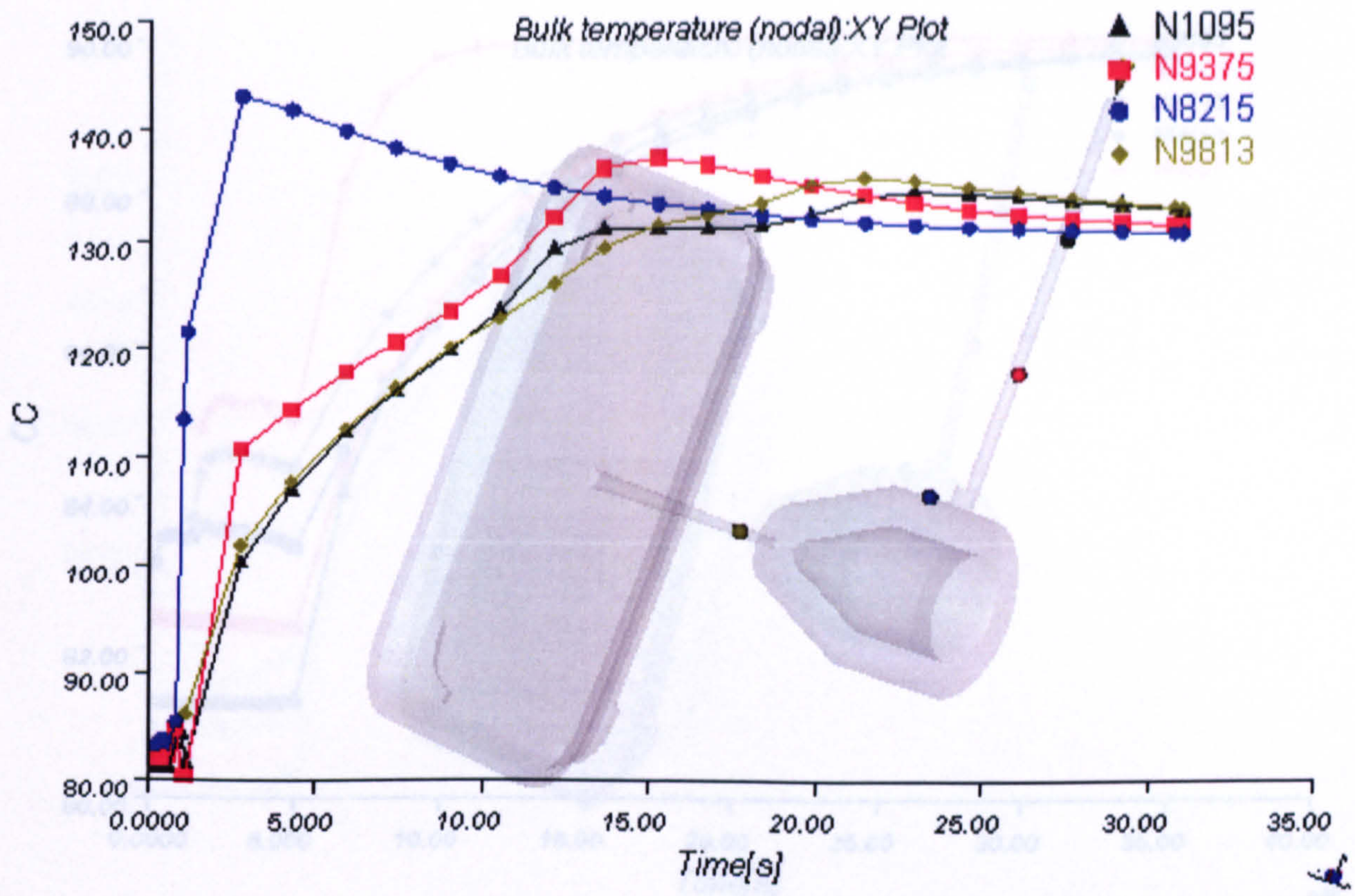

Figure App4.5 Injection time-melt temperature plot at 5-second injection time and mould temperatures is varied from 80 to 130°C

Figure App4.5 a.) Mould temperature 80°C

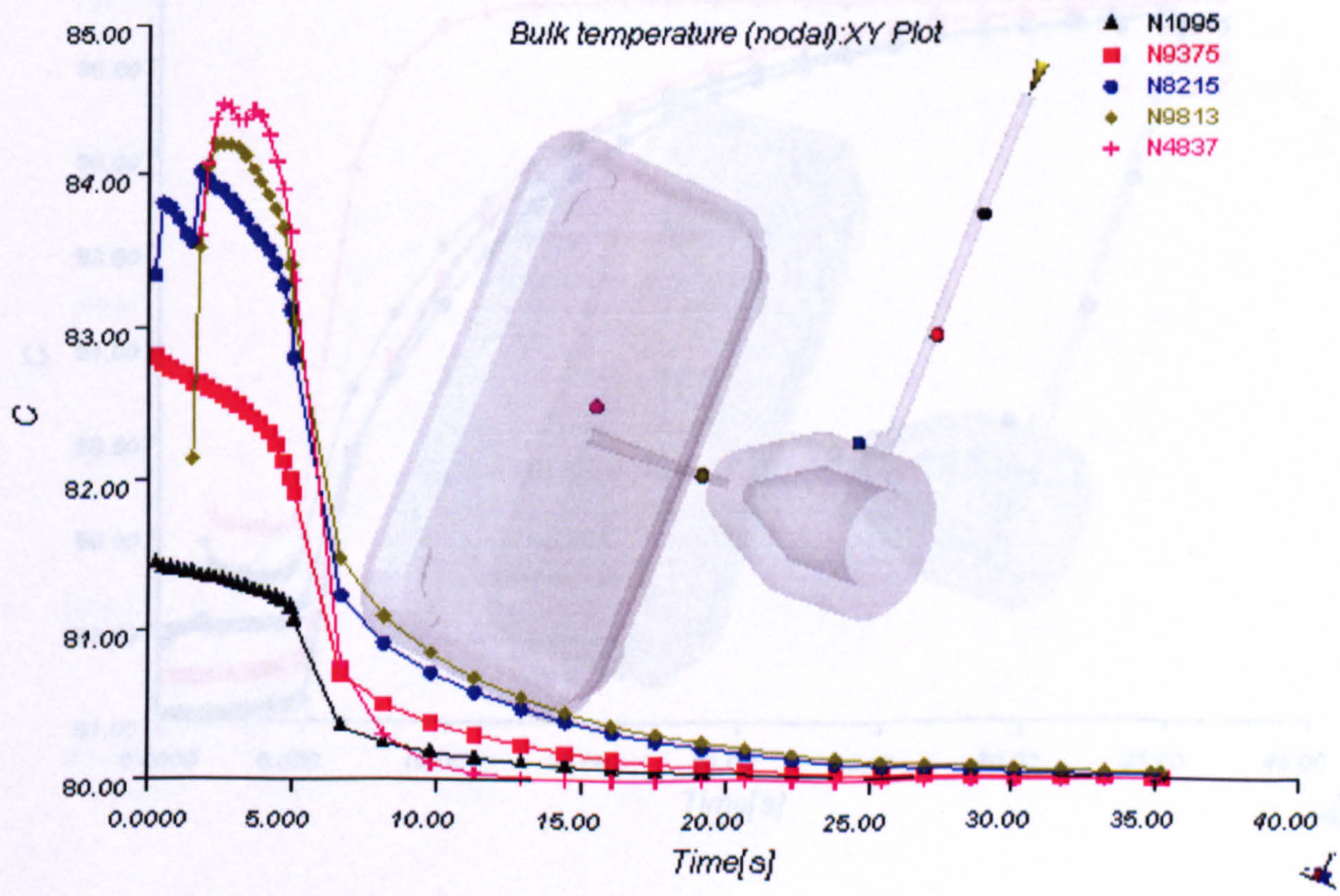

Figure App4.5 b.) Mould temperature 90°C

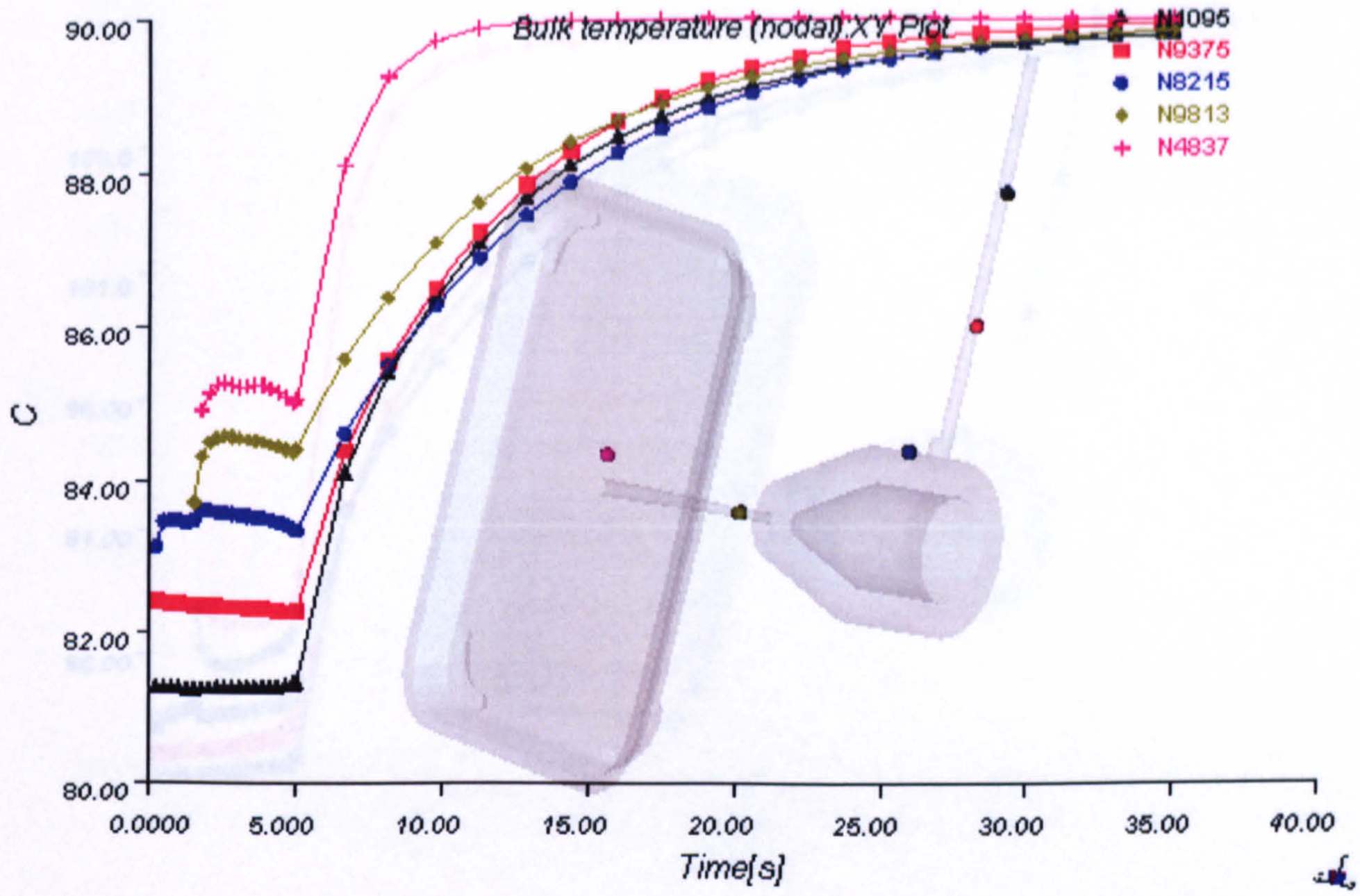

Figure App4.5 c.) Mould temperature 100°C

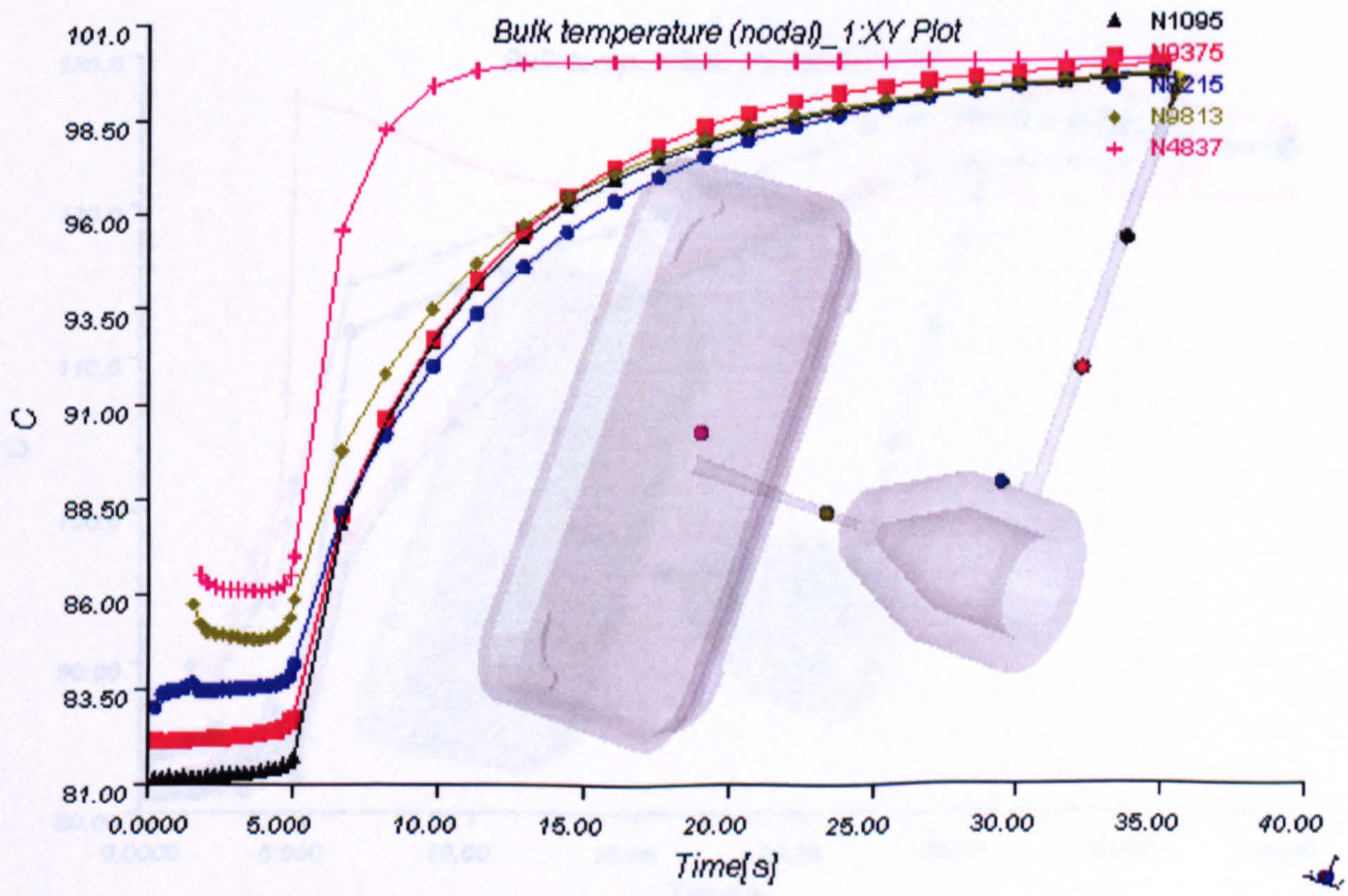

Figure App4.5 d.) Mould temperature 110°C

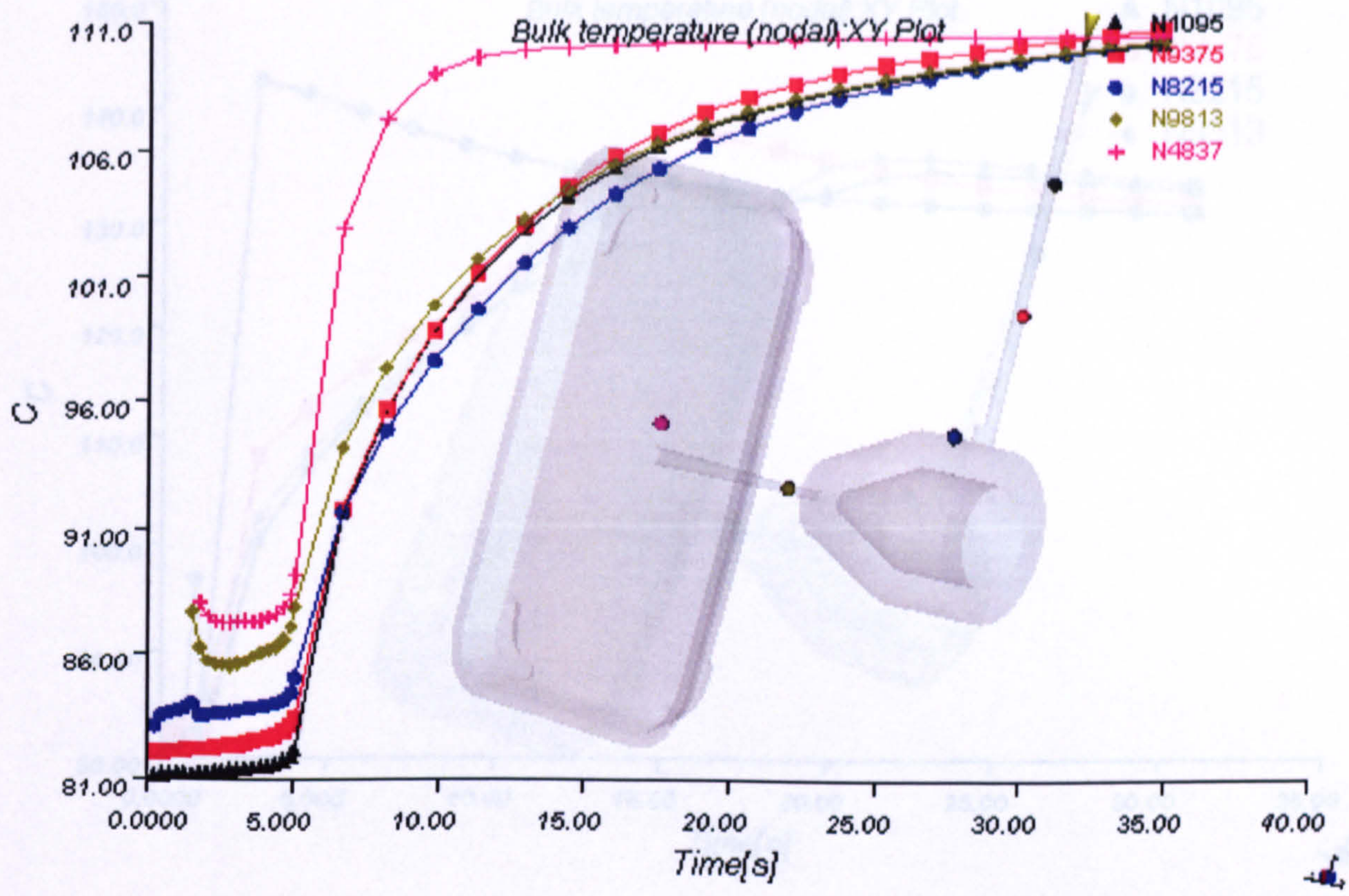

Figure App4.5 e.) Mould temperature 120°C

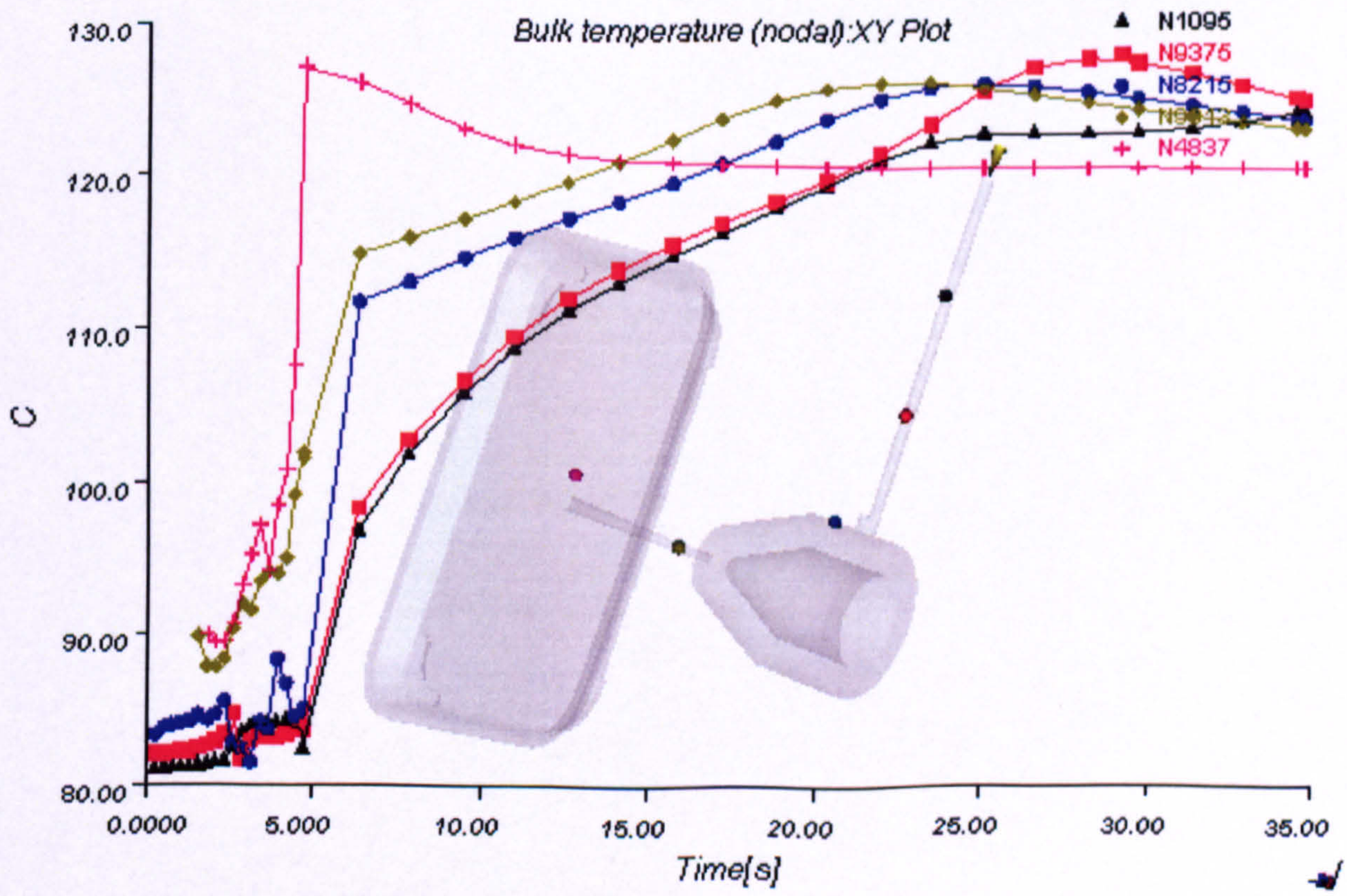

Figure App4.5 f.) Mould temperature 130°C

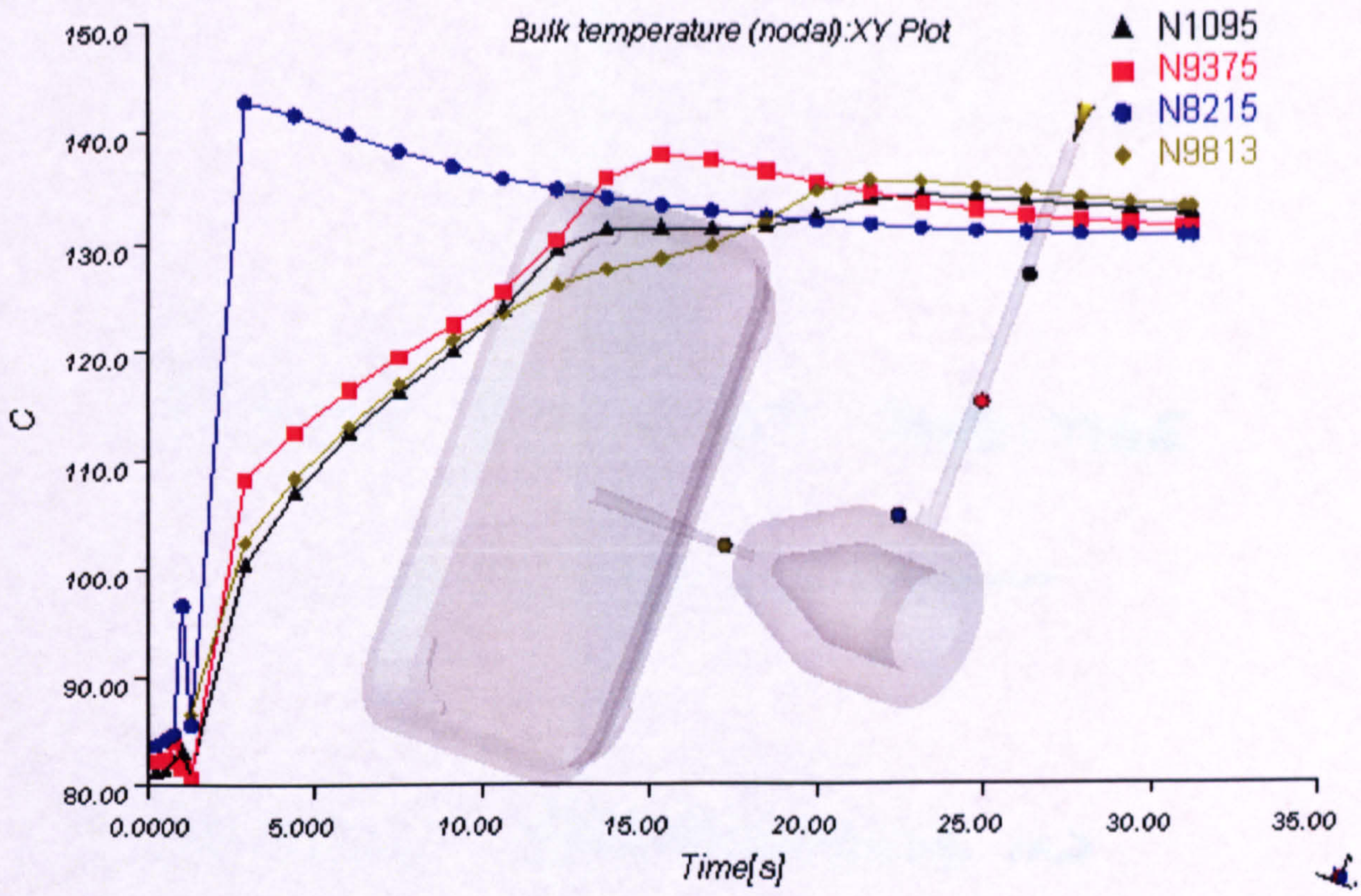

PAGE/PAGES
EXCLUDED
UNDER
INSTRUCTION
FROM
UNIVERSITY